STUDIES ON SECONDARY METABOLITES OF *C. LONGA* AND *A. RACEMOSUS* INFLUENCED BY PLANT GROWTH PROMOTING RHIZOBACTERIA

A THESIS SUBMITTED TO

SHIVAJI UNIVERSITY, KOLHAPUR

FOR THE DEGREE OF

DOCTOR OF PHILOSOPHY

IN

MICROBIOLOGY

UNDER THE FACULTY
OF
SCIENCE AND TECHNOLOGY

BY

MISS. RUDDHI RAJENDRA JAGTAP
M.Sc., SET, NET-ICAR

UNDER THE GUIDANCE OF

Dr. GAJANAN VISHNU MALI
M. Sc., Ph. D
Rayat Institute of Research and Development, Satara

AND

CO-GUIDANCE OF

Prof. (Dr.) KAILAS DASHRATH SONAWANE
M. Sc., Ph. D
Head,
Department of Biochemistry,
Shivaji University, Kolhapur.

2023

CERTIFICATE

This is to certify that the thesis entitled "**Studies on Secondary Metabolites of *C. longa* and *A. racemosus* influenced by Plant Growth Promoting Rhizobacteria**" is being submitted herewith for the award of the Degree of Doctor of Philosophy in Microbiology under the Faculty of Science and Technology of Shivaji University, Kolhapur. The work reported in this thesis is based upon the results of original experimental work carried out by **Ms. Ruddhi Rajendra Jagtap** under our supervision and guidance and the papers published are included under UGC approved journal list. To the best of my knowledge and belief the work embodied in this thesis has not formed earlier the basis for the award of any degree or similar title of this or any other university or examining body.

In view of university Grants Commission (Promotion of Academic Integrity and Prevention of plagiarism in Higher Educational Institutions) Regulations, 2018 dated 31st July 2018, this is also to certify that the work done by the **Ms. Ruddhi Rajendra Jagtap** is plagiarism free.

Place: Kolhapur
Date:

Prof. (Dr.) K. D. Sonawane
(Research Co-guide)

Dr. G. V. Mali
(Research Guide)

Dr. B. T. Jadhav
Director
Rayat Institute of Research and Development, Satara

Dr. P. M. Gurao
Head I/C
Department of Microbiology, Shivaji University, Kolhapur

DECLARATION AND UNDERTAKING

I hereby declare that the thesis entitled "**Studies on Secondary Metabolites of *C. longa* and *A. racemosus* influenced by Plant Growth Promoting Rhizobacteria**" completed and written by me has not previously formed the basis for the award of any degree or similar title of this or any other university or examining body. Further, I declare that I have not violated any of the provisions under the acts of Copyright/Piracy/Cyber/IPR etc. amended from time to time.

In view of university Grants Commission (Promotion of Academic Integrity and Prevention of plagiarism in Higher Educational Institutions) Regulations, 2018 dated 31st July 2018, I hereby submit an undertaking that this thesis is my original work and it is free of any plagiarism. Further, it is also to state that this thesis has been duly checked through a Plagiarism detection tool approved by Shivaji University.

Place: Kolhapur
Date:

Miss. Ruddhi Rajendra Jagtap
(Research Student)

Acknowledgements

First and foremost I would like to record my gratitude and heartfelt thanks to my guide Dr. G. V. Mali , Rayat Institute of Research and Development (Associate Professor, UG & PG Department of Microbiology, Bharati Vidyapeeth (Deemed to be University) Yashwantrao Mohite College, Pune, India) and co-guide Prof. (Dr) Kailas D. Sonawane, Head, Department of Biochemistry and Co-Ordinator of Post Graduate Diploma in Bioinformatics, Shivaji University, Kolhapur, India, for joining and giving me an opportunity to study on a topic related to plant growth promoting rhizobacteria. Their valuable guidance, help and support has been always helpful to complete my research work positively. I hope that their energy, attention to detail, and enthusiasm have been instilled in me.

My sincere thanks to Dr. P. M. Gurao, In-charge Head, Department of Microbiology, Shivaji University, Kolhapur for providing laboratory facilities and encouragement and for his kind support, guidance and invaluable advice. I am also thankful to Prof. & Head (Mrs.). J. P. Jadhav, Department of Biotechnology, Shivaji University Kolhapur, India for providing the laboratory facility, support and timely inspiration. I would also like to thank Dr. M. S. Nimbalkar, Department of Botany, Shivaji University Kolhapur, India for providing instrumental facilities and valuable guidance. My sincere thanks to all my respected teachers Dr. (Mrs.). P. B. Dandge, Dr. N. H. Nadaf and late Dr. S. R. Waghmare whose valuable guidance, suggestions, and support always inspired and helped me.

I am also thankful to the Director of the Rayat Institute of Research and Development in Satara, Maharashtra, India, for allowing me to work at their institute. Also grateful to Mr. Bapu Awatade, Superintendent, RIRD, for his assistance throughout the research process, as well as teachers and research colleagues from Yashavantrao Chavan Institute of Science, Satara.

I am also grateful to the Authorities of Chhatrapati Shahu Maharaj Research, Training and Human Development Institute (SARTHI) for providing financial support for this research in the form of Junior Research Fellowships (JRF) and Senior Research Fellowships (SRF). I was greatly helped by the financial assistance I received from SARTHI for my ongoing

research. The Ph.D. training, I received from SARTHI in its early stages was extremely motivating for me to complete my research work.

I would also like to thank all the non-teaching staff from the Department of Microbiology for their timely support and cooperation. I sincerely express my thanks to all research colleagues from my Department and University campus for providing continuous inspiration and support during this study. I would also like to thank all my friends who supported me and incented me to strive toward my goal. I think it has been a nice place to work due to the healthy environment and good discussions within us to carry out scientific activities. At last with heartfelt emotions, I would like to dedicate my thesis to my beloved Gurudev, my Parents, my Husband, and my family members.

Ms. Ruddhi Rajendra Jagtap

ABBREVIATIONS

PGPR	Plant growth promoting rhizobacteria
Ca-P	Calcium phosphate
Fe-P	Iron phosphate
Mn-P	Manganese phosphate
Al-P	Aluminium phosphate
Zn	Zinc
P	Phosphate
K	Potassium
HCN	Hydrogen Cyanide
IAA	Indole-3-acetic acid
ACC	1-aminocyclopropane-1-carboxylic acid
N	Nitrogen
NH3	Ammonia
EPS	Exopolysaccharides
ISR	Induced systemic resistance
PGPB	Plant growth promoting bacteria
CNS	Central nervous system
NA	Nutrient agar
MHA	Calcium-adjusted Muller Hinton agar
BHI	Brain heart infusion
PDA	Potato Dextrose Agar
$CaCl_2$	Calcium chloride
NaCl	Sodium chloride
AlCl3	Aluminium chloride
DPPH	2,2-Diphenyl-1-picrylhydrazyl
K_2HPO_4	Dipotassium phosphat
KH_2PO_4	Potassium dihydrogenphosphate
NH_4NO_3	Ammonium nitrate
$MgSO_4.7H_2O$	Magnesium sulfate
$MnSO_4$	Manganese sulfate
$FeSO_4.2H_2O$	Ferrous sulfate
CFU	Centrifugal unit
rRNA	ribosomal RNA
NCIM	National Center for Industrial Microorganisms
BLAST	Basic Local Alignment Search Tool
NCBI	National Center for Biotechnology Information
ZnO	Zinc oxide

TLC	Thin layer chromatography
RP-HPLC	Reverse phase High performance liquid chromatography
GC-MS/MS	Gas Chromatography Mass Spectrophotometry
LC-MS/MS	LCMS Liquid Chromatography Mass Spectrometry
MIC	Minimum inhibitory concentration
SEM	Scanning electron microscopy
SrtA	Sortase A
ADMET	Absorption Distribution Metabolism Excretion Toxicity
PDB	Protein Data Bank
Rg	Radius of gyration
RMSD	Root Mean Square Deviation
RMSF	Root Mean Square Fluctuation
MD	Molecular Dynamics
MM-GBSA	Molecular mechanics Generalized Born/surface area
CUR	Curcumin
DMC	Demethoxycurcumin
BDMC	Bisdemethoxycurcumin
µl	Microliter
µg	Microgram
ml	Mililiter
mm	Millimeter
gm	Gram
mg	Milligram
nm	Nanometer
mM	Millimolar
OD	Optical density
hrs	Hours

INDEX

INDEX

INDEX

INDEX

INDEX

INDEX

INDEX

INDEX

List of Figures and Tables

List of Figures and Tables

List of Figures and Tables

List of Figures and Tables

List of Figures and Tables

List of Figures and Tables

CHAPTER I

INTRODUCTION

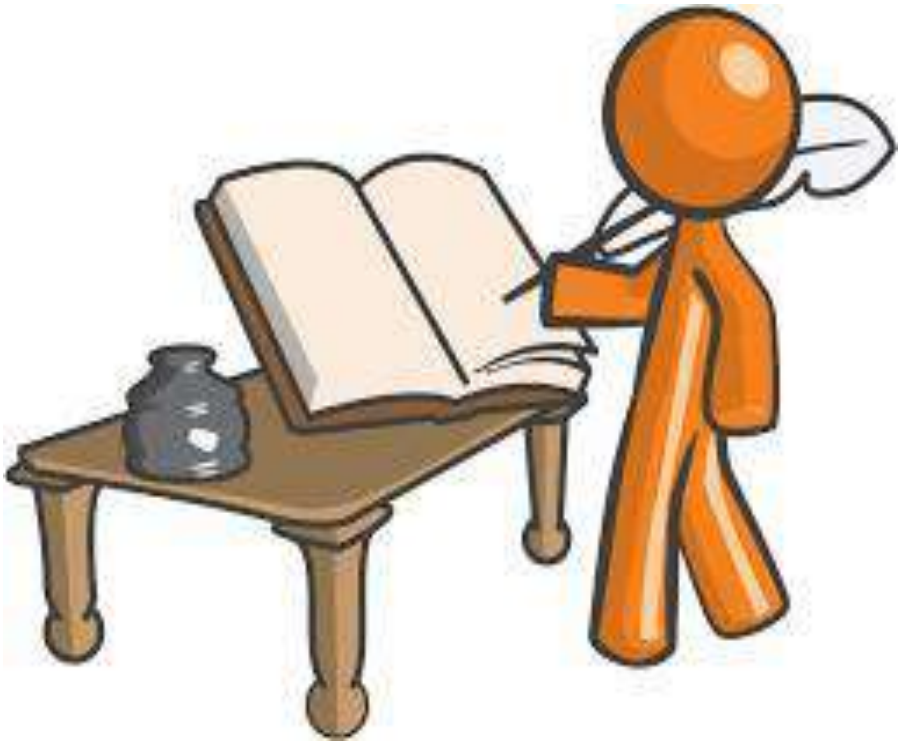

1. INTRODUCTION:

1.1 Plant growth promoting rhizobacteria (PGPR)

Plant growth-promoting rhizobacteria (PGPR) are a diverse group of rhizosphere-dwelling bacteria that colonies plant roots and stimulate plant growth through direct or indirect mechanisms (Kang et al., 2020). Direct mechanisms involve phosphorous solubilization, auxin, cytokinin, gibberellin production, nitrogen fixation, and iron sequestration. Indirect mechanisms include hydrogen cyanide, ISR, competition, antibiotic production, cell wall-degrading enzymes, and quorum quenching. They can also inhibit one or more plant pathogenic organisms (fungi and bacteria) (Glick B, 1995; Rizvi et al., 2022). ACC deaminase production and siderophores synthesis are also found in both these direct as well as indirect mechanisms (Ramamoorthy et al., 2001).

Common PGPR includes the strains in the genera, *Alcaligenes, Azospirillum, Bacillus, Acinetobacter, Burkholderia, Arthrobacter, Beijerinckia, Enterobacter, Azotobacter, Erwinia, Flavobacterium, Rhizobium* and *Serratia* (Andy et al., 2020). These rhizobacteria are then characterized as "extracellular plant growth rhizobacteria (ePGPR)" and "intracellular plant growth rhizobacteria (known as iPGPR)" based on their interaction with plants. The ePGPR predominantly present in the rhizosphere and between cells of the root cortex majorly from bacteria of genera such as *Agrobacterium, Azotobacter, Caulobacter, Chromobacterium,* etc. (Gray and Smith, 2005). iPGPR is found in specific nodular structures for root cells of some endophytes such as *Azorhizobium, Mesorhizobium, Bradyrhizobium, Allorhizobium*, and *Frankia* species (Verma et al., 2010; Wang and Romero, 2000).

1.2 PGPR interaction with Medicinal plants

The health and growth of plants are substantially influenced by bacteria associated with plants. PGPR has been employed for increasing biologically active phytocompounds from aromatic and medicinal plants. More research is being directed toward the use of PGPRs in the cultivation of medicinal and aromatic plants in order to increase plant yield (Karthikeyan et al., 2013; Tchakounte et al., 2018). Various rhizospheric microorganisms are linked to medicinal plants, thus it is important to isolate them, characterize them and research how to utilize them to produce a biofertilizer that's environmentally friendly or as a biocontrol agent (Vasudha et

al., 2013; Ipek et al., 2014). The application of biofertilizers on plant growth has demonstrated that they are superior to chemical fertilizers in terms of promoting plant growth, yield, and essential oil composition (Gharib et al., 2008).

According to Schmidt et al. (2014), *P. polymyxa* Mc5Re-14 and *B. subtilis* Co1-6 influence the phytocompounds and local microbiota of the chamomile plant, as well as enhance the major phytocompound, apigenin-7-O-glucoside (Schmidt et al., 2014). Similarly, Banchio et al. (2008) studied the effect of root-colonizing PGPRs on *Origanum majorana* plant and discovered that only *Bradyrhizobium* sp. and *P. fluorescens* significantly improved overall plant growth parameters when compared to control plants (Banchio et al., 2008). Previously, Toussaint et al. (2008) demonstrated that inoculating *Ocimum basilicum* with *G. mosses* increased the weights of the shoots and roots by up to 60% (Toussaint et al., 2008). According to Kumar et al. (2016), inoculation of *P. fluorescens* CL12 exhibited an increase in curcumin content by 18% as compared to control, which is a significant compound of the Turmeric plant (Kumar et al., 2016).

1.3 Turmeric

Medicinal plants contain a high concentration of bioactive compounds, which are thought to be safer for humans and the environment than synthetic medicines used to treat cancer and other disorders (Egamberdieva et al., 2015). Turmeric (*Curcuma longa* L.) has been used medicinally forcenturies in Ayurvedic medicine. Chemically complex turmeric products may also have different pharmacodynamic and pharmacokinetic profiles, which may support their ethnobotanical use (Meng et al., 2018). Turmeric, a perennial plant that belongs to Zingiberaceae family is famous for its colouring, flavouring, and digestive properties. Curcuminoids and essential oils are majorly found in Turmeric. Curcuminoids are group of Curcumin (~77%), Demethoxycurcumin (DMC) (~18%), and Bisdemethoxycurcumin (BDMC) (~5%) with different functional groups on the aromatic rings having various medicinal properties (Kita et al., 2008; Guerra et al., 2019; Rodrigues et al., 2015). Curcuminoids are yellow pigments having beneficial biological activities but curcumin is the primary component among the curcuminoids (Mostert et al., 2000). Curcumin has a high potential as a treatment for a variety of inflammatory illnesses and malignancies (Aggarwal et al., 2013).

The dried rhizome of Turmeric contains ~26% essential oil, ~58 % of which is turmerones.Turmeric essential oil contains α-phellandrene, sabinene, zingiberene, borneol, 1,8- cineole, sesquiterpene alcohols, bisabolene, and two monoterpenes, pinene, in addition to pcymene, β- sesquiphellandrene, and ar-turmerone (Raina et al., 2002). Turmeric oil shows insect-repellent activity against the stored grain insect *Tribolium castaneum* (Mostert et al., 2000). Essential oils of Turmeric were shown to have anti-angiogenic activities (Yue et al., 2015)

1.4 Asparagus

The usage of medicinal herbs is related to one of the most ancient, diversified, and rich cultural traditions in India. Medicinal plants are essential for the health of individuals and entire communities (Kishore et al., 2018). The medicinal plant *Asparagus racemosus* Willd from Asparagaceae family is native to tropical and subtropical India. Its medicinal usage is documented in the Indian and British Pharmacopoeias, as well as traditional medical systems like Ayurveda, Unani, and Siddha. *A. racemosus* Willd. is also known as Satavari, Satawar, and Satmuli (Bopanaand Saxena, 2007; Onlom et al., 2017). The roots of this plant have been used to cure schistosomiasis and tuberculosis. It also has a lot of chemical components such as steroidal saponins, flavonoids, oligosaccharides, and amino acid derivatives (Kasai and Sakamura, 1981; Taufique etal., 2014). The crown and root system of the plant accumulates carbohydrates, which act as food reserves, increasing the size and vigour of the buds and succeeding spears. The roots are used to cure gonorrhoea, tuberculosis, skin conditions, leprosy, dysentery, and diarrhoea (Mandal et al., 2000).

The primary active components of *A. racemosus* are the root steroidal saponins (Shatavarins I-IV) (Alok et al., 2013). Asparagus also contains essential oils, arginine, flavonoids (rutin, quercetin, kaempferol), asparagine, tyrosine tannin and resins. Saponins are anti-oxidants, anti-hepatotoxic, immunostimulants, helpful in diabetic retinopathy, anti-bacterial, anti-carcinogenic, anti-ulcerogenic, anti-diarrheal, and reproductive agents. Many types of saponins are antibacterial, preventing mould and shielding plants from insects (Negi et al., 2010; Patil et al., 2014).

1.5 *In-silico* study of Plant Secondary Metabolites (Phytocompounds)

Plant-based medicine, which has been practiced since antiquity, is the source of many commercially important drugs. Traditional methods of plant-based drug discovery can take a longtime and money. Bioinformatics allows for the analysis and interpretation of huge volumes of datagenerated by molecular biology-based techniques (Sharma and Sarkar, 2013). Such approaches are now required when it comes to analyzing and integrating large amounts of data due to high-throughput techniques. To improve our understanding of plant cellular processes, genomic, proteomic, and metabolomic data must be thoroughly examined. The use of bioinformatics techniques is critical in identifying genes and pathways associated with biologically active secondary metabolites from medicinal plants (Saito and Matsuda, 2010; Sharma and Sarkar, 2013).

The medicinal plants contain a significant amount of antioxidants, which include polyphenols, which aid in the adsorption and neutralization of harmful free radicals (Saleem et al., 2020). These biological processes can be studied with computational techniques. The biological activity of the molecule was verified by docking studies, which determined the binding free energies and elucidated the interactions with the active site (Saleem et al., 2020). Molecular docking and molecular dynamics simulation studies are useful tools for predicting binding activity and interactions with enzymes (Dhanavade et al., 2013; Bansode et al., 2019; Dhanavade and Sonawane 2014; Gao et al., 2016; Thappeta et al., 2020). This information is crucial when developing new lead molecule (Sivaramakrishnan et al.,2019).

1.6 Aspects of the study

Turmeric and Asparagus plants were chosen as the experimental material in this study because turmeric has been used in Indian households for centuries as a spice and traditional medicine. Curcuminoids and sesquiterpenoids, which are active components of turmeric, are useful in pharmaceuticals. Asparagus was traditionally used in India to stimulate fertility, alleviatemenstrual pains, and enhance milk production in nursing mothers. Shatavarin and diosgenin are important components of Asparagus. Both plants contain major phytocompounds that are widely used as antioxidants, antipyretics, anti-inflammatory agents, and anticancer agents. Both plant rhizomes interact with the large microbial population present in the rhizosphere. These bacterial strains have the potential to influence the immune system of

the plant.

The aim of this study was to find a potent PGPR strain by screening the rhizospheric soil of the Turmeric and Asparagus plants. The effects of these PGPR strains on medicinal plants were investigated, and secondary metabolites produced by those plants were purified using various methods, including silica gel column chromatography and high-performance liquid chromatography. These secondary metabolites were characterized and identified using TLC, GC-MS/MS, and LC-MS/MS. All of the metabolites exhibited antibacterial activity against pathogens such as *Staphylococcus aureus*, *Escherichia coli*, *Proteus vulgaris*, and *Streptococcus mutans*. Furthermore, biofilm inhibition studies showed that isolated secondary metabolites prevent the formation of biofilms. Computational analysis of secondary metabolites induced biofilm inhibition could help researchers to better understand the underlying mechanism.

Thus, the potent strains of PGPR are reported in this thesis to enhance the growth, yield, and phytocompounds of Turmeric and Asparagus plants. Further, enhanced phytocompounds demonstrated various biological applications and the computational approach used in this study elucidated the mechanism of inhibition of the SortaseA enzyme which is a key adhesion protein involved in biofilm formation. Therefore, this study would pave the way for the development of PGPR-induced phytocompounds therapeutic approaches by targeting SrtA to control biofilm-related infectious diseases.

CHAPTER II

REVIEW OF LITERATURE

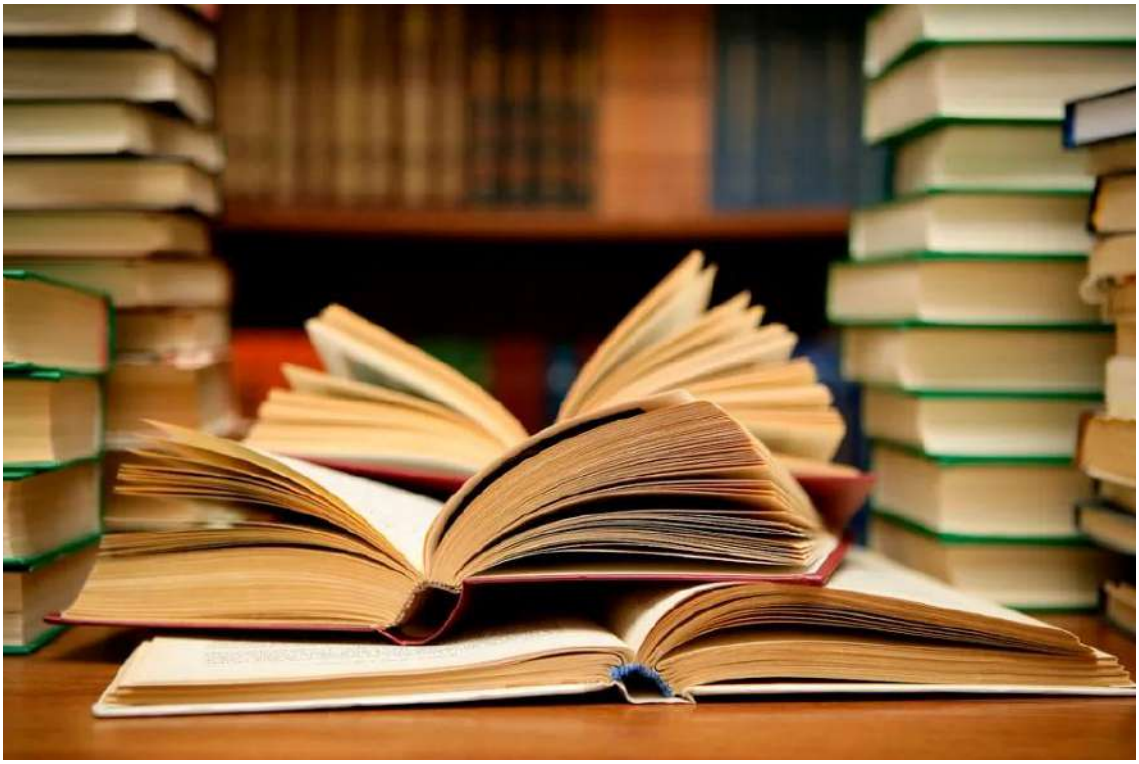

2. Review of literature:

2.1 Plant growth promoting rhizobacteria (PGPR)

Rhizospheric bacteria known as "plant growth-promoting rhizobacteria" (PGPR) canbenefit plant growth through various processes or mechanisms. PGPR can employ both direct and indirect channels (Fig. 2.1). The list of direct ways includes production of IAA, gibberellin, cytokinin, phosphate solubilization, biological nitrogen fixation, including siderophore production whereas hydrogen cyanide, ACC deaminase, induced systemic resistance, antibiotics, competition, cell wall-degrading enzymes and synthesis of siderophores are the examples of indirect ways (Olanrewaju et al., 2017; Maheshwari and Dheeman, 2014).

The application of PGPR in agriculture is becoming more and more likely as it provides adesirable substitute for the use of chemical fertilizers, pesticides, and other additives (Perez- Montano et al., 2014). These PGPR are expected to produce significant amounts of growth- promoting compounds, which could affect the general morphology of the plants both directly and indirectly. Recent research on the many varieties of PGPR in the rhizosphere, as well as their colonization potential and mode of action, should make it easier to use them as a reliable management tool for sustainable agriculture practices (Shah et al., 2021; Kumar et al., 2014a). Previous research thus demonstrated the progress made in the use of rhizosphere bacteria in many applications for agricultural improvement, as well as their mode of action, with a focus on characteristics that encourage plant development. There are several methods in which PGPR might encourage the growth of their plant symbionts and provide cross-protection against different stresses (Bhattacharyya & Jha, 2012).

The use of PGPR can help to increase eco-friendly practices for sustainable agriculture because it promotes plant growth under both biotic and abiotic stresses (Passari et al., 2018). Many Gram-negative and Gram-positive bacterial genera have been reported to induce plant growth, including coryneform bacteria, *Azospirillum*, *Azotobacter*, *Arthrobacter*, *B. subtilis*,*Burkholderia*, *Enterobacter*, *Klebsiella*, *Micrococcus*, *P. gladioli*, *P. cepacia*, and *Xanthomonas*(El-Sayed et al., 2014; Bal et al., 2013). PGPR have also been widely documented in the previous era from various medicinal plants such as *Ocimum* spp. (*Glomus fasciculatum*, *Azotobacter chroococcum*), *Withania somnifera* (*Azospirillum*, *Azotobacter chroococcum*, *Pseudomonas fluorescens*, *Bacillus megaterium*)

(Egamberdieva & Teixeira da Silva, 2015), *Mentha piperita* (*Bacillus amyloliquefaciens, Pseudomonas fluorescence*) (Cappellari et al., 2015), *Trachyspermum ammi* (*Azotobacter chroococcum*) (Hashemi et al., 2022). However, PGPR from Turmeric and Asparagus rhizospheres is still being studied. Thus, the purpose of this work was to isolate and describe rhizobacterial strains living in naturally occurring plant species.

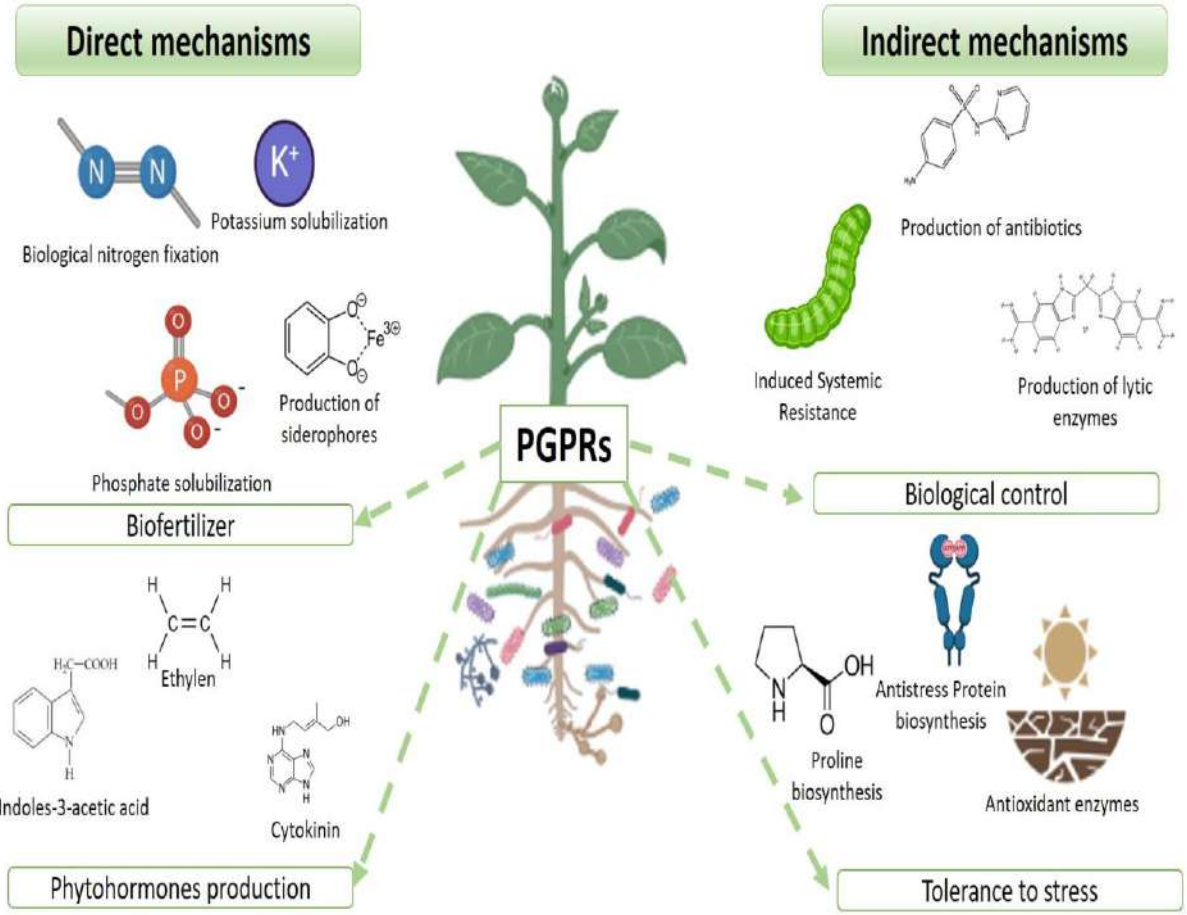

Fig. 2.1: Direct and indirect mechanisms of PGPRs (Jacquelin et al., 2022)

2.2 Mechanism of PGPR action:

2.2.1 Phosphate solubilization

Next to nitrogen, phosphorus is the most crucial essential component in plant nutrition. Almost all main metabolic processes, such as photosynthesis, respiration, signal transduction, energy transfer, and macromolecular biosynthesis, depend on it in some way (Anand et al., 2016).Despite being plentiful, phosphorus reserve does not exist in plant-friendly forms. Only the soluble forms of mono and dibasic phosphate can be absorbed by plants (Bhattacharyya & Jha, 2012). *Bacillus*, *Achromobacter*, *Rhizobium*, *Pseudomonas*,

Agrobacterium, *Burkholderia*, *Flavobacterium*, *Chryseobacterium*, *Aerobacter*, *Micrococcus*, and *Erwinia* are just a few of the numerous bacteria from various genera that may solubilize phosphate (Khan et al., 2014). There are two ways that bacteria solubilize phosphate: The release of phosphatases, which liberate phosphate groups attached to organic matter, and the release of organic acids that, through ionic interactions with the cations of the phosphate salt, liberate phosphorus. Most of these bacteria are capable of dissolving the mineral phosphate complexes. In general, these systems work better in simple soils (Rodriguez and Fraga, 1999; Hayat et al., 2010).

In contrast to non-rhizosphere soil, the rhizosphere frequently contains a significantly higher concentration of phosphate-solubilizing bacteria (Rodriguez & Fraga, 1999). These bacterial inoculations can sometimes enhance plant development and other times be utterly ineffective. Without a doubt, understanding their mechanics and rhizosphere ecology will reform their application in sustainable agriculture (Prasad et al., 2019).

2.2.2 Zinc solubilization

For healthy development and reproduction, plant tissues must have relatively small amounts of zinc (Zn), one of the essential micronutrients (Shaikh & Saraf, 2017). There are several soil-specific characteristics that are associated to the availability of P and Fe at pH (7.0) where Zn solubility decreases as the pH rises, including a large quantity of organic matter and bicarbonate concentration, high availability of P and Fe and high magnesium to calcium ratio (Kamran et al., 2017). In order to make zinc available, a bacterial strain that can solubilize it must be inoculated into the crop because it is a restricting factor in crop productivity (Saravanan et al., 2004). According to earlier studies, PGPR inoculation improves plant nutrition, promotes vigor in plant growth, and gives a higher amount of yield (Shakeel et al., 2015).

2.2.3 Potassium solubilization

The third most vital nutrient for plants, potassium (K) is necessary for enzyme function, protein synthesis, and photosynthesis. Since more than 90% of potassium is found in insoluble rock and silicate minerals, the amount of soluble potassium present in soil is often rather low (Parmar and Sindhu, 2013). Potassium deficiency is now a major hindrance to agricultural productivity. Without enough potassium, plants have weak roots,

limited growth, lower yields, and fewer seeds. A different indigenous source of potassium needs to be discovered in order to maintain soil plant uptake and agricultural production (Kumar and Dubey, 2012).

The capability of the PGPR to generate and secrete organic acids to dissolve potassium rock has been thoroughly investigated (Etesami et al., 2017). It has been proven that PGPR, including *B. edaphicus*, *B. mucilaginosus*, *Ferrooxidans* sp., *Burkholderia* sp., *Pseudomonas* sp., *Paenibacillus* sp., and *Acidothiobacillus* sp. release potassium from potassium-containing minerals in soils. Applying potassium-solubilizing PGPR as a biofertilizer can enhance sustainable crop output while reducing the need for agrochemicals (Meena et al., 2014; Prasad et al., 2019).

2.2.4 Siderophore production

A siderophore is defined as a low molecular weight organic compound produced by bacteria under low iron conditions. (Schwyn and Neilands, 1987). The fungus and bacteria need Fe for heme creation, ATP synthesis, and other critical processes. Siderophores can be classified according to their moieties such as catecholate, hydroxamate, carboxylate and diazeniumdiolate (Hermenau etal., 2018). The PGPR produces a variety of siderophores, including *P. fluorescens*, which produces pyoverdine (Behnsen and Raffatellu, 2016). Rhizobactin, a structurally unique form of siderophore produced by *Pseudomonas* to obtain iron from dissolved organic matter in peatlands (Kugler et al., 2020). Bacillibactin is the mainly well-known triscatetholate siderophore produced by *Bacillus* spp (Nithyapriya et al., 2021). In the rhizosphere, siderophore-synthesizing PGPR suppresses phyto-pathogens via iron deficiency or competitive exclusion in iron-deficient conditions (Arora and Verma, 2017). Additionally, fluorescent *Pseudomonads* have been reported to inhibit soil-borne fungi through the release of siderophores that chelate iron (Beneduzi et al., 2012).

2.2.5 HCN production

PGPR produces the deadly chemical cyanide, which has lethal effects. While cyanide functions as a common metabolic inhibitor, numerous species involving bacteria, fungus, algae, insects, and plants produce, secrete, and utilize it as a defense against competition or predation (Kumar et al., 2015; Lastra et al., 2021). Hydrogen cyanide (HCN), an effective volatile secondary metabolite frequently synthesized by rhizospheric bacteria, is known to adversely influence on growth and metabolism of root and represents

a possible and ecologically friendly strategy for the biological control of weeds (Schippers et al., 1990). The HCN synthetase enzyme, which is connected to the rhizobacterial plasma membrane, converts glycine into HCN (Shameer and Prasad, 2018).

Numerous studies have demonstrated the potential for HCN production by many genera of *Aeromonas, Pseudomonas, Alcaligenes, Rhizobium,* and *Bacillus* (Olanrewaju et al., 2017). The nematodes *Meloidogyne javanica* and *Thielaviopsis basicota*, respectively, induce root-knot and black rot in tomato and tobacco roots, which have been suppressed by HCN, according to several investigations (Siddiqui et al., 2006). According to research, roughly 50% of *pseudomonads* isolated from the potato and wheat rhizosphereare capable of producing HCN *in vitro*, whereas HCN production is a general characteristic shared by the group of *Pseudomonas* from the rhizosphere (Syed Shameer, 2018). It has been discovered that *Pseudomonas* (88.89%) and *Bacillus* (50%) both produce HCN as a biocontrol metabolite in a root nodules of plant and the rhizospheric soil (Ahmad et al., 2008).

2.2.6 Phytohormone production

Plant hormones, like auxins, abscisic acid, gibberellin, cytokinin, and ethylene, are tiny, structurally unrelated molecules found in nature that control the development and growth of plants (Chen et al., 2017; Hayat et al., 2010). IAA (indole-3-acetic acid) is the primary auxin produced by plants. It is essential for several plant activities, including seed and tuber germination, regulation of vegetative growth processes, accelerated development of xylem and root, and initiation of lateral and adventitious root formation. IAA also facilitates responses to light, gravity, and florescence (Ali et al., 2017; Kumar et al., 2019). Plants and microorganisms synthesize IAA via several interconnected pathways, the most well-studied of which is the tryptophan-dependent system (Chandra et al., 2018).

Plant roots exude the amino acid tryptophan, which is subsequently broken down by PGPR in the rhizoplane and transformed into IAA which is then absorbed by plant roots (Mohite,2013; Shameer and prasad, 2018). A various bacterial species from the genera *Alcaligenes, Azospirillum Acinetobacter, Arthrobacter, Bacillus, Bradyrhizobium, Burkholderia, Enterobacter, Flavobacterium, Erwinia, Rhizobium, Serratia* and *Pseudomonas* have been discovered to be rhizosphere-associated and capable of synthesizing IAA that promote growth of plant (Egamberdieva et al., 2015; Shah et al.,

2021).

2.2.7 Cytokinin production

Cytokinin's are another class of phytohormone that influences development and growth of the plant by controlling physiological processes like division of cell, seed germination, apical dominance, flower and fruit production, development of root and shoot, aging of leaves, plant-pathogen interactions, nutrient mobilization and absorption (Akhtar et al., 2020; Shah et al., 2021). Cytokinins produced by rhizospheric bacteria which are living near the roots can also impact on growth and development of plant (Salamone et al., 2001). In addition, seed inoculationwith cytokinin-producing bacteria usually results in increased cytokinin levels in plants, which affects plant growth and development (Gamalero and Glick, 2011).

In contrast, it has been observed that PGPR, such as *Azospirillum, Rhizobium, Azotobacter, Pseudomonas* and *Bacillus* spp., may produce cytokinin in pure culture (Salamone et al., 2001). Cytokinin mediates responses to biotic and abiotic stresses, as well as a variety of extrinsic variables like light conditions in the shoot, also nutrition and water availability in the root. These activities collaborate to fine-tune quantitative growth regulation in plants (Wernerand Schmulling, 2009; Gupta and Rashotte, 2012).

2.2.8 Gibberilic acid production

Gibberellins, a large class of phytohormone with specific roles throughout the life cycle of higher plants. These are tetracyclic diterpenoid carboxylic acids with carbon skeletons of C20 or C19 (Alori and Babalola, 2018). Gibberellins play a role in a variety of physiological and developmental processes, such as seed germination, stem and leaf growth, flower or fruit growth, seedling emergence, floral induction, control of vegetative and reproductive (bud) dormancy, and postponement of senescence (Bottini et al., 2004; Kang et al., 2015). Gibberellins, when combined with other phytohormones, are directly beneficial in promoting shoot elongation in plants (Crozier et al., 2000). When bacteria are grown on artificial culture medium, very few of them synthesize Gibberlic acid (Kaminek et al.,1997). PGPR such as *Bacillus, Pseudomonas, Azotobacter, Acetobacter, Azospirillum,* and *Burkholderia,* are able to produce gibberellins (Lotfi et al., 2022).

2.2.9 Nitrogen fixation and ammonia production

Nitrogen serves as a crucial nutrient for plant development and yield. Nitrogen

fixation is the process by which nitrogen-fixing microorganisms use an enzyme nitrogenase to convert molecular or atmospheric nitrogen into a form that plants can use (Alori and Babalola, 2018). Agricultural practices have utilized both symbiotic and asymbiotic/associative bacteria to support plant growth (Ahmad et al., 2013). Rhizobacteria that facilitate plant growth have been isolated as free-living soil bacteria from plant rhizosphere, and when associated with plant roots and other plant parts, can decrease the requirement for chemical fertilizer and increase plant growth and yield (Roychowdury et al., 2015). Therefore, several nitrogen-fixing bacteria, such as *Azospirillum, Klebsiella, Burkholderia, Bacillus*, and *Pseudomonas* have been discovered as PGPR for maize plants (Kuan et al., 2016; Singh et al., 2020).

Production of gaseous products like ammonia is one of the methods used by rhizobacteria to encourage plant development (Laslo et al., 2012). The capability of PGPR to produce ammonia, which indirectly promotes plant development, is another crucial characteristic (Sayyed R, 2019). In general, it has been shown that PGPR produces ammonia that supplies nitrogen to the host plants, promoting the overall growth of the plant (Bhattacharyya et al., 2020). Earlier reports showed that, *Bacillus* strains produce ammonia when grown in nitrogen sources, which aids host plant growth and biomass production (Singh et al., 2020). Similarly, Malleswari and Bagyanarayana, (2013) found that inoculating sorghum, maize, and green gram with ammonia-producing *Pantoea* sp., *Bacillus* sp., and *Pseudomonas* sp. improved growth promotion (Malleswari and Bagyanarayana, 2013).

2.2.10 Salt tolerance

In agriculture, salt stress is a major problem that inhibits plant growth. Stress factors that are both biotic and abiotic have a significant influence on plants and seriously harm crop production globally (Varma et al., 2017). Salinity is a harsh environment with limited organic matter and very low nitrogen levels in the soil (Malik K, 1997). Salinity has other issues that have an impact on the environment's biodiversity in addition to having an impact on agriculture (Mohammed A, 2018). Beneficial bacteria have a great chance of improving crop production and environmentally friendly resource management by promoting plant growth and stress tolerance (Mohammed A, 2018). The use of drought-tolerant PGPR is thought to be a successful substitute method for sustainable agriculture under water deficit

conditions (Mayak et al., 2004). Inoculation of plants with PGPR promotes seedling emergence and increases growth rate, it also confers tolerance to several stresses and plant pathogens (Khan and Bano, 2019).

2.2.11 Exopolysaccharides production

Exopolysaccharides (EPS) are a very important component of the extracellular matrix, and frequently account for 40-95% of bacterial weight. Bacteria can produce two types of exopolysaccharides: Slime exopolysaccharide and capsular exopolysaccharide (Naseem and Bano, 2014). Exopolysaccharides play important roles in surface attachment, microbial aggregation, biofilm formation, plant-microbe interaction, protection, and bioremediation (Manca et al., 1985). Similarly, an important feature of EPS is its biodegradability, it can be released in extreme environmental conditions such as temperature and pH Microbial EPS improve soil aggregation, which benefits plants by retaining moisture and trapping nutrients (Vasagade et al., 2021). Some exopolysaccharide-producing bacteria, such as *Pseudomonas*, can survive under drought conditions and protect themselves from desiccation by rising water holding (Sandhya et al., 2009a). Similar to this, plants have shown resistance to water stress when treated with exopolysaccharide-producing bacteria, like *Azospirillum* (Bensalim et al., 1998).

2.2.12 Induction of Systemic Disease Resistance by PGPR

Induced systemic resistance, or ISR, is the rise in defense mechanisms brought on by an inducer agent in response to a pathogen infection. It is the condition in which plants develop an enhanced defensive ability when appropriately stimulated (Beneduzi et al., 2012). Several nonpathogenic PGPR strains can make plants resistant to a wide range of phytopathogens by inducing systemic disease resistance (Egamberdieva et al., 2015). For instance, the application of PGPR as a sett-treatment in sugarcane resulted in the development of systemic resistance to *C. falcatum* (Ramamoorthy et al., 2001). Similarly, Alstroem (1991) noticed that PGPR-induced systemic resistance to bacterial diseases. He reported that *Pseudomonas fluorescens* treated bean seeds shielded the plant from the disease called as halo blight caused by *Pseudomonas syringae pv. phaseolicola* (Bhattacharyya and Jha, 2012). Similar to this, Kloepper et al. (1993) discovered that when cucumber seeds were treated with rhizobacterial strains such as *Pseudomonas putida* and *Serratia marcescens*, the occurrence of bacterial wilt was significantly decreased (Kloepper et al., 1993).

2.3 PGPR in relation to medicinal plants:

Medicinal plants contain a high concentration of bioactive compounds which are thought to be safer for humans and the environment than synthetic medicines that have been used to treat cancer and other various diseases since ancient times (Zhao et al., 2022; Egamberdieva et al., 2015). However, natural products, especially medicinal plants, continue to be a substantial source of new drugs, drug leads, and chemical entities because they are more socially acceptable, have a high level of compatibility, and can adapt to the human body than synthetic chemicals (Garg et al., 2021; Zhao et al., 2022). Similarly, medicinal plants are associated with various rhizospheric microbes, which improve plant growth parameters and secondary metabolite content of the plant (Vasudha et al., 2013).

PGPRs have the ability to increase the synthesis of biologically active phytocompounds in aromatic and medicinal plants. More research is being directed toward the use of PGPRs in the cultivation of these plants in order to increase plant productivity (Karthikeyan et al., 2013). Hence, plant-associated bacteria perform a crucial role for the health and growth of plants. However, we know very little about how bacterial treatments affect the physiology and microbiome of host plant (Schmidt et al., 2014). At the moment, the various studies on plant-associated microbes demonstrate the entire influence of ongoing research as well as the tremendous interest in this area (Berendsen et al., 2012; Bakker et al., 2013). Similarly, the growing concerns of medicinal and aromatic plants on a wide scale can be overcome by discovering and choosing suitable useful bacteria to be employed as biofertilizers that promote plant growth without damaging the environment (Ipek et al., 2014).

Banchio et al. (2008) examined the considerable enhancement in leaf number, shoot weight, nodal number, shoot length, root dry weight and biomass of *Origanum majorana* after treatment with *Bradyrhizobium* sp. and *P. fluorescens* (Banchio et al., 2008). Similarly, Gharib et al. (2008) discovered that biofertilizers increase overall growth and essential oil content in *Majorana hortensis* L. when compared to control plants which may be treated with chemical fertilizers (Gharib et al., 2008). When PGPRs such as *Bacillus, Azotobacter*, and *Pseudomonas* were inoculated to *Catharanthus roseus*, either alone or in combination, they dramatically boosted root length, nutrient concentration, secondary metabolite concentration, and plant height, when compared to non-inoculated control plants (Karthikeyan et al., 2009). Similar to this, according to Mishra et al. (2010), the synthesis

of ammonia by rhizobacterial strains (*B. subtilis* and *P. fluorescens*) isolated from the aromatic herb *P. graveolens* L. shown a considerable increase in plant growth and biomass (Mishra et al., 2010).

Ruth Schmidt et al. (2014) studied the impact of bacterial inoculants on the native microbiome and secondary metabolites of the chamomile plant. They found that *B. subtilis* Co1-6 and *P. polymyxa* Mc5Re-14 enhance the bioactive phytocompound apigenin-7-O-glucoside (Schmidt et al., 2014). According to Santoro et al. (2011), using PGPRs like *B. subtilis*, *P. fluorescens*, and *A. brasilense* increased essential oil content in *Mentha piperita* by doubling monoterpene synthesis (Santoro et al., 2011). Similar to this, Ghorbanpour et al. (2013) found that treatment of *Pseudomonas* spp. to Black henbane (*Hyoscyamus niger*) in water-stressed environments increased the production of tropane alkaloids like scopolamine and daturine (Ghorbanpour et al., 2013). Additionally, following PGPB inoculation, medicinal plants showed an increase in the content of several alkaloid and terpenoid compounds with pharmaceutical importance (Cakmakc et al., 2020). However, Bharti et al. (2013) stated that the yield was increased by 138% and the amount of bacoside A was increased by 376% when *B. monnieri* (Brahmi) was inoculated with *B. pumilus* and *E. oxidotolerans* under saline conditions (Bharti et al., 2013). Similarly, Darzi et al. (2012) found that PGPB inoculations in *Coriandrum sativum* increased the amount of geranyl acetate, limonene, and beta pinene (Darzi et al., 2012).

The important secondary metabolites in medicinal plants may be enhanced by PGPR treatment, a few examples are given here. In case of *Curcuma longa* which was inoculated with *Bacillus* spp. and *P. fluorescens*, showed increased plant growth, fresh rhizome biomass, morphological yield, and the plant's main bioactive component curcumin (Cakmakc et al., 2020). Kumar et al. (2016) discovered a similar result such as increase in biological properties, yield attributes, and curcumin content in turmeric plant bacterized with *P. fluorescens* (Kumar et al., 2016). Similar to this, *Panax ginseng* inoculation with PGPR demonstrated significantly improved growth, root activity, and the content of total ginsenoside (Ji et al., 2019). In addition to this various studies have shown increased levels of flavonoids in *Withania somnifera* under metal stress (Khanna et al., 2019). In medicinal plant like Aloe vera, it has been observed that PGPR (*Azospirillum, Azotobacter, Bacillus,* and *Pseudomonas*) either alone or in combination, increase the aloin content (Rizvi et al., 2022). Similarly, applying microbial consortia to the roots of medicinal plants has been

demonstrated to enhance phytocompounds and can be understood as a plant defense reaction to microbial colonization (Egamberdieva and Teixeira da Silva, 2015). In general, PGPR applications to *Withania somnifera* showed increased plant dry matter accumulation, N and P concentration in roots and shoots, withaferin-A concentration in roots, and total withanolide content in plants when compared to controls (Rizvi et al., 2022).

Bacterial mechanisms for stimulating plant growth, nutrient uptake, phytochemical constituents, and alleviating abiotic stresses include number of enzymes, nutrient mobilization, induction of systemic resistance, nitrogen fixation, and synthesis of plant hormones such as indole-3-acetic acid (IAA), cytokinin and gibberellic acid (Mishra et al., 2010; Egamberdieva and Lugtenberg, 2014; Hameed et al., 2014). However, our understanding regarding PGPR's potential to increase plant secondary metabolites is restricted. Additional research is needed to explore the potential methods by which bacteria enhance phytochemical contents in medicinally significant plants at the cell, tissue, or molecular level.

2.4 Plant secondary metabolites:

Secondary metabolites (phytocompounds) are organic compounds synthesized inside the cell and do not play role in direct growth and development of plant. They are synthesized due to the heritable mutations in basic primary metabolite pathways by natural selection. They are used against herbivory and pathogens like bacteria, viruses and fungi. They have crucial role in symbiotic nitrogen fixation, attract pollinators, and reduce plant-plant competition. They are nota part of the basic structure of the cell. There are mainly 3 classes of secondary metabolites (Bourgaud et al., 2001) which are given below:

1. Terpenes
2. Phenolic compounds
3. Nitrogen containing compounds

2.5 Scientific classification of *Curcuma longa* (Turmeric)

Kingdom : Plantae
Phylum : Tracheophyta
Division : Angiosperms
Class : Monocots
Order : Zingiberales
Family : Zingiberaceae
Genus: Curcuma
Species: *Curcuma longa*

Fig. 2.2: Turmeric plant

2.5.1 Curcuminoids

The most significant active component of Turmeric is curcuminoids. These are phenolic compounds which are frequently employed in a wide range of foods as a spice, pigment, additive, and therapeutic agent (Amalraj et al., 2016). In *Curcuma longa*, crude extract curcuminoid accounts for 1-6% of the total weight of the Turmeric (Cas and Ghidoni, 2019). The pharmacological activity of Turmeric has been attributed primarily to curcuminoids, which include curcumin (CUR) and two related compounds, demethoxycurcumin (DMC) and bisdemethoxycurcumin (BDMC) (Kadam et al., 2018). They are robust complex forming agents, with the keto-enol units acting as the molecule's reactive units. Curcuminoids with absorption wavelengths ranging from 420nm to 430nm, are extracted from Curcuma species (primarily *Curcuma longa* L.) (Tonnesen, 1992). As curcuminoids having complex chemical structures hence less soluble in water at acidic and neutral pH levels, but much more soluble in organic solvents such as methanol, ethanol, dimethyl sulfoxide, and acetone (Amalraj et al., 2016). Additionally, they possess a wide range of biological attributes, including anti-oxidative, anti-diabetic, anti-inflammatory, anti-cancer, anticholinesterase, anti-mutagenic, cytotoxic, neuroprotective, and anti-Alzheimers properties (Xu et al., 2020; Kalaycıoglu et al., 2017; Chen et al., 2017; Jayaprakasha et al., 2005).

2.5.2 Curcumin

One of the primary chemical compound of *Curcuma longa* L. is "curcumin," which accounts for approximately 71.5% and is also known as diferuloylmethane, has the chemical formula (1,7-bis-4-hydroxy-3-methoxyphenyl-1,6-heptadiene-3,5-dione) (Beevers & Huang, 2011; Li and Wang, 2011). Over the past six decades, there has been extensive research on the pharmacokinetic, pharmacodynamic, and clinical pharmacological properties of curcumin (Aggarwal et al., 2003). These investigations have shown that curcumin functions as an anti-inflammatory, antioxidant, anti-cancer agent, anti-atherosclerotic, inhibits scarring, promotes wound healing and muscle regeneration, prevents kidney toxicity and liver injury, shown therapeutic effect on diabetes, septic shock, multiple sclerosis, cardiovascular disease, HIVdisease, arthritis, lung fibrosis, and Alzheimer's disease (Sharma et al., 1976; Li et al., 2004; Aggarwal et al., 2006). Besides, Turmeric treated with PGPR showed increased concentration of curcumin (Chauhan et al., 2017).

2.5.3 Demethoxycurcumin

Demethoxycurcumin (curcumin II) also known as p-hydroxycinnamoyl, feruloylmethane is the second most important compound within the group of curcuminoids and accounts for 19.4% (Beevers and Huang, 2011). According to Mustarichie et al. (2013), demethoxycurcumin has inhibitory actions against two isoforms of monoamine oxidase (MAO), which is involved in the catalysis of neurotransmitting monoamines, as well as acting as a whitening agent (Baek et al., 2018). Demethoxycurcumin was reported to be the most effective inhibition of MCF-7 cells (Agan et al., 2002). Additionally, it has greater effects on the Bcl-2-controlled apoptotic pathways (Luthra et al., 2009). Similar to this, it has antitubercular properties (Agrawal et al., 2008), antibiofilm activity against *Staphylococcus aureus* (Park et al., 2005), and antiparkinsonian effects (Mazumder et al., 2020). It also has been shown that demethoxycurcumin to be a potential COVID-19 Mpro inhibitor in *in silico* studies (Khaerunnisa et al., 2020).

2.5.4 Bisdemethoxycurcumin

Bisdemethoxycurcumin (curcumin III), also known as di-p-hydroxycinnamoylmethane, is the third major component of the curcuminoid group, accounting for 9.1% (Agan et al., 2002). Various biological activities of

bisdemethoxycurcumin, such as cytotoxicity, anti-inflammatory, antioxidant properties, and activity against leukemia, CNS, colon, melanoma, renal, and breast cancer cell lines, were reported (Rarnsewak et al., 2000; Kim et al., 2016). It also inhibited sortase A, an enzyme responsible for biofilm formation (Park et al., 2005). The effectiveness of bisdemethoxycurcumin against ulcers was reported by Mahattanadul et al. (2009). It has been stated that bisdemethoxycurcumin may act as an antioxidant agent and may function as atherapeutic target for oral hypoglycemic medications in type-2 diabetes (Ponnusamy et al., 2012; Jayaprakasha et al., 2005). According to Kalaycioglu et al. (2017), the noteworthy properties of bisdemethoxycurcumin compared to its isomers may serve as a starting point for the development of new medications for diabetes and Alzheimer's disease (Kalaycioglu et al., 2017). In addition to this, the bisdemethoxycurcumin showed an inhibitory effect on liver lipogenes (Kim et al., 2016). Fig 2.2 depicts the picture of Turmeric plant.

2.5.5 Pathway for curcuminoid synthesis

Curcuminoids, primarily curcumin, demethoxycurcumin, and bisdemethoxycurcumin, are found in the rhizome of turmeric. Type III polyketide synthases (PKSs), which are homodimers of ketosynthase and are structurally simple enzymes, are involved in the biosynthesis of the majority of plant polyketides (Austin and Noel, 2003). However, curcuminoids in the herb *Curcuma longa* are produced by the collaboration of two type III Polyketide synthases diketide-CoA synthase (DCS) and curcumin synthase (CURS) (Katsuyama et al., 2009). The pathway begins with phenylalanine, an aromatic amino acid that produces p-coumaroyl-CoA, and the reaction is catalyzed by the enzyme phenylalanine ammonia liase (PAL). Feruloyl-CoA is produced from P-coumaryl-CoA. Then, the DCS reacts with these two molecules to produce p- coumaroyldiketide-CoA and feruloyldiketide-CoA. A series of CURS then reacts with this to generate the three main curcuminoid components: 1. Curcumin 2. Demethoxycurcumin 3. Bisdemethoxycurcumin. (Fig. 2.3)

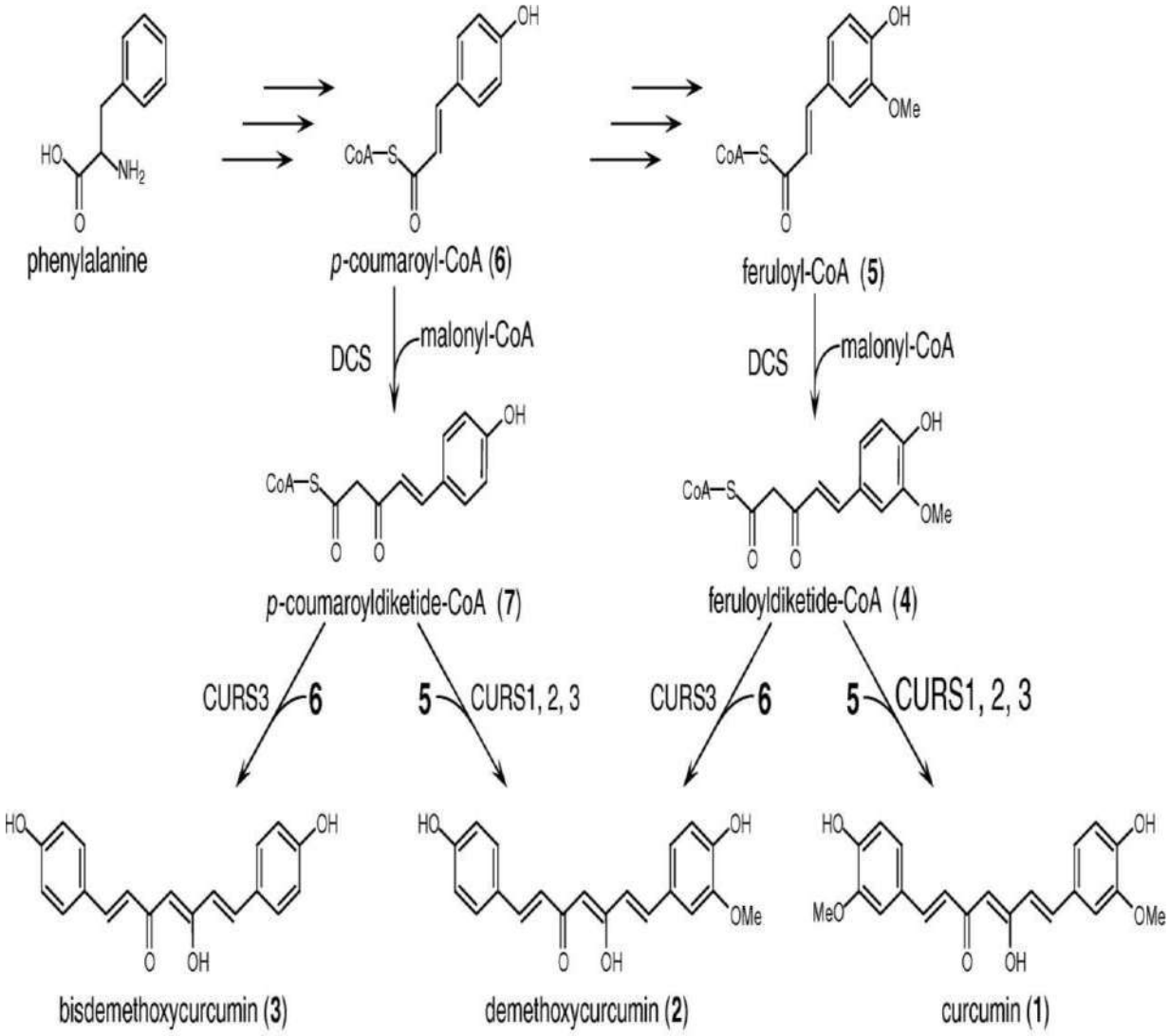

Fig. 2.3: Pathway of curcuminoid synthesis of *C. longa* (Katsuyama et al., 2009)

2.6 Scientific Classification of *Asparagus racemosus* (Shatavari)

Fig. 2.4: Asparagus plant

Kingdom : Plantae
Phylum : Tracheophyta
Division : Angiosperms
Class : Monocots
Order : Asparagales
Family : Asparagaceae
Genus: Asparagus
Species: *Asparagus racemosus*

There are several species of Asparagus grown in India, but *Asparagus racemosus* (Willd) is the one most frequently used in traditional medicine (Fig. 2.4). It is also known as Satavari, Satawar, or Satmuli in Hindi, Satavari in Sanskrit, and Shatamuli in Bengali (Kumar et al., 2008). A variety of plant parts in the Asparagus genus are a great source of sapogenins and saponins (Hayes et al.,2008). In traditional Indian medicine, the tuberous root of *A. racemosus* is used to treat a wide range of ailments, including dysentery, tumors, neuropathy, inflammations, nervous disorders, hyperacidity, bronchitis, some infectious diseases, chronic fevers, conjunctivitis, and rheumatism. Similarly, Pharmacological tests on animals have also shown that *A. racemosus* extract is effective as an antioxidant and anti-anaphylactic (Upadhyay et al., 2014; Hayes et al., 2008).

When medicinal plants were treated with a consortium of PGPR under saline conditions, it was demonstrated that the plant parameters had improved (Varma et al., 2017). In addition to this the plants grown in soil treated with compost showed the highest antioxidant activit (Sharafzadeh & Ordookhani, 2011). An analysis of *Asparagus racemosus* roots grown in soil treated with vermicompost, compost, cow dung, and other organic manures without the use of mineral or chemical fertilizers revealed that the plants from this soil had the uppermost levels of total phenol and total flavonoid content (Saikia and Upadhyaya, 2011). Similarly, Ge et al. (2016) found improved plant growth characteristics of asparagus when treated with a combination of PGPR, vermicompost and cow manure (Ge et al., 2016).

Steroid saponins, or Shatavarins I–IV, are phytoestrogen compounds present in the roots of *Asparagus racemosus* Willd. they are the main biologically active components of the plant. (Mfengwana and Mashele, 2020). Shatavarin IV is a sarsasapogenin glycoside made up of two rhamnose molecules and one glucose molecule, as well as starch and mucilage (Hayes et al., 2008). In 2001, Saxena and Chourasia extracted a new isoflavone called 8-methoxy-5,6,4′-trihydroxyisoflavone from the roots of *Asparagus racemosus* Willd. They identified a novel antioxidant compound named racemofuran in addition to well-known substances like asparagamine A and racemosol and flavonoids such glycosides of quercetin, hyperoside, rutin, kaempferol, and polycyclic alkaloids (Saxena and Chourasia, 2001). As a result of the presence of secondary metabolites *Asparagus racemosus* is used as a dietary supplement because it

also has some nutritional qualities. Additionally, it has anticancer, galactagogue, and immunomodulatory properties (Patil et al., 2014).

2.6.1 Shatavarin

The root and fruit of *A. racemosus* both contain steroidal saponins, which are the active ingredients. Shatavarins I to X, which are major steroidal glucosides (saponins), were discovered in the roots of *A. racemosus* but Shatavarins I and IV have been identified as the primary steroidal saponins (Haghi et al., 2012; Mitra et al., 2012). Shatavarin IV has been demonstrated to have significant inhibitory activity against Core Golgi enzymes such as transferases as well as immunomodulatory activity against specific T-dependent antigens in immunodeficient animals (Pandiyan et al., 2022). The medicinal properties of *A. racemosus*, including its anticancer activity, are due to the presence of saponin glycosides (Onlom et al., 2017). An earlier study demonstrated that Shatavarin IV had antioxytocic activity and Shatavarin I had anti-abortifacient activity, and both were used to treat infertility (Gohel et al., 2015).

2.6.2 Diosgenin

Diosgenin serves as a major raw material in the manufacture of synthetic hormones. It belongs to the steroidal saponins that are found in *A. racemosus* (Alok et al., 2013; Wang et al., 2011). Diosgenin has been demonstrated to have anti-proliferative activities against human coloncancer and to induce apoptosis in a number of human cancer cell lines (Bhutani et al., 2010). Clinical studies revealed that diosgenin-induced increases in biliary cholesterol output have a significant effect on the solubility and transport of biliary cholesterol (Thewles et al., 1993). Diosgenin has been discovered to be effective in treating conditions such as diabetes, hyperlipidemia, various cancers, osteoporosis, cardiovascular diseases, skin conditions, and neurological disorders (Paramesha et al., 2021). In fact, this compound is known to have anti-inflammatory and antioxidant properties and may be helpful for a variety of conditions, including blood and cerebral disorders, allergic diseases, obesity, and menopausal symptoms (Jesus et al., 2016).

2.6.3 Pathway for Diosgenin synthesis

In a number of plants, cholesterol is converted into steroidal sapogenins (spirostanols), such as diosgenin, but the exact biosynthetic processes that take place in

between have not yet been fully understood (Mehrafarin et al., 2010). Two processes can result in the formation of diosgenin from squalene-2,3-oxide: one is the formation of cholesterol from lanosterol and the other is the production of sitosterol from cycloartenol (Ciura et al., 2017). According to an *in vitro* study by Tal et al. (1984), naturally occurring glycosides in a number of plant species include steroidal saponins (furostanols), in which the side chain is held open by glycoside formation. These glycosides are converted to spirostanols by the action of glucosidases. These results provided evidence in favor of the theory that, in the biosynthesis of sapogenin, and also suggest that furostanol is utilized in the biosynthesis of diosgenin from cholesterol in a manner similar to that suggested by the proposed biosynthetic pathways (Tal et al., 1984) (Fig. 2.5).

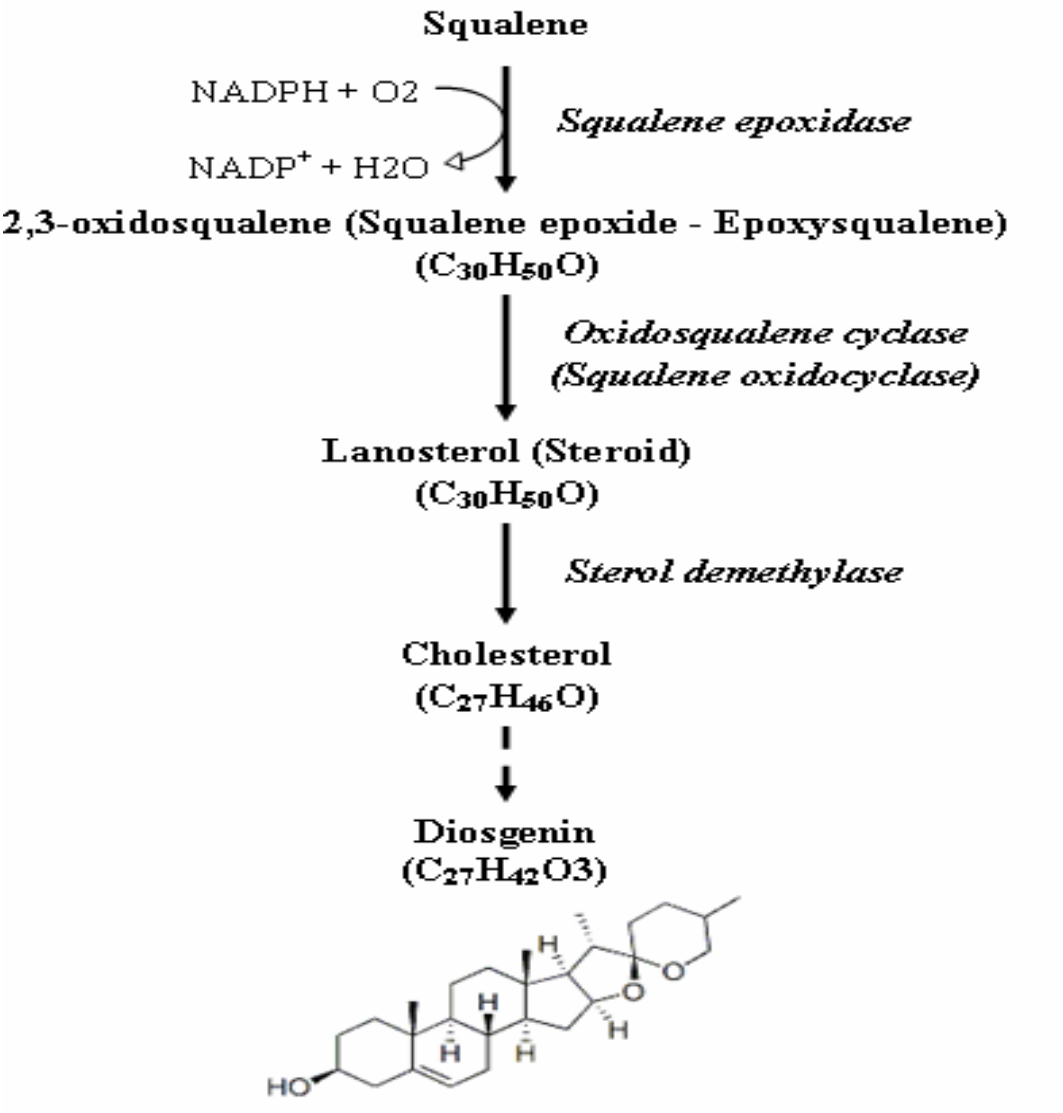

Fig. 2.5: Pathway of Diosgenin synthesis of Asparagus (Mehrafarin et al., 2010).

2.7 Pharmacological properties of secondary metabolites from Turmeric

Curcuminoids, which make up the turmeric rhizome, reveal a variety of advantageous biological properties, including antitumor, anticarcinogenic, and antioxidant properties. Curcumin is now viewed as a secure, innovative, and promising medication for the prevention and treatment of cancer, chronic inflammation, and other illnesses (Rodrigues et al., 2015). Some of the pharmacological properties of the metabolites are listed in Table 2.1.

Table 2.1: Pharmacological properties of secondary metabolites from Turmeric

Name of compound	Source	Biological activity	Reference
Curcumin	*C. longa*	Neuroprotective activity	Cas and Ghidoni, 2019
Curcumin	*C. longa*	Premenstrual syndrome	Fanaei et al., 2016
Curcumin	*C. longa*	Antibacterial, antiviral, antifungal	Moghadamtousi et al., 2014
Curcumin	*C. longa*	Antibacterial	Zheng et al., 2020
Curcuminoids	*C. xanthorrhiza*	Oxidative stress	Masuda et al., 1992
Curcuminoids	*C. longa*	Antitumor activity	Agarwal et al 2013
Curcuminoids	*C. longa*	Antimalaria	Nandakumar et al., 2006
Curcuminoids	*C. longa*	Cytotoxic Activity	Chen et al., 2017
Curcuminoids	C. *mangga*	Gastric ulcer, chest pain, fever	Blagojevic et al., 2011
DMC	*C. longa*	Anticancer activity	Yodkeeree et al., 2009
BDMC	*C. longa*	Anti-inflammatory	Kim et al., 2016
Ar-turmerone	*C. longa*	Anti-angiogenic effects Human	Yue et al., 2015
Ar turmerone	*C. longa*	Selective induction of apoptosis	Aratanechemuge et al., 2002
Ar-turmerone	*C. longa*	Anti-plasmodial	Hamizah et al., 2020
Ar-Turmerone	*C. longa*	Inhibits key enzymes linked to type 2 diabetes	Lekshmi et al., 2012
ar-turmerone	*C. longa*	To control cucumber	Fu et al., 2021

		powdery mildew	
ar-turmerone	*C. longa*	Antibacterial	Negi et al., 1999
Turmerone	*C. longa*	Larvicidal activity	Setzer et al., 2008
Turmerone	*C. longa*	Antifungal	Ferreira et al., 2013
Turmeronol A and TurmeronolB	*C. longa*	Anti-inflammatory mechanism	Okuda-hanafusa et al., 2019
Monoterpenoids, sesquiterpenoids	*C. longa*	Antiradical properties	Dutta and Neog, 2016
Phellandrene	*C. longa*	Insecticidal activity	Chaaban et al., 2019
Phellandrene	-	Wound healing activity	Scherer et al., 2019
Curcumenol	*C. phaeocaulis*	Anti-inflammatory	Tanaka et al., 2008
Curcumenol	*C. longa*	Antibacterial	Wagner et al., 2020
Curlone	*C. longa*	Antibacterial	Jayaprakasha et al., 2005
Curlone	*C. longa*	Insecticidal activity	Mehrotra et al., 2009
Furanodienone	*C. phaeocaulis*	Anti-inflammatory	Tanaka et al., 2008

2.8 Pharmacological properties of secondary metabolites from Asparagus

Traditional and Ayurvedic scriptures frequently refer to the roots of the Asparagus plant. The ancient classical Ayurvedic literature recommended it as a galactagogues and for the treatment of reproductive disorders and threatened abortion. Additionally, *A. racemosus* root is used to treat mental, neurological, and hepatic disorders as well as it works as an anti-ulcer, anti-inflammatory, antidiabetic, anti-aging, and anti-tumor agent (Hazra et al., 2020). Table 2.2 includes a list of some of the pharmacological characteristics of Asparagus metabolites.

Table 2.2: Pharmacological properties of secondary metabolites from Asparagus

Name of compound	Source	Biological activity	Reference
Shatavarin IV	*A. racemosus* root	Anticancer	Mitra et al., 2015
Shatavarin-IV	*A. racemosus*	Immuno-modulation activity	Kamat et al., 2000
Shatavarin I–IV	*A. racemosus*	Gastric ulcer healing effects	Sairam et al., 2002
Shatavarin I	*A. racemosus*	Anti-abortifacient	Patel, 2015
Shatavarin IX, Shatavarin IV	*A. racemosus*	Against prostate-carcinoma cell lines	Onlom et al., 2017
Diosgenin	*A. racemosus* root	Anti-inflammatory	Jung et al., 2010
Diosgenin	*A. racemosus* root	Induce apoptosis in human1547 osteosarcoma	Corbiere et al., 2003
Immunoside	*A. racemosus*	Induced apoptosis was	Bhutani et al., 2010
Sapogenin	*A. racemosus*	Control of cholesterol metabolism	Upadhyay et al., 2014
Sarsasapogenin	*A. officinalis* L	Improving memory	Hu et al., 2005
Asparanin A	*A. officinalis L*	Induce cell cycle arrest	Liu et al., 2009
Asparacoside	*A. racemosus*	Against hepato-carcinoma cell lines	Onlom et al., 2017
8-methoxy-5,6,4′-trihydroxyisoflavone-7-O-β-d-glucopyranoside	*A. racemosus* root	Antidiarrhoeal	Mandal et al., 2000
Methyl protodioscin and protodioscin	*A. officinalis* seed	Cytotoxic	Shao et al., 1997
Spirostanol glycoside	*A. officinalis* fruits	Immobilization of human spermatozoa	Pant et al., 1988
Racemosol	*A. racemosus* Fruits Roots	Antioxidant, Anticarcinogenic	Velavan et al., 2007
Racemoside A	*A. racemosus*	Inducer of apoptosis	Onlom et al., 2017
Norlignans	*A. gobicus* root	Cytotoxic	Yang et al., 2004
Yamogenin glycosides I, II,	*A. plumosus* root	Spermicidal	Pant et al., 1988

2.9 Computational study of Phytocompounds:

For the discovery of organic ligands, bioinformatics methods for the identification of novel protein binding molecules and the variety of available compound databases have proven to be powerful resources (Luthra et al., 2009; Parulekar et al., 2018; Sonawane et al., 2021; Bansode et al., 2019). Phenolics, flavonoids, coumarins, sterols, and lignans are examples of secondary metabolites that exhibit significant pharmacological properties. To treat various diseases, numerous *in-silico* studies on plant metabolites have been carried out. This includes a step-by-step analysis of the structure-property relationship, the use of structural information about metabolite targets, and the use of structural information of known active compounds to establish a structure-activity relationship (Wase and Wright, 2008). One can study the physicochemical properties that affect drug absorption and excretion, such as stability, solubility, and lipophilicity, with the aid of bioinformatics (Vijayalakshmi et al., 2014). Usually, when considering any compound for lead optimization, these characteristics are taken into account. This classification is based on a limit on molecular weight, lipophilicity, and hydrophilicity, and is known as Lipinski's "rule-of-five," which encodes a basic profile for orally bioavailable compounds (Wase and Wright, 2008).

Many proteins in the body have their activity controlled by small ligands that interact with key proteins in metabolic pathways (Wase & Wright, 2008). The Protein Database contains information about them,and bioinformatics can be used to examine their interactions. A set of predicted binding models of each compound against the corresponding receptor is the result of receptor-ligand docking (Su et al., 1982). The study by Ogungbe and Setzer (2016) presents molecular docking of phytochemical ligands with potential parasitic protein targets as an *in-silico* attempt at natural product therapeutic development for neglected parasitic protozoal illnesses (Ogungbe and Setzer, 2016). There are a few metabolite examples that have been studied *in silico*, such as study of *Moringa oleifera* Lam. metabolites as an anti-diabetic agent was reported by (Zainab et al., 2020). Similarly, Salanin, astragalin, and epoxyazadirone, three significant neem metabolites, exhibit the strongest antibacterial activity against *Staphylococcus aureus* cell surface proteins in an *in silico* screening (Gunamalai and Vanila, 2014). In addition to that, the rich variety of phytochemicals in beach spider lily demonstrated antibiofilm activity, which is thought to be one of the key factors responsible for drug resistance in microorganisms. Therefore, learning more about the lily's therapeutic potential may help to reduce the spread

of pathogens that produce biofilms (Nadaf et al., 2018).

To gain insight into the molecular level binding interactions between the drug and polymer, *in silico* docking study was followed by molecular dynamic simulations (Gangurde et al., 2015). Through *in silico* studies, Jagatha et al. (2008) explained the therapeutic implications for Parkinson's disease. They used an *in-silico* screening tool to evaluate the effectiveness of all other natural compounds/products for therapeutic benefit (Jagatha et al., 2008). The most often suggested substances from medicinal plants that may act as COVID-19 major protease inhibitors include quercetin, oleuropein, catechin, luteolin-7-glucoside, demethoxycurcumin, naringenin, apigenin-7-glucoside, epicatechin-gallate, and curcumin (Khaerunnisa et al., 2020).

Likewise, an *in-silico* study provides insight into how chitin and chitosan-based nanoparticles deliver insulin and curcumin (Dhanasekaran et al., 2018). Earlier study by Mohankumaret al, (2015) has been shown that an analogue of curcumin, BDMC-A, to be more effective than curcumin in inhibiting the NF-kB signalling network and related markers in a breast cancer cell line than curcumin itself (Mohankumar et al., 2015). Another study by Guller et al. (2021) revealed that studies on the inhibition of the glutathione reductase enzyme by curcumin, quercetin, and resveratrol were carried out both *in vitro* and *in silico* (Guller et al., 2021). With the *in silico*, *in vitro*, and *in vivo* efficacy study, which thoroughly demonstrates curcumin's potency, the anti-inflammatory and anti-allergic efficacy of curcumin was confirmed by (Venkata et al., 2012). According to the earlier report, curcumin, demethoxycurcumin, and xanthorrizol spontaneously interact with the amino acids in the active enzyme tyrosinase sac and α-MSH, suggesting that they may have skin-whitening properties (Mustarichie et al., 2013). According to Baek et al. (2018), demethoxycurcumin and bisdemethoxycurcumin may be effective treatments for conditions like depression, Parkinson's disease, and Alzheimer's disease (Baek et al., 2018). Previously Meizarini et al, (2018) stated that curcuminoids are more effective than eugenol, according to *in vivo* studies. *In silico* studies that forecast the potential anti-inflammatory effect of curcuminoid provide support for these findings (Meizarini et al., 2018).

Diosgenin, a promising natural compound, has been studied *in silico* for its biological properties including antioxidant, anti-hyperglycemic, and antilipidemic effects (Sangeetha et al., 2013). It is a sapogenin and has anti-diabetic, anti-inflammatory, chemopreventive, and anticancer properties. Through the targeting of numerous tissues-specific pathways, numerous *in vitro* and *in vivo* studies show that it has a great deal of

potential for treating diabetes and its complications (Nazir et al., 2022). Sarsasapogenin significantly inhibits key enzymes involved in the pathogenesis of AD, including acetylcholinesterase, butyrylcholinesterase, BACE1, and MAO-B, according to an *in vitro* and *in silico* study by (Kashyap et al., 2020). Overall, Singh et al, (2014) showed that diosgenin analogues inhibit the production of pro-inflammatory cytokines in both *in vitro* and *in vivo* conditions (Singh et al., 2014).

Similarly, diosgenin demonstrated a positive impact on type 2 diabetes by interacting with the PPARγ (Peroxisome proliferated-activated receptor γ). These results suggest that the insulin-sensitizing effects of trigonelline and diosgenin are mediated through modulation of ER stress and oxidative stress in the pancreas as well as by PPARc activation in adipose tissue in *in vivo, in vitro*, and *in silico* study (Rani S, 2014). According to Tap et al, (2018) there is evidence that the enzyme phospholipase 2 (Pla2) is inhibited by bromelain, asisticoside, and diosgenin. However, using a single anti-inflammatory drug for treatment frequently results in a number of side effects, including hepatotoxicity, gastrointestinal bleeding, meningitis, and asthma. Therefore, a novel approach combining two or more potential compounds that have inhibitory effects on Pla2 activity has been suggested to solve the issue (Tap et al., 2018).

In the present investigation, *in silico* study of the potent PGPR induced secondary metabolites of *C. longa* has been carried out with respect to the nature of interactions, binding mode and selectivity of biofilm producing protein such as sortaseA from *Staphylococcus aureus* and *Streptococcus mutans.*

2.10 Scope and Objectives of Research:

Plant growth-promoting rhizobacteria (PGPR) are significantly playing role in sustainable development of agricultural sector. Efforts are being continuously undertaken to increase the crop yields with reduction in the use of chemical fertilizers and pesticides. The use of PGPR is an eco-friendly way of increasing the yield of various crops. The mechanism of action of different PGPR varies in different plants and it depends upon the type of host plants. In recent days, an innovative way of using PGPR for medicinal plant production and sustainable agriculture is being developed. Many studies have established the historic usage of medicinal plants to treat a wide range of disorders, as herbal medicine is often regarded to have fewer adverse effects when used on humans. Furthermore, utilization of natural products has risen, both as therapeutically active

medicines and as lead molecules in drug development practices.

With this background, the present research was undertaken which includes the screening of potent PGPR strains from the rhizospheric soil of the Turmeric and Asparagus plants. These potent strains were tested to identify their effects on different parameters of Turmeric and Asparagus plants. Further, the secondary metabolites (phytocompounds) produced by these plants were extracted and purified. The purified phytocompounds were characterized and identified using TLC, GC-MS/MS, and LC-MS/MS. These PGPR induced phytocompounds were then tested for their antimicrobial activity *in vitro* against a variety of Gram-positive and Gram-negative bacterial pathogens as well as fungi and biofilm inhibition property. Additionally, *in silico* study was carried out in which we targeted the adhesion protein SortaseA (SrtA) from both *S. aureus* and *S. mutans* to study the inhibition mechanism using molecular modelling methods. The docking studies revealed that the combination of phytocompounds binding significantly lowers the binding energy of the overall complex. MD simulation and MM-GBSA binding energy calculation studies showed the stability of SrtA in all phytocompounds specifically for ternary complexes with combination of phytocompounds. Thus, the objectives of the present research work were –

Objectives:

1. Screening and identification of potent PGPR from rhizosphere of medicinal plants.
2. Effect of potent PGPR on the growth parameters and secondary metabolites of selected medicinal plants.
3. Extraction and purification of secondary metabolites from medicinal plants.
4. Pharmacological applications and bioinformatics studies of secondary metabolites.

CHAPTER III

MATERIALS AND METHODS

3. MATERIALS AND METHODS:

3.1 Introduction

This chapter describes the methodology employed in this work, including the screening and isolation of Plant Growth Promoting Rhizobacteria from rhizospheric soil of medicinal plants such as Turmeric and Asparagus. Afterwards, using a pot culture experiment, it was determined how PGPR affected plant metrics and biological contents. Plant metabolites that were influenced by PGPR were then extracted and purified using different methods. Computational and experimental techniques are applied to delve deeper into its pharmacological characteristics.

3.2 Materials:

3.2.1 Soil

The rhizospheric soil samples were collected from the cultivated Turmeric farms of the Turmeric Research Section, "Mahatma Phule Krishi Vidyapeeth's Agriculture Research Centre", Kasbe Digraj, Dist. Sangli and from cultivated Asparagus farms of various localities in Kolhapur District.

3.2.2 Plant material

Turmeric rhizomes of the Salem variety and two months old cultivated plantlets of Asparagus were used for the pot culture experiments.

3.2.3 Chemicals and culture media

All the chemicals used in this study were highly purified and of analytical grade. All bacterial and fungal culture media such as nutrient agar (NA), calcium-adjusted Muller Hinton agar (MHA), brain heart infusion (BHI) broth, potato dextrose agar (PDA) and other media components were purchased from Himedia, India. Standard antibiotics discs, standard curcumin, curcuminoids, diosgenin were also purchased from HiMedia, India. Standard 4 Hydroxy 2 methylacetophenone was obtained from TCI, India while ascorbic acid (AR Grade), rutin, 2,2- Diphenyl-1-picrylhydrazyl (DPPH) were obtained from Himedia India. Filtration assembly and equipment were obtained from Axiva. Analytical grade TLC plates were obtained from Merck Millipore.

3.2.4 Bacterial cultures

Gram positive organisms: *Staphylococcus aureus* NCIM 2654, *Streptococcus mutans* NCIM 5660 and Gram negative: *Escherichia coli* NCIM 2832, *Proteus vulgaris* NCIM 2813 were purchased from National Collection of Industrially important Microorganism (NCIM) Pune, India and were maintained with refrigeration at the Department of Microbiology, Shivaji University, Kolhapur.

3.3 Screening of PGPR from rhizospheric soil of Medicinal plants

For the isolation of rhizome and root associated soil bacteria, the adhering soil (1 gm) was suspended in 100 ml of nutrient broth in an Erlenmeyer flask and shaken for 24 hrs on shaker at room temperature for enrichment. It was then serially diluted upto 10^{-5} to 10^{-10}, and from that 0.1 ml suspension was added to the Petri plate containing sterile nutrient agar media and spread by the sterile glass spreader in the laminar flow hood. Petri dishes were incubated at 30°C till visible growth appeared on the plates. Bacterial colonies were isolated following the standard microbiological techniques. The pure isolates were isolated after repeated streaking on the nutrient agar plate. The pure isolates were inoculated on the respective medium slants and after growth, they were maintained at 4°C in a freeze for further use in the Department of Microbiology, Shivaji University, Kolhapur.

3.4 Plant growth promoting attributes of PGPR:

3.4.1 Phosphate solubilization

The Pikovskay's agar medium containing tricalcium phosphate was spot-inoculated with the bacterial isolates, and the plates were then incubated at 28±2ºC for 2 to 3 days. The appearance of a transparent halo zone surrounding the bacterial isolates demonstrated their capacity to solubilize phosphate (Laslo et al., 2012).

3.4.2 Zinc solubilization

The bacterial isolates were grown separately on basal medium (Glucose-1gm, Ammonium sulphate-0.1gm, Potassium chloride-0.02gm, Dipotassium hydrogen phosphate-0.01gm, Magnesium sulphate-0.02gm, Distilled water -100ml, pH 7.0) supplemented with 0.1% insoluble zinc oxide. 10µl bacterial suspension was placed on a basal medium containing plates and plates were incubated at room temperature for 24, 48 and 72 hrs. After incubation zone of clearance were observed around

bacterial growth (Saravanan et al., 2004).

3.4.3 Potassium solubilization

To check potassium solubilization, isolates were inoculated on the modified Alexondrov's medium (Glucose- 0.5gm, Magnesium sulphate- 0.05gm, Ferric chloride- 0.0005gm, Calcium carbonate- 0.01gm, Tri- calcium phosphate- 0.2gm, Potassium alumino silicate- 0.2gm, Agar 1.5-2gm, distilled water- 100 mL) containing 0.2 % potassium alumino silicate as a potassium source and phenol red 0.05% as a pH indicator. The test organisms were inoculated on the media and incubated at 28 ± 2ºC for 24-72 hrs. After incubation the color change was observed due to the presence of pH indicator (Dhaked et al., 2017).

3.4.4 Production of IAA

Bacterial cultures were grown in the flasks containing Yeast extract mineral medium supplemented with 1 % mannitol, 0.01% $CaCl_2$ and different concentrations of L-Tryptophan (12.5, 37.5, 62.5, 75 mg/25ml) and kept at dark conditions for 48 hrs at room temperature on shaker. After incubation broth were centrifuged at (8000rpm, 10 min). 2 ml supernatant bacterial cultures were mixed with 2 drops of orthophosphoric acid and 4 ml of Salkowski reagent (50 ml, 35% of per chloric acid, 1 ml 0.5 M, $FeCl_3$ solution). Development of pink colour confirmed the Production of IAA (Brick et al.,1991).

3.4.5 Nitrogen fixation

The freshly grown potent isolates were streaked on N-free Asbhy's agar medium plates. The plates were incubated at room temperature for 48 hrs. formation of creamy white colonies indicates nitrogen fixation by the isolates. The Kjeldahl method was used to further quantify the fixed nitrogen. After adding a fresh inoculum of isolated PGPR to sterile, nitrogen-free Ashby's broth, the mixture was incubated for five days at 28 ±2°C and 120 rpm on a rotary shaker. The uninoculated broth was served as a control. Following incubation, the inoculated broth was centrifuged for 10 minutes at 5000 rpm to remove biomass, and the amount of Total Kjeldahl Nitrogen (TKN) was calculated by titration (Kumar et al., 2014).

3.4.6 NH_3 Production

To estimate NH3 production, the method suggested by Cappuccino and Sherman, (1992) was used. In brief, 50 µl of bacterial cell suspension was grown for 72 hours at 25°C in 30 ml of peptone broth (4%). Following incubation, 1 ml Nessler's reagent (50 gm potassium iodide, 35 ml saturated mercuric chloride, 25 ml distilled water, 400 ml potassium hydroxide (40%) was added. The presence of NH3 was demonstrated by the production of yellow to brown precipitate.

3.4.7 HCN Production

HCN Production was detected by the method of Kloepper et al. (1991). The bacterial cultures were streaked on King's B medium that contains 0.4% glycine. The plate's lid was lined with a Whatman filter paper No. 1 that had been dipped in a solution of 0.5% picric acid (in 2% sodium carbonate). Parafilm was used to seal the plates, which were then incubated for 72 hours at 28 ±2°C. HCN production was detected by the color changing from light brown to dark brown.

3.4.8 Siderophore Production

The Schwyn and Neilands (1987) approach was used to determine siderophore production. Bacterial suspension (10 µl) was inoculated on the Chrome azurol- S agar plate and incubated at 28 ±2ºC for 24, 48 and 72 hrs. The formation of a yellow orange hallow zone around the bacterial spot is the indication of siderophore production.

3.4.9 Salt tolerance

To test the salt tolerance of bacterial isolates, 100µl of 24 hrs old culture of isolates was inoculated into 10 ml Luria Broth containing 1%, 2%, 3%, 4%, 5%, 6%, 7%, 8%, 9%, 10% NaCl. After 24-48 hrs, the growth was examined by taking absorbance at 600 nm in a Spectrophotometer (UV/Vis) and their range of stress tolerance was detected (Tirry et al., 2021).

3.4.10 Exopolysaccharides (EPS) production

To detect exopolysaccharide production, the samples were cultured in optimized mineral salts medium with K_2HPO_4- 1.26gm, KH_2PO_4- 1.82gm, NH_4NO_3- 1gm, $MgSO_4.7H_2O$- 0.1gm, $MnSO_4$- 0.06gm, $CaCl_2.2H_2O$- 0.1gm, $FeSO_4.2H_2O$- 0.006gm, sodium molybdate- 0.1gm, NaCl- 0.15gm and Glucose- 0.02gm in 100 ml

of distilled water for 7 days incubation (Bramchari and Dubey, 2006). Following that, the 250 ml bacterial cultures were centrifuged for 20 minutes at 4°C and 10,000 rpm. Double the quantity of 95% ice-cold ethanol was added to the supernatant in order to remove the exopolysaccharides (Naseem & Bano, 2014).

3.5 Morphological, Cultural and Biochemical characteristics of bacterial isolates

Morphological, Cultural and Biochemical characteristics of bacterial isolates were studied on the basis of colony characters, Gram staining, motility, and biochemical tests such as citrate utilization, starch hydrolysis, nitrate reduction, catalase, oxidase and sugar fermentations including glucose, adonitol, arabinose. Further, antibiotic sensitivity testing was carried out utilizing the antibiotic impregnated discs method. The organisms have been categorized as resistant or sensitive based on their zone of inhibition, according to the DIFCO Manual, 10^{th} edition (1984).

3.6 Genotypic characterization of PGPR

The genomic DNA of potent PGPR were extracted using the conventional phenol/chloroform extraction method (Sambrook et al., 1989) and the 16S rRNA gene were amplified using universal primers 16F27 [5'-CCAGAGTTTGATCMTGGCTCAG-3'] and 16R1492 [5'-TACGGYTACCTTGTTACGACTT-3']. PEG-NaCl precipitation was used to purify the amplified 16S rRNA gene PCR products and it was then sequentially sequenced on an ABI®3730XL automated DNA sequencer (Applied Biosystems, Inc., Foster City, CA) as per the manufacturer's recommendations. The assembly was performed with the Lasergene package, andthe identification was done with the EzBioCloud database (Riera et al., 2017). Using the Nucleotide Basic Local Alignment Search Tool (BLAST) programme, the resulting sequences were processed and searched to find the best fit to sequences at the National Center for Biotechnology Information (NCBI) BLAST server (www.ncbi.nlm.nih.gov/BLAST). Multiple sequence alignment was performed using CLUSTALW software (Thompson et al., 1997) on the sequences that showed >98% resemblance. MEGA X was used to create a phylogenetic tree based on molecular analyses. Identified 16S rRNA sequence were deposited in GenBank with Accession number **MZ452064**, **OL739684, OL771442** and **OL656822.**

3.7 Pot culture experiment:

3.7.1 Inoculum preparation for Turmeric

With minor modifications, the inoculum was made as described Kaur et al. (2012). To maintain cell density at 10^8 CFU/ml of bacterial suspension, 1% activated charcoal powder was combined with 1% glucose and 0.5% NaCl. Turmeric rhizomes were surface sterilized with 70% alcohol and washed five to six times with sterile distilled water. Then coated with this inoculum and sowed in pots containing natural soil and sterile soil each.

3.7.2 Inoculum preparation for Asparagus

1 gm of carboxy methyl cellulose (adhesive), 10^8 CFU/ml of bacterial suspension, 1% glucose, and 0.5% NaCl were added into 90 ml of sterile distilled water to make the inoculum. Asparagus roots were surface sterilized with 70% alcohol and rinsed with sterile distilled water five to six times. The roots were then covered with inoculum and sown in pots containing naturaland sterile soil each.

3.7.3 Effect of PGPR on Turmeric

To demonstrate effect of PGPR on Turmeric, pot culture experiment was performed. The isolates used in present study were *Serratia nematodiphila* RGK and *Pseudomonas plecoglossicida* RGK. To study the influence of treatment of these isolates, the experiment was carried out in randomized block design (RBD) in triplicate by using air dried, sieved natural as well as sterile soil. Total 72 pots were used for experiment from that 36 for natural soil and 36 for sterile soil. Four types of treatments were given to rhizome before sowing -

T1 : Treatment with *Serratia nematodiphila* RGK

T2 : Treatment with *Pseudomonas plecoglossicida* RGK

T3: Co-culture of *Serratia nematodiphila* RGK and *Pseudomonas plecoglossicida* RGK

T4 : Control (Uninoculated)

The morphological parameters of plants were examined at 45, 90 and 180 days of sowing (Ambardar and Vakhlu, 2013).

3.7.4 Effect of PGPR on Asparagus

A pot culture experiment was carried out to demonstrate the effect of PGPR on Asparagus. The isolates used in this experiment were *Exiguobacterium acetylicum* RGK and *Enterobacter mori* RGK1. To study the influence of treatment of these isolates, the experiment was carried out in randomized block design (RBD) in triplicate by using air dried, sieved natural as well as sterile soil. Total 72 pots were used for experiment from that 36 for natural soil and 36 for sterile soil. Four types of treatments were given to plantlets before sowing

T1 : Treatment with *Exiguobacterium acetylicum* RGK

T2 : Treatment with *Enterobacter mori* RGK1

T3 : Co-culture of *Exiguobacterium acetylicum* RGK and *Enterobacter mori* RGK1

T4 : Control (Uninoculated)

The morphological parameters of plants were examined at 45, 90 and 180 days of sowing(Ambardar and Vakhlu, 2013).

3.7.5 Plant parameters:

The morphological plant parameters such as number of leaves, rhizome biomass, shoot length, root number, root biomass of both the plants from each pot were examined at 45, 90 and 180 days of sowing.

3.7.5.1 Plant parameters for Turmeric

Number of leaves- The leaf number was measured after 45, 90, and 180 days in net house conditions. All leaves, regardless of size, were counted, and the average number of leaves per plant were calculated.

Rhizome biomass- The extra water was removed by pressing it between the filter paper's folds. Following a 60°C drying process, the rhizomes' weight was measured and represented as gm/dry plant weight.

Shoot length- The plant's shoot length was measured in centimeters (cm) from the soil line tothe highest point of the plant.

3.7.5.2 Plant parameters for Asparagus

Root number - The data on root number was recorded after 45, 90 and 180 days in net house conditions. All the roots, regardless of their size were counted and average number of root per plant were calculated.

Root biomass - The roots were thoroughly washed and wiped off by putting them between the folds of filter paper. The roots were then dried at 60°C, and the weight was recorded in gm/dry weight of plant.

Shoot length - The plant's shoot length was measured in centimeters (cm) from the soil line to the highest point of the plant.

3.8 Extraction of secondary metabolites:

The uprooting of plants was done after 45, 90 and 180 days and proceeded for secondary metabolite extraction. After uprooting rhizomes and roots were washed with distilled water to remove adhered soil. It was then cut into small pieces and dried in oven at 40℃ to make fine powder. This powder was used for the metabolite extraction process. Different solvents and extraction techniques were used to extract plant secondary metabolites. Below are some additional effective extraction techniques.

3.8.1 Soxhlet Extraction

Soxhlet extraction was carried out using standard apparatus. 1 gm of powdered rhizomes with 250 ml of each hexane, methanol, acetone, petroleum ether, diethyl ether and ethanol as solvent were used with the extraction time of 8 hrs. The organic extracts were concentrated using hot plate and stored at 4℃ for further analysis.

3.8.2 Sonication for Turmeric and Asparagus

1 gm of sample was added to 10 ml of methanol in sealed tube and solution was treated in bath sonicator for 1 hr at room temperature, centrifuged at 5000 rpm at 4℃ for 10 min. Supernatant was collected for further analysis.

3.9 Preliminary qualitative phytochemical screening of crude extracts:

Preliminary qualitative phytochemical screening was performed with the prepared crude extracts of PGPR treated plants and control plants in natural and sterile soil, to assess the presence or absence of various classes of medicinally important secondary metabolites.

3.9.1 Analysis of total phenolic content

Wolfe et al. (2003) assessed the extracts' total phenolic content using the Folin-Ciocalteu technique. 12.5µl of plant extracts and 50µl of distilled water were

added to a 96-well microtiter plate. Following the addition of 12.5µl of Folin-Ciocalteu's phenol reagent, the plate was left at room temperature for 10 minutes. Following a 10 minute duration, 125µl of sodium carbonate 7% and 100µl of distilled water were added, resulting in a final volume of 300µl. The entire mixture was then allowed to stand at room temperature for 90 minutes in dark conditions. The total phenolic acid content was measured at 750 nm and represented as mg gallic acid equivalents (mg GA/gm) of the dry samples (Ahmad et al., 2015).

3.9.2 Analysis of flavonoids content

The method of Luximan and Rama (2002) was used to calculate the total flavonoid content of plant extracts. 150 µl of extracts and 150 µl 2% $AlCl_3$ was added to 96 well microtiter plate. Following a 10 minute dark incubation period, the plate was measured for absorbance at 367 nm. Rutin equivalents (RE)/gm of dry weight samples were used to express the total flavonoid content.

3.9.3 Analysis of saponins content

Using the method described by Hiai et al. in 1976, the saponin content was calculated. 5 ml of ice cold H_2SO_4 (72%) and 0.5 ml of 8% methanolic vanillin were added to 0.5 ml of asparagus plant extract and then the mixture was incubated in a water bath for 10 minutes at 60°C. After cooling, the absorbance at 544 nm was measured. The amount of total saponin was calculated as quil-A equivalents (QE)/gm of dry weight samples.

3.10 Purification of plant secondary metabolites:

Separation and purification of secondary metabolites from PGPR treated and non-treated plantswere done using following techniques

3.10.1 Purification of curcuminoids

Methanolic extract was subjected to silica gel column chromatography (60-120 mesh). To pack the column, silica gel was dissolved in chloroform: methanol (98:2) and filled upto 46 cm. Then sample was added on the top of gel and eluted with chloroform followed by chloroform: methanol with increasing polarity. All fractions were collected and subjected to UVspectrophotometry at 425 nm (Heffernan et al., 2017).

3.10.2 Thin layer chromatography (TLC) for curcuminoids

The collected fractions were tested on pre-coated Silica gel (Merck, Darmstadt, Germany) TLC plates along with standard curcuminoids. The plates were developed using pre- saturated TLC chamber for 1 hr. chloroform: methanol: formic acid (96:4:0.8 v/v/v) was used as mobile phase. Each plate was developed up to the height of about 12 cm. The plates were then removed and dried. Spots were analyzed and Rf values calculated (Zhang et al., 2008).

3.10.3 Purification of curcumin

Curcumin was further purified from separated spots on TLC. The uppermost spot which was of curcumin (based on Rf value) was scrapped, dissolved in methanol and kept in refrigerator overnight. The supernatant was then collected, evaporated and concentrated. It was used for further purification by silica gel column chromatography (Revathy et al., 2011).

3.10.4 Purification of diosgenin by acid hydrolysis

5 gm of Asparagus plant powder was hydrolyzed in 50 ml of 2 M sulphuric acid by heating under refluxation for 2 hrs. When the solution had cooled, 40% sodium hydroxide was added to neutralize it. The hydrolyzed product was then extracted with an equal quantity of chloroform (Wang et al., 2011; Yang et al., 2015). The extract was separated by a separating funnel and concentrated by evaporation at 60°C. The residue was dissolved in methanol and used for TLC on precoated silica gel for TLC analysis along with the standards.

3.10.5 Thin layer chromatography (TLC) for diosgenin

Thin-layer chromatography was performed on plates precoated with silica gel (Merck, Darmstadt, Germany). The samples were developed with hexane-acetone (8:2) as the mobile phase with a few minor modifications, dried to ensure that all solvents had evaporated, and detected with a 0.5:5 mixture of ethanol (8% vanillin) and sulfuric acid solution (70%) (Hardman, 1968).

3.10.6 High Performance Liquid Chromatography (HPLC)

For the purification of small organic molecules like drugs, peptides, microbial metabolites, plant metabolites and antibiotics, high-performance liquid chromatography (HPLC) is a highly effective and high-resolution technique (Smyth et

al., 2014; Dhanarajan et al., 2015). As part of the recovery of the purification method, HPLC was also used to quantify the metabolites.

3.10.6.1 For Curcumin

This method involves the interaction of liquid solvent in the tightly packed solid column or a liquid column. Parameter used during HPLC purification of Curcumin are given below in Table 3.1

Table 3.1: Parameter used for purification of Curcumin

Parameter used during HPLC purification of Curcumin

Column	C_{18}
Detector	Diode Array detector
Solvent system/Mobile phase	The mobile phase was 50:50 (v/v) acetonitrile and 2% acetic acid
Flow rate	0.5ml/min
Wavelength of detection	425nm
Sample volume	20 µl
Working temperature	25℃
Standard curcumin	100- 500 µg/ml

3.10.6.2 For Diosgenin

Parameter used during HPLC purification of Diosgenin are given below in Table 3.2

Table 3.2: Parameter used for purification of Diosgenin

Parameter used during HPLC purification of Diosgenin

Column	C_{25}
Detector	Diode Array detector
Solvent system/Mobile phase	The mobile phase was 10:90 (v/v) HPLC-grade water and acetonitrile
Flow rate	0.8ml/min
Wavelength of detection	194 nm
Sample volume	25 µl
Working temperature	27^0C
Standard diosgenin	20 – 100 µg/ml

3.10.7 Gas Chromatography-Mass spectroscopy (GC-MS/MS)

Phytocompounds were analyzed both qualitatively and quantitatively using Gas Chromatography Mass Spectroscopy (GC-MS/MS). Following the conversion of the materials to a gaseous form, analysis was done using the mass-to-charge ratio (Balamurugan et al., 2019). Curcuminoid fractions were subjected to GC-MS/MS analysis for compound identification. Helium was used as a carrier gas for the GC-MS/MS study of metabolites, which was performed utilizing an HS 2010 Plus (SHIMADZU) MS TQ 8050 mass detector, column, and SH-Rxi-5Sil MS (30mm × 0.25mm ID × 0.25µm). 1 µl of the sample was injected at a temperature of 250℃; the auxiliary was set at 290℃; the ion source was set at 280℃; the oven was set between 50℃ and 275℃; the GC ran for 38 minutes. The metabolites were identified by National Institute of Standard and Technology (NIST) database.

3.10.8 Liquid chromatography and mass spectroscopy (LC-MS/MS)

HPLC-Quadrupole-Orbitrap MS an Ultimate 3000-series HPLC hyphenated to a QExactive MS (ThermoFisher Scientific, Bremen, Germany) was used with a Waters HSST3 C18 (100 × 2.1 mm, 2.7 µm) column (Waters, USA), thermostated at 30°C. The mobile phase comprised the following: A: water and B: Acetonitrile, each containing 0.1% formic acid. With aflow rate of 0.4 mL/min, the gradient programme was set at 0–10 min/98% A, 11.1 min/2 % A, 16 min/2% A. The heated electrospray ionization (H-ESI, positive mode) parameters were as follows: sheath gas flow rate, 45; auxiliary gas flow rate, 8; sweep gas flow rate, 1; spray voltage, 3.50 kV; capillary temperature, 320 °C; S-lens RF level, 50.0 and heater temperature, 300°C. The MS analysis was performed in the ddMS2 mode. At three different resolutions of 70000 "Full Width at Half Maxima" (FWHM) (at m/z 200), FS was performed in the mass rangeof 100–1000 Da. This was followed by ddMS2 at 17500 resolution (at m/z 200) with stepped collision energy, operated at 10, 30 and 70 V. The automatic gain control (AGC)- targets for the ddMS2 methods were maintained at 1e6. In ddMS2 the m/z with scan range 100-1500 was used. (Originally developed by ThermoFisher Scientific). The software compound discoverer 3.2.0.421 was used for the data processing.

3.11 Analysis of Antioxidant Activity:

The total antioxidant capacity was calculated by measuring the sample's ability to scavenge free radicals using 2,2-Diphenyl-1-picrylhydrazyl (DPPH) according to the procedure described by Aquino et al. (2001). A 0.1 mM methanol DPPH solution was made, and a UV-vis spectrophotometer was used to detect the absorbance at 517 nm. A mixture of 10 µl plant extract and 290 µl DPPH was added to each well of 96-well microtiter plates. Following that, methanol was kept as a blank and the plate was incubated for 20 minutes at room temperature in the dark. Using a UV-vis spectrophotometer, the absorbance was determined at 517 nm. The experiment was conducted in triplicate. Percentage inhibition was calculated using the formula-

$$\% \text{ inhibition } = \frac{\text{A517Control – A517 Sample}}{\text{A517 control}} \; x\,100$$

The antioxidant capacity of the extracts using DPPH for free radical scavenging ability wasexpressed as mg ascorbic acid equivalent per gram of dry weight of sample.

3.12 Antimicrobial and antifungal activity of Phytocompounds:

Turmeric and Asparagus has long been considered as to have natural medicinal properties (Hoe seon lee, 2002). Antimicrobial studies were carried out on the pathogens included *Proteus vulgaris*, *Escherichia coli*, *Streptococcus mutans* and *Staphylococcus aureus.* Antifungal activity was checked by using *Pythium aphanidermatum*, *Aspergillus niger* and *Candida albicans* strains of fungus. The antimicrobial and antifungal activity was monitored in terms of zone of inhibition observed on agar plates of nutrient medium with 1.8% agar by using agar well diffusion method. The plates were incubated for 24 hrs at 37°C for bacteria and 48 hrs at 37°C for fungal cultures. Curcumin, curcuminoids, 4 hydroxy 2 methyl acetophenone, purified curcumin, purified curcuminoids, a combination of curcumin + 4 hydroxy 2 methyl acetophenone and diosgenin standard and purified diosgenin were used for testing purpose. After incubation results were recorded.

3.13 Minimum inhibitory concentration:

The Minimum inhibitory concentration (MIC) of purified metabolites (curcumin, curcuminoid and diosgenin), standard metabolites (curcumin, curcuminoid, 4 hydroxy 2 methyl acetophenone and diosgenin) and their combination (curcumin + 4 hydroxy 2 methyl acetophenone) was determined by using test pathogens as *P.*

vulgaris, E. coli, S. mutans and *S. aureus.* It was determined by twofold serial dilutions of metabolites in a Mueller-Hinton Broth medium. The test was carried out in 96 well microtitre plate with a standardized bacterial suspension of 0.5 McFarland's turbidity. The lowest concentration that completely inhibited the growth of the bacteria after 24 hrs was considered as the minimum inhibitory concentration (Bahari et al., 2017).

3.14 Effect of phytocompounds on test pathogen:

To assess the effect of these metabolites on pathogen growth, the test pathogen *S. aureus* NCIM 2654 was grown in the presence of purified metabolites (curcumin, curcuminoid, and diosgenin), standard metabolites (curcumin, curcuminoid, 4 hydroxy 2 methyl acetophenone, and diosgenin), and their combination (curcumin + 4 hydroxy 2 methyl acetophenone). Their effect on the development of bacteria was measured using an hourly interval of OD at 660 nm. The test culture with initial concentration of 0.5 McFarland was incubated for 12 hours in the presence of these metabolites. The OD values were compared with the control sample and a sterile BHI medium was used as blank. By taking absorbance readings every hour, the growth trend was obtained.

3.15 Biofilm inhibition study by using crystal violet assay:

The microtiter plate assay was used to optimize the conditions for biofilm production. Four human pathogenic strains were used for the study of biofilm inhibition by different phytocompounds. The experiment was performed with some modifications on pre-sterilized 96 well flat bottom polystyrene microtitre plates in triplicates as described earlier (Sharifian et al., 2020). Briefly, a 50µl of cell suspension with 0.5 OD at 600nm was inoculated in 150µl sterile BHI broth in each well. 100µl of purified metabolites (curcumin, curcuminoid and diosgenin), standard metabolites (curcumin, curcuminoid, 4 hydroxy 2 methyl acetophenone and diosgenin) and their combination (curcumin plus 4 hydroxy 2 methyl acetophenone) was added in respective wells. Then microtiter plate was incubated for 24 hrs at 37°C. Biofilms were fixed with 99% methanol after aspiration of planktonic cells. After two sterile phosphate buffer saline washes, the plates were dried. All wells were then filled with 200µl of crystal violet solution (0.1%). After 15 minutes, the extra crystal violet was removed, and the plates were washed twice and air dried. In order

to dissolve the cell-bound crystal violet, 33% acetic acid was used. Using a micro plate reader, the growth of the biofilm was observed in terms of OD 578 nm (Erba scan).

3.16 Biofilm inhibition study by scanning electron microscopy (SEM):

The effect of purified metabolites (curcumin, curcuminoid and diosgenin), standard metabolites (curcumin, curcuminoid, 4 hydroxy 2 methyl acetophenone and diosgenin) and their combination (curcumin + 4 hydroxy 2 methyl acetophenone) on biofilm inhibition was also investigated by the SEM technique. In this, a clean glass was cut into a square having dimensions 1 cm^2. They were washed in a 5% (v/v) Hiclean (Liquid soap, Hi-Media) solution for 30 minutes before being rinsed in ultrapure water to eliminate any leftover detergent. After airdrying for 30 minutes, the surfaces were immersed in 96% (v/v) ethanol for 10 minutes to eliminate any contaminants.

To prepare a sample for SEM, 2% glutaraldehyde solution was taken on slide. A test bacterial culture along with metabolites were used for the preparation of smear. The slides were kept in freezer overnight to fix the smear. On next day smear was washed with an ethanol dehydration series of 20 to 100% (v/v) (Ansari et al., 2021). The samples were then analyzed by SEM using VEGA3 TESCAN instrument.

3.17 *In silico* study:

3.17.1 Biological database

Since biological databases are an essential component of bioinformatics research, they offer structural data on macromolecules that can be used to study biological processes. Recent developments in computational technology and *in vitro* research have accelerated the development of biological databases and improved their quality. Databases can be categorized based on the types of data they contain. For example, there are several protein and peptide databases that include information on protein sequence, protein 3D structure, and protein families. These databases include Uniprot, Swiss-prot, and Protein Data Bank (PDB) (Ma L, 2015).

3.17.2 Protein Data Bank (PDB)

The ‘Protein Data Bank (PDB)’ was started in the 1970’s. Later, PDB was created by Brookhaven National Laboratory in 1971 as a global archive to store 3D

structural data of macromolecules (Berman et al., 2000). Before 1999, Brookhaven managed the PDB, but later that year a group called the Research Collaboratory of Structural Bioinformatics (RCSB PDB) took over management. The PDB contains the experimentally determined 3D structures of proteins, nucleic acids, carbohydrates, and complex assemblies (Burley et al., 2018). The PDB contains the xyz Cartesian coordinates of a macromolecule along with some additional details about the small-molecule ligands, some information about the data collection and structure refinement, and some structural descriptors (Berman et al., 2003).

3.17.3 Molecular Docking

The primary goal of a molecular docking study is to predict the structure of intramolecular complexes generated between two or more molecules (Thomsen and Christensen, 2006; Meyer and Schomburg 2008). Molecular docking is an effective technique for structure-based drug design and discovery, according to Sousa et al. (2006). The availability of more known protein crystal structures has driven interest in moleculardocking. The field of computational biology has advanced more recently. Molecular docking is a technique for predicting the preferred orientation of a receptor and ligand when they combine to create a stable complex (Lengauer and Rarey 1996). Molecular docking is a computational technique used to find possible binding conformation of ligand for interaction within binding pocket, most of docking protocols one of the partner is a protein and the other is a macromolecule such as DNA, RNA, protein, lipids and small organic molecules either natural or artificial (Ferreira et al.,2015). Depending on type of ligand different computational model with their search algorithm are required to solve the docking problem, genetic algorithm is most commonly used in many docking programs such as AutoDock, Gold is a type of stochastic algorithm apply theories of evolution and natural selection. In this study dock 6 program is used to predict binding mode and intramolecular interaction with the help of genetic algorithm and appropriate scoring function. Descriptor score, Hawkins generalized born (GB)/surface area (SA) score, and Amber score. The lowest score in each method was chosen for further examination. These algorithms were based on the Grid score in DOCK6. DOCK 6.7 was reasonably accurate and might be used to carry out additional extensive screening.

3.17.4 Molecular Dynamics (MD) simulation

Molecules are dynamic in nature this dynamic nature is essential for their functioning of protein, they exhibit variety of motion in both solution in the crystalline state (McCammon et. al.,1977). Molecular dynamics (MD) simulations are performed to investigate the structural conformation and stability of the protein and ligand bound state (Sivaramakrishnan et al., 2019). MD simulation is not only to study structure-function relationships of proteins at atomic level butalso behavior of the system in atomic detail that is the position of every atom as a function of time is computed by an algorithm that solves in an iterative fashion Newton's classical equation of motion.

$$F_i = m_i \, a_I$$

Where,

F_i- Force exerted on particle i,

m_i- Mass of particle i, and

a_i– Acceleration of particle i.

The equations are solved concurrently in small time steps. The system applies classical mechanics to describe the motion of atoms keeping temperature and pressure at defined values. These coordinates as a function of time are written to an output file at predefined time intervals and represented as the trajectory of the system to confirm the stability of the system.

3.17.5 MD simulation algorithm

There are numerous simulation algorithms that incorporate Newton's equation of motion. Among the most popular algorithms are the Verlet algorithm (Verlet, 1967) and its modification, the leap frog algorithm (Hockney, 1970), the Gear predictor-corrector algorithm (Gear et al., 1971), and the Beemann algorithm (Beemann, 1976). The reliable physical behavior of constraints is represented by bond vibrations and there are numerous algorithms are available. The SETTLE algorithm (Miyamoto and Kollman, 1992) is an analytical variant of the SHAKE algorithm, which is primarily used for small molecules. The SHAKE algorithm (Ryckaert et al., 1977) is a widely used algorithm for large molecules. Following an unconstrained update, LINear Constraint Solver (LINCS) algorithms reorder various bonds according to their exact lengths (Hess et al., 1997). Particle mesh Ewald (PME) was used to calculate long

rage Coulomb interactions between biomolecules (Essmann et al., 1995).

3.17.6 Topology generation

There are more atom types than elements, however the force field only covers atom types present in biological systems. The topology file illustrates the positions of the atoms as well as their interactions, such as bonds, angles, and dihedrals. These interactions are defined as fixed lists that are stored in the topology file (Spoel et al., 2005). Topology files are essential for nonstandard atoms, ions, and molecules. During the MD simulation, the topology file settings are applied to the atoms. As a result, additional molecular topology data are required for MD simulations of non-standard molecules such as ligands, ions, and lipids. The topology files for these non-standard molecules were included in the appropriate topology file after being directly downloaded from online servers or using AmberTools.

3.17.7 Force field (FF)

The term force field refers to the collection of variables and equations that are used to describe the characteristics of atoms and their bonded and nonbonded interactions. The potential function and parameter set for the force field are generated from either ab initio/semi-empirical quantum mechanical calculations or data from neutron electron, neutron and X-ray diffraction, Raman, NMR, and neutron spectroscopy studies (Gonzalez, 2011). The potential uses of the force field are classified into three categories: bonded, nonbonded, and restraints. The three types of bonding interactions that covalent bonds retain are bond distance, bond angle, and dihedral angles. Electrostatic and van der Waals interactions are examples of nonbonded interactions. Non-bonded potentials are described by the Lennard-Jones potential and the Coulomb interaction, according to Mackerell et al. (1998). Force fields such as AMBER (Cornell et al., 1995), CHARMM (Mackerell et al., 1998), GROMOS (Oostenbrink et al., 2004), and OPLS (Jorgensen et al., 1996) have been widely employed for biomolecule simulation over the last few years. The force field Amber ff99SBIldn was used in the present study.

3.17.8 Periodic boundary condition (PBC)

To minimise the effect of edges, periodic boundary conditions are used in finite and cubic systems (Fig. 3.1). GROMACS calculates far-off electrostatic interactions using the more precise lattice sum techniques, such as PME, Ewald Sum, and PPME (Berendsen et al., 1995; Darden et al., 1993). During the simulation, every direction of an atom in a PBC's primary cell is repeated. According to Bernendsen et al. (1995), an image cell that resembles an atom in terms of size, number, shape, location, and momentum is said to form an infinite lattice. It is simpler to compute the interactions between two given atoms when you have a graphic that illustrates the shortest path between them. Therefore, molecules act as an infinite system and are unrestricted in their movement inside the box (Hansson et al., 2002; Van der Spoel et al., 2005). MD simulation software provides numerous shapes of boxes but frequently used are cubic box.

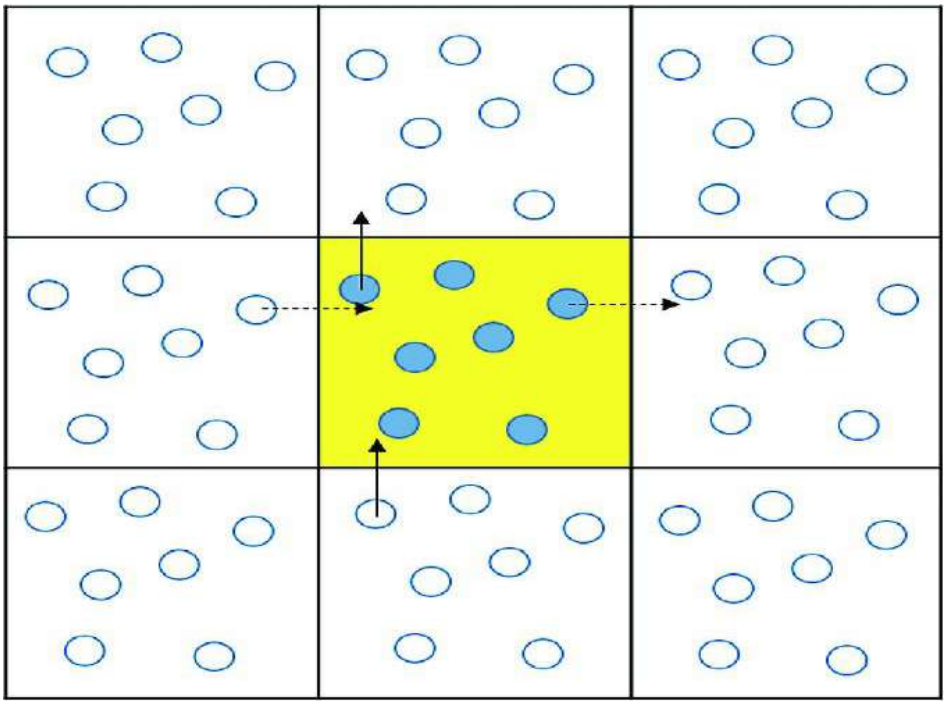

Fig. 3.1: Schematic representation of the idea of periodic boundary conditions. A particle which goes out from the simulation box by one side is reintroduced in the box by the opposite side. (Available from: https://www.researchgate.net/figure/Two-dimensional-representation-of-periodic-boundary-condition-The-central-cell-filled_fig3_322868494)

3.17.9 Thermodynamic ensembles and water model

A collection of all possible systems with a large variety of microscopic states and highly comparable thermodynamic states is called an ensemble. A system's thermodynamic state is composed of a small set of parameters known as thermodynamic ensembles (Brooks, 1995). Temperature (T), volume (V), pressure (P), energy (E), number of particles (N), and pressure (P) are some of these factors. Numerous configurations of thermodynamic ensembles exist, such as isothermal-isobaric (Gibbs) ensemble (NPT), microcanonical (NVE), and canonical ensembles (NVT) (Hunenberger 2005). An isothermal-isobaric, constant pressure and temperature (NPT) ensemble is frequently used to simulate macromolecules because it precisely resembles experimental circumstances. The number of molecules, pressure, and temperature are constant in this ensemble. As a result, it is critical to ensure that the temperature and pressure remain stable throughout the MD simulation time (Evans and Morriss 1983, Eslami and Plathe-Muller 2007).

Water is regarded as the most important solvent in nature. To explore a variety of perceptions, such as solvent dynamic behavior at protein surfaces and solvent effect related to biomolecule structural behavior, biomolecules are dissolved in water in the MD simulation (Marechal 2004, Fornili et al., 2012). The models TIP3-P (Transferable Intermolecular Potential 3-Point), TIP4-P (Transferable Interatomic Potential-4 Point) (Jorgensen et al., 1983), SPC (Simple Point Charge) (Berendsen et al., 1981), SPC/E (Extended Simple Point Charge) (Berendsen et al., 2005) were created for molecular simulations of water. These models feature three basically identical interaction fields with different Lennard-Jones (LJ) and Coulombic parameters in an attempt to replicate the bulk properties of water as shown in tests (Mark and Nilsson, 2001). Choice of water model depends on the nature of system and force field.

3.17.10 Energy minimization

Optimal molecule geometry can be obtained by minimizing energy by changing atomic potions in the molecule. In order to eliminate bad contacts, energy minimization can be used during system setup for MD simulation. The steepest-descent (SD) minimization method locates minima on the molecular potential energy surface using a first order derivative scheme (Wiberg 1965; van der Sopel et al., 2005). The steepest-descent approach uses the first order derivative to calculate the direction towards the

minimum, and this direction is always the inverse of the direction in which the gradient is steepest at the initial point. When the structure is far from the minimal configuration, the robust SD method is used to minimize the initial configuration. Energy minimization aims to relax the system by removing steric clashes. Energy minimization can also be done using the Newton-Raphson and conjugate-gradient methods, respectively. In order to find the best direction, the conjugate gradient method uses line search from the first derivative. As opposed to this, the Newton-Raphson method uses the second order derivative and the Hessian matrix to describe the curvature of the function (Hestenes and Eduard, 1952; Leach, 2001).

3.17.11 Binding energy calculation

MM-PBSA and MM-GBSA methods generally used to calculate binding energy between protein ligand complexes (Kumari et al., 2014), which is based on molecular mechanics Poisson−Boltzmann surface area (MM-PBSA) and Generalized Born/surface area (MM-GBSA) mostly used for calculation of interaction energy in biomolecule complexes.

Interaction free energy represent in equation as follows

$$\Delta G_{binding} = \Delta E_{MM} + \Delta G_{Solv}$$

Where, $G_{binding}$ is total binding energy of system

$$\Delta E_{MM} = E_{bonded} + E_{non}bonded = E_{bonded} + (\Delta G_{vdw} + \Delta G_{elec})$$

ΔG_{MM} is mean molecular mechanics includes van der waals interactions (ΔG_{vdw}) and electrostatic energies (ΔG_{elec})

$$\Delta G_{Solv} = \Delta G_{nps} + \Delta G_{ps}$$

ΔG_{Solv} is solvation energy includes both polar solvation energy (ΔG_{ps}) and non-polar solvationenergy (ΔG_{nps}).

3.17.12 MD simulation and analysis software

Various software used for performing molecular dynamic simulation. These are freelyand routinely used from GROMACS 2021.5 package. Commercial softwares such as AMBER and CHARMM are also used. Molecular visualization software used to visualize MD trajectories and molecules are Chimera, Rasmol, VMD, and PyMol.

3.18 Statistical analysis:

The obtained data were analyzed by one way Analysis of Variance (ANOVA). Values in figures and tables represent the arithmetic mean of the three replicates. Graph-pad prism software used for data analysis.

CHAPTER IV

RESULTS AND DISCUSSION

4.1 Screening, isolation and identification of plant growth promoting rhizobacteria

The part of this study published as:

YMER || ISSN : 0044-0477 http://ymerdigital.com

ISOLATION, CHARACTERIZATION AND IDENTIFICATION OF POTENT PLANT GROWTH PROMOTING RHIZOBACTERIA FROM *ASPARAGUS RACEMOSUS*

Ruddhi. R. Jagtap[1], Gajanan. V. Mali*[3,4], Kailas. D. Sonawane[1,2]

[1]Department of Microbiology, Shivaji University, Kolhapur (416004), Maharashtra, India.

[2]Department of Biochemistry, Shivaji University, Kolhapur (416004), Maharashtra, India

[3]Rayat Institute of Research and Development, Satara (415001), Maharashtra, India.

[4]Department of Microbiology, Bharati Vidyapeeth Deemed to be University, Yashwantrao Mohite College, Pune (411038), Maharashtra, India.

4.1.1 Introduction:

There are numerous types of microorganisms present in the soil, including bacteria, fungus, actinomycetes, and algae, which help to improve the soil's general quality and health. A source of microbial activity can be found in the rhizosphere, which receives nutrition from root secretions. Moreover, isolates from several genera, including *Bacillus, Serratia, Azospirillum, Pseudomonas, Clostridium, Azotobacter, Enterobacter,* and *Arthobacter,* have been demonstrated to possess PGPR properties (Kumar et al., 2014; Kloepper and Beauchamp, 1992). There are numerous ways that PGPR can directly and indirectly increase plant productivity. The direct mechanism involved the capability to fix nitrogen, synthesis of siderophores and phytohormones, solubilization of phosphate, and the biological regulation of diseased plants (Maougal et al., 2021). Plant- associated bacteria may provide an indirect benefit to plants by deterring the progress or interaction of plant pathogenic organisms through various mechanisms (such as rivalries for nutrition and space, antibiosis, formation of hydrolytic enzymes, and suppression of pathogen produced enzymes or toxins).

Plant-associated bacteria may induce plant defence mechanisms, which may also benefit plants (Laslo et al., 2012). PGPR, interact with plants and other microbes that can be either antagonistic or synergistic (Chauhan et al., 2021). PGPRs are useful to plants, as they arealso essential for maintaining the balance of the ecosystem. In recent years, PGPR has been extremely prevalently used as soil inoculants in environmentally friendly agriculture because they have a smaller negative influence on the surrounding environment and produced the highest possible crop yield (Kumar et al., 2016). According to Parveen et al, (2018) PGPR is aconstituent of the defensive microflora. They are beneficial to plants because they improve rootactivities, prevent disease, and speed up growth and development (Parveen et al., 2018). PGPRalso can potentially break down pesticides like endosulfan (Rani et al., 2021). In addition to this, they have antifungal properties (Kavitha et al., 2012). According to reports, they play a significant part in the production of secondary metabolites in plants (Kabera et al., 2014). Theeffects of PGPR on the phytoconstituents of medicinal plants are also documented (Egamberdieva and Teixeira, 2015).

Native medicinal shrubs of the genus Asparagus are members of the family Liliaceae and are valued for the therapeutic benefits of their stems, leaves, and roots. Around the globe,around 300 different species belong to the genus Asparagus (Negi et al.,

2010). Shatavari is thegeneric term for the plant that bears the scientific name *Asparagus racemosus* willd. This planthas a long history of usage as a female reproductive tonic because of its ability to protect the health of mothers and the developing fetus and stimulate increased lactation in breastfeeding women (Mfengwana and Mashele, 2020). *Asparagus racemosus* wild possesses curative properties that can be applied to treat a diverse range of diseases. According to the Ayurvedic literature (the database of Indian traditional remedies), it is a potent substance that can boost memory and intelligence and retain physical vigor and vitality. Additionally, the plant can be used as a demulcent to cure dyspepsia as well as a number of skin problems, wounds, and otherconditions (Patil, 2020). According to Sharafzadeh and Ordookhani (2011), the total phenol and flavonoid content was highest in plants grown in organic manure-treated soil, compost, and vermicompost-without using mineral or chemical fertilizer (Sharafzadeh and Ordookhani, 2011). According to research by Lastra et al, (2021), PGPR can inhibit fungal infections that reduce Asparagus productivity.

The current investigation demonstrates that inoculation of PGPR is an important agricultural approach that plays a significant role in protecting crops and promoting plant development in control of the diseases. As these isolates can tolerate high salt concentrations,they can be used as a biofertilizer in saline soil. They provide an option in place of conventionalagricultural practices that rely on synthetic fertilizers, antibiotics, herbicides and insecticides.

4.1.2. Material and method:

4.1.2.1 Isolation of PGPR from soil

Samples of soil (*A. racemosus* rhizospheric area) were collected from different locations in the districts of Kolhapur and Satara. To isolate PGPR, 100 ml of sterile nutrient broth was enriched with 1 gm of soil in a separate 250 ml Erlenmeyer flask. These flasks were continuously shaken at 30°C (at 120 rpm) for 24 hours. Following that, a 0.1 ml aliquot of a 10^{-5} to 10^{-8} dilution was spread on a sterile nutrient agar plate and incubated at 30°C for 24 hours.

4.1.2.2 Screening for Plant Growth-Promoting Activities:

4.1.2.3 Phosphate Solubilization

To assess their phosphate solubilization potential, all bacterial isolates were

streaked on Pikovskaya's agar plates and plates were incubated at 30°C for 48 hrs (Pikovskaya, 1948). After incubation, the transparent zone around the growth suggested that inorganic phosphate had been solubilized. Bacteria growing in Pikovskaya's broth were quantified, with a sterile uninoculated medium serving as a control. After 48 hours, the culture was collected by centrifuging it at 6000 rpm for 15 minutes to assess how much soluble phosphate was present in the supernatant (Fiske and Subbarow, 1925). Using the KH_2PO_4 standard curve, the amount of soluble phosphate was calculated.

4.1.2.4 Potassium solubilization

Potassium solubilizing isolates were inoculated in a modified Alexandrov's medium (Glucose- 0.5 gm, Magnesium sulfate- 0.05 gm, Ferric chloride- 0.005 gm, Calcium carbonate- 0.01 gm, Tricalcium phosphate- 0.2 gm, Potassium aluminosilicate- 0.2 gm, agar 1.5-2.0 gm, Double distilled water100 ml). The test organisms were seeded on the media and incubated for 48-72 hours at 28˚C. The colony's color variation and the diameter of the zone around it were both measured (Mahadevamurthy et al., 2016).

4.1.2.5 Zinc solubilization

To investigate the solubility of zinc, the isolates were spot-inoculated into an agar medium that included 0.1% of insoluble zinc compounds, like ZnO. Plates containing test microorganisms were incubated at 30°C for 48 hours. Further, the zone of clearance around the colonies were measured (Shakeel et al., 2015).

4.1.2.6 Production of indole-3-acetic acid (IAA)

Culturing the PGPR in yeast extract-mannitol-mineral salts broth enriched with various concentrations of tryptophan, at 28±1°C with constant shaking and it was used to quantify IAA production. Further, 5 ml of cultures were centrifuged at 10,000 rpm for 15 minutes at 4°C after 48 hours, and the supernatant was extracted (Brick et al., 1991). Two drops of orthophosphoricacid and 4 ml of Salkowski reagent (50 ml, 35% of perchloric acid, 1 ml 0.5 M $FeCl_3$ solution) were added to the supernatant (2 ml). IAA production is signified by the appearance of the cherry red color. A UV–Vis spectrophotometer was used to assess color at 540 nm. The concentration of IAA

was determined from a standard curve of IAA (50–300 µg/ml).

4.1.2.7 Ammonia Production

An actively growing PGPR culture was added in 30 ml of 4% peptone water. The entire set was then placed in an incubator at 30℃ for 48 hours. Following the completion of the bacterial growth, 0.3 ml of Nessler's reagent was added to each flask. The presence of a color range from brown to yellow indicates a successful ammonia production assay (Cappuccino and Sherman, 1992).

4.1.2.8 Siderophore Production

The chrome azurol S agar (CAS) was used to test the siderophore synthesis of isolates(Louden et al., 2011). All isolates were inoculated on chrome azurol S agar plates and incubated for 48 to 72 hrs at 30°C. After incubation, the emergence of a yellow-to-orange halo zone around the colony was considered positive for siderophore production

4.1.2.9 Hydrogen Cyanide Production

Using King's B medium, the isolates were tested for cyanide formation (King and Weinhold, 1995). Each bacterial isolate was placed on King's B agar plates amended with 1% glycine. The Petri plates were covered in parafilm and incubated at 30°C with a cover made of filter paper that had been moistened with a few drops of 10% NaCO3 and 1% picric acid (Lorck, 1948). Control plates without inoculation have been prepared. A change from yellow to brown filter paper was predicted to facilitate the production of HCN.

4.1.2.10 Exopolysaccharide Production

According to Nicolaus and team (1999), the exopolysaccharides production by isolates was evaluated qualitatively (Nicolaus et al., 1999). For that, bacterial strains were cultivated in 250 ml Erlenmeyer flasks containing 100 ml medium supplemented with Yeast extract- 1gm, Casamino acids- 0.75gm, Trisodium citrate- 0.3gm, KCl- 0.2gm, $MgSO_4.7H_2O$- 2 gm, $MnCl_2.4H_2O$- 0.036 mg, $FeSO_4.7H_2O$- 5 gm at 30°C for 48 hrs under shaking conditions at 120 rpm. After incubation the supernatant was extracted by centrifuging for 15 minutes at 4°C at 8000 rpm. The development of a precipitate was deemed positive for the synthesis of exopolysaccharidesafter adding

cold 100% ethanol dropwise under agitation.

4.1.2.11 Salt tolerance

To test for inherent resistance to salt stress, the isolated plant growth-promoting bacteria were used. The isolates were grown up for this purpose in flasks containing a nutrient broth supplemented with varying NaCl (1-7%) concentrations. Growth in NaCl-supplemented media was observed after the flasks had been incubated at 30°C for 48 hours (Bhise and Dandge, 2019).

4.1.2.12 Biochemical Characterization and Identification of isolates

A carbohydrate utilization test kit (KB 009, Hi-Media) was used to assess the PGPR's capacity to consume different types of carbohydrates, and 16S rRNA gene sequence analysis was used to identify the isolates showing the highest PGPR performance. The evolutionary history was ascertained by utilizing the neighbor-joining method and evolutionary analysis was conducted using MEGA X (Tamura et al., 2021). The partial 16S rRNA gene sequences were deposited into the GenBank database with accession numbers **OL771442** and **OL656822**.

4.1.2.13 Statistical analysis

The data is presented as means ± standard deviation (SD) for each of the three replicates. The data were analyzed by analysis of variance (ANOVA) utilizing the graph pad software in compliance with the Tukey comparison test ($p < 0.05$).

4.1.3. Results and Discussion:

4.1.3.1 Isolation of rhizobacterial strains PGPR

PGPR strains were isolated from soil attached to Asparagus roots employing the culture-dependent standard plate method. 20 rhizobacterial isolates were chosen based ondistinct colony morphologies and biochemical assays. Two PGPR isolates (Asp-A and Asp-B) with the highest plant growth promotion activity were preferred for physiological and biochemical investigation among the 20 isolates. Earlier studies also showed that plant symbiosis with rhizospheric microorganisms is an essential and critical component of environmentally friendly and efficient agriculture systems. Many bacteria found in the rhizosphere help plants thrives (Santoyo et al., 2021).

4.1.3.2 Phosphate solubilization

Phosphate solubilization was tested on all isolates. In Pikovskaya's agar plates, six isolates displayed a distinct zone, but the diameter of the zone was significant in Asp-A and Asp-B isolates. In a continuous culture medium, quantitative phosphate solubilization was carried out for 48 hrs. After 48 hours of incubation, Asp-A and Asp-B had the highest phosphate solubilization of 84.24 ±0.01 and 86.16 ±0.02 µg/ml. Data are shown as mean ± SD of three replicates (Table 4.1.1 Fig. 4.1.1, 4.1.2).

Hence, we observed that both PGPR strains, *Exiguobacterium acetylicum* strain RGK and *Enterobacter mori* strain RGK1, had an ability for P-solubilization. Phosphorus (P) is the second most important macronutrient after nitrogen (N), and it plays a significant function in plant growth and productivity. Due to insoluble forms of phosphorus, even in phosphorus-richsoil, the majority of the P is inaccessible to plants (Meena et al., 2015). *Pseudomonas, Enterobacter, Bacillus,* and endosymbiotic *Rhizobium* strains have been found to be highly efficient P- solubilizers in soil microbial flora.

Table 4.1.1: Solubilization of Phosphate and IAA production by *Exiguobacterium acetylicum* RGK (Asp-A) and *Enterobacter mori* RGK1 (Asp-B) after 48hrs. Data are shownas mean ± SD of three replicates.

Organism names	Solubilization of Phosphate µg/ml	IAA Production in µg/ml
Asp-A	84.24 ±0.01	90.11 ±0.1
Asp-B	86.16 ±0.02	253.45 ±0.01
Asp-C	31.35 ±0.01	8.45 ±0.02
Asp-D	24.30 ±0.03	33.45 ±0.01
Asp-E	25.90 ±0.01	6.55 ±0.03
Asp-F	31.67 ±0.02	38.45 ±0.02

Fig. 4.1.1: Solubilization of Phosphate on Pikovskaya's agar after 48 hrs where A) *Exiguobacterium acetylicum* RGK B) *Enterobacter mori* RGK1

4.1.3.3 Potassium and Zinc solubilization

Potassium releasing capacity was found in Asp-A and Asp-B isolates. The colour of the pH indicator changes as potassium was solubilized, and the resulting solubilization zone was recorded. After 72 hours of incubation at 28±2˚C, a range of diameter zone 20 mm to 30 mm was noted. The zinc solubilizing isolates were examined for effectiveness on TRIS minimal medium enriched with zinc source ZnO. The maximal solubilization zone of Asp-A was 18 mm where Asp-B was 22 mm in size. As a result, both isolates were capable of solubilizing potassium and zinc data presented in (Fig. 4.1.3, Table 4.1.2).

Earlier studies showed that *Burkholderia, Bacillus spp., Enterobacter spp., Paenibacillus mucilaginosus,* and other rhizospheric bacteria have been described as K-solubilizers and have a great capacity for mobilizing and solubilizing K from minerals (Meenaet al., 2016). According to Singh et al. (1998), increasing potassium application rates had a favorable and significant influence on fresh rhizome output (Singh et al., 1998). Similarly, zinc plays several dynamic roles in plants as crop growth, maturity, vigor, yield, and many physiological functions (Singh et al., 2020). Inoculating plants with various PGPR has resulted in improved growth and zinc content. This includes different strains of PGPR such as *Pseudomonas, Rhizobium, Bacillus, Azospirillum* (Kamran et al., 2017). Our results also showed that both the strains have ability to solubilize potassium and zinc.

4.1.3.4 Production of indole-3-acetic acid (IAA)

Rhizobacterial strains were examined for IAA quantification in tryptophan levels of 25, 50, 150, 200 and 250 µg/ml concentrations. The colorimetric investigations revealed that distinctive PGPR isolates differed substantially in their ability to produce IAA in the broth; isolates Asp-A and Asp-B produced the maximum IAA (Table 4.1.1, Fig. 4.1.2). Earlier study by Ghosh et al (2013) reported that increasing L-tryptophan concentration increased symbiotic growth and IAA production (Ghosh et al., 2013). IAA play a critical role in controlling plant development and growth. In many herbaceous plants, PGPR producing IAA in the rhizospheric soil is crucial for increasing the number of root tips and root surface area (Han et al., 2005).

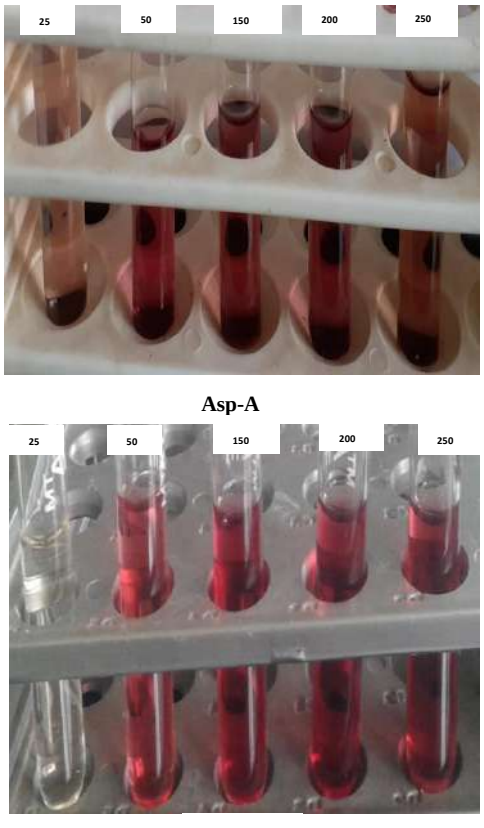

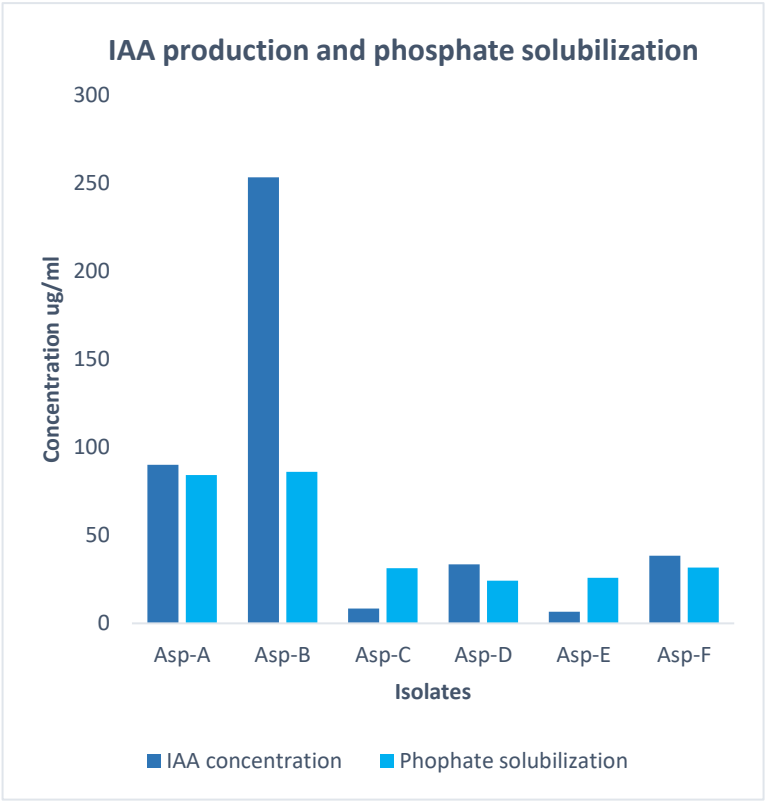

Fig. 4.1.2: A-Production of IAA (Qualitative), B- Production of IAA and solubilization of phosphate (Quantitative) after 48 hrs.

Table 4.1.2: Solubilization of Potassium and Zinc, Exopolysaccharide synthesis by *Exiguobacterium acetylicum* RGK (Asp-A) and *Enterobacter mori* RGK1(Asp-B) after 48hrs

Organism names	Exopolysaccharide production	Solubilization of Potassium	Solubilization of Zinc
Asp-A	+	+	+
Asp-B	+	+	+
Asp-C	+	-	-
Asp-D	-	-	-
Asp-E	-	+	-
Asp-F	-	-	-

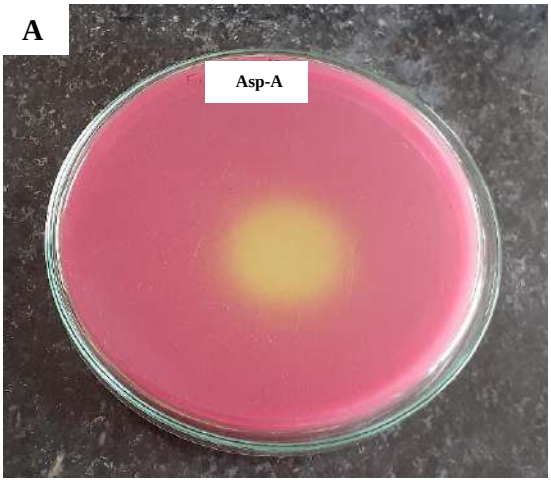

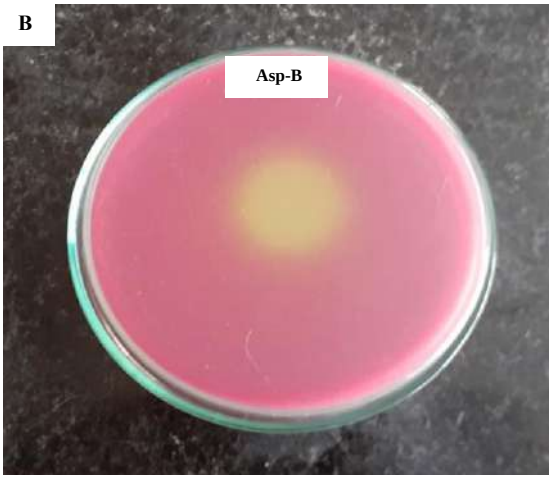

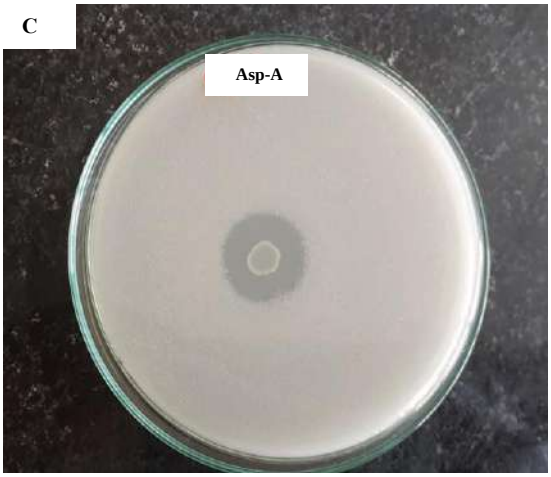

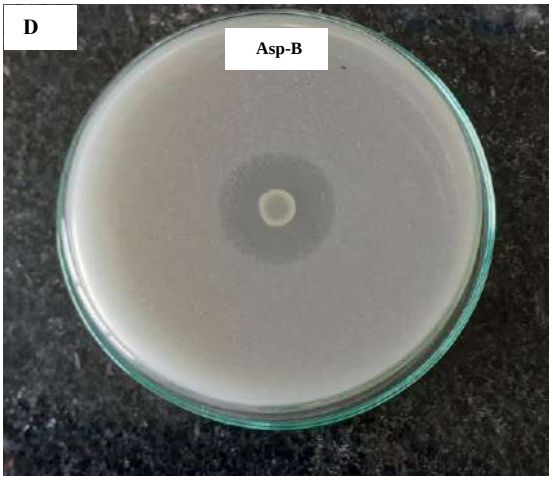

Fig. 4.1.3: A, B are solubilization of Potassium on modified Aleksandrov's k medium by *Exiguobacterium acetylicum* RGK (Asp-A) and *Enterobacter mori* RGK1(Asp-B) and C, D are Zinc solubilization by Asp-A and Asp-B after 72 hrs of incubation.

4.1.3.5 Siderophore, Ammonia, and Hydrogen Cyanide Production

Among the six isolates Asp-A and Asp-B can produce ammonia, hydrogen cyanide and siderophore on CAS agar medium, as illustrated in Fig. 4.1.4. Iron is one of the crucial elements for plant and microorganism development and appropriate functioning. Siderophore-producing isolates can improve plant growth by increasing iron availability to plants while decreasing iron availability to pathogenic fungi (Ahmad et al., 2008). Numerous studies have shown the critical function that bacterial strains that produce siderophores play in both biocontrol and growth promotion (Kumar et al., 2016a). Venkat et al. (2017) found that isolates of *Bacillus* and *Enterobacter* from soil that had been iron-enriched were good candidates to synthesize siderophores (Venkat et al., 2017).

PGPR converted organic nitrogen residues into soil organic matter, such as ammonia nitrifiers. Through ammonification, this PGPR releases ammonia (Geisselera et al., 2010). Similarly, hydrogen cyanide is a secondary metabolite that can be used to manage weeds biologically. The ability of HCN to block essential metalloenzymes, such as cytochrome c oxidase, impacts its toxicity (Alori and Babalola, 2018). In the current study, both PGPR isolates can synthesize siderophore, ammonia, and hydrogen cyanide.

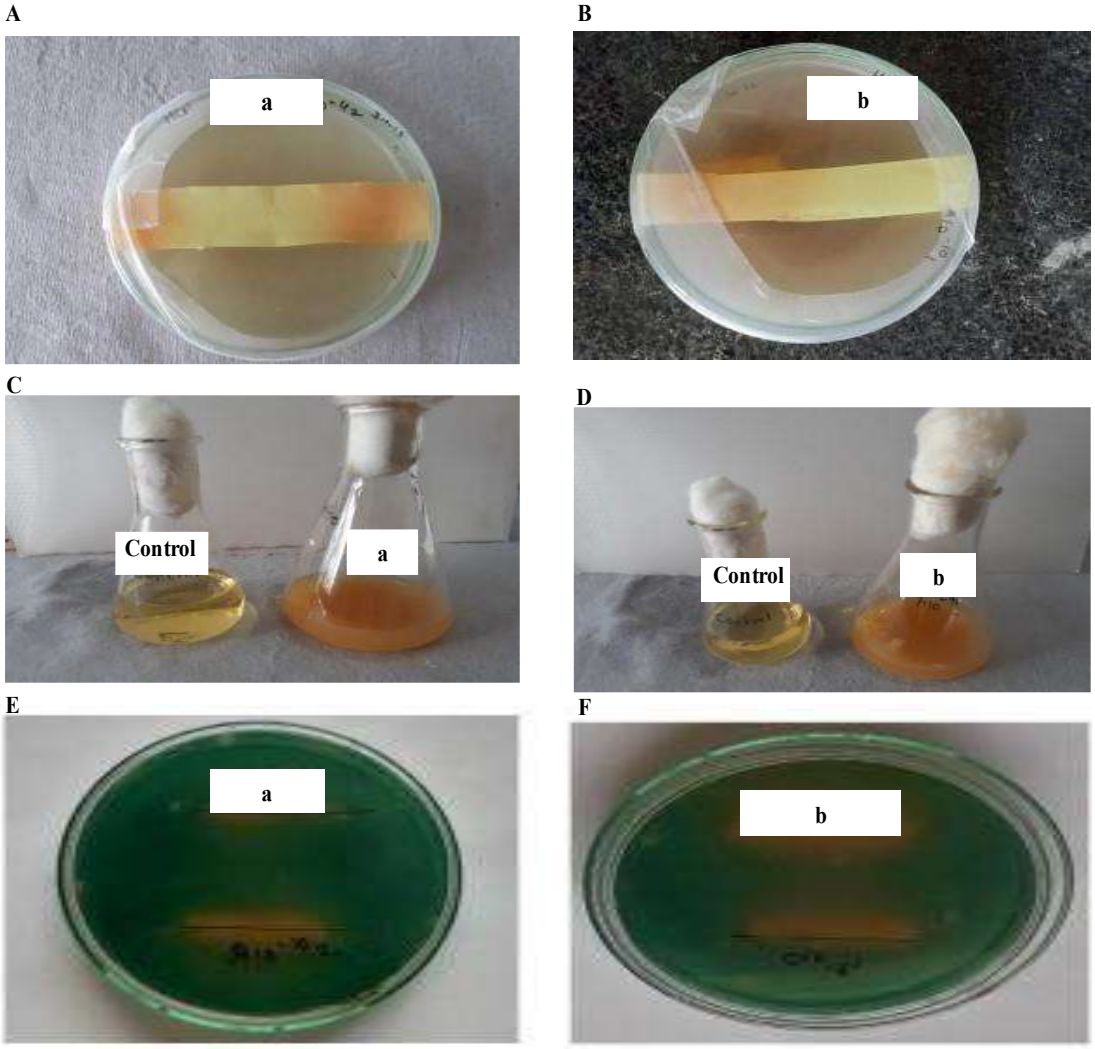

Fig. 4.1.4: A, B are HCN production, C, D are Ammonia production and E, F are Siderophore production by *E. acetylicum* RGK (a) and *E. mori* RGK1(b) respectively after 48 hrs of incubation.

4.1.3.6 Exopolysaccharide Production and Salt tolerance

After 72 hours, isolates were able to produce exopolysaccharides in the minimal medium. Asp-A and Asp-B were two of the six isolates that produced exopolysaccharides. Datarepresents in (Table 4.1.2). Earlier reports revealed that, exopolysaccharides generated by PGPR have been proven to impact plant growth and drought tolerance significantly. Exopolysaccharides have important roles in microbial aggregation, surface adhesion, desiccation resistance, plant-microbe interaction, and bioremediation (Khan and Bano, 2019).

In the presence of NaCl, six out of twenty bacteria showed a 3 % salt tolerance

capacity. Asp-A, on the other hand, could withstand up to a 5% salt concentration, whereas Asp-B could tolerate up to a 6% salt concentration. The trend indicates that these PGPR grows in high salt concentrations or high ionic strength environments and may provide salt tolerance to the host. Salt tolerance by endophytic plant growth promoting bacteria also reported by (Heydarian et al., 2018). Treatments with salt-tolerant PGPR like *B. pumilus* and *E. oxidotolerans* can be an effective approach in increasing biomass production and saponin levels in medicinal plants like *B. monnieri*, reported by (Bharti et al., 2013)

4.1.3.7 Biochemical Characterization and Identification of isolates

The most efficient plant growth-promoting rhizobacterial isolates were Asp-A (*E. acetylicum* RGK) and Asp-B (*E. mori* RGK1) (Table 4.1.3) summarizes the biochemical profile of the isolates. 16S rRNA sequencing analysis identified the isolates as *E. acetylicum* RGK and *E. mori* RGK1**.** (Fig. 4.1.5) shows the evolutionary tree of both the organisms.

Table 4.1.3: Biochemical characters of *Exiguobacterium acetylicum* RGK (Asp-A) and *Enterobacter mori* RGK1(Asp-B).

Biochemical activity	***Exiguobacterium acetylicum* RGK**	***Enterobacter mori* RGK1**
Gram nature	Gram positive	Gram negative
Glucose	+	+
Sucrose	+	+
Fructose	+	-
Maltose	+	-
Lactose	-	-
Starch utilization	-	-
Catalase	+	-
Gelatin hydrolysis	+	-
Raffinose utilization	-	+
Nitrate reduction	-	-

Citrate utilization	+	-
Urease	+	-
Oxidase	+	-
Salinity tolerance	5	6

+ present, - absent

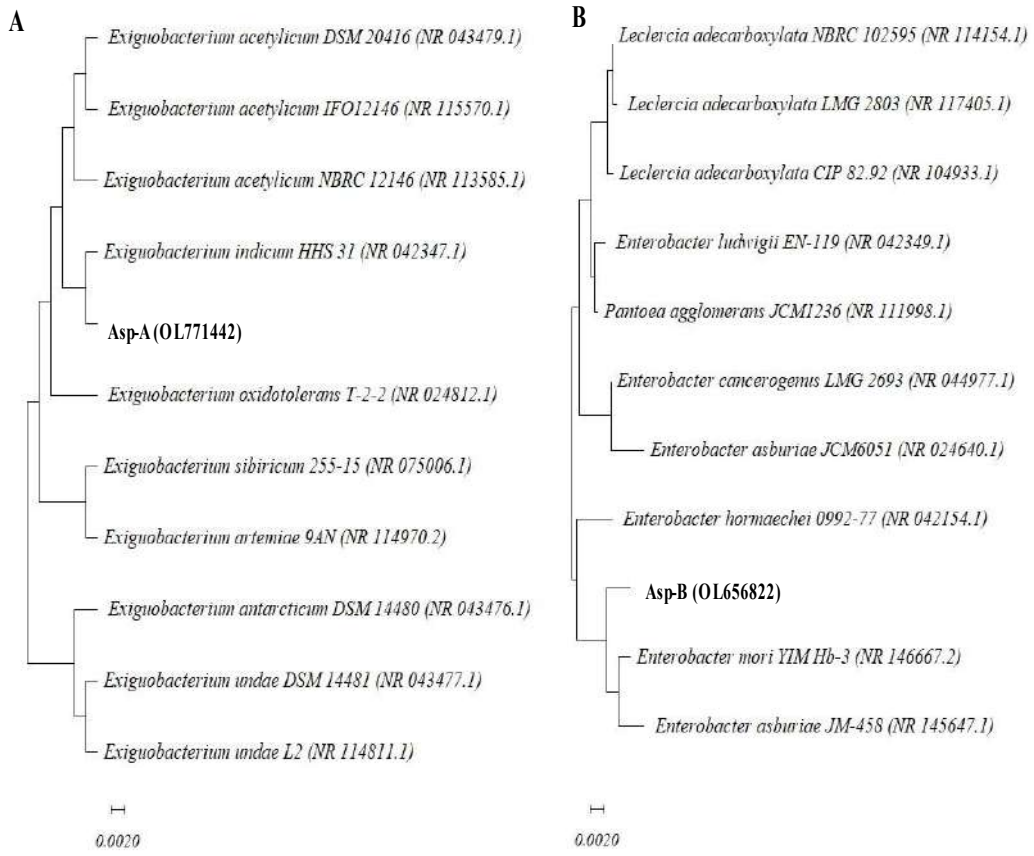

Fig. 4.1.5: Neighbor-joining phylogenetic tree based on16S rRNA gene sequence of the closely related isolates of (A) *Exiguobacterium acetylicum* RGK (B) *Enterobacter mori* RGK1, bootstrap values on each branch point indicates 1000 pseudo replicates.

4.1.4. Conclusions:

The current study involved the screening, isolation, and characterization of PGPR from the Asparagus plant's rhizosphere. By using the 16s rRNA method, the isolates were identified as *Exiguobacterium acetylicum* strain RGK and *Enterobacter mori* strain RGK1. The results of this study showed that the bacteria *Exiguobacterium acetylicum* RGK and *Enterobacter mori* RGK1 possess a variety of traits that aid in plant growth, such as the ability to solubilize phosphate, zinc and potassium, produce auxin, HCN, and ammonia, synthesize siderophores, and have a high tolerance to salt. The PGPR are appealing as biofertilizers and biopesticides as well as a cost-effective solution to sustainable agriculture. PGPR protects plants from phytopathogens and helps them grow and perform better. Although chemical fertilizers and pesticides are useful and practical for managing diseases and producing plants, they are hazardous to the environment, soil, plants, and human health. As a result, using these PGPR isolates as an inoculant can promote plant development. In conclusion, these PGPR could also be used as a biofertilizer in the future.

4.2 Impact of plant growth promoting rhizobacteria *Exiguobacterium acetylicum* RGK and *Enterobacter mori* RGK1 on secondary metabolites of *Asparagus racemosus*

Manuscript under preparation:

4.2.1 Introduction:

A significant variety of bacterial species have been investigated and proved to be advantageous to crop quality, plant growth, and yield, largely from the plant rhizosphere. These bacteria are referred to as Plant growth promoting rhizobacteria (PGPR) (Adnezhad et al., 2016). Rhizospheric bacteria that promote plant growth, including associative and symbiotic bacteria such as *Azotobacter* sp., *Alcaligenes* sp., *Azospirillum* sp., *Arthrobacter* sp., *Pseudomonas*sp., *Burkholderia* sp., *Klebsiella* sp., *Enterobacter* sp., and *Rhizobium* sp. (Mitra et al., 2016). Furthermore, some rhizospheric bacteria can induce plant growth by synthesizing plant growth promoting compounds like plant hormones or accelerating the uptake of specific nutrients from the environment like phosphorus, potassium, or nitrogen, which may help the plant fight pathogens (Lastra et al., 2021). They are also involved in a variety of key ecosystem processes (Adnezhad et al., 2016). PGPR has also proven to be an effective in addressing salinity and drought. The soil structure is altered by PGPR, which includes the growth of bacteria like *Azospirillum, Bacillus* sp., and *Pseudomonas*, as well as the production of EPS, which accumulates qualities that aid in the easy absorption of minerals and water (Kumar et al., 2022).

Asparagus racemosus is a member of the Asparagaceae family, often known as Shatavari. It is a woody climber that can reach heights of 1-2 metres. It is a popular herb in conventional medicine since steroidal saponins and sapogenins can be detected in many parts of the plant. (Jediya et al. 2022). The root of *A. racemosus* has numerous medicinal characteristics, according to the research of ancient classical Ayurvedic literature, and has been specifically indicated in situations of imminent abortion and as a galactagogue (Alok et al., 2013). It also has nutritive, anti-stress, antioxidant, antiulcer, antidiabetic, adaptogenic, anabolic, and immunomodulatory properties andis used in a variety of medicinal preparations have been reported (Sairam et al., 2003).

Asparagus is associated with several types of PGPR, which affect plant development directly or indirectly. The findings of various researchers demonstrated the ability of PGPR to actas a positive regulator. Under water-stressed conditions, seeds treated with PGPR produced excellent results in a variety of crop plants, including chickpea, maize, and asparagus (Umair et al., 2018). Similarly, *B. subtilis* PMB-034 was effective in controlling Fusarium wilt of asparagus bean and promoting crop growth (Ha et al., 2008). In addition to that vermicompost, have been shown to improve plant growth,

yields and germination, in greenhouse crops reported by Edwardsand Burrows, (1988).

The current study aimed to isolate and characterize potent PGPR from the Asparagus plant's rhizosphere, as well as to investigate the effects of their treatment on the growth parameters and biochemical content of Asparagus, both individually and in co-culture.

4.2.2 Materials and method:

4.2.2.1 Materials

Chemicals and solvents of the analytical grade were bought from Hi Media Laboratories in Mumbai, India. A standard diosgenin sample (20-100µg/ml) was prepared in methanol. Then, it was filtered using a 0.2 m Millipore filter that was obtained from Sigma Aldrich (Bangalore, India) to get rid of contaminants. For the pot culture experiments, 2 months old planlets of Asparagus were obtained from agriculture field at Sarud, Dist. Kolhapur, Maharashtra, India.

4.2.2.2 Screening and identification of PGPR

4.2.2.2.1 Sample collection and Screening of PGPR

For the current study, 20 soil samples were collected from Asparagus rhizospheres in Kolhapur and Satara districts of Maharashtra. The samples were brought to the lab for PGPR isolation in sterile polypropylene bags. For the purpose of enrichment, 100 ml of sterile nutrient broth were added to Erlenmeyer flasks containing 1 gm of soil from each sample. The flasks were then shaken at 120 rpm for 24 hrs at room temperature (27°C±2). In order to produce well-isolated colonies, the enriched samples were serially diluted in sterile distilled water. Then, 0.1 ml of each dilution was spread on sterile nutrient agar plates, and the plates were incubated for 24 hours at room temperature (27°C±2). After incubation well isolated colonies were obtained. To get pure cultures well isolated and pigmented colonies were selected and streaked over the same media. All bacterial isolates were stored at 4°C and phenotypic characterization was performed by examining their morphological, cultural, and biochemical properties according to Bergey's Manual of Determinative Bacteriology (Holt et al., 1994; Ahmad et al., 2008; Santoyo et al., 2021). The 16SrRNA gene sequence analysis was used to confirm the identification.

4.2.2.2.2 Genotypic identification of PGPR

The standard phenol/chloroform extraction procedure was used to extract the genomic DNA of potent PGPR, and universal primers 16F27 [5'-

CCAGAGTTTGATCMTGGCTCA G-3'] and 16R1492 [5'-TACGGYTACCTTGTTACGACTT-3'] were used for amplification of the 16S rRNA genes. After the amplification 16S rRNA gene, PCR products were purified using PEG-NaCl precipitation, and they were sequentially sequenced using an ABI®3730XL automated DNA sequencer (Applied Biosystems, Inc., Foster City, CA) in accordance with the manufacturer's instructions. The Lasergene package was used for assembly, and the EzBioCloud database was used for identification (Yoon et al., 2017). The obtained sequences were processed and searched using the Nucleotide Basic Local Alignment Search Tool (BLAST) programme to determine which sequences matched the results at the National Centre for Biotechnology Information (NCBI) BLAST server. (www.ncbi.nlm.nih.gov/BLAST). Multiple sequence alignment was performed using CLUSTALW software (Thompson et al., 1997) on the sequences that showed >98% resemblance. The phylogenetic tree was built using Mega X software(Tamura et al., 2021).

4.2.2.2.3 Plant growth promoting attributes of isolates

Bacterial isolates were examined for the growth promoting attributes such phosphate solubilization (Pikovskaya, 1948), zinc solubilization (Shakeel et al., 2015), Indole acetic acid (IAA) production (Bric et al., 1991), potassium solubilization (Mahadevamurthy et al., 2016), nitrogen fixation (Dashti et al., 1998), siderophore production (Louden et al., 2011), hydrogen cyanide (HCN) production (King and Weinhold, 1995), ammonia production (Cappuccino and Sherman, 1992), exopolysaccharide production (Nicolaus et al., 1999). Enzyme production in the isolates, including those of amylase, cellulase, and chitinase, was also examined. The ability of isolates to tolerate salt was tested using various NaCl concentrations (Tirry et al., 2021).

4.2.2.3 Antibiotic sensitivity test

Antibiotic impregnated paper disc diffusion method in seeded agar medium was used to test the antibiotic sensitivity of the bacterial isolates to drugs like Amikacin, Netilin, Co-trimaxazole, Streptomycin, Furazolidone, Kanamycin, Nalidixic acid, Nitrofurantoin, Tobramycin, Oxytetracyclin, Chloramphenicol, and Gentamycin (Barale et al., 2022). After an incubation period at room temperature (27^0C), plates were observed for zones of inhibition. The organisms were classified as resistant or sensitive based on the size of the zone of inhibition.

4.2.2.4 Pot culture experiment

4.2.2.4.1 Inoculum preparation

1 gm of carboxy methyl cellulose (adhesive), 10^8 CFU/ml of bacterial suspension, 1% glucose, and 0.5% NaCl were added into 90 ml of sterile distilled water to make the inoculum. Asparagus roots were surface sterilized with 70% alcohol and rinsed with sterile distilled water five to six times. The roots were then covered with inoculum and sown in pots containing natural and sterile soil each (Kumar et al., 2016).

4.2.2.4.2 Method of inoculation

The 2-month-old, healthy Asparagus plantlets were thoroughly cleaned with sterile distilled water at least 5 times, and they were surface sterilized with 70% ethanol 4 to 5 times. Before being sown in pots, the roots were kept in inoculum for 2 to 3 hours. The experiment was conducted in pots that were filled with sterile and naturally occurring soil that had been air-dried and sieved. The pots were arranged in naturalistic settings in a random pattern with 72 repetitions (36 for each treatment with natural soil and 36 for each treatment with sterile soil with corresponding controls), and they were periodically irrigated. Using a randomized block design (RBD), the experiment was run in triplicate to investigate the impact of treatment of both- the individual isolates and their co-culture. Four types of treatments were given to the rhizome before sowing-

T1 : Treatment with *Exiguobacterium acetylicum* RGK

T2: Treatment with *Enterobacter mori* RGK1

T3: Co-culture of *Exiguobacterium acetylicum* RGK and *Enterobacter mori* RGK1

T4: Control (Uninoculated)

The morphological parameters of plants were examined at 45, 90 and 180 days of sowing as perthe earlier report (Ambardar & Vakhlu, 2013).

4.2.2.5 Extraction and purification of secondary metabolites from Asparagus

In order to extract secondary metabolites, Asparagus plants were taken away from the pots after 45, 90, and 180 days. The roots were thinly sliced, dried at 40ºC in the oven, and then crushed into a fine powder. After adding 1 gm of sample to 10 ml of methanol in a sealed tube, the mixture was treated for 1 hour at room temperature in a bath sonicator. It was then centrifuged for 10 minutes at 5000 rpm and 4°C. For further analysis, supernatant was collected.

For purification 5 gm of Asparagus plant powder was hydrolysed in 50 ml of 2 M sulphuric acid by heating under refluxation for 2 hrs. 40% sodium hydroxide was used to neutralize the solution once it had cooled. Following hydrolysis, the product was extracted using an equal amount of chloroform (Wang et al., 2011; Yang et al., 2015). The extract was concentrated by evaporating it at 60°C after being separated using a separating funnel. The residue was dissolved in methanol and utilized for TLC on precoated silica gel with the standards, and the product was quantified using RP-HPLC.

4.2.2.6 Phytochemical analysis of Asparagus root extract

The Folin Ciocalteu reagent test (Lamuela-ravents, 1999) was used to assess the total phenolic content (TPC), using gallic acid as a standard. The measurement was given in mg gallic acid equivalents (GAE)/g of dry weight. Using rutin as a standard, the total flavonoid content (TFC) was calculated and represented as mg rutin equivalents (RE)/g dry weight (Zhishen et al., 1999). The capacity of each sample to scavenge free radicals in the presence of DPPH was also examined (Surveswaran et al., 2007).

4.2.2.7 Separation, detection and quantification of phytocompounds

Metabolites were separated using pre-coated silica gel thin layer chromatography (TLC) plates (Merck, Darmstadt, Germany). Samples were spotted on the plate, processed in a TLC chamber using hexane-acetone (8:2) as the mobile phase with a few minor modifications, dried to make sure all solvents had evaporated, and detected with a 0.5:5 mixture of ethanol (8% vanillin) and sulfuric acid solution (70%) and the RF values of metabolites were determined (Hardman, 1968). After that, the metabolites were recognized and quantified using HPLC on the methanolic extracts as well as GC-MS/MS analysis of the samples.

4.2.2.8 GC-MS / MS analysis of extracts

Samples were analyzed using GC-MS/MS utilizing GCMS-TQ8050Plus with HS 20 (SHIMADZU, Japan) that was outfitted with an MS detector. Helium was employed as a carrier gas at a flow rate of 1 ml per minute in a SH -Rxi - 5Sil MS column (30 mm × 0.25 mm ID × 0.25 µm). Method: Q3, scan, range: m/z 45–600, 1 µl sample was injected at 250°C, interphase temperature: 290°C, ion source temperature: 280°C, oven temperature: 50°C to 275°C, and GC running time: 52 min. The National Institute of Standards and Technology (NIST) Database was used to identify the metabolites.

4.2.2.9 Reverse phase high performance liquid chromatographic (RP-HPLC) analysis of diosgenin

JASCO's RP-HPLC system, which includes a quaternary pump, autosampler, and UV detector, was used to purify and measure diosgenin. As previously described (Schieffer, 2002), diosgenin purification was performed on a semi-preparative scale Hiber C25 column (250 4.6 mm, 5 m). With a flow rate of 0.8 ml/min and a total injection volume of 25 µl, the mobile phase was composed of acetonitrile and HPLC-grade water in a ratio of 10:90 (v/v). A UV detector detected the diosgenin at 194 nm. The linearity range of standards is determined by the standard diosgenin. Test solutions containing (20–100 µg/ml of standard diosgenin) have been prepared and injected three times as part of the linearity test. Diosgenin's correlation value (R2) was 0.9945.

4.2.2.10 Statistical analysis

The results were presented as mean values ± SD. Graph pad Prism version 5 software was used to do analysis of variance (ANOVA) techniques in order to detect variation differences. Tukey's comparison test showed significance at $p \leq 0.05$.

4.2.3 Results and discussion:

4.2.3.1 Phenotypic characterization and identification of PGPR

From the diverse soil samples, 20 different bacterial isolates were obtained. Based on their capacities to promote plant growth, 2 notable isolates were chosen for phenotypic characterization and identification. One of them was Gram negative and the other was Gram positive, both of them were rod-shaped and demonstrated the biochemical traits that are previously listed in Table 4.1.3 of Chapter 4.1. Based on 16S rDNA sequence analysis, they were identified as strains of *Exiguobacterium acetylicum* and *Enterobacter mori* and named *Exiguobacterium acetylicum* RGK and *Enterobacter mori* RGK1. The sequences has been deposited in the NCBI GenBank database under the accession numbers **OL771442** and **OL656822**, respectively (Fig. 4.1.5 from chapter 4.1). In the current investigation, strains of *Enterobacter mori* RGK1 and *Exiguobacterium acetylicum* RGK have been identified from the Asparagus rhizosphere to have the ability to promote plant growth. According to previous reports, PGPR produces a variety of vital metabolites for plants that support nutrient uptake and general plant vigour (Jabborova et al., 2020). In earlier investigations, plant growth-promoting *Enterobacter* spp. have been found in the rhizosphere of the Asparagus plant (Plate et al., 2010). Similarly,

Exiguobacterium spp. were isolated from the medicinal plant *Bacopa monnieri* (Bharti et al., 2013). These two PGPR strains were chosen based on a variety of their PGPR characteristics.

4.2.3.2 Plant growth promoting attributes of isolates

As mentioned in Chapter 4.1, these two isolates exhibited the highest levels of plant growth promoting properties such as phosphate solubilization, potassium solubilization, zinc solubilization, nitrogen fixation, indole acetic acid (IAA) production, hydrogen cyanide (HCN) production, ammonia production, siderophore production and exopolysaccharide synthesis. These isolates showed negative result for amylase and chitinase production where cellulase production was shown by *Exiguobacterium* spp. They were both resistant to salt concentration. *Exiguobacterium acetylicum* RGK tolerated up to 5.00% NaCl, while *Enterobacter mori* RGK1 tolerated up to 6.00% NaCl.

Many other studies have shown that PGPR has the ability to dissolve phosphorus, zinc, and potassium (Soto et al., 2019; Bagyalakshmi et al., 2017; Shakeel et al., 2015). Phosphate solubilization by numerous *Exiguobacterium* and *Enterobacter* species has also been documented (Saengsanga, 2018; Rajendran et al., 2012). Similar to phosphorus, potassium is a crucial macronutrient, and Meena et al. (2016) found that solubilizing potassium by PGPR improves plant development in a variety of commercial crops. According to Parveen et al. (2018), zinc also contributes to the metabolism of plants by acting as a cofactor in several enzyme activities.

In this work, both rhizobacteria strains synthesize siderophores and generate IAA when tryptophan is present. According to Kumari et al. (2018), IAA synthesis stimulates root system expansion and lengthening, which facilitates water and nutrient uptake. Our results are in line with earlier research which shows that PGPR, including *Exiguobacterium, Enterobacter, Pseudomonas,* and *Bacillus* can synthesizes IAA and siderophores (Lopez et al., 2019; Emmert & Handelsman, 1999; Rajendran et al., 2012). Both of the PGPRs used in this study are capable of fixing nitrogen and producing ammonia and HCN. Devi et al. (2022) claim that PGPR can produce siderophores, ammonia, and HCN, as well as able to fix nitrogen.

Both isolates in this investigation produced exopolysaccharides, which may be crucial for desiccation resistance, plant-microbe interactions, bioremediation and microbial aggregation. Under drought stress conditions, it has been shown that

inoculating plants with EPS-producing bacterial strains increases soil moisture content, leaf area, root and shoot length, plant biomass, and the amount of protein and sugar in the leaves (Naseem et al., 2014; Khan et al.,2017). Additionally, the salt tolerance of *Exiguobacterium acetylicum* RGK and *Enterobacter mori* RGK1 was up to 5% and 6%, respectively. Salinity is one of the most detrimental abiotic variables impacting crop development and output. Plant characteristics like root and shoot growth drought tolerance, and germination rate, are all enhanced by PGPR under salt stress. Previously, it was shown that plants exposed to salt were protected by PGPR, such as *Bacillus* sp. and *Pseudomonas* sp. (Chauhan et al., 2017).

4.2.3.3 Antibiotic sensitivity test

Results showed that both isolates were sensitive to Gentamycin, Kanamycin, Streptomycin, Tobramycin, furazolidone, Nalidixic acid, Co-trimoxazole and Amikacin where *Enterobacter mori* RGK1 resistant to nitrofurantoin. As listed in Table 4.2.1, *Exiguobacterium acetylicum* RGK showed 19 ±0.07mm, 19 ±0.05mm, 11 ±0.05mm, 21 ±0.07mm, 24 ±0.07mm, 17 ±0.07mm, 25 ±0.05mm, 17 ±0.04mm zone of inhibition respectively. In contrast, *Enterobacter mori* RGK1 showed 35 ±0.05mm, 23 ±0.07mm, 20 ±0.05mm, 6 ±0.04mm, 15 ±0.02mm, 2 ±0.08mm, 22 ±0.03mm, 30 ±0.07mm respectively. However, *Enterobacter mori* RGK1 was resistant to Nitrofurantoin (Saengsanga, 2018)

Table 4.2.1: Antibiotic resistivity of isolated PGPR strains against standard antibiotics and zone of inhibition (mm) given below

Antibiotics	***Exiguobacterium acetylicum* RGK**	***Enterobacter mori* RGK1**
Streptomycin	11 ± 0.05	20 ± 0.05
Oxytetracyclin	27 ± 0.06	30 ± 0.07
Gentamycin	19 ± 0.07	35 ± 0.05
Furazolidone	24± 0.07	15 ± 0.02
Co-trimoxazole	25 ± 0.05	22 ± 0.03
Amikacin	17 ± 0.04	30 ± 0.07
Tobramycin	21 ± 0.07	6 ± 0.04

Nitrofurantoin	19 ± 0.03	-
Kanamycin	19 ± 0.05	23 ± 0.07
Nalidixic acid	17 ±0.07	20±0.08

4.2.3.4 Pot culture experiment

A study on pot cultivation was conducted to determine the individual effect and the function of these PGPR in co-culture as well. The results showed that the co-culture's effect is superior to the individual application. Furthermore, the effect was more significant in natural soil than in sterile soil. Table 4.2.2a, 4.2.2b, and 4.2.2c show that after 45, 90, and 180 days of treatment, plants treated independently with *Exiguobacterium acetylicum* RGK, *Enterobacter mori* RGK1, and co-culture of both showed progressive increases in the shoot height, root number, and root biomass as compared to the control.

Previous research found that inoculating pea seeds with *Exiguobacterium* in pot trial conditions improved germination and growth parameters (Mishra et al., 2009). Similarly, co- inoculation of *Exiguobacterium* strains with *Trigonella foenum-graecum* promoted plant growth in terms of increased chlorophyll content, nodulation efficiency, root and shoot length, and noduledry weight (Rajendran et al., 2012). As with earlier research, *Enterobacter* could be used as a plant growth promoter to enhance crop production and yield. In addition to increasing plant growth, these bacteria were discovered to be antagonistic to plant pathogens (Lopez et al., 2019; Saengsanga, 2018). Similarly, inoculation with PGPR enhance seedling germination in asparagus reported by Liddycoat et al. (2009).

4.2.3.4.1 Effect on shoot height

E. acetylicum RGK, had shown the increment as 54, 102 and 109 % after 45, 90 and 180 days respectively in natural soil, while in sterile soil it showed the increment as 33, 82 and 105 % after same interval of days. Similarly, *E.mori* RGK1 it showed the increase in shoot height by 33, 54 and 79 % after 45, 90 and 180 days in natural soil. While in sterile soil it showed 15, 46 and 64 % of rise in the shoot height. Similarly, in case of treatment with co-culture of these PGPRs(*E.mori* RGK1+ *E. acetylicum* RGK) it showed the increase in the shoot height after 45, 90 and180 days as 120, 128 and 135% in natural soil while in sterile soil it showed as 106, 123 and 130 % increase after 45, 90 and 180 days when compared with its control (Table 4.2.2a).

4.2.3.4.2 Effect on root number

E. acetylicum RGK, had shown the enhanced root number after 45, 90 and 180 days as 35, 47 and 50% respectively in natural soil while in sterile soil it showed the increment as 33, 45 and57% after 45, 90 and 180 days. Similarly in case of treatment with *E.mori* RGK1 showed increament on the root number by 32, 35 and 39 % after 45, 90 and 180 days in natural soil. Whilein sterile soil it showed 22, 26 and 38 % increase in the root number. When Asparagus plant treated with co-culture of these PGPRs (*E.mori* RGK1 + *E. acetylicum* RGK) it showed increased root number after 45, 90 and 180 days as 58, 60 and 72% in natural soil while in sterile soil it showed as 53, 55 and 71 % increase after 45, 90 and 180 days when compare with its control (Table 4.2.2b).

4.2.3.4.3 Effect on root biomass

In case of treatment with *E. acetylicum* RGK, it showed the increment as 30, 35 and 56 % after 45, 90 and 180 days respectively in natural soil, while in sterile soil it showed the incrementas 25, 27 and 46 % after same interval of days, that is 45, 90 and 180. Similarly, *E.mori* RGK1, had shwon the increment in root biomass by 15, 17 and 37 % after 45, 90 and 180 days in naturalsoil, while in sterile soil it showed 12, 14 and 23 % of increase in the root biomass. When a Asparagus plant treated with co-culture of these PGPRs (*E.mori* RGK1+ *E. acetylicum* RGK) it showed the increased in root biomass after 45, 90 and 180 days as 54, 73 and 106% in natural soilwhile in sterile soil it showed as 50, 71 and 92 % increase after 45, 90 and 180 days when comparewith its control (Table 4.2.2c).

4.2.3.5 Phytochemical analysis of Asparagus extract

The phytochemical analysis of Asparagus extract is provided in Table 4.2.3a, 4.2.3b, 4.2.3c, and 4.2.3d in terms of total phenolic content (TPC) in mg/gm, total flavonoid content (TFC) in mg/gm, total saponin (SAP) mg/gm, and DPPH radical scavenging activity in percent inhibition. It reveals that after 45, 90, and 180 days the co-culture treated plants had higher phenolic, flavonoid, and saponin contents than the untreated plants. Furthermore, all of the samples demonstrated strong DPPH-targeting free radical scavenging activity. After 180 days, plants treated with individual PGPRs and co-cultures of PGPRs in natural soil showed higher TPC, TFC, SAP, and DPPH levels.

In the current investigation, we discovered that bacterial co-culture treatment raises the levels of total phenolic content, flavonoid content, saponin content, DPPH

radical scavenging, and diosgenin content. After 180 days, the combination of these PGPR enhanced the phenolic and flavonoid contents of natural and sterile soil by 31.6% and 27.1%, respectively, and by 46.2% and 42.8%, respectively. After 180 days, a co-culture treatment in natural and sterile soil revealed increased saponin content by 132% and 104.7%. The co-cultured plants showed increased antioxidant activity of between 55% and 36.6% in both types of soil.

According to Mitra et al. (2016), PGPR treatment increased phenolic content in *A.racemosus* (Mitra et al., 2016). There are a few reports on saponin content enhancement by PGPR. One of them is increased saponin content in *B. monnieri* plants after treatment with *Exiguobacterium oxidotolerans* (Bharti et al., 2013). Similarly, Jain et al. (2014) reported that the total phenolic and flavonoid content was increased in pea plants by *T. harzianum*, *P. aeruginosa*, and *B. subtilis*, both individually and in combination (Jain et al., 2014). Dobosz et al. (2011) reported an increase in *A officinalis* antioxidant capacity after fusarium treatment (Doboszet al., 2011). In the same way, Liu et al. (2018) reported increased antioxidant activity after treatment with single and consortium PGPR (Liu et al., 2018).

Table 4.2.2a: Shoot height of Asparagus after inoculation with PGPR

Parameter	Shoot height (cm) after 45, 90 and 180 days											
	Control			*E. acetylicum* RGK			*E.mori* RGK1			Co-culture of both these PGPR		
	Days			Days			Days			Days		
	45	90	180	45	90	180	45	90	180	45	90	180
Natural soil	20.83 ±0.6	22.5 ±0.4	45.9 ±0.9	32.17 ±0.8	45.5 ±0.4	96.33 ±3.9	27.83 ±0.2	34.83 ±0.6	82.67 ±2.5	45.83 ±2.3	51.5 ±1.8	108 ±4.3
Sterile soil	11 ±0.8	18.6 ±1.2	31 ±0.8	14.6 ±0.4	34 ±0.8	63.6 ±1.7	12.6 ±1.7	27.3 ±1.2	51 ±0.8	22.6 ±2.4	41.6 ±1.2	71.3 ±2.6
% Increase over control(N)	-	-	-	54	102	109	33	54	79	120	128	135
% Increase over control (S)	-	-	-	33	82	105	15	46	64	106	123	130

(N)=natural soil (S)=sterile soil. The values represent the average of three experiments ± SD. ANOVA using Tukey's comparison test yielded a significant difference from control group at $p \leq 0.05$, and the relative standard deviation for all values are less than 10

Table 4.2.2b: Root number of Asparagus after inoculation with PGPR

Parameter	Root number after 45, 90 and 180 days											
	Control			*E.acetylicum* RGK			*E.mori* RGK1			Co-culture of both these PGPR		
	Days			Days			Days			Days		
	45	90	180	45	90	180	45	90	180	45	90	180
Natural soil	5.67 ±0.4	11.83 ±1.3	18 ±0.4	7.6 ±0.6	17.5 ±1.8	27 ±1.6	7.5 ±0.4	15.1 ±0.8	25 ±1.3	9 ±0.4	19 ±2.1	31 ±0.8
Sterile soil	4.5 ±0.4	10.3 ±0.3	14 ±0.8	6 ±0.4	15 ±0.4	22 ±0.8	5.5 ±0.4	13 ±0.8	19 ±0.4	6.9 ±0.04	16 ±0.8	24 ±1.4
% Increase over control (N)	-	-	-	35	47	50	32	35	39	58	60	72
% Increase over control (S)	-	-	-	33	45	57	22	26	38	53	55	71

(N)=natural soil (S)=sterile soil. The values represent the average of three experiments ± SD. ANOVA using Tukey's comparison test yielded a significant difference from control group at $p \leq 0.05$, and the relative standard deviation for all values are less than 10.

Table 4.2.2c: Root biomass of Asparagus after inoculation with PGPR

Parameter	Root biomass (gm) after 45, 90 and 180 days											
	Control			*E. acetylicum* RGK			*E.mori* RGK1			Co-culture of both these PGPR		
	Days			Days			Days			Days		
	45	90	180	45	90	180	45	90	180	45	90	180
Natural soil	0.13 ±0.01	2.3 ±0.1	16 ±0.1	0.17 ±0.01	3.12 ±0.01	25 ±0.2	0.15 ±0.04	2.7 ±0.02	22 ±0.3	0.2 ±0.01	4 ±0.13	33 ±0.2
Sterile soil	0.08 ±0.08	1.57 ±0.04	13 ±0.1	0.1 ±0.01	2 ±0.02	19 ±0.2	0.09 ±0.01	1.80 ±0.08	16 ±0.1	0.12 ±0.05	2.7 ±0.03	25 ±0.2
% Increase over control(N)	-	-	-	30	35	56	15	17	37	54	73	106
% Increase over control (S)	-	-	-	25	27	46	12	14	23	50	71	92

(N)=natural soil (S)=sterile soil. The values represent the average of three experiments ± SD. ANOVA using Tukey's comparison test yielded a significant difference from control group at $p \leq 0.05$, and the relative standard deviation for all values are less than 10.

Table 4.2.3a: Total phenolic content of Asparagus plant inoculated with PGPR

	Phenolic content after 45, 90 and 180 days											
	Control			***E. acetylicum* RGK**			***E. mori* RGK1**			**Co-culture of both these PGPR**		
	Days			**Days**			**Days**			**Days**		
	45	**90**	**180**	**45**	**90**	**180**	**45**	**90**	**180**	**45**	**90**	**180**
Natural soil	3.46 ±0.02	4.60 ±0.04	5.32 ±0.01	3.7 ±0.01	5.1 ±0.07	6.1 ±0.09	3.5 ±0.01	4.9 ±0.06	5.7 ±0.09	3.8 ±0.05	5.9 ±0.01	7 ±0.02
Sterile soil	3.6 ±0.02	4.5 ±0.02	5.2 ±0.03	3.2 ±0.02	4.8 ±0.04	6 ±0.02	3.1 ±0.03	4.6 ±0.01	5.7 ±0.07	3.3 ±0.01	5.9 ±0.03	6.6 ±0.09
% Increase over control(N)	-	-	-	8	11.3	15.1	3.18	6.5	7.3	12.4	30	31.6
% Increase over control(S)	-	-	-	4.5	8.2	14	1.3	3.7	9.5	9.4	13.1	27.1

(N)=natural soil (S)=sterile soil. The values represent the average of three experiments ± SD. ANOVA using Tukey's comparison test yielded a significant difference from control group at $p \leq 0.05$, and the relative standard deviation for all values are less than 10.

Table 4.2.3b: Total flavonoid content of Asparagus plant inoculated with PGPR

	Flavonoid content after 45, 90 and 180 days											
	Control			***E. acetylicum* RGK**			***E. mori* RGK1**			**Co-culture of both these PGPR**		
	Days			**Days**			**Days**			**Days**		
	45	**90**	**180**	**45**	**90**	**180**	**45**	**90**	**180**	**45**	**90**	**180**
Natural soil	8.92 ±0.05	26.6 ±0.3	40 ±0.01	11.1 ±0.04	33.5 ±0.07	52.3 ±0.02	10 ±0.05	30.5 ±0.1	46 ±0.02	12 ±0.04	37.5 ±0.03	58.5 ±0.02
Sterile soil	6.6 ±0.03	20 ±0.02	35 ±0.05	8.2 ±0.03	24 ±0.09	43 ±0.02	7.2 ±0.05	22.2 ±0.1	40 ±0.01	8.2 ±0.03	27.2 ±0.02	50 ±0.03
% Increase over control(N)	-	-	-	24.8	25.5	30.7	12.1	14.2	15	34.5	40.5	46.2
% Increase over control (S)	-	-	-	23.8	20	22.8	8.7	11.5	14.2	24.3	36	42.8

(N)=natural soil (S)=sterile soil. The values represent the average of three experiments ± SD. ANOVA using Tukey's comparison test yielded a significant difference from control group at $p \leq 0.05$, and the relative standard deviation for all values are less than 10.

Table 4.2.3c: Total saponin content of Asparagus plant inoculated with PGPR

	Saponin content after 45, 90 and 180 days											
	Control			***E. acetylicum* RGK**			***E. mori* RGK1**			**Co-culture of both these PGPR**		
	Days			**Days**			**Days**			**Days**		
	45	**90**	**180**	**45**	**90**	**180**	**45**	**90**	**180**	**45**	**90**	**180**
Natural soil	84 ±0.08	100 ±0.02	115 ±0.05	92 ±0.3	132 ±0.3	158 ±1.2	89 ±0.2	118 ±0.03	140 ±0.1	100 ±0.4	189 ±0.4	267 ±2.1
Sterile soil	71 ±0.03	89 ±0.02	105 ±0.05	76 ±0.03	112 ±0.09	130 ±0.02	74 ±0.05	100 ±0.1	123 ±0.01	79 ±0.03	135 ±0.02	215 ±0.03
% Increase over control(N)	-	-	-	9.5	32	37.3	5.9	18	21.7	19	89	132
% Increase over control(S)	-	-	-	7.4	25.8	23.8	4.2	12.3	17.1	11.2	51.6	104.7

(N)=natural soil (S)=sterile soil. The values represent the average of three experiments ± SD. ANOVA using Tukey's comparison test yielded a significant difference from control group at $p \leq 0.05$, and the relative standard deviation for all values are less than 10.

Table 4.2.3d: Percent inhibition for DPPH activity of Asparagus plant inoculated with PGPR

	Percent inhibition for DPPH activity after 45, 90 and 180 days											
	Control			***E. acetylicum* RGK**			***E.mori* RGK1**			**Co-culture of both these PGPR**		
	Days			**Days**			**Days**			**Days**		
	45	**90**	**180**	**45**	**90**	**180**	**45**	**90**	**180**	**45**	**90**	**180**
Natural soil	25.2 ±0.06	30.7 ±0.04	38.2 ±0.14	28.7 ±0.01	36.02 ±0.04	48.5 ±0.01	28.3 ±0.06	35.9 ±0.1	45 ±0.07	29.3 ±0.04	36.2 ±0.06	59.5 ±0.07
Sterile soil	22.16 ±0.03	31.84 ±0.04	37.73 ±0.1	25 ±0.04	35 ±0.05	47.3 ±0.07	24 ±0.06	34 ±0.01	42 ±0.07	25 ±0.06	36 ±0.06	51 ±0.05
% Increase over control(N)	-	-	-	14.11	17.02	25.52	12.5	16.73	18	16.13	17.8	55
% Increase over control (S)	-	-	-	12.8	12.7	26.3	8.3	9.8	13.91	14.1	13.1	36.6

(N)=natural soil (S)=sterile soil. The values represent the average of three experiments ± SD. ANOVA using Tukey's comparison test yielded a significant difference from control group at $p \leq 0.05$, and the relative standard deviation for all values are less than 10

4.2.3.6 Separation and purification of PGPR induced phytocompounds

Diosgenin was purified using acid hydrolysis followed by solvent extraction. The obtained sample was evaporated and dissolved in methanol before being used for additional analyses such as TLC, GC-MS/MS, and RP-HPLC. The TLC profile revealed that the extracted compound matched with the standard diosgenin band on the pre-coated TLC silica-gel plate with an Rf value of 0.49. Similarly, GC-MS/MS results revealed that when Asparagus extracts were compared to untreated controls, the percent area of diosgenin in co-culture treated plants increased(5.71% area). Table 4.2.4 showed the GC-MS/MS identification of the compounds using the Wiley- NIST database based on retention time, peak area, molecular mass, and molecular formula. Fig.4.2.1. Previous research has also shown that acid hydrolysis followed by extraction in non-polar solvents yields a higher yield than traditional methods (Yang et al., 2016)**.** Similarly, in an earlier study of phytochemical analysis, a GC-MS based method was used to analyze *Asparagus racemosus* (Janani and Singaravadivel, 2014).

4.2.3.7 HPLC for diosgenin

Diosgenin was isolated from *A. racemosus* root by acid hydrolysis and analyzed with HPLC-UV detection. The retention time was noted at 17 min, and UV absorption of diosgenin occurs at 194 nm. Table 4.2.5 shows the concentrations of diosgenin after 45, 90, and 180 days and HPLC chromatograms are given in Fig. 4.2.2 Quantification of diosgenin was performed by using HPLC UV detection. Asparagus plant treated with *E. acetylicum* RGK had shown the enhanced diosgenin content after 45, 90 and 180 days as 0.05, 0.09 and 0.15 % respectively in natural soil while in sterile soil it showed the increment as 0.05, 0.09 and 0.13 % after 45, 90 and 180 days respectively. Further, treatment with *E. mori* RGK1 had shown the increment on the diosgenin content by 0.04, 0.09 and 0.12 % after 45, 90 and 180 days respectively in natural soil. While in sterile soil it showed 0.04, 0.09 and 0.11 % of the increase in the diosgenin content after 45, 90 and 180 days respectively. When an Asparagus plant treated with co-culture of these PGPRs (*E. acetylicum* RGK + *E. mori* RGK1) it showed the increased diosgenin content after 45, 90 and 180 days as 0.06, 0.09, and 0.28 % respectively in natural soil while in sterile soil it showed as 0.06, 0.09 and 0.19 % increase after 45, 90 and 180 days when compared with its control. An earlier study reported that the quantification of diosgenin was performed by using HPLC (Peiqin Li,2012).

Table 4.2.5: Diosgenin content after 45, 90 and 180 days

	Diosgenin content in percentage (%)					
	45 days		**90 days**		**180 days**	
	Natural soil	**Sterile soil**	**Natural soil**	**Sterile soil**	**Natural soil**	**Sterile soil**
Control	0.02	0.02	0.08	0.07	0.11	0.10
***E. acetylicum* RGK**	0.05	0.05	0.09	0.09	0.15	0.13
***E. mori* RGK1**	0.04	0.04	0.09	0.09	0.12	0.11
Co-culture of these PGPR	0.06	0.06	0.09	0.09	0.28	0.19

Table 4.2.4: Secondary metabolite profile identified by GC-MS/MS from PGPR treated Asparagus

Sr. No.	Name of Identified Compounds	Category	Retention time	Area%	Control	*Exiguobacterium acetylicum* RGK	*Enterobacter mori* RGK1	Co-culture of both PGPR
1	n-Hexadecanoic acid	Fatty acid	31.35	4± 21*	+	+	+	+
2	9,12-Octadecadienoic acid (Z,Z)-, methyl este	Fatty acid	34.89	5± 29.09*	+	+	+	-
3	Octadec-9-enoic acid	Fatty acid	48.24	7.24	+	-	+	+
4	Glycidyl palmitate	Fatty acid	38.01	0.2± 2.77*	+	+	+	-
5	n-Propyl 9,12-octadecadienoate	Fatty acid	33.68	0.71± 1.80*	+	-	+	-
6	Methyl 3-cis,9-cis,12-cis-octadecatrienoate	Fatty acid	41.08	1.10	-	+	-	+
7	Glycidyl oleate	Fatty acid	41.17	0.14± 2.77*	+	+	+	-
8	Glycidyl palmitate	Fatty acid	41.62	0.24± 3.78*	+	+	+	-
9	Butyl 9,12,15-octadecadienoate	Fatty acid	41.08	1.87	-	-	-	+
10	2,2-Dimethoxybutane	Alkane	3.2	0.37± 3.75*	-	+	+	+

11	Bicyclo[2.2.1]heptan-2-ol, 1,7,7-trimethyl-, (1S	Fatty acid	13.57	0.19± 1.19*	-	+	+	-
12	5-Hydroxymethylfurfural	furans	16.09	4.7 ± 55.41*	+	+	-	+
13	Oleic Acid	Fatty acid	35.01	0.66± 2.90	-	+	+	-
14	Octadecanoic acid	Fatty acid	35.55	0.7± 2.4	-	+	+	-
15	1,3-Propanediol, 2-(hydroxymethyl)-2-nitro-	Fatty acid	22.05	8± 26	-	+	-	+
16	Glycidol stearate	Fatty acid	41.64	0.83	-	-	-	+
17	Methyl 3-cis,9-cis,12-cis-octadecatrienoate	***methyl*** ester fatty acid	41.08	1.10	-	+	-	-
18	Sucrose	Disaccharide	49.25	73.69	-	+	-	-
19	Diosgenin	Saponin	44.09	1.27± 5.71*	-	+	-	+

Note: + denotes present, - denotes absent, *Exiguobacterium acetylicum* RGK+, Co-culture of both PGPR*

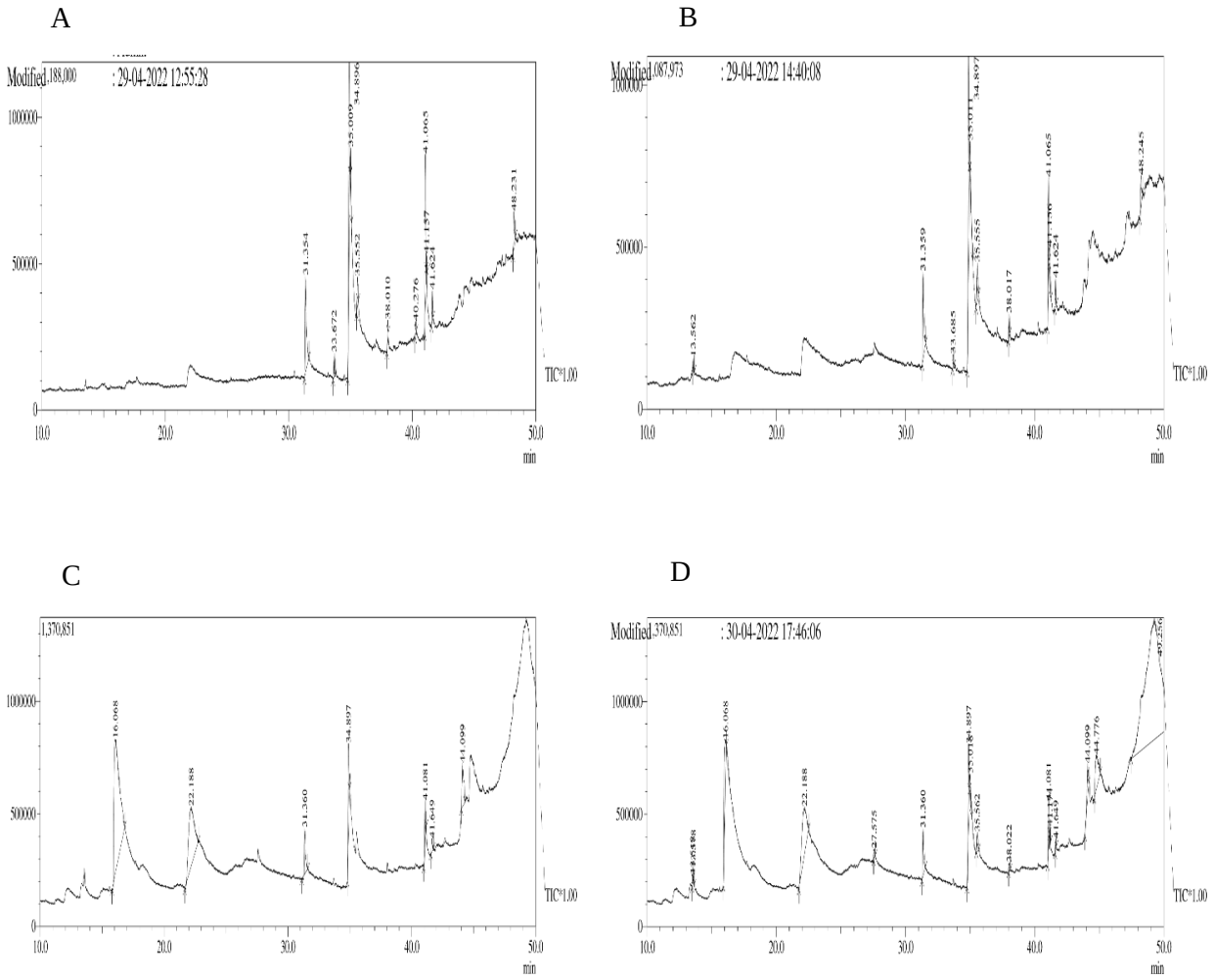

Fig.4.2.1: The gas chromatography–tandem mass spectrometry graph with various peaks of Asparagus where (a) Chromatogram of control Asparagus (uninoculated) (b) Chromatogram of *Enterobacter mori* RGK1 inoculated Asparagus (c) Chromatogram of *Exiguobacterium acetylicum* RGK inoculated Asparagus (d) Chromatogram of co-culture of both inoculated Asparagus

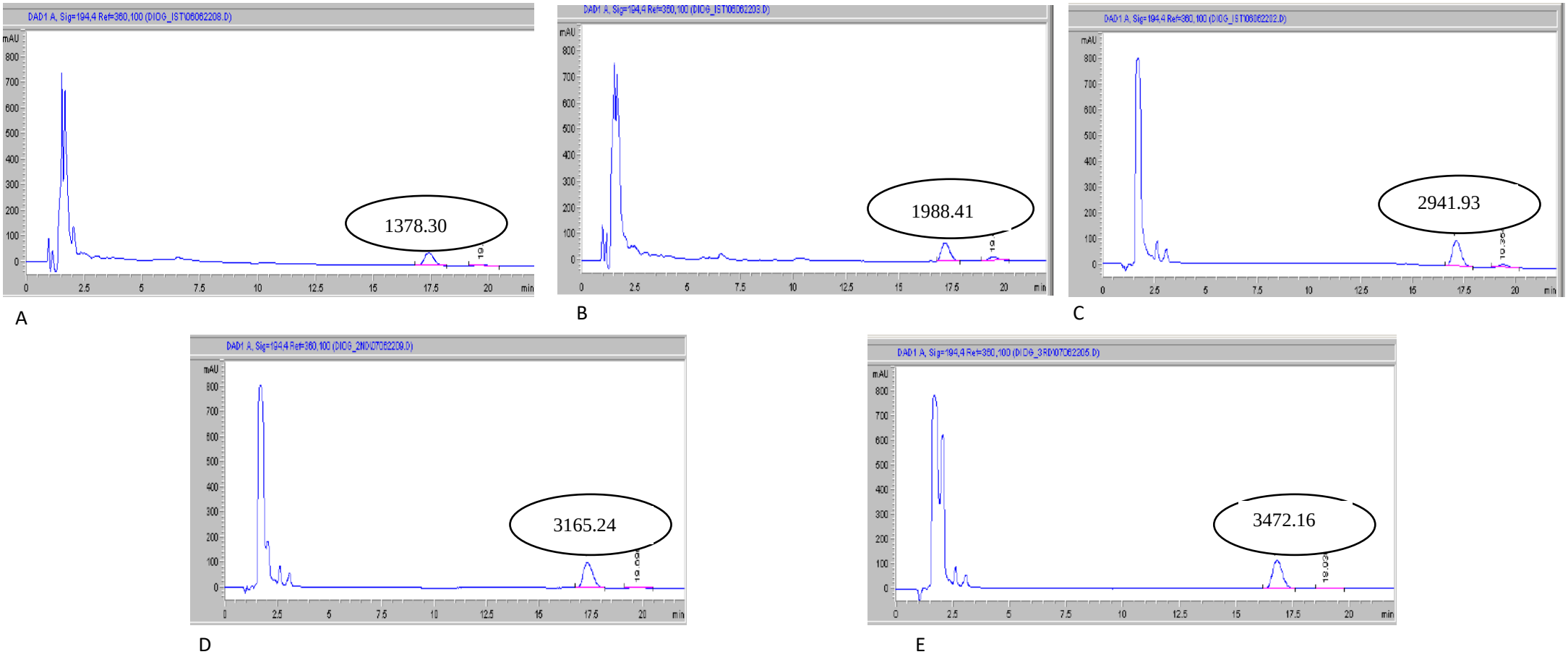

A B C D E

Fig.4.2.2: HPLC chromatogram of purified diosgenin at 194 nm. (A) Chromatogram of standard of diosgenin. (B) Chromatogram of control Asparagus (uninoculated). (C) Chromatogram of *Enterobacter mori* RGK1 inoculated Asparagus. (D) Chromatogram of *Exiguobacterium acetylicum* RGK noculated Asparagus. (E) Chromatogram of co-culture inoculated Asparagus

4.2.4 Conclusions:

In the present investigation, we found that PGPR treatment improved plant metrics and phytocompounds. Additionally, co-culture inoculations yielded better outcomes than a single inoculation. Furthermore, these findings reveal that the amount of phenolic compounds, flavonoids, and saponins has a positive relationship with anti-radical activities, meaning that the bioinoculants used on the Asparagus rhizosphere are effective. In the future, these phytocompounds could be employed as an effective treatment for a variety of diseases and therapeutic formulations, either alone or in combination with other relevant agents. This PGPR co-culture inoculation would be one of the best alternatives for a long-term Asparagus agroindustry.

The fundamental benefit of utilizing PGPR is that they have a twofold positive impact, working as both a full biofertilizer and a plant biofortifier, addressing nutritional shortages as well as agro-environmental concerns. In natural soil rather than sterile soil, we detected better plant metrics and phytocompounds in Asparagus after PGPR inoculation, both individualy and in co-culture. Although there have been a few publications on the presence of diosgenin in *A. racemosus* roots, we are the first to indicate that co-culture treatment increases diosgenin concentration in *A. racemosus* roots.

4.3 Impact of plant growth promoting rhizobacteria *Serratia nematodiphila* RGK and *Pseudomonas plecoglossicida* RGK on secondary metabolites of turmeric rhizome

The part of this study Published as:

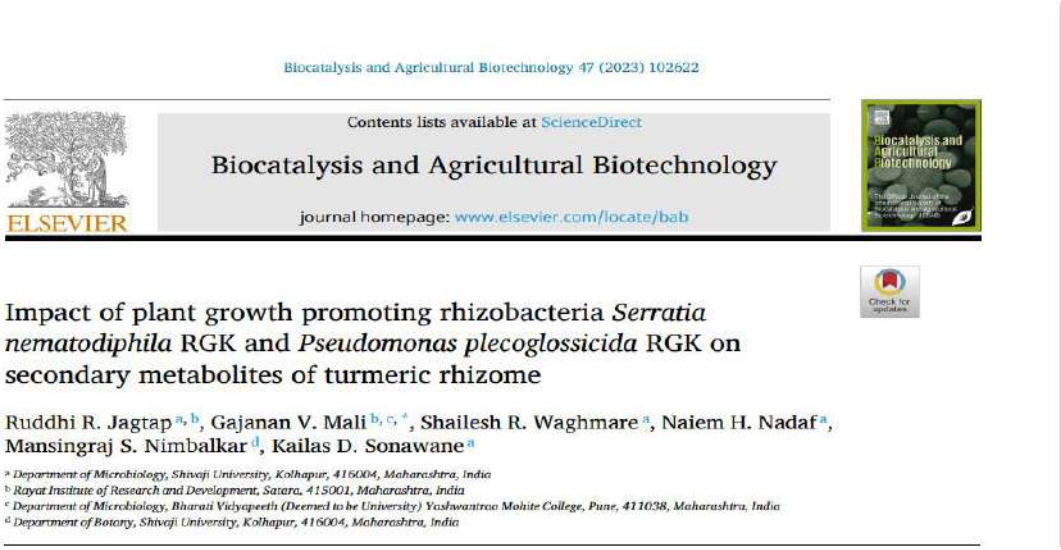

Biocatalysis and Agricultural Biotechnology 47 (2023) 102622

Contents lists available at ScienceDirect

Biocatalysis and Agricultural Biotechnology

journal homepage: www.elsevier.com/locate/bab

Impact of plant growth promoting rhizobacteria *Serratia nematodiphila* RGK and *Pseudomonas plecoglossicida* RGK on secondary metabolites of turmeric rhizome

Ruddhi R. Jagtap [a, b], Gajanan V. Mali [b, c, *], Shailesh R. Waghmare [a], Naiem H. Nadaf [a], Mansingraj S. Nimbalkar [d], Kailas D. Sonawane [a]

[a] Department of Microbiology, Shivaji University, Kolhapur, 416004, Maharashtra, India
[b] Rayat Institute of Research and Development, Satara, 415001, Maharashtra, India
[c] Department of Microbiology, Bharati Vidyapeeth (Deemed to be University) Yashwantrao Mohite College, Pune, 411038, Maharashtra, India
[d] Department of Botany, Shivaji University, Kolhapur, 416004, Maharashtra, India

4.3.1 Introduction:

Plant growth-promoting rhizobacteria (PGPR) are naturally existing soil bacteria that colonize plant roots actively and promote plant growth. Plant growth, plant health, soil fertility,carbon sequestration and phytoremediation are aided by these microbiomes colonizing the soiland plant surfaces (Adamczyk et al., 2019). These organisms are primarily associated with plant roots and help them to grow (Kloepper & Beauchamp, 1992). PGPR has recently become a viable approach considering its potential to produce essential phytohormones such as indoleacetic acid, gibberellic acid, cytokines, ethylene, and siderophores (Bharucha et al., 2013; Lotfiet al., 2022). PGPRs are also employed in the treatment of garbage (Yuan et al., 2020). Their ability to produce biofilms aids in their survival under stressful situations (Ansari et al., 2021).Moreover, some PGPR have demonstrated their ability to degrade pesticides (Rani et al., 2021). They also can withstand abiotic stress, which has beneficial impact on plant growth characteristics (Prasad, 2018). They are utilized as biofertilizers in many countries due to their capacity to solubilize potassium and zinc, and their usage is both environmentally and economically acceptable (Dhaked et al., 2017a). For decades, PGPR has piqued curiosity due to their multifunctional activities. They exhibit chemotactic behavior, as well as antagonism and synergism, with plant roots (Santoyo et al., 2021: Chauhan et al., 2021). Bacteria produceexopolysaccharides as well as function as a biocontrol agent (Chenniappan et al., 2019; Mohammed, 2018). *Bacillus subtilis*, one of the PGPR, is also recognized for its quorum sensing ability (Rosier et al., 2021).

Turmeric (*Curcuma longa*), a medicinally valuable plant, is a member of the *Zingiberaceae* family. It is a perennial spice with palmate leaves arranged alternately in two rows and an aromatic rhizome that is yellow to orange in color (Baranska et al., 2004). The rhizome includes a variety of secondary metabolites, the most common are curcuminoids, which are phenolic chemical compounds (Kumar et al., 2014). It is primarily well known for its therapeutic value. Even though curcumin has a long scientific history, it continues to attract scientist's interest.

Turmeric is associated with a number of PGPR, which influences plant development through direct or indirect mechanisms (Kumar et al., 2016). *Agrobacterium, Alcaligenes, Arthrobacter, Azotobacter, Azospirillum, Bacillus, Burkholderia, Enterobacter, Klebsiella, Pseudomonas,* and *Serratia* are the most

prevalent PGPR associated with turmeric (Kumar et al., 2018). Through an induced systemic resistance mechanism, PGPR increases secondary metabolites in plants. PGPR's synthesizes enzymes and secondary metabolites essential for the host's defence mechanisms (Kavitha et al., 2012). Many researchers have explored several biotechnological applications of PGPR. It includes an increase in the concentration of curcumin after treatment of *Pseudomonas fluorescens* and *Bacillus megaterium* (Boominathan and Sivakumaar, 2012). The co-culture application of PGPR is also more efficient than a single one(Kumar et al., 2019).

The current research work was undertaken with the objective of isolation and characterization of potent PGPR from the rhizosphere of the Turmeric plant and to investigate the effects of their treatment on the growth parameters and biochemical content of turmeric, both individually and in combination.

4.3.2 Material and method:

4.3.2.1 Materials

Analytical grade solvents and chemicals were purchased from Hi Media Laboratories, (Mumbai, India). A standard sample of curcumin was prepared in methanol (100-500µg/ml). To remove impurities, it was then filtered using a 0.2 µm Millipore filter obtained from SigmaAldrich (Bangalore, India). For the pot culture experiments, turmeric rhizomes of the Salem variety were obtained from Turmeric Research Department of Mahatma Phule Krishi Vidyapeeth's Agriculture Research Station at Kasabe Digraj, Dist. Sangli, Maharashtra, India.

4.3.2.2 Screening and identification of PGPR

4.3.2.2.1 Sample collection and Screening of PGPR

20 soil samples were obtained from Tumeric rhizospheres in Kolhapur, Sangli, andSatara districts of Maharashtra for the current study. Among them, five were from Kolhapur, eleven from Sangli while four were from Satara districts. The samples were transported to the laboratory in sterile polypropylene bags for the isolation of PGPR. 1 gm of soil from each sample was then transferred to Erlenmeyer flasks having 100 ml of sterile nutrient broth and shaken at 120 rpm for 24 hours at room temperature (270C±2) for enrichment. Serial dilutions of the enriched samples were carried out in sterile distilled water and 0.1 ml from each dilution was spread on the sterile nutrient agar plates and kept for incubation at room temperature (270C±2) for 24 hours to get well isolated colonies. Colonies with

diverse morphologies such as size, shape, margin, elevation, consistency, opacity, surface and pigmentation were picked and streaked over the same media to obtain the pure cultures. All the isolates of bacteria were preserved at 4°C and phenotypic characterization of isolates was carried out by studying their morphological, cultural and biochemical properties as per the Bergey's Manual of Determinative Bacteriology (Holt et al.,1994; Ahmad et al., 2008). Further identification was done by 16S rRNA gene sequence analysis.

4.3.2.2.2 Genotypic identification of PGPR

The genomic DNA of potent PGPR was extracted using the conventional phenol/chloroform extraction method, and the 16S rRNA genes were amplified using universal primers 16F27 [5'-CCAGAGTTTGATCMTGGCTCA G-3'] and 16R1492 [5'-TACGGYTACCTTGTTACGACTT-3']. Following amplification, the 16S rRNA gene PCR products were purified using PEG-NaCl precipitation, and ABI®3730XL automated DNA sequencer (Applied Biosystems, Inc., Foster City, CA) was used to sequence the results sequentially in accordance with the manufacturer's instructions. The EzBioCloud database was used for identification, and the Lasergene software was used for assembly (Yoon et al., 2017). The resultant sequences were processed and searched using the Nucleotide Basic Local Alignment Search Tool (BLAST) programme to determine which sequences matched the ones at the National Centre for Biotechnology Information (NCBI) BLAST server (www.ncbi.nlm.nih.gov/BLAST). For the sequences with >98% similarity, multiple sequence alignment was carried out using the CLUSTALW programme (Thompson et al., 1997). Using the neighbour joining approach and the Mega XI version of the distance matrix alignment tool (Tamura et al., 2021) with two different bootstrap values (*Serratia nematodiphila* RGK 0.50, and *Pseudomonas plecoglossicida* RGK 0.0010), the phylogenetic tree was constructed.

4.3.2.2.3 Plant growth promoting attributes of isolates

Bacterial isolates were screened for the growth promoting attributes such as Indole acetic acid (IAA) production (Bric et al., 1991), phosphate solubilization (Laslo et al., 2012), zinc solubilization (Saravanan et al., 2004)**,** potassium solubilization (Dhaked et al., 2017b), nitrogen fixation (Dashti et al., 1998), hydrogen cyanide (HCN) production (Lorck, 1948), siderophore production

(Schwyn & Neilands, 1987), ammonia production (Dhaked et al., 2017a), exopolysaccharide production (Naseem & Bano, 2014). The isolates were also checkedfor synthesis of enzymes such as chitinase, cellulase and amylase. Salinity tolerance of isolates was checked by using different concentrations of NaCl (Tirry et al., 2021).

4.3.2.3 Antibiotic sensitivity test

The bacterial isolates were tested for their sensitivity to the antibiotics such as Gentamycin, Amikacin, Kanamycin, Streptomycin, Netilin, Tobramycin, Co-trimaxazole, Furazolidone, Oxytetracyclin, Nitrofurantoin, Chloramphenicol and Nalidixic acid using antibiotic impregnated paper disc diffusion method in seeded agar medium (Barale et al., 2022). Plates were examined for zones of inhibition after incubation at room temperature (270C±2). Based on the diameter of zone of inhibition, the organisms were categorized as resistant or sensitive.

4.3.2.4 Antifungal activity

In vitro antifungal activity of bacterial isolates against fungal pathogen of Turmeric wastested. The pathogen was *Pythium aphanidermatum*, isolated and identified in the laboratory from naturally infected Turmeric plants (Kavitha et al., 2012). The bacterial isolates were streaked at one side of the potato dextrose agar medium in petri dish, and a mycelial disc (8 mm diameter) of five days old culture of *Pythium aphanidermatum* was put at the other side (Kavitha et al., 2010). The plates were incubated at room temperature (27 ±2°C) for 4 days andthe zone of inhibition was measured.

4.3.2.5 Pot culture experiment

4.3.2.5.1 Inoculum preparation

For the treatment of rhizomes, inoculum of each isolate was prepared in medium containing 1% activated charcoal powder, 1% glucose, and 0.5% NaCl. The cell density was adjusted to 10^8 CFU/ml as per MacFarland's standard (Teles et al., 2019)

4.3.2.5.2 Method of inoculation

The young and healthy rhizomes Salem variety were surface sterilized with 70% ethanol (4-5 times) and completely rinsed with sterile distilled water at least

five times. The rhizomes were kept in an inoculum for 2 to 3 hrs before sowing in pots. Experiment was carried out in pots filled with air dried and sieved natural as well as sterile soil. The pots were placed randomly with 72 repeats (36 for each treatment with natural soil and 36 for each treatment with sterile soil with their respective controls) in naturalistic environments and periodically irrigated. The experiment was performed in triplicate using a randomized block design (RBD) to examine the effects of treatment of both - the individual isolates and their co-culture. Four types of treatments were given to the rhizome before sowing -

T1 : Treatment with *Serratia nematodiphila* RGK

T2 : Treatment with *Pseudomonas plecoglossicida* RGK

T3 : Co-culture of *Serratia nematodiphila* RGK and *Pseudomonasplecoglossicida* RGK

T4 : Control (Uninoculated)

The morphological parameters of plants were examined at 45, 90 and 180 days of sowing as per the earlier report (Ambardar & Vakhlu, 2013).

4.3.2.6 Extraction of secondary metabolites from Turmeric

Rhizomes were uprooted from pots after 45, 90, and 180 days and cleaned to extract secondary metabolites. They were sliced into tiny pieces, dried in the oven at 40ºC and grindedto obtain a fine powder. The powder was used to extract secondary metabolites by an ultrasound assisted extraction procedure using methanol as a solvent. In this, 100 mg of dried rhizome powder was mixed with 10 ml of methanol in screw cap tube. The tubes were incubated at room temperature for 60 minutes in an ultrasonic clean bath (230 Volts, 50 Hz, Rivotek, RivieraGlass Pvt. Ltd., Mumbai, India). After centrifuging the solution for 10 minutes at 4500 rpm, the supernatant was recovered and evaporated to concentrate the sample. To evaluate secondary metabolite concentration, 2 ml methanol was added to dissolve the sample. Then, the samples were filtered through a 0.2 µm (Millipore) filter to eliminate contaminants before being used (Zhang et al., 2008).

4.3.2.7 Phytochemical analysis of Turmeric extract

Total phenolic content (TPC) was determined utilizing the Folin Ciocalteu reagent assay (Lamuela-ravents, 1999) using gallic acid as a standard and was

represented in mg gallic acid equivalents (GAE)/g dry weight. Using rutin as a standard, total flavonoid content (TFC)was calculated and reported as mg rutin equivalents (RE)/g dry weight (Zhishen et al., 1999). All the samples were also examined for their ability to scavenge free radicals in the presence of DPPH (Surveswaran et al., 2007).

4.3.2.8 Separation, detection and quantification of secondary metabolites

Pre-coated silica gel thin layer chromatography (TLC) plates were used to separate metabolites (Merck, Darmstadt, Germany). After saturation with mobile phase vapors for 1 hour, samples were spotted on the plate and processed in a TLC chamber with chloroform- methanol-formic acid (96:4:0.8 v/v/v) as a solvent system in a 20×20 cm glass (Borosil) flat bottom chamber. After the development of yellow colour spots, it was retrieved, air dried and the RF values of metabolites were determined. The metabolites were subsequently detected and quantified using HPLC on the methanolic extracts as well as GC-MS/MS analysis of samples were done.

4.3.2.9 GC-MS / MS analysis of extracts

The GC-MS/MS analysis of samples was carried out using GCMS-TQ8050Plus with HS 20 (SHIMADZU, Japan) equipped with an MS detector. Column used was SH -Rxi – 5SilMS with (30 mm × 0.25 mm ID × 0.25 μm) and helium as a carrier gas with flow rate 1ml/min.1 μl sample was injected at 250℃ temperature, interphase temperature was 290℃, ion sourcetemperature was set to 280℃, the oven temperature was 50℃ to 275℃ and GC running time was 38 min, Method-Q3, scan used and range-m/z 45–600. The metabolites were identified by National Institute of Standard and Technology (NIST) Database.

4.3.2.10 Reverse phase high performance liquid chromatographic (RP-HPLC) analysis of curcumin

Curcumin was purified and quantified using an RP-HPLC system by JASCO, including a quaternary pump, autosampler, and UV detector. Curcumin purification was carried out on asemi-preparative scale Hiber C18 column (250×4.6 mm, 5 μm) as previously reported with some modifications (Schieffer, 2002). The mobile phase was 50:50 (v/v) acetonitrile and 2% acetic acid, with a 0.5 ml/min flow rate and a

total injection volume of 20 µl. The peak of curcumin was detected by a UV detector at 425 nm. The standard curcumin determines the linearity range of standards. For the linearity test, test solutions containing (100- 500 µg/ml of curcumin) were produced and injected three times. It was found with high reproducibility inthe concentration range of 2-10 µg. Curcumin's correlation value (R2) was 0.9979.

4.3.2.11 Statistical analysis

The results were expressed as the mean values ± SD. Analysis of variance (ANOVA) techniques were used to determine variation differences by using Graph pad Prism version 5 Software. Significance was determined at $p \leq 0.05$ by Tukey's comparison test.

4.3.3 Results and discussion

4.3.3.1 Phenotypic characterization and identification of PGPR

A total number of 85 isolates of bacteria were obtained from the different soil samples. Among them two prominent isolates based on their plant growth promoting attributes were selected for phenotypic characterization and identification. Both of these were Gram negative,rod shaped showing biochemical characteristics as listed in Table 4.3.1. They were identified as strains of *Serratia nematodiphila* and *Pseudomonas plecoglossicida* based on 16S rDNA sequence analysis and named as *Serratia nematodiphila* RGK and *Pseudomonas plecoglossicida* RGK. The sequences were deposited in the NCBI GenBank database under the accession numbers **MZ452064** and **OL739684**, respectively (Fig. 4.3.1). PGPR is reported to generate a variety of essential metabolites for plants, which contribute in plant nutrition and overall plant vigor (Jabborova et al., 2020). In the present study strains of *Serratia nematodiphila* and *Pseudomonas plecoglossicida* having plant growth promoting potential areconfirmed from the Turmeric rhizosphere. In earlier studies also plant growth promoting *Pseudomonas* spp. were isolated from rhizosphere of Turmeric, Tomato and Wheat plant (Ansari et al., 2021; Takishita et al., 2018) whereas *Serratia nematodiphila* were isolated from pepperand rice plant (Kang et al., 2015; Khoa et al., 2016). These two PGPR strains were selected onthe basis of their various PGPR properties.

Table 4.3.1: Biochemical properties of potent isolates

Biochemical characters	*Pseudomonas plecoglossicida* RGK	*Serratia nematodiphila* RGK
Glucose	+	+
Adonitol	+	+
Arabinose	-	+
Catalase	+	+
Oxidase	-	+
Nitrate reduction	+	+
Starch hydrolysis	+	+
Citrate utilization	+	+

Note: + denotes Positive, - denotes Negative

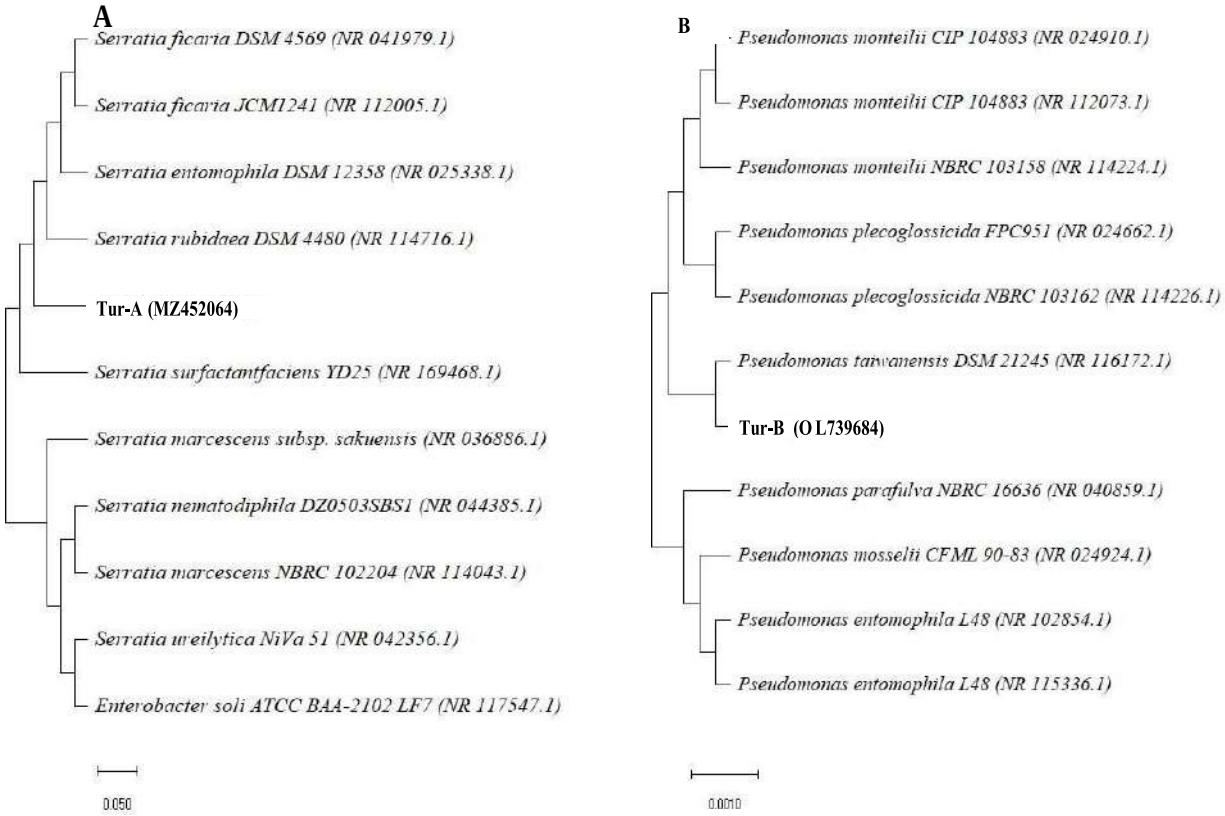

Fig. 4.3.1: Neighbor-joining phylogenetic tree based on16S rRNA gene sequence of the closelyrelated isolates of (A) *Serratia nematodiphila* RGK, (B) *Pseudomonas plecoglossicida* RGK bootstrap values on each branch point indicates 1000 pseudo replicates.

4.3.3.2 Plant growth promoting attributes of isolates

As indicated in Table 4.3.2, these two isolates showed maximum plant growth promoting characters such as phosphate solubilization, zinc solubilization, potassium solubilization, indole acetic acid (IAA) production, siderophore production, nitrogen fixation, hydrogen cyanide (HCN) production, ammonia production and exopolysaccharide synthesis. These isolates also showed amylase production, however *Serratia nematodiphila* RGK showed negative result for cellulase and chitinase production and *Pseudomonas plecoglossicida* RGK showed positive for these two enzymes production. Both of them were tolerant to high salt concentration. *Serratia nematodiphila* RGK tolerated up to 6.00% NaCl and *Pseudomonas plecoglossicida* RGK tolerated salt up to 7.00% NaCl.

Many other researchers also have demonstrated the potential of PGPR to dissolve phosphorus, potassium, and zinc (Soto et al., 2019; Bagyalakshmi et al., 2017; Shakeel et al., 2015). The solubilization of phosphate by numerous species of *Pseudomonas* and *Serratia* have also been documented (Sayyed et al., 2009; Khoa et al., 2016). Like phosphorous, potassium is also an important macronutrient, and its solubilization by PGPR enhances plant growth in anumber of commercial crops (Meena et al., 2016; Ajmal et al., 2021) has reported the solubilization of potassium by *Pseudomonas* and *Serratia*. Zinc also plays role in the plant metabolism by serving as a cofactor in number of enzyme processes (Parveen et al., 2018). Increase in zinc mobilization in wheat and soybean plants was found to be increased by treatment with *Bacillus, Pseudomonas,* and *Serratia* (Shakeel et al., 2015).

Both the strains of rhizobacteria in this work are producing IAA in the presence of tryptophan (Kumari et al., 2018) has reported the favorable impact of IAA synthesis on growthand elongation of root system, which aids in water and vital nutrients absorption. The results in our investigation are also in line with the earlier reports that shows the synthesis of IAA byPGPR such as *Serratia nematodiphila* NII-0928, *Pseudomonas* sp., *Agrobcterium tumifaciens, Burkholderia sp.,* and *Bacillus sp*. (Dastager & Ashok, 2011; Zhao et al., 2014).

Both the strains in our study are producing siderophores. Siderophores produced by rhizobacteria chelate Fe+3 and make it accessible to plants for growth. Several reports with regard to siderophore production by PGPR are well

documented. *P. fluorescence* NCIM5096 isolated from the groundnut field rhizosphere produced siderophores (Sayyed et al.,2009); *P. aeruginosa* isolated from the rhizosphere of a banana farm produced siderophore (Shaikh et al.,2014); ability of *S. nematodiphila* to produce siderophores helped to improve growth metrics of pepper plants (Kang et al.,2015).

Both the PGPRs in this work have ability to fix nitrogen as well as produce ammonia. Further *Serratia nematodiphila* RGK has the potential to produce HCN. According to Devi etal. (2022), PGPR can generate ammonia, siderophores, HCN, and N2 fixation. In one more study, bacteria isolated bacteria from the rhizosphere of the *L. hypogaea* plant were capable ofproducing HCN and fix nitrogen (Felestrino et al., 2017). Similarly, both the isolates in this study were producing exopolysaccharides, which may be crucial for bioremediation, microbialaggregation, plant-microbe interactions, and protection against desiccation. Enhanced soil moisture content, plant biomass, root and shoot length, leaf area, and leaf protein and sugar contents under drought stress conditions due to inoculation with EPS producing bacterial strains in plants such as maize and wheat is also previously reported (Naseem et al., 2014; Khanet al.,2017).

Isolates have also demonstrated enzyme synthesis which is in line with Jabborova et al., (2020) which demonstrated endophytic PGPR from ginger synthesize several enzymes. Further, *Serratia nematodiphila* RGK and *Pseudomonas plecoglossicida* RGK demonstrated up to 6% and 7% salt tolerance, respectively. Salinity is one of the most severe abiotic factors that affect crop development and yield. Under salt stress, PGPR has beneficial impacts on plant characteristics such as germination rate, drought tolerance, and root and shoot growth. Plants exposed to salt were protected by PGPR such as *Bacillus sp*. and *Pseudomonas sp*., (Chauhanet al., 2017).

Table 4.3.2: Plant growth promoting attributes of bacterial isolates

PGPR traits	***Pseudomonas plecoglossicida* RGK (OL739684)**	***Serratia nematodiphila* RGK (MZ452064)**
Phosphate solubilization	+	+
IAA production	+	+
Ammonia production	+	+
HCN production	-	+

Nitrogen fixation	+	+
Zinc solubilization	+	+
Potassium solubilization	+	+
Siderophore production	+	+
Salinity tolerance	7 %	6 %
Cellulase	+	-
Chitinase	+	-
Amylase	+	+
Exopolysaccharide production	+	+

Note: + denotes Positive, - denotes Negative

4.3.3.3 Antibiotic sensitivity test

Results showed that both isolates were sensitive to Gentamycin, Kanamycin, Streptomycin, Tobramycin and Amikacin. As listed in Table 4.3.3, *Serratia nematodiphila* RGK showed 20± 0.07mm, 24 ± 0.06mm,24 ± 0.07mm, 8 ± 0.04mm, 22 ± 0.07mm zone of inhibition respectively. In contrast, *Pseudomonas plecoglossicida* RGK showed 20 ± 0.05mm, 22 ± 0.07mm, 6 ± 0.02mm, 20 ± 0.03mm, 25 ± 0.06mm respectively. However, *Serratia nematodiphila* RGK was resistant to Oxytetracyclin, Furazolidone, Nitrofurantoin, and *Pseudomonas plecoglossicida* RGK shown resistance to Nitrofurantoin, Co-trimoxazole, Nalidixic acid. According to some previous reports, *Pseudomonas* and *Serratia* were likewise susceptible to the aforementioned drugs (Singh & Jha,2016; Capatina et al., 2022).

Table 4.3.3: Antibiotic resistivity of isolated PGPR strains against standard antibiotics andzone of inhibition (mm) given below

Antibiotics	***Pseudomonas plecoglossicida* RGK**	***Serratia nematodiphila* RGK**
Streptomycin	6 ± 0.02	24 ± 0.07
Oxytetracyclin	18 ± 0.07	-
Gentamycin	20 ± 0.05	20 ± 0.07
Furazolidone	15 ± 0.04	-
Co-trimoxazole	-	18 ± 0.05

Amikacin	25 ± 0.06	22 ± 0.07
Tobramycin	20 ± 0.03	8 ± 0.04
Nitrofurantoin	-	-
Kanamycin	22 ± 0.07	24 ± 0.06
Nalidixic acid	-	29 ± 0.07

4.3.3.4 Antifungal activity

As regard to the antifungal activity, fungistatic action was seen as a zone of growth inhibition in the area of the agar plate with bacterial inoculation. *Pseudomonas plecoglossicida* RGK shown antifungal activity against the fungus *Pythium aphanidermatum* while *Serratia nematodiphila* RGK doesn't showed it. *Pythium aphanidermatum* fungus, is responsible for rhizome rot of Turmeric. According to earlier study numerous species of *Pseudomonas* and *Serratia* have been demonstrated to exhibit antagonistic behavior towards different fungi and bacteria (Kumari et al., 2018; Passari et al., 2018; Khoa et al., 2016).

4.3.3.5 Pot culture experiment

Pot culture study was performed to determine the individual effect and the role of these PGPR in co-culture as well, and results revealed that the effect of co-culture is better than the individual application. Further, the effect was more in the natural soil than sterile soil. As demonstrated in Table 4.3.4a, 4.3.4b, 4.3.4c, rhizomes treated separately with *S. nematodiphila* RGK, *P. plecoglossicida* RGK and co-culture of both demonstrated progressive increase in the shoot height, leaf number, and rhizome biomass as compared to the control after45, 90 and 180 days. However, only the results after 180 days are described below.

The co-culture of *Serratia nematodiphila* RGK and *Pseudomonas plecoglossicida* RGK considerably increased the plant parameters in the pot culture experiment, and it was more than either strain alone and uninoculated control in both natural and sterile soil. Kumar et al., (2016) found that treatment with *P. fluorescens* CL12 improved plant development metrics including shoot height, leaf number, rhizome biomass, and curcumin content in *Curcuma longa*. Inoculation with diazotroph bacterial suspension (1:1 ratio of *Pseudomonas* and *Bacillus* sp.)

demonstrated considerable improvement in rhizome production (21%), plant height (5%), rhizome weight (60%) and soil microbial population over respective controls by (Suryadevara and Ponmurugan,2012) in natural soil. In another study it is found that when *Azotobacter, Bacillus, and Pseudomonas* were co-inoculated on a maize crop rather than whenthey were inoculated separately, the consortium significantly increased the dry weight of the maize (0.50 g plant-1) (Jarak et al., 2012). Under the pot culture experiment and field circumstances, the microbial consortia significantly affected the physiological and growth characteristics of the *Amaranthus* crop, as reported by Devi et al., (2022). As per the literature and practical investigations, combined inoculation produces successful outcomes when thereis a synergistic link between the microorganisms.

4.3.3.5.1 Shoot height

S. nematodiphila RGK had shwon the increament in shoot height by 61, 83 and 85 % after 45, 90 and 180 days in natural soil. While in sterile soil it showed 46, 80 and 81 % of rise in the shoot height. Similarly in case of treatment with *P. plecoglossicida* RGK the increment was 74, 90 and 95 % after 45, 90 and 180 days respectively in natural soil, while in sterile soil it showed the incerement as 65, 86 and 90 % after same interval of days. When a Turmeric plant treated with co-culture of these PGPRs (*S. nematodiphila* RGK + *P. plecoglossicida* RGK) it showed the increased in shoot height after 45, 90 and 180 days as 97, 110 and 116% in natural soil while in sterile soil it showed as 84, 100 and 113 % increase after 45, 90 and 180 days when compare with its control (Table 4.3.4a)

4.3.3.5.2 Leaf number

As regard to the leaf number, treatment with *S. nematodiphila* RGK showed the increment by 40, 46 and 60 % after 45, 90 and 180 days in natural soil. While in sterile soil it showed 25, 37.5 and 46 % of increase in the leaf numbers. Similarly in case of treatment with *P. plecoglossicida* RGK, it showed the enhanced leaves number after 45, 90 and 180 days as 32, 60 and 79% respectively in natural soil while in sterile soil it showed the increment as 25, 50 and 70 % after 45, 90 and 180 days. When a Turmeric plant treated with co-culture of these PGPRs (*S. nematodiphila* RGK + *P. plecoglossicida* RGK) it showed the increased leaves

number after 45, 90 and 180 days as 60, 66 and 114% in natural soil while in sterile soil it showed as 50, 62.5 and 106 % increase after 45, 90 and 180 days when compare with its control (Table 4.3.4b)

4.3.3.5.3 Rhizome biomass

In contrast, *S. nematodiphila* RGK had shown the increament in rhizome biomass by 29, 48 and 78 % after 45, 90 and 180 days in natural soil. While in sterile soil it showed 25, 45 and 56 % of increase in the rhizome biomass. Similarly in case of treatment with *P. plecoglossicida* RGK, it showed the increment as 41, 73 and 105 % after 45, 90 and 180 days respectively in natural soil, while in sterile soil it showed the increase as 37, 62 and 88 % after same interval of days, that is 45, 90 and 180. When a Turmeric plant treated with co-culture of these PGPRs (*S. nematodiphila* RGK + *P. plecoglossicida* RGK) it showed the increased in rhizome biomass after 45, 90 and 180 days as 76, 130 and 208 % in natural soil while in sterile soil it showed as 87, 127 and 188 % increase after 45, 90 and 180 days when compare with its control (Table 4.3.4c).

Table 4.3.4a: Shoot height of Turmeric after inoculation with PGPR

Parameter	Shoot height (cm) after 45, 90 and 180 days											
	Control			*S. nematodiphila* RGK			*P. plecoglossicida* RGK			Co-culture of both these PGPR		
	Days			Days			Days			Days		
	45	90	180	45	90	180	45	90	180	45	90	180
N	22.83 ±0.13	47.33 ±0.5	60.5 ±0.3	36.83 ±0.13	87 ±0.86	112 ±0.4	39.83 ±0.1	90.24 ±1.02	118 ±0.23	45 ±0.4	99.5 ±0.4	131 ±0.7
S	19.83 ±0.14	43 ±0.8	47 ±0.8	29 ±0.8	77.5 ±0.8	85.4 ±0.4	32.83 ±0.1	80 ±0.4	89.5 ±0.4	36.5 ±0.4	86.3 ±0.6	100 ±0.4
% Increase over control(N)	-	-	-	61	83	85	74	90	95	97	110	116
% Increase over control (S)	-	-	-	46	80	81	65	86	90	84	100	113

N (natural soil) S (sterile soil). The values represent the average of three experiments ± SD. ANOVA using Tukey's comparison test yielded a significant difference from control group at $p \leq 0.05$, and the relative standard deviation for all values are less than 10.

Table 4.3.4b: Leaf number of Turmeric after inoculation with PGPR

Parameter	Leaf number after 45, 90 and 180 days											
	Control			*S. nematodiphila* RGK			*P. plecoglossicida* RGK			Co-culture of both these PGPR		
	Days			Days			Days			Days		
	45	90	180	45	90	180	45	90	180	45	90	180
N	2.5 ±0.4	5 ±0.4	6 ±0.4	3.5 ±0.4	7.3 ±0.6	9.6 ±0.2	3.3 ±0.2	8 ±0.4	12.5 ±0.5	4 ±0.4	8.3 ±0.2	15 ±0.4
S	2 ±0.4	4 ±0.3	5 ±0.4	2.5 ±0.2	5.5 ±0.4	7.3 ±0.2	2.5 ±0.4	6 ±0.4	8.5 ±0.6	3 ±0.7	6.5 ±0.1	10.3 ±1.2
% Increase over control (N)	-	-	-	40	46	60	32	60	79	60	66	114
% Increase over control (S)	-	-	-	25	37.5	46	25	50	70	50	62.5	106

N (natural soil) S (sterile soil). The values represent the average of three experiments ± SD. ANOVA using Tukey's comparison test yielded a significant difference from control group at $p \leq 0.05$, and the relative standard deviation for all values are less than 10.

Table 4.3.4c: Rhizome biomass of Turmeric after inoculation with PGPR

Parameter	Rhizome biomass (gm) after 45, 90 and 180 days											
	Control			*S. nematodiphila* RGK			*P. plecoglossicida* RGK			Co-culture of both these PGPR		
	Days			Days			Days			Days		
	45	90	180	45	90	180	45	90	180	45	90	180
N	0.17 ±0.08	1.3 ±0.04	3.8 ±0.08	0.22 ±0.08	1.93 ±0.08	5.51 ±0.008	0.24 ±0.008	2.2 ±0.8	6.33 ±0.01	0.3 ±0.08	3 ±0.08	9.5 ±0.4
S	0.08 ±0.05	0.77 ±0.08	2.23 ±0.4	0.1 ±0.02	1.12 ±0.01	3.5 ±0.4	0.1 ±0.05	1.2 ±0.2	4.21 ±0.2	0.15 ±0.05	1.75 ±0.08	6.43 ±0.4
% Increase over control(N)	-	-	-	29	48	78	41	73	105	76	130	208
% Increase over control (S)	-	-	-	25	45	56	37	62	86	87	127	188

N (natural soil) S (sterile soil). The values represent the average of three experiments ± SD. ANOVA using Tukey's comparison test yielded a significant difference from control group at $p \leq 0.05$, and the relative standard deviation for all values are less than 10

4.3.3.6 Phytochemical analysis of Turmeric extract

In terms of total phenolic content (TPC), total flavonoid content (TFC) in mg/gm and DPPH radical scavenging activity in percent inhibition, the phytochemical analysis of Turmeric extract is given in Table 4.3.5a, 4.3.5b and 4.3.5c. It demonstrates that the co-culture treated plants had greater phenolic and flavonoid contents than untreated plants after 45, 90, and 180 days. Further, all of the samples showed significant free radical scavenging activity against DPPH. Plants treated with individual PGPRs and co-culture of PGPRs in natural soil had elevated TPC, TFC, and DPPH levels after 180 days.

In the current study we found that the treatment with bacterial co-culture increases the levels of total phenolic content, flavonoid content, DPPH radical scavenging, and curcumin content. In natural and sterile soil, a combination of these PGPR increased phenolic content by 42.5% and 39.2%, respectively, after 180 days while increase in flavonoid content was by 38.7% and 27.5%. In both types of soil, the plants treated with a co-culture demonstrated improved antioxidant activity by 53% and 51%. Devi et al., (2022) found that the co-culture increases total content of phenolics and flavonoids in the range of 0.67 to 1.07 and 0.998 to 1.029, respectively, in seeds of *Amaranthus hypochondrius* L. The results of Ham et al., (2022) demonstrated that the PGPR treatment of *G.aleppicum* increased the total phenol and flavonoid content. According to Dutta et al., (2016), the inoculation of turmeric plants with a bacterial and fungal consortia led to an increase in the total phenolic, flavonoid, antioxidant and curcumin contents in the rhizomes. As per the work by Jain et al., (2014), *Trichoderma harzianum*, *Pseudomonas aeruginosa*, and *Bacillus subtilis* individually and in consortia increased the amount of phenolic and flavonoids in pea plants. Similarly, *S. nematodiphila* has been shown to stimulate the antioxidative enzyme activity in *Solanum nigrum* (Wan et al., 2012).

Table 4.3.5a: Total phenolic content of Turmeric inoculated with PGPR

	Phenolic content after 45, 90 and 180 days (mg/gm)											
	Control			***S. nematodiphila* RGK**			***P. plecoglossicida* RGK**			**Co-culture of both these PGPR**		
	Days			**Days**			**Days**			**Days**		
	45	**90**	**180**	**45**	**90**	**180**	**45**	**90**	**180**	**45**	**90**	**180**
N	62.31 ±0.02	87 ±0.7	103.3 ±0.01	64.2 ±0.03	98.2 ±0.01	122.5 ±0.02	65.5 ±0.01	99 ±0.03	123 ±0.04	68.4 ±0.02	120 ±0.01	147.2 ±0.08
S	39.2 ±0.02	54.6 ±0.02	61.3 ±0.03	40 ±0.03	59 ±0.01	69 ±0.07	40.5 ±0.02	62 ±0.04	71.5 ±0.02	43 ±0.01	74 ±0.03	85 ±0.09
% Increase over control(N)	-	-	-	3.16	12.8	18.6	5.2	13.7	19	9.7	37.9	42.3
% Increase over control(S)	-	-	-	1.96	8.02	13.6	3.24	13.51	16.42	9.61	35.4	39.2

(N) natural soil (S) sterile soil. The values represent the average of three experiments ± SD. ANOVA using Tukey's comparison test yielded a significant difference from control group at $p \leq 0.05$, and the relative standard deviation for all values are less than 10

Table 4.3.5b: Total flavonoid content of Turmeric inoculated with PGPR

	Flavonoid content after 45, 90 and 180 days (mg/gm)											
	Control			***S. nematodiphila* RGK**			***P. plecoglossicida* RGK**			**Co-culture of both these PGPR**		
	Days			**Days**			**Days**			**Days**		
	45	**90**	**180**	**45**	**90**	**180**	**45**	**90**	**180**	**45**	**90**	**180**
N	203 ±0.07	217 ±0.03	239 ±0.06	213 ±0.05	231 ±0.02	284 ±0.01	205 ±0.01	248 ±0.01	292 ±0.01	221 ±0.06	265 ±0.01	332 ±0.05
S	170 ±0.01	201 ±0.05	235 ±0.06	175 ±0.08	213 ±0.05	282 ±0.08	172 ±0.06	225 ±0.08	278 ±0.06	185 ±0.04	240 ±0.01	300 ±0.04
% Increase over control(N)	-	-	-	5.1	6.5	18.1	0.8	14.1	21.9	8.6	22.3	38.7
% Increase over control(S)	-	-	-	2.7	5.6	19.8	0.6	11.5	18.1	8.3	19	27.5

(N) natural soil (S) sterile soil. The values represent the average of three experiments ± SD. ANOVA using Tukey's comparison test yielded a significant difference from control group at $p \leq 0.05$, and the relative standard deviation for all values are less than 10

Table 4.3.5c: Percent inhibition for DPPH activity of Turmeric inoculated with PGPR

	Percent inhibition for DPPH activity after 45, 90 and 180 days											
	Control			**S. *nematodiphila* RGK**			***P. plecoglossicida* RGK**			**Co-culture of both these PGPR**		
	Days			**Days**			**Days**			**Days**		
	45	**90**	**180**	**45**	**90**	**180**	**45**	**90**	**180**	**45**	**90**	**180**
N	11 ±0.03	34 ±0.08	41 ±0.02	14 ±0.2	43 ±0.01	52 ±0.1	13 ±0.1	49 ±0.06	59 ±0.02	15 ±0.2	52 ±0.6	63 ±0.5
S	10.35 ±0.02	30.13 ±0.02	39 ±0.03	12 ±0.01	34 ±0.02	47 ±0.07	11 ±0.01	41 ±0.03	54 ±0.5	14 ±0.02	43 ±0.06	59 ±0.01
% Increase over control(N)	-	-	-	25	22	26	10	42	43	35	48	53
% Increase over control (S)	-	-	-	15	12	20	6	36	38	35	42	51

(N) natural soil (S) sterile soil. The values represent the average of three experiments ± SD. ANOVA using Tukey's comparison test yielded a significant difference from control group at $p \leq 0.05$, and the relative standard deviation for all values are less than 10.

4.3.3.7 Separation of secondary metabolites

The TLC profile revealed three distinct spots with RF values of 0.28, 0.54 and 0.77. They were confirmed as bisdemethoxycurcumin, demethoxycurcumin and curcumin by comparison with the values in mixed standards. All of these spots showed fluorescence under UV light. Fig.4.3.2.

The curcumin and two additional curcuminoids, demethoxycurcumin and bisdemethoxycurcumin, are the most bioactive secondary metabolites and constitute the active component of turmeric (Wichitnithad & Rojsitthisak, 2009). In the present study separation ofthese compounds with the help of TLC was carried out.

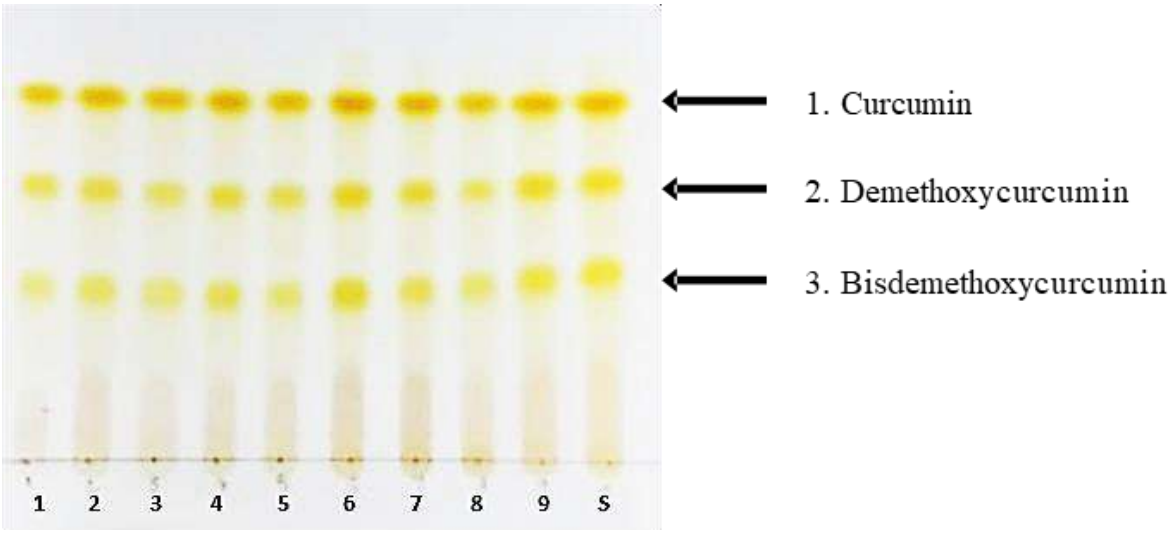

Fig.4.3.2: TLC profile showing separation of methanol extracts of *Curcuma longa* on silica gel TLC plate (20cm x 20cm). Where, S is mixed standards and 1-9 are rhizome extracts.

4.3.3.8 Extraction and analysis of secondary metabolites

4.3.3.8.1 GC-MS/MS analysis

The GC chromatogram shows retention durations, whereas MS analysis looks at compound fragmentation patterns, mass peaks, base peaks, m/z values, peak intensities and soon. A matching number of peaks were used in conjunction with these m/z values to confirm compound identification. The retention time, approximate concentration in the extract (peak area %), molecular weight, molecular formula and structures of identified secondary metabolites are depicted in the chromatograms Fig. 4.3.3 Total 22 metabolites were found in PGPR treated plant extracts. Control plants were showing 7 compounds, *P. plecoglossicida* RGK treated were showing 7, *S. nematodiphila* RGK treated plants were showing 12 compounds and consortia treated were showing 15 compounds. Among these, four were

sesquiterpenoids, one was triterpene, one was a derivative of hydrocarbon and two were phenols. The metabolites were identified by National Institute of Standard and Technology (NIST) Database and its abundance in percentage given in Table 4.3.6

In our investigation, we found that, in addition to curcumin, a few essential oils such as turmerone, phenolics such as 4-hydroxy 2-methyl acetophenone (ethanone), and sesquiterpenoids such as curlone (bisabolane) are elevated in co-culture treated plants as compared to untreated plants with biological activities. The analysis of these metabolites was performed with the assistance of GCMS. According to earlier research, PGPR inoculation with *Exiguobacterium oxidotolerans* increases the secondary metabolite bacoside-A in *Bacopa monnieri* L. (Bharti et al., 2013). A recently reported PGPR has also shown that rose scented geranium has enhanced plant characteristics and essential oil content in *Pelargonium graveolens cv. Bourbon*. (Dharni et al., 2014; Rahmoune et al., 2017). One of the known PGPRs, *Serratia sp*., can promote the development of plants by a variety of processes, including the synthesis of secondary metabolites including auxins, cytokinin, gibberellins, and HCN, as well as the solubilization of phosphate minerals. In a previous investigation, it was also shown that *S. nematodiphila* PEJ1011 can produce the plant hormone gibberellin (Kang et al., 2015).

4.3.3.8.2 RP-HPLC analysis

Curcumin content determined after 45, 90 and 180 days has been given in Table 4.3.7 UV absorbance was also examined at 425 nm. The UV detector showed curcumin peak at 425nm. Curcumin has an 11 minutes retention time. The purity of compound was determined by comparing it to a curcumin standard peak Fig.4.3.4 The HPLC analysis showed that increased curcumin content in individual PGPR treated plant as well as co-culture treated plant in natural soil after 180 days. Turmeric plant treated with *S. nematodiphila* RGK had shown the increment in the curcumin content by 5.8 % and 4.6% in natural and sterile soil respectively after 180 days. While, *P. plecoglossicida* RGK showed the enhanced curcumin content after 180 days by 4.8 % and 4.3% in natural and sterile soil respectively. Treatment with co-culture showed the increased curcumin content after 180 days in natural and sterile soil by 8.2% and 6.3% respectively.

In this study, co-culture inoculation significantly increased curcumin content as compared to a single bacterial treatment and a control. Dutta et al, (2016) found a considerably greater concentration of secondary metabolites (total phenolics, total flavonoids, and

curcumincontent) in turmeric rhizome. According to Kumar et al, (2016), *P. fluorescens* inoculations increased curcumin concentrations in Turmeric by 18% as compared to a control. The route of action of PGPR is currently not well understood, however in tomato, *P. fluorescens* exhibited chemotactic sensitivity to several amino acids (Oku et al., 2012). Turmeric rhizome contains phenolics like curcuminoids and sesquiterpenoids that may attract PGPR to the roots, resultingin improved nutrient intake and growth (Kumar et al., 2014). It is feasible to obtain a favorable response to *Pseudomonas plecoglossicida* RGK and *Serratia nematodiphila* RGK inoculation for curcumin production because PGPR serves as potent elicitors of key enzymes involved in secondary metabolite biosynthesis pathways, which are associated to plant defensive responsesagainst pathogenic infections (Wan et al., 2012).

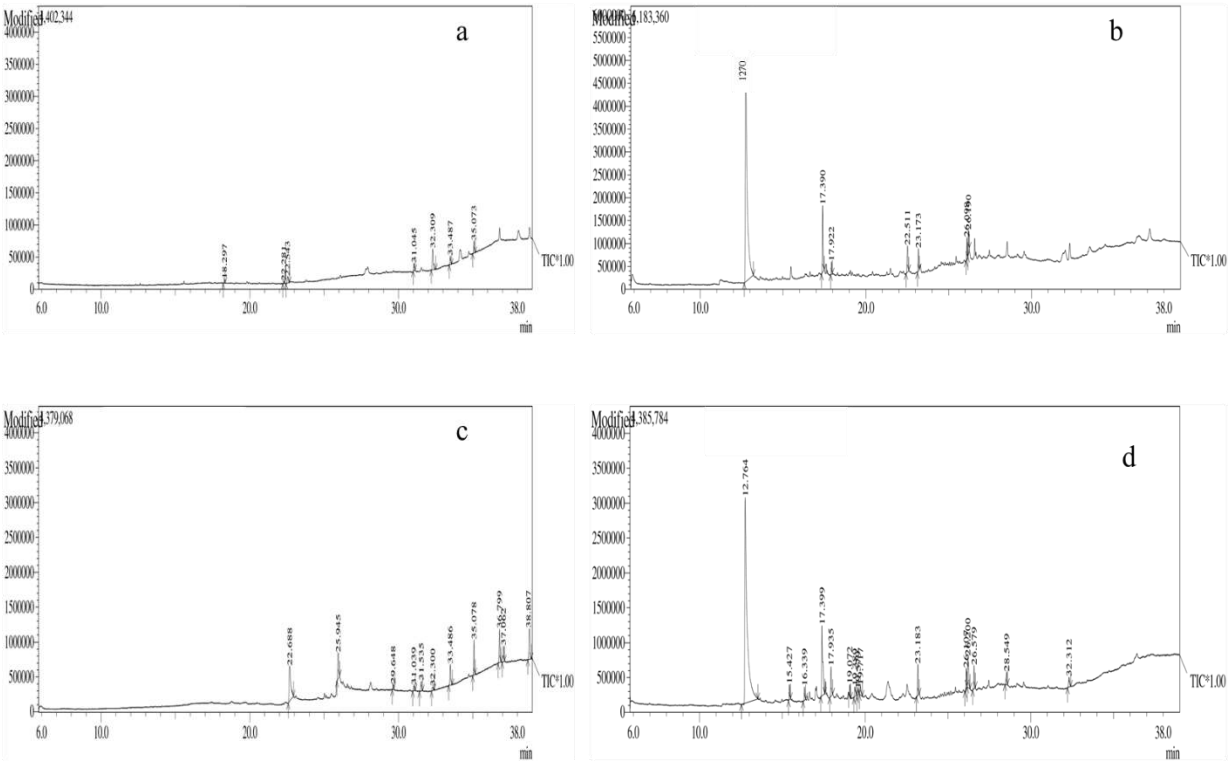

Fig. 4.3.3: The gas chromatography–tandem mass spectrometry graph with various peaks of *C. longa* where (a) Chromatogram of control Turmeric(uninoculated) (b) Chromatogram of *Pseudomonas plecoglossicida* RGK inoculated Turmeric (c) Chromatogram of *Serratia nematodiphila* RGK inoculated Turmeric (d) Chromatogram of co-culture of both inoculated Turmeric.

Table 4.3.6: Secondary metabolite profile of Turmeric identified by GC-MS/MS

S. No.	Name of Identified Compounds	Category	Retention time	Area%	Control	*P. plecoglossicida* RGK	*S. nematodiphila* RGK	Co-culture of both
1	Ethanone, 4-Hydroxy-2-methylacetophenone	Phenol	12.75	65± 77*	-	+	-	+
2	2,4-Di-tert-butylphenol	Phenol	15.42	1.35	-	-	-	+
3	Butyric acid, 2-phenyl-, dodec-2-en-1-yl ester	Fatty acid	16.33	1.18	-	-	-	+
4	aR-Turmerone	Sesquiterpene	17.93	8±10*	-	+	-	+
5	2-Methyl-6-(4-methyl enecyclohex-2-en-1-yl), curlone	Bisabolane	17.92	1± 3*	-	+	-	+
6	(Z)-.gamma.-Atlantone	Bisabolane	19.38	1.38	-	-	-	+
7	Isopropyl myristate	Fatty acid	19.57	0.44	-	-	-	+
8	Ethyl 14-methyl-hexa decanoate	Fatty acid	23.18	3.24	-	+	-	+
9	trans, trans-9,12-Octa decadienoic acid, propyl	Fatty acid	26.10	1.57	-	-	-	+
10	Ethyl Oleate	Ester of fatty acid	26.20	4.94	-	+	-	+

11	1-Hexadecanethiol	Alkane	26.57	2.05	-	-	-	+
12	Bis(2-ethylhexyl) phthalate	Esters of phthalic acid	32.13	1± 2*	+	-	+	+
13	Eicosane	Derivative of hydrocarbon	18.29	1± 4*	+	-	+	-
14	Tetracontane	N alkane	35	11± 16	+	-	+	-
15	Tetrapentacontane	N alkane	22.28	2.68	-	-	+	-
16	1, ,4-Cyclohexanediol, (Z)-,TMS derivative	Polyester resin	31.04	11.28	+	-	-	-
17	n-Hexadecanoic acid	Fatty acid	22.68	27.21	-	-	+	-
18	Dichloroacetic acid	Acid	25.94	12.13	-	-	+	-
19	1,3,5-Trisilacyclohexane	Acid	31.03	1.79	-	-	+	-
20	Dotriacontane	N alkane	33.48	7.09	-	-	+	-
21	Squalene	Triterpene	37.06	6.09	-	-	+	-
22	11,14-Eicosadienoic acid, methyl ester	Fatty acid	26.09	2.29	-	+	-	-

Note: + denotes present, - denotes absent, *P. plecoglossicida* RGK +, Co-culture of both *

Table 4.3.7: Curcumin content after 45, 90 and 180 days

	Curcumin content in percentage (%)					
	45 days		**90 days**		**180 days**	
	N	**S**	**N**	**S**	**N**	**S**
Control	0.6	0.12	2.6	2.1	4.01	2.4
***S. nematodiphila* RGK**	1.27	1.1	3.09	2.09	5.88	4.66
***P. plecoglossicida* RGK**	1.25	1.1	3.04	2.04	4.08	4.03
Co-culture of both PGPR	2.0	1.55	4.08	3.55	8.02	6.03

Note: N denotes (natural soil), S denotes (sterile soil).

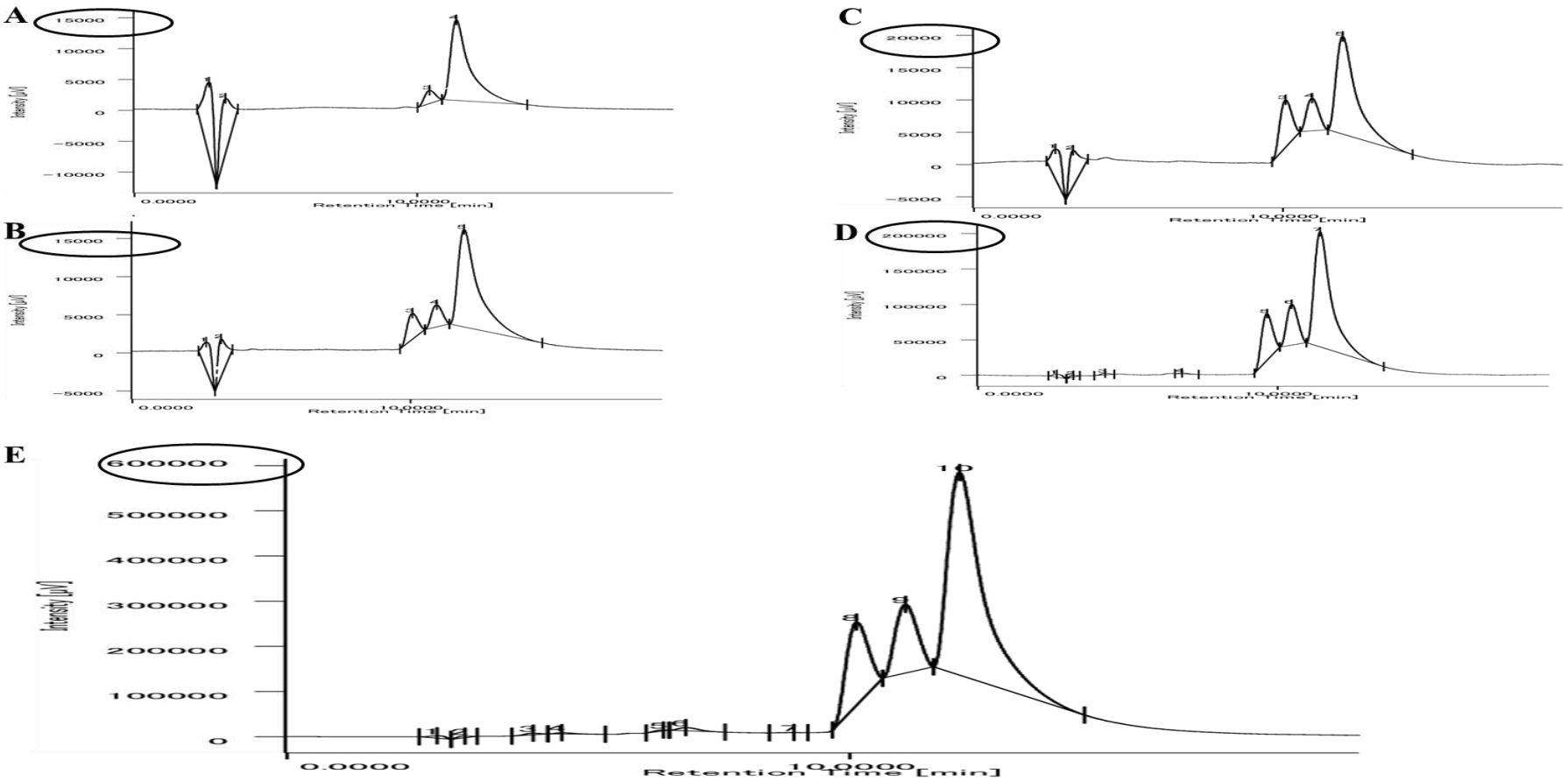

Fig. 4.3.4: HPLC chromatogram of Turmeric extracts at 425. (A) Chromatogram of standard ofcurcumin. (B) Chromatogram of control Turmeric (uninoculated). (C) Chromatogram of *Serratia nematodiphila* RGK inoculated Turmeric. (D) Chromatogram of *Pseudomonas plecoglossicida* RGK inoculated Turmeric. (E) Chromatogram of co-culture inoculated Turmeric.

4.3.4 Conclusions:

In the present study, we found that combination of both the PGPR inoculations yielded better effects than a single inoculation. Furthermore, these findings suggest that phenolic compounds and flavonoids have a favorable link with anti-radical activities, implying that the bioinoculants utilized on the Turmeric rhizosphere are efficacious. These phytochemicals can be used as an effective remedy for various ailments and drug formulations in the future, either alone or in combination with other suitable agents. This co-culture of PGPR inoculation would be one of the finest solutions for a sustained Turmeric agroindustry.

The primary benefit of employing PGPR is that they have a dual positive impact, acting as both a full biofertilizer and a biofortifier of plants, giving a remedy for nutritional deficiency and agro-environmental issues. Here we found enhanced plant parameters and phytocompounds in Turmeric following PGPR individually and in combination inoculation in natural soil rather than sterile soil. Our research revealed an interesting finding that after 180 days, the co-culture treated plant has a greater quantity of the secondary metabolite 4-hydroxy-2-methylacetophenone. We report here for the first time that 4-hydroxy-2-methylacetophenone is found in *Curcuma longa*, combined with a high percentage of curcumin.

4.4 Extraction, purification, quantification and bioactivity of secondary metabolites from PGPR treated *C. longa* and *A. racemosus*

Manuscript under preparation:

4.4.1 Introduction:

Plant secondary metabolites are mostly biosynthesized via three major pathways: the isoprenoid pathway, the shikimate pathway, and the polyketide pathway (Joulain 2021). The defense against biotic and abiotic stress is primarily mediated by the secondary metabolites of plants (Sun et al., 2019). Secondary metabolites and their derivatives such as phenolics, flavonoids, terpenes, saponins, alkaloids, glycosides, tannins, anthraquinones, essential oils, and steroids are examples of biologically active compounds (Egamberdieva & Teixeira da Silva, 2015). Plants are renewable resources that provide raw materials (such as lignocellulosic biomass) and phytochemicals (particularly secondary metabolites) for a variety of industrial applications, including textiles, building materials, pharmaceuticals, nutraceuticals, and cosmetics. Plants are thought to be essential for promoting the transition to a bio-economy that is less reliant on fossil fuels because of these characteristics (Guerriero et al., 2018).

A significant quantity of secondary metabolites are present in medicinal plants (John et al., 2014). According to Anandet al. (2019), these plants generate a wide range of secondary metabolites as a result of numerous metabolic processes, which are essential for enhancing the immune system in the treatment of illnesses. For instance, curcumin, a key ingredient in turmeric (Kumar et al., 2016 a, b), has been frequently used to both treat and prevent diabetes. It has been demonstrated that to maintain stable blood glucose levels, it increases postprandial serum insulin levels (Meng et al., 2013). Since the dawn of civilization, plant secondary metabolites (natural compounds) have been employed to treat a wide range of human illnesses, including chronic disorders (Kumar et al., 2021). These active compounds produced from plants are widely employed as secretagogues or insulin mimics(Patel et al., 2012). More than 25% of current medications are derived from plants, while natural product derivatives account for 60% of anti-cancer and 60% of anti-tumor drugs (Kumar et al., 2021).

The discovery of therapeutic agents and the identification of new sources of bioactive compounds depend on the phytochemical analysis of ethnomedicinal plants for secondary metabolites, which is a crucial area of fundamental research (Dutta, 2015). Several extraction methods were carried out in isolation of phytocompounds (Ibanez and Blazquez, 2021).For example, secondary metabolites such as phenolics, flavonoids and tannins can be separated and purified with help of repeated silica gel, RP-8, diaion, sephadex-LH20, MCI-gel, RP-18, and toyopearl chromatography columns (Chen et al.,

2017). Anticancer constituents that have been detected and isolated from terrestrial plants include brassinosteroids, polyphenols, and taxols (Greenwell & Rahman, 2015).

C. longa and *A. racemosus* were used in this study, and previously several extraction processes were used to isolate secondary metabolites from Turmeric, including steam distillation, soxhlet extraction, ultrasonic extraction, and solvent extraction (Ibanez and Blazquez, 2021). Traditionally, curcuminoids which are major component of Turmeric were extracted using solid-liquid or liquid-liquid extraction, followed by isolation using repeated column chromatography technology (Verghese and Joy, 1989). The separation of metabolites on column chromatography, such as silica gel column chromatography, is essentially based on polarity, with phenolic compounds containing more hydroxyl groups being more firmly adsorbed (Chen et al., 2017). Many studies have employed and reported on column chromatography for the discovery and identification of novel compounds, some of which have been associated to antibacterial, antimicrobial, and antifungal characteristics. Similarly, gas chromatography (GC and GC-MS) is a very potent analytical method for distinguishing the different components of essential oils. Mass spectrometry and retention indices have both been used to precisely identify the makeup of essential oils (Agostini-costa et al., 2012). Chaudhary et al, (2018) previously reported, the methods of diosgenin extraction from yams and high-performance liquid chromatography (HPLC)analysis are well-known and frequently employed (Chaudhary et al., 2018). A number of standard methods for detecting diosgenin and curcuminoids have been developed, including thin-layer chromatography (TLC). This technique has also been used successfully to obtain sufficient amounts of a substance to investigate its biological properties and detect its olfactory properties (Agostini-costa et al., 2012; Pushpakumari et al., 2014)

This study was designed to use an easy and effective method for extracting curcuminoidsand diosgenin from *C. longa* and *A. racemosus*, respectively. Curcumin was also purified by silicagel column chromatography, and diosgenin was acid hydrolyzed, and their quantification using HPLC was carried out as well. Furthermore, antibacterial, antifungal, and antibiofilm studies wereconducted.

4.4.2 Material and method:

4.4.2.1 Extraction of plant secondary metabolites

The uprooting of plants was done after 45, 90 and 180 days and proceeded for

secondary metabolite extraction. After uprooting rhizomes and roots were rinsed with distilled water to eliminate adhered soil. It was then cut into small pieces and dried in oven at 40℃ to make a fine powder. This powder was used for the metabolite extraction process. Different solvents and extraction techniques were used to extract plant secondary metabolites. Below are some additional effective extraction techniques.

4.4.2.1.1 Soxhlet Extraction

Soxhlet extraction was carried out using standard apparatus. 1 gm of powdered rhizomes with 250 ml of each hexane, methanol, acetone, petroleum ether, diethyl ether and ethanol as solvent were used with the extraction time of 8 hrs. The organic extracts were concentrated usinghot plate and stored at 4℃ for further analysis.

4.4.2.1.2 Sonication for Turmeric and Asparagus

In a sealed tube, 1 gm of sample was added to 10 ml of methanol. The mixture was then treated in a bath sonicator for 1 hour at room temperature and centrifuged at 5000 rpm for 10 minutes at 4 °C. Supernatant was collected for further analysis.

4.4.2.2 Purification of plant secondary metabolites

Separation and purification of secondary metabolites from PGPR treated and non-treated plantswere done using following techniques

4.4.2.2.1 Purification of curcuminoids by silica gel column chromatography

Methanolic extract was subjected to silica gel column chromatography (60-120 mesh). Topack the column, silica gel was dissolved in chloroform: methanol (98:2) and filled upto 46 cm. Then sample was added on the top of gel and eluted with chloroform followed by chloroform: methanol with increasing polarity. All fractions were collected and subjected to UV spectrophotometry at 425 nm (Heffernan et al., 2017).

4.4.2.2.2 Thin layer chromatography (TLC) for curcuminoids

The collected fractions were tested on pre-coated Silica gel (Merck, Darmstadt, Germany) TLC plates along with standard curcuminoid. The plates were developed using pre-saturated TLCchamber for 1 hr. chloroform: methanol (95:5 v/v) was used as mobile phase. Each plate was developed up to the height of about 12 cm. The plates were then removed and dried. Spots were analyzed and Rf values were calculated (Zhang et al., 2008; Peret-Almeida et al., 2005).

4.4.2.2.3 Purification of curcumin

Curcumin was further purified from separated spots on TLC. The uppermost spot which was of curcumin (based on Rf value) was scrapped, dissolved in methanol and kept in refrigeratorovernight. The supernatant was then collected, evaporated and concentrated. It was used for furtherpurification by silica gel column chromatography (Revathy et al., 2011).

4.4.2.2.4 High Performance Liquid Chromatography for curcumin

For the purification of small organic molecules like drugs, peptides, microbial metabolites,plant metabolites and antibiotics, high-performance liquid chromatography (HPLC) is a highly effective and high-resolution technique (Smyth et al., 2014; Dhanarajan et al., 2015). As part of the recovery of the purification method, HPLC was also used to quantify the metabolites. This method involves the interaction of liquid solvent in the tightly packed solid column or a liquid column. Parameter used during HPLC purification of Curcumin are given below in Table 4.4.1

Table 4.4.1: Parameter used for purification of Curcumin

Parameter used during HPLC purification of Curcumin

Column	C_{18}
Detector	Diode Array detector
Solvent system/Mobile phase	The mobile phase was 50:50 (v/v) acetonitrile and 2% acetic acid
Flow rate	0.5ml/min
Wavelength of detection	425nm
Sample volume	20 µl
Working temperature	25°C
Standard curcumin	100– 500 µg/ml

4.4.2.2.5 Purification of diosgenin by acid hydrolysis

5 gm of Asparagus plant powder was hydrolyzed in 50 ml of 2 M sulphuric acid by heating under refluxation for 2 hrs. After cooling, 40% sodium hydroxide was added to the solution to neutralize it. The hydrolysis product was then extracted using an equal

amount of chloroform (Wang et al., 2011; Yang et al., 2015). The extract was separated by a separating funnel and concentrated by 60°C evaporation. The residue was combined with the standards for TLC analysis after being dissolved in methanol and applied to precoated silica gel.

4.4.2.2.6 Thin layer chromatography (TLC) for diosgenin

Thin-layer chromatography was performed on plates precoated with silica gel (Merck, Darmstadt, Germany). The samples were developed with hexane-acetone (8:2) as the mobile phase with a few minor modifications, dried to ensure that all solvents had evaporated, and detected witha 0.5:5 mixture of ethanol (8% vanillin) and sulfuric acid solution (70%) (Hardman, 1968

4.4.2.2.7 High Performance Liquid Chromatography for Diosgenin

Parameter used during HPLC purification of Diosgenin are given below in Table 4.4.2

Table 4.4.2: Parameter used for purification of Diosgenin

Parameter used during HPLC purification of Diosgenin

Column	C_{25}
Detector	Diode Array detector
Solvent system/Mobile phase	The mobile phase was 10:90 (v/v) HPLC-grade water and acetonitrile
Flow rate	0.8ml/min
Wavelength of detection	194 nm
Sample volume	25 µl
Working temperature	27℃
Standard diosgenin	20 – 100 µg/ml

4.4.2.2.8 Gas Chromatography-Mass spectroscopy (GC-MS/MS)

Phytochemicals were analyzed qualitatively and quantitatively using gas chromatography-mass spectrometry (GC-MS/MS). The samples were transformed into a gaseous condition, and analysis based on the mass-to-charge ratio was then completed (Balamurugan et al., 2019). Curcuminoid fractions were subjected to GC-MS/MS analysis

for the purpose of compound identification. The HS 2010 Plus (SHIMADZU) MS TQ 8050 mass detector, column SH-Rxi-5Sil MS with (30mm 0.25mm ID 0.25m), and helium as a carrier gas were utilized in the GC-MS/MS study of metabolites. The temperature of the sample injection was 250°C, the auxiliary temperature was 290°C, the ion source temperature was set to 280°C, the oven temperature ranged from 50°C to 275°C, and the GC ran for 38-52 minutes. The metabolites were identified by National Institute of Standard and Technology (NIST) database.

4.4.2.2.9 Liquid chromatography and mass spectroscopy (LC-MS/MS)

ThermoFisher Scientific's Ultimate 3000-series MS was used for the HPLC-Quadrupole-Orbitrap analysis (Bremen, Germany). The subsequent was a part of the mobile phase: Formic acid is present in water and acetonitrile at 0.1% each. With a flow rate of 0.4 mL/min, the gradient programme was adjusted to 0-10 min/98% A, 11.1 min/2% A, and 16 min/2% A. The following values were used to calculate the heated electrospray ionisation (H-ESI, positive mode) parameters: capillary temperature, 320 °C; S-lens RF level, 50.0; sheath gas flow rate, 45; auxiliary gas flow rate, 8; sweep gas flow rate, 1; spray voltage, 3.50 kV; and heater temperature, 300 °C. The MS analysis was performed in ddMS2 mode. The mass range of 100-1000 Da was employed for FS at three different resolutions of 70000 "Full Width at Half Maxima" (FWHM) (at m/z 200). Then came ddMS2, which had stepped collision energy with a resolution of 17500 (at m/z 200) and operated at 10, 30, and 70 V. The 1e6 goals of the automatic gain control (AGC) were maintained for the ddMS2 approaches. The m/z was employed in ddMS2, which was initially created by ThermoFisher Scientific, and had a scan range of 100–1500. The data processing utilized the compound discoverer 3.2.0.421 programme.

4.4.2.3 Antimicrobial and antifungal activity of purified phytocompounds

Turmeric and Asparagus has long been considered as to have natural medicinal properties (Hoe seon lee, 2006). Antimicrobial studies were carried out on the pathogens including *Proteus vulgaris*, *Escherichia coli*, *Streptococcus mutans* and *Staphylococcus aureus.* Antifungal activity was checked by using *Pythium aphanidermatum*, *Aspergillus niger* and *Candida albicans* strains of fungus. The antimicrobial and antifungal activity was monitored in terms of zone of inhibition observed on agar plates of nutrient medium with 1.8% agar by using agar well diffusion method. The plates were incubated for 24 hrs

at 37℃ for bacteria and 48-72 hrs at 37℃ for fungal cultures. Curcumin, curcuminoids, 4 hydroxy 2 methyl acetophenone, purified curcumin, purified curcuminoids, combination of curcumin + 4 hydroxy 2 methyl acetophenone and diosgenin standard and purified diosgenin were used for testing purpose. After incubation results were recorded.

4.4.2.4 Minimum inhibitory concentration of phytocompounds

The Minimum inhibitory concentration (MIC) of purified metabolites (curcumin, curcuminoid and diosgenin), standard metabolites (curcumin, curcuminoid, 4 hydroxy 2 methyl acetophenone and diosgenin) and their combinations (curcumin + 4 hydroxy 2 methyl acetophenone) was determined by using test pathogens as *P. vulgaris, E. coli, S. mutans* and *S. aureus.* It was determined by twofold serial dilutions of metabolites in a Mueller-Hinton Broth medium. The test was carried out in 96 well microtitration plate with a standardized bacterial suspension of 0.5 McFarland's turbidity. The lowest concentration that completely inhibited the growth of the bacteria after 24 hrs was considered as the minimum inhibitory concentration (Bahariet al., 2017).

4.4.2.5 Effect of phytocompounds on test pathogen

The effect of phytocompounds on the growth of test pathogen *S. aureus* NCIM 2654 was assessed in the presence of purified plant metabolites (curcumin, curcuminoid and diosgenin), standard metabolites (curcumin, curcuminoid, 4 hydroxy 2 methyl acetophenone and diosgenin) and their combinations (curcumin + 4 hydroxy 2 methyl acetophenone). Their effect on bacterial growth was assessed by measuring OD at 660 nm against a time interval of 1 hr. The test culture at the initial concentration of 0.5 McFarland was incubated for 12 hours in the presence of these metabolites. The OD values were compared with the control sample. A sterile BHI medium was used as a blank. The growth pattern was obtained by taking absorbance at the time interval of 1 hr.

4.4.2.6 Biofilm inhibition study by using crystal violet assay

To improve the conditions for biofilm production, the microtiter plate assay was carried out. Four human pathogenic strains were employed in the study of biofilm suppression by various phytocompounds. As previously stated, (Sharifian et al., 2020), the experiment was carried out with a few changes on 96 well flat bottom polystyrene micro-titre plates that were previously sterilized. In each well, 150 µl of sterile BHI broth and 50 µl of cell suspension with 0.5 OD at 600 nm were used as inoculants. 100 µl of

purified metabolites (curcumin, curcuminoid and diosgenin), standard metabolites (curcumin, curcuminoid, 4 hydroxy 2 methyl acetophenone and diosgenin) and their combinations (curcumin plus 4 hydroxy 2 methyl acetophenone) was added in respective wells. Following that, the microtiter plate was incubated for 24 hours at 37°C. Planktonic cells were aspirated, and biofilms were then fixed in 99% methanol. Plates were air dried after being cleaned twice in sterile phosphate buffer saline. Then, 200 µl of 0.1 percent crystal violet solution was added to each well. After 15 minutes, the extra crystal violet was removed, the plates were cleaned twice, and they were air dried. Finally, 33% acetic acid was used to dissolve the cell-bound crystal violet. Using a micro plate reader (Erba scan), the growth of the biofilm was observed in terms of OD 578 nm.

4.4.2.7 Biofilm inhibition study by scanning electron microscopy (SEM)

The effect of purified metabolites (curcumin, curcuminoid and diosgenin), standard metabolites (curcumin, curcuminoid, 4-hydroxy 2-methylacetophenone and diosgenin) and their combinations (curcumin + 4- hydroxy 2 -methylacetophenone) on biofilm inhibition was also investigated by the SEM technique. In this, a clean glass was cut into a square having dimensions1 cm2. They were washed for 30 minutes in an ultrapure water rinse after being cleaned with a 5%(v/v) Hiclean (Liquid soap, Hi-Media) solution. The surfaces were immersed in 96% (v/v) ethanolfor 10 minutes to remove all impurities after being air dried for 30 minutes.

To prepare a sample for SEM, 2% glutaraldehyde solution was taken on slide. A test bacterial culture along with metabolites were used for the preparation of smear. The slides were kept in freezer overnight to fix the smear. On next day smear was washed with an ethanol dehydration series of 20 to 100% (v/v) (Galabova et al., 1996). The samples were then analyzed by SEM using VEGA3 TESCAN instrument.

4.4.3 Results and discussion:

4.4.3.1 Extraction of plant secondary metabolites

In the current study, Soxhlet extraction and sonication were used, and the resulting extract was used for purification and analysis of metabolites. Previously, Soxhlet extraction is used to ensure that curcumin and related compounds are extracted as completely as possible from turmeric root powder. Additionally, it eliminates the need to operate heavy glassware, heating, and cooling systems (Schieffer, 2002). To assess the

efficacy of the curcuminoid extraction methods under consideration, Soxhlet extraction was used as the baseline method. Soxhlet extraction is one of the most important and widely used extraction techniques, in which long extraction times at high temperatures aid in the extraction of the target compound, additionally, repeated contact of the solvent with turmeric can increase the extraction yield (Sahne et al., 2016). Although simpler, single or multiple ultrasonically-assisted extractions appear to leave a small but significant amount of secondary metabolites (Schieffer, 2002).

4.4.3.2 Purification of curcuminoids by silica gel column chromatography

In current study curcumin and curcuminoids were purified using silica gel column chromatography. Adsorption chromatography was performed for methanolic extracts using silica gel (60-120 mesh) and stepwise elution with chloroform and methanol CHCl3:CH3OH with increasing polarity with the flow rate of 1 ml/min. In our study, the chromatographic separation was done for curcumin as well as curcuminoids. A total of 40 fractions were collected and their OD was taken at 425 nm. Among the 40 fractions, fractions 10 to 25 demonstrated bioactivity and high absorbance at 425 nm, indicating that they contained purified curcuminoids. According to previous reports, separating curcumin and curcuminoids using silica gel column chromatography results in good yields (Peret-Almeida et al., 2005; Pushpakumari et al., 2014).

4.4.3.3 Thin layer chromatography

In the present study the TLC profile for the *C. longa* secondary metabolites shown three separate spots with retention factor (Rf) of 0.28, 0.54, and 0.77 for bisdemethoxycurcumin, demethoxycurcumin, and curcumin respectively (Fig. 4.3.2 from chapter 4.3) and were verified when compared to the levels in mixed standards. Under UV light, all of these dots fluoresced in comparison with standards. Similarly, in the case of diosgenin different solvent systems were used to conduct TLC analysis. In chloroform extracts produced from acid hydrolysis of roots of *A. racemosus*, retention factor for the diosgenin spot was 0.49 (Rf). (Fig.4.4.1). TLC is a simple and frequently used technique for purifying and identifying antibiotics, peptides, amino acids, plant pigments, and secondary metabolites in plants. Our findings are in line with previous reports for curcumin, curcuminoid and diosgenin (Laila et al., 2014; Peret-Almeida et al., 2005; Brain and hardman, 1968).

Fig. 4.4.1: TLC profile showing separation of purified secondary metabolites on Silica gel TLC plate where, S-standard diosgenin, D- purified diosgenin

4.4.3.4 Purification of curcumin

The spot with Rf value 0.77 was removed from the TLC separation as above mentioned, dissolved in methanol, and purified using silica gel column chromatography. A non isocratic elution profile was utilized with a constant mobile phase flow rate of 0.5 ml/min by progressively increasing the concentration of methanol in the chloroform-methanol mobile phase. Pure curcumin was extracted from the column using a pure chloroform solvent as a starting point. Subsequently increasing the methanol concentration, which elutes a mixture of remaining compounds. Fractions containing curcumin were collected, concentrated, and their UV absorbance at 425 nm was measured. These were then utilized for additional biological activities. As per earlier reports, curcumin has a wide range of therapeutic approaches. To examine the biological characteristics of individual curcumin, isolate compound of high purity is required (Heffernan et al., 2017).

4.4.3.5 Purification of diosgenin by acid hydrolysis

The acid concentration was an important factor in the hydrolysis reaction because it directly affected saponin yield. It was discovered that 50 ml of chloroform was sufficient to extract diosgenin, and that increasing the chloroform consumption did not increase the yield any further. Purified diosgenin is present in the upper layer of chloroform in the separating funnel, and the chloroform is evaporated at 60°C to yield a residual compound, which is then dissolved in methanol and used for TLC analysis. Previous research has also shown that acid hydrolysis followed by extraction in non-polar solvents yields a higher

yield than traditional methods (Yanget al., 2016).

4.4.3.6 HPLC analysis for curcumin and diosgenin

The HPLC approach was used to detect and quantify curcuminoids from the fractions of silica gel column chromatography. Separation by HPLC was done on reverse phase column by using mixtures of water and acetonitrile. Due to difference in the chemical structures of curcuminoids, their physicochemical properties and their functional qualities might differ. As a result, analysis of pure compounds and characterizing them separately in order to study their biological features is critical. Curcumin had eluted at 425 nm when analyzed with UVdetection by retention time of 11 min. The purity of the compound was assessed by comparing the extracted curcumin with curcumin standard. Curcumin content determined after 45, 90 and 180 days of each PGPR treated plant as depicted in chapter 4.3**.** Similar kind of work done by kumar et al. (2015) the reports stated that increased curcumin content after single and consortial treatment with PGPR to turmeric rhizome. Inoculations with *Pseudomonas fluorescens* raised turmeric's curcumin levels by 18% in comparison to a control, reported by Kumar et al. (2016).

HPLC results for diosgenin were shown in chapter 4.2 under results and discussion section. Earlier study reported that quantification of diosgenin was performed by using HPLC (Peiqin Li, 2012).

4.4.3.7 GC-MS/MS and LC-MS/MS analysis for curcumin and diosgenin

Analysis through GC-MS/MS to assess the similar compounds present in the fractions. The results for GC-MS/MS for Turmeric and Asparagus are given in chapter 4.3 and 4.2 respectively under results and discussion section. GC-MS/MS results revealed that when plant samples were compared to untreated control plants, the percent area of important phytocompounds in co-culture treated plants increased. Similar to this, we discovered a newer compound (4-hydroxy-2-methylacetophenone) in the co-culture and *Pseudomonas plecoglossicida*-treated *C. longa.* In an earlier study of phytochemical analysis, a GC-MS-based method was used to analyze *Asparagus racemosus* (Janani and Singaravadivel, 2014; Wang et al., 2011). Previous studies have shown that PGPR inoculation with *Exiguobacterium oxidotolerans* increases the secondary metabolite bacoside-A in *Bacopa monnieri* L. (Bharti et al., 2013).

Identification of curcumin and diosgenin were performed by using LC-MS/MS. The full scan in positive mode was used (scan range from m/z 200→m/z 700) to identify

the curcumin. With full scan mass spectra for the determination of curcumin precursor ion is [M+H]+ m/z 369. Under optimized HPLC and MS conditions, curcumin was detected. After optimization, the mass transitions were m/z 369→m/z 759 for curcumin. Fig.4.4.2 The earlier research by Xie et al. (2009) represents a verified LC-MS/MS based approach for figuring out how much curcumin is present in *Curcuma longa.* Because chromatographic separation coupled to mass spectrometry detection (LC- MS/MS) technologies offer great accuracy, repeatability, and sensitivity, they should be employed for precise measurement and detection of tiny quantities of curcuminoids and metabolites.

The voltage for the most significant abundance of diosgenin is [M+H]+ m/z 415.3. Fig.4.4.3 The retention time of 2.44 min was detected for diosgenin. These results led to the identification of the diosgenin by using the full scan in positive mode (scan range from m/z 200– m/z 450) and the precursor/product ion pair with a transition mass of m/z415.3/271.2. Similarly, earlier studies reported the determination of diosgenin from various plant sources by using LC- MS (Sarvin et al., 2018).

Fig.4.4.2: TIC of Curcumin

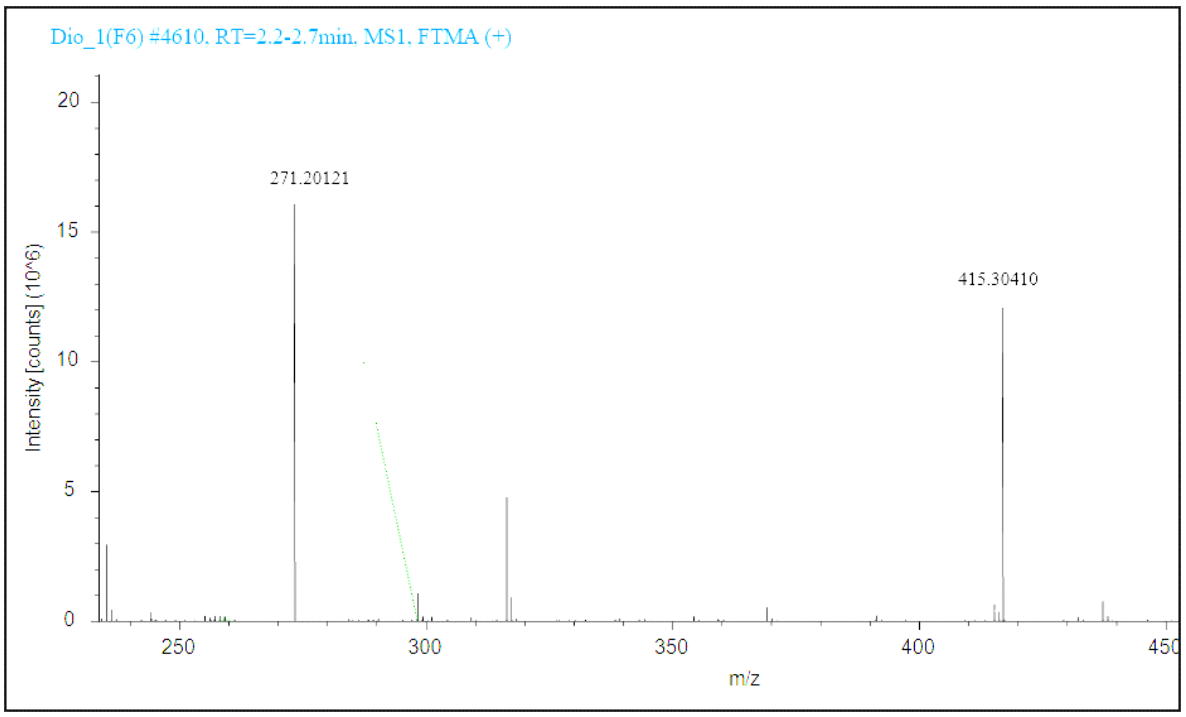

Fig.4.4.3: TIC of Diosgenin

4.4.3.8 Antibacterial and antifungal activity of phytocompounds

Curcumin, curcuminoids, 4-hydroxy-2-methylacetophenone, purified curcumin, purified curcuminoids, combination of curcumin + 4-hydroxy-2-methylacetophenone and diosgenin standard and purified diosgenin were tested against a variety of pathogens including *E. coli* NCIM2832, *Staphylococcus aureus* NCIM 2654, *Streptococcus mutans* NCIM 5660 and *Proteus vulgaris* NCIM 2813. Agar well diffusion method employed to check the antibacterial activity. The results are depicted in Table 4.4.3 Curcumin, curcuminoids, 4-hydroxy-2-methylacetophenone, purified curcumin, purified curcuminoids, combination of curcumin + 4-hydroxy-2-methylacetophenone and diosgenin standard and purified diosgenin showed highest antibacterial activity against *S. aureus* among all pathogens with diameter of zone of inhibition as 23.8 ±1.2, 23 ±2.7, 22.3 ±2.0, 24 ±0.5, 19.5 ±0.7, 27.8 ±0.70, 12.5 ±0.7 and 11 ±0.2 mm respectively. These results indicate that the combinational effect of curcumin + 4-hydroxy- 2-methylacetophenone is more inhibitory than the individual compound. We also demonstrated that purified compounds have inhibitory values close to the standard. Antifungal activity was tested against *Pythium aphanidermatum*, *Aspergillus niger* and *Candida albicans*, and findings were recorded in a Table 4.4.4. Curcumin, curcuminoids,

4-hydroxy-2-methylacetophenone, purified curcumin, purified curcuminoids, combination of curcumin + 4-hydroxy-2-methylacetophenone and diosgenin standard and purified diosgenin showed the highest antifungal activity against *A. niger* among all pathogens and the zone of inhibition was observed and noted as 13.8 ±1.2, 13 ±2.7, 12.3 ±2.0, 14 ±0.5, 14.5 ±0.7, 17.8 ±0.70, 14.5 ±0.7 and 11 ±0.2 mm respectively. According to our findings, the combined effect is more significant than a single treatment.

Many studies reported the antibacterial activity of Turmeric extracts, essential oil extracted from Turmeric and curcumin against pathogenic organisms (Khatun et al., 2021; Negi et al., 1999).Combinational effect of curcumin along with other phytocompounds showed the antibacterial effect against human pathogen (Sharma et al., 2013). Antifungal activity of *C. longa* against different fungi were also reported (Moghadamtousi et al., 2014).

Table 4.4.3: Antimicrobial activity of phytocompounds against Gram-positive and Gram-negative bacteria by agar well diffusion assay

Phytocompounds	**Inhibition zone in mm**			
	***S. aureus* NCIM 2654**	***S. mutans* NCIM 5660**	***P. vulgaris* NCIM 2813**	***E. coli* NCIM 2832**
Curcumin	23.8 ± 1.2	23.00±1.3	19 ±0.7	20 ±0.5
Curcuminoid	23.0 ± 2.7	22.5 ± 0.7	18 ±0.8	19 ±0.8
4-hydroxy-2-methylacetophenone	22.3±2.0	22 ± 0.2	16 ±1	17 ±0.7
Purified Curcumin	24.0 ± 0.5	23.5 ±0.3	18.5 ±0.8	19 ±0.3
Purified Curcuminoid	19.5 ± 0.7	22 ± 0.8	17 ±0.5	18 ±0.2
Curcumin+4-hydroxy-2-methylacetophenone	27.8 ± 0.70	26.00±1.4	20 ±0.6	21 ±0.2
Diosgenin	12.5 ± 0.7	10.12±0.3	12 ±1.2	11.5 ±0.6
Purified diosgenin	11 ± 0.2	10 ± 0.3	12 ±0.2	10 ±0.5

Table 4.4.4: Antifungal activity of phytocompounds against different fungi by agar well diffusion assay.

Phytochemicals	Inhibition zone in mm		
	Aspergillus niger	***Pythium aphanidermatum***	***Candida albicans***
Curcumin	13.8 ± 1.2	10.00 ± 1.3	17 ±0.7
Curcuminoid	13.0 ± 2.7	12.5 ± 0.7	15 ±0.8
4-hydroxy-2-methylacetophenone	12.3±2.0	08 ± 0.2	12 ±1
Purified Curcumin	14.0 ± 0.5	13.5 ± 0.3	15.5 ±0.8
Purified Curcuminoid	14.5 ± 0.7	12 ± 0.8	14 ±0.5
Curcumin + 4-hydroxy-2-methylacetophenone	17.8 ± 0.70	13.00 ± 1.4	17 ±0.6
Diosgenin	14.5 ± 0.7	12.12 ± 0.3	22 ±1.2
Purified diosgenin	11 ± 0.2	12± 0.3	20 ±0.2

4.4.3.9 Minimal Inhibitory concentration of phytocompounds

Minimum inhibitory concentration (MIC) was performed against a variety of human pathogens, including *S. aureus* NCIM 2654, *S. mutans* NCIM 5660, *P. vulgaris* NCIM 2813, and *E. coli* NCIM 2832. We continued our further investigation with *S. aureus* because among these pathogens, significant results were found for this species. *S. aureus* is an aerobic Gram-positive bacterium and has been found in a variety of diseases, including skin infections, endocarditis, toxic shock syndrome, osteomyelitis, and septicemia (Niu et al., 2018; Ippolito et al., 2010). MIC of curcumin, curcuminoids, 4-hydroxy-2-methylacetophenone, purified curcumin, purified curcuminoids, combination of curcumin + 4-hydroxy-2-methylacetophenone and diosgenin standard and purified diosgenin were 180, 200, 200, 200, 220, 160, 200 and 240 µg/ml respectively against *S. aureus* (Table 4.4.5).

Earlier studies reported the minimum inhibitory concentrations of curcumin against human pathogens (Gunes et al., 2016). MIC against *S. aureus* was reported by Park et al. (2005). Our results of MIC are in accordance to these findings.

Table 4.4.5: MIC against human pathogens

Phytocompounds	MIC in µg/ml			
	S. aureus **NCIM 2654**	***S. mutans*** **NCIM 5660**	***P. vulgaris*** **NCIM 2813**	***E. coli*** **NCIM2832**
Curcumin	180	200	220	300
Curcuminoid	200	220	240	300
4-hydroxy-2 methylacetophenone	200	240	240	310
Purified curcumin	200	220	260	320
Purified curcuminoid	220	240	240	340
Curcumin +4-hydroxy-2-methylacetophenone	160	200	240	280
Diosgenin	200	240	260	320
Purified diosgenin	240	260	260	300

4.4.3.10 Effect of phytocompounds on test pathogen

Growth curve experiment was performed to check the effect of purified metabolites (curcumin, curcuminoid and diosgenin), standard metabolites (curcumin, curcuminoid, 4-hydroxy-2-methylacetophenone and diosgenin) and their combinations (curcumin + 4-hydroxy-2-methylacetophenone) on the growth of *S. aureus* NCIM 2654. On the basis of MIC values of each metabolite, we selected *S. aureus* NCIM 2654 for this experiment. The experiment was performed to check inhibition potential of phytocompounds. The observed growth curve patterns (Fig. 4.4.4) showed the effective inhibition of *S. aureus* in presence of curcumin+4-hydroxy- 2-methylacetophenone over individual phytocompounds and control. The decrease in absorbance at 660 nm by *S. aureus* in the occurrence of phytocompounds showed that inhibition of growth of pathogen. Earlier reports also showed that growth of *S. aureus* was inhibited in the presence of curcumin (Wang et al., 2016).

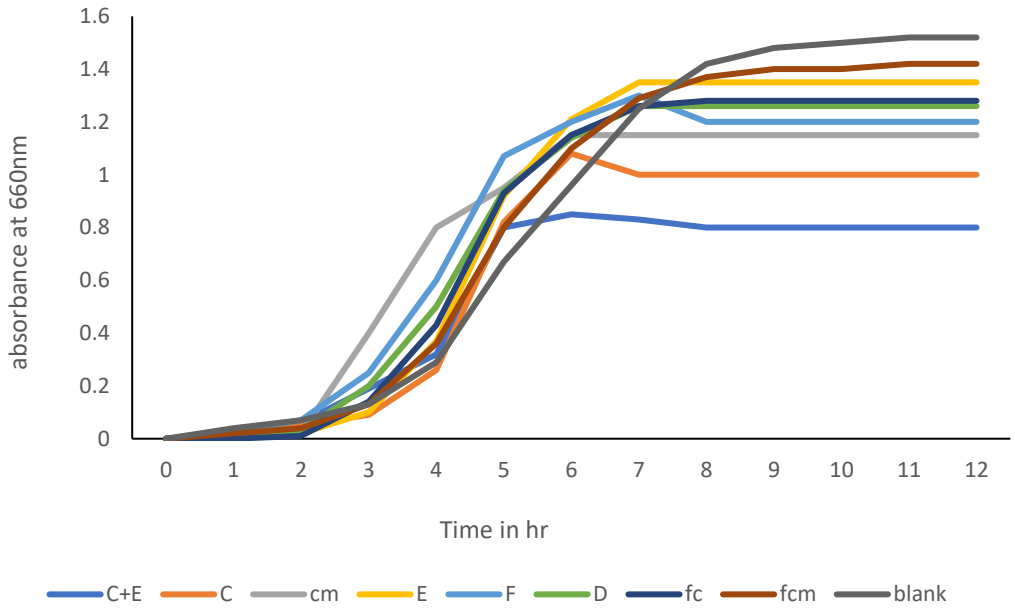

Fig.4.4.4: Growth curve of *S. aureus* in presence of different phytocompounds where C+E - curcumin+4-hydroxy-2-methylacetophenone, C-curcumin, cm- curcuminoids, E-4-hydroxy-2-methylacetophenone, F- purified diosgenin, D- diosgenin standard, fc- purified curcumin, fcm- purified curcuminoids.

4.4.3.11 Antibiofilm activity by using Crystal violet Assay

In order to investigate the biofilm inhibition activity of all phytocompounds, crystal violet assay was performed against biofilm forming pathogens. Biofilms in the wells containing curcumin, curcuminoids, 4-hydroxy-2-methylacetophenone, purified curcumin, purified curcuminoids, combination of curcumin + 4-hydroxy-2-methylacetophenone and diosgenin standard and purified diosgenin were easily detached from the base. It may be said that biofilms in the absence of phytocompounds were less disturbed by the staining process and adhered to the microplate wells more firmly. The OD was higher in the group lacking phytocompounds than in the group containing phytocompounds due to biofilm development. The combinational effect of curcumin + 4-hydroxy-2-methylacetophenone had shown better biofilm inhibition than individual treatment of metabolites as illustrated in Fig.4.4.5. These metabolites were showed better biofilm inhibition in case of *S. aureus* and *S. mutans* under *in vitro* and *in silico* studies.

S. aureus is known for biofilm-related infections, particularly in nosocomial infections (Jinet al., 2019), but *S. mutans* is more commonly connected with dental carries (Caroline et al., 2018). Bacteria associated with biofilm are resistant to the majority of

regularly used antibiotics, and they create extracellular polymeric substance (EPS) for cell-to-cell adhesion and biofilm growth, slowing the diffusion of conventional antibiotics (Nadaf et al., 2018). Attachment to cell surfaces, matrix development, and maturation are the phases in biofilm formation (Nadar and colleagues, 2022). Numerous earlier studies demonstrated that curcumin inhibits the growth of organisms that produce biofilms (Hu et al., 2013; Park et al., 2005).

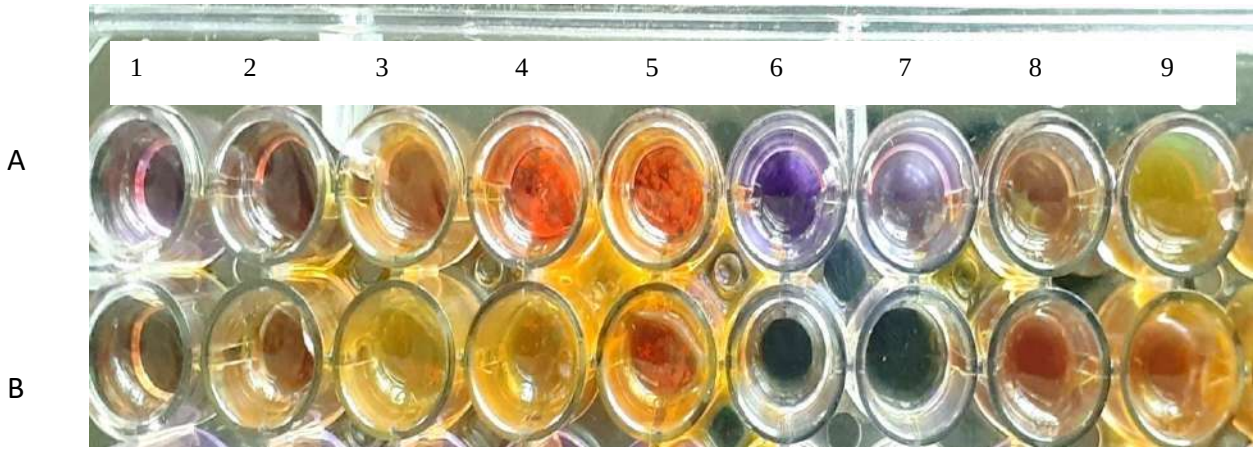

Fig.4.4.5: Crystal violet assay of biofilm for *S. mutans* (A) and *S. aureus* (B) where, 1) is control untreated cells 2) cells treated with curcumin 3) cells treated with curcuminoids 4) cells treated with purified curcumin 5) purified curcuminoid 6) cells treated with 4-hydroxy-2-methylacetophenone 7) cells treated with diosgenin 8) cells treated with curcumin + 4-hydroxy-2-methylacetophenone 9) cells treated with purified diosgenin.

4.4.3.12 Scanning electron microscopy (SEM) study for biofilm inhibition

The antibiofilm action of phytocompounds on *S. aureus* NCIM 2654 Fig. 4.4.6 was confirmed by SEM analysis. The disorganized adhesion of the organisms treated with phytocompounds is clearly visible, indicating a failure in aggregate formation and an inability to maintain their normal morphology in the presence of phytocompounds. The untreated cells had a smooth, undamaged surface that was spherical in shape, and they had a strong adherence to one another (Fig. 4.4.6-A). Cells lose their adhesion after being treated with all phytocompounds, and alterations to their morphology occur, with a combinational impact producing better results than an individualone. These observations lend credence to the results of the growth curve investigations.

One of the key steps in the production of biofilms, called quorum sensing or cell-to-cell communication, is where microorganisms may interact. Gram-positive and Gram-

negative microbes have been the subject of the most thorough research in this process (Waters and Bassler,2005; Eberhard et al., 1981; Sheikh et al., 2013; Vendeville et al., 2005). According to reports, the inhibitory effect of phytocompounds on quorum sensing and the formation of biofilms is a phenomenon that depends on the density of the bacteria (Filomena et al., 2013). Our findings, however, suggest that inhibiting adhesion may halt the development of biofilms right at their beginning, which may be more useful when developing fresh therapeutic approaches.

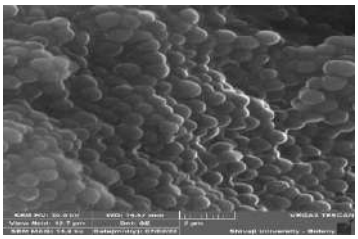

A

B

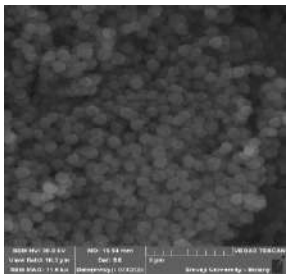

C

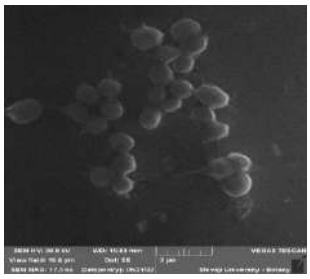

D

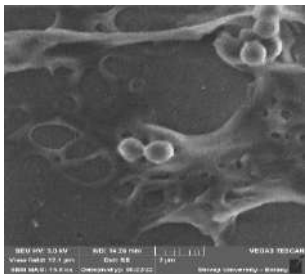

E

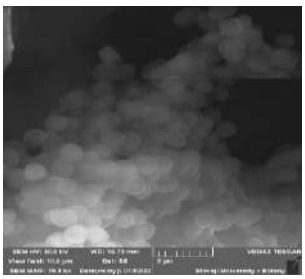

F

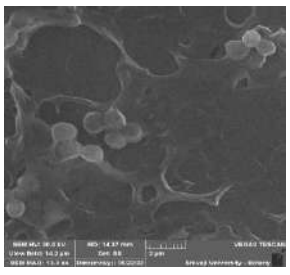

G

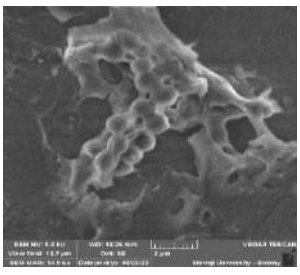

H

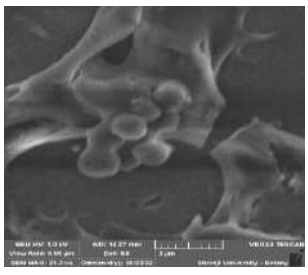

I

Fig.4.4.6: Scanning electron microscopic images of *S. aureus* cells after treatment with phytocompounds A) Untreated control cells B) cells treated with curcumin C) cells treated with curcuminoids D) cells treated with 4-hydroxy-2-methylacetophenone E) cells treated with purified curcumin F) cells treated with purified curcuminoid G) cells treated with combination of curcumin + 4-hydroxy-2-methylacetophenone H) cells treated with diosgenin I) cells treated with purified diosgenin

4.4.4 Conclusions:

The secondary metabolites from plants were extracted by using liquid, reflux, or ultrasonic extraction methods with an alcoholic solvent. The phytocompounds present in the extracts were separated by chromatographic method linked to mass spectrometer detection (LC-MS/MS) which offered accurate and reliable quantification and recognition of trace quantities of metabolites. Similarly, GC-MS/MS analysis provided insight into the variety of phytocompounds present in the extracts.

Individual and combinational effect of phytocompounds was investigated on Gram-positive and Gram-negative pathogens such as *S. aureus* NCIM 2654, *S. mutans* NCIM 5660 and *E. coli* NCIM 2832, *P. vulgaris* NCIM 2813 respectively. Further, we studied the inhibition of biofilm forming pathogens such as *S. aureus* and *S. mutans* by using phytocompounds. In this context, our biofilm inhibition experiment with crystal violet assay and SEM showed the inhibition of biofilm formation for all the phytocompounds significantly against *S. aureus*. Notably, the combinational effect of curcumin + 4-hydroxy-2-methylacetophenone showed significant antibacterial, antifungal, and anti-biofilm forming activity. Hence it concludes that the combinational effect of phytocompounds provides a better inhibition as compared to individual one.

4.5 Inhibition of *S. Aureus* and *S. Mutans* Sortase A by PGPR induced secondary metabolites from *C. longa: In-vitro* and *in-silico* approaches

The part of this study communicated to:

International Journal of Biological Macromolecules

Inhibition of S. Aureus and S. Mutans Sortase A by PGPR induced secondary metabolites from C. longa: In-vitro and in-silico approaches

--Manuscript Draft--

Manuscript Number:	
Article Type:	Research Paper
Section/Category:	Proteins and Nucleic acids

International Journal of Biological Macromolecules (Manuscript ID: IJBIOMAC-D-23-16762), Under Review

4.5.1 Introduction:

Staphylococcus aureus is an aerobic Gram-positive bacteria and has been found in a variety of diseases, including skin infections, endocarditis, toxic shock syndrome, osteomyelitis, and septicaemia (Niu et al., 2018; Ippolito et al., 2010; Lowy et al., 1998). Another Gram-positive endogenous pathogen, *Streptococcus mutans*, cariogenic bacteria live in biofilm and consequence in dental caries and other related disorders (Hu et al., 2013; Luo et al., 2017). Previously, it has been shown that *S. aureus* causes nosocomial infections, whereas *S. mutans* causes a variety of mild to severe infections (Chenna et al., 2008; Cvitkovitch et al., 2003). It has been found that cell adhesion protein sortases (SrtA) are extracellular transpeptidases highly conserved in Gram-positive bacteria that covalently attaches the secreted proteins to the peptidoglycan cell wall and essential for initiation of biofilm formation (McCafferty et al., 2010). So far, four isoforms of sortase have been identified: SrtA, SrtB, SrtC, and SrtD (Si et al., 2016; Nitulescu et al., 2021). Among them, the structure and catalytic mechanism of highly conserved SrtA has received promising target for anti-infective agents (Niu et al., 2018; Stoica et al., 2017). SrtA also plays an important role in the pathogenesis, invasions and biofilm formation in both of *S. aureus* and *S. mutans* (Hu et al., 2013). The biofilm is defined as dense aggregates of surface adherent microorganisms embedded in extracellular matrix composed by exopolysaccharide (EPS), and it is estimated that biofilms are reason for 65 percent of human bacterial infections (Cvitkovitch et al., 2003). The formation of biofilm involves two major steps: adhesion and maturation with proliferation (Fux et al., 2005; Costerton et al., 2003). SrtA catalyzed three steps sorting reaction: recognition, transesterification, and transpeptidation of LPXTG motif sorting signal (Ha et al., 2020; Cascioferro et al., 2015). Earlier studies of SrtA knockout *S. mutans* showed the decrease in adhesion, colonization, and biofilm formation and associated dental caries (Lee et al., 1989; Levesque et al., 2005). Hence, SrtA is being considered as a promising target in the development of drugs to treat these biofilm associated bacterial infections (Wang et al., 2019; Shulga et al., 2021).

The SrtA inhibition lead to diminution of attachment of various surface proteins that involved in cell adhesion, colonization and inhibition of biofilm formation (Nadaf et al., 2018; Richards et al., 2015;). Curcumin and its analogues have recently shown great *in-vitro* potential for reversing methicillin resistance in *Staphylococcus aureus* (Nitulescu et al., 2021). Several molecular modeling studies showed that curcumin analogues (Niu

et al., 2018; Park et al., 2005; Das et al., 2018; Nitulescu et al., 2017; Li et al., 2018) and other plant secondary metabolites inhibit SortaseA (Bi et al., 2016; He et al., 2017; Oniga et al., 2017; Salmanli et al., 2021; Nitlescue et al., 2017). SrtA's primary sequence includes an N-terminal signal peptide, a surface protein and a C-terminal sorting signal (Suree et al., 2009; Zong et al., 2004). The C-terminal sorting domain contains three subdomains: a LPXTG motif, second hydrophobic domain, and third charged tail (Si et al., 2016). These subdomains aid in the anchoring of microbial surface components recognizing adhesive matrix molecules (Cascioferro et al., 2015). In previous studies of sortase inhibition assay, it was discovered that curcumin effectively inhibited SrtA (Park et al., 2005). As per previous reports several SrtA conformations were observed, including the immobilized β 6/7 loop (formed by residues Thr156 to Lys177) in few docked complexes and open state conformations in apo form (Gao et al., 2016). The analysis of conformational diversity and binding pocket fluctuations assumes that the active site is not always the preferred site for binding for lead molecules reported (Gao et al., 2016). However, additional curcumin analogues have also been shown to inhibit SrtA (Sivaramakrishnan et al., 2019). Earlier studies showed the crude extracts of *C. longa* and *Psoralea* in methanol, inhibit the *S. aureus* (80%) and *S. mutans* (44.2%), respectively (Nitulescu et al., 2021). The SrtA inhibitor does not kill the bacteria, but it inhibits virulence and thus prevents infection caused by Gram-positive bacteria (Stoica et al., 2015.).

PGPR has also demonstrated their ability to increase the yield and content of plant secondary metabolites (Kumar et al., 2016; Bharati et al., 2013; Jagtap et al., 2023). When PGPR-treated plants are compared to untreated plants, they show a significant increase in plant growth and secondary metabolite production (Yadav et al., 2022; Cappellari et al., 2015). Considering pathogenic potential of biofilm forming pathogen and the great potential of PGPR in producing novel secondary metabolites which could inhibit the biofilm formation. Hence, our *in-vitro* and *in-silico* approaches to investigate the biofilm inhibition potential and molecular mechanism of SrtA inhibition by PGPR induced phytocompounds. It has been found that the all phytocompounds specifically in synergistic action showed significant biofilm inhibition activity. Hence, phytocompounds in synergy curcumin and 4 hydroxy 2 methyl acetophenone would pave the way for the development of novel lead molecules targeting Srt A to control biofilm formation by *S. aureus* and *S. mutans*.

4.5.2 Materials and methods:

4.5.2.1 Chemicals, bacterial strains and culture conditions

Chemicals such as glutaraldehyde, and crystal violet were purchased from (SRL, INDIA and Himedia,). Similarly, Muller hinton agar (MHA) and brain heart infusion (BHI) broth were bought from Himedia in India. The cultures of *Streptococcus mutans* NCIM 5660 and *Staphylococcus aureus* NCIM 2654 were bought from NCIM (National Collection of Industrial Microorganisms) Pune, India. These bacterial cultures were transferred to MHA plates, which were then incubated for 24 hours at 37°C. On the next day, pure cultures were obtained, transferred to slants, and maintained at 4°C in a refrigerator at the Department of Microbiology, Shivaji University in Kolhapur.

4.5.2.2 Molecular properties of phytocompounds

Phytocompounds such as curcumin, curcuminoids, 4-hydroxy 2-methylacetophenone isolated and identified in our previous study were used in this study (Jagtap et al., 2023). In order to predict pharmacological and toxicological prediction an *in-silico* approaches were used using ADME Lab2.0 online server (Bansode et al., 2019; Xiong et al., 2021).

4.5.2.3 Antibiofilm activity of PGPR induced phytocompounds

The microtiter plate assay based on crystal violet was performed for optimizing biofilm formation conditions (Toole et al., 1999). The biofilm formation assay was performed in triplicates using pre-sterilized 96 well flat bottom polystyrene micro-titre plates as described previously with minor modifications (Sharifian et al., 2020). Briefly, a 50 µl of cell suspension with optical density 0.5 at 600nm was inoculated in 150 µl sterile BHI broth in each well. The phytocompounds (curcumin, curcuminoids, 4 hydroxy 2 methyl acetophenone and their combinations- curcumin plus 4 hydroxy 2 methyl acetophenone) at 100 µl (300µg/ml) were added in respective wells. Then microtiter plates were incubated for 24 hrs at 37°C. After incubation media and planktonic cells were carefully aspirated then biofilms in microtitter plate was fixed with of 99% methanol. Thereafter, plates were rinsed with sterile phosphate buffer saline twice and air-dried. Then attached bacterial cells stained with 200 µl of 0.1 % (w/v) crystal violet solution and incubated at 15 min at room temperature. After incubation the excess stain was removed and plates were washed with PBS for twice and then air dried. Finally, the cell bound crystal violet was release by 33% acetic acid. Biofilm growth was monitored

by measuring absorbance at 578 nm using micro plate reader (Erba scan) (Thappeta et al., 2020).

4.5.2.4 Biofilm inhibition study by scanning electron microscopy (SEM)

In this, a clean glass was cut into a square having dimensions 1 cm^2 and washed with a solution of 5% (v/v) Hiclean (Liquid soap, Hi-Media) for 30 min and then rinsed in an ultrapure water to remove any remaining detergent. After air drying the surfaces for 30 min, they were immersed in 96% (v/v) ethanol for 10 min to remove all impurities. To prepare a sample for SEM, 2% glutaraldehyde solution was flood on slide. The bacteria *S. aureus* treated at 300µg/ml concentration of phytocompounds alone and in combination (curcumin and 4-hydroxy-2-methylacetophenone) were used for the preparation of smear. The slides were kept in freezer overnight to fix the smear. On next day smear was washed with an ethanol dehydration series of 20 to 100% (v/v) (Galabova et al., 1996). The samples were then analyzed by SEM using VEGA3 TESCAN instrument.

4.5.2.5 Structural analysis, refinement and validation of SrtA

The three-dimensional structures of SrtA of Gram positive *S. aureus* ($SrtA_{staph}$; PDB ID: 1T2P) and *S. mutans* ($SrtA_{strepto}$; PDB ID: 4TQX) were retrieved from the RCSB structural database (Zong et al., 2004; Richards et al., 2015). The residues from the missing loop region were constructed (5 conformations/loop) using the chimera modeler interface. The structure of SrtA from *S. mutans* had mutated residues, such as H139A, which were changed to wild type using the chimera's 'swapaa' module. The structures with the lowest DOPE (discrete optimised potential energy) scores were chosen and structural refinement was done using the Gromacs version 2018.2. The structural refinement parameters were derived from previous studies (Dhanavade et al., 2013; Parulekar and Sonawane 2017; Barale et al., 2019). The bad contacts along with steric clashes formed during modelling were removed through energy minimization using the steepest descent algorithm, followed by conjugate gradient. The both SrtA protein model with rebuilt loop from trajectories of unrestrained molecular dynamics (MD) simulation were stereochemicaly validated and secondary structural assignment were done using Structure Analysis and Verification Server 6 (SAVES) and by generating a Ramachandran plot (Sonawane et al., 2015; Laskowski et al., 1993; Cavaturu et al., 2019)

4.5.2.6 Binding mode analysis and intermolecular interactions of phytocompounds with SrtA

UCSF's dock6.9 docking tool was used to investigate the binding poses of phytocompounds to SrtA and their detailed intermolecular interactions. The energy minimised and validated structures of both SrtA from MD simulations trajectories were subjected to local docking and then blind docking. Both SortaseA protein were prepared using 'dockprep' module of UCSF chimera by adding hydrogens and assigning charges. Three-dimensional structures of all the phytocompounds were obtained from the PubChem small molecule database in SDF format and open babel was used to converted in pdb (Singh et al., 2014; Kim et al., 2016; O'Boyle et al., 2011), Curcumin (CID 969516), demethoxycurcumin (CID 5324476), Bisdemethoxycurcumin (CID 5315472), 4-hydroxy 2-methyl acetophenone (CID 160512), and ar-turmerone (CID 70133). For convenience, we have referred to these phytocompounds as C1, C2, C3, C4, and C5 respectively, throughout the manuscript.

The known SrtA inhibitors Carvone (Car) for $SrtA_{Staph}$ and Transchalcone (TC) for $SrtA_{Strepto}$ were chosen as controls for comparison with phytocompounds of *C. longa*. All Ligands (Phytocompounds) and Car, TC for docking protocol were prepared using UCSF Chimera 'dockprep' tool. The spheres (grid) were generated using the 'sphgen' tool, and the binding pocket was defined using both the largest sphere and active site residues, Cys184, His120, Arg197 of $SrtA_{Staph}$ and His139, Cys205, Arg213 of $SrtA_{Strepto}$ (Maia et al., 2020). To study detailed binding modes, the conformations were clustered based on grid score and conformation with lowest grid score subjected for investigation of intermolecular interactions. Docking studies of Curcumin (C1) and 4-hydroxy 2-methyl acetophenone (C4) with both SrtA in synergistic were also implemented, as our experimental studies showed significant anti-biofilm activity of C1 and C4 in synergistic as compare to alone. The efficacy of dual inhibitors is well established (Mannu et al., 2014), earlier studies also suggest the binding of compounds other than active site of SrtA alter its activity (Gao et al., 2016). The Maestro suite was used to construct the 2D SrtA and phytocompounds interaction diagrams (Hajbabaie et al., 2021). The structural stability, intermolecular interactions, and binding affinity of docked complexes ($SrtA_{Staph}$-Car, $SrtA_{Staph}$-C1, $SrtA_{Staph}$-C2, $SrtA_{Staph}$-C3, $SrtA_{Staph}$ -C4, $SrtA_{Staph}$ -C5, $SrtA_{Staph}$ -C1+C4) were investigated by performing all atom MD simulation in explicit solvent.

4.5.2.7 MD simulations of SrtA in complex with phytocompounds to assess structural stability

All the $SrtA_{Staph}$-Car, $SrtA_{Staph}$-C1, $SrtA_{Staph}$-C2, $SrtA_{Staph}$-C3, $SrtA_{Staph}$-C4, $SrtA_{Staph}$-C5, $SrtA_{Staph}$-C1+C4, $SrtA_{Strepto}$-TC, and $SrtA_{Strepto}$-C1, $SrtA_{Strepto}$-C2, $SrtA_{Strepto}$-C3, $SrtA_{Strepto}$-C4, $SrtA_{Strepto}$-C5, $SrtA_{Strepto}$-C1+C4 complexes from lowest grid score were selected for MD simulation using GROMACS 2018.2 on Linux platform (Abraham et al., 2015). The partial charges on the ligand structures were calculated in antechamber using the quantum mechanics method (Katsori et al., 2011), and the force field parameters for all ligands were generated using the generalised amber force field (GAFF). The topology files for all 14 docked complexes (listed above) were generated using the Amber ff99SB-ILDN force field in Ambertool21's 'xleap' module (Niu et al., 2018; Gao et al., 2016). ParmEd tool was used to convert Amber topology files to Gromacs (http://parmed.github.io/ParmEd)). TIP3P water model was used to solvate the docked complexes, and the required numbers of counter ions were added to neutralise charges on the solvated systems. The energy of these systems were minimised using the steepest descent method, followed by the conjugate gradient method. Energy-minimized systems were equilibrated over 1ns using a canonical 'NVT' ensemble and an isothermal-isobaric 'NPT' ensemble. Furthermore, for each of the systems under consideration, an unrestrained MD simulation was run for 100ns. The cut-off values for treating long/short range interactions, as well as other input parameters for MD, were derived from previous studies (Parulekar and Sonawane, 2018; Dhanavade and Sonawane, 2014; Jalkute et al., 2013; Sonawane et al., 2021; Bansode et al., 2019; Dhanavade et al., 2013). The simulation trajectories were recorded every 2fs, and the trajectories were analysed for structural stabilities using Gromacs tools such as 'gmx_rms', 'gmx_rmsf', gmx_hbond and so on. Other third-party tools, such as 'vmd,' were also used where necessary. UCSF Chimera1.15 was used to analyse the individual snapshots and to generate quality images. Biovia Discovery studio visualizer 2021 was used to investigate intermolecular interactions at the atomic level.

4.5.2.8 Binding energy calculation and key residue contributions in binding energy of phytocompounds with SrtA

Binding free energy estimation provides a measure of binding affinities between protein-ligand complexes. With a single trajectory approach and either the MMPBSA or MMGBSA methods, it is now possible to estimate relative binding energy effectively. To

calculate relative binding free energy, we used the recently released 'gmx MMGBSA' tool (Tresanco et al., 2021; Miller et al, 2012).

To calculate the binding free energy, the MMGBSA method employs the following equations:

$$\Delta G_{Bind} = < G_{com} > - < G_{Rec} > - < G_{Lig} >$$

However, classical thermodynamic equation of binding energy is;

$$\Delta G_{Bind} = \Delta H - T\Delta S$$

Where ΔH is enthalpy of binding and $T\Delta S$ is conformational entropy after ligand binding.

$$\Delta H = \Delta E_{MM} + \Delta G_{sol}$$

The enthalpic contribution in the binding free energy ΔE_{MM} is calculated by;

$\Delta E_{MM} = \Delta E_{bonded+\Delta E_{nonbonded}} = \left(\Delta E_{bond} + \Delta E_{angle} + \Delta E_{dihedral}\right) + (\Delta E_{ele} + \Delta E_{vdW})$

and, $$\Delta G_{sol} = \Delta G_{polar\ (GB)} + \Delta G_{non-polar}$$

After reimaging the periodic boundary conditions, the stable trajectory observed between 60ns and 100ns of the entire MD simulation period was extracted and used for binding free energy calculation. By performing residue decomposition energy, the contribution of individual residues to the binding free energy was also investigated. This would aid in the investigation of conserved binding pocket interactions in our docked complexes versus their respective controls.

4.5.2.9 Principle component analysis (PCA) and dynamic cross correlation map

We looked for dynamic differences during stable complex formations by both the sortases $SrtA_{staph}$ and $SrtA_{strepto}$, which would provide key insights into the significant dynamic information and inter residue / inter domain correlation of proteins in 2D, in addition to structural stability and intermolecular interactions. Dynamic cross correlation matrices over representative snapshots from stable trajectories (60 to 100 ns) were plotted using the CPPTRAJ module of antechamber to observe the correlation in the dynamics of $SrtA_{staph}$ and $SrtA_{strepto.}$ GNUPLOT was used to create the 2D plot. Principal component analysis (PCA) is a well-established statistical method for studying protein dynamics and describing functionally important protein motions. To test the collective motion and obtain extreme conformations from stable trajectories, principal component analysis was used.

4.5.3. Results and Discussion:

4.5.3.1 Molecular properties of phytocompounds

The phytocompounds such as curcumin, demethoxycurcumin, bisdemethoxycurcumin, 4-hydroxy-2-methylacetophenone, and ar-turmerone were detected in our previous studies of GC-MS/MS and RP-HPLC analysis of PGPR treated *C. longa* (Jagtap et al., 2023). These compounds individually and in combination were investigated for anti-biofilm activity in this study. To determine drug-likeness of physicochemical, pharmacological, Lipinski rule and toxicity properties of these selected compounds have been assessed using ADME Lab2.0 online server. It has been discovered that the molecules of all five compounds pass through the Lipinski rule and exhibit drug-like behaviour. The ADMET profile highlights the therapeutic potential of all of the chosen molecules (Table 4.5.1). Fig. 4.5.1A depicts the 2D structures of the PGPR-treated phytocompounds with PubChem ID.

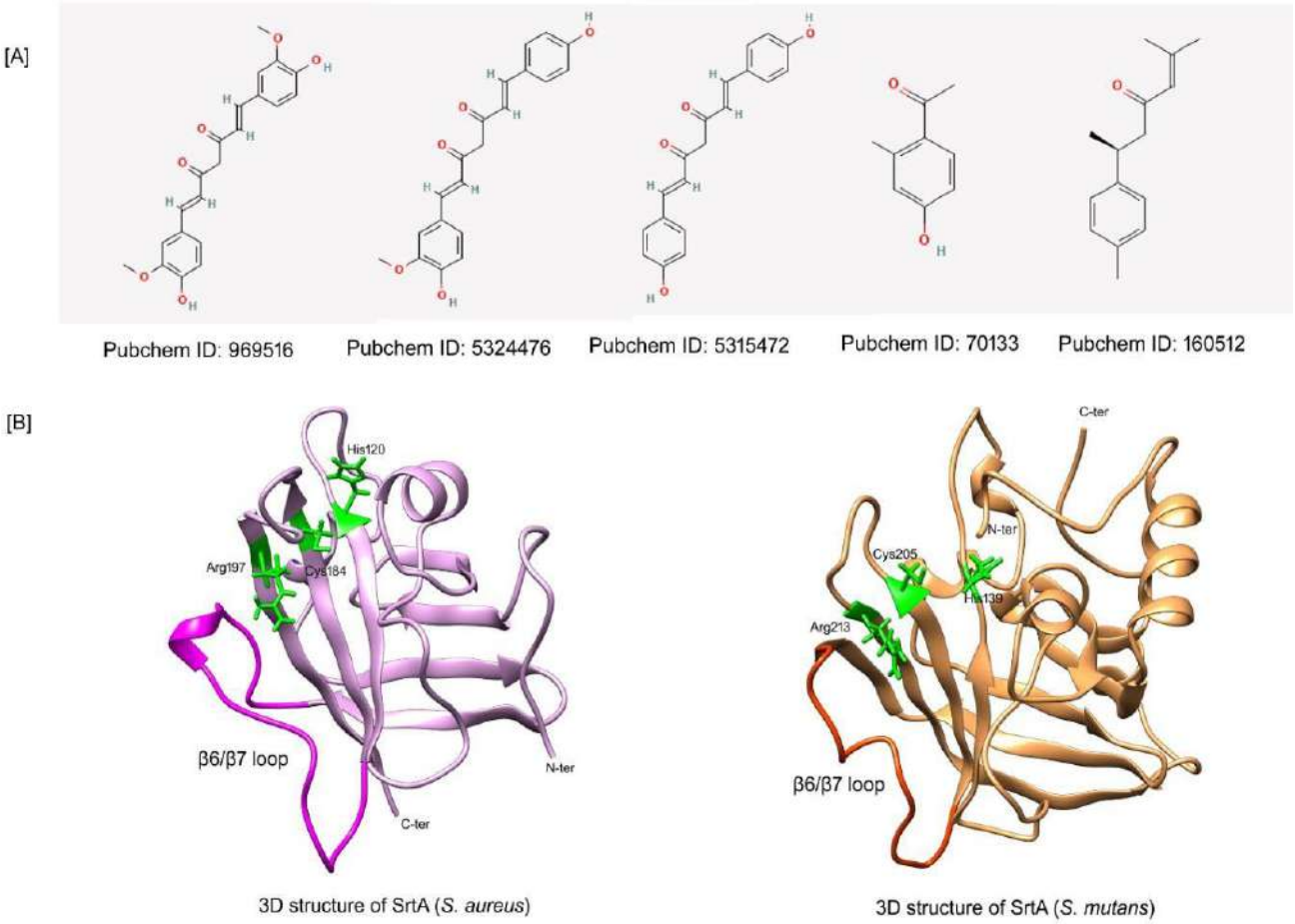

Fig. 4.5.1: The 2D representation of the PGPR treated phytocompounds with PubChem ID and the three-dimensional representation of the relaxed conformation of $SrtA_{staph}$ and $SrtA_{strepto}$.

Table 4.5.1: The ADMET profile of PGPR induced phytocompounds, as well as their PubChem ID, are listed below

Name	PubChem ID	Molecular weight	LogP	SkinSen	Ames	DILI	Carcinogenicity	LC_{50}	Lipinski	Pfizer
Carvone	7439	150.22	2.136	0.041	0.029	0.455	0.432	3.777	Accepted	Accepted
Transchalcone	139036268	208.26	2.987	0.952	0.818	0.668	0.627	5.908	Accepted	Accepted
Curcumin	969516	368.38	2.742	0.958	0.234	0.895	0.706	6.191	Accepted	Accepted
Demethoxycurcumin	5324476	338.36	2.786	0.96	0.41	0.877	0.611	6.13	Accepted	Accepted
Bisdemethoxycurcumin	5315472	308.33	2.847	0.967	0.613	0.843	0.457	6.05	Accepted	Accepted
4 hydroxy 2 methyl acetophenone	160512	150.17	1.771	0.347	0.12	0.462	0.556	3.515	Accepted	Accepted
Ar turmerone	70133	216.32	4.11	0.925	0.015	0.259	0.475	4.57	Accepted	Rejected

4.5.3.2 Antibiofilm activity of PGPR induced phytocompounds from *C. longa*

In order to investigate the biofilm inhibition activity of all phytocompounds, crystal violet assay was performed against biofilm forming *S. aureus* and *S. mutans*. The wells containing curcumin, curcuminoids, 4 hydroxy 2 methyl acetophenone, along with combination of curcumin and 4 hydroxy 2 methyl acetophenone showed the biofilm inhibition activity. Notably, profound anti-biofilm activity was observed for synergistic action of curcumin and 4 hydroxy 2 methyl acetophenone. It may be stated that biofilms without phytocompounds were more securely adhered to the micro plate wells and were less disrupted in staining procedure. The higher absorbance of crystal violet of untreated well of bacteria indicate well established biofilm. However, when bacteria in well treated with curcumin, curcuminoids, 4-hydroxy- 2-methylacetophenone at 300µg/ml concentration the decrease in absorbance was observed which implies the inhibition of biofilm. The profound biofilm inhibition activity was observed for the combination of curcumin and 4 hydroxy 2 methyl acetophenone. These results suggest that the combination of curcumin and 4 hydroxy 2 methyl acetophenone are more effective than alone of phytocompounds as an anti-biofilm activity (Fig. 4.5.2). Hence, these metabolites alone and in their combination are manifested to inhibit the biofilm formation by *S. aureus* and *S. mutans*.

S. aureus is known for biofilm-related infections, particularly in nosocomial infections (Gould 2009), but *S. mutans* is more commonly connected with dental carries (Caroline et al., 2018). Bacteria associated with biofilm are resistant to the majority of regularly used antibiotics, and they create extracellular polymeric substance (EPS) for cell-to-cell adhesion and biofilm growth, slowing the diffusion of conventional antibiotics (Nadaf et al., 2018). Attachment to cell surfaces, matrix development, and maturation are the phases in the biofilm formation (Nadar et al., 2022). Several earlier studies demonstrated that alone curcumin inhibits the growth of biofilm producing organisms (Hu et al., 2013; Park et al., 2005). However, our both *in-vitro* and *in-silico* studies showed significant biofilm inhibition activity of phytocompounds in combination against *S. aureus* as compare to alone targeting adhesion protein SrtA.

4.5.3.3 Biofilm inhibition study by scanning electron microscopy (SEM)

To confirm the anti-biofilm activity of phytocompounds on *S. aureus* NCIM

2654, SEM analysis was implemented. The SEM analysis of untreated *S. aureus* showed more organised and dense bacterial biofilm (chapter 4- Fig.4.4.6A). The untreated cells had a smooth, undamaged surface that was spherical in shape, contributing in their strong adherence to one another (chapter 4-Fig. 4.4.6A). The disorganized adhesion of the bacteria was clearly visible in bacteria treated with phytocompounds (chapter 4-Fig. 4.4.6 B-D,G), indicating impediment in formation of aggregate and an inability to maintain their normal morphology. SEM analysis also revealed that, after the treatment of curcumin and 4-hydroxy-2-methylacetophenone alone cell number get drastically reduced as compare to control (chapter 4-Fig. 4.4.6 A, B, G). Notably, combination of curcumin and 4-hydroxy-2-methylacetophenone showed profound effect on cell morphology and cell number, the cell number get reduced as compared to all experiment in this study. Similarly, cells loses their adhesion after being treated with all phytocompounds, and alterations to their morphology was observed, our results suggest the synergistic impact of phytocompounds better than an individual on biofilm inhibition. These observations lend credence to the results of the growth curve investigations.

One of the key steps in the production of biofilms, called quorum sensing or cell-to-cell communication, where microorganisms may interact with each other. Gram positive and Gram-negative microbes have been the subject of the most thorough research in this process (Waters and Bassler, 2005; Eberhard et al., 1981; Sheikh et al., 2013; Vendeville et al., 2005). According to reports, the inhibitory effect of phytocompounds on quorum sensing and the formation of biofilms is a phenomenon that depends on the density of the bacteria (Filomena et al., 2013). Our findings, however, suggest that inhibiting adhesion may halt the development of biofilms right at their beginning, which may be more useful when developing fresh therapeutic approaches. Earlier several studies showed the role of sortaseA (SrtA) in attachment of surface protein involved in adhesion of cell to host and subsequent biofilm formation (Hu et al., 2013; Wang et al., 2019; He et al., 2017).

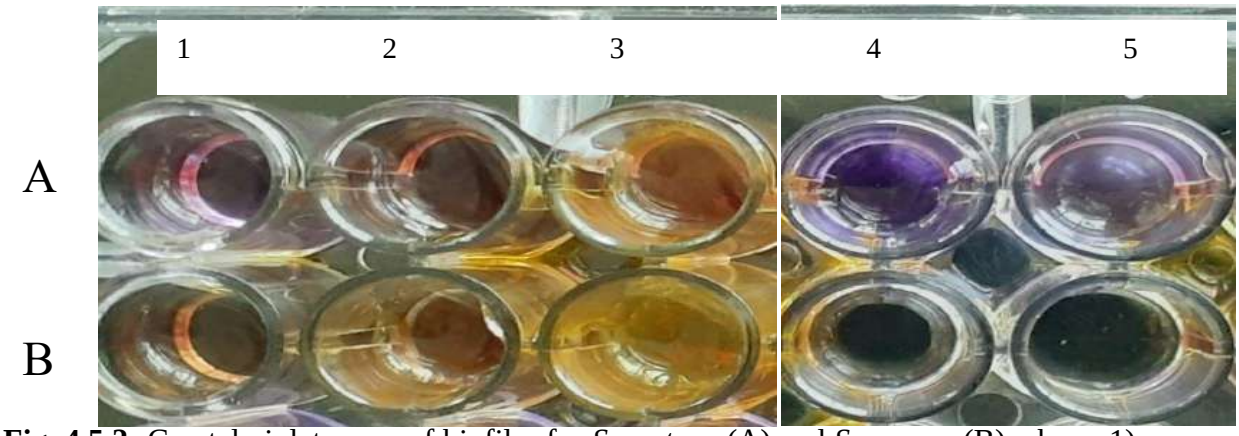

Fig. 4.5.2: Crystal violet assay of biofilm for *S. mutans* (A) and *S. aureus* (B) where, 1) is control untreated cells 2) cells treated with curcumin 3) cells treated with curcuminoids 4) cells treated with 4-hydroxy-2-methylacetophenone 5) cells treated with curcumin + 4-hydroxy-2 methylacetophenone

4.5.3.4 Structural analysis, refinement and validation of SrtA

In order to investigate the mechanism of inhibition of sortaseA (SrtA) from both *S. aureus* and *S. mutans* by phytocompounds molecular modelling techniques were used. The structural stability of SrtA was evaluated by MD simulation and analysis of conformational stability parameters such as root mean square deviation (RMSD), root mean square fluctuation (RMSF) and radius of gyration (Rg). The overall quality of SrtA structure was validated using, the ERRAT score, ramachandran plot along with the stereochemical properties of $SrtA_{staph}$ and $SrtA_{strepto}$. The ERRAT scores of $SrtA_{staph}$ and $SrtA_{strepto}$ conformations are 97 and 95 percent, respectively, indicating that the tertiary structure is of high quality. The Ramachandran plot shows that 98.6 percent of the residues ($SrtA_{staph}$) and 98.9 percent of the residues ($SrtA_{strepto}$) occupy the most allowed and additionally allowed region in the plot (Fig.4.5.3). It is worth noting that after structural refinement in free form of $SrtA_{staph}$ and $SrtA_{strepto}$, no single residue occupies a disallowed region in either sortases.

The N-terminal signal peptide of SrtA was removed in this study due to its flexibility and positioned away from the primary binding pocket. The result, suggests that both of these models of $SrtA_{staph}$ and $SrtA_{strepto}$ have good stereochemical properties as well as native secondary structural folds in the tertiary structure (Fig.4.5.1B). The calculated Q-means of $SrtA_{staph}$ and $SrtA_{strepto}$ are 0.7 and 0.62, respectively, indicating

the model's reliability. The ProSA analysis results of SrtA$_{staph}$'s showed Z-score of -5.93, and -4.89 for SrtA$_{strepto}$, confirming the good overall quality of the 3D structures. The structural quality of protein is also supported by the local quality, which is estimated using the knowledge-based energy value for all amino acids in SrtA$_{staph}$ and SrtA$_{strepto}$ which are less than 0. These results suggest both SrtA$_{staph}$ and SrtA$_{strepto}$ have fewer high energy regions in their relaxed conformations. The relaxed conformation of SrtA$_{staph}$ and SrtA$_{strepto}$ (Fig. 4.5.1B) is represented in three dimensions, highlighting the β 6/7 loop and key active residues in stick form (shown in green).

4.5.3.5 Binding mode analysis and intermolecular interactions of phytocompounds with SrtA

Docking studies aid in elucidating binding poses and estimating binding affinity as observed in previous studies (Dhanavade et al., 2013; Parulekar and Sonawane 2017; Barale et al., 2019). SrtA$_{Staph}$ and SrtA$_{strepto}$ energetically refined structures were used to investigate binding mode and explore intermolecular interactions of phytocompounds at the atomic level using UCSF's dock6.9. The docking studies were also conducted using carvone (car) as control for SrtA$_{Staph}$ and transchalcone (TC) for SrtA$_{strepto}$. Our docking protocol reproduced and showed similar type of binding and interaction of carvone (Car) and transchalcone (TC) molecules with SrtA$_{Staph}$ and SrtA$_{strepto}$ respectively, validating our docking protocol also. Curcumin, demethoxy curcumin, bisdemethoxy curcumin, 4 hydroxy 2 methyl acetophenone, and ar-turmerone bind to the binding pocket residues of SrtA$_{staph}$ and SrtA$_{strepto}$ and represented as SrtA$_{Staph}$-C1, SrtA$_{Staph}$-C2, SrtA$_{Staph}$-C3, SrtA$_{Staph}$-C4, SrtA$_{Staph}$-C5, and in combination SrtA$_{Staph}$-C1+C4, and for SrtA$_{strepto}$-C1, SrtA$_{strepto}$-C2, SrtA$_{strepto}$-C3, SrtA$_{strepto}$-C4, SrtA$_{strepto}$-C5 and in combination SrtA$_{Strepto}$-C1+C4 respectively. Binding affinity to the SrtA$_{Staph}$ was estimated in decreasing order to be C1 > C2 > C3 > C5 > Car > C4 > C1+C4 and for SrtA$_{Strepto}$ it was estimated to be C2 > C3 > C1 > C1+C4 > TC > C5 > C4. The grid score, van der Waals energy, and repulsive energy of phytocompounds Car, TC, C1, C2, C3, C4, C5, C1+C4 (combination) and bound to both the SrtA$_{Staph}$ and SrtA$_{strepto}$ are listed in Table 4.5.2. These result showed the curcumin (C1) has a much stronger binding to SrtA$_{Staph}$ than car (control), however, curcumin analogue demethoxy curcumin (C2) reflects much stronger binding towards SrtA$_{strepto}$ than TC (control), the binding mode of all phytocompounds depicted in Fig. 4.5.4A and 4.5.4B The analysis of intermolecular interactions suggests that the

formation of stable complexes is primarily triggered by conserved non-bonded contacts with the key binding pocket residues reported in previous studies (Nadaf et al., 2018; Bi et al., 2016; Chenna et al., 2008). The fact that hydrophobic and hydrogen bonding interactions facilitates the formation of stable complexes in all complexes (Table 4.5.3). In both SrtA$_{Staph}$ and SrtA$_{strepto}$ complexes, the residues Thr, Lys, Ala, and Glu (156 to 177) of the β 6/7 loop play a critical role in loop opening and closing as compared to other neighbouring residues. Docking results showed interacting residues of SrtA$_{Staph}$ Glu105, Cys184, Arg 197, Lys62 and for SrtA$_{strepto}$ Cys205, His139, Arg213, Ser138 found in interaction with phytocompounds.

C4 binds at the active site of SrtA in complex SrtA$_{Staph}$-C1+C4, whereas C1 binds at an alternate binding pocket adjacent to the primary binding pocket of SrtA. Previous studies showed the compounds have been bind at other than active site of SrtA (Gao et al., 2016). Our findings of forming a stable ternary complex with SrtA$_{Staph}$ and SrtA$_{strepto}$ of C1 and C4 respective are consistent with previous reports. In the complex SrtA$_{Strepto}$-C1+C4, both C1 and C4 occupy in same binding pocket and exhibit conserved non-bonded interactions, as reported in the crystal structure (Wallock et al., 2015). Fig. 4.5.5 depicts non-bonded interactions in the studied complexes in two dimensions.

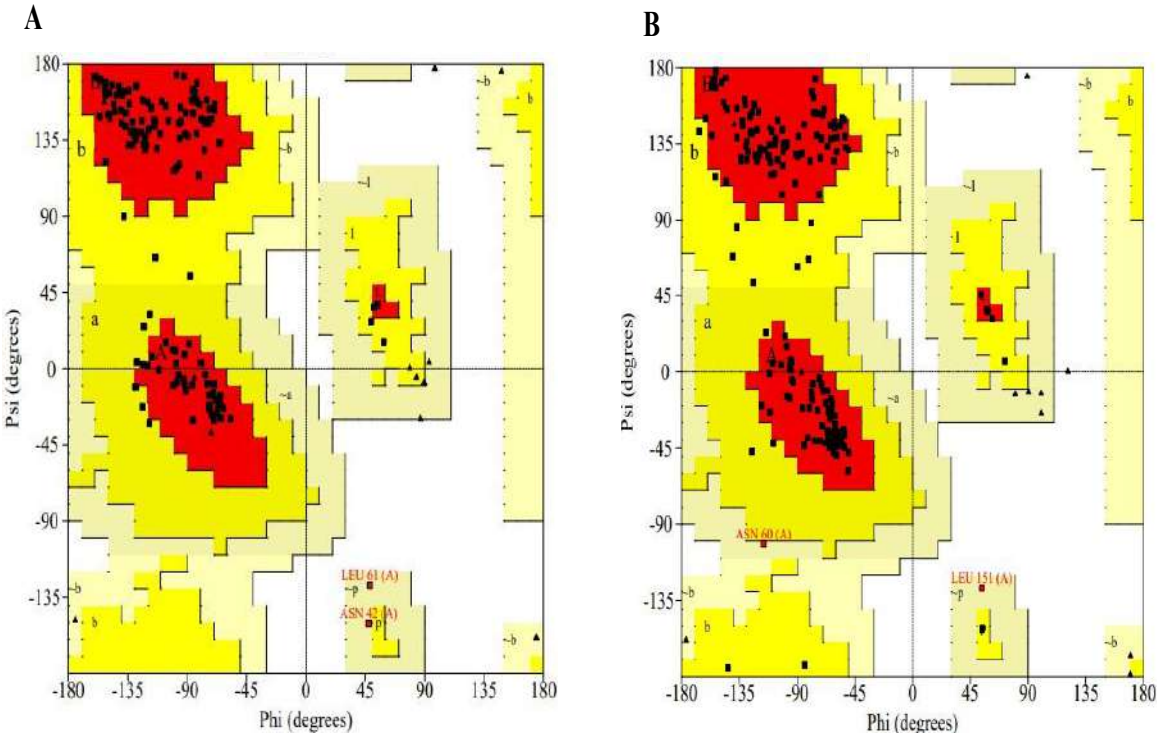

Fig. 4.5.3: Ramachandran plot of SrtA$_{staph}$ (A) and SrtA$_{strepto}$ (B) model with rebuilt loop.

Table 4.5.2: Molecular docking of phytocompounds with active site residues of $SrtA_{staph}$ and $SrtA_{strepto}$-using Dock6.9

	Compound name	**Grid Score**	**Vwd energy**	**Energy repulsive**
$SrtA_{staph}$	Carvone (Car)	-21.06	-21.31	3.97
	Curcumin(C1)	-34.55	-29.10	14.18
	Demethoxycurcumin(C2)	-32.29	-28.02	10.49
	Bisdemethoxycurcumin(C3)	-31.24	-27.11	4.85
	4-hydroxy-2-methylacetophenone (C4)	-19.49	-17.28	2.60
	Ar-turmerone(C5)	-21.47	-21.03	9.79
	Curcumin + 4-hydroxy-2-methylacetophenone (C1+C4)	-18.74	-18.74	2.12
$SrtA_{strepto}$	Transchalcone (Tc)	-23.05	-22.21	2.85
	Curcumin(C1)	-31.38	-29.96	11.39
	Demethoxycurcumin(C2)	-32.73	-30.33	4.30
	Bisdemethoxycurcumin(C3)	-31.99	-28.46	3.64
	4-hydroxy-2-methylacetophenone (C4)	-18.59	-15.55	1.76
	Ar-turmerone(C5)	-21.40	-20.08	8.01
	Curcumin + 4-hydroxy-2-methylacetophenone (C1+C4)	-23.31	-23.31	13.99

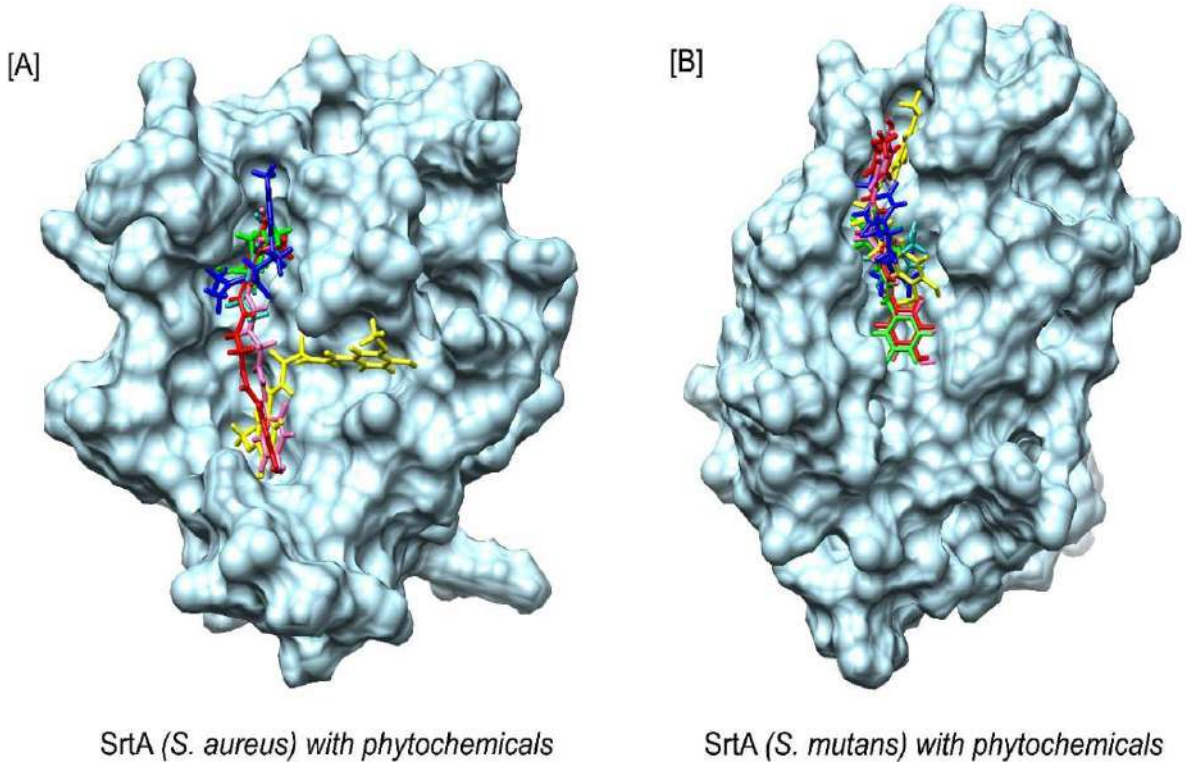

Fig. 4.5.4: The surface view depicts the binding mode of all phytocompounds bound to $SrtA_{staph}$ and $SrtA_{strepto}$

Table 4.5.3: Hydrogen bonding interactions of phytocompounds with $SrtA_{staph}$ and $SrtA_{strepto}$ in docking

	Compound name	**Interaction**	**Distance(Å)**
$SrtA_{staph}$	Carvone (Car)	ALA92 HN…O1 UNK	3.07726
	Curcumin(C1)	LEU169 HN… O3 UNK GLY167 O … H13 UNK VAL168 H… O3 UNK	2.68979 2.4078 2.00886
	Demethoxycurcumin(C2)	LEU169 HN…O5 UNK ARG197 H…O3 UNK ALA104 O…H15 UNK	2.04411 2.64559 2.71909
	Bisdemethoxycurcumin(C3)	LEU169 HN…O3 UNK	2.51404
	4-hydroxy-2-methylacetophenone C4)	GLY192 O…H10 UNL TRP194 HD1… C5 UNL ILE182 HD12… O2	2.22369 2.788 2.854

		UNL	
	Ar-turmerone(C5)	-	-
	Curcumin + 4-hydroxy-2-methylacetophenone (C1+C4)	LEU169 H …O3 UNK VAL168 H…H UNK VAL166 C20… H UNK SER109 HB2… O4 UNK ALA 92 HB3…H UNL TRP194 H… O2 UNL ARG 197 HD2… O2 UNL GLY192 O… H5 UNL	1.737 1.654 2.630 2.009 2.674 2.369 2.941 2.688
SrtA*strepto*	Transchalcone (Tc)	HIS140 H…O1 UNK THR204 H… O1UNK CYS205 H… O1 UNK HIS139 HA… O1 UNK	2.35582 2.71581 2.42955 2.94051
	Curcumin(C1)	ALA210 H… O5 UNK SER138 O… H15 UNK ASP68 O… H18 UNK	3.04136 3.03284 2.56842
	Demethoxycurcumin(C2)	HIS140 H…O4 UNK	2.41686
	Bisdemethoxycurcumin(C3)	HIS140 H… O2UNK HIS139 H…O2 UNK	2.24961 2.88918
	4-hydroxy-2-methylacetophenone (C4)	THR204 H… O1 UNL CYS205 H… O1 UNL SER138 O… H10 UNL HIS139 H… O2 UNL	2.56819 2.32768 2.66199 2.91423
	Ar-turmerone(C5)	ASN113 H… O1 UNK HIS139 H… O1UNK	2.91684 2.47309
	Curcumin + 4-hydroxy-2-methylacetophenone (C1+C4)	CYS205 H… O1 UNK SER138 O… H1 UNK HIS139 H… O2 UNK HIS139 HE1… O2 UNL CYS205 H… H1 UNL THR204 HG1… H1 UNL	2.32768 2.172 2.91423 2.914 2.599 1.920

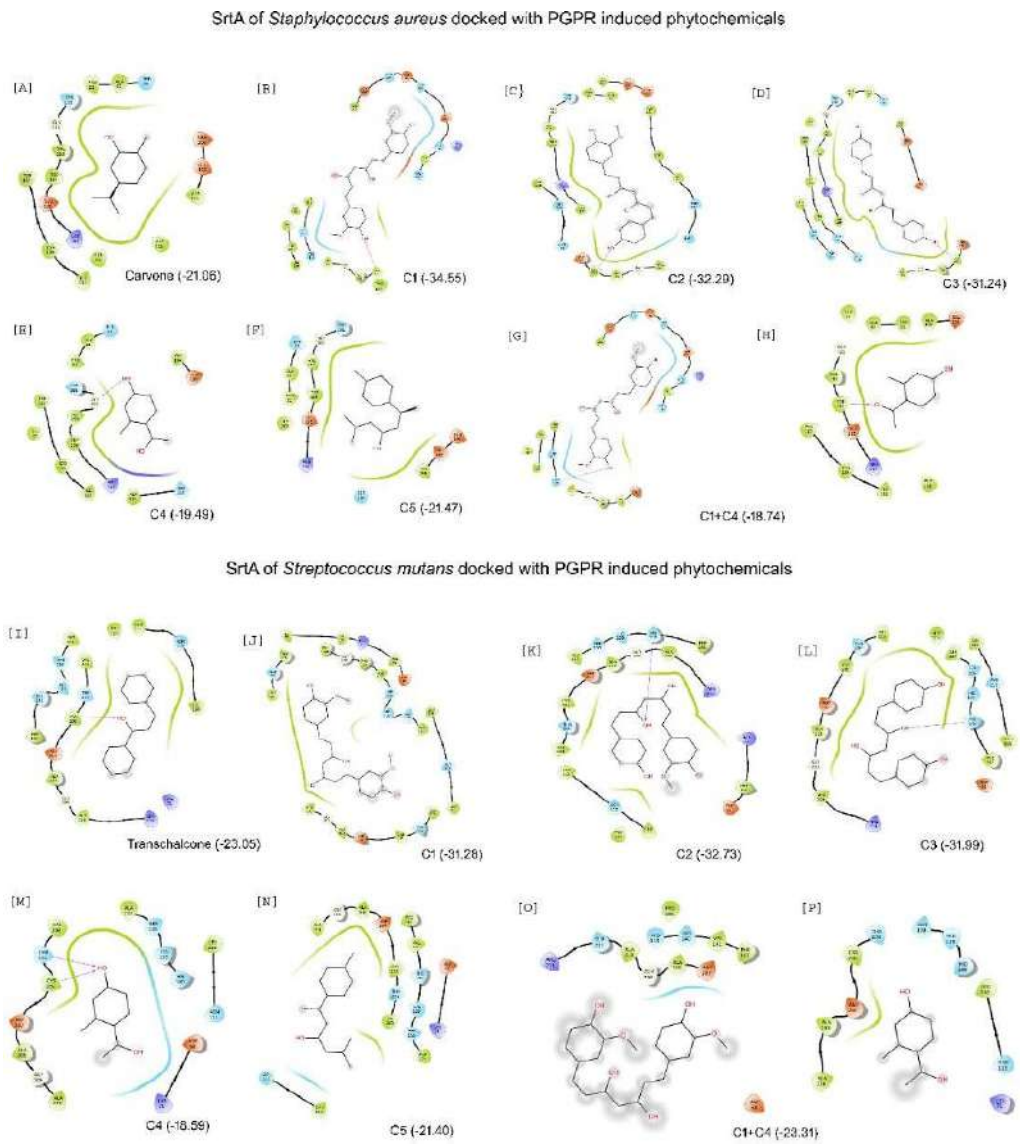

Fig. 4.5.5: Nonbonded interactions in the complexes studied are represented in 2D

4.5.3.6 MD simulations of SrtA in complex with phytocompounds to assess structural stability

MD simulation helps to generate ensemble of configurations, assessment of structural stability of ligand bound proteins, further in free energy calculations and ligand induced conformational changes. MD simulations of 100 ns performed for all the docked complexes namely SrtA$_{Staph}$-Car, SrtA$_{Strepto}$-TC, SrtA$_{Staph}$-C1, SrtA$_{Staph}$-C2, SrtA$_{Staph}$-C3, SrtA$_{Staph}$-C4, SrtA$_{Staph}$-C5, SrtA$_{Staph}$-C1+C4, SrtA$_{Strepto}$-C1, SrtA$_{Strepto}$-C2, SrtA$_{Strepto}$-C3, SrtA$_{Strepto}$-C4, SrtA$_{Strepto}$-C5, SrtA$_{Strepto}$-C1+C4 to investigate their structural stability and

intermolecular interactions. The trajectories of all simulated complexes were examined for the quality and dependability of the MD parameters. Throughout the simulation, the potential energy, temperature, and pressure were all analysed to ensure the quality of all the trajectories. The data show that the pressure and temperature remained constant at 300K and 1bar, respectively, and that the potential energy fluctuated less during MD. As a result, we believe that all of the MD simulation trajectories are properly equilibrated.

The parameters that explain structural stability have been studied, including RMSD, RMSF, Rg, and solvent accessible surface area (SASA). Calculating the RMSD of proteins allows for the quantification of the degree of conformational changes that may occur during MD simulations with respect to the starting structure as a reference. An average RMSD of SrtA$_{Staph}$ and SrtA$_{Strepto}$ in complex with all phytocompounds fall within a range of 2 and 2.5Å, respectively (Fig. 4.5.6A and 4.5.6B; Table 4.5.4). This RMSD analysis of SrtA from both the pathogens reflects the structural stability. The complex of SrtA$_{Staph}$-Car has a higher RMSD of 2.3 when compared to other complexes bound to SrtA$_{Staph}$. Overall, we found that after the equilibrium period of 0 ns to 60 ns, all of the simulated complexes were well stabilized. The complexes SrtA$_{Staph}$-C5 and SrtA$_{Strepto}$-C5 have higher RMSD values, owing to the flexibility of the N-terminal domain (NTD). RMSF analysis of C-alpha of residues of SrtA from both pathogens in complex with all phytocompounds showed similar kind of residue fluctuation except for the complex SrtA$_{Strepto}$-C5 (Fig. 4.5.6D). In SrtA$_{Staph}$ complexed with phytocompounds, the N-terminal region shows maximum fluctuations with RMSF values up to 5.5 Å, whereas the fluctuation of SrtA$_{Strepto}$ shows the highest RMSF value of 12 Å. As seen in the RMSF plot, the maximum RMSF value in SrtA$_{Strepto}$ is primarily due to the N-terminal flexibility of the SrtA$_{Strepto}$-C5 complex. Overall, the stability of SrtA was attained during MD simulation due to facilitation of stable complexation of phytocompounds with the residues Thr156 to Lys177 of SrtA$_{Staph}$ and Thr184 to Asn198 of SrtA$_{Strepto}$ within the loop β 6/7 (Fig. 4.5.6C and 4.5.6D). Additionally, our results highlight the much lower fluctuations and more stability of SrtA from both the pathogen, when complexed with both curcumin and 4-hydroxy 2-methyl acetophenone (C1and C4). The reported key residues of both SrtA$_{Staph}$ and SrtA$_{Strepto}$ His, Cys, and Arg, show less fluctuation. This emphasises the importance of these binding pocket residues in the formation of stable protein-ligand complexes.

Another parameter that contributes to overall spatial arrangement of secondary structure in protein is Rg, which represents the folding and unfolding pattern and compactness of protein-ligand complexes. A comparison of the Rg values of all the complexes shows that the control complexes in our study, SrtA$_{Staph}$-Car and SrtA$_{Strepto}$-TC, have larger deviation in Rg values, indicating that these complexes are unstable, most likely due to poor binding pocket interactions (Fig. 4.5.7A and 4.5.7B). The SrtA$_{Strepto}$-C5 complex exhibits partial unfolding for up to 30ns before adopting compact globular shapes during the simulation (Fig. 4.5.7B). As a result, we believe that the partial unfolding at the N-terminus of SrtA$_{Strepto}$ may cause some conformational changes at the binding pocket, enhancing the interactions. The Rg value of the ternary complexes SrtA$_{Staph}$-C1+C4 and SrtA$_{Strepto}$-C1+C4 is relatively stable, indicating that the binding of curcumin (C1) and 4-hydroxy 2-methyl acetophenone (C4) promotes the formation of compact globular conformations (Fig. 4.5.7A and 4.5.7B). Except for SrtA$_{Strepto}$ -C5 and SrtA$_{Strepto}$-TC, the complexes of phytocompounds bound to SrtA$_{Strepto}$ showing similar folding pattern as revealed by a steady decrease in Rg values during the simulation from 16.15 to 15.8. (Fig. 4.5.7B). However, phytocompounds bound to SrtA$_{Staph}$ exhibit Rg value variations (Rg value ranges between 14.5 and 15.1), resulting in a different folding pattern in all complexes. As a result, we propose that SrtA$_{Staph}$ undergoes significant conformational changes during MD simulations, resulting in the formation of stable complexes. In order to evaluate compactness of SrtA, we calculate solvent accessible surface area (SASA), which is thought to be important for intermolecular interactions within globular molecules. It aids in determining the protein's accessibility to the solvent. The stability of SrtA was observed in a similar trend of hydrophobic SASA as that of Rg values which was observed in all complexes (Fig. 4.5.7C and 4.5.7D). Increased SASA has been observed for complexes SrtA$_{Strepto}$-C5 and SrtA$_{Strepto}$-TC, revealing the unfolding caused by interruption of hydrophobic interactions in non-polar residues. The SASA plot reveals a moderate fluctuation in the SASA of all complexes, indicating its importance in the formation of stable complexes

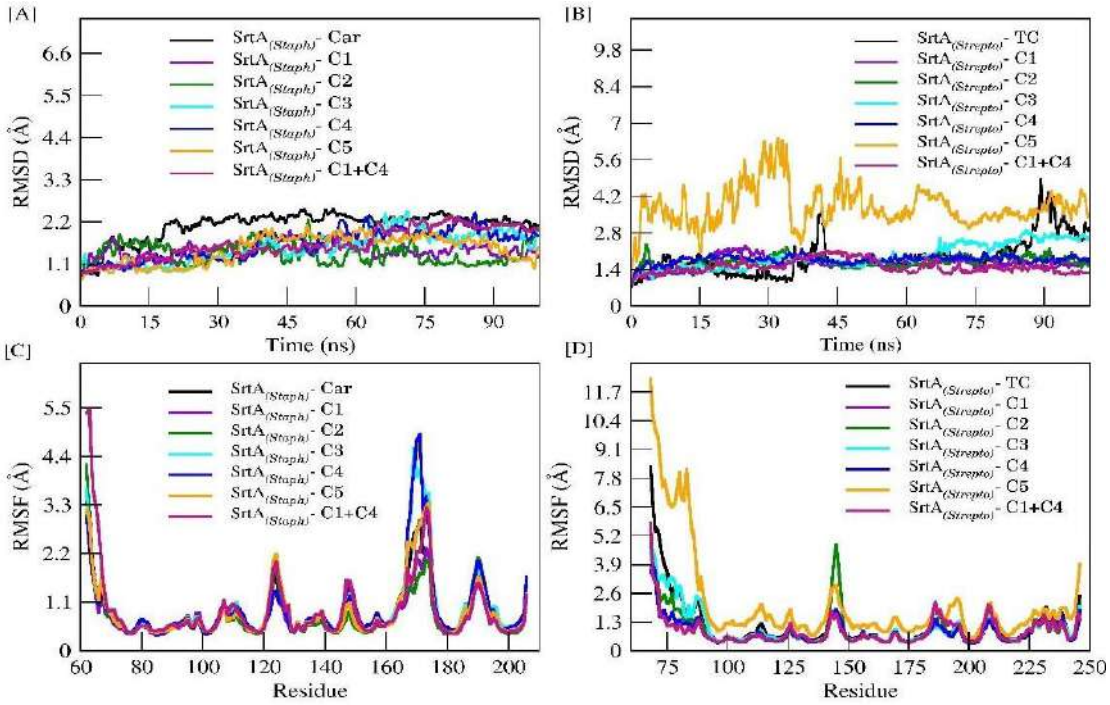

Fig. 4.5.6: The structural stability of simulated complexes was investigated by plotting the backbone RMSD of all complexes. A) $SrtA_{staph}$ B) $SrtA_{strepto}$ and C) $SrtA_{staph}$ D) $SrtA_{strepto}$ and their comparative RMSF

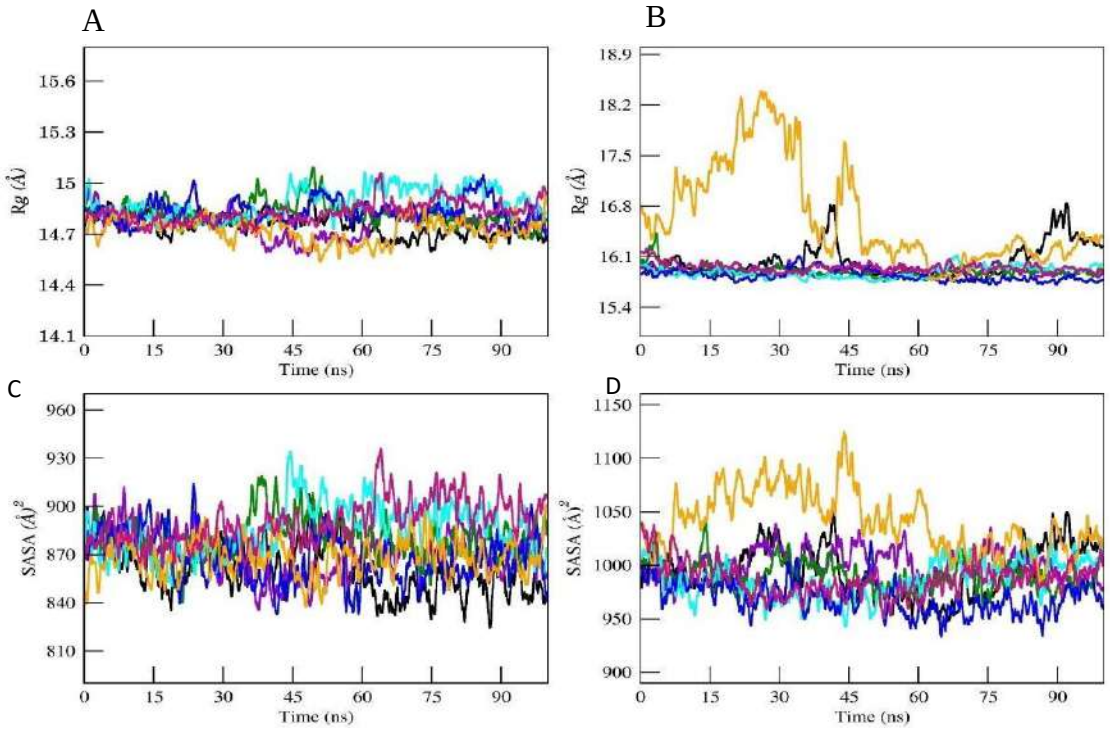

Fig. 4.5.7: The radius of gyration of A) $SrtA_{staph}$ B) $SrtA_{strepto}$ and solvent accessible area of all C)$SrtA_{staph}$ D) $SrtA_{strepto}$ complexes.

Table 4.5.4: Analysis of MD trajectories for average RMSD, RMSF and Rg of SrtA*staph* and SrtA*strepto* over 100 ns.

	Name of organisms					
	Staphylococcus aureus			*Streptococcus mutans*		
	RMSD(Å)	**RMSF(Å)**	**Rg**	**RMSD(Å)**	**RMSF(Å)**	**Rg**
C1	1.4 ±0.02	0.8 ±0.04	14.7 ±0.009	1.6 ±0.02	0.9 ±0.05	15.9 ±0.006
C2	1.3 ±0.02	0.7 ±0.04	14.8 ±0.008	1.6 ±0.02	0.9 ±0.07	15.8 ±0.009
C3	1.5 ±0.04	0.9 ±0.07	14.8 ±0.01	1.9 ±0.04	1.0 ±0.07	15.8 ±0.008
C4	1.6 ±0.04	0.9 ±0.07	14.8 ±0.008	1.7 ±0.01	0.8 ±0.05	15.8 ±0.008
C5	1.4 ±0.03	0.8 ±0.06	14.7 ±0.008	3.8 ±0.07	2.1 ±0.19	16.6 ±0.06
C1+C4	1.6 ±0.04	0.9 ±0.07	14.8 ±0.007	1.6 ±0.02	0.8 ±0.05	15.9 ±0.008
Car	2.1 ±0.03	0.8 ±0.05	14.7 ±0.008	-	-	-
Tc	-	-	-	1.8 ±0.07	1.1 ±0.09	16.0 ±0.02

4.5.3.7 Molecular interactions contributes in inhibition of SrtA

Hydrogen bonding interactions are crucial in protein-ligand interactions among the other non-bonded interactions. The number of hydrogen bonds formed with SrtA*Staph* and SrtA*Strepto* by phytocompounds during the MD simulation was plotted against time (Fig. 4.5.8). The hydrogen bond analysis showed the complexes SrtA*Strepto*-C1, SrtA*Strepto* -C2, and SrtA*Strepto* -C1+C4 maximum number of H-bonds with SrtA, with a total of six, four of which are consistent during the MD simulation. Compound C5 (ar-turmerone) interacts poorly with both sortases, SrtA*Staph* and SrtA*Strepto*. The calculated minimum distance between the ligand and protein demonstrates that in complex SrtA*Staph*–C1,

$SrtA_{Staph}$–C4, $SrtA_{Staph}$–C1+C4, $SrtA_{Strepto}$-C1, $SrtA_{Strepto}$-C1+C4 phytocompounds maintain close contacts with SrtA forming stable non-bonded contacts during the MD simulation. The compound C5 exhibits increased distance in both the sortases $SrtA_{Staph}$ and $SrtA_{Strepto}$ due to significant conformational changes expressed during the dynamics (RMSD, RMSF, Rg, and SASA) responsible for the weak non-bonded interactions. Overall, the complexes such as $SrtA_{Staph}$-C1+C4 and $SrtA_{Strepto}$-C1+C4 have the minimum distances, indicating the stability of ternary complex formed by C1 and C4 further these interactions are stable and conserved during the simulation. In conclusion, the results of analysis of molecular interactions during docking, MD simulation showed the structural stability of SrtA in complex with Curcumin (C1), and 4-hydroxy 2-methyl acetophenone (C4) and in their combination. These results are consistent with our biofilm inhibition assay by crystal violet and SEM, hence we believe that Curcumin, and 4 hydroxy 2 methyl acetophenone in combination would be effective to inhibit SrtA and for biofilm inhibition.

The number of contacts quantifies interactions between spatially closed amino acids that are not sequentially next to each other in the protein's primary sequence. The percentage of contacts that are preserved reflects the stability of the protein-ligand complexes. We looked at the total number of contacts to learn more about the structural stability of the simulated complexes. Except for phytocompounds C5 complexed with both $SrtA_{Staph}$ and $SrtA_{Strepto,}$ all complexes showed a steady increase in the number of contacts. In $SrtA_{Staph}$ and $SrtA_{Strepto}$, the number of contacts formed by C1, C2, C3, and C4 are significantly greater than that of the controls, Car and TC. However, the ternary complex formed by C1 and C4 in $SrtA_{Staph}$ and $SrtA_{Strepto}$ shows a consistent number of contacts with relatively less fluctuations, highlighting the importance of both of these compounds in SrtA inhibition. The non-bonded interactions between phytocompounds and SrtA following MD simulation are illustrated in Fig. 4.5.9A and Fig.4.5.9B.

In order to evaluate the consistency of non-bonded interactions of phytocompounds with SrtA we compare the starting docked conformation of SrtA and final confirmation from MD simulation. Table 4.5.5 list all of the important hydrogen and non-bonded interactions that influence stable complex formation. The interactions observed in our simulated SrtA complexes with phytocompounds were also compared to the control complexes and previously reported interactions (Katsipis et al., 2020, Bi et

al., 2016, Zong et al., 2004). This analysis reveals that residues from the β 6/7 loop, such as Lys, Asp, Gly, Gln, Leu, Val, and Thr, play an important role in the formation of stable complexes. During the MD simulations, we observed that hydrophobic interactions outweighed the H-bonding interactions. In addition, number of intermolecular interactions in all complexes has increased at the end of MD simulation as compared to the initial starting conformation.

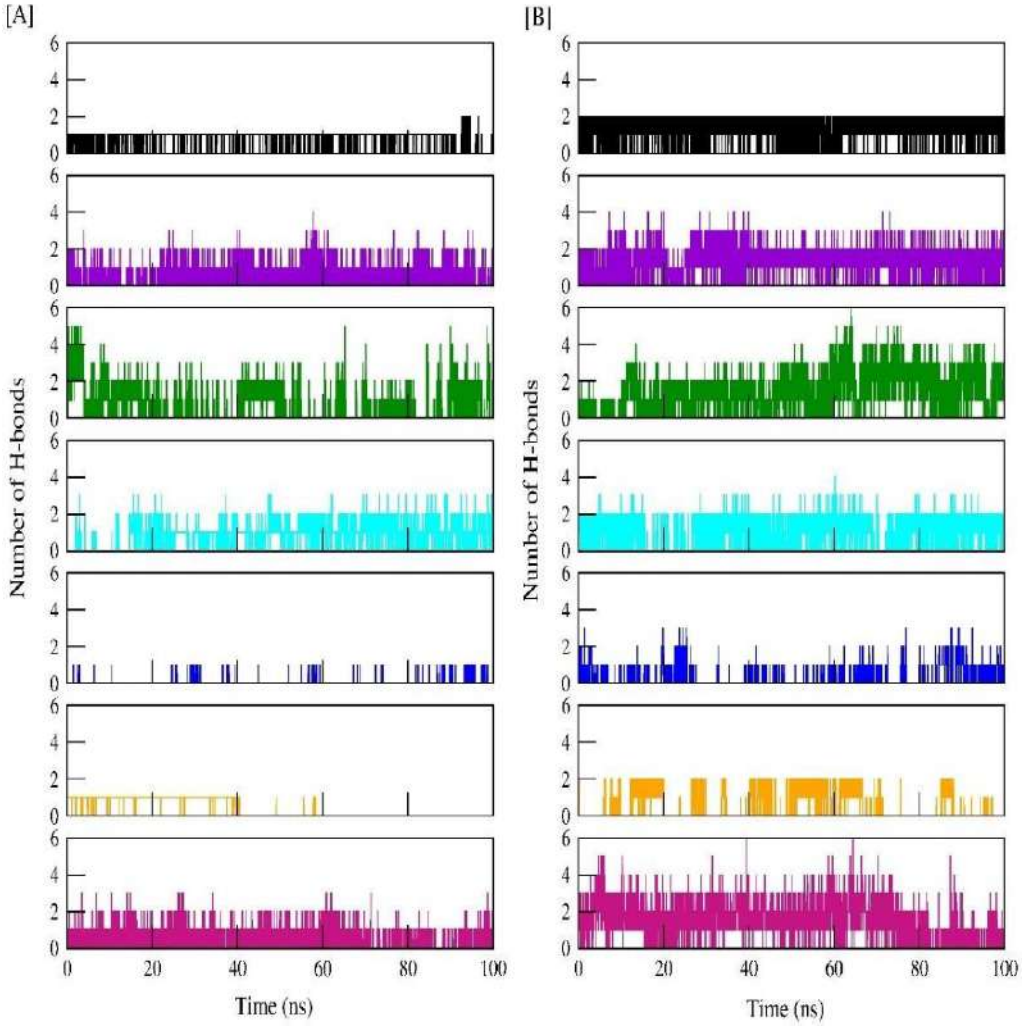

Fig. 4.5.8: Hydrogen bond interactions observed in complexes of PGPR induced phytocompounds in A)$SrtA_{staph}$ B) $SrtA_{strepto}$

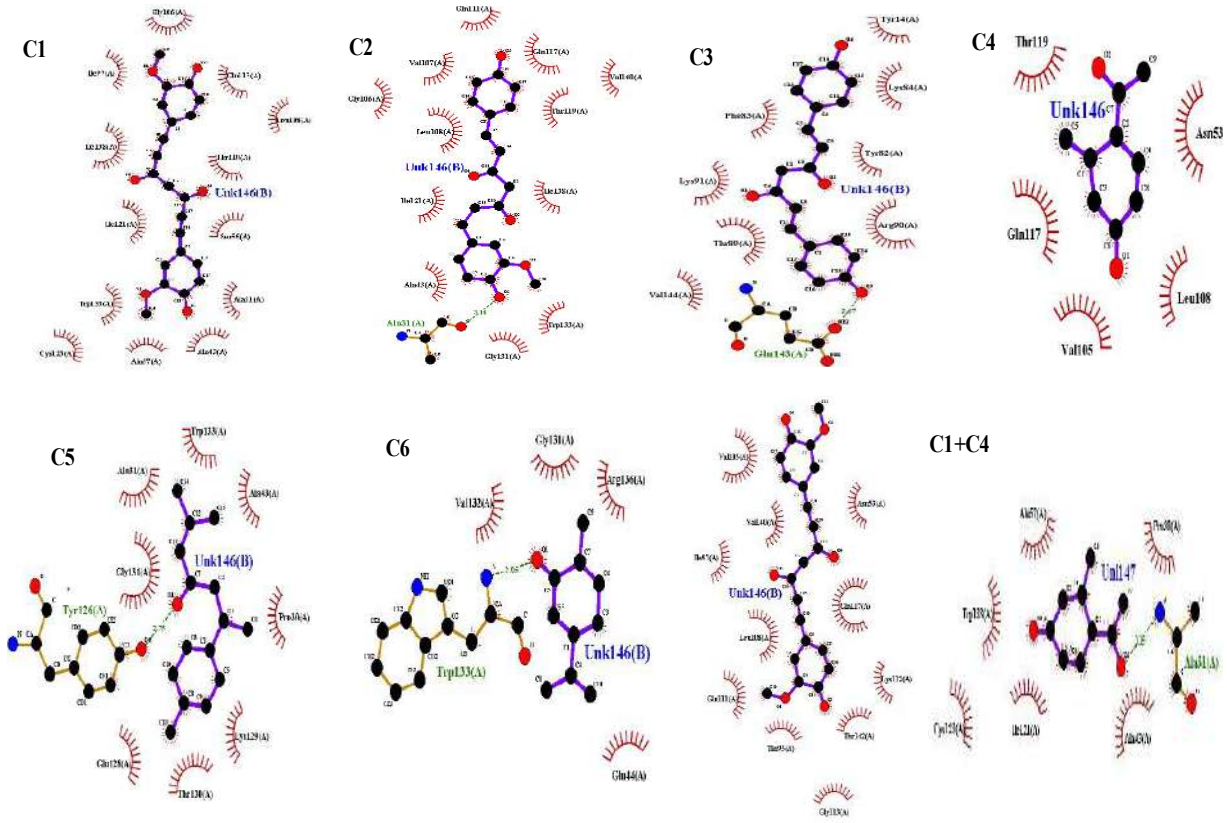

Fig. 4.5.9A: Nonbonded interactions in the complexes of $SrtA_{staph}$ studied after MD simulation are represented in 2D

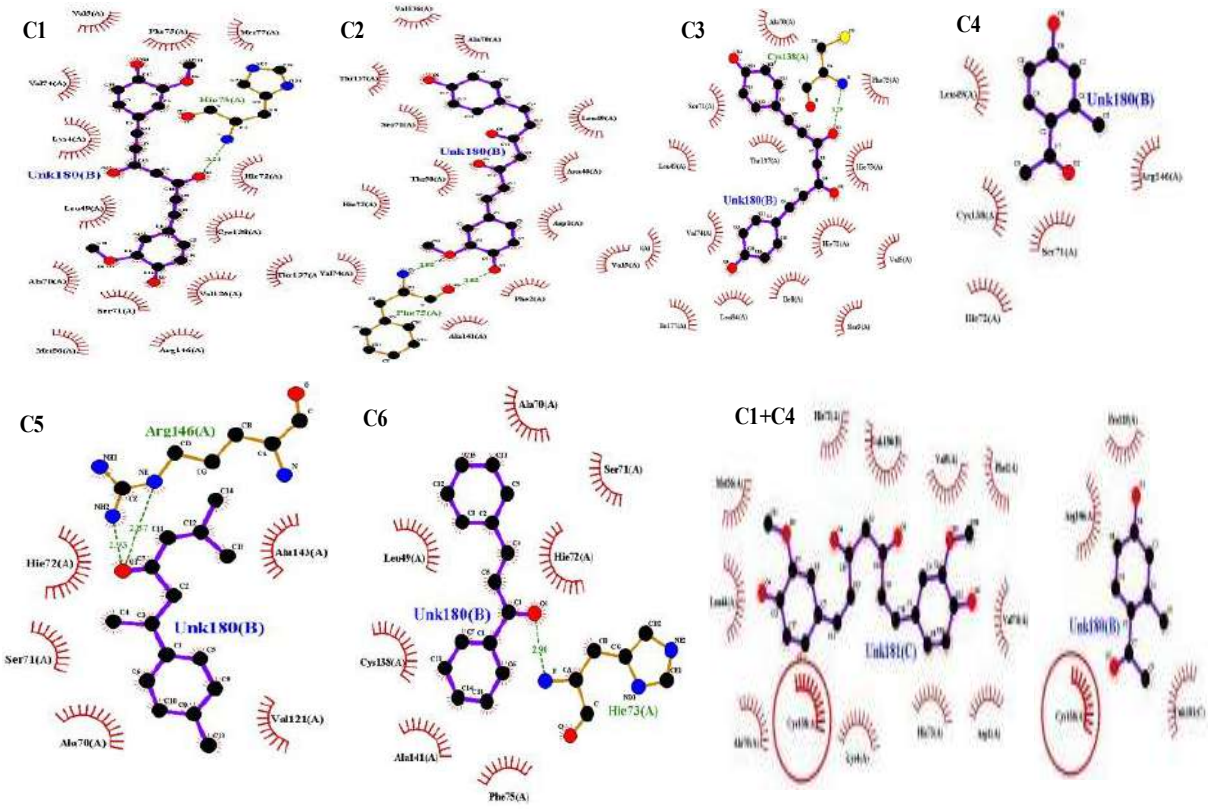

Fig. 4.5.9B: Nonbonded interactions in the complexes of $SrtA_{strepto}$ studied after MD simulation are represented in 2D.

Table 4.5.5: Hydrogen bond interactions of phytocompounds with $SrtA_{staph}$ and $SrtA_{strepto}$ during MD simulations.

	Compound name	**Interaction**	**Distance(Å)**
$SrtA_{staph}$	Carvone (Car)	TRP194 H… O1 UNK VAL193 H… O1 UNK TRP194 HD… O1 UNK	1.99652 2.88217 2.72136
	Curcumin(C1)	GLY167 HN… O1 UNK SER116 OG…O6 UNK TRP194 HD1… O2 UNK	2.41154 3.0304 2.7939
	Demethoxycurcumin(C2)	ALA92 H… O2 UNK TRP194 HE1…O2 UNK ARG197 HE… O2 UNK	2.88586 2.65387 2.66132 2.38455

		GLY192 O… H17 UNK	
	Bisdemethoxycurcumin(C3)	GLU204 OE2…H15 UNK	1.72421
	4-hydroxy-2-methylacetophenone (C4)	ILE182 HD12 … O2 UNL TRP194 HD1… C5 UNL GLY192 O… H10 UNL	2.854 2.788 2.224
	Ar-turmerone(C5)	TYR187 HH…O1 UNK	1.81662
	Curcumin + 4-hydroxy-2-methylacetophenone (C1+C4)	ASN114 HD22… O6 UNK GLY174 HA1… O3 UNK VAL166 HB… O4 UNK VAL201 HG12… O6 UNK GLN178 HG3… O6 UNK ALA 92 H… O2 UNL TRP194 HD1… O1 UNL PRO91 HB2… O1 UNL	3.09247 2.66458 2.682 2.838 2.792 2.586 2.297 2.406
SrtA*strepto*	Transchalcone (Tc)	HIS140 H…O1 UNK CYS205 H…O1 UNK HIS139 HA…O1 UNK	1.90111 2.76199 2.64532
	Curcumin(C1)	HIS140 HN…O5 UNK CYS205 HN… O5 UNK LYS71 HE1… O6 UNK	2.31886 2.36848 2.26958
	Demethoxycurcumin(C2)	PHE142 H… O1 UNK PHE142 O…H14 UNK VAL141 HA… O1 UNK PHE142 O…H16 UNK	2.00704 2.10119 2.71378 2.92132
	Bisdemethoxycurcumin(C3)	HIS140 HN…O2 UNK CYS205 HN… O2 UNK	2.53223 2.38858
	4-hydroxy-2-methylacetophenone (C4)	ALA137 H…C5 UNL LEU111 HD1…H10 UNL	2.25865 2.781
	Ar-turmerone(C5)	ARG213 HE… O1 UNK	1.93355 2.08737

		ARG213 HH21…O1 UNK	
	Curcumin + 4-hydroxy-2-methylacetophenone (C1+C4)	LEU111 HD1… H14 UNK MET123 HE… CH10 UNK HIS139 HE1… CH1 UNK ALA137 HB1… CH10 UNK PRO185 O… H1 UNL ARG213 HD3… O2 UNL	2.968 2.125 2.512 2.054 1.896 2.902

4.5.3.8 Effect of phytocompounds on secondary structure of SrtA$_{staph/strepto.}$

The Dictionary of secondary structure of protein (DSSP) tool was used to analyse the distortions in the secondary structural changes during the MD simulation. Complexes of phytocompounds C1, C2, C3, C4, and C5 with SrtA$_{staph}$ exhibit fewer deviations at the secondary structural level; interestingly, all of the β-sheets maintain their structures throughout the simulations (Fig. 4.5.10A). The β 6/7 loop formed by the residues Thr156-Lys177 undergoes structural transitions during the MD and contributes significantly to stable interactions with phytocompounds. SrtA$_{staph}$ also formed a short-lived helix in this β 6/7 loop in a ternary complex of C1+C4). This short-lived helix is expected to give the binding pocket rigidity by forming stable H-bonding interactions. Furthermore, complex SrtA$_{staph}$-C1+C4 exhibits closure movement by the β 6/7 loop and N-terminal helix, whereas complex SrtA$_{staph}$- Car β 6/7 loop and N-terminus move away from each other. As a result of the closure movement of β 6/7 at the active site, we observed the most non-bonded interactions in SrtA$_{staph}$–C1+C4. During the MD simulation of complex SrtA$_{Strepto}$–C5, the N-terminal helix loses its helicity completely and transitions to turn. As seen in the RMSD, RMSF, and Rg plots, increased flexibility of the N-terminal region is responsible for the larger deviation in structural stability of the SrtA$_{Strepto}$–C5 complex. This N-terminal helix's helicity varies moderately in other complexes, namely SrtA$_{Strepto}$-C1, SrtA$_{Strepto}$–C2, SrtA$_{Strepto}$–C3, and SrtA$_{Strepto}$–C4, whereas in complex SrtA$_{Strepto}$-C1+C4 helicity is well maintained throughout the simulation (Fig. 4.5.10B). The complex N-terminal helix in complexes SrtA$_{Strepto}$– C2 and SrtA$_{Strepto}$-C1+C4 exhibits scissoring movement, promoting the opening and closing of the binding pocket and enhancing non-bonded interactions during simulation. Other secondary structure components exhibit the

fewest variations in the structure. The minimum distance between the residues has also been used to estimate the local conformational changes at the binding pocket. As a result, the SrtA*Strepto*–C1+C4 complex is more stable than other complexes.

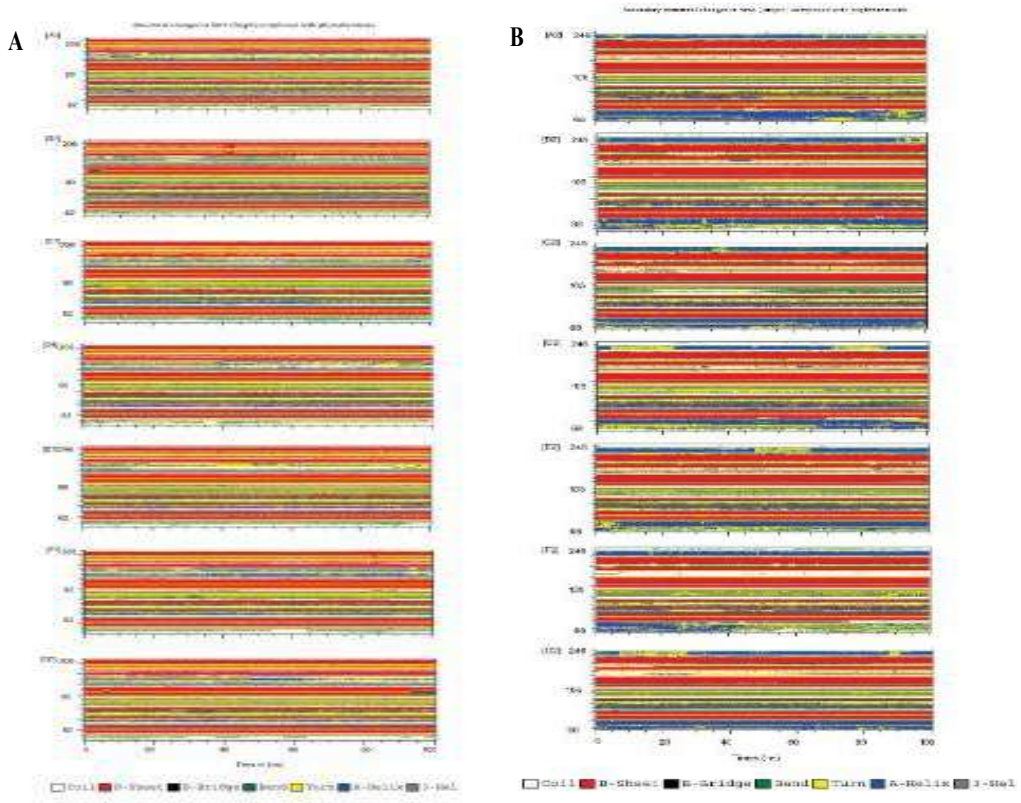

Fig. 4.5.10: The distortions in the secondary structure observed during MD simulation were noted in SrtA*staph*(A) and SrtA*strepto*(B) using DSSP of all the studied phytocompounds.

4.5.3.9 Binding energy calculation using MM/GBSA and SrtA residue contribution in binding

The binding free energy provides a reliable estimate of the protein-ligand binding affinities. In this context we used the MM/GBSA method to calculate binding free energy; the individual components that contribute to binding energy are listed in (Table 4.5.6a and 4.5.6b). The compounds in complex with SrtA*staph* are found the binding energy order of in descending order C1+C4>, C1>C3>C5>C2>Car>C4, whereas compounds in complex with SrtA*Strepto* showed a binding energy order of C3>C1>C1+C4>C2>TC>C5>C4. In our study, the majority of the compounds have

higher binding affinity than the control (Car and TC) to $SrtA_{staph}$ and $SrtA_{Strepto}$, respectively. A newer phytocompound 4-hydroxy 2-methyl acetophenone from our previous study with the smallest molecular weight of 150.17 and the smallest size has the lowest binding affinity with $SrtA_{staph}$ and $SrtA_{Strepto}$. However, when compared to the other compounds studied, the combination of C1 and C4 complexed with $SrtA_{staph}$ ($SrtA_{staph}$–C1+C4) exhibits significantly higher binding affinity. The compounds C1, C3, and C1+C4 with comparable binding energy values were observed to $SrtA_{strepto}$, but based on the overall MD analysis e.g. structural stability, intermolecular interactions, and conformational changes at the structural level. Thus, we propose that the combination of curcumin and 4-hydroxy 2-methyl acetophenone is more effective and favours the formation of stable complexes. As a result, the curcumin and 4-hydroxy 2-methyl acetophenone combination of these compounds would be regarded as the best possible inhibition for both sortases, $SrtA_{staph}$ and $SrtA_{strepto}$. We also performed residue decomposition analysis to determine the contribution of individual residues to the binding energy (Fig.4.5.11A and 4.5.11B). According to this data, the residues involved in the stable non-bonded interactions such as van der Waals and electrostatic during the MD which contribute significantly in the total binding energy. The β 6/7 loop residues for $SrtA_{staph}$ and $SrtA_{strepto}$ are Ile 158, Gly 167, Leu 169, Gln 178, and Pro 185, Val 188, and Thr 204, respectively. Similarly, the active site residues for $SrtA_{staph}$ and $SrtA_{strepto}$ are Cys 184, Arg 197, and His 139, Cys 205, Arg 213, contributes the most to the binding energy, emphasising the importance of this flexible loop in the formation of stable complexes.

Table 4.5.6 a: The relative binding energy of phytocompounds in binding with $SrtA_{staph}$.

Compound name	**ΔTOTAL(SD)**	**ΔVDWAALS**	**ΔEEL**	**ΔEGB**	**ΔESURF**	**ΔGGAS**	**ΔGSOLV**
Carvone	-18.97±0.21	-20.29	-8.11	12.17	-2.75	-28.40	9.43
Curcumin	-31.84±2.83	-36.75	-17.05	27.21	-5.24	-53.81	21.97
Demethoxycurcumin	-22.71±3.92	-29.63	-9.38	20.67	-4.37	-39.01	16.30
Bisdemethoxycurcumin	-27.90±1.79	-32.18	-16.02	25.13	-4.83	-48.20	20.30
4-hydroxy-2-methylacetophenone	-13.47±0.82	-17.10	-8.44	14.64	-2.57	-25.54	12.07
Ar-turmerone	-23.62±0.44	-21.47	-2.78	3.53	-2.90	-24.25	0.63
Curcumin + 4-hydroxy-2-methylacetophenone	-62.34±0.36	-71.23	-5.16	22.43	-8.38	-76.39	14.05

Table 4.5.6 b: The relative binding energy of phytocompounds in binding with SrtA*strepto*.

Compound name	ΔTOTAL	ΔVDWAALS	ΔEEL	ΔEGB	ΔESURF	ΔGGAS	ΔGSOLV
Transchalcone	-29.55± 0.75	-5.24	0.0	13.73	-4.18	-34.79	9.55
Curcumin	-53.84±1.46	-60.24	-9.62	22.10	-6.08	-69.86	16.02
Demethoxycurcumin	-36.85± 2.04	-41.98	-26.55	37.85	-6.17	-68.53	31.68
Bisdemethoxycurcumin	-56.81±0.46	-61.86	-1.45	12.38	-5.87	-63.31	6.50
4-hydroxy-2-methylacetophenone	-16.37±1.24	-14.95	-1.99	2.97	-2.39	-16.95	0.58
-Ar-turmerone	-25.79±1.80	-26.48	-14.70	19.14	-3.76	-41.18	15.38
Curcumin + 4-hydroxy-2-methylacetophenone	-51.39±0.42	-45.71	-3.87	5.02	-6.82	-49.59	-1.80

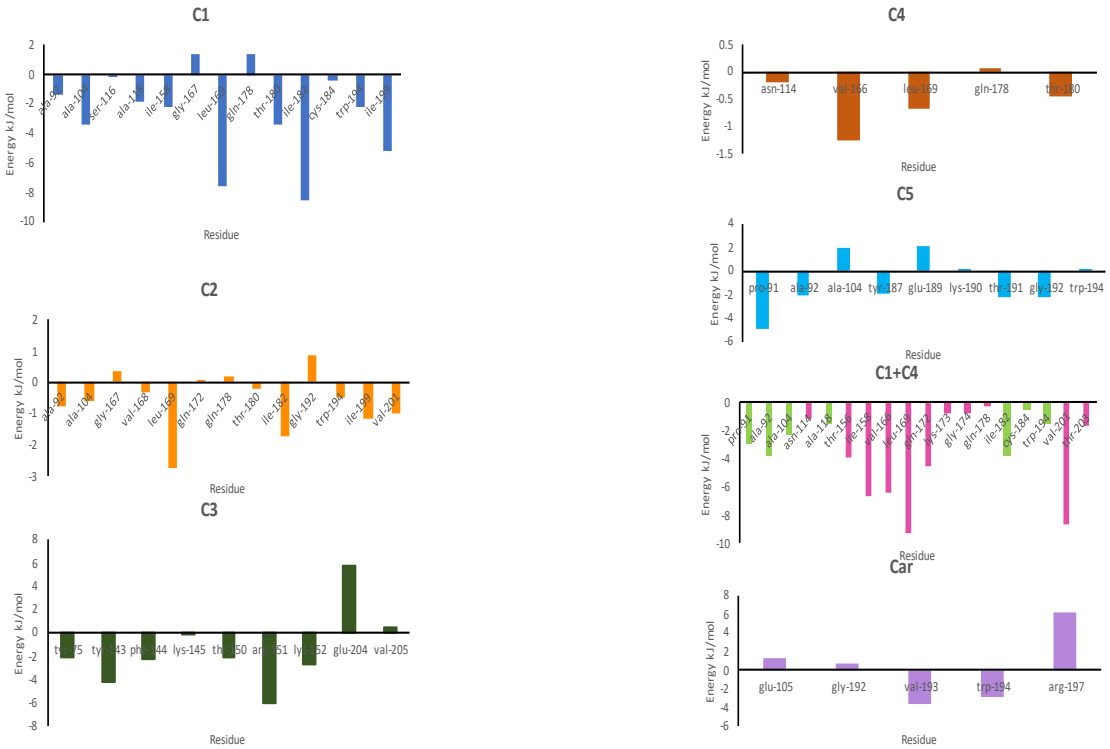

Fig. 4.5.11A: The energy contribution of residues from SrtA*staph* complexes to binding free energy in kJ/mol

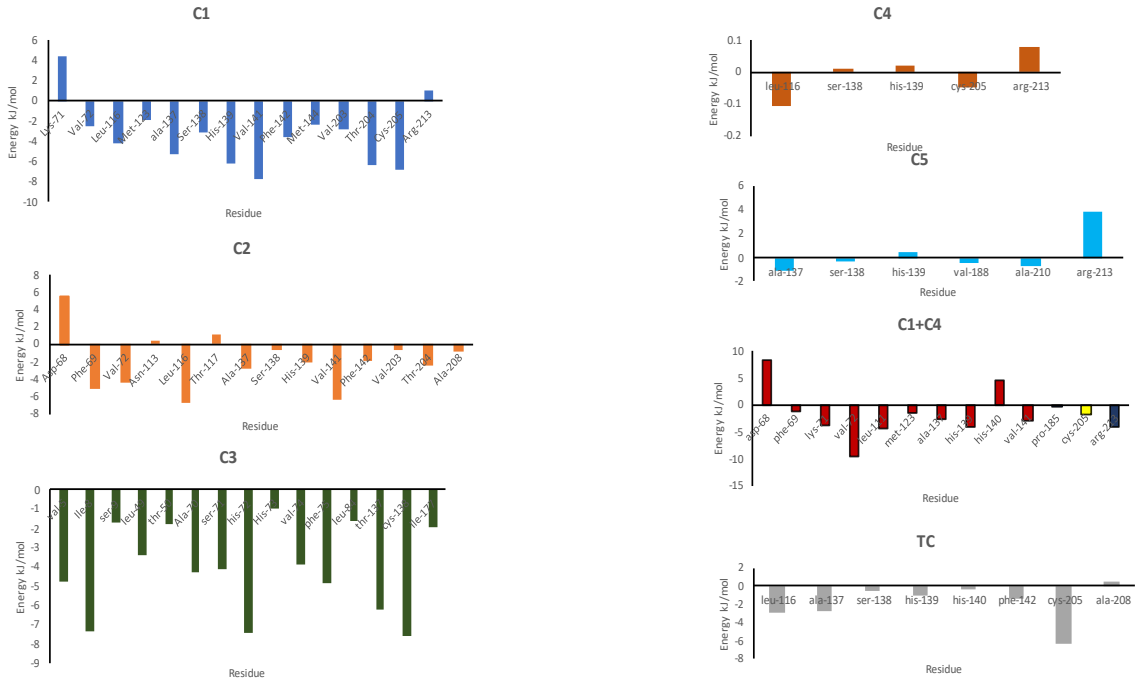

Fig. 4.5.11B: The energy contribution of residues from SrtA*strepto* complexes to binding free energy in kJ/mol

4.5.3.10 Principle component analysis (PCA) and dynamic cross correlation map

The coordinated motions of SrtA*staph* and SrtA*strepto* caused by the binding of phytocompounds from *C. longa* were recorded in order to gain important insights into the significant dynamic information and inter residue and inter domain correlation of SrtA*staph* and SrtA*strepto*. The dynamic cross correlation map in 2D for all complexes is depicted in Fig. 4.5.12 Individual residue self-correlation in all complexes shows a strong positive correlation with itself (Fig.4.5.12). The control complex i.e. SrtA*staph* – Car exhibits overall negative correlation in various regions of the SrtA*staph*, whereas the amplitude of negative correlation in complex SrtA*strepto*–TC is relatively smaller. The ternary complex SrtA*strepto*–C1+C4 has a negative correlation with the N-terminal region, indicating that the β 6/7 loop has a significant dynamic nature that facilitates the stable interactions of curcumin and 4-hydroxy 2-methyl acetophenone at the primary and alternate binding pockets of SrtA*staph*. A similar negative correlation has been observed in another ternary complex, SrtA*staph*–C1+C4, but the amplitude of the negative correlation is much lower. However, the SrtA*staph*–C5 and SrtA*strepto*–C5 show a moderately positive correlation with the N-terminal region at β 6/7 loop and our MD results show that the dynamics of these

two complexes are unstable. Thus, the negative co-operative motion of the β 6/7 loop with the N-terminal region has a significant influence on the stability of SrtA complexes with phytocompounds.

In order to observe the conformational dynamics, we extracted the extreme conformations of SrtA using PCA from the stable trajectory observed during the simulation. The compact globular shape has been adopted in complexes SrtA$_{strepto}$–C1+C4 and SrtA$_{strepto}$–C2, owing to the scissoring motion exerted by bending the N-terminal domain towards the binding pocket. The extended conformation of the β 6/7 loop has been observed in complex SrtA$_{staph}$–C1+C4, which promotes proper folding of this SrtA$_{staph}$ to form a compact globular shape. The open and close states have been observed in the binding pocket region of SrtA$_{staph}$ and SrtA$_{strepto}$ complexes where large phytocompounds such as C1, C2, and C3 occupy the binding pocket.

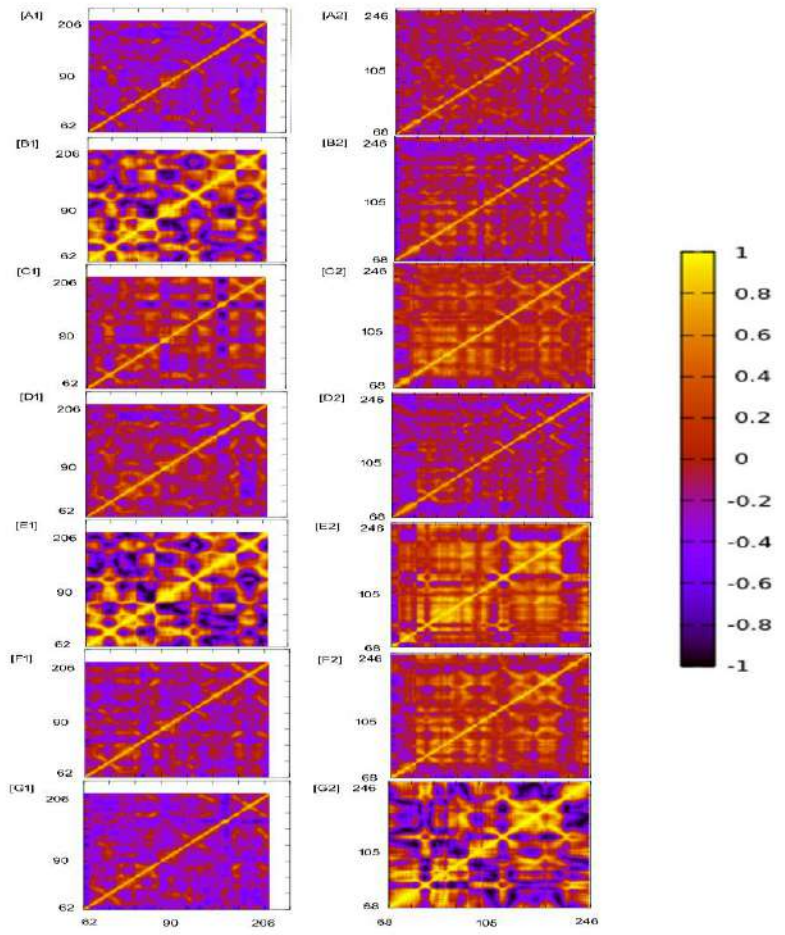

Fig. 4.5.12: Concerted motion analysed using dynamic cross corelation map for all complexes where (A1 to G1) for SrtA$_{staph}$ and (A2 to G2) for SrtA$_{strepto}$

4.5.4 Conclusions:

Thus, in the present work, we studied the inhibition of biofilm forming pathogens such as *S. aureus* and *S. mutans* by using PGPR induced phytocompounds of *C. longa*. In this context, our biofilm inhibition experiment with crystal violet and SEM showed the inhibition of biofilm formation for all the phytocompounds from *C. longa*. Notably, the synergistic action of curcumin and 4-hydroxy 2 methylacetophenone showed significant anti-biofilm forming activity. Further, we targeted the adhesion protein SrtA from both the *S. aureus* and *S. mutans* to study the inhibition mechanism using molecular modelling methods. Our docking studies revealed varying binding sites for phytocompounds and combination of binding of phytocompounds significantly lowers the binding energy of overall complex implies the synergistic inhibition mechanism of phytocompounds. MD simulation and MM-GBSA binding energy calculation studies showed the stability of SrtA in all phytocompounds specifically for ternary complexes of combined curcumin and 4-hydroxy-2-methylacetophenone.

Thus, we propose that binding of Curcumin and 4-hydroxy-2-methylacetophenone to the binding pocket and alternate site, respectively, attains a high stability in ternary complex of SrtA as compare to other phytocompounds alone that inhibits SrtA more effectively than individual compounds. Thus, this study would pave the way for the development of PGPR-induced secondary metabolite therapeutic approaches by targeting SrtA to control biofilm related infectious diseases.

CHAPTER V

SUMMARY AND CONCLUSIONS

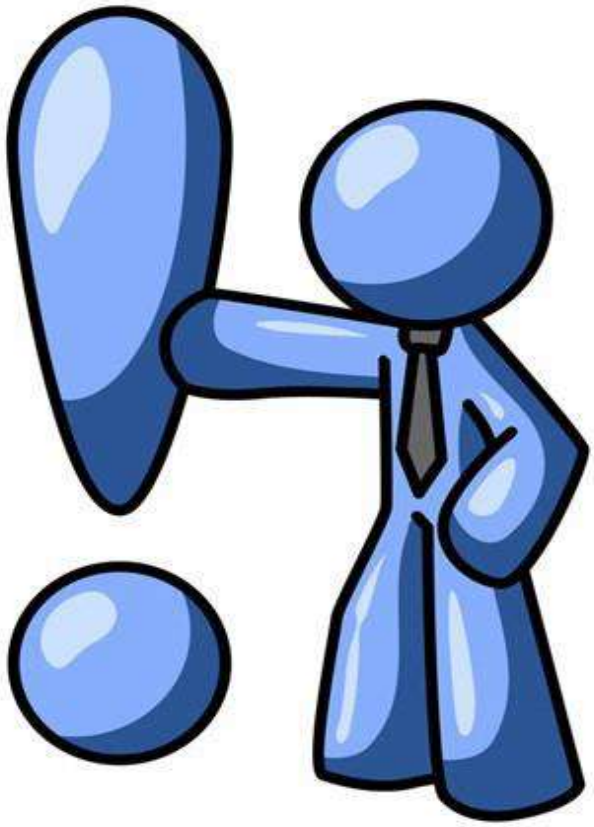

SUMMARY AND CONCLUSIONS:

5.1 Summary:

In the present study, we have selected two medicinal plants - namely are *Curcuma longa* (Turmeric) and *Asparagus racemosus* (Asparagus). Phytochemical analysis of Turmeric has revealed a large number of compounds, including curcumin, volatile oil, and curcuminoids, all of which have potent pharmacological properties. Curcuminoid which is a group of phenolic compounds, represented in the quantities ranging from 2 to 5 % of the dry weight, as a functional secondary metabolite. Asparagus has saponins ranging from 5 to 7 % of dry weight as a major secondary metabolite.

The present work resulted in the isolation of novel strains of plant growth-promoting rhizobacteria from the rhizosphere of two medicinal plants - Turmeric and Asparagus with maximum plant growth-promoting traits. The isolated PGPR strains were characterized on the basis of their morphological and biochemical properties. Further, they were identified by the molecular characterization by 16S rRNA analysis. The Turmeric rhizosphere isolates were identified as strains of *Serratia nematodiphila* and *Pseudomonas plecoglossicida* while Asparagus rhizosphere isolates were identified as the strains of *Exiguobacterium acetylicum* and *Enterobacter mori*. These isolates were designated as *Serratia nematodiphila* RGK, *Pseudomonas plecoglossicida* RGK, *Exiguobacterium acetylicum* RGK and *Enterobacter mori* RGK1. These strains were used for pot culture studies. A pot culture study demonstrated that PGPR treatment improved the growth, yield, and phytocompounds of Asparagus and Turmeric. Additionally, these phytocompounds were purified after extraction and tested for different *in vitro* biological activities as well as *in silico* study.

Curcumin and curcuminoids were purified and separated by using chromatographic techniques such as silica gel chromatography, TLC and by using RP-HPLC-UV detection. Additionally, diosgenin was purified by acid hydrolysis and quantified on RP-HPLC-UV detection. Furthermore, phytocompounds were identified by using GC-MS/MS, and LC-MS/MS as well, the results showed an increase in the concentration of chief phytocompounds such as curcumin and diosgenin. The computational approach used in this study elucidated the mechanism of inhibition of the SortaseA enzyme which is a key adhesion protein involved in biofilm formation.

These phytocompounds individually as well as in combination also showed

antibacterial and antifungal activity. Additionally, antibiofilm activity of these phytocompounds against Gram positive pathogens like *S. aureus* and *S. mutans* was also checked in the current study. Crystal violet assay revealed the biofilm formed by bacteria as well as inhibitory action of phytocompounds against these pathogenic organisms, so these phytocompounds may be used as drug molecules in the future.

The combinational effect of phytocompounds (Curcumin + 4-hydroxy-2 methylacetophenone) inhibits the enzyme (SrtA) by forming a ternary complex which shows better results over control inhibitors and this combination also gives similar results in wet-lab experiments. Hence, the present work opens a new avenue and creates scope for evaluation of other applications of PGPR-induced plant secondary metabolites from Turmeric and Asparagus in pharmaceutical applications, agricultural and food industries.

5.2 Conclusions:

- The screening of PGPR from the rhizospheric soil of two medicinal plants such as *C. longa* and *A. racemosus* resulted in the isolation of four potent PGPRs which were used for further studies based on their PGPR traits.
- The phenotypic and genotypic characterization of isolated PGPR identified them as strains of *Serratia nematodiphila*, *Pseudomonas plecoglossicida*, *Exiguobacterium acetylicum* and *Enterobacter mori*. These isolates were designated as *Serratia nematodiphila* RGK, *Pseudomonas plecoglossicida* RGK, *Exiguobacterium acetylicum* RGK and *Enterobacter mori* RGK1.
- The 16S rRNA sequences were submitted to the NCBI GenBank and Accession Numbers were obtained as - **MZ452064, OL739684, OL771442** and **OL656822** respectively.
- Biochemical characterization of these strains shows that they are capable to utilize various sugars.
- *Pseudomonas plecoglossicida* RGK can tolerate 7% NaCl along with exopolysaccharide production.
- A pot culture study revealed that PGPR treatment improved the growth and yield of Turmeric and Asparagus. These plants are then subjected to extraction and purification procedures.
- Soxhlet extraction and sonication used here may give several metabolites from PGPR-treated and control plants. Further, these extracts were used for purification.

- Silica gel column chromatography and TLC method yielded good results for curcumin purification, while RP-HPLC determination revealed the maximum amount of curcumin (8.02%) produced in co-culture treated plants.
- Similarly, acid hydrolysis yields a significant amount of diosgenin, and RP-HPLC results showed that the largest level of diosgenin (0.28%) was found in co-culture treated plants.
- GC-MS/MS analysis of the purified extracts gave an idea about the diversity of known and established phytocompounds in the plant extracts. In this study, we report for the first time a presence and elevated concentration of a new phytocompound (4-hydroxy-2 methylacetophenone) in the co-culture treated Turmeric plant.
- PGPR treated plants also showed strong free-radical scavenging activity and its inoculation enhanced phenolic content in Turmeric rhizome while saponin content in Asparagus root mainly co-culture treatment gives these kinds of results. An overall increase in phenolic and flavonoid content in both plants was observed.
- Individual and combinational effect of purified phytocompounds was checked on Gram-positive and Gram-negative pathogens such as *S. aureus* NCIM 2654, *S. mutans* NCIM 5660 and *E. coli* NCIM 2832, *Proteus vulgaris* NCIM 2813 respectively. The minimum inhibitory concentration of each phytocompounds against these pathogens was checked and it concludes that the combinational effect of phytocompounds provided a better inhibition as compared to an individual one.
- The bacterial growth curve assay was performed for *S. aureus* which is prominent organism in biofilm formation. It was performed in presence of standard plant metabolites and purified fractions to investigate the inhibition effect of phytocompounds. The obtained growth curve patterns showed the effective inhibition of the microorganism in presence of individual and combination of phytocompounds as compare control.
- The result of biofilm biomass assay indicated a reduced production of biofilm biomass in pathogens when treated with individual and combinational phytocompounds. These phytocompounds not only reduced the biofilm biomass but also reduced the microcolony formation.
- The present study also includes *in silico* study of biofilm-forming protein SrtA from *S. aureus* and *S. mutans.* The binding mode analysis by using molecular docking and MD simulation showed that phytocompounds may be bound to other site than the active site in combinational effect.

- Docking with dock 6 explored the molecular interactions, showing the involvement of hydrogen bonding and hydrophobic contacts of phytocompounds with SrtA.
- MD simulation showed ligand-induced conformational changes. We also emphasize the significance of the β 6/7 loop's scissoring and closure movement, which facilitates the opening and closing of the binding pocket region for stable complex formation in SrtA.
- As a result, we believe that PGPR-treated plant secondary metabolites would be great candidates for SrtA suppression and that combining curcumin and 4-hydroxy 2-methyl acetophenone would encourage better control of these pathogens.
- Thus, this study would pave the way for the development of PGPR-induced secondary metabolite therapeutic approaches by targeting SrtA to control biofilm related infectious diseases.

CHAPTER VI

REFERENCES

Abraham, M., Murtola, T., Schulz, R., Pall, S., Smith, J., Hess, B., Lindah, E. (2015). Gromacs: high-performance molecular simulations through multi-level parallelism from laptops to supercomputers, *SoftwareX* **1**, 219–25.

Adamczyk, M., Hagedorn, F., Wipf, S., Donhauser, J., Vittoz, P., Rixen, C., Frossard, A., Theurillat, J. P., & Frey, B. (2019). The soil microbiome of Gloria Mountain summits in the Swiss Alps. *Frontiers in Microbiology* **10**, 1080.

Agan, L. and Akariah, K. (2002). Improved HPLC Method for the Determination of Curcumin, Demethoxycurcumin, and Bisdemethoxycurcumin. *Journal of Agricultural and Food Chemistry* **50**, 3668–3672.

Agarwal, E., Brattain, M., Chowdhury, S. (2013). Cell survival and metastasis regulation by Akt signaling in colorectal cancer. *Cellular Signalling* **25**, 1711–1719.

Aggarwal, B., Yuan, W., Li, S., Gupta, S. (2013). Curcumin-free turmeric exhibits anti-inflammatory and anticancer activities : Identification of novel components of turmeric. *Molecular Nutrition Food Research* **57,** 1529–1542.

Aggarwal, S., Ichikawa, H., Takada, Y., Sandur, S.K., Shishodia, S., Aggarwal, B.B., (2006). Curcumin (diferuloylmethane) down-regulates expression of cell proliferation and antiapoptotic and metastatic gene products through suppression of I-kappa B-alpha kinase and Akt activation. *Molecular Pharmacology* **69**, 195–206.

Agostini-Costa, S., Vieira, R., Bizzo, H., Silveira, D., Gimenes, M. (2012). Secondary metabolites. *Chromatography and its applications* **1**, 131-164.

Agrawal, D., Saikia, D., & Tiwari, R. (2008). Demethoxycurcumin and its Semisynthetic Analogues as Antitubercular Agents. *Planta Med*. **74,** 1828-1831.

Ahmad, A., Robinson, A., Duensing, A., van Drunen, E., Beverloo, H., Weisberg, D., Hasty, P., Hoeijmakers, J., & Niedernhofer, L. (2008). ERCC1-XPF Endonuclease Facilitates DNA Double-Strand Break Repair. *Molecular and Cellular Biology* **28,** 5082–5092.

Ahmad, F., Ahmad, I., Khan, M. (2005). Indole acetic acid production by the indigenous isolates of *Azotobacter* and Flourescent *Pseudomonas* in the presence and absence of tryptophan. *Turk J Biol* **29,** 29–34.

Ahmad, F., Ahmad, I., Khan, M. (2008). Screening of free-living rhizospheric bacteria for their multiple plant growth promoting activities. *Microbiol Research* **163,**173–181.

Ahmad, S., Maziah, M. (2015). Total Antioxidant Capacity, Total Phenolic Compounds and the Effects of Solvent Concentration on Flavonoid Content in *Curcuma longa* and *Curcuma xanthorhhiza* Rhizomes. *Medicinal & Aromatic Plants* **3,** 156.

Ajmal, A., Saroosh, S., Mulk, S., Hassan, M., Yasmin, H., Jabeen, Z., Nosheen, A., Shah, S., Naz, R., Hasnain, Z., Qureshi, T., Waheed, A., & Mumtaz, S. (2021). Bacteria

isolated from wastewater irrigated agricultural soils adapt to heavy metal toxicity while maintaining their plant growth promoting traits. *Sustainability* **13,** 7792.

Akhtar, S., Mekureyaw, M., Pandey, C., and Roitsch, T. (2020). Role of cytokinins for interactions of plants with microbial pathogens and pest insects. *Front. Plant Sci*. **10,** 1777.

Alibi, S., Crespo, D., Navas, J. (2021). Plant-Derivatives Small Molecules with Antibacterial Activity. *Antibiotics* (Basel) **10,** 231.

Alok, S., Jain, S., Verma, A., Kumar, M., Mahor, A., & Sabharwal, M. (2013). Plant profile, phytochemistry and pharmacology of *Asparagus racemosus* (Shatavari): A review. *Asian Pacific Journal of Tropical Disease* **3,** 242–251.

Alori, E., & Babalola, O. (2018). Microbial inoculants for improving crop quality and human health in Africa. *Frontiers in Microbiology* **9,** 1–12.

Al-snafi, A. E. (2015). The pharmacological importance of *Asparagus officinalis* - A review. *Pharm. Biol* **5,** 93–98.

Amalraj, A., Pius, A., Gopi, S. (2016). Biological activities of curcuminoids, other biomolecules from turmeric and their derivatives e A review. Journal of Traditional and Complementary Medicine. **7,** 205-233.

Ambardar, S., and Vakhlu, J. (2013). Plant growth promoting bacteria from *Crocus sativus* rhizosphere. *World Journal of Microbiology and Biotechnology* **29,** 2271–2279.

Anand, K., Kumari, B., and Mallick M. (2016). Phosphate solubilizing microbes: An effective and alternative approach as bio-fertilizers. *International Journal of Pharmacy and Pharmaceutical Sciences* **8**, 37–40.

Anand, U., Jacobo-Herrera, N., Altemimi, A., Lakhssassi, N., (2019). A comprehensive review on medicinal plants as antimicrobial therapeutics: potential avenues of biocompatible drug discovery. *Metabolites* **9,** 258.

Anandaraj, M., and Dinesh, R. (2008). Use of microbes for spices production. In: Parthasarathy VA, Kandiannan K, Srinivasan V, editors. *Organic spices* New Delhi: New India Publishing Agency, 101–32.

Andy, A., Masih, S., & Gour, V. (2020). Isolation, screening and characterization of plant growth promoting rhizobacteria from rhizospheric soils of selected pulses. *Biocatalysis and Agricultural Biotechnology* **27,** 101685.

Ansari, F., Jabeen, M., & Ahmad, I. (2021). *Pseudomonas azotoformans* FAP5, a novel biofilm-forming PGPR strain, alleviates drought stress in wheat plant. *International Journal of Environmental Science and Technology* **18,** 3855–3870.

Aquino, R., Morellis, S., Lauro, M., Abdo, S., Saija, A., Tomaino, A. (2001). Phenolic constituents and antioxidant activity of an extract of Anthurium vesicular leaves. *Journal of Natural Products* **64,** 1019-1023.

Aratanechemuge, Y., Komiya, T., & Moteki, H. (2002). Selective induction of apoptosis by ar-turmerone isolated from turmeric (*Curcuma longa* L) in two human leukemia cell lines, but not in human stomach cancer cell line. *International Journal of Molecular Medicine* **9,** 481–484.

Arora, N., & Verma, M. (2017). Modified microplate method for rapid and efficient estimation of siderophore produced by bacteria. *3 Biotech* **7,** 381.

Austin, M., and Noel, J. (2003). The chalcone synthase superfamily of type III polyketide synthases. *Nat Prod Rep* **20,** 79–110.

Baek, S., Choi, B., Nam, S., Kim, H. (2018). Inhibition of monoamine oxidase A and B by demethoxycurcumin and bisdemethoxycurcumin. *Journal of Applied Biological Chemistry* **61,** 187–190.

Bagyalakshmi, B., Ponmurugan, P., & Balamurugan, A. (2017). Potassium solubilization, plant growth promoting substances by potassium solubilizing bacteria (KSB) from southern Indian Tea plantation soil. *Biocatalysis and Agricultural Biotechnology* **12,** 116–124.

Bahari, S., Zeighami, H., Mirshahabi, H., Roudashti, S., Haghi, F. (2017). Inhibition of *Pseudomonas aeruginosa* quorum sensing by subinhibitory concentrations of curcumin with gentamicin and azithromycin. *Integrative Medicine Research* **10,** 21–28.

Bajpai, V., Majumder, R., Park, J. (2016). Isolation and purification of plant secondary metabolites using column-chromatographic technique. *Bangladesh Journal of Pharmacology **11,*** 844–848.

Bakker, P., Doornbos, R., Zamioudis, C., Berendsen, R., Pieterse, C. (2013). Induced Systemic Resistance and the rhizosphere microbiome. *Plant Pathology Journal* **29,** 136–143.

Bal, H., Nayak, L., Das, S., and Adhya, K. (2013). Isolation of ACC deaminase producing PGPR from rice rhizosphere and evaluating their plant growth promoting activity under salt stress. *Plant and Soil* **366,** 93–105.

Balamurugan V, Sheerin F, Velurajan S. (2019). A guide to phytochemical analysis. *IJARIIE* **5,** 236-245.

Banchio, E., Bogino, P., Zygadlo, J., Giordano, W. (2008). Plant growth promoting rhizobacteria improve growth and essential oil yield in *Origanum majorana* L. *Biochemical* Systematics and *Ecology* **36,** 766–771.

Bandopadhyay, S. (2019). Optimization of biofertilizer production and its application in plants using pot culture technique. *Journal of Pure and Applied Microbiology* **13,** 2159–2167.

Bandyopadhyay, P., Yadav, B., Kumar, S., Kumar, R., Kogel, K., Kumar, S. (2022). *Piriformospora indica* and *Azotobacter chroococcum* consortium facilitates higher

acquisition of N, P with improved carbon allocation and enhanced plant growth in *Oryza sativa*. *Journal of Fungi* **8,** 453.

Bansode, P., Anantacharya, R., Dhanavade, M., Kamble, S., Barale, S. Sonawane, K., Nayak, D., Rashinkar, G. (2019). Evaluation of drug candidature: In silico ADMET, binding interactions with CDK7 and normal cell line studies of potentially anti-breast cancer enamidines, *Computational Biology and Chemistry*, **83**, 107-124.

Barale, S., Ghane, S., Sonawane, K. (2022). Purification and characterization of antibacterial surfactin isoforms produced by *Bacillus velezensis* SK. AMB Express **12,** 7.

Barale, S., Parulekar, R., Fandilolu, P., Dhanavade, M., and Sonawane, K. (2019). Molecular Insights into Destabilization of Alzheimer's Aβ Protofibril by Arginine Containing Short Peptides: A Molecular Modeling Approach. *ACS Omega* **4,** 892-903.

Baranska, M., Schulz, H., Rosch, P., Strehle, M. A., & Popp, J. (2004). Identification of secondary metabolites in medicinal and spice plants by NIR-FT-Raman microspectroscopic mapping. *Analyst* **129,** 926–930.

Batista, J., Pessoa, V., Brito F., Rocha, C., Gurgel L., Ramos, A., Barbosa, M., Silva, J., Marinho, E., Cavalcanti, B. (2021). Anti-mrsa activity of curcumin in planktonic cells and biofilms and determination of possible action mechanisms. *Microbial Pathogenesis* **155,** 104892.

Beattie G. (2006). Survey, molecular phylogeny, genomics and recent advances. *Plant-Associated Bacteria* 1-56.

Bednarikova, Z., Gancar, M., Wang, R., Zheng, L., Tang, Y., Luo, Y., Huang, Y., Spodniakova, B., Ma, L., Gazova, Z. (2021). Extracts from Chinese herbs with anti-amyloid and neuroprotective activities. *International Journal of Biological Macromolecules* **179**, 475–484.

Beemann, D. (1976). Some multistep methods for use in molecular dynamics simulations. *Journal of Computational Physics* **20,** 130-139.

Beevers, C., and Huang, S. (2011). Pharmacological and clinical properties of curcumin. *Botanics: Targets and Therapy* **1,** 5-18.

Begum, A., Knv, R., Dutt, R. Giri, K., Sindhu, K., Umera, f., Gowthami, G., Kumar, V., Naveen N., and Shaffath, S. (2017). Phytochemical screening and thin layer chromatography of indian *Asparagus officinalis* Linn. *International Journal of Advanced Research* **5,** 1520-1528.

Behnsen, J., and Raffatellu, M. (2016). Siderophores: More than stealing iron. *M Bio* **15,** 1906-1916.

Beneduzi A, Ambrosini A, Passaglia L. (2012). Plant growth-promoting rhizobacteria (PGPR): Their potential as antagonists and biocontrol agents. *Genetics and Molecular Biology* **35,** 1044–1051.

Bensalim, S., Nowak, J., Asiedu, S. (1998). A plant growth promoting rhizobacterium and temperature effects on performance of 18 clones of potato. *Am J Potato Res* **75,** 145–152.

Berendsen, R., Pieterse, C., Bakker, P. (2012). The rhizosphere microbiome and plant health. *Trends Plant Sci* **17,** 478–486.

Berman, H., Henrick, K., Nakamura, H. (2003). Announcing the worldwide Protein Data Bank. *Nat Struct Mol Biol* **10,** 980–980.

Berman, H., Westbrook, J., Feng, Z., Gilliland, G., Bhat, T., Weissig, H., Shindyalov, I., Bourne, P. (2000). The Protein Data Bank. *Nucleic Acids Research* **28,** 235–242.

Bhandare, V. & Ramaswamy, A. (2016). Identification of possible siRNA molecules for TDP43 mutants causing amyotrophic lateral sclerosis: in silico design and molecular dynamics study. *Comput Biol Chem* **61**, 97-108.

Bharti, N., Yadav, D., Barnawal, D., Maji, D., Kalra, A. (2013). *Exiguobacterium oxidotolerans*, a halotolerant plant growth promoting rhizobacteria, improves yield and content of secondary metabolites in *Bacopa monnieri* (L.) Pennell under primary and secondary salt stress. *World Journal of Microbiology and Biotechnology* **29,** 379–387.

Bharucha, U., Patel, K., & Trivedi, U. B. (2013). Optimization of Indole Acetic Acid Production by *Pseudomonas putida* UB1 and its Effect as Plant Growth-Promoting Rhizobacteria on Mustard (*Brassica nigra*). *Agriculture research* **2,** 215–221.

Bhattacharyya, C., Banerjee, S., Acharya, U., Mitra, A., Mallick, I., Haldar, A., Haldar, S., Ghosh, A. (2020). Evaluation of plant growth promotion properties and induction of antioxidative defense mechanism by tea rhizobacteria of Darjeeling, India. *Scientific Reports*, **10,** 1–19.

Bhattacharyya, P., & Jha, D. (2012). Plant growth-promoting rhizobacteria (PGPR): Emergence in agriculture. *World Journal of Microbiology and Biotechnology* **28,** 1327–1350.

Bhise, K., and Dandge, B. (2019). Mitigation of salinity stress in plants using plant growth promoting bacteria. *Symbiosis* **79,** 191-204.

Bhutani, K., Paul, A., Fayad, W., Linder, S. (2010). Apoptosis inducing activity of steroidal constituents from *Solanum xanthocarpum* and *Asparagus racemosus*. *Phytomedicine* **17,** 789–793.

Bi, C., Dong, X., Zhong, X., Cai, H., Wang, D., Wang, L. (2016). Acacetin Protects Mice from *Staphylococcus aureus* Bloodstream Infection by Inhibiting the Activity of Sortase A, *Molecules.* **21**, 1285.

Bijitha, P., and Suseela, R. (2019). *Burkholderia cepacia* strain iisrclrb5, a promising bioagent for the management of rhizome rot of turmeric (*Curcuma longa* L.) *International Journal of Agricultural Science and Research* **9,** 2250-0057.

Blagojevic, P., Radulovic, N., Boylan, F., & Resources, N. (2011). Volatiles of *Curcuma mangga* Val & Zijp (Zingiberaceae) from Malaysia. *Chemistry and Biodiversity* **8,** 2005–2014.

Boominathan, U., Sivakumaar, P. (2012). A liquid chromatography method for the determination of curcumin in PGPR inoculants *Curcuma longa* L. plant. *Int J Pharm Sci Res* **3,** 4438–4441.

Boominathan, U., Sivakumaar, P. (2012). Induction of systemic resistance by mixtures of rhizobacterial isolates against *Pythium aphanidermatum*. *Res J Biotechnol* **7,** 192–197.

Bopana, N., Saxena, S. (2007). *Asparagus racemosus*- Ethnopharmacological evaluation and conservation needs. *Journal of Ethnopharmacology* **110,** 1–15.

Bottini, R., Cassan, F., Piccoli, P. (2004). Gibberellin production by bacteria and its involvement in plant growth promotion and yield increase. Appl Microbiol Biotechnol **65,** 497–503.

Bourgaud, F., Gravot, A., Milesi, S. and Gonteir, E. (2001). Production of plant secondary metabolites: a historical perspective. *Plant Science* **161,** 839-851.

Bramchari, P. and Dubey, S. (2006). Isolation and characterization of exopolysaccharides produced by *Vibrio harveyi* strain VB23. *Lett Appl Microbiol* **43,** 571-577.

Brick, J., Bostock, R., Silverstone, S., (1991). Rapid in situ assay for indole acetic acid production by bacteria immobilized on nitrocellulose membrane. *Appl Environ Microbiol* **57,** 535-538.

Brooks, C. (1995). Methodological advances in molecular dynamics simulations of biological systems. *Curr Opin Struct Biol* **5,** 211-215.

Burley, S., Berman, H., Christie, C., Duarte, J., Feng, Z., Westbrook, J., Zardecki, C., (2018). RCSB Protein Data Bank: Sustaining a living digital data resource that enables breakthroughs in scientific research and biomedical education: RCSB Protein Data Bank. *Protein Science* **27,** 316–330.

Cakmakc, R., Mosber, G., Hazal, A., Firat, M., & Baboo, A. (2020). The Effect of Auxin and Auxin - Producing Bacteria on the Growth, Essential Oil Yield, and Composition in Medicinal and Aromatic Plants. *Current Microbiology* **77,** 564-577.

Cao, L., Zhou, Z., Sun, J., Li, C., Zhang, Y. (2021) Altering Sterol Composition Implied That Cholesterol is Not Physiologically Associated With Diosgenin Biosynthesis in *Trigonella foenum-graecum*. *Frontiers in Plant Science* **12,** 1-11.

Capatina, D., Feier, B., Hosu, O., Tertis, M., & Cristea, C. (2022). Analytical methods for the characterization and diagnosis of infection with *Pseudomonas aeruginosa*: A critical review. *Analytica Chimica Acta* **1204,** 1-33.

Cappuccino, J.G., Sherman, N. (1992). Biochemical activities of microorganisms. Microbiology, A Laboratory Manual. The Benjamin/Cummings Publishing Co, California, USA

Caroline, A., Dias, P., Aparecida, S., Corona, M., Cristina, M. (2018). Photodiagnosis and Photodynamic Therapy Effect of aPDT on *Streptococcus mutans* and *Candida albicans* present in the dental biofilm :Systematic review. *Photodiagnosis and Photodynamic Therapy* **21,** 363–366.

Cas, M., & Ghidoni, R. (2019). Dietary curcumin: Correlation between bioavailability and health potential. *Nutrients* **11,** 1–14.

Cascioferro, S., Ra, D., Maggio, B., Raimondi, M., Schillaci, D., & Daidone, G. (2015). Sortase A Inhibitors : Recent Advances and Future Perspectives. *Journal of Medicinal Chemistry* **58,** 9108–9123.

Cavuturu, B., Bhandare, V., Ramaswamy, A., & Arumugam, N. (2019). Molecular dynamics of interaction of Sesamin and related compounds with the cancer marker β-catenin: an in silico study. *Journal of Biomolecular Structure and Dynamics* **37,** 877–891.

Chaaban, A., Richardi, V., Carrer, A., Brum, J., Cipriano, R., Martins, C., Silva, M., Deschamps, C., & Molento, M. (2019). Insecticide activity of *Curcuma longa* (leaves) essential oil and its major compound α-phellandrene against *Lucilia cuprina* larvae (Diptera: Calliphoridae): Histological and ultrastructural biomarkers assessment. *Pesticide Biochemistry and Physiology* **153**, 17–27.

Chandra, S., Askari, K., & Kumari, M. (2018). Optimization of indole acetic acid production by isolated bacteria from *Stevia rebaudiana* rhizosphere and its effects on plant growth. *Journal of Genetic Engineering and Biotechnology* **16,** 581–586.

Chaudhary, S., Chaudhary, P., Syed, B., Misra, R., Bagali, P., Vitalini, S., & Iriti, M. (2018). Validation of a method for diosgenin extraction from fenugreek (*Trigonella foenum-graecum* L.). *Acta Scientiarum Polonorum, Technologia Alimentaria* **17,** 377–385.

Chauhan, A., Maheshwari, D., Dheeman, S., Bajpai, V. (2017). Termitarium-Inhabiting *Bacillus* spp. Enhanced Plant Growth and Bioactive Component in Turmeric (*Curcuma longa* L.). *Current Microbiology* **74,** 184–192.

Chauhan, A., Saini, R., Sharma, C. (2021). Plant growth promoting rhizobacteria and their biological properties for soil enrichment and growth promotion. *Journal of Plant Nutrition* **45,** 273– 299.

Chen, B., Luo, S., Wu, Y., Ye, J., Wang, Q., Xu, X., Pan, F., Khan, K., Feng, Y., & Yang, X. (2017). The effects of the endophytic bacterium *Pseudomonas fluorescens* Sasm05

and IAA on the plant growth and cadmium uptake of Sedum alfredii hance. *Frontiers in Microbiology* **8,** 1–13.

Chen, C., Jin, S., Xiang, X., Wang, X., Shi, Q., Yang, M., Ji, S., Huang, R., & Song, C. (2017). Enrichment and Cytotoxic Activity of Curcuminoids from Turmeric Using Macroporous Resins. *Journal of Food Science* **82,** 2024–2030.

Chenna, B., Shinkre, B., King, J., Lucius, A., Narayana, S. & Velu, S. (2008). Identification of novel inhibitors of bacterial surface enzyme *Staphylococcus aureus* Sortase A. *Bioorganic & Medicinal Chemistry Letters* **18,** 380–385.

Chenniappan, C., Narayanasamy, M., Daniel, G., Ramaraj, G., Ponnusamy, P., Sekar, J., Ramalingam, P. (2019). Biocontrol efficiency of native plant growth promoting rhizobacteria against rhizome rot disease of turmeric. *Biol. Control* **129,** 55–64.

Ciura, J., Szeliga, M., Grzesik, M., & Tyrka, M. (2017). Next-generation sequencing of representational difference analysis products for identification of genes involved in diosgenin biosynthesis in fenugreek (*Trigonella foenum - graecum*). *Planta* **245,** 977–991.

Clancy, K., Melvin, J., McCafferty, D. (2010). Sortase transpeptidases: insights into mechan- ism, substrate specificity, and inhibition. *Biopolymers* **94,** 385–396.

Corbiere, C., Liagre, B., Bianchi, A., Bordji, K., Dauca, M., Netter, P., Beneytout, J. (2003). Different contribution of apoptosis to the antiproliferative effects of diosgenin and other plant steroids, hecogenin and tigogenin, on human 1547 osteosarcoma cells. *International Journal of Oncology* **22,** 899–905.

Cornell, W., Cieplak, P., Bayly, C., Gould, I., Merz, K., Ferguson, D., Spellmeyer, D., Fox, T., Caldwell, J., Kollman, P. (1995). A second generation force field for the simulation of proteins, nucleic acids, and organic molecules. *J Am Chem Soc* **117,** 5179-5197.

Costerton, W., Veeh, R., Shirtliff, M, Pasmore. M., Post, C., Ehrlich, G. (2003). The application of biofilm science to the study and control of chronic bacterial infections. *J. Clin Invest* **112,** 1466–1477.

Crozier, A., Kamiya, Y., Bishop, G., Yokota, T. (2000). Biosynthesis of hormones and elicitor molecules. Biochemistry and molecular biology of plants. *American Society of Plant Physiology* 850–929.

Cvitkovitch, D., Li, Y., Ellen, R., Cvitkovitch, D., & Ellen, R. (2003). Quorum sensing and biofilm formation in *Streptococcal infections*. *The Journal of Clinical Investigation* **112,** 1626–1632.

Darden, T., York, D., Pedersen, L. (1993). Particle mesh Ewald: An N -log(N) method for Ewald sums in large systems. *J Chem Phys* **98**, 10089-10092.

Darzi, M. (2012). Effect of biofertilizers application on quantitative and qualitative yield of fennel (*Foeniculum vulgare*) in a sustainable production system. *IJACS* **4,**187–192.

Das, R., & Mehta, D. (2018). Microbial Biofilm and Quorum Sensing Inhibition: Endowment of Medicinal Plants to Combat Multidrug-Resistant Bacteria. *Current Drug Targets*, **19,** 1916–1932.

Dashti, N., Zhang, F., Hynes, R., Smith, D. & Bellevue, S. (1998). Plant growth promoting rhizobacteria accelerate nodulation and increase nitrogen fixation activity by field grown soybean (*Glycine max* L.) under short season conditions. *Plant and Soil* **200,** 205–213.

Dastager, S. & Ashok, C. (2011). Potential plant growth-promoting activity of *Serratia nematodiphila* NII-0928 on black pepper (*Piper nigrum* L.). *World J Microbiol Biotechnol* **27,** 259–265.

De Christo Scherer, M., Marques, F., Figueira, M., Peisino, M., Schmitt, E., Kondratyuk, T., Endringer, D., Scherer, R. & Fronza, M. (2019). Wound healing activity of terpinolene and α-phellandrene by attenuating inflammation and oxidative stress in vitro. *Journal of Tissue Viability* **28,** 94–99.

De la Lastra, E., Camacho, M. & Capote, N. (2021). Soil bacteria as potential biological control agents of Fusarium species associated with asparagus decline syndrome. *Applied Sciences* **11,** 8356.

Del Rosario Cappellari, L., Santoro, M., Reinoso, H., Travaglia, C., Giordano, W. & Banchio, E. (2015). Anatomical, Morphological, and Phytochemical Effects of Inoculation with Plant Growth- Promoting Rhizobacteria on Peppermint (*Mentha piperita*). *Journal of Chemical Ecology* **41,** 149–158.

Devi, R., Kaur, T., Kour, D. & Nath, A. (2022). Microbial consortium of mineral solubilizing and nitrogen fixing bacteria for plant growth promotion of amaranth (*Amaranthus hypochondrius* L.). *Biocatalysis and Agricultural Biotechnology* **43,** 102404.

Dhaked, B., Triveni, S., Reddy, R. & Padmaja, G. (2017a). Isolation and Screening of Potassium and Zinc Solubilizing Bacteria from Different Rhizosphere Soil. *International Journal of Current Microbiology and Applied Sciences* **6**, 1271–1281.

Dhanarajan, G., Rangarajan, V., Sridhar, P., Sen, R. (2016). Development and Scale- up of an Efficient and Green Process for HPLC purification of antimicrobial homologues of commercially important microbial lipopeptides. *ACS Sustain Chem Eng* **4,** 6638–6646.

Dhanasekaran, S., Rameshthangam, P., Venkatesan, S., Singh, S. & Vijayan, S. (2018). In Vitro and In Silico Studies of Chitin and Chitosan Based Nanocarriers for Curcumin and Insulin Delivery. *Journal of Polymers and the Environment,* **26,** 4095–4113.

Dhanavade, M. and Sonawane, K. (2014). Insights into the molecular interactions between aminopeptidase and amyloid beta peptide using molecular modeling techniques. *Amino acids* **46,**1853–1866.

Dhanavade, M., Jalkute, C., Barage, S., Sonawane, K. (2013). Homology modeling, molecular docking and MD simulation studies to investigate role of cysteine protease from *Xanthomonas campestris* in degradation of Aβ peptide, *Computers in Biology and Medicine*. **43**, 2063-2070.

Dharni, S., Kumar, A., Samad, A. & Dhar, D. (2014). Impact of plant growth promoting *Pseudomonas monteilii* PsF84 and *Pseudomonas plecoglossicida* PsF610 on metal uptake and production of secondary metabolite (monoterpenes) by rose-scented geranium (*Pelargonium graveolens* cv. bourbon) grown. Chemosphere **117,** 433–439.

Dobbelaere, S., Croonenborghs, A., Thys, A., Ptacek, D., Vanderleyden, J., Dutto, P., Labandera-Gonzalez, C., Caballero-Mellado, J., Aguirre, J., Kapulnik, Y. (2001). Responses of agronomically important crops to inoculation with *Azospirillum*. *Australian Journal of Plant Physiology* **28,** 871–879.

Dobbelaere, S., Vanderleyden, J., Okon, Y. (2003). Plant growth-promoting effects of diazotrophs in the rhizosphere. *Critical Review of Plant Science* **22,** 107–149.

Dobosz, B., Drzewiecka, K., Waskiewicz, A., Irzykowska, L., Bocianowski, J., Karolewski, Z., Kostecki, M., Kruczynski, Z., Krzyminiewski, R., Weber, Z., Golinski, P. (2011). Free Radicals, Salicylic Acid and Mycotoxins in *Asparagus* after Inoculation with Fusarium. *Applied Magnetic Resonance* **41,**19–30.

Dutta, B. (2015). Study of secondary metabolite constituents and curcumin contents of six different species of genus Curcuma. *Journal of Medicinal Plants Studies* **3,** 116–119.

Dutta, S. & Neog, B. (2016). Accumulation of secondary metabolites in response to antioxidant activity of turmeric rhizomes co-inoculated with native arbuscular mycorrhizal fungi and plant growth promoting rhizobacteria. *Scientia Horticulturae* **204,** 179–184.

Eberhard, A., Burlingame, L., Eberhard, C., Kenyon, L., Nealson, H., Oppenheimer, J. (1981). Structural identification of autoinducer of *Photobacterium fischeri* luciferase. *Biochem* **20,** 2444–2449.

Edwards, C. and Burrows, I. (1988). The potential of earthworm composts as plant growth media In: Earthworms in Environmental and Waste Management. SPB Academic Publ. b.v, The Netherlands, 211-220.

Egamberdieva, D., Shrivastava, S., Varma, A. (2015). Plant-Growth-Promoting Rhizobacteria (PGPR) and Medicinal Plants. *Soil Biology* **42,** 1-16.

Egamberdieva, D., Teixeira da Silva, J. (2015). Medicinal Plants and PGPR: A New Frontier for Phytochemicals. *Soil Biology* **42,** 287–303.

El, S., Koraichi, S., Latrache, H., Hamadi, F. (2012). Scanning Electron Microscopy (SEM) and Environmental SEM: Suitable Tools for Study of Adhesion Stage and Biofilm Formation. *Scanning Electron Microscopy* **35,** 717-730.

Emmert, E. & Handelsman, J. (1999). Biocontrol of plant disease: A Gram-positive perspective. *FEMS Microbiology Letters*, **171,** 1–9.

Eslami, H., Muller-Plathe F. (2007). Molecular dynamics simulation in the grand canonical ensemble. *J Comput Chem* **28,** 1763-1773.

Essmann, U., Perera, L., Berkowitz, M., Darden, T., Lee, H., Pedersen, L. (1995). A smooth particle mesh Ewald method. *The Journal of Chemical Physics* **103,** 8577–8593.

Etesami, H., Emami, S., & Alikhani, H. A. (2017). Potassium solubilizing bacteria (KSB): Mechanisms, promotion of plant growth, and future prospects - a review. *Journal of Soil Science and Plant Nutrition* **17**, 897–911.

Evans, D. and Morriss, G. (1983). Isothermal/Isobaric molecular dynamics ensemble. *Physics Letter* **98,** 433-436.

Falcinelli, B., Marconi, O., Maranghi, S., Lutts, S., Rosati, A., Famiani, F., Benincasa, P. (2017). Effect of Genotype on the Sprouting of Pomegranate (*Punica granatum* L.) Seeds as a Source of Phenolic Compounds from Juice Industry by-Products. *Plant Foods for Human Nutrition* **72**, 432–438.

Fanaei, H., Khayat, S., Kasaeian, A., Javadimehr, M. (2016). Effect of curcumin on serum brain-derived neurotrophic factor levels in women with premenstrual syndrome: a randomized, double-blind, placebo-controlled trial. *Neuropeptides* **56,** 25-31.

Fatahiya, M., Fadzilah, A., Hassan, F., Tet, S., Kamyar, S., Mikio, M. and Nurul B. (2018). In Silico and In Vitro Study of the Bromelain-Phytochemical Complex Inhibition of Phospholipase A2 (Pla2). *Molecules* **23,** 73.

Felestrino, E., Santiago, I., Freitas, L., Rosa, L., Ribeiro, S. & Moreira, L. (2017). Plant growth promoting bacteria associated with *Langsdorffia Hypogaea* Rhizosphere-Host biological interface: A neglected model of bacterial prospection. *Frontiers in Microbiology* **8,** 1–15.

Ferreira, F., Aparecida, S., Mossini, G., Maery, F., Ferreira, D., Arrotéia, C., Luciana, C., Nakamura, C. & Junior, M. (2013). The inhibitory Effects of *Curcuma longa* L . Essential Oil and Curcumin on *Aspergillus flavus* Link Growth and Morphology *Scientific World Journal* **20**, 343804.

Ferreira, L., Santos, R., Oliva, G. and Andricopulo, A. (2015). Molecular Docking and Structure-Based Drug Design Strategies. *Molecules* **20,** 13384-13421.

Filomena, N., Florinda, F., Raffaele, C., (2013). Quorum Sensing and Phytochemicals. *Int. J. Mol. Sci*. **14,** 12607-12619.

Fiske H, and Subbarow Y. (1925). The colorimetric determination of phosphorus. *J. biol. Chem* **66**, 375-400.

Fornili, A., Autore, F., Chakroun, N., Martinez, P., Fraternali, F. (2012). Protein-Water

Interactions in MD Simulations: POPS/POPSCOMP Solvent Accessibility Analysis, Solvation Forces and Hydration Sites. *Methods Mol Biol* **819,** 375-392.

Fu, W., Liu, J., Zhang, M., Li, J., Hu, J., Xu, L. & Dai, G. (2018). Isolation, purification and identification of the active compound of turmeric and its potential application to control cucumber powdery mildew. *The Journal of Agricultural Science* **156,** 358–366.

Fumes, A., da Silva Telles, P., Corona, S., Borsatto, M. (2018). Effect of aPDT on *Streptococcus mutan*s and *Candida albicans* present in the dental biofilm: Systematic review, *Photodiagnosis Photodyn Ther.* **21**, 363-366.

Fux, C., Costerton, J., Stewart, P., Stoodley, P. (2005). Survival strategies of infectious biofilms. Trends *Microbiology* **13,** 34-40.

Galabova, D., Tuleva, B., Spasova, D. (1996). Permeabilization of *Yarrowia lipolytica* cells by triton X-100. *Enzyme and Microbial Technology* **18,** 18–22.

Gamalero, E. & Glick, B. (2011). Plant Nutrient Management. *Bacteria in Agrobiology* Book

Gangurde, A., Kundaikar, H., Javeer, S., Jaiswar, D., Degani, M. & Amin, P. (2015). Enhanced solubility and dissolution of curcumin by a hydrophilic polymer solid dispersion and its insilico molecular modeling studies. *Journal of Drug Delivery Science and Technology* **29,** 226–237.

Gao, C., Uzelac, I., Gottfries, J., Eriksson, A. (2016). Exploration of multiple Sortase A protein conformations in virtual screening. *Scientific reports* **6**, 1–14.

Garg, A., Faheem, M. and Singh, S. (2021). Role of medicinal plant in human health disease. *Asian J Plant Sci Res* **11,**19-21.

Ge, C., Radnezhad, H., Abari, M., Sadeghi, M. and Kashi, G. (2016). Effect of biofertilizers and plant growth promoting bacteria on the growth characteristics of the herb Asparagus officinalis. *Applied Ecology and Environmental Research* **14**, 547–558.

Gear, C. (1971). Numerical initial value problems in ordinary differential equations Prentice-Hall, Inc., Englewood cliffs N. J., Chapter 2. 17-253.

Geisselera, D., Horwath, R., Joergensen, G. and Ludwig, B. (2010). Pathways of nitrogen utilization by soil microorganisms. *Soil Biology* **42,** 2058– 2067.

Gharib, F., Moussa L. and Massoud, O. (2008). Effect of compost and bio-fertilizers on growth, yield and essential oil of sweet marjoram (*Majorana hortensis*) plant. *International Journal of Agricultural Biology* **10,** 381-387.

Ghorbanpour, M., Hatami, M. and Khavazi, K. (2013). Role of plant growth promoting rhizobacteria on antioxidant enzyme activities and tropane alkaloid production of Hyoscyamus niger under water deficit stress. *Turk J Biol* **37,** 350–360.

Glick, B. (1995). The enhancement of plant growth by free living bacteria. *Canadian Journal of Microbiology* **41,** 109–114.

Gohel, R., Solanki, B., Gurav, N., Patel, G., Patel, B. (2015). Isolation and characterization of shatavarin iv from root of asparagus. *Innovare academic sciences* **7**, 6–9.

González, M. (2011). Force fields and molecular dynamics simulations. *Collection SFN* **12,** 169-200.

Gould, I. (2009). Antibiotic resistance: the perfect storm, *Int J Antimicrob Agents.* **34,** Suppl 3:S2-5.

Gray, E., Smith, D. (2005). Intracellular and extracellular PGPR: commonalities and distinctions in the plant–bacterium signaling processes. *Soil biology and Biochemistry* **37,** 395–412.

Greenwell, M. and Rahman, P. (2015). Medicinal Plants: Their Use in Anticancer Treatment. *International Journal of Pharmaceutical Sciences* and *Research* **6,** 4103–4112.

Guerra, A., Hoyos, C., Velasquez, J., Acosta, L., Rojo, P., Maria, A., Giraldo, V. & Mar, A. (2019). The nanotech potential of turmeric (*Curcuma longa* L.) in food technology : A review. *Critical Reviews in Food Science and Nutrition* **0,** 1–13.

Guerriero, G., Berni, R., Munoz-sanchez, J., Apone, F., Abdel-salam, E., Qahtan, A., Alatar, A. & Cantini, C. (2018). Production of Plant Secondary Metabolites: Examples, Tips and Suggestions for Biotechnologists. *Genes* **9,** 309.

Guller, P., Karaman, M., Guller, U., Aksoy, M. & Kufrevioglu, O. (2021). A study on the effects of inhibition mechanism of curcumin, quercetin, and resveratrol on human glutathione reductase through in vitro and in silico approaches. *Journal of Biomolecular Structure and Dynamics* **39**, 1744–1753.

Gunamalai, L. & Vanila, D. (2014). Insilico analysis of neem secondary metabolites against clumping factor A of *Staphylococcus aureus*. *International Journal of Pharmaceutical Sciences Review and Research* **29**, 232–235.

Gunes, H., Gulen, D., Mutlu, R., Gumus, A., Tas, T. and Topkaya A. (2016). Antibacterial effects of curcumin : An in vitro minimum inhibitory concentration study. *Toxicology and Industrial Health* **32**, 246–250.

Gupta, S. and Rashotte, A. (2012). Down-stream components of cytokinin signaling and the role of cytokinin throughout the plant. *Plant Cell Rep* **31,** 801–812.

Gupta, S., Sung, B., Kim, J., Prasad, S., Li, S., Aggarwal, B. (2013). Multitargeting by turmeric, the golden spice: From kitchen to clinic. *Mol. Nutr. Food Res* **57,** 1510–1528.

Ha, M., Huang, Y., & Huang, J. (2008). Influence of organic amendment and *Bacillus subtilis* on mineral nutrient uptake of asparagus bean in two field soils. *Plant*

Pathology Bulletin 17, 289–296.

Ha, M., Yi, S. & Paek, S. (2020). Design and Synthesis of Small Molecules as Potent Staphylococcus aureus Sortase A Inhibitors. *Antibiotics* **9,** 706.

Haghi, G., Hatami, A. and Mehran, M. (2012). Determination of Shatavarin IV in Root Extracts of Asparagus racemosus by HPLC-UV. *Analytical Chemistry Letters* **2**, 1–6.

Hajbabaie, R., Harper, M., Rahman, T. (2021). Establishing an Analogue Based In Silico Pipeline in the Pursuit of Novel Inhibitory Scaffolds against the SARS Coronavirus 2 Papain-Like Protease, *Molecules.* **26,** 1134.

Hakeem, K. and Akhtar, M. (2016). Plant, soil and microbes: Mechanisms and molecular interactions. *Plant, Soil Microbes* **2,** 1–439.

Ham, S., Yoon, A., Oh, H. & Park, Y. (2022). Plant Growth-Promoting Microorganism *Pseudo arthrobacter* sp. NIBRBAC000502770 Enhances the Growth and Flavonoid Content of *Geum aleppicum*. *Microorganisms* **10,** 1241.

Hameed, A., Egamberdieva, D., Abd-Allah, E., Hashem, A., Kumar, A., Ahmad, P. (2014). Salinity stress and arbuscular mycorrhizal symbiosis in plants. In: Miransari M (ed) Use of microbes for the alleviation of soil stresses. Springer, New York, pp 139–159.

Hamizah, A., Kartini, H., Izzaty, N., Latip, J., & Embi, N. (2020). Data on antiplasmodial and stage-specific inhibitory effects of Aromatic (Ar)-Turmerone against Plasmodium falciparum 3D7. *Data in Brief* **33,** 106592.

Han, J., Sun, L., Dong, X., Cai, Z., Sun, X., Yang, H., Wang, Y., Song, W. (2005). Characterization of a novel plant growth-promoting bacteria strain *Delftia tsuruhatensis* HR4 both as a diazotroph and a potential biocontrol agent against various plant pathogens. *Syst Appl Microbiol* **28,** 66–76.

Hansson, T., Oostenbrink, C., van Gunsteren, W. (2002). Molecular dynamics simulations. *Curr Opin Chem Biol* **12,** 190-196.

Hardman, K. and R. (1968). An improved method of densitometric thin layer chromatography as applied to the determination of sapogenin in dioscorea tubers *Determination sapogenin*. **38,** 355–363.

Hashemi, M., Behboodian, B., Karimi, E. (2022). Enhancing biosynthesis and bioactivity of *Trachyspermum ammi* seed essential oil in response to drought and *Azotobacter chroococcum* stimulation. *Chem. Biol. Technol. Agric*. **9**, 26.

Hayat, R., Ali, S., Amara, U., Khalid, R., & Ahmed, I. (2010). Soil beneficial bacteria and their role in plant growth promotion: A review. *Annals of Microbiology* **60**, 579–598.

Hayes P, Jahidin, A, Lehmann R, Penman K, Kitching W, De Voss J. (2008). Steroidal saponins from the roots of *Asparagus racemosus*. *Phytochemistry* **69,** 796–804.

Hazra, K., Mandal, A., Mondal, D., Ravte, R., Hazra, J., & Rao, M. (2020). Seasonal dynamics of shatavarin-iv, a potential biomarker of asparagus racemosus by HPTLC: Possible validation of the ancient ayurvedic text. *Indian Journal of Traditional Knowledge* **19,** 174–181.

He, W., Zhang, Y., Bao, J., Deng, X., Batara, J., Casey, S., Guo, Q., Jiang, F., Fu, L. (2017) Synthesis, biological evaluation and molecular docking analysis of 2-phenyl-benzofuran-3-carboxamide derivatives as potential inhibitors of *Staphylococcus aureus* Sortase A, Bioorg *Med Chem*. **25,** 1341-1351,

Heffernan, C., Ukrainczyk, M., Gamidi, R., Hodnett, B., Rasmuson, A. (2017). Extraction and Purification of Curcuminoids from Crude Curcumin by a Combination of Crystallization and Chromatography. *Organic Process Research & Development* **21,** 821-826.

Hermenau R. (2018). Gramibactin is a bacterial siderophore with a diazeniumdiolate ligand system. *Nat Chem Biol* **14,** 841–843.

Hess, B., Bekker, H., Berendsen, H. and Fraaije, J. (1997). LINCS: a linear constraint solver for molecular simulations. *J Comput Chem* **18,** 1463–1472.

Hestenes, M. and Eduard, S. (1952). Methods of Conjugate Gradients for Solving Linear Systems. *J Res Natl Bur Stand* **49,** 410-436.

Heydarian, Z., Gruber, M., Glick, B., Hegedus, D. (2018). Gene expression patterns in roots of *Camelina sativa* with enhanced salinity tolerance arising from inoculation of soil with plant growth promoting bacteria producing 1-aminocyclopropane-1-carboxylate deaminase or expression the corresponding acds gene. *Frontiers in Microbiology* **9,** 1–15.

Hiai, S., Oura, H. and Nakajima, T. (1976). Color Reaction of Some Sapogenins and Saponins with Vanillin Sulfuric Acid. *Planta Medica* **29,** 116-122.

Hildah, M., & Sitheni M. (2020). Medicinal Properties of Selected Asparagus Species: A Review. In Phytochemicals in Human Health. *Intech Open*.

Hockney R. (1970). The potential calculation and some applications, in: Alder, B., Fernbach, S., Rotenberg, M. (eds.): *Methods in Computational Physics* **9,** 136.

Hofstad, G., Van Der Marugg, J., Verjans, G. (1986). Characterization and structural analysis of the siderophore produced by the PGPR *Pseudomonas putida* strain wcs358. Plenum press 71–75.

Holt, J., Krieg, N. and Sneath, P. (1994). Berger's manual of determinative bacteriology. 9th ed. Williams & Wilkins, Baltimore, MD, USA

Hu, P., Huang, P., Chen, M. (2013). Curcumin reduces *Streptococcus mutans* biofilm formation by inhibiting sortase A activity. *Archives of Oral Biology* **58,** 1343–1348.

Hu, Y., Xia, Z., Sun, Q., Orsi, A., Rees, D. (2005). A new approach to the pharmacological regulation of memory: sarsasapogenin improves memory by elevating the low

muscarinic acetylcholine receptor density in brains of memory-deficit rat models. *Brain Res* **1060,** 26–39.

Hunenberger, P. (2005). Thermostat Algorithms for Molecular Dynamics Simulations. *Adv Polym Sci* **173,** 105-149.

Huyskens-keil, S., Hassenberg, K., Herppich. (2011). Impact of postharvest UV-C and ozone treatment on textural properties of white asparagus (*Asparagus officinalis* L.). *Journal of Applied Botany and Food Quality* **84,** 229 – 234.

Ilangovan, U., Ton-That, H., Iwahara, J., Schneewind, O., & Clubb, R. (2001). Structure of sortase, the transpeptidase that anchors proteins to the cell wall of *Staphylococcus aureus*. *Proc Natl Acad Sci* **98**, 6056-6061.

Inghorn A. (2004). Constituents of *Asparagus officinalis* Evaluated for Inhibitory Activity against Cyclooxygenase *Journal of Agricultural and Food Chemistry* **52,** 2218−2222.

Ipek, M., Pirlak, L., Esitken, A., Figen, D., Turan M., Sahin, F. (2014). Plant growth promoting rhizobacteria (PGPR) increase yield, growth and nutrition of strawberry under high-calcareous soil conditions. *Journal of Plant Nutrition* **37,** 990–1001.

Ippolito, G., Leone, S., Lauria, F., Nicastri E, Wenzel R. (2010). Methicillin-resistant *Staphylococcus aureus*: the superbug. *International Journal of Infectious Disease* **14,** S7–S11.

Islam, F., Yasmeen, T., Ali, Q., Ali, S., Arif, S., Hussain, S., Rizvi, H. (2014). Influence of *Pseudomonas aeruginosa* as PGPR on oxidative stress tolerance in wheat under Zn stress. *Ecotoxicology and Environmental Safety* **104**, 285–293.

Islam, S., Akanda, A., Prova, A., Islam, M., Hossain, M. (2016). Isolation and identification of plant growth promoting rhizobacteria from cucumber rhizosphere and their effect on plant growth promotion and disease suppression. *Frontiers in Microbiology* **6,** 1360.

Itatiaia, S., Samambaia, C., Itatiaia, S. (2016). Physicochemical/photophysical characterization and angiogenic properties of *Curcuma longa* essential oil. *Annals of the Brazilian Academy of Sciences* **88,** 1889–1897.

Jabborova, D., Wirth, S., Kannepalli, A., Narimanov, A., Desouky, S., Davranov, K., Sayyed, R., Enshasy, H., Malek, R., Syed, A., & Bahkali, A. (2020). Co-inoculation of rhizobacteria and biochar application improves growth and nutrientsin soybean and enriches soil nutrients and enzymes. *Agronomy* **10,** 1142.

Jackson, K., Brown M. (1966). Behaviour of *Azotobacter chroococcum* introduced into the plant rhizosphere. Ann. Inst. Pasteur, Paris. **3**, 108–112.

Jacqueline, L., Luis, J., Ignacio, R., & Martín, J. (2022). A Look at Plant-Growth-Promoting Bacteria. *Plants*, **12**, 1668.

Jagatha, B., Mythri, R., Vali, S., & Bharath, M. (2008). Curcumin treatment alleviates the effects of glutathione depletion in vitro and in vivo: Therapeutic implications for

Parkinson's disease explained via in silico studies. *Free Radical Biology and Medicine* **44**, 907–917.

Jagtap, R., Mali, G., Waghmare, S., Nadaf, N., Nimbalkar, M., Sonawane, K. (2023). Impact of plant growth promoting rhizobacteria *Serratia nematodiphila* RGK and *Pseudomonas plecoglossicida* RGK on secondary metabolites of turmeric rhizome, *Biocatalysis and Agricultural Biotechnology.* **47,** 102622.

Jain, A., Singh, A., Chaudhary, A., Singh, S., Singh, H. (2014). Modulation of nutritional and antioxidant potential of seeds and pericarp of pea pods treated with microbial consortium. *Food Res. Int.* **64,** 275–282.

Jain, A., Verma, S., Kumar, A., Mahor, M., Sabharwal, M. (2013). Plant profile, phytochemistry and pharmacology of *Asparagus racemosus* (Shatavari): A review. *Asian Pacific J. Trop. Dis.* **3,** 242–251.

Janani, S. R., Analytical, A. F., & Kunjithapatham, S. (2014). Screening of Phytochemical and GC-MS Analysis of some Bioactive constituents of *Asparagus racemosus. International Journal of PharmTech Research* **6**, 428-432.

Jarak, M., Mrkovacki, N., Bjelic, D., Joscaron, D., Hajnal-Jafari, T., Stamenov, D. (2012). Effects of plant growth promoting rhizobacteria on maize in greenhouse and field trial. *African Journal of Microbiology Research* **6,** 5683–5690.

Jasim, B., Joseph, A., John, C., Mathew, J., Radhakrishnan, E. (2014). Isolation and characterization of plant growth promoting endophytic bacteria from the rhizome of *Zingiber officinale. 3 Biotech* **4**, 197204.

Jayaprakasha, G., Jagan Mohan Rao, L., & Sakariah, K. (2005). Chemistry and biological activities of *C. longa*. *Trends in Food Science and Technology* **16**, 533–548.

Jediya, H., Joshi, M., Sharma, S., Gurjar, M., Aalam, H. (2022). Effect of phytobiotic feed additives garlic (*Allium sativum*), Ashwagandha (*Withania somnifera*) and Shatavari (*Asparagus racemosus*) on haematology in broiler. *The Pharma Innovation Journal* **11**, 1908–1911.

Jenardhanan, P., Mannu, J., Mathur, P. (2014). The structural analysis of MARK4 and the exploration of specific inhibitors for the MARK family: a computational approach to obstruct the role of MARK4 in prostate cancer progression. *Molecular BioSystems*, **10,** 1845.

Jesus, M., Martins, A., Gallardo, E., & Silvestre, S. (2016). Diosgenin: Recent Highlights on Pharmacology and Analytical Methodology. *Journal of Analytical Methods in Chemistry*, **2016,** 16.

Jha, Y., Dehury, B., Kumar, S., Chaurasia, A., Singh, U., Yadav, M., Angadi, U., Ranjan, R., Tripathy, M., Subramanian, R., Kumar, S., & Simal-Gandara, J. (2022). Delineation of molecular interactions of plant growth promoting bacteria induced β-1,3-glucanases and guanosine triphosphate ligand for antifungal response in rice: a molecular dynamics approach. *Molecular Biology Reports* **49**, 2579–2589.

Ji, S., Kim, J., Lee, C., Seo, H., Chun, S., Oh, J., Park, G., (2019). Enhancement of vitality and activity of a plant growth-promoting bacteria (PGPB) by atmospheric pressure non-thermal plasma. *Scientific Reports* **9,** 1–16.

Jin, S., Song, C., Jia, S., Li, S., Zhang, Y., Chen, C., Feng, Y., Xu, Y., Xiong, C., Xiang, Y., & Jiang, H. (2017). An integrated strategy for establishment of curcuminoid profile in turmeric using two LC–MS / MS platforms. *Journal of Pharmaceutical and Biomedical Analysis* **132,** 93–102.

John, K., Ayyanar, M., Jeeva, S., Suresh, M., Enkhtaivan, G., & Kim, D. (2014). Metabolic Variations, Antioxidant Potential, and Antiviral Activity of Different Extracts of *Eugenia singampattiana* (an Endangered Medicinal Plant Used by Kani Tribals, Tamil Nadu, India) Leaf. *BioMed Research International* **2014,** 11.

Jorgensen, W., Maxwell, D., Tirado-Rives, J. (1996). Development and testing of the OPLS all-atom force field on conformational energetics and properties of organic liquids. *Journal of American Chemical Society* **118,** 11225-11236.

Joulain, D. (2021). Jasminum grandiflorum flowers- Phytochemical complexity and its capture in extracts: a review. *Flavour and Fragrance Journal* **36,** 526-553.

Jung, D., Park, H., Byun, H., Park, Y., Kim, T., Kim, B., Um, S., & Pyo, S. (2010). Diosgenin inhibits macrophage-derived inflammatory mediators through downregulation of CK2, JNK, NF-κB and AP-1 activation. *International Immunopharmacology* **10**, 1047–1054.

Jurenka, J, Ascp, M. (2009). Anti-inflammatory Properties of Curcumin, a Major Constituent of *Curcuma longa*: A Review of Preclinical and Clinical Research. *Alternative Medicine Review* **14,** 141-153.

Kabera, N., Semana, E., Mussa, R. and He X. (2014). Plant secondary metabolites: biosynthesis, classification, function and pharmacological properties. *J Pharm Pharmacol* **2,** 377-392.

Kahlon, A., Negi, A., Kumari, R., (2014). Identification of 1-chloro-2- formyl indenes and tetralenes as novel anti-staphylococcal agents exhibiting sortase A inhibition. *Applied Microbiology and Biotechnology* **98,** 2041–51.

Kalaycıoglu, Z., Gazioglu, I., & Erim, F. (2017). Comparison of antioxidant, anticholinesterase, and antidiabetic activities of three curcuminoids isolated from *Curcuma longa* L. *Natural Product Research* **31,** 2914-2917.

Kamat, J., Boloor, K., Devasagayam, P., Venkatachalam, S. (2000). Antioxidant properties of *Asparagus racemosus* against damage induced by gamma-radiation in rat liver mitochondria. *Journal of Ethnopharmacology* **71,** 425–435.

Kaminek, M., Motyka, V., Vankova, R. (1997). Regulation of cytokinin content in plant cells. *Physiol Plant* **101,** 689–700.

Kamran, S., Shahid, I., Baig, D., Rizwan, M., Malik, K. & Mehnaz, S. (2017).

Contribution of zinc solubilizing bacteria in growth promotion and zinc content of wheat. *Frontiers in Microbiology* **8,** 2593.

Kang, S., Bilal, S., Shahzad, R., Kim, Y. & Park, C. (2020). Producing Endophytic *Klebsiella pneumoniae* YNA12 as a Bio-Herbicide for Weed Inhibition : Special Reference with Evening Primroses. *Plants* **9,** 761.

Kang, S., Latif, A., Waqas, M., You, Y., Hamayun, M., Joo, G., Shahzad, R., Choi, K., & Lee, I. (2015). Gibberellin-producing *Serratia nematodiphila* PEJ1011 ameliorates low temperature stress in *Capsicum annuum* L . *European Journal of Soil Biology* **68**, 85–93.

Kankate, M., Tekale, V., Thakare, P. (2018). Adoption of Improved Cultivation Practices of Turmeric in Yavatmal District. *International Journal of Current Microbiology and Applied Science* **7,** 640–647.

Karnwal A. (2011) Plant growth promoting activity of *Bacillus* spp. on turmeric. The annals of "valahia" university of targoviste.

Karthikeyan, B., Joe, M., Jaleel, C. (2009). Response of some medicinal plants to vesicular arbuscular mycorrhizal inoculations. *Journal of Scientific Research* **1,** 381–386.

Karthikeyan, B., Sakthivel, U., Narayanan, J. (2013). Role of plant growth promoting rhizobacteria for commercially grown medicinal plants. *Bacteria in agrobiology: crop productivity* **2,** 65–76.

Kasai, T. and Sakamura, S. (1981). N-Carboxymethyl-L-serine, a new acidic amino acid from Asparagus (*Asparagus officinalis*) shoots. *Agriculture and Biological Chemistry* **45,** 1483-1485.

Kashyap, P., Muthusamy, K., Niranjan, M., Trikha, S., & Kumar, S. (2020). Sarsasapogenin : A steroidal saponin from *Asparagus racemosus* as multi target directed ligand in Alzheimer ' s disease. *Steroids* **153,** 108529.

Katsipis, G., Tsalouxidou, V., Halevas, E., Geromichalou, E., Geromichalos, G., & Pantazaki, A. (2021). In vitro and in silico evaluation of the inhibitory effect of a curcumin-based oxovanadium (IV) complex on alkaline phosphatase activity and bacterial biofilm formation. *Applied Microbiology and Biotechnology* **105**, 147–168.

Katsori, M., Chatzopoulou, M., Dimas, K., Kontogiorgis, C., Patsilinakos, A., Trangas, T., & Hadjipavlou-Litina, D. (2011). Curcumin analogues as possible anti-proliferative & anti-inflammatory agents. *European Journal of Medicinal Chemistry*, **46,** 2722–2735.

Katsuyama, Y., Kita, T., & Horinouchi, S. (2009). Identification and characterization of multiple curcumin synthases from the herb *Curcuma longa*. *FEBS Letters* **583**, 2799–2803.

Kaur, S., Anu, G., & Satinder, K. (2012). Assessing the Benefits of Azotobacter Bacterization in Sugarcane : A Field Appraisal. *Sugar Tech* **14,** 61–67.

Kavitha, K., Nakkeeran, S., & Chandrasekar, G. (2012). Rhizobacterial-mediated induction of defense enzymes to enhance the resistance of turmeric (*Curcuma longa* L) to *Pythium aphanidermatum* causing rhizome rot. *Archives of Phytopathology and Plant Protection* **45,** 199–219.

Khaerunnisa, S., Kurniawan, H., Awaluddin, R., Suhartati, S., Soetjipto, S. (2020). Potential Inhibitor of COVID-19 Main Protease (Mpro) From Several Medicinal Plant Compounds by Molecular Docking Study Molecular Docking, ADME-Toxicity Prediction, and Evaluation of Curcumin Derivative Compound as Inhibitor Inflamation on Rheumathoid Arth. *Preprints.org*.

Khan, & Bano, A. (2019). Exopolysaccharide producing rhizobacteria and their impact on growth and drought tolerance of wheat grown under rainfed conditions. Plos One **12,** 1–19.

Khan, F., Bamunuarachchi, N. I., Tabassum, N., & Kim, Y. M. (2021). Caffeic Acid and Its Derivatives: Antimicrobial Drugs toward Microbial Pathogens. *Journal of Agricultural and Food Chemistry* **69,** 2979–3004.

Khan, M., Zaidi, A., & Musarrat, J. (2014). Phosphate solubilizing microorganisms: Principles and application of microphos technology. *Phosphate Solubilizing Microorganisms: Principles and Application of Microphos Technology* 1–297.

Khanna, K., Lakshmi, V., Sharma, A., Gandhi, S., Ali, H. & Ahmad, P. (2019). Supplementation with plant growth promoting rhizobacteria (PGPR) alleviates cadmium toxicity in *Solanum lycopersicum* by modulating the expression of secondary metabolites. *Chemosphere* **230**, 628–639.

Khatun, M., Nur, A., Biswas, S., Khan, M., Amin, Z. (2021). Assessment of the anti-oxidant, anti-inflammatory and anti-bacterial activities of different types of turmeric (*Curcuma longa*) powder in Bangladesh. *Journal of Agriculture and Food Research* **6,** 100201.

Khoa, N., Giau, N., Tuan, T. (2016). Effects of *Serratia nematodiphila* CT-78 on rice bacterial leaf blight caused by *Xanthomonas oryzae* pv.oryzae. *Biological Control* **103,** 1–10.

Khorasani, A., Sani, W., Philip, K., Taha, R., Rafat, A. (2010). Antioxidant and antibacterial activities of ethanolic extracts of *Asparagus officinalis* cv. Mary Washington: Comparison of in vivo and in vitro grown plant bioactivities *African journal of biotechnology* **9,** 8460–8466.

Kim, J., Mistry, B., Shin, H. & Kang, S. (2021). Anti-biofilm activity of N-Mannich bases of berberine linking piperazine against *Listeria monocytogenes*. *Food Control*, **121**,107668.

Kim, S., Kang, O., Lee, Y., Han, S., & Ahn, Y. (2016). Hepatoprotective Effect and

Synergism of Bisdemethoycurcumin against MCD Diet-Induced Nonalcoholic Fatty Liver Disease in Mice. *Plos one* **16,** 1–15.

Kim, S., Thiessen, P., Bolton, E., Chen, J., Fu, G., Gindulyte, A., Han, L., He, J., He, S., Shoemaker, B., Wang, J., Yu, B., Zhang, J., Bryant, S. (2016). PubChem Substance and Compound databases. *Nucleic acids Res.* **44**, D1202–D1213

King, F., Weinhold, F. (1995). Structure and spectroscopy of (HCN) n clusters: Cooperative and electronic delocalization effects in C–H···N hydrogen bonding. *The Journal of chemical physics* **103,** 333-347.

Kishore, A., Kumar, S., Pratap, P., Kumar, A., Pandey, K., Kumar, A. & Yadav, H. (2018). Biotechnological aspects of plants metabolites in the treatment of ulcer : A new prospective. *Biotechnology Reports* **18,** 256.

Kita, T., Imai, S., Sawada, H., Kumagai, H., Seto, H. (2008). The biosynthetic pathway of curcuminoid in turmeric (*Curcuma longa*) as revealed by 13C-labeled precursors. *Bioscience, Biotechnology and Biochemistry* **72,** 1789–1798.

Kloepper, J. & Beauchamp, C. (1992). A review of issues related to measuring colonization of plant roots by bacteria. *Canadian Journal of Microbiology* **38,** 1219–1232.

Kloepper, J. (1993). Plant growth promoting rhizobacteria as biological agents. In: FB Metting (eds) Soil microbial ecology: application in agricultural and environmental management, *Jr. Marcel Dekker* 255-274.

Kloepper, J., Lifshitz, R., Zablotowicz, R. (1989). Free-living bacterial inocula for enhancing crop productivity. *Trends Biotechnol* **7,** 39-43.

Knobloch, J. & Horstkotte, M. (2002). Evaluation of different detection methods of biofilm formation in *Staphylococcus aureus*. *Medical Microbiology and Immunology* **191,** 101–106.

Kuan, K., Othman, R., & Rahim, K. (2016). Plant Growth-Promoting Rhizobacteria Inoculation to Enhance Vegetative Growth, Nitrogen Fixation and Nitrogen Remobilisation of Maize under Greenhouse Conditions. *PLoS One* **11,** 1–19.

Kugler, S., Cooper, R., Boessneck, J., Kusel, K., & Wichard, T. (2020). Rhizobactin B is the preferred siderophore by a novel *Pseudomonas* isolate to obtain iron from dissolved organic matter in peatlands. *BioMetals* **33**, 415–433.

Kumar, A., Maurya, B., Raghuwanshi, R. (2014a). Isolation and characterization of PGPR and their effect on growth, yield and nutrient content in wheat (*Triticum aestivum* L.). *Biocatalysis and Agricultural Biotechnology* **3**, 121–128.

Kumar, A., Singh, A., Kaushik, M., Mishra, S., Raj, P., Singh, P., Pandey, K. (2017). Interaction of turmeric (*Curcuma longa* L.) with beneficial microbes: a review. *3 Biotech* **7,** 1–8.

Kumar, A., Singh, R., Giri, D., Singh, P. & Pandey, K. (2014). Effect of *Azotobacter*

chroococcum CL13 inoculation on growth and curcumin content of turmeric (*Curcuma longa* L). *International Journal of Current Microbiology and Applied Sciences* **3**, 275–283.

Kumar, A., Singh, V., Singh, M., Singh, P., Singh, S., Pandey, K. (2016). Isolation of plant growth promoting rhizobacteria and their impact on growth and curcumin content in *Curcuma longa* L. *Biocatalysis and Agricultural Biotechnology* **8,** 1–7.

Kumar, P., and Dubey R. (2012). Plant Growth Promoting Rhizobacteria for biocontrol of phytopathogens and yield enhancement of *Phaseolus vulgaris*. *Journal of Current Perspectives in Applied Microbiology* **1,** 6–38.

Kumar, P., Kamle, M., Maurya, P., Singh, R. (2019). Beneficial Uses and Applications of Plant Growth-Promoting Rhizobacteria in Sustainable Agriculture. *Microbiology for Sustainable Agriculture, Soil Health, and Environmental Protection* 81–104.

Kumar, R., Swapnil, P., Meena, M., Selpair, S., & Yadav, B. (2022). Plant Growth-Promoting Rhizobacteria (PGPR): Approaches to Alleviate Abiotic Stresses for Enhancement of Growth and Development of Medicinal Plants. *Sustainability* **14,** 15514.

Kumar, S., Mehla, R., Dang, A. (2008). Use of Shatavari *Asparagus Racemosus* as a Galactopoietic and Therapeutic Herb a Review. *Agricultural Reviews* **29,** 132 – 138.

Kumar, V., Kumar, A., Pandey, K. & Roy, B. (2015). Isolation and characterization of bacterial endophytes from the roots of *Cassia tora* L. *Annals of Microbiology*, **65,** 1391–1399.

Kumari, P., Meena, M., & Upadhyay, R. (2018). Characterization of plant growth promoting rhizobacteria (PGPR) isolated from the rhizosphere of *Vigna radiata* (mung bean). *Biocatalysis and Agricultural Biotechnology* **16,** 155–162.

Kumari, R., Kumar, R., Lynn, A. (2014). G-mmpbsa-A GROMACS tool for high-throughput MM-PBSA calculations. *Journal of Chemical Information and Modeling* **54**, 1951–1962.

Lamuela-ravents, R. (1999). 2,6-di-tert-butyl-4-hydroxytoluene. *Methods in enzymology* **299,** 152–178.

Lan, C., Chen, X., Zhang, Y., Wang, W., Liu, Y., Cai, Y., Ren, H., Zheng, S., Zhou, L., Zeng, C. (2018). Curcumin prevents strokes in stroke-prone spontaneously hypertensive rats by improving vascular endothelial function. *BMC Cardiovasc. Disord.* **18,** 1–10.

Laskowski, R., MacArthur, M., Moss, D., Thornton, J. (1993) PROCHECK—a program to check the stereochemical quality of protein structures, *J Appl Cryst.* **26**, 283–291.

Laslo, E., Gyorgy, E., Mara, G., Tamas, E., Abraham, B., & Lanyi, S. (2012). Screening of plant growth promoting rhizobacteria as potential microbial inoculants. *Crop Protection* **40,** 43–48.

Lastra, D., Camacho, M., Capote, N. (2021). Soil bacteria as potential biological control agents of Fusarium species associated with asparagus decline syndrome. *Applied Sciences* **11,** 8356.

Leach A. (2001). Molecular Modelling: Principles and Applications, second edition

Lee, H. (2006). Antimicrobial Properties of Turmeric (*Curcuma longa* L.) Rhizome-Derived ar-Turmerone and Curcumin. *Food science Biotechnology* **15,** 559-563.

Lee, J., Park, J., Cho, H., Joo, S., Cho, M., Lee, J. (2013). Anti-biofilm activities of quercetin and tannic acid against *Staphylococcus aureus. Biofouling* **29,** 491-499.

Lee, K., Shin, D., Yoon, J., Kang, H., Oh, K. (2002). Expression of a transpeptidase for cell wall sorting reaction, from sortase, *Staphylococcus aureus* ATCC 6538p in *Escherichia coli J. Microbiol. Biotechnol* **12,** 530-533.

Lee, S., Progulske, A., Erdos, G., Piacentini, D., Ayakawa, G., Crowley, P., Bleiweis, A. (1989) Construction and characterization of isogenic mutants of *Streptococcus mutans* deficient in major surface protein antigen P1 (I/II), *Infect Immun*. **57**, 3306-13.

Lee, S., Song, I., Lee, J., Yang, W., Oh, K. & Shin, J. (2014). Sortase A inhibitory metabolites from the roots of *Pulsatilla koreana*. *Bioorganic and Medicinal Chemistry Letters* **24**, 44–48.

Lekshmi, P., Arimboor, R., Indulekha, P. & Menon, A. (2012). Turmeric (*Curcuma longa* L.) volatile oil inhibits key enzymes linked to type 2 diabetes. *International Journal ofFood Sciences and Nutrition* **63**, 832–834.

Levesque, C., Voronejskaia, E., Huang, Y., Mair, R., Ellen, R., Cvitkovitch, D. (2005). Involvement of sortase anchoring of cell wall proteins in biofilm formation by *Streptococcus mutans, Infect Immun*. **73** 3773-7.

Li, B., Li, X., Lin, H., & Zhou, Y. (2018). Curcumin as a Promising Antibacterial Agent: Effects on Metabolism and Biofilm Formation in *S. mutans*. *BioMed Research International* **2018,** 4508709.

Li, L., Aggarwal, B., Shishodia, S., Abbruzzese, J., Kurzrock, R., (2004). Nuclear factor-kappaB and I-kappaB kinase are constitutively active in human pancreatic cells, and their down-regulation by curcumin (diferuloylmethane) is associated with the suppression of proliferation and the induction of apoptosis. *Cancer* **101,** 2351–2362.

Li, R., Xiang, C., Zhang, X., Guo, D., Ye, M. (2010). Chemical Analysis of the Chinese Herbal Medicine Turmeric (*Curcuma longa* L). *Current Pharmaceutical Analysis* **6,** 256–268.

Li, S., & Wang, P. (2011). Chemical composition and product quality control of turmeric (*Curcuma longa* L). *Pharmaceutical Crops* **2,** 28-54.

Liddycoat S, Wolyn D. (2009). Field evaluation of asparagus crowns and germinating seeds inoculated with plant growth-promoting rhizobacteria. *Canadian Journal of*

Plant Science **89**, 1133–1138.

Liu, W., Huang, X., Qi, Q., Dai, Q.S., Yang, L., Nie, F., Lu, N., Gong, D., Kong, L., Guo, Q., (2009). Asparanin A induces G2/M cell cycle arrest and apoptosis in human hepatocellular carcinoma HepG2 cells. *Biochem. Biophys. Res. Commun*. **381**, 700–705.

Lopez, S., Pastorino, G., Malbran, I., & Balatti, P. (2019). Enterobacteria isolated from an agricultural soil of Argentina promote plant growth and biocontrol activity of plant pathogens. *Revista de La Facultad de Agronomia* **118**, 022.

Lorck, H. (1948). Production of Hydrocyanic Acid by Bacteria. *Physiologia Plantarum* **1**, 142–146.

Lotfi, N., Soleimani, A., Cakmakcı, R., Vahdati, K., & Mohammadi, P. (2022). Characterization of plant growth-promoting rhizobacteria (PGPR) in Persian walnut associated with drought stress tolerance. *Scientific Reports* **12**, 1–13.

Louden, C., Haarmann, D., Lynne, M. (2011). Use of blue agar CAS assay for siderophore detection. *Journal of microbiology & biology education* **12**, 51-53.

Lowy F. (1998). *Staphylococcus aureus* infections. *N Engl J Med* **8,** 520–532.

Lucy, M., Reed, E., Glick, B. (2004). Applications of free living plant growth promoting rhizobacteria. *Antonie Van Leeuwenhoek* **86,** 1– 25.

Luo, H., Liang, D., Bao, M., Sun, R., Li, Y., Li, J., Wang, X., Lu, K., & Bao, J. (2017). In silico identi fi cation of potential inhibitors targeting *Streptococcus mutans* sortase A. *International Journal of Oral Science* **9,** 53–62.

Luthra, P., Kumar, R., & Prakash, A. (2009). Demethoxycurcumin induces Bcl-2 mediated G2/M arrest and apoptosis in human glioma U87 cells. *Biochemical and Biophysical Research Communications* **384**, 420–425.

Luximon-Ramma, A., Bahorun, T., Soobrattee, M., Aruom, O. (2002). Antioxidant activities of phenolic, proanthocyanidin, and flavonoid components in extracts of *Cassia fistula*. *Journal of Agricultural and Food Chemistry* **50,** 5042-5047.

Ma, L. (2015). Biological Databases for Human Research. *Genomics, Proteomics & Bioinformatics* **13**, 55–63.

Mack, D., Becker, P., Chatterjee, I., Dobinsky, S., Knobloch, J., Peters, G., Rohde, H., & Herrmann, M. (2004). Mechanisms of biofilm formation in Staphylococcus epidermidis and *Staphylococcus aureus*: functional molecules, regulatory circuits, and adaptive responses. *International Journal of Medical Microbiology* **294,** 203–212.

MacKerell, A., Bashford, D., Bellott, Dunbrack R., Evanseck, J., Field, M., Fischer, S., Gao, J., Guo, H., Ha, S., Joseph-McCarthy, D. (1998). All-atom empirical potential for molecular modeling and dynamics studies of proteins. *J Phys Chem B* **102,** 3586-3616.

Mahadevamurthy, M., Channappa, M., Sidappa, M., Raghupathi, S., Nagaraj, K. (2016). Isolation of phosphate solubilizing fungi from rhizosphere soil and its effect on seed growth parameters of different crop plants. *J. Appl. Biol. Biotechnol,* **4**, 22-26.

Mahattanadul, S., Nakamura, T., Panichayupakaranant, P., & Phdoongsombut, N. (2009). Comparative antiulcer effect of Bisdemethoxycurcumin and Curcumin in a gastric ulcer model system. *Phytomedicine* **16,** 342–351.

Maheshwari, D, and Dheeman, S. (2014). Phytohormone-Producing PGPR for Sustainable Agriculture. *Bacterial Metabolites in Sustainable Agroecosystem, Sustainable Development and Biodiversity* 12.

Maia, E., Medaglia, L., da Silva, A., Taranto, A. (2020). Molecular Architect: A User-Friendly Workflow for Virtual Screening, *ACS Omega*. **5**, 6628-6640.

Malik, K., Bilal, R., Mehnaz, S., Rasul, G., Mirza, M., & Ali, S. (1997). Association of nitrogen-fixing, plant-growth-promoting rhizobacteria (PGPR) with kallar grass and rice. *Plant and Soil* **194,** 37–44.

Malleswari, D., Bagyanarayana, G. (2013). In vitro screening of rhizobacteria isolated from the rhizosphere of medicinal and aromatic plants for multiple plant growth promoting activities. *J Microbiol Biotech Res* **3,** 84–91.

Manca de Nadra, M., Strasser, A., de Saad A., de Ruiz Holgado, P., Oliver, G. (1985). Extracellular polysaccharide production by *Lactobacillus bulgaricus* CRL 420. *Milchwissenschaft* **40,** 409-411.

Mandal, S., Nandy, A., Pal, M., Saha, B. (2000). Evaluation of antibacterial activity of *Asparagus racemosus* Willd. root. *Phytotherapy Research* **14,** 118–119.

Maougal, T., Kechid, M., Ladjabi, C., Djekoun, A. (2021). PGPR Characteristics of Rhizospheric Bacteria to Understand the Mechanisms of Faba Bean Growth. *Proceedings* **66,** 27.

Marechal, Y. (2004). Water and biomolecules: an introduction. *J Mol Struct* **70,** 207-210.

Maria D. and Maria A. (2021). *Curcuma longa L.* Rhizome Essential Oil from Extraction to Its Agri-Food Applications: A Review. *Plants* **10,** 44.

Mark, P. and Nilsson, L. (2001). Structure and dynamics of the TIP3P, SPC, and SPC/E water models 298 K. *J Phys Chem A* **105,** 9954-9960.

Masuda, T., Isobe, J., Jitoe, A., Nakatani, N. (1992). Antioxidative curcuminoids from rhizomes of *Curcuma xanthorrhiza*. *Phytochemistry* **31,** 3645–3647.

Matloubi, Z., Hassan, Z. (2020). HSA-curcumin nanoparticles: a promising substitution for Curcumin as a Cancer chemoprevention and therapy. *J. Pharm. Sci.* **28,** 209–219.

Mattos, J., Castro, H., Alves, G. & Amorim, L. (2015). The Use of DNA Extraction for Molecular Biology and Biotechnology Training : A Practical and Alternative Approach. *Creative Education* **6,** 762-772.

Mayak, S., Tirosh, T., Glick, B. (2004). Plant growth-promoting bacteria that confer resistance to water stress in tomatoes and peppers. *Plant Science* **166,** 525–530.

Mazumdar, D., Saha, S., Ghosh, S. (2019). Isolation, screening and application of a potent PGPR for enhancing growth of Chickpea as affected by nitrogen level. *International Journal of Vegetable Science* **0**, 1–18.

Mazumder, M., Borah, A., & Choudhury, S. (2020). Inhibitory potential of plant secondary metabolites on anti-Parkinsonian drug targets: Relevance to pathophysiology, and motor and non-motor behavioural abnormalities. *Medical Hypotheses* **137**, 109544.

McCammon, J., Gelin, B. and Karplus, M. (1977). Dynamics of folded proteins. *Nature* **267**, 585-590.

Meena, V., Maurya, B. and Verma, J. (2014a). Does a rhizospheric microorganism enhance K^+ availability in agricultural soils. *Microbiological Research* **169,** 337-347.

Meena, V., Maurya, B., Verma, J., & Meena, R. (2016). Potassium-Solubilizing Microorganism in Evergreen Agriculture: An Overview. *Potassium solubilizing microorganisms for sustainable agriculture* 1–331.

Mehrafarin, A., Ghaderi, A., Rezazadeh, S., Naghdi, B., Nourmohammadi, G., (2010). Bioengineering of important secondary metabolites and metabolic pathways in fenugreek (*Trigonella foenum-graecum* L.). *J. Med. Plant*. **9**, 1–18.

Mehrotra, N., Sabarinath, S., Suryawanshi, S., Raj, K., & Gupta, R. (2009). LC – UV Assay for Simultaneous Estimation of Aromatic Turmerone, a/b-Turmerone and Curlone : Major Bisabolane Sesquiterpenes of Turmeric Oil in Rabbit Plasma for Application to Pharmacokinetic Studies. *Chromatographia* **69,** 1077–1082.

Meizarini, A., Siswandono, Riawan, W., & Rahayu, R. (2018). In silico and in vivo anti-inflammatory studies of curcuminoids, turmeric extract with zinc oxide, and eugenol. *Tropical Journal of Pharmaceutical Research* **17**, 269–275.

Meng, B., Li, J., Cao, H. (2013). Antioxidant and anti-inflammatory activities of curcumin on diabetes mellitus and its complications. *Cur. Phar. Des*. **19,** 2101–2113.

Meng, F., Zhou, Y., Ren, D., & Wang, R. (2018). Turmeric : A Review of Its Chemical. In Natural and Artificial Flavoring Agents and Food Dyes. Elsevier Inc. London, UK, 299–350.

Meyer, M., & Schomburg, D. (2008). Protein Interactions. *Biotechnology*, **5,** 87–108.

Miller, B., McGee, T., Swails, J., Homeyer, N., Gohlke, H., Roitberg, A. (2012). MMPBSA.py: An Efficient Program for End-State Free Energy Calculations, *J Chem Theory Comput***. 8**, 3314-21.

Mishra P. (2009). Isolation, spectroscopic characterization and molecular modeling studies of mixture of *Curcuma longa*, ginger and seeds of fenugreek. *Int. J. Pharm Tech Res*. **1,** 79–95.

Mishra, P., Kundu, E. & Gupta, A. (2009). *Exiguobacterium acetylicum* strain 1P (MTCC 8707) a novel bacterial antagonist from the North Western Indian Himalayas. *World J Microbiol Biotechnol* **25,** 131–137.

Mishra, R., Prakash, O., Alam, M., Dikshit, A. (2010). Influence of plant growth promoting rhizobacteria (PGPR) on the productivity of *Pelargonium graveolens* L. herit. *Recent Res Sci Technol* **2,** 53–57.

Mitra, D., Sharma, K., Uniyal, N., Chauhan, A., & Sarkar, P. (2016). Study on Plant Hormone (Indole-3-Acetic Acid) Producing Level and Other Plant Growth Promotion Ability (PGPA) by *Asparagus racemosus* L. Rhizobacteria. *Journal of Chemical and Pharmaceutical Research* **8**, 995–1002.

Mitra, S., Prakash, N. & Sundaram, R. (2012). Shatavarins (containing Shatavarin IV) with anticancer activity from the roots of *Asparagus racemosus*. *Indian Journal of Pharmacology* **44,** 732–736.

Miyamoto, S., Kollman, P. (1992). Settle: An analytical version of the SHAKE and RATTLE algorithm for rigid water models. *J Comput Chem* **13,** 952-962.

Moghadamtousi, S., Kadir, H., Hassandarvish, P., Tajik, H., Abubakar, S., Zandi, K. (2014). Review on antibacterial, antiviral, and antifungal activity of curcumin. *BioMed Research International*. **2014,** 186864.

Mohamed, F., Abd Majid, F., Ismail, H., Wong, T., Shameli, K., Miyake, M., Ahmad Khairudin, N. (2018). In Silico and In Vitro Study of the Bromelain-Phytochemical Complex Inhibition of Phospholipase A2 (Pla2) Fatahiya. *Molecules* **23,** 73.

Mohammed, A. (2018). Effectiveness of exopolysaccharides and biofilm forming plant growth promoting rhizobacteria on salinity tolerance of faba bean (*Vicia faba* L.). *African Journal of Microbiology Research* **12**, 399–404.

Mohankumar, K., Sridharan, S., Pajaniradje, S., Singh, V., Ronsard, L., Banerjea, A., Somasundaram, D., Coumar, M., Periyasamy, L. & Rajagopalan, R. (2015). BDMC-A, an analog of curcumin, inhibits markers of invasion, angiogenesis, and metastasis in breast cancer cells via NF-κB pathway-A comparative study with curcumin. *Biomedicine and Pharmacotherapy* **74**, 178–186.

Mohite, B. (2013). Isolation and characterization of indole acetic acid (IAA) producing bacteria from rhizospheric soil and its effect on plant growth. *Journal of Soil Science and Plant Nutrition* **13**, 638–649.

Mostert, M., Schoeman, A., Van Merwe, M. (2000). Isolation, characterization and insect growth inhibitory activity of major turmeric constituents and their derivatives against *Schistocerca gregaria* (Forsk) and *Dysdercus koenigii* (Walk). *Pest Management Science* **56**, 1086–1092.

Mustarichie, R., Levita, J. and Febriani, D. (2013). In-Silico Study of Curcumin, Demethoxycurcumin and Xanthorrizol as Skin Whitening Agents. *World Journal of Pharmaceutical Sciences* **1,** 72-80.

Nadaf, N., Parulekar, R., Patil, R., Gade, T., Momin, A., Waghmare, S., Dhanavade, M., Akalpita, U., Sonawane, K. (2018). Biofilm inhibition mechanism from extract of *Hymenocallis littoralis*. *Journal of Ethnopharmacology* **222,** 121-132.

Nadar, S., Khan, T., Patching, S. & Omri, A. (2022). Development of Antibiofilm Therapeutics Strategies to Overcome Antimicrobial Drug Resistance. *Microorganisms* **10**, 1–28.

Nagaraju, Y., Triveni, S., Reddy, R., Sagar, B., Kumar, B., Chari, K., Jhansi, P. (2016). Screening of zinc solubilizing, potassium releasing bacterial and fungal isolates from different rhizosphere soils *International Journal for Research in Applied Science & Engineering Technology* **11,** 2187–2192.

Nandakumar, D., Nagaraj, V., Vathsala, P., Rangarajan, P. and Padmanaban, G. (2006). Curcumin-artemisinin combination therapy for Malaria. *Antimicrobial Agents and Chemotherapy* **50,** 1859–1860.

Naseem, H., Bano, A. (2014). Role of PGPR and their Exopolysaccharide (EPS) in drought tolerance of maize. *Journal of Plant Interactions* **9**, 689-701.

Nazir, R., Gupta, S., Dey, A., Kumar, V., Gupta, A., Shekhawat, M., Goyal, P., & Pandey, D. (2022). In vitro tuberization, genetic, and phytochemical fidelity assessment of *Dioscorea deltoidea*. *Industrial Crops and Products* **175**, 114174.

Nazzaro, F., Fratianni, F., Coppola, R. (2013). Quorum sensing and phytochemicals, *Int J Mol Sci*. **14,** 12607-12619.

Negi, J., Singh, P., Joshi, G., Rawat, M., Bisht, V. (2010). Chemical constituents of Asparagus. *Pharmacognosy reviews* **8,** 215-220.

Negi, P., Jayaprakasha, G., Rao, L., & Sakariah, K. (1999). Antibacterial Activity of Turmeric Oil : A Byproduct from Curcumin Manufacture. *Journal of agricultural and food chemistry* **47,** 4297−4300.

Nicolaus, B., Panico, A., Lama, L., Romano, I., Manca, C., De Giulio A., Gambacorta, A. (1999). Chemical composition and production of exopolysaccharides from representative members of heterocystous and non-heterocystous cyanobacteria. *Phytochemistry* **52**, 639-647.

Nithyapriya, S., Lalitha, S., Sayyed, R., Reddy, M., Dailin, D., El Enshasy, H., Luh Suriani, N., & Herlambang, S. (2021). Production, purification, and characterization of bacillibactin siderophore of *Bacillus subtilis* and its application for improvement in plant growth and oil content in sesame. *Sustainability* **13,** 5394.

Nitulescu, G., Margina, D., Zanfirescu, A., Olaru, O., & Nitulescu, G. (2021). Targeting bacterial sortases in search of anti-virulence therapies with low risk of resistance development. *Pharmaceuticals* **14,** 415.

Nitulescu, G., Nicorescu, I., Olaru, O. & Ungurianu, A. (2017). Molecular Docking and Screening Studies of New Natural Sortase A Inhibitors. *International Journal of Molecular Sciences* **18,** 2217.

Niu, X., Gao, Y., Yu, Y., Yang, Y., Wang, G., & Sun, L. (2018). Molecular Modeling reveals the inhibition mechanism and structure-activity relationship of curcumin and its analogues to *Staphylococcal aureus* Sortase A. *Journal of Biomolecular Structure and Dynamics* **37,** 1220-1230.

O'Boyle, N., Banck, M., James, C., Morley, C., Vandermeersch, T., Hutchison, G. (2011). Open Babel: An open chemical toolbox. *J. Cheminform.* **3,** 33.

Ogungbe, I. & Setzer, W. (2016). The Potential of secondary metabolites from plants as drugs or leads against protozoan neglected diseases-Part III: In-Silico molecular docking investigations. *Molecules* **21,** 1389.

Oku, S., Komastu, A., Tajima, T., Nakashimada, Y., Kato, J., (2012). Identification of chemotaxis sensory proteins for aminoacids in *Pseudomonas fluorescens* Pf0-1 and their involvement in chemotaxis to tomato root exudates and root colonization. *Microbes Environ*. **27,** 462-469.

Okuda-hanafusa, C., Uchio, R., Fuwa, A., Kawasaki, K., Muroyama, K., Yamamoto, Y., & Murosaki, S. (2019). Turmeronol A and turmeronol B from *Curcuma longa* prevent inflammatory mediator production by lipopolysaccharide-stimulated RAW264.7 macrophages, partially via reduced NF-κB signaling. *Food and function* **10,** 5779-5788.

Olanrewaju, O., Glick, B., & Babalola, O. (2017). Mechanisms of action of plant growth promoting bacteria. *World Journal of Microbiology and Biotechnology* **33**, 1–16.

Oniga, S., Araniciu, C., Palage, M., Popa, M., Chifiriuc, M., Marc, G., Pirnau, A., Stoica, C., Lagoudis, I., Dragoumis, T., Oniga, O. (2017). New 2-Phenylthiazoles as Potential Sortase A Inhibitors: Synthesis, Biological Evaluation and Molecular Docking. *Molecules* **27,** 1827.

Onlom, C., Nuengchamnong, N., Phrompittayarat, W., Putalun, W., Waranuch, N., Ingkaninan, K. (2017). Quantification of saponins in *Asparagus racemosus* by HPLC-Q-TOF-MS/MS. *Nat. Prod. Commun.* ***12***, 7–10.

Oostenbrink, C., Villa, A., Mark, A., Van Gunsteren, W. (2004). Biomolecular Force Field Based on the Free Enthalpy of Hydration and Solvation: The GROMOS ForceField Parameter Sets 53A5 and 53A6. *Journal of Computational Chemistry* **25,** 1656– 76.

O'Toole, G., Pratt, L., Watnick, P., Newman, D., Weaver, V., Kolter, R. (1999). Genetic approaches to study of biofilms, *Methods Enzymol*. **310**, 91-109.

Pandiyan, G., Leela, V., Eswari, S., Ramachandran, M., Ranganathan, V., Visha, P. (2022). Evaluation of Shatavarin IV Compound from Methanolic Extract of *Asparagus racemosus* by High Performance Thin Layer Chromatography. *J. Phytopharm*. **11,** 89–91.

Pant, G., Panwar, M., Negi, D., Rawat, M., Morris, G. (1988). Spirostanol glycoside from fruits of *Asparagus officinalis*. *Phytochemistry* **27,** 3324–3325.

Paramesha, M., Priyanka, N., Crassina, K., Shetty, N. (2021). Evaluation of diosgenin content from eleven different Indian varieties of fenugreek and fenugreek leaf powder fortified bread. *J. Food Sci. Technol*. **58,** 4746–4754.

Parewa, H., Yadav, J., Rakshit, A., Meena, V., Karthikeyan, N. (2014). Plant Growth Promoting Rhizobacteria Enhance Growth and Nutrient Uptake of Crops. *Agric Sustain Dev*. **2,**101-116.

Park, B., Kim, J., Kim, M., Lee, S., Takeoka, G., Oh, K. (2005). *Curcuma longa* L. constituents inhibit sortase A and *Staphylococcus aureus* cell adhesion to fibronectin. *Journal of Agricultural and Food* **53**, 9005–9009.

Parmar, P., Sindhu, S. (2013). Potassium solubilization by rhizosphere bacteria: influence of nutritional and environmental conditions. *J. Microbiol. Res.* **3,** 25-31.

Parulekar, R., Sonawane, K. (2018). Molecular modeling studies to explore the binding affinity of virtually screened inhibitor toward different aminoglycoside kinases from diverse MDR strains. *Journal of Cellular Biochemistry* **119**, 2679–2695.

Parveen, H., Singh, A., Khan, A., Prasad, B., & Pareek, N. (2018). Influence of plant growth promoting rhizobacteria on seed germination and seedling vigour of green gram. *Int J Chem Stud* **6**, 611–618.

Passari, A., Lalsiamthari, P., Zothanpuia, Leo, V., Mishra, V., Yadav, M., Gupta, V. & Singh, B. P. (2018). Biocontrol of Fusarium wilt of *Capsicum annuum* by rhizospheric bacteria isolated from turmeric endowed with plant growth promotion and disease suppression potential. *European Journal of Plant Pathology* **150**, 831–846.

Patel, B. (2015). Isolation and characterization of shatavarin IV from root of *Asparagus racemosus* willd. *International Journal of Pharmacy and Pharmaceutical Sciences* **7,** 362-365.

Patel, D., Prasad, S., Kumar, R., Hemalatha, S., (2012). An overview on antidiabetic medicinal plants having insulin mimetic property. *Asi.Pac.J.Trop.biomed*. **2,** 320–333.

Patil D, (2020). Shatpushpa: One solution for various female health issues: A Review. *Natl. J. Res. Ayurved Sci*. **8,** 1105–1114.

Patil, D., Gautam, M., Gairola, S., Jadhav, S., & Patwardhan, B. (2014). HPLC/Tandem mass spectrometric studies on steroidal saponins: An example of quantitative

determination of shatavarin IV from dietary supplements containing *Asparagus racemosus*. *Journal of AOAC International* **97,** 1497–1502.

Peiqin, Li. (2012). Quantitative determination of diosgenin in *Dioscorea zingiberensis* cell cultures by microplate-spectrophotometry and high-performance liquid chromatography. *African Journal of Pharmacy and Pharmacology* **6,** 15.

Peret-Almeida, L., Cherubino, A., Alves, R., Dufosse, L., & Gloria, M. (2005). Separation and determination of the physico-chemical characteristics of curcumin, demethoxycurcumin and bisdemethoxycurcumin. *Food Research International* **38**, 1039–1044.

Perez-Montano, F., Alias-Villegas, C., Bellogin, R., Cerro, P., Espuny, M., Guerrero, I., Baena, F., Ollero, F., Cubo, T. (2014). Plant growth promotion in cereal and leguminous agricultural important plants: from microorganism capacities to crop production. *Microbiol. Res*. **169**, 325–336.

Pikovskaya, I. (1948). Mobilization of phosphorus in soil in connection with vital activity of some microbial species. *Microbiologiya* **17,** 362-370.

Ponnusamy, S., Zinjarde, S., Bhargava, S., Rajamohanan, P. & Ravikumar, A. (2012). Discovering Bisdemethoxycurcumin from *Curcuma longa* rhizome as a potent small molecule inhibitor of human pancreatic alpha-amylase, a target for type-2 diabetes. *Food Chemistry* **135,** 2638–2642.

Prabhukarthikeyan, S., Manikandan, R., Durgadevi, D., Keerthana, U., Harish, S., Karthikeyan, G., Raguchander, T. (2017). Bio-suppression of turmeric rhizome rot disease and understanding the molecular basis of tripartite interaction among *Curcuma longa*, *Pythium aphanidermatum* and *Pseudomonas fluorescens*. *Biol. Control* **111,** 23–31.

Prasad, M., Srinivasan, R. & Chaudhary, M. (2019). Plant Growth Promoting Rhizobacteria (PGPR) for Sustainable Agriculture: Perspectives and Challenges. *PGPR Amelioration in Sustainable Agriculture* 129-157.

Prasad, S., Aggarwal, B. (2011). Turmeric, the Golden spice from traditional medicine to modern medicine. In: Benzie IFF, Wachtel-Galor S (eds) Herbal medicine. *Biomolecular and clinical aspects*, 2nd edn. CRC Press, Boca Raton, 1-26.

Pushpakumari, K., Naijo, Varghese. and Kavitha, Kottol. (2014). Purification and separation of individual curcuminoids from spent. *International Journal of Pharmaceutical Sciences and Research* **5,** 3246–3254.

Rahman, M., Khan, K. (2019). In silico based unraveling of New Delhi metallo- β - lactamase (NDM-1) inhibitors from natural compounds : a molecular docking and molecular dynamics simulation study. *J. Biomol. Struct. Dyn***. 0,** 1–11.

Rahmoune, B., Morsli, A., Khelifi-Slaoui, M., Khelifi, L., Strueh, A., Erban, A., Kopka, J., Prell, J. & Van Dongen, J. (2017). Isolation and characterization of three new PGPR and their effects on the growth of Arabidopsis and Datura plants. *Journal of*

Plant Interactions **12,** 1–6.

Raina, V., Srivastava, S., Jain, Ł., Ahmad, A., Syamasundar, K. & Aggarwal, K. (2002). Essential oil composition of *Curcuma longa* L . roma from the plains of northern India. *Flavour And Fragrance Journal* **17,** 99–102.

Rajendran, G., Patel, M. & Joshi, S. (2012). Isolation and characterization of nodule-associated *Exiguobacterium* sp. from the root nodules of fenugreek (*Trigonella foenum-graecum*) and their possible role in plant growth promotion. *International Journal of Microbiology* **2012,** 8.

Ramamoorthy, V., Viswanathan, R., Raguchander, T., Prakasam, V. & Samiyappan, R. (2001). Induction of systemic resistance by plant growth promoting rhizobacteria in crop plants against pests and diseases. *Crop Protection* **20,** 1-11.

Rani, R., Kumar, V., Gupta, P., Chandra, A. (2021). Potential use of *Solanum lycopersicum* and plant growth promoting rhizobacterial (PGPR) strains for the phytoremediation of endosulfan stressed soil. *Chemosphere* **279,** 130589.

Rani, S. (2014). Trigonelline and diosgenin attenuate ER stress, oxidative stress-mediated damage in pancreas and enhance adipose tissue PPAR c activity in type 2 diabetic rats *Mol Cell Biochem* **396,**161–174.

Rarey, M., Kramer, B., Lengauer, T., Klebe, G. (1996). A fast flexible docking method using an incremental construction algorithm. *J. Mol. Biol*. **261,** 470-489.

Rarnsewak, R., Dewitt, D. & Nair, M. (2000). activities of Curcumins I-III from *Curcuma longa*. *Phytomedicine* **7**, 303–308.

Reiter, B., Sessitsch, A. (2006). Bacterial endophytes of the wildflower *Crocus albiflorous* analyzed by characterization of isolates and by a cultcultivation-independent roach. *Can J Microbiol* **52,**140–149.

Revathy, S., Elumalai, S., Benny, M., & Antony, B. (2011). Isolation, Purification and Identification of Curcuminoids from Turmeric (*Curcuma longa* L.) by Column Chromatography. *Journal of Experimental Sciences* **2**, 21–25.

Riaz, U., Murtaza, G., Anum, W., Samreen, T., Sarfraz, M., Nazir, M. (2021). Plant Growth-Promoting Rhizobacteria (PGPR) as Biofertilizers and Biopesticides. *Microbiota and Biofertilizers* 181-196.

Riera, N., Handique, U., Zhang, Y., Dewdney, M. & Wang, N. (2017). Characterization of antimicrobial-producing beneficial bacteria isolated from Huanglongbing escape citrus trees. *Frontiers in Microbiology* **8**, 1–12.

Rizvi, A., Ahmed, B., Khan, M., El-Beltagi, H., Umar, S. & Lee, J. (2022). Bioprospecting Plant Growth Promoting Rhizobacteria for Enhancing the Biological Properties and Phytochemical Composition of Medicinally Important Crops. *Molecules* **27**, 1–31.

Rodrigues, J., Prather, K., Kluskens, L. & Rodrigues, L. (2015). Heterologous Production

of Curcuminoids. *Microbiology and Molecular Biology Reviews* **79**, 39–60.

Rodriguez, H. & Fraga, R. (1999). Phosphate solubilizing bacteria and their role in plant growth promotion. *Biotechnology Advances* **17,** 319–339.

Rosier, A., Beauregard, P. & Bais, H. (2021). Quorum Quenching Activity of the PGPR *Bacillus subtilis* UD1022 Alters Nodulation Efficiency of Sinorhizobium meliloti on *Medicago truncatula*. *Frontiers in Microbiology* **11,** 596299.

Roychowdury, D., Paul, M. & Banerjee, S. (2015). Isolation Identification and Partial Characterization of Nitrogen Fixing Bacteria from Soil and then the Production of Biofertilizer. *International Journal of Current Microbiology and Applied Sciences* **4**, 808-815.

Ryckaert, J., Ciccotti, G., Berendsen, H. (1977). Numerical integration of the cartesian equations of motion of a system with constraints; molecular dynamics of n-alkanes. *J Comput Phys* **23,** 327-341.

Saengsanga, T. (2018). Isolation and Characterization of Indigenous Plant Growth-Promoting Rhizobacteria and Their Effects on Growth at the Early Stage of Thai Jasmine Rice (*Oryza sativa* L. KDML105). *Arabian Journal for Science and Engineering* **43**, 3359–3369.

Saharan, B. & Nehra, V. (2011). Plant Growth Promoting Rhizobacteria: A Critical Review. *Life Sci. Med. Res* **2011**, 1–30.

Sahne, F., Mohammadi, M., Najafpour, G. & Moghadamnia, A. (2016). Enzyme-assisted ionic liquid extraction of bioactive compound from turmeric (*Curcuma longa* L.): Isolation, purification and analysis of curcumin. *Industrial Crops & Products* **95**, 686-694.

Saikia, L. & Upadhyaya, S. (2011). Antioxidant activity, phenol and flavonoid content of *A. racemosus* Willd. a medicinal plant grown using different organic manures. *Res. J. Pharm. Biol. Chem. Sci* **2**, 457-463.

Sairam, K., Priyambada, N. & Goel, R. (2003). Gastroduodenal ulcer protective activity of *Asparagus racemosus.* An experimental, biochemical and histological study. *Journal of Ethnopharmacology* **86**, 1-10.

Saito, K. & Matsuda, F. (2010). Metabolomics for functional genomics, systems biology, and biotechnology. *Annu Rev Plant Bio* **l61**, 463–89.

Salamone, I., Hynes, R. & Nelson, L. (2001). Cytokinin production by plant growth promoting rhizobacteria and selected mutants. *Can J Microbiol* **47**, 404–411.

Saleem, H., Sarfraz, M., Ahsan, H., Khurshid, U., Kazmi, S., Zengin, G., Locatelli, M., Ahmad, I., Abdallah, H., Mahomoodally, M., Rengasamy, K. & Ahemad, N. (2020). Secondary metabolites profiling, biological activities and computational studies of *Abutilon figarianum* webb (Malvaceae). *Processes* **8**, 336.

Salmanli, M., Tatar Yilmaz, G., Tuzuner, T. (2021). Investigation of the antimicrobial activities of various antimicrobial agents on *Streptococcus Mutans* Sortase A through computer-aided drug design (CADD) approaches, *Comput Methods Programs Biomed.* **212**, 106454.

Sanchita, Singh, G. & Sharma, A. (2014). In silico study of binding motifs in squalene synthase enzyme of secondary metabolic pathway Solanaceae family. *Molecular Biology Reports* **41**, 7201–7208.

Sandhya, V., Ali, S., Grover, M., Kishore, N. & Venkateswarlu, B. (2009). *Pseudomonas* sp. strain P45 protects sunflowers seedlings from drought stress through improved soil structure. *J Oilseed Res* **26**, 600–601.

Sangeetha, M., Mal, N., Atmaja, K., Sali, V. & Vasanthi, H. (2013) Chemico-Biological Interactions PPAR's and Diosgenin a chemico biological insight in NIDDM. *Chem. Biol. Interact* **206**, 403–410.

Santoro, M., Zygadlo, J., Giordano, W. & Banchio, E. (2011). Volatile organic compounds from rhizobacteria increase biosynthesis of essential oils and growth parameters in peppermint (*Mentha piperita*). *Plant Physiol Biochem* **49**, 1177–1182.

Santoyo, G., Urtis-Flores, C., Loeza-Lara, P., Orozco-Mosqueda, M. & Glick, B. (2021). Rhizosphere colonization determinants by plant growth-promoting rhizobacteria (Pgpr). *Biology* **10**, 1–18.

Saravanan, V., Subramoniam, S. & Raj, S. (2004). Assessing in vitro solubilization potential of different zinc solubilizing bacterial (zsb) isolates. *Brazilian journal of microbiology* **35**, 121–125.

Sarvin, B., Fedorova, E., Shpigun, O., Titova, M. & Nikitin, M. (2018). LC-MS determination of steroidal glycosides from *Dioscorea deltoidea* Wall cell suspension culture: Optimization of pre-LC-MS procedure parameters by Latin Square design. *Journal of Chromatography B*, **1080**, 64–70.

Sattari, N., Pahlavan, Y. & Bozorg, A. (2018). Effects of humic acid and plant growth-promoting rhizobacteria (PGPR) on induced resistance of canola to *Brevicoryne brassicae* L. *Bulletin of Entomological Research* **109**, 479-489.

Saxena, V. & Chourasia, S. (2001). A new isoflavone from the roots of *Asparagus racemosus. Fitoterapia* **72**, 307-309.

Sayyed, R. Z. (Ed.). (2019). Plant Growth Promoting Rhizobacteria for Sustainable Stress Management. *Rhizobacteria in Biotic Stress Management* Springer Nature **13.**

Schieffer, G. (2002). Pressurized liquid extraction of curcuminoids and curcuminoid degradation products from turmeric (*Curcuma longa*) with subsequent HPLC assays. *Journal of Liquid Chromatography and Related Technologies* **25**, 3033–3044.

Schippers, B., Bakker, A., Bakker, P. & Van, P. (1990). Beneficial and deleterious effects of HCN-producing *Pseudomonad*s on rhizosphere interactions. *Plant and Soil* **129,** 75-83.

Schmidt, R., Koberl, M., Mostafa, A., Ramadan, E., Monschein, M., Jensen, K., Bauer, R. & Berg, G. (2014). Effects of bacterial inoculants on the indigenous microbiome and secondary metabolites of chamomile plants. *Frontiers in Microbiology* **5**, 1–11.

Schwyn, B. & Neilands, J. (1987). Universal chemical assay for the detection and determination of siderophores. *Analytical Biochemistry* **160**, 47–56.

Setzer, W., Sama, W., Essien, E., Olayemi, J., Ekundayo, O., Ajaiyeoba, E., Sama, W., Walker, T. & Setzer, W. (2008). Larvicidal Activity of Turmerone-Rich Essential Oils of *Curcuma longa,* Leaf and Rhizome from Nigeria on Anopheles gambiae. Pharmaceutical Biology **46**, 279-282.

Shah, A., Nazari, M., Antar, M., Msimbira, L., Naamala, J., Lyu, D., Rabileh, M., Zajonc, J. & Smith, D. (2021). PGPR in Agriculture: A Sustainable Approach to Increasing Climate Change Resilience. *Frontiers in Sustainable Food Systems* **5**, 1–22.

Shaikh, S. & Saraf, M. (2017). Biofortification of *Triticum aestivum* through the inoculation of zinc solubilizing plant growth promoting rhizobacteria in field experiment. *Biocatalysis and Agricultural Biotechnology* **9**, 120–126.

Shakeel, M., Rais, A., Hassan, M. & Hafeez, F. (2015). Root Associated *Bacillus* sp. Improves Growth, Yield and Zinc Translocation for Basmati Rice (*Oryza sativa*) Varieties. *Frontiers in Microbiology* **6**, 1–12.

Shameer, S., Prasad, T.N.V.K.V (2018). Plant growth promoting rhizobacteria for sustainable agricultural practices with special reference to biotic and abiotic stresses. *Plant Growth Regulation* **84**, 603–615.

Shao, Y., Poobrasert, O., Kennelly, E., Chin, C., Ho, C., Huang, M., Garrison, S. & Cordell, G. (1997). Steroidal saponins from *Asparagus officinalis* and their cytotoxic activity. *Planta. Med.* **63**, 258-262.

Sharafzadeh, S. & Ordookhani, K. (2011). Organic and bio fertilizers as a good substitute for inorganic fertilizers in medicinal plants farming. *Australian Journal of Basic and Applied Sciences* **5**, 1330–1333.

Sharifian, P., Yaslianifard, S., Fallah, P., Aynesazi, S., Bakhtiyari, M. & Mohammadzadeh, M. (2020). Investigating the effect of nano-curcumin on the expression of biofilm regulatory genes of *Pseudomonas aeruginosa*. *Infection and Drug Resistance* **13**, 2477–2484.

Sharma, O. (1976). Antioxidant activity of curcumin and related compounds. *Biochemical Pharmacology* **25**, 1811–1812.

Sharma, V. & Sarkar, I. (2013). Bioinformatics opportunities for identification and study of medicinal plants. *Briefings in Bioinformatics* **14**, 238–250.

Sheikh, I., Capoor, M. & Khatoon, F. (2013). Phytochemical analysis and growth inhibiting effects of *Cinnamomum cassia* bark on some pathogenic fungal isolates. *J Chem. Pharma. Res* **5**, 25-32.

Shulga, D., Kudryavtse, K. (2021). Selection of Promising Novel Fragment Sized *S. aureus* SrtA Noncovalent Inhibitors Based on QSAR and Docking Modeling Studies, *Molecules*. **26** 7677,

Si, L., Li, P., Liu, X. & Luo, L. (2016). Chinese herb medicine against Sortase A catalyzed transformations, a key role in gram-positive bacterial infection progress, *Journal of Enzyme Inhibition and Medicinal Chemistry* **31,** 184-196.

Siddiqui, I., Shaukat, S., Sheikh, I. & Khan, A. (2006). Role of cyanide production by *Pseudomonas fluorescens* CHA0 in the suppression of root-knot nematode, Meloidogyne javanica in tomato. *World J Microbiol Biotechnol* **22**, 641–650.

Singh, M., Hamid, A., Maurya, A., Prakash, O., Khan, F., Kumar, A., Aiyelaagbe, O., Negi, A. & Bawankule, D. (2014). Journal of Steroid Biochemistry and Molecular Biology Synthesis of diosgenin analogues as potential anti-inflammatory agents. *Journal of Steroid Biochemistry and Molecular Biology* **143**, 323–333.

Singh, M., Singh, D., Gupta, A. & Pandey, K. (2019). Plant Growth Promoting Rhizobacteria: Application in Biofertilizers and Biocontrol of Phytopathogens. *PGPR Amelioration in Sustainable Agriculture* Chapter **3,** 41-66.

Singh, R. & Jha, P. (2016). The Multifarious PGPR *Serratia marcescens* CDP-13 Augments Induced Systemic Resistance and Enhanced Salinity Tolerance of Wheat (*Triticum aestivum* L). PLoS ONE **11,** e0155026.

Singh, R., Singh, P., Li, H., Song, Q., Guo, D., Solanki, M., Verma, K., Malviya, M., Song, X., Lakshmanan, P. & Yang, L. (2020). Diversity of nitrogen-fixing rhizobacteria associated with sugarcane : a comprehensive study of plant-microbe interactions for growth enhancement in *Saccharum* spp. *BMC Plant Biology* **20,** 1–21.

Singh, T., Sahai, V., Goyal, D., Prasad, M., Yadav, A., Shrivastav, P., Ali, A. & Dantu, P. (2020). Identification, Characterization and Evaluation of Multifaceted Traits of Plant Growth Promoting Rhizobacteria from Soil for Sustainable Approach to Agriculture. *Current Microbiology* **77**, 3633–3642.

Sivaramakrishnan, M., Jagadeesan, V. & Ruban, S. (2019). Screening of curcumin analogues targeting Sortase A enzyme of *Enterococcus faecalis* : a molecular dynamics approach. *Journal of Proteins and Proteomics* **10**, 245–255.

Siviero, A., Gallo, E., Maggini, V., Gori, L., Mugelli, A., Firenzuoli, F. & Vannacci, A. (2015). Curcumin, a golden spice with a low bioavailability. *J Herb Med* **5**, 57–70.

Smyth, T., Rudden, M., Tsaousi, K., Marchant, R. & Banat, I. (2014). Protocols for the Isolation and Analysis of Lipopeptides and Bioemulsifiers. In: McGenity T, Timmis K, Nogales B (eds) Hydrocarbon and Lipid Microbiology Protocols. *Springer*

Protocols Handbooks, Springer, Heidelberg.

Sonawane, K., Barale, S., Dhanavade, M., Waghmare, S., Nadaf, N., Kamble, S., Mohammed, A., Makandar, A., Fandilolu, P., Dound, A., Naik, N., More, V. (2021). Structural insights and inhibition mechanism of TMPRSS2 by experimentally known inhibitors Camostat mesylate, Nafamostat and Bromhexine hydrochloride to control SARS-coronavirus-2: a molecular modeling approach, *Inform. Med. Unlocked* **24**, 100597.

Soni, V., Mehta, A., Ratre, Y., Tiwari, A., Amit, Singh, R., Sonkar, S., Chaturvedi, N., Shukla, D. & Vishvakarma, N. (2020). Curcumin, a traditional spice component, can hold the promise against COVID-19. *Eur. J. Pharmacol* **886**, 173551.

Soto, J., Ortiz, J., Herrera, H., Fuentes, A., Almonacid, L. & Charles, T. (2019). Enhanced arsenic tolerance in *Triticum aestivum* inoculated with arsenic-resistant and plant growth promoter microorganisms from a heavy metal-polluted soil. *Microorganisms* **7**, 348.

Sousa, S., Fernandes, P. & Ramos, M. (2006). Protein–ligand docking: current status and future challenges. *Proteins* **65**, 15–26.

Srivastava, P., Shukla, A. & Kalunke, R. (2018). Comprehensive metabolic and transcriptomic profiling of various tissues provide insights for saponin biosynthesis in the medicinally important *Asparagus racemosus. Sci. Rep*. **8**, 1–13.

Su, H., Horvat, R. & Jilani, G. (1982). Isolation, Purification, and Characterization of Insect Repellents from Curcuma. *J. Agric. Food Chem.* **30,** 290-292.

Su, Z., Cai, S., Liu, J., Zhao, J., Liu, Y., Yin, J. & Zhang, D. (2021). Root-Associated Endophytic Bacterial Community Composition of *Asparagus officinalis* of Three Different Varieties. *Indian J. Microbiol* **61**, 160–169.

Sun, J., Cui, G., Ma, X., Zhan, Z., Ma, Y., Teng, Z., Gao, W., Wang, Y., Chen, T., Lai, C., Zhao, Y., Tang, J., Lin, H., Shen, Y., Zeng, W., Guo, J. & Huang, L. (2019). An integrated strategy to identify genes responsible for sesquiterpene biosynthesis in turmeric. *Plant Molecular Biology* **101**, 221–234.

Suree, N., Liew, C., Villareal, V., Thieu, W., Fadeev, E., Clemens, J. & Clubb, R. (2009). The structure of the *Staphylococcus aureus* sortase- substrate complex reveals how the universally conserved LPXTG sorting signal is recognized. *J Biol Chem* **284**, 24465-24477.

Surveswaran, S., Cai, Y., Corke, H. & Sun, M. (2007). Systematic evaluation of natural phenolic antioxidants from 133 Indian medicinal plants. *Food Chemistry* 102, 938–953.

Suryadevara, N., Ponmurugan, P. (2012). Response of turmeric to plant growth promoting rhizobacteria (PGPR) inoculation under different levels of nitrogen. *Int J Biol Technol* **3,** 39–44.

Swamy, M., Pokharen, N., Dahal, S. & Anuradha, M. (2011). Phytochemical and antimicrobial studies of leaf extract of *Euphorbia neriifolia*. *J Med Plants Res* **5**, 5785–5788.

Takishita, Y., Charron, J. & Smith, D. (2018). Biocontrol rhizobacterium Pseudomonas sp. 23S induces systemic resistance in Tomato (*Solanum lycopersicum* L.) against bacterial Canker *Clavibacter michiganensis* subsp. michiganensis. *Frontiers in Microbiology* **9**, 1–14.

Tal, B., Tamir, I., Rokem, J. & Goldberg, I. (1984). Isolation and characterization of an intermediate steroid metabolite in diosgenin biosynthesis in suspension cultures of *Dioscorea deltoidea* cells. *Biochem. J* **219**, 619 - 24.

Tamura, K., Stecher, G. & Kumar, S. (2021). MEGA11: Molecular Evolutionary Genetics Analysis Version 11. *Mol Biol Evol* **38**, 3022–3027.

Tanaka, K., Kuba, Y., Ina, A., Watanabe, H. & Komatsu, K. (2008). Prediction of cyclooxygenase inhibitory activity of Curcuma rhizome from chromatograms by multivariate analysis. *Chemical and Pharmaceutical Bulletin* **56**, 936–940.

Taufique, T., Mayda, U. & Mehraj, H. (2014). Yield performance and phytochemical screening of three asparagus varieties. *Bangladesh Research Publication Journal* **10**, 196-201.

Taylor, P., Joe, B., Vijaykumar, M., Lokesh, B., Joe, B. (2004). Biological Properties of Curcumin-Cellular and Molecular Mechanisms of Action of Curcumin. *Crit Rev Food Sci Nutr* **44**, 97-111.

Tchuisseu, G., Berger, B., Patz, S., Fankem, H. & Ruppel, S. (2018). Data on molecular identification, phylogeny and in vitro characterization of bacteria isolated from maize rhizosphere in Cameroon. *Data in Brief* **19**, 1410–1417.

Teles, A., Dulce, T., Mouchrek, A., Abreu-silva, A., Calabrese, S. & Almeida-souza, F. (2019), Cinnamomum zeylanicum, Origanum vulgare, and Curcuma longa Essential Oils: Chemical Composition, Antimicrobial and Antileishmanial Activity. *Evid Based Complement Alternat Med* **2019**, 2421695.

Thappeta, K., Zhao, L., Nge, C., Crasta, S., Leong, C., Ng, V., Kanagasundaram, Y., Fan, H. & Ng, S. (2020). In-silico identified new natural sortase a inhibitors disrupt *S. aureus* biofilm formation. *International Journal of Molecular Sciences* **21**, 1–18.

Thewles, A., Parslow, R. & Coleman, R. (1993). Effect of diosgenin on biliary cholesterol transport in the rat. *Biochemical Journal* **291**, 793–798.

Thompson, J., Gibson, T., Plewniak, F., Jeanmougin, F. & Higgins, D. (1997). The CLUSTAL_X windows interface: flexible strategies for multiple sequence alignment aided by quality analysis tools. *Nucleic Acids Res* **25**, 4876–4882.

Thomsen, R., Christensen, M. (2006). MolDock: a new technique for high-accuracy molecular docking. *J Med Chem.* **49,** 3315–3321.

Tirry, N., Kouchou, A., Laghmari, G., Lemjereb, M., Hnadi, H., Amrani, K., Bahafid, W. & El Ghachtouli, N. (2021). Improved salinity tolerance of *Medicago sativa* and soil enzyme activities by PGPR. *Biocatalysis and Agricultural Biotechnology* **31,**101914.

Tonnesen, H.H. (1992). Chemistry of curcumin and curcuminoids. *Phenolic Compounds in Food and their Effect on Health. I*: **506,** 143 153.

Toussaint, J., Kraml, M., Nell, M., Smith, S., Smith, F., Steinkellner, S., Schmiderer, C., Vierheilig, H. & Novak, J. (2008). Effect of *Glomus mosseae* on concentrations of rosmarinic and caffeic acids and essential oil compounds in basil inoculated with *Fusarium oxysporum* f. sp. basilici. *Plant Pathol* **57**, 1109–1116.

Tsai, S., Huan, C., Chyau, C., Weng, C. & Mau, J. (2011). Composition and Antioxidant Properties of Essential Oils from Curcuma rhizome. *Asian Journal of Arts and Sciences* **2,** 57–66.

Umair, M., Muhammad, I., Muhammad, S., Adeela, A., Farooq, A. & Sikandar, H. (2018). A brief review on plant growth promoting rhizobacteria (PGPR): a key role in plant growth promotion. *Plant Protection* **2**, 77–82.

Upadhyay, S., Phukan, U., Mishra, S. & Shukla, R. (2014). De novo leaf and root transcriptome analysis identified novel genes involved in Steroidal sapogenin biosynthesis in *Asparagus racemosus.* *BMC Genomics* **15**, 746.

Valdes-Tresanco, M., Valiente, P., Moreno, E. (2021). gmx_MMPBSA: A New Tool to Perform End-State Free Energy Calculations with GROMACS, *J Chem Theory Comput.* **17**, 6281-6291.

Van Loon, L. & Glick, B. (2004). Increased plant fitness by rhizobacteria. In *Molecular ecotoxicology of plants* 170, 177–205.

Van, Der., Lindahl, E., Hess, B., Groenhof, G., Mark, A. & Berendsen, H. (2005). GROMACS: fast, flexible, and free. *J Comput Chem* **26**, 1701-1718.

Varma, A., Prasad, R. & Tuteja, N. (2017). Promotion and Value Addition to Some Important Medicinal Plants Under Saline Condition by Intervention of a Novel Mycorrhizal Formulation. *Mycorrhiza - eco-physiology, secondary metabolites, nanomaterials: Fourth Edition* 1–334.

Vasagade, S., Patil, S., Patil, S. & Shubham, A. (2021). Study on Rhizospheric Bacterial Exopolysaccharide and Its Application in Plant Growth Promoters and Antimicrobial Activity. *International Journal of Research in Engineering and Science (IJRES)* **9**, 59–66.

Vasudha, S., Shivesh, S. & Prasad, S. (2013). Harnessing PGPR from rhizosphere of prevalent medicinal plants in tribal areas of Central India. *Res J Biotechnol* **8**, 76–85.

Velavan, S., Nagulendran, K., Mahesh, R. & Begum, H. (2007). In vitro antioxidant

activity of *Asparagus racemosus* root. *Pharmacognecy* **3**, 26–33.

Velhal, C. (2014). Effect of Rhizobium Based Biofertilizer Combined with *Saccharomyces cerevisiae* on the Growth of Hyacinth Bean. *International Journal of Plant & Soil Science* **3**, 959–968.

Vendeville, A., Winzer, K., Heurlier, K., Tang, C. & Hardie, K. (2005). Making 'sense' of metabolism: autoinducer-2, LuxS and pathogenic bacteria. *Nat Rev Microbiol* **3,** 383-96.

Vendeville, A., Winzer, K., Heurlier, K., Tang, C., Hardie, K. (2005). Making 'sense' of metabolism: autoinducer-2, LuxS and pathogenic bacteria, *Nat Rev Microbiol*. **3,** 383-96.

Venkat, S., Soumya, S., Agarwal, H. & Divya, D. (2017). Characterization and optimization of bacterium isolated from soil samples for the production of siderophores. *Resour Effic Technol* **3**, 434-439.

Venkata, M., Sripathy, R., Anjana, D., Somashekara, N., Krishnaraju, A., Krishanu, S., Murali, M., RamaVerma, S. & Ramchand, C. (2012). In silico, in vitro and in vivo assessment of safety and anti-inflammatory activity of curcumin. *American Journal of Infectious Diseases* **8**, 26–33.

Verghese, J. & Joy, M. (1989). Isolation of the colouring matter from dried turmeric (*Curcuma longa* L.) with ethyl acetate. *Flavour Frag J* **4**, 31–2.

Verlet, L. (1967). Computer experiments on classical fluids. I. Thermodynamical properties of Lenard-Jones molecules. *Physical Review* **159**, 98-103.

Verma, H., Sonbhadra, D., Singh, S., White, J. & Kumar, A. (2021). Biocontrol Potential of Microbial Consortia: Approaches in Food Security and Disease Management. In: Kumar, A. (eds) *Microbial Biocontrol: Sustainable Agriculture and Phytopathogen Management*. Springer, Cham. 187-203

Verma, J. (2010). Impact of plant growth promoting rhizobacteria on crop production. *Int J Agric Res* **5**, 954–983.

Verma, V., Patel, R., Deshmukh, N., Jha, A., Ngachan, S., Singha, A. & Deka, B. (2019). Response of ginger and turmeric to organic versus traditional production practices at different elevations under humid subtropics of north-eastern India. *Ind. Crops Prod* **136**, 21–27.

Vijayalakshmi, K., Nadhiya, K., Haripriya, D. & Ranjani, R. (2014). In silico docking analysis of secondary metabolites of *Bauhinia variegata* and *Garcinia cambogia* with retinol-binding protein 4 as target for obesity. *International Journal of Pharmacognosy and Phytochemical Research* **6**, 636–642.

Vinayarani, G. & Prakash, H. (2018). Growth Promoting Rhizospheric and Endophytic Bacteria from *Curcuma longa* L. as Biocontrol Agents against Rhizome Rot and Leaf Blight Diseases *Plant Pathol. J.* **34**, 218–235.

Vinayarani, G., Madhusudhan, K. & Prakash, H. (2019). Induction of systemic resistance in turmeric by rhizospheric isolate *Trichoderma asperellum* against rhizome rot disease. *J. Plant Pathol* **101**, 965–980.

Wagner, L., Jonatas, F., Oliveira, R., Esteves, S. & Camargo, A. (2020). *Curcuma longa* L. (turmeric), *Rosmarinus officinalis* L. (rosemary), and *Thymus vulgaris* L. (thyme) extracts aid murine macrophages (RAW 264.7) to fight *Streptococcus mutans* during in vitro infection. *Archives of Microbiology* **202**, 2269-2277.

Walia, M., Batra, N. & Goyal, S. (2014). Isolation and characterization of plant growth promoting rhizobacteria and their application in plant growth. *Legume Research* **37**, 72–78.

Wallock, R., Marles, W., Clarke, D., Maitra, A., Dodds, M., Hanley, B. & Campopiano, D. (2015). Molecular basis of *Streptococcus mutans* sortase A inhibition by the flavonoid natural product trans-chalcone. *Chem Commun (Camb)* **51**, 10483-10485.

Wan, Y., Luo, S., Chen, J., Xiao, X., Chen, L. & Zeng, G. (2012). Chemosphere Effect of endophyte-infection on growth parameters and Cd-induced phytotoxicity of Cd-hyperaccumulator *Solanum nigrum* L . *Chemosphere* **89**, 743–750.

Wang, E. & Martinez, R. (2000). *Sesbania herbacea*-Rhizobium huautlense nodulation in flooded soils and comparative characterization of *S. herbacea*-nodulating rhizobia in different environments. *Microb Ecol* **40**, 25–32.

Wang, J., Li, H., Pan, J., Dong, J., Zhou, X. Niu, X., Deng, X. (2018). Oligopeptide Targeting Sortase A as Potential Anti-infective Therapy for *Staphylococcus aureus*, *Front Microbiol***. 9,** 245.

Wang, J., Shi, Y., Jing, S., Dong, H., Wang, D., Wang, T. (2019). Astilbin Inhibits the Activity of Sortase A from *Streptococcus mutans. Molecules.* **24,** 465.

Wang, L., Wang, X. & Zhao, B. (2011). Simultaneous Analysis of Diosgenin and Sarsasapogenin in *Asparagus officinalis* Byproduct by Thin-layer Chromatography. *Phytochem Anal* **22,** 14–17.

Wang, N., Wang, Z., Tootle, S., Philip, T. & Zhao, Z. (2012). Curcumin promotes cardiac repair and ameliorates cardiac dysfunction following myocardial infarction. *Br. J. Pharmacol* **167**, 1550–1562.

Wase, N. & Wright, P. (2008). Systems biology of cyanobacterial secondary metabolite production and its role in drug discovery. *Expert Opinion on Drug Discovery* **3**, 903–929.

Waters, C. & Bassler, B. (2005). Quorum sensing: cell-to-cell communication in bacteria. *Ann Rev Cell Developmental Biol* **21**, 319-46.

Werner, T. & Schmulling, T. (2009). Cytokinin action in plant development. *Curr Opin Plant Biol* **12**, 527-38.

Weyens, N., Van, L., Taghavi, S., Newman, L. & Vangronsveld, J. (2009). Exploiting plant microbe partnerships to improve biomass production and remediation. *Trends Biotechnol* **27**, 591-598.

Wiberg, K. (1965). A scheme for strain energy minimization application to the cycloalkanes. *J Am Chem Soc* **87**, 1070-1078.

Wichitnithad, W., Rojsitthisak, P., Ichitnithad, W., Jongaroonngamsang, N., Pummangura, S. and Rojsitthisak, P. (2009). A simple isocratic HPLC method for the simultaneous determination of curcuminoids in commercial turmeric extracts. *Phytochem. Anal* **20**, 314-319.

Wolfe, K., Wu, X. & Liu, R. (2003). Antioxidant Activity of Apple Peels. *Journal of Agricultural and Food Chemistry* **51**, 609-614.

Xekarfotakis, N., Chatzistathis, T., Mola, M., Demirtzoglou, T. & Monokrousos, N. (2021). The effects of different fertilization practices in combination with the use of PGPR on the sugar and amino acid content of *Asparagus officinalis*. *Horticulturae* **7**, 507.

Xie, Z., Ma, X. & Gang, D. (2009). Modules of co-regulated metabolites in turmeric (*Curcuma longa*) rhizome suggest the existence of biosynthetic modules in plant specialized metabolism. *Journal of Experimental Botany* **60**, 87–97.

Xiong, G., Wu, Z., Yi, J., Fu, L., Yang, Z., Hsieh, C., Yin, M., Zeng, X., Wu, C., Lu, A., Chen, X., Hou, T., Cao, D. (2021). ADMETlab 2.0: an integrated online platform for accurate and comprehensive predictions of ADMET properties. *Nucleic Acids Res*. **49**, W5-W14.

Xu, L., Shang, Z., Lu, Y., Li, P., Sun, L., Guo, Q., Bo, T., Le, Z., Bai, Z., Zhang, X., Qiao, X., & Ye, M. (2020). Analysis of curcuminoids and volatile components in 160 batches of turmeric samples in China by high-performance liquid chromatography and gas chromatography-mass spectrometry. *Journal of Pharmaceutical and Biomedical Analysis* **188**, 1–7.

Yadav, P., Kadam, K., Bhingare K. & Patil, M. (2018). Standardization and quantification of curcumin from *Curcuma longa* extract using UV visible spectroscopy and HPLC. *Journal of Pharmacognosy and Phytochemistry* **7,** 1913–1918.

Yang, C., Huang, S., Yang, X. & Jia, Z. (2004). Nor-lignans and steroidal saponins from *Asparagus gobicus*. *Planta Med* **70**, 446-51.

Yang, H., Yin, H., Shen, Y., Xia, G., Zhang, B., Wu, X., Cai, B. & Tam, J. (2016). A more ecological and efficient approach for producing diosgenin from *Dioscorea zingiberensis* tubers via pressurized biphase acid hydrolysis. *Journal of Cleaner Production* **131**, 10–19.

Yang, H., Yin, H., Wang, X., Li, Z., Shen, Y. & Jia, X. (2015). In situ pressurized biphase acid hydrolysis, a promising approach to produce bioactive diosgenin from the

tubers of *Dioscorea Zingiberensis*. *Pharmacognosy Magazine* **11**, 636–642.

Yilmaz, A. & Karik, U. (2022). AMF and PGPR enhance yield and secondary metabolite profile of basil (*Ocimum basilicum* L.). *Industrial Crops and Products*, **176**, 114327.

Yodkeeree, S., Chaiwangyen, W., Garbisa, S. & Limtrakul, P. (2009). Curcumin, demethoxycurcumin and bisdemethoxycurcumin differentially inhibit cancer cell invasion through the down-regulation of MMPs and uPA. *J. Nutr. Biochem*. **20**, 87–95.

Yoon, S., Ha, S., Kwon, S., Lim, J., Kim, Y., Seo, H. & Chun, J. (2017). Introducing EzBioCloud : a taxonomically united database of 16S rRNA gene sequences and whole-genome assemblies. *Int J Syst Evol Microbiol* **67**, 1613–1617.

Yuan, Y., Chu, D., Fan, J., Zou, P., Qin, Y., Geng, Y., Cui, Z., Wang, X., Zhang, C., Li, X., Clark, J., Li, Y. & Wang, X. (2020). Ecofriendly conversion of algal waste into valuable plant growth- promoting rhizobacteria (PGPR) biomass. *Waste Management* **120**, 576 – 584.

Yue, G., Kwok, H. & Lee, J. (2015). Novel anti-angiogenic effects of aromatic- turmerone, essential oil isolated from spice. *Journal of Functional Foods* **15**, 243–253.

Zainab, B., Ayaz, Z., Alwahibi, M., Khan, S., Rizwana, H., Soliman, D., Alawaad, A. & Mehmood A. (2020). In-silico elucidation of *Moringa oleifera* phytochemicals against diabetes mellitus. *Saudi Journal of Biological Sciences* **27**, 2299–2307.

Zhang, S., Guan, J., Yang, Q., Liu, G., Cheng, J. & Li, P. (2008). Analysis Qualitative and quantitative analysis of four species of Curcuma rhizomes using twice development thin layer chromatography. *Journal of Pharmaceutical and Biomedical* **48**, 1024–1028.

Zhao, Y., Cartabia, A., Lalaymia, I. & Declerck, S. (2022). Arbuscular mycorrhizal fungi and production of secondary metabolites in medicinal plants. *Mycorrhiza* **32**, 3–4.

Zhishen, J., Mengcheng, T., Jianming, W., The determination of flavonoid contents in mulberry and their scavenging effects on superoxide radicals, *Food Chemistry* **64**, 555-559.

Zong, Y., Bice, T., Ton-That, H., Schneewind, O. & Narayana, S. (2004). Crystal structures of *Staphylococcus aureus* Sortase A and its substrate complex. *Journal of Biological Chemistry* **279**, 31383–31389.

CHAPTER VII

RESEARCH PUBLICATIONS AND PRESENTATIONS

Paper Published (02):

1. **Ruddhi R. Jagtap**, Gajanan V. Mali and Kailas D. Sonawane. (2022) Isolation, characterization and identification of potent plant growth promoting rhizobacteria from *Asparagus racemosus.* **YMER, 21,** || ISSN : 0044-0477

2. **Ruddhi R. Jagtap**, Gajanan V. Mali, Shailesh R. Waghmare, Naiem H. Nadaf, Mansingraj S. Nimbalkar, and Kailas D. Sonawane. (2023) Impact of plant growth promoting rhizobacteria *Serratia nematodiphila* RGK and *Pseudomonas plecoglossicida* RGK on secondary metabolites of turmeric rhizome. **Biocatalysis and Agricultural Biotechnology, 47**, 102622. DOI: 10.1016/j.bcab.2023.102622.

Manuscript Communicated (01):

3. **Ruddhi. R. Jagtap**, Gajanan. V. Mali, Sagar S. Barale and Kailas. D. Sonawane. Inhibition of *S. Aureus* and *S. Mutans* Sortase A by PGPR induced secondary metabolites from *C. longa: In-vitro* and *in-silico* approaches **International Journal of Biological Macromolecules (Manuscript ID: IJBIOMAC-D-23-16762),** Under Review

Conferences Attended/ Paper Presented:

1. Participated in two days National conference-2019: Research and innovations in healthcare & Business Management Organised by Rashtriya Shikshan Mandal's CDGIM, Pune, 5 & 6th November 2019
2. **Ruddhi. R. Jagtap**, Gajanan.V. Mali, Kailas. D. Sonawane, Effect of Plant Growth Promoting Rhizobacteria on Turmeric. Interdisciplinary International Conference on 'Research Interventions and Technological Advancements In Plant Sciences (RITAPS,2021)' jointly organized by Association of Plant Science Researchers, Dehradun and PG department of Botany, Shri Pancham Khemraj Mahavidyalaya, Sawantwadi on 26th and 27th March, 2021.
3. Participated in two days International conference on 'Infectious Diseases and Immunopathology', organized by Department of Biotechnology, Savitribai Phule Pune University, Pune, 22nd to 24thApril 2021.

4. Completed one online certificate course on HPC Shiksha -Basics of High Performance Computing, conducted by Indian Institute of Technology Goa.
5. Participated in two days 3rd International Multidisciplinary Conference on Emerging Trends in Humanities, Commerce, Management, Science and Technology (IMCET-2021) organized by the Balwant College, Vita Dist. Sangli (MS) on 23rd – 24th December 2021.
6. **Ruddhi. R. Jagtap**, Gajanan.V. Mali, Kailas. D. Sonawane, Effect of Plant Growth Promoting Rhizobacteria on Secondary Metabolites of Medicinal Plant. International E-conference on the "Frontiers in Microbiology" organized by Vasantdada Patil Arts, commerce and science college in association with Microbiologists society, India on 17th and 18th January 2022.
7. **Ruddhi. R. Jagtap**, Gajanan.V. Mali, Kailas. D. Sonawane, Effect of Plant Growth Promoting Rhizobacteria on Secondary Metabolites of Medicinal Plant. National Conference on Recent trends in pure and applied sciences (RTPAS-2022) organized by internal quality assurance cell, Bharati Vidyapeeth's Dr. Patangrao Kadam Mahavidyalaya, Sangli. on 21st and 22nd January 2022.
8. **Ruddhi. R. Jagtap,** Gajanan.V. Mali, Kailas. D. Sonawane, Effect of Plant Growth Promoting Rhizobacteria on Secondary Metabolites of *Asparagus racemosus* one-day national conference on "Biodiversity and biosciences" organized by Rayat Shikshan Sanstha's Balwant College, Vita on 29 th December 2022.
9. **Ruddhi. R. Jagtap,** Gajanan.V. Mali, Kailas. D. Sonawane, SrtA inhibition by PGPR treated plant secondary metabolites from *C. longa*: A Structural perspectives, Symposium on "Accelerating Biology 2023: Discovery to Delivery" organized by HPC M & BA Group, C-DAC, Pune, India from 28th Feb to 2nd March 2023.
10. Participated in the workshop cum hands-on training on techniques on biogenic synthesis of nanomaterials organized by the School of Nanoscience and Biotechnology, Department of Biochemistry, and Department of Botany, Shivaji University, Kolhapur held during 20-24 Feb 2023 under the DBT-BUILDER SUK program.

STUDIES ON SECONDARY METABOLITES OF *C. LONGA* AND *A. RACEMOSUS* INFLUENCED BY PLANT GROWTH PROMOTING RHIZOBACTERIA

A THESIS SUBMITTED TO

SHIVAJI UNIVERSITY, KOLHAPUR

FOR THE DEGREE OF

DOCTOR OF PHILOSOPHY

IN

MICROBIOLOGY

UNDER THE FACULTY
OF
SCIENCE AND TECHNOLOGY

BY

MISS. RUDDHI RAJENDRA JAGTAP
M.Sc., SET, NET-ICAR

UNDER THE GUIDANCE OF

Dr. GAJANAN VISHNU MALI
M. Sc., Ph. D
Rayat Institute of Research and Development, Satara

AND

CO-GUIDANCE OF

Prof. (Dr.) KAILAS DASHRATH SONAWANE
M. Sc., Ph. D
Head,
Department of Biochemistry,
Shivaji University, Kolhapur.

2023

1. Recommendations:

Plant growth promoting rhizobacteria (PGPR) are naturally occurring soil bacteria that aggressively colonise plant roots and benefit plants by promoting growth. Several PGPR inoculants that are currently on the market appear to stimulate growth through at least one mechanism, including the prevention of plant disease (Bioprotectants), enhanced nutrient uptake (Biofertilizers), siderophore production (Biostimulants), and phytohormone production (Biofertilizers). The use of PGPR offers a desirable alternative to chemical fertilizers, pesticides, and dietary supplements, and the majority of these isolates significantly increase overall plant growth. The use of PGPRs for medicinal plant cultivation is a promising approach. These medicinal plants and their secondary metabolites have been used as one of the key sources for medicines and other health-related issues.

2. Conclusions:

The present work has resulted in the isolation of potent PGPR strains from the rhizosphere of medicinal plants such as *Curcuma longa* L. and *Asparagus racemosus* Willd. These PGPR identified as strains of *Serratia nematodiphila* RGK, *Pseudomonas plecoglossicida* RGK, *Exiguobacterium acetylicum* RGK and *Enterobacter mori* RGK1. The strain showed broad-spectrum antimicrobial activity against both Gram-positive and Gram-negative human pathogens. Biochemical characterization of these strains shows that they are capable to utilize various sugars. *Serratia nematodiphila* RGK and *Pseudomonas plecoglossicida* RGK can tolerate 7% NaCl along with exopolysaccharide production. Further these PGPR used for pot cultures studies, individually and in combination and found that PGPR treatment improved the growth and yield of Asparagus and Turmeric plants. Further, these plants were taken in order to extract secondary metabolites. Following extraction, metabolites were purified using acid hydrolysis and silica gel column chromatography. After that, HPLC, GC-MS/MS, and LC-MS/MS analysis were performed on the purified metabolites. One new phytocompound with increased level was found in the turmeric plant treated by the co-culture of both the isolated PGPR. In addition to this, studies on the antimicrobial, antifungal, antioxidant, and anti-biofilm properties of purified metabolites gave good results. Individual and combined effect of phytocompounds against Gram-positive and Gram-negative pathogens were also gave good results. The present study also includes *in silico* study of biofilm-forming protein SrtA from *S. aureus* and *S. mutans.* Thus, the present study will serve as a foundation for the development of similar therapeutic approaches (PGPR-induced phytocompounds) for controlling biofilm production by the Gram-positive pathogens such as *S. aureus* and *S. mutans*

3. Summary:

The present thesis was aimed to isolate bacterial strains of potent PGPR from the rhizosphere of *Curcuma longa* L. and *Asparagus racemosus* Willd. The *in-vitro* studies showed that these PGPR have ability to enhance plant growth and secondary metabolites of Asparagus and Turmeric plants. The present study includes extraction, purification, quantification and identification of plant secondary metabolites which was influenced by PGPR. The various analytical techniques were used to study these secondary metabolites. Purification of these metabolites were carried out by silica gel column chromatography and acid hydrolysis. Furthermore, phytocompounds were identified by using GC-MS/MS, and LC-MS/MS as well, the results showed an increase in the concentration of chief phytocompounds such as curcumin and diosgenin. These purified metabolites were tested for antimicrobial activity using a variety of microbiological assays, including Agar well diffusion and MIC, as well as antifungal and anti-biofilm inhibition activity. The mechanism of inhibition of Sortase A enzyme, which is essential for biofilm formation, was elucidated using molecular modelling techniques. The combinational effect of phytocompounds (curcumin + 4-hydroxy-2 methylacetophenone) inhibits the enzyme by forming a ternary complex which shows better results over control inhibitors and this combination also gives similar results in wet-lab experiments.

4.Future Findings:

- In this study, pot culture experiments were conducted, but it will be interesting to see if the potent PGPR, such as *Serratia nematodiphila* RGK, *Pseudomonas plecoglossicida* RGK, *Exiguobacterium acetylicum* RGK, and *Enterobacter mori* RGK1, will have the same effects in field trials.
- It will be fascinating to see these potent strains of isolated PGPRs used on a large scale by the production of biofertilizer in future research.
- According to the current study, isolated PGPR influenced plant secondary metabolites, and these enhanced metabolites were used for a variety of purposes. It will be interesting to see if these metabolites can be used for various purposes, such as anti-cancer and anti-insecticidal, as in the previous study, a variety of uses for plant secondary metabolites were reported.
- The antimicrobial activity and selectivity of secondary metabolites can be improved by combining them with nanoparticles.
- Hence, the present work opens a new avenue and creates scope for evaluation of other applications of PGPR-induced plant secondary metabolites from Turmeric and Asparagus in pharmaceutical applications, agricultural and food industries.

1. University Name : Shivaji University.
2. Department of : Microbiology.
3. Name of Researcher : Ms. Ruddhi Rajendra Jagtap.
4. Name of Research Guide : Dr. Gajanan Vishnu Mali.
5. Name of Research Co-guide : Prof. (Dr.) Kailas Dashrath Sonawane.
6. Type of Degree : Doctor of Philosophy in Microbiology.
7. Registration Date : 01/07/2018
8. Completion Date :21/11/2023
9. Thesis Title : “Studies on Secondary Metabolites of *C. longa* and *A. racemosus* influenced by Plant Growth Promoting Rhizobacteria”
10. Size of Thesis : Total Number Pages 1-228 (6.92 MB)

STUDIES ON SECONDARY METABOLITES OF *C. LONGA* AND *A. RACEMOSUS* INFLUENCED BY PLANT GROWTH PROMOTING RHIZOBACTERIA

A THESIS SUBMITTED TO

SHIVAJI UNIVERSITY, KOLHAPUR

FOR THE DEGREE OF

DOCTOR OF PHILOSOPHY

IN

MICROBIOLOGY

UNDER THE FACULTY
OF
SCIENCE AND TECHNOLOGY

BY

MISS. RUDDHI RAJENDRA JAGTAP
M.Sc., SET, NET-ICAR

UNDER THE GUIDANCE OF

Dr. GAJANAN VISHNU MALI
M. Sc., Ph. D
Rayat Institute of Research and Development, Satara

AND

CO-GUIDANCE OF

Prof. (Dr.) KAILAS DASHRATH SONAWANE
M. Sc., Ph. D
Head,
Department of Biochemistry,
Shivaji University, Kolhapur.

2023

DECLARATION AND UNDERTAKING

I hereby declare that the thesis entitled "**Studies on Secondary Metabolites of *C. longa* and *A. racemosus* influenced by Plant Growth Promoting Rhizobacteria**" completed and written by me has not previously formed the basis for the award of any degree or similar title of this or any other university or examining body. Further, I declare that I have not violated any of the provisions under the acts of Copyright/Piracy/Cyber/IPR etc. amended from time to time.

In view of university Grants Commission (Promotion of Academic Integrity and Prevention of plagiarism in Higher Educational Institutions) Regulations, 2018 dated 31st July 2018, I hereby submit an undertaking that this thesis is my original work and it is free of any plagiarism. Further, it is also to state that this thesis has been duly checked through a Plagiarism detection tool approved by Shivaji University.

Place: Kolhapur
Date:

Miss. Ruddhi Rajendra Jagtap
(Research Student)

CERTIFICATE

This is to certify that the thesis entitled "**Studies on Secondary Metabolites of *C. longa* and *A. racemosus* influenced by Plant Growth Promoting Rhizobacteria**" is being submitted herewith for the award of the Degree of Doctor of Philosophy in Microbiology under the Faculty of Science and Technology of Shivaji University, Kolhapur. The work reported in this thesis is based upon the results of original experimental work carried out by **Ms. Ruddhi Rajendra Jagtap** under our supervision and guidance and the papers published are included under UGC approved journal list. To the best of my knowledge and belief the work embodied in this thesis has not formed earlier the basis for the award of any degree or similar title of this or any other university or examining body.

In view of university Grants Commission (Promotion of Academic Integrity and Prevention of plagiarism in Higher Educational Institutions) Regulations, 2018 dated 31st July 2018, this is also to certify that the work done by the **Ms. Ruddhi Rajendra Jagtap** is plagiarism free.

Place: Kolhapur
Date:

Prof. (Dr.) K. D. Sonawane
(Research Co-guide)

Dr. G. V. Mali
(Research Guide)

Dr. B. T. Jadhav
Director
Rayat Institute of Research and Development, Satara

Dr. P. M. Gurao
Head I/C
Department of Microbiology,
Shivaji University, Kolhapur

Acknowledgements

First and foremost I would like to record my gratitude and heartfelt thanks to my guide Dr. G. V. Mali , Rayat Institute of Research and Development (Associate Professor, UG & PG Department of Microbiology, Bharati Vidyapeeth (Deemed to be University) Yashwantrao Mohite College, Pune, India) and co-guide Prof. (Dr) Kailas D. Sonawane, Head, Department of Biochemistry and Co-Ordinator of Post Graduate Diploma in Bioinformatics, Shivaji University, Kolhapur, India, for joining and giving me an opportunity to study on a topic related to plant growth promoting rhizobacteria. Their valuable guidance, help and support has been always helpful to complete my research work positively. I hope that their energy, attention to detail, and enthusiasm have been instilled in me.

My sincere thanks to Dr. P. M. Gurao, In-charge Head, Department of Microbiology, Shivaji University, Kolhapur for providing laboratory facilities and encouragement and for his kind support, guidance and invaluable advice. I am also thankful to Prof. & Head (Mrs.). J. P. Jadhav, Department of Biotechnology, Shivaji University Kolhapur, India for providing the laboratory facility, support and timely inspiration. I would also like to thank Dr. M. S. Nimbalkar, Department of Botany, Shivaji University Kolhapur, India for providing instrumental facilities and valuable guidance. My sincere thanks to all my respected teachers Dr. (Mrs.). P. B. Dandge, Dr. N. H. Nadaf and late Dr. S. R. Waghmare whose valuable guidance, suggestions, and support always inspired and helped me.

I am also thankful to the Director of the Rayat Institute of Research and Development in Satara, Maharashtra, India, for allowing me to work at their institute. Also grateful to Mr. Bapu Awatade, Superintendent, RIRD, for his assistance throughout the research process, as well as teachers and research colleagues from Yashavantrao Chavan Institute of Science, Satara.

I am also grateful to the Authorities of Chhatrapati Shahu Maharaj Research, Training and Human Development Institute (SARTHI) for providing financial support for this research in the form of Junior Research Fellowships (JRF) and Senior Research Fellowships (SRF). I was greatly helped by the financial assistance I received from SARTHI for my ongoing

research. The Ph.D. training, I received from SARTHI in its early stages was extremely motivating for me to complete my research work.

I would also like to thank all the non-teaching staff from the Department of Microbiology for their timely support and cooperation. I sincerely express my thanks to all research colleagues from my Department and University campus for providing continuous inspiration and support during this study. I would also like to thank all my friends who supported me and incented me to strive toward my goal. I think it has been a nice place to work due to the healthy environment and good discussions within us to carry out scientific activities. At last with heartfelt emotions, I would like to dedicate my thesis to my beloved Gurudev, my Parents, my Husband, and my family members.

Ms. Ruddhi Rajendra Jagtap

List of Figures and Tables

ABBREVIATIONS

PGPR	Plant growth promoting rhizobacteria
Ca-P	Calcium phosphate
Fe-P	Iron phosphate
Mn-P	Manganese phosphate
Al-P	Aluminium phosphate
Zn	Zinc
P	Phosphate
K	Potassium
HCN	Hydrogen Cyanide
IAA	Indole-3-acetic acid
ACC	1-aminocyclopropane-1-carboxylic acid
N	Nitrogen
NH3	Ammonia
EPS	Exopolysaccharides
ISR	Induced systemic resistance
PGPB	Plant growth promoting bacteria
CNS	Central nervous system
NA	Nutrient agar
MHA	Calcium-adjusted Muller Hinton agar
BHI	Brain heart infusion
PDA	Potato Dextrose Agar
$CaCl_2$	Calcium chloride
NaCl	Sodium chloride
AlCl3	Aluminium chloride
DPPH	2,2-Diphenyl-1-picrylhydrazyl
K_2HPO_4	Dipotassium phosphat
KH_2PO_4	Potassium dihydrogenphosphate
NH_4NO_3	Ammonium nitrate
$MgSO_4.7H_2O$	Magnesium sulfate
$MnSO_4$	Manganese sulfate
$FeSO_4.2H_2O$	Ferrous sulfate
CFU	Centrifugal unit
rRNA	ribosomal RNA
NCIM	National Center for Industrial Microorganisms
BLAST	Basic Local Alignment Search Tool
NCBI	National Center for Biotechnology Information

ZnO	Zinc oxide
TLC	Thin layer chromatography
RP-HPLC	Reverse phase High performance liquid chromatography
GC-MS/MS	Gas Chromatography Mass Spectrophotometry
LC-MS/MS	LCMS Liquid Chromatography Mass Spectrometry
MIC	Minimum inhibitory concentration
SEM	Scanning electron microscopy
SrtA	Sortase A
ADMET	Absorption Distribution Metabolism Excretion Toxicity
PDB	Protein Data Bank
Rg	Radius of gyration
RMSD	Root Mean Square Deviation
RMSF	Root Mean Square Fluctuation
MD	Molecular Dynamics
MM-GBSA	Molecular mechanics Generalized Born/surface area
CUR	Curcumin
DMC	Demethoxycurcumin
BDMC	Bisdemethoxycurcumin
µl	Microliter
µg	Microgram
ml	Mililiter
mm	Millimeter
gm	Gram
mg	Milligram
nm	Nanometer
mM	Millimolar
OD	Optical density
hrs	Hours

INDEX

INDEX

INDEX

INDEX

INDEX

INDEX

INDEX

INDEX

CHAPTER I

INTRODUCTION

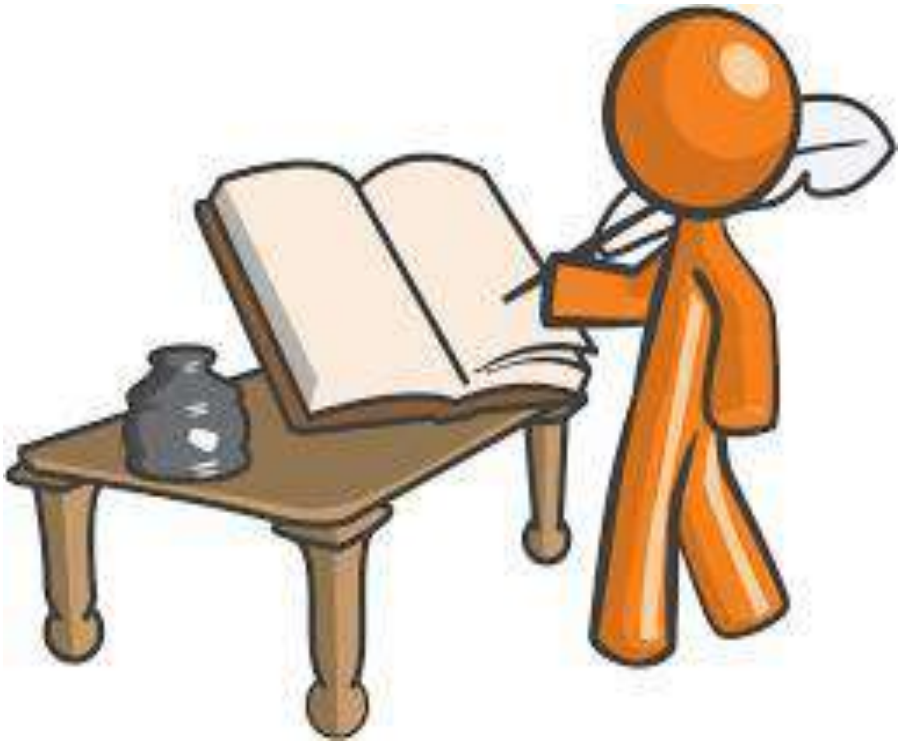

1. INTRODUCTION:

1.1 Plant growth promoting rhizobacteria (PGPR)

Plant growth-promoting rhizobacteria (PGPR) are a diverse group of rhizosphere-dwelling bacteria that colonies plant roots and stimulate plant growth through direct or indirect mechanisms (Kang et al., 2020). Direct mechanisms involve phosphorous solubilization, auxin, cytokinin, gibberellin production, nitrogen fixation, and iron sequestration. Indirect mechanisms include hydrogen cyanide, ISR, competition, antibiotic production, cell wall-degrading enzymes, and quorum quenching. They can also inhibit one or more plant pathogenic organisms (fungi and bacteria) (Glick B, 1995; Rizvi et al., 2022). ACC deaminase production and siderophores synthesis are also found in both these direct as well as indirect mechanisms (Ramamoorthy et al., 2001).

Common PGPR includes the strains in the genera, *Alcaligenes, Azospirillum, Bacillus, Acinetobacter, Burkholderia, Arthrobacter, Beijerinckia, Enterobacter, Azotobacter, Erwinia, Flavobacterium, Rhizobium* and *Serratia* (Andy et al., 2020). These rhizobacteria are then characterized as "extracellular plant growth rhizobacteria (ePGPR)" and "intracellular plant growth rhizobacteria (known as iPGPR)" based on their interaction with plants. The ePGPR predominantly present in the rhizosphere and between cells of the root cortex majorly from bacteria of genera such as *Agrobacterium, Azotobacter, Caulobacter, Chromobacterium,* etc. (Gray and Smith, 2005). iPGPR is found in specific nodular structures for root cells of some endophytes such as *Azorhizobium, Mesorhizobium, Bradyrhizobium, Allorhizobium*, and *Frankia* species (Verma et al., 2010; Wang and Romero, 2000).

1.2 PGPR interaction with Medicinal plants

The health and growth of plants are substantially influenced by bacteria associated with plants. PGPR has been employed for increasing biologically active phytocompounds from aromatic and medicinal plants. More research is being directed toward the use of PGPRs in the cultivation of medicinal and aromatic plants in order to increase plant yield (Karthikeyan et al., 2013; Tchakounte et al., 2018). Various rhizospheric microorganisms are linked to medicinal plants, thus it is important to isolate them, characterize them and research how to utilize them to produce a biofertilizer that's environmentally friendly or as a biocontrol agent (Vasudha et

al., 2013; Ipek et al., 2014). The application of biofertilizers on plant growth has demonstrated that they are superior to chemical fertilizers in terms of promoting plant growth, yield, and essential oil composition (Gharib et al., 2008).

According to Schmidt et al. (2014), *P. polymyxa* Mc5Re-14 and *B. subtilis* Co1-6 influence the phytocompounds and local microbiota of the chamomile plant, as well as enhance the major phytocompound, apigenin-7-O-glucoside (Schmidt et al., 2014). Similarly, Banchio et al. (2008) studied the effect of root-colonizing PGPRs on *Origanum majorana* plant and discovered that only *Bradyrhizobium* sp. and *P. fluorescens* significantly improved overall plant growth parameters when compared to control plants (Banchio et al., 2008). Previously, Toussaint et al. (2008) demonstrated that inoculating *Ocimum basilicum* with *G. mosses* increased the weights of the shoots and roots by up to 60% (Toussaint et al., 2008). According to Kumar et al. (2016), inoculation of *P. fluorescens* CL12 exhibited an increase in curcumin content by 18% as compared to control, which is a significant compound of the Turmeric plant (Kumar et al., 2016).

1.3 Turmeric

Medicinal plants contain a high concentration of bioactive compounds, which are thought to be safer for humans and the environment than synthetic medicines used to treat cancer and other disorders (Egamberdieva et al., 2015). Turmeric (*Curcuma longa* L.) has been used medicinally forcenturies in Ayurvedic medicine. Chemically complex turmeric products may also have different pharmacodynamic and pharmacokinetic profiles, which may support their ethnobotanical use (Meng et al., 2018). Turmeric, a perennial plant that belongs to Zingiberaceae family is famous for its colouring, flavouring, and digestive properties. Curcuminoids and essential oils are majorly found in Turmeric. Curcuminoids are group of Curcumin (~77%), Demethoxycurcumin (DMC) (~18%), and Bisdemethoxycurcumin (BDMC) (~5%) with different functional groups on the aromatic rings having various medicinal properties (Kita et al., 2008; Guerra et al., 2019; Rodrigues et al., 2015). Curcuminoids are yellow pigments having beneficial biological activities but curcumin is the primary component among the curcuminoids (Mostert et al., 2000). Curcumin has a high potential as a treatment for a variety of inflammatory illnesses and malignancies (Aggarwal et al., 2013).

The dried rhizome of Turmeric contains ~26% essential oil, ~58 % of which is turmerones.Turmeric essential oil contains α-phellandrene, sabinene, zingiberene, borneol, 1,8- cineole, sesquiterpene alcohols, bisabolene, and two monoterpenes, pinene, in addition to pcymene, β- sesquiphellandrene, and ar-turmerone (Raina et al., 2002). Turmeric oil shows insect-repellent activity against the stored grain insect *Tribolium castaneum* (Mostert et al., 2000). Essential oils of Turmeric were shown to have anti-angiogenic activities (Yue et al., 2015)

1.4 Asparagus

The usage of medicinal herbs is related to one of the most ancient, diversified, and rich cultural traditions in India. Medicinal plants are essential for the health of individuals and entire communities (Kishore et al., 2018). The medicinal plant *Asparagus racemosus* Willd from Asparagaceae family is native to tropical and subtropical India. Its medicinal usage is documented in the Indian and British Pharmacopoeias, as well as traditional medical systems like Ayurveda, Unani, and Siddha. *A. racemosus* Willd. is also known as Satavari, Satawar, and Satmuli (Bopanaand Saxena, 2007; Onlom et al., 2017). The roots of this plant have been used to cure schistosomiasis and tuberculosis. It also has a lot of chemical components such as steroidal saponins, flavonoids, oligosaccharides, and amino acid derivatives (Kasai and Sakamura, 1981; Taufique etal., 2014). The crown and root system of the plant accumulates carbohydrates, which act as food reserves, increasing the size and vigour of the buds and succeeding spears. The roots are used to cure gonorrhoea, tuberculosis, skin conditions, leprosy, dysentery, and diarrhoea (Mandal et al., 2000).

The primary active components of *A. racemosus* are the root steroidal saponins (Shatavarins I-IV) (Alok et al., 2013). Asparagus also contains essential oils, arginine, flavonoids (rutin, quercetin, kaempferol), asparagine, tyrosine tannin and resins. Saponins are anti-oxidants, anti-hepatotoxic, immunostimulants, helpful in diabetic retinopathy, anti-bacterial, anti-carcinogenic, anti-ulcerogenic, anti-diarrheal, and reproductive agents. Many types of saponins are antibacterial, preventing mould and shielding plants from insects (Negi et al., 2010; Patil et al., 2014).

1.5 *In-silico* study of Plant Secondary Metabolites (Phytocompounds)

Plant-based medicine, which has been practiced since antiquity, is the source of many commercially important drugs. Traditional methods of plant-based drug discovery can take a longtime and money. Bioinformatics allows for the analysis and interpretation of huge volumes of datagenerated by molecular biology-based techniques (Sharma and Sarkar, 2013). Such approaches are now required when it comes to analyzing and integrating large amounts of data due to high-throughput techniques. To improve our understanding of plant cellular processes, genomic, proteomic, and metabolomic data must be thoroughly examined. The use of bioinformatics techniques is critical in identifying genes and pathways associated with biologically active secondary metabolites from medicinal plants (Saito and Matsuda, 2010; Sharma and Sarkar, 2013).

The medicinal plants contain a significant amount of antioxidants, which include polyphenols, which aid in the adsorption and neutralization of harmful free radicals (Saleem et al., 2020). These biological processes can be studied with computational techniques. The biological activity of the molecule was verified by docking studies, which determined the binding free energies and elucidated the interactions with the active site (Saleem et al., 2020). Molecular docking and molecular dynamics simulation studies are useful tools for predicting binding activity and interactions with enzymes (Dhanavade et al., 2013; Bansode et al., 2019; Dhanavade and Sonawane 2014; Gao et al., 2016; Thappeta et al., 2020). This information is crucial when developing new lead molecule (Sivaramakrishnan et al.,2019).

1.6 Aspects of the study

Turmeric and Asparagus plants were chosen as the experimental material in this study because turmeric has been used in Indian households for centuries as a spice and traditional medicine. Curcuminoids and sesquiterpenoids, which are active components of turmeric, are useful in pharmaceuticals. Asparagus was traditionally used in India to stimulate fertility, alleviatemenstrual pains, and enhance milk production in nursing mothers. Shatavarin and diosgenin are important components of Asparagus. Both plants contain major phytocompounds that are widely used as antioxidants, antipyretics, anti-inflammatory agents, and anticancer agents. Both plant rhizomes interact with the large microbial population present in the rhizosphere. These bacterial strains have the potential to influence the immune system of

the plant.

The aim of this study was to find a potent PGPR strain by screening the rhizospheric soil of the Turmeric and Asparagus plants. The effects of these PGPR strains on medicinal plants were investigated, and secondary metabolites produced by those plants were purified using various methods, including silica gel column chromatography and high-performance liquid chromatography. These secondary metabolites were characterized and identified using TLC, GC-MS/MS, and LC-MS/MS. All of the metabolites exhibited antibacterial activity against pathogens such as *Staphylococcus aureus*, *Escherichia coli*, *Proteus vulgaris*, and *Streptococcus mutans*. Furthermore, biofilm inhibition studies showed that isolated secondary metabolites prevent the formation of biofilms. Computational analysis of secondary metabolites induced biofilm inhibition could help researchers to better understand the underlying mechanism.

Thus, the potent strains of PGPR are reported in this thesis to enhance the growth, yield, and phytocompounds of Turmeric and Asparagus plants. Further, enhanced phytocompounds demonstrated various biological applications and the computational approach used in this study elucidated the mechanism of inhibition of the SortaseA enzyme which is a key adhesion protein involved in biofilm formation. Therefore, this study would pave the way for the development of PGPR-induced phytocompounds therapeutic approaches by targeting SrtA to control biofilm-related infectious diseases.

CHAPTER II

REVIEW OF LITERATURE

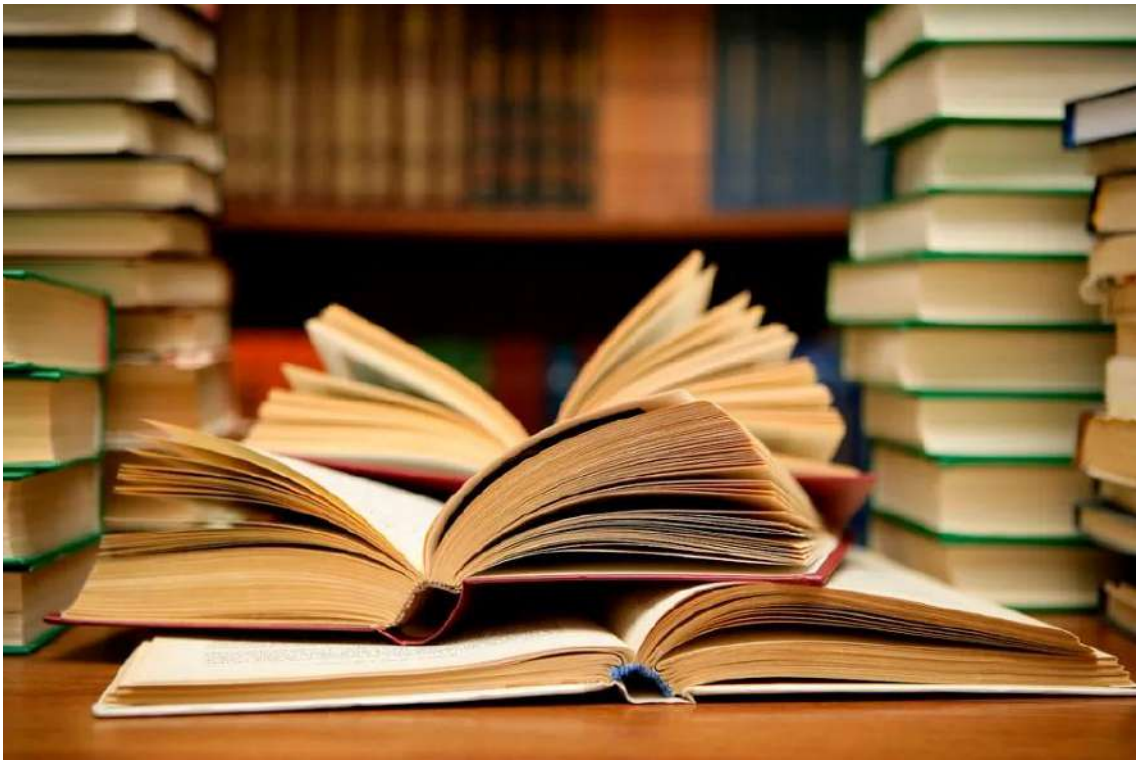

2. Review of literature:

2.1 Plant growth promoting rhizobacteria (PGPR)

Rhizospheric bacteria known as "plant growth-promoting rhizobacteria" (PGPR) canbenefit plant growth through various processes or mechanisms. PGPR can employ both direct and indirect channels (Fig. 2.1). The list of direct ways includes production of IAA, gibberellin, cytokinin, phosphate solubilization, biological nitrogen fixation, including siderophore production whereas hydrogen cyanide, ACC deaminase, induced systemic resistance, antibiotics, competition, cell wall-degrading enzymes and synthesis of siderophores are the examples of indirect ways (Olanrewaju et al., 2017; Maheshwari and Dheeman, 2014).

The application of PGPR in agriculture is becoming more and more likely as it provides adesirable substitute for the use of chemical fertilizers, pesticides, and other additives (Perez- Montano et al., 2014). These PGPR are expected to produce significant amounts of growth- promoting compounds, which could affect the general morphology of the plants both directly and indirectly. Recent research on the many varieties of PGPR in the rhizosphere, as well as their colonization potential and mode of action, should make it easier to use them as a reliable management tool for sustainable agriculture practices (Shah et al., 2021; Kumar et al., 2014a). Previous research thus demonstrated the progress made in the use of rhizosphere bacteria in many applications for agricultural improvement, as well as their mode of action, with a focus on characteristics that encourage plant development. There are several methods in which PGPR might encourage the growth of their plant symbionts and provide cross-protection against different stresses (Bhattacharyya & Jha, 2012).

The use of PGPR can help to increase eco-friendly practices for sustainable agriculture because it promotes plant growth under both biotic and abiotic stresses (Passari et al., 2018). Many Gram-negative and Gram-positive bacterial genera have been reported to induce plant growth, including coryneform bacteria, *Azospirillum*, *Azotobacter*, *Arthrobacter*, *B. subtilis*,*Burkholderia*, *Enterobacter*, *Klebsiella*, *Micrococcus*, *P. gladioli*, *P. cepacia*, and *Xanthomonas*(El-Sayed et al., 2014; Bal et al., 2013). PGPR have also been widely documented in the previous era from various medicinal plants such as *Ocimum* spp. (*Glomus fasciculatum*, *Azotobacter chroococcum*), *Withania somnifera* (*Azospirillum*, *Azotobacter chroococcum*, *Pseudomonas fluorescens*, *Bacillus megaterium*)

(Egamberdieva & Teixeira da Silva, 2015), *Mentha piperita* (*Bacillus amyloliquefaciens, Pseudomonas fluorescence*) (Cappellari et al., 2015), *Trachyspermum ammi* (*Azotobacter chroococcum*) (Hashemi et al., 2022). However, PGPR from Turmeric and Asparagus rhizospheres is still being studied. Thus, the purpose of this work was to isolate and describe rhizobacterial strains living in naturally occurring plant species.

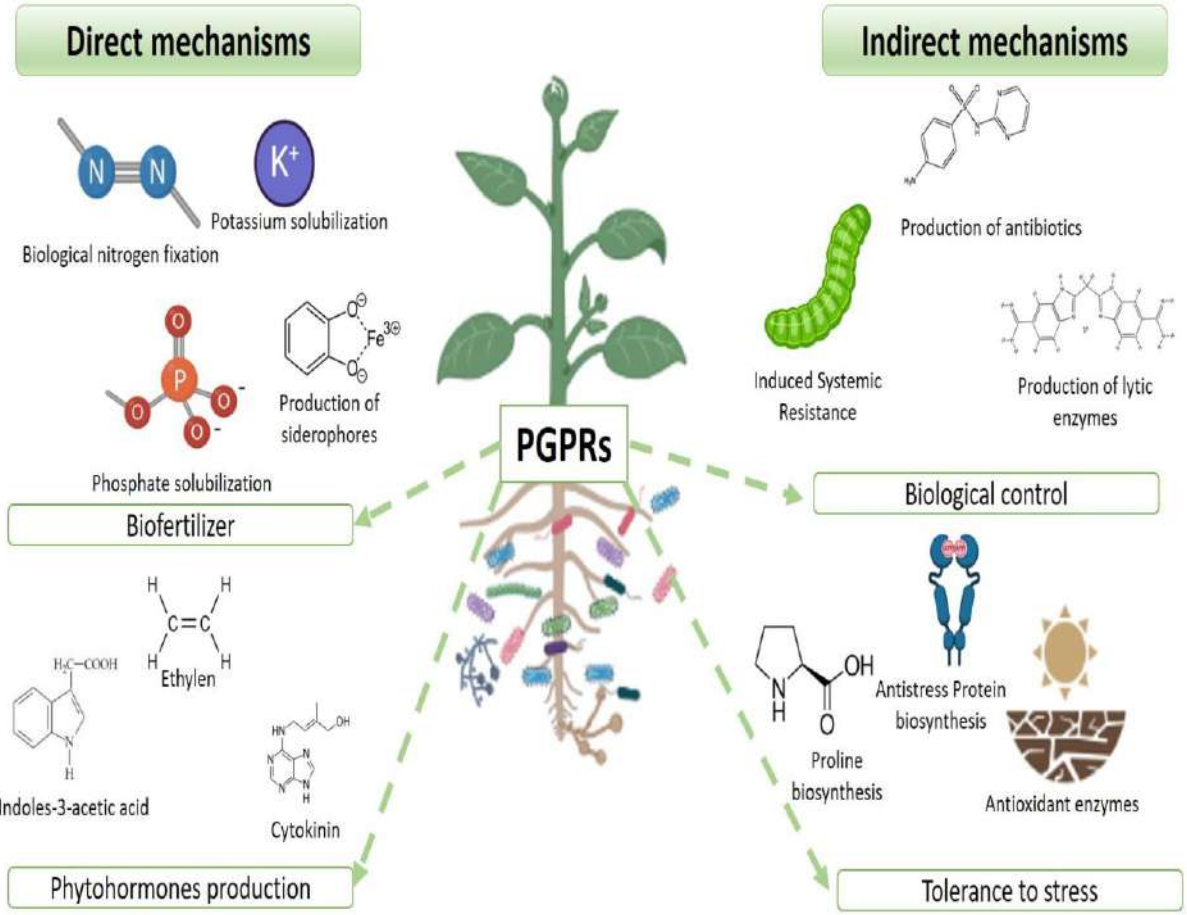

Fig. 2.1: Direct and indirect mechanisms of PGPRs (Jacquelin et al., 2022)

2.2 Mechanism of PGPR action:

2.2.1 Phosphate solubilization

Next to nitrogen, phosphorus is the most crucial essential component in plant nutrition. Almost all main metabolic processes, such as photosynthesis, respiration, signal transduction, energy transfer, and macromolecular biosynthesis, depend on it in some way (Anand et al., 2016).Despite being plentiful, phosphorus reserve does not exist in plant-friendly forms. Only the soluble forms of mono and dibasic phosphate can be absorbed by plants (Bhattacharyya & Jha, 2012). *Bacillus*, *Achromobacter*, *Rhizobium*, *Pseudomonas*,

Agrobacterium, *Burkholderia*, *Flavobacterium*, *Chryseobacterium*, *Aerobacter*, *Micrococcus*, and *Erwinia* are just a few of the numerous bacteria from various genera that may solubilize phosphate (Khan et al., 2014). There are two ways that bacteria solubilize phosphate: The release of phosphatases, which liberate phosphate groups attached to organic matter, and the release of organic acids that, through ionic interactions with the cations of the phosphate salt, liberate phosphorus. Most of these bacteria are capable of dissolving the mineral phosphate complexes. In general, these systems work better in simple soils (Rodriguez and Fraga, 1999; Hayat et al., 2010).

In contrast to non-rhizosphere soil, the rhizosphere frequently contains a significantly higher concentration of phosphate-solubilizing bacteria (Rodriguez & Fraga, 1999). These bacterial inoculations can sometimes enhance plant development and other times be utterly ineffective. Without a doubt, understanding their mechanics and rhizosphere ecology will reform their application in sustainable agriculture (Prasad et al., 2019).

2.2.2 Zinc solubilization

For healthy development and reproduction, plant tissues must have relatively small amounts of zinc (Zn), one of the essential micronutrients (Shaikh & Saraf, 2017). There are several soil-specific characteristics that are associated to the availability of P and Fe at pH (7.0) where Zn solubility decreases as the pH rises, including a large quantity of organic matter and bicarbonate concentration, high availability of P and Fe and high magnesium to calcium ratio (Kamran et al., 2017). In order to make zinc available, a bacterial strain that can solubilize it must be inoculated into the crop because it is a restricting factor in crop productivity (Saravanan et al., 2004). According to earlier studies, PGPR inoculation improves plant nutrition, promotes vigor in plant growth, and gives a higher amount of yield (Shakeel et al., 2015).

2.2.3 Potassium solubilization

The third most vital nutrient for plants, potassium (K) is necessary for enzyme function, protein synthesis, and photosynthesis. Since more than 90% of potassium is found in insoluble rock and silicate minerals, the amount of soluble potassium present in soil is often rather low (Parmar and Sindhu, 2013). Potassium deficiency is now a major hindrance to agricultural productivity. Without enough potassium, plants have weak roots,

limited growth, lower yields, and fewer seeds. A different indigenous source of potassium needs to be discovered in order to maintain soil plant uptake and agricultural production (Kumar and Dubey, 2012).

The capability of the PGPR to generate and secrete organic acids to dissolve potassium rock has been thoroughly investigated (Etesami et al., 2017). It has been proven that PGPR, including *B. edaphicus*, *B. mucilaginosus*, *Ferrooxidans* sp., *Burkholderia* sp., *Pseudomonas* sp., *Paenibacillus* sp., and *Acidothiobacillus* sp. release potassium from potassium-containing minerals in soils. Applying potassium-solubilizing PGPR as a biofertilizer can enhance sustainable crop output while reducing the need for agrochemicals (Meena et al., 2014; Prasad et al., 2019).

2.2.4 Siderophore production

A siderophore is defined as a low molecular weight organic compound produced by bacteria under low iron conditions. (Schwyn and Neilands, 1987). The fungus and bacteria need Fe for heme creation, ATP synthesis, and other critical processes. Siderophores can be classified according to their moieties such as catecholate, hydroxamate, carboxylate and diazeniumdiolate (Hermenau etal., 2018). The PGPR produces a variety of siderophores, including *P. fluorescens*, which produces pyoverdine (Behnsen and Raffatellu, 2016). Rhizobactin, a structurally unique form of siderophore produced by *Pseudomonas* to obtain iron from dissolved organic matter in peatlands (Kugler et al., 2020). Bacillibactin is the mainly well-known triscatetholate siderophore produced by *Bacillus* spp (Nithyapriya et al., 2021). In the rhizosphere, siderophore-synthesizing PGPR suppresses phyto-pathogens via iron deficiency or competitive exclusion in iron-deficient conditions (Arora and Verma, 2017). Additionally, fluorescent *Pseudomonads* have been reported to inhibit soil-borne fungi through the release of siderophores that chelate iron (Beneduzi et al., 2012).

2.2.5 HCN production

PGPR produces the deadly chemical cyanide, which has lethal effects. While cyanide functions as a common metabolic inhibitor, numerous species involving bacteria, fungus, algae, insects, and plants produce, secrete, and utilize it as a defense against competition or predation (Kumar et al., 2015; Lastra et al., 2021). Hydrogen cyanide (HCN), an effective volatile secondary metabolite frequently synthesized by rhizospheric bacteria, is known to adversely influence on growth and metabolism of root and represents

a possible and ecologically friendly strategy for the biological control of weeds (Schippers et al., 1990). The HCN synthetase enzyme, which is connected to the rhizobacterial plasma membrane, converts glycine into HCN (Shameer and Prasad, 2018).

Numerous studies have demonstrated the potential for HCN production by many genera of *Aeromonas, Pseudomonas, Alcaligenes, Rhizobium,* and *Bacillus* (Olanrewaju et al., 2017). The nematodes *Meloidogyne javanica* and *Thielaviopsis basicota*, respectively, induce root-knot and black rot in tomato and tobacco roots, which have been suppressed by HCN, according to several investigations (Siddiqui et al., 2006). According to research, roughly 50% of *pseudomonads* isolated from the potato and wheat rhizosphereare capable of producing HCN *in vitro*, whereas HCN production is a general characteristic shared by the group of *Pseudomonas* from the rhizosphere (Syed Shameer, 2018). It has been discovered that *Pseudomonas* (88.89%) and *Bacillus* (50%) both produce HCN as a biocontrol metabolite in a root nodules of plant and the rhizospheric soil (Ahmad et al., 2008).

2.2.6 Phytohormone production

Plant hormones, like auxins, abscisic acid, gibberellin, cytokinin, and ethylene, are tiny, structurally unrelated molecules found in nature that control the development and growth of plants (Chen et al., 2017; Hayat et al., 2010). IAA (indole-3-acetic acid) is the primary auxin produced by plants. It is essential for several plant activities, including seed and tuber germination, regulation of vegetative growth processes, accelerated development of xylem and root, and initiation of lateral and adventitious root formation. IAA also facilitates responses to light, gravity, and florescence (Ali et al., 2017; Kumar et al., 2019). Plants and microorganisms synthesize IAA via several interconnected pathways, the most well-studied of which is the tryptophan-dependent system (Chandra et al., 2018).

Plant roots exude the amino acid tryptophan, which is subsequently broken down by PGPR in the rhizoplane and transformed into IAA which is then absorbed by plant roots (Mohite,2013; Shameer and prasad, 2018). A various bacterial species from the genera *Alcaligenes, Azospirillum Acinetobacter, Arthrobacter, Bacillus, Bradyrhizobium, Burkholderia, Enterobacter, Flavobacterium, Erwinia, Rhizobium, Serratia* and *Pseudomonas* have been discovered to be rhizosphere-associated and capable of synthesizing IAA that promote growth of plant (Egamberdieva et al., 2015; Shah et al.,

2021).

2.2.7 Cytokinin production

Cytokinin's are another class of phytohormone that influences development and growth of the plant by controlling physiological processes like division of cell, seed germination, apical dominance, flower and fruit production, development of root and shoot, aging of leaves, plant-pathogen interactions, nutrient mobilization and absorption (Akhtar et al., 2020; Shah et al., 2021). Cytokinins produced by rhizospheric bacteria which are living near the roots can also impact on growth and development of plant (Salamone et al., 2001). In addition, seed inoculationwith cytokinin-producing bacteria usually results in increased cytokinin levels in plants, which affects plant growth and development (Gamalero and Glick, 2011).

In contrast, it has been observed that PGPR, such as *Azospirillum, Rhizobium, Azotobacter, Pseudomonas* and *Bacillus* spp., may produce cytokinin in pure culture (Salamone et al., 2001). Cytokinin mediates responses to biotic and abiotic stresses, as well as a variety of extrinsic variables like light conditions in the shoot, also nutrition and water availability in the root. These activities collaborate to fine-tune quantitative growth regulation in plants (Wernerand Schmulling, 2009; Gupta and Rashotte, 2012).

2.2.8 Gibberilic acid production

Gibberellins, a large class of phytohormone with specific roles throughout the life cycle of higher plants. These are tetracyclic diterpenoid carboxylic acids with carbon skeletons of C20 or C19 (Alori and Babalola, 2018). Gibberellins play a role in a variety of physiological and developmental processes, such as seed germination, stem and leaf growth, flower or fruit growth, seedling emergence, floral induction, control of vegetative and reproductive (bud) dormancy, and postponement of senescence (Bottini et al., 2004; Kang et al., 2015). Gibberellins, when combined with other phytohormones, are directly beneficial in promoting shoot elongation in plants (Crozier et al., 2000). When bacteria are grown on artificial culture medium, very few of them synthesize Gibberlic acid (Kaminek et al.,1997). PGPR such as *Bacillus, Pseudomonas, Azotobacter, Acetobacter, Azospirillum,* and *Burkholderia,* are able to produce gibberellins (Lotfi et al., 2022).

2.2.9 Nitrogen fixation and ammonia production

Nitrogen serves as a crucial nutrient for plant development and yield. Nitrogen

fixation is the process by which nitrogen-fixing microorganisms use an enzyme nitrogenase to convert molecular or atmospheric nitrogen into a form that plants can use (Alori and Babalola, 2018). Agricultural practices have utilized both symbiotic and asymbiotic/associative bacteria to support plant growth (Ahmad et al., 2013). Rhizobacteria that facilitate plant growth have been isolated as free-living soil bacteria from plant rhizosphere, and when associated with plant roots and other plant parts, can decrease the requirement for chemical fertilizer and increase plant growth and yield (Roychowdury et al., 2015). Therefore, several nitrogen-fixing bacteria, such as *Azospirillum, Klebsiella, Burkholderia, Bacillus*, and *Pseudomonas* have been discovered as PGPR for maize plants (Kuan et al., 2016; Singh et al., 2020).

Production of gaseous products like ammonia is one of the methods used by rhizobacteria to encourage plant development (Laslo et al., 2012). The capability of PGPR to produce ammonia, which indirectly promotes plant development, is another crucial characteristic (Sayyed R, 2019). In general, it has been shown that PGPR produces ammonia that supplies nitrogen to the host plants, promoting the overall growth of the plant (Bhattacharyya et al., 2020). Earlier reports showed that, *Bacillus* strains produce ammonia when grown in nitrogen sources, which aids host plant growth and biomass production (Singh et al., 2020). Similarly, Malleswari and Bagyanarayana, (2013) found that inoculating sorghum, maize, and green gram with ammonia-producing *Pantoea* sp., *Bacillus* sp., and *Pseudomonas* sp. improved growth promotion (Malleswari and Bagyanarayana, 2013).

2.2.10 Salt tolerance

In agriculture, salt stress is a major problem that inhibits plant growth. Stress factors that are both biotic and abiotic have a significant influence on plants and seriously harm crop production globally (Varma et al., 2017). Salinity is a harsh environment with limited organic matter and very low nitrogen levels in the soil (Malik K, 1997). Salinity has other issues that have an impact on the environment's biodiversity in addition to having an impact on agriculture (Mohammed A, 2018). Beneficial bacteria have a great chance of improving crop production and environmentally friendly resource management by promoting plant growth and stress tolerance (Mohammed A, 2018). The use of drought-tolerant PGPR is thought to be a successful substitute method for sustainable agriculture under water deficit

conditions (Mayak et al., 2004). Inoculation of plants with PGPR promotes seedling emergence and increases growth rate, it also confers tolerance to several stresses and plant pathogens (Khan and Bano, 2019).

2.2.11 Exopolysaccharides production

Exopolysaccharides (EPS) are a very important component of the extracellular matrix, and frequently account for 40-95% of bacterial weight. Bacteria can produce two types of exopolysaccharides: Slime exopolysaccharide and capsular exopolysaccharide (Naseem and Bano, 2014). Exopolysaccharides play important roles in surface attachment, microbial aggregation, biofilm formation, plant-microbe interaction, protection, and bioremediation (Manca et al., 1985). Similarly, an important feature of EPS is its biodegradability, it can be released in extreme environmental conditions such as temperature and pH Microbial EPS improve soil aggregation, which benefits plants by retaining moisture and trapping nutrients (Vasagade et al., 2021). Some exopolysaccharide-producing bacteria, such as *Pseudomonas*, can survive under drought conditions and protect themselves from desiccation by rising water holding (Sandhya et al., 2009a). Similar to this, plants have shown resistance to water stress when treated with exopolysaccharide-producing bacteria, like *Azospirillum* (Bensalim et al., 1998).

2.2.12 Induction of Systemic Disease Resistance by PGPR

Induced systemic resistance, or ISR, is the rise in defense mechanisms brought on by an inducer agent in response to a pathogen infection. It is the condition in which plants develop an enhanced defensive ability when appropriately stimulated (Beneduzi et al., 2012). Several nonpathogenic PGPR strains can make plants resistant to a wide range of phytopathogens by inducing systemic disease resistance (Egamberdieva et al., 2015). For instance, the application of PGPR as a sett-treatment in sugarcane resulted in the development of systemic resistance to *C. falcatum* (Ramamoorthy et al., 2001). Similarly, Alstroem (1991) noticed that PGPR-induced systemic resistance to bacterial diseases. He reported that *Pseudomonas fluorescens* treated bean seeds shielded the plant from the disease called as halo blight caused by *Pseudomonas syringae pv. phaseolicola* (Bhattacharyya and Jha, 2012). Similar to this, Kloepper et al. (1993) discovered that when cucumber seeds were treated with rhizobacterial strains such as *Pseudomonas putida* and *Serratia marcescens*, the occurrence of bacterial wilt was significantly decreased (Kloepper et al., 1993).

2.3 PGPR in relation to medicinal plants:

Medicinal plants contain a high concentration of bioactive compounds which are thought to be safer for humans and the environment than synthetic medicines that have been used to treat cancer and other various diseases since ancient times (Zhao et al., 2022; Egamberdieva et al., 2015). However, natural products, especially medicinal plants, continue to be a substantial source of new drugs, drug leads, and chemical entities because they are more socially acceptable, have a high level of compatibility, and can adapt to the human body than synthetic chemicals (Garg et al., 2021; Zhao et al., 2022). Similarly, medicinal plants are associated with various rhizospheric microbes, which improve plant growth parameters and secondary metabolite content of the plant (Vasudha et al., 2013).

PGPRs have the ability to increase the synthesis of biologically active phytocompounds in aromatic and medicinal plants. More research is being directed toward the use of PGPRs in the cultivation of these plants in order to increase plant productivity (Karthikeyan et al., 2013). Hence, plant-associated bacteria perform a crucial role for the health and growth of plants. However, we know very little about how bacterial treatments affect the physiology and microbiome of host plant (Schmidt et al., 2014). At the moment, the various studies on plant-associated microbes demonstrate the entire influence of ongoing research as well as the tremendous interest in this area (Berendsen et al., 2012; Bakker et al., 2013). Similarly, the growing concerns of medicinal and aromatic plants on a wide scale can be overcome by discovering and choosing suitable useful bacteria to be employed as biofertilizers that promote plant growth without damaging the environment (Ipek et al., 2014).

Banchio et al. (2008) examined the considerable enhancement in leaf number, shoot weight, nodal number, shoot length, root dry weight and biomass of *Origanum majorana* after treatment with *Bradyrhizobium* sp. and *P. fluorescens* (Banchio et al., 2008). Similarly, Gharib et al. (2008) discovered that biofertilizers increase overall growth and essential oil content in *Majorana hortensis* L. when compared to control plants which may be treated with chemical fertilizers (Gharib et al., 2008). When PGPRs such as *Bacillus, Azotobacter*, and *Pseudomonas* were inoculated to *Catharanthus roseus*, either alone or in combination, they dramatically boosted root length, nutrient concentration, secondary metabolite concentration, and plant height, when compared to non-inoculated control plants (Karthikeyan et al., 2009). Similar to this, according to Mishra et al. (2010), the synthesis

of ammonia by rhizobacterial strains (*B. subtilis* and *P. fluorescens*) isolated from the aromatic herb *P. graveolens* L. shown a considerable increase in plant growth and biomass (Mishra et al., 2010).

Ruth Schmidt et al. (2014) studied the impact of bacterial inoculants on the native microbiome and secondary metabolites of the chamomile plant. They found that *B. subtilis* Co1-6 and *P. polymyxa* Mc5Re-14 enhance the bioactive phytocompound apigenin-7-O-glucoside (Schmidt et al., 2014). According to Santoro et al. (2011), using PGPRs like *B. subtilis*, *P. fluorescens*, and *A. brasilense* increased essential oil content in *Mentha piperita* by doubling monoterpene synthesis (Santoro et al., 2011). Similar to this, Ghorbanpour et al. (2013) found that treatment of *Pseudomonas* spp. to Black henbane (*Hyoscyamus niger*) in water-stressed environments increased the production of tropane alkaloids like scopolamine and daturine (Ghorbanpour et al., 2013). Additionally, following PGPB inoculation, medicinal plants showed an increase in the content of several alkaloid and terpenoid compounds with pharmaceutical importance (Cakmakc et al., 2020). However, Bharti et al. (2013) stated that the yield was increased by 138% and the amount of bacoside A was increased by 376% when *B. monnieri* (Brahmi) was inoculated with *B. pumilus* and *E. oxidotolerans* under saline conditions (Bharti et al., 2013). Similarly, Darzi et al. (2012) found that PGPB inoculations in *Coriandrum sativum* increased the amount of geranyl acetate, limonene, and beta pinene (Darzi et al., 2012).

The important secondary metabolites in medicinal plants may be enhanced by PGPR treatment, a few examples are given here. In case of *Curcuma longa* which was inoculated with *Bacillus* spp. and *P. fluorescens*, showed increased plant growth, fresh rhizome biomass, morphological yield, and the plant's main bioactive component curcumin (Cakmakc et al., 2020). Kumar et al. (2016) discovered a similar result such as increase in biological properties, yield attributes, and curcumin content in turmeric plant bacterized with *P. fluorescens* (Kumar et al., 2016). Similar to this, *Panax ginseng* inoculation with PGPR demonstrated significantly improved growth, root activity, and the content of total ginsenoside (Ji et al., 2019). In addition to this various studies have shown increased levels of flavonoids in *Withania somnifera* under metal stress (Khanna et al., 2019). In medicinal plant like Aloe vera, it has been observed that PGPR (*Azospirillum, Azotobacter, Bacillus,* and *Pseudomonas*) either alone or in combination, increase the aloin content (Rizvi et al., 2022). Similarly, applying microbial consortia to the roots of medicinal plants has been

demonstrated to enhance phytocompounds and can be understood as a plant defense reaction to microbial colonization (Egamberdieva and Teixeira da Silva, 2015). In general, PGPR applications to *Withania somnifera* showed increased plant dry matter accumulation, N and P concentration in roots and shoots, withaferin-A concentration in roots, and total withanolide content in plants when compared to controls (Rizvi et al., 2022).

Bacterial mechanisms for stimulating plant growth, nutrient uptake, phytochemical constituents, and alleviating abiotic stresses include number of enzymes, nutrient mobilization, induction of systemic resistance, nitrogen fixation, and synthesis of plant hormones such as indole-3-acetic acid (IAA), cytokinin and gibberellic acid (Mishra et al., 2010; Egamberdieva and Lugtenberg, 2014; Hameed et al., 2014). However, our understanding regarding PGPR's potential to increase plant secondary metabolites is restricted. Additional research is needed to explore the potential methods by which bacteria enhance phytochemical contents in medicinally significant plants at the cell, tissue, or molecular level.

2.4 Plant secondary metabolites:

Secondary metabolites (phytocompounds) are organic compounds synthesized inside the cell and do not play role in direct growth and development of plant. They are synthesized due to the heritable mutations in basic primary metabolite pathways by natural selection. They are used against herbivory and pathogens like bacteria, viruses and fungi. They have crucial role in symbiotic nitrogen fixation, attract pollinators, and reduce plant-plant competition. They are nota part of the basic structure of the cell. There are mainly 3 classes of secondary metabolites (Bourgaud et al., 2001) which are given below:

1. Terpenes
2. Phenolic compounds
3. Nitrogen containing compounds

2.5 Scientific classification of *Curcuma longa* (Turmeric)

Kingdom : Plantae
Phylum : Tracheophyta
Division : Angiosperms
Class : Monocots
Order : Zingiberales
Family : Zingiberaceae
Genus: Curcuma
Species: *Curcuma longa*

Fig. 2.2: Turmeric plant

2.5.1 Curcuminoids

The most significant active component of Turmeric is curcuminoids. These are phenolic compounds which are frequently employed in a wide range of foods as a spice, pigment, additive, and therapeutic agent (Amalraj et al., 2016). In *Curcuma longa*, crude extract curcuminoid accounts for 1-6% of the total weight of the Turmeric (Cas and Ghidoni, 2019). The pharmacological activity of Turmeric has been attributed primarily to curcuminoids, which include curcumin (CUR) and two related compounds, demethoxycurcumin (DMC) and bisdemethoxycurcumin (BDMC) (Kadam et al., 2018). They are robust complex forming agents, with the keto-enol units acting as the molecule's reactive units. Curcuminoids with absorption wavelengths ranging from 420nm to 430nm, are extracted from Curcuma species (primarily *Curcuma longa* L.) (Tonnesen, 1992). As curcuminoids having complex chemical structures hence less soluble in water at acidic and neutral pH levels, but much more soluble in organic solvents such as methanol, ethanol, dimethyl sulfoxide, and acetone (Amalraj et al., 2016). Additionally, they possess a wide range of biological attributes, including anti-oxidative, anti-diabetic, anti-inflammatory, anti-cancer, anticholinesterase, anti-mutagenic, cytotoxic, neuroprotective, and anti-Alzheimers properties (Xu et al., 2020; Kalaycıoglu et al., 2017; Chen et al., 2017; Jayaprakasha et al., 2005).

2.5.2 Curcumin

One of the primary chemical compound of *Curcuma longa* L. is "curcumin," which accounts for approximately 71.5% and is also known as diferuloylmethane, has the chemical formula (1,7-bis-4-hydroxy-3-methoxyphenyl-1,6-heptadiene-3,5-dione) (Beevers & Huang, 2011; Li and Wang, 2011). Over the past six decades, there has been extensive research on the pharmacokinetic, pharmacodynamic, and clinical pharmacological properties of curcumin (Aggarwal et al., 2003). These investigations have shown that curcumin functions as an anti-inflammatory, antioxidant, anti-cancer agent, anti-atherosclerotic, inhibits scarring, promotes wound healing and muscle regeneration, prevents kidney toxicity and liver injury, shown therapeutic effect on diabetes, septic shock, multiple sclerosis, cardiovascular disease, HIVdisease, arthritis, lung fibrosis, and Alzheimer's disease (Sharma et al., 1976; Li et al., 2004; Aggarwal et al., 2006). Besides, Turmeric treated with PGPR showed increased concentration of curcumin (Chauhan et al., 2017).

2.5.3 Demethoxycurcumin

Demethoxycurcumin (curcumin II) also known as p-hydroxycinnamoyl, feruloylmethane is the second most important compound within the group of curcuminoids and accounts for 19.4% (Beevers and Huang, 2011). According to Mustarichie et al. (2013), demethoxycurcumin has inhibitory actions against two isoforms of monoamine oxidase (MAO), which is involved in the catalysis of neurotransmitting monoamines, as well as acting as a whitening agent (Baek et al., 2018). Demethoxycurcumin was reported to be the most effective inhibition of MCF-7 cells (Agan et al., 2002). Additionally, it has greater effects on the Bcl-2-controlled apoptotic pathways (Luthra et al., 2009). Similar to this, it has antitubercular properties (Agrawal et al., 2008), antibiofilm activity against *Staphylococcus aureus* (Park et al., 2005), and antiparkinsonian effects (Mazumder et al., 2020). It also has been shown that demethoxycurcumin to be a potential COVID-19 Mpro inhibitor in *in silico* studies (Khaerunnisa et al., 2020).

2.5.4 Bisdemethoxycurcumin

Bisdemethoxycurcumin (curcumin III), also known as di-p-hydroxycinnamoylmethane, is the third major component of the curcuminoid group, accounting for 9.1% (Agan et al., 2002). Various biological activities of

bisdemethoxycurcumin, such as cytotoxicity, anti-inflammatory, antioxidant properties, and activity against leukemia, CNS, colon, melanoma, renal, and breast cancer cell lines, were reported (Rarnsewak et al., 2000; Kim et al., 2016). It also inhibited sortase A, an enzyme responsible for biofilm formation (Park et al., 2005). The effectiveness of bisdemethoxycurcumin against ulcers was reported by Mahattanadul et al. (2009). It has been stated that bisdemethoxycurcumin may act as an antioxidant agent and may function as atherapeutic target for oral hypoglycemic medications in type-2 diabetes (Ponnusamy et al., 2012; Jayaprakasha et al., 2005). According to Kalaycioglu et al. (2017), the noteworthy properties of bisdemethoxycurcumin compared to its isomers may serve as a starting point for the development of new medications for diabetes and Alzheimer's disease (Kalaycioglu et al., 2017). In addition to this, the bisdemethoxycurcumin showed an inhibitory effect on liver lipogenes (Kim et al., 2016). Fig 2.2 depicts the picture of Turmeric plant.

2.5.5 Pathway for curcuminoid synthesis

Curcuminoids, primarily curcumin, demethoxycurcumin, and bisdemethoxycurcumin, are found in the rhizome of turmeric. Type III polyketide synthases (PKSs), which are homodimers of ketosynthase and are structurally simple enzymes, are involved in the biosynthesis of the majority of plant polyketides (Austin and Noel, 2003). However, curcuminoids in the herb *Curcuma longa* are produced by the collaboration of two type III Polyketide synthases diketide-CoA synthase (DCS) and curcumin synthase (CURS) (Katsuyama et al., 2009). The pathway begins with phenylalanine, an aromatic amino acid that produces p-coumaroyl-CoA, and the reaction is catalyzed by the enzyme phenylalanine ammonia liase (PAL). Feruloyl-CoA is produced from P-coumaryl-CoA. Then, the DCS reacts with these two molecules to produce p- coumaroyldiketide-CoA and feruloyldiketide-CoA. A series of CURS then reacts with this to generate the three main curcuminoid components: 1. Curcumin 2. Demethoxycurcumin 3. Bisdemethoxycurcumin. (Fig. 2.3)

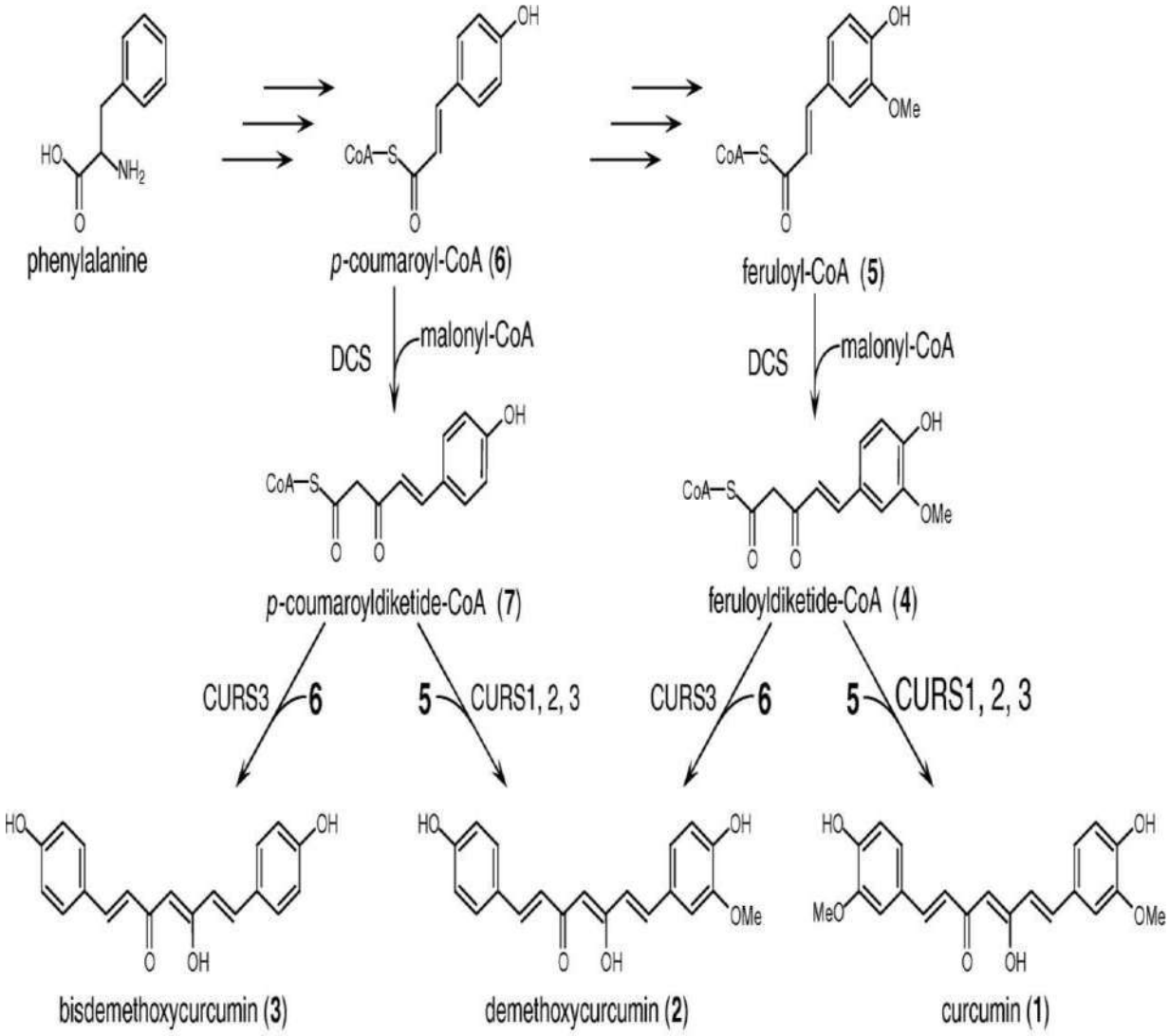

Fig. 2.3: Pathway of curcuminoid synthesis of *C. longa* (Katsuyama et al., 2009)

2.6 Scientific Classification of *Asparagus racemosus* (Shatavari)

Fig. 2.4: Asparagus plant

Kingdom : Plantae
Phylum : Tracheophyta
Division : Angiosperms
Class : Monocots
Order : Asparagales
Family : Asparagaceae
Genus: Asparagus
Species: *Asparagus racemosus*

There are several species of Asparagus grown in India, but *Asparagus racemosus* (Willd) is the one most frequently used in traditional medicine (Fig. 2.4). It is also known as Satavari, Satawar, or Satmuli in Hindi, Satavari in Sanskrit, and Shatamuli in Bengali (Kumar et al., 2008). A variety of plant parts in the Asparagus genus are a great source of sapogenins and saponins (Hayes et al.,2008). In traditional Indian medicine, the tuberous root of *A. racemosus* is used to treat a wide range of ailments, including dysentery, tumors, neuropathy, inflammations, nervous disorders, hyperacidity, bronchitis, some infectious diseases, chronic fevers, conjunctivitis, and rheumatism. Similarly, Pharmacological tests on animals have also shown that *A. racemosus* extract is effective as an antioxidant and anti-anaphylactic (Upadhyay et al., 2014; Hayes et al., 2008).

When medicinal plants were treated with a consortium of PGPR under saline conditions, it was demonstrated that the plant parameters had improved (Varma et al., 2017). In addition to this the plants grown in soil treated with compost showed the highest antioxidant activit (Sharafzadeh & Ordookhani, 2011). An analysis of *Asparagus racemosus* roots grown in soil treated with vermicompost, compost, cow dung, and other organic manures without the use of mineral or chemical fertilizers revealed that the plants from this soil had the uppermost levels of total phenol and total flavonoid content (Saikia and Upadhyaya, 2011). Similarly, Ge et al. (2016) found improved plant growth characteristics of asparagus when treated with a combination of PGPR, vermicompost and cow manure (Ge et al., 2016).

Steroid saponins, or Shatavarins I–IV, are phytoestrogen compounds present in the roots of *Asparagus racemosus* Willd. they are the main biologically active components of the plant. (Mfengwana and Mashele, 2020). Shatavarin IV is a sarsasapogenin glycoside made up of two rhamnose molecules and one glucose molecule, as well as starch and mucilage (Hayes et al., 2008). In 2001, Saxena and Chourasia extracted a new isoflavone called 8-methoxy-5,6,4′-trihydroxyisoflavone from the roots of *Asparagus racemosus* Willd. They identified a novel antioxidant compound named racemofuran in addition to well-known substances like asparagamine A and racemosol and flavonoids such glycosides of quercetin, hyperoside, rutin, kaempferol, and polycyclic alkaloids (Saxena and Chourasia, 2001). As a result of the presence of secondary metabolites *Asparagus racemosus* is used as a dietary supplement because it

also has some nutritional qualities. Additionally, it has anticancer, galactagogue, and immunomodulatory properties (Patil et al., 2014).

2.6.1 Shatavarin

The root and fruit of *A. racemosus* both contain steroidal saponins, which are the active ingredients. Shatavarins I to X, which are major steroidal glucosides (saponins), were discovered in the roots of *A. racemosus* but Shatavarins I and IV have been identified as the primary steroidal saponins (Haghi et al., 2012; Mitra et al., 2012). Shatavarin IV has been demonstrated to have significant inhibitory activity against Core Golgi enzymes such as transferases as well as immunomodulatory activity against specific T-dependent antigens in immunodeficient animals (Pandiyan et al., 2022). The medicinal properties of *A. racemosus*, including its anticancer activity, are due to the presence of saponin glycosides (Onlom et al., 2017). An earlier study demonstrated that Shatavarin IV had antioxytocic activity and Shatavarin I had anti-abortifacient activity, and both were used to treat infertility (Gohel et al., 2015).

2.6.2 Diosgenin

Diosgenin serves as a major raw material in the manufacture of synthetic hormones. It belongs to the steroidal saponins that are found in *A. racemosus* (Alok et al., 2013; Wang et al., 2011). Diosgenin has been demonstrated to have anti-proliferative activities against human coloncancer and to induce apoptosis in a number of human cancer cell lines (Bhutani et al., 2010). Clinical studies revealed that diosgenin-induced increases in biliary cholesterol output have a significant effect on the solubility and transport of biliary cholesterol (Thewles et al., 1993). Diosgenin has been discovered to be effective in treating conditions such as diabetes, hyperlipidemia, various cancers, osteoporosis, cardiovascular diseases, skin conditions, and neurological disorders (Paramesha et al., 2021). In fact, this compound is known to have anti-inflammatory and antioxidant properties and may be helpful for a variety of conditions, including blood and cerebral disorders, allergic diseases, obesity, and menopausal symptoms (Jesus et al., 2016).

2.6.3 Pathway for Diosgenin synthesis

In a number of plants, cholesterol is converted into steroidal sapogenins (spirostanols), such as diosgenin, but the exact biosynthetic processes that take place in

between have not yet been fully understood (Mehrafarin et al., 2010). Two processes can result in the formation of diosgenin from squalene-2,3-oxide: one is the formation of cholesterol from lanosterol and the other is the production of sitosterol from cycloartenol (Ciura et al., 2017). According to an *in vitro* study by Tal et al. (1984), naturally occurring glycosides in a number of plant species include steroidal saponins (furostanols), in which the side chain is held open by glycoside formation. These glycosides are converted to spirostanols by the action of glucosidases. These results provided evidence in favor of the theory that, in the biosynthesis of sapogenin, and also suggest that furostanol is utilized in the biosynthesis of diosgenin from cholesterol in a manner similar to that suggested by the proposed biosynthetic pathways (Tal et al., 1984) (Fig. 2.5).

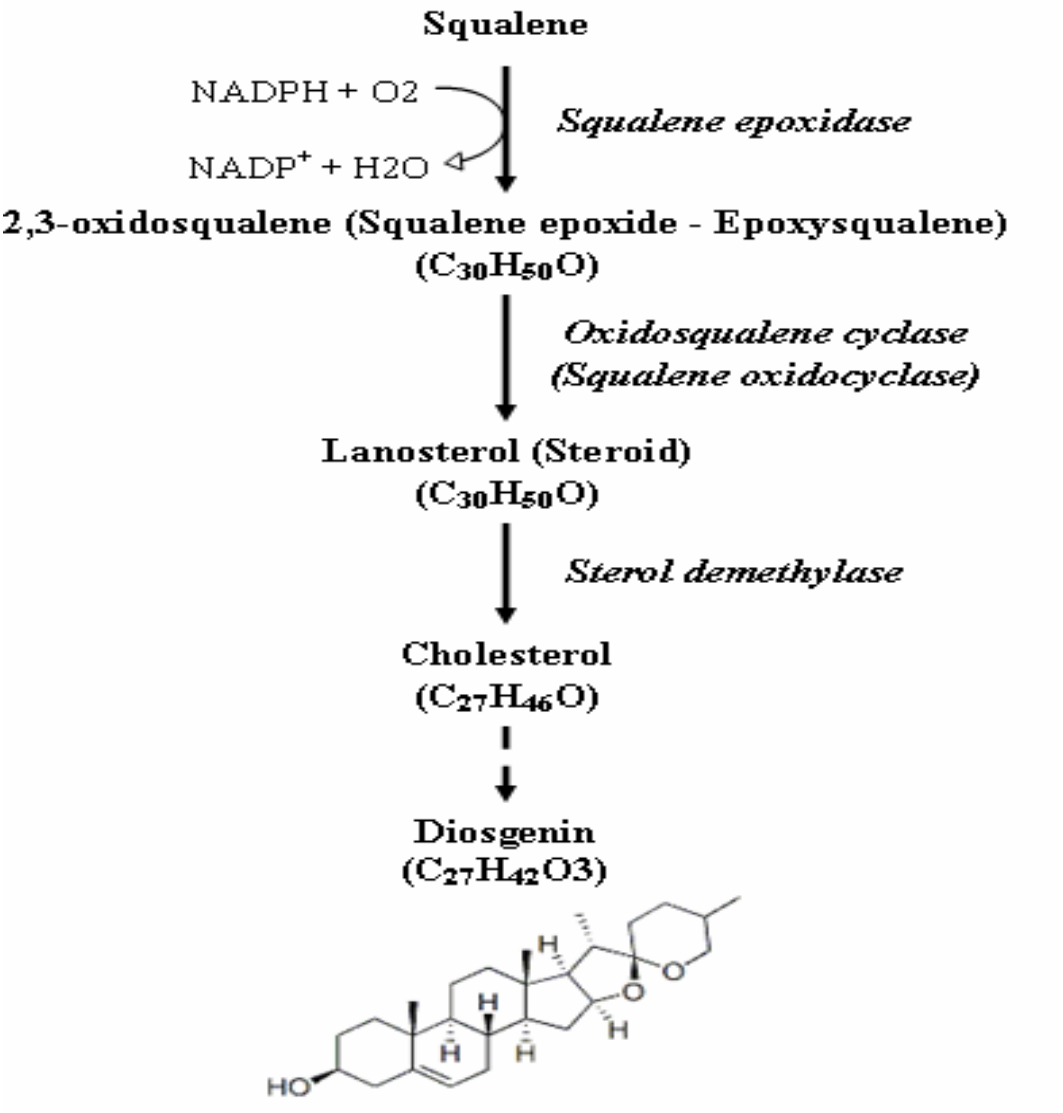

Fig. 2.5: Pathway of Diosgenin synthesis of Asparagus (Mehrafarin et al., 2010).

2.7 Pharmacological properties of secondary metabolites from Turmeric

Curcuminoids, which make up the turmeric rhizome, reveal a variety of advantageous biological properties, including antitumor, anticarcinogenic, and antioxidant properties. Curcumin is now viewed as a secure, innovative, and promising medication for the prevention and treatment of cancer, chronic inflammation, and other illnesses (Rodrigues et al., 2015). Some of the pharmacological properties of the metabolites are listed in Table 2.1.

Table 2.1: Pharmacological properties of secondary metabolites from Turmeric

Name of compound	Source	Biological activity	Reference
Curcumin	*C. longa*	Neuroprotective activity	Cas and Ghidoni, 2019
Curcumin	*C. longa*	Premenstrual syndrome	Fanaei et al., 2016
Curcumin	*C. longa*	Antibacterial, antiviral, antifungal	Moghadamtousi et al., 2014
Curcumin	*C. longa*	Antibacterial	Zheng et al., 2020
Curcuminoids	*C. xanthorrhiza*	Oxidative stress	Masuda et al., 1992
Curcuminoids	*C. longa*	Antitumor activity	Agarwal et al 2013
Curcuminoids	*C. longa*	Antimalaria	Nandakumar et al., 2006
Curcuminoids	*C. longa*	Cytotoxic Activity	Chen et al., 2017
Curcuminoids	C. *mangga*	Gastric ulcer, chest pain, fever	Blagojevic et al., 2011
DMC	*C. longa*	Anticancer activity	Yodkeeree et al., 2009
BDMC	*C. longa*	Anti-inflammatory	Kim et al., 2016
Ar-turmerone	*C. longa*	Anti-angiogenic effects Human	Yue et al., 2015
Ar turmerone	*C. longa*	Selective induction of apoptosis	Aratanechemuge et al., 2002
Ar-turmerone	*C. longa*	Anti-plasmodial	Hamizah et al., 2020
Ar-Turmerone	*C. longa*	Inhibits key enzymes linked to type 2 diabetes	Lekshmi et al., 2012
ar-turmerone	*C. longa*	To control cucumber	Fu et al., 2021

		powdery mildew	
ar-turmerone	*C. longa*	Antibacterial	Negi et al., 1999
Turmerone	*C. longa*	Larvicidal activity	Setzer et al., 2008
Turmerone	*C. longa*	Antifungal	Ferreira et al., 2013
Turmeronol A and TurmeronolB	*C. longa*	Anti-inflammatory mechanism	Okuda-hanafusa et al., 2019
Monoterpenoids, sesquiterpenoids	*C. longa*	Antiradical properties	Dutta and Neog, 2016
Phellandrene	*C. longa*	Insecticidal activity	Chaaban et al., 2019
Phellandrene	-	Wound healing activity	Scherer et al., 2019
Curcumenol	*C. phaeocaulis*	Anti-inflammatory	Tanaka et al., 2008
Curcumenol	*C. longa*	Antibacterial	Wagner et al., 2020
Curlone	*C. longa*	Antibacterial	Jayaprakasha et al., 2005
Curlone	*C. longa*	Insecticidal activity	Mehrotra et al., 2009
Furanodienone	*C. phaeocaulis*	Anti-inflammatory	Tanaka et al., 2008

2.8 Pharmacological properties of secondary metabolites from Asparagus

Traditional and Ayurvedic scriptures frequently refer to the roots of the Asparagus plant. The ancient classical Ayurvedic literature recommended it as a galactagogues and for the treatment of reproductive disorders and threatened abortion. Additionally, *A. racemosus* root is used to treat mental, neurological, and hepatic disorders as well as it works as an anti-ulcer, anti-inflammatory, antidiabetic, anti-aging, and anti-tumor agent (Hazra et al., 2020). Table 2.2 includes a list of some of the pharmacological characteristics of Asparagus metabolites.

Table 2.2: Pharmacological properties of secondary metabolites from Asparagus

Name of compound	Source	Biological activity	Reference
Shatavarin IV	*A. racemosus* root	Anticancer	Mitra et al., 2015
Shatavarin-IV	*A. racemosus*	Immuno-modulation activity	Kamat et al., 2000
Shatavarin I–IV	*A. racemosus*	Gastric ulcer healing effects	Sairam et al., 2002
Shatavarin I	*A. racemosus*	Anti-abortifacient	Patel, 2015
Shatavarin IX, Shatavarin IV	*A. racemosus*	Against prostate-carcinoma cell lines	Onlom et al., 2017
Diosgenin	*A. racemosus* root	Anti-inflammatory	Jung et al., 2010
Diosgenin	*A. racemosus* root	Induce apoptosis in human1547 osteosarcoma	Corbiere et al., 2003
Immunoside	*A. racemosus*	Induced apoptosis was	Bhutani et al., 2010
Sapogenin	*A. racemosus*	Control of cholesterol metabolism	Upadhyay et al., 2014
Sarsasapogenin	*A. officinalis* L	Improving memory	Hu et al., 2005
Asparanin A	*A. officinalis L*	Induce cell cycle arrest	Liu et al., 2009
Asparacoside	*A. racemosus*	Against hepato-carcinoma cell lines	Onlom et al., 2017
8-methoxy-5,6,4′-trihydroxyisoflavone-7-O-β-d-glucopyranoside	*A. racemosus* root	Antidiarrhoeal	Mandal et al., 2000
Methyl protodioscin and protodioscin	*A. officinalis* seed	Cytotoxic	Shao et al., 1997
Spirostanol glycoside	*A. officinalis* fruits	Immobilization of human spermatozoa	Pant et al., 1988
Racemosol	*A. racemosus* Fruits Roots	Antioxidant, Anticarcinogenic	Velavan et al., 2007
Racemoside A	*A. racemosus*	Inducer of apoptosis	Onlom et al., 2017
Norlignans	*A. gobicus* root	Cytotoxic	Yang et al., 2004
Yamogenin glycosides I, II,	*A. plumosus* root	Spermicidal	Pant et al., 1988

2.9 Computational study of Phytocompounds:

For the discovery of organic ligands, bioinformatics methods for the identification of novel protein binding molecules and the variety of available compound databases have proven to be powerful resources (Luthra et al., 2009; Parulekar et al., 2018; Sonawane et al., 2021; Bansode et al., 2019). Phenolics, flavonoids, coumarins, sterols, and lignans are examples of secondary metabolites that exhibit significant pharmacological properties. To treat various diseases, numerous *in-silico* studies on plant metabolites have been carried out. This includes a step-by-step analysis of the structure-property relationship, the use of structural information about metabolite targets, and the use of structural information of known active compounds to establish a structure-activity relationship (Wase and Wright, 2008). One can study the physicochemical properties that affect drug absorption and excretion, such as stability, solubility, and lipophilicity, with the aid of bioinformatics (Vijayalakshmi et al., 2014). Usually, when considering any compound for lead optimization, these characteristics are taken into account. This classification is based on a limit on molecular weight, lipophilicity, and hydrophilicity, and is known as Lipinski's "rule-of-five," which encodes a basic profile for orally bioavailable compounds (Wase and Wright, 2008).

Many proteins in the body have their activity controlled by small ligands that interact with key proteins in metabolic pathways (Wase & Wright, 2008). The Protein Database contains information about them,and bioinformatics can be used to examine their interactions. A set of predicted binding models of each compound against the corresponding receptor is the result of receptor-ligand docking (Su et al., 1982). The study by Ogungbe and Setzer (2016) presents molecular docking of phytochemical ligands with potential parasitic protein targets as an *in-silico* attempt at natural product therapeutic development for neglected parasitic protozoal illnesses (Ogungbe and Setzer, 2016). There are a few metabolite examples that have been studied *in silico*, such as study of *Moringa oleifera* Lam. metabolites as an anti-diabetic agent was reported by (Zainab et al., 2020). Similarly, Salanin, astragalin, and epoxyazadirone, three significant neem metabolites, exhibit the strongest antibacterial activity against *Staphylococcus aureus* cell surface proteins in an *in silico* screening (Gunamalai and Vanila, 2014). In addition to that, the rich variety of phytochemicals in beach spider lily demonstrated antibiofilm activity, which is thought to be one of the key factors responsible for drug resistance in microorganisms. Therefore, learning more about the lily's therapeutic potential may help to reduce the spread

of pathogens that produce biofilms (Nadaf et al., 2018).

To gain insight into the molecular level binding interactions between the drug and polymer, *in silico* docking study was followed by molecular dynamic simulations (Gangurde et al., 2015). Through *in silico* studies, Jagatha et al. (2008) explained the therapeutic implications for Parkinson's disease. They used an *in-silico* screening tool to evaluate the effectiveness of all other natural compounds/products for therapeutic benefit (Jagatha et al., 2008). The most often suggested substances from medicinal plants that may act as COVID-19 major protease inhibitors include quercetin, oleuropein, catechin, luteolin-7-glucoside, demethoxycurcumin, naringenin, apigenin-7-glucoside, epicatechin-gallate, and curcumin (Khaerunnisa et al., 2020).

Likewise, an *in-silico* study provides insight into how chitin and chitosan-based nanoparticles deliver insulin and curcumin (Dhanasekaran et al., 2018). Earlier study by Mohankumaret al, (2015) has been shown that an analogue of curcumin, BDMC-A, to be more effective than curcumin in inhibiting the NF-kB signalling network and related markers in a breast cancer cell line than curcumin itself (Mohankumar et al., 2015). Another study by Guller et al. (2021) revealed that studies on the inhibition of the glutathione reductase enzyme by curcumin, quercetin, and resveratrol were carried out both *in vitro* and *in silico* (Guller et al., 2021). With the *in silico*, *in vitro*, and *in vivo* efficacy study, which thoroughly demonstrates curcumin's potency, the anti-inflammatory and anti-allergic efficacy of curcumin was confirmed by (Venkata et al., 2012). According to the earlier report, curcumin, demethoxycurcumin, and xanthorrizol spontaneously interact with the amino acids in the active enzyme tyrosinase sac and α-MSH, suggesting that they may have skin-whitening properties (Mustarichie et al., 2013). According to Baek et al. (2018), demethoxycurcumin and bisdemethoxycurcumin may be effective treatments for conditions like depression, Parkinson's disease, and Alzheimer's disease (Baek et al., 2018). Previously Meizarini et al, (2018) stated that curcuminoids are more effective than eugenol, according to *in vivo* studies. *In silico* studies that forecast the potential anti-inflammatory effect of curcuminoid provide support for these findings (Meizarini et al., 2018).

Diosgenin, a promising natural compound, has been studied *in silico* for its biological properties including antioxidant, anti-hyperglycemic, and antilipidemic effects (Sangeetha et al., 2013). It is a sapogenin and has anti-diabetic, anti-inflammatory, chemopreventive, and anticancer properties. Through the targeting of numerous tissues-specific pathways, numerous *in vitro* and *in vivo* studies show that it has a great deal of

potential for treating diabetes and its complications (Nazir et al., 2022). Sarsasapogenin significantly inhibits key enzymes involved in the pathogenesis of AD, including acetylcholinesterase, butyrylcholinesterase, BACE1, and MAO-B, according to an *in vitro* and *in silico* study by (Kashyap et al., 2020). Overall, Singh et al, (2014) showed that diosgenin analogues inhibit the production of pro-inflammatory cytokines in both *in vitro* and *in vivo* conditions (Singh et al., 2014).

Similarly, diosgenin demonstrated a positive impact on type 2 diabetes by interacting with the PPARγ (Peroxisome proliferated-activated receptor γ). These results suggest that the insulin-sensitizing effects of trigonelline and diosgenin are mediated through modulation of ER stress and oxidative stress in the pancreas as well as by PPARc activation in adipose tissue in *in vivo, in vitro*, and *in silico* study (Rani S, 2014). According to Tap et al, (2018) there is evidence that the enzyme phospholipase 2 (Pla2) is inhibited by bromelain, asisticoside, and diosgenin. However, using a single anti-inflammatory drug for treatment frequently results in a number of side effects, including hepatotoxicity, gastrointestinal bleeding, meningitis, and asthma. Therefore, a novel approach combining two or more potential compounds that have inhibitory effects on Pla2 activity has been suggested to solve the issue (Tap et al., 2018).

In the present investigation, *in silico* study of the potent PGPR induced secondary metabolites of *C. longa* has been carried out with respect to the nature of interactions, binding mode and selectivity of biofilm producing protein such as sortaseA from *Staphylococcus aureus* and *Streptococcus mutans.*

2.10 Scope and Objectives of Research:

Plant growth-promoting rhizobacteria (PGPR) are significantly playing role in sustainable development of agricultural sector. Efforts are being continuously undertaken to increase the crop yields with reduction in the use of chemical fertilizers and pesticides. The use of PGPR is an eco-friendly way of increasing the yield of various crops. The mechanism of action of different PGPR varies in different plants and it depends upon the type of host plants. In recent days, an innovative way of using PGPR for medicinal plant production and sustainable agriculture is being developed. Many studies have established the historic usage of medicinal plants to treat a wide range of disorders, as herbal medicine is often regarded to have fewer adverse effects when used on humans. Furthermore, utilization of natural products has risen, both as therapeutically active

medicines and as lead molecules in drug development practices.

With this background, the present research was undertaken which includes the screening of potent PGPR strains from the rhizospheric soil of the Turmeric and Asparagus plants. These potent strains were tested to identify their effects on different parameters of Turmeric and Asparagus plants. Further, the secondary metabolites (phytocompounds) produced by these plants were extracted and purified. The purified phytocompounds were characterized and identified using TLC, GC-MS/MS, and LC-MS/MS. These PGPR induced phytocompounds were then tested for their antimicrobial activity *in vitro* against a variety of Gram-positive and Gram-negative bacterial pathogens as well as fungi and biofilm inhibition property. Additionally, *in silico* study was carried out in which we targeted the adhesion protein SortaseA (SrtA) from both *S. aureus* and *S. mutans* to study the inhibition mechanism using molecular modelling methods. The docking studies revealed that the combination of phytocompounds binding significantly lowers the binding energy of the overall complex. MD simulation and MM-GBSA binding energy calculation studies showed the stability of SrtA in all phytocompounds specifically for ternary complexes with combination of phytocompounds. Thus, the objectives of the present research work were –

Objectives:

1. Screening and identification of potent PGPR from rhizosphere of medicinal plants.
2. Effect of potent PGPR on the growth parameters and secondary metabolites of selected medicinal plants.
3. Extraction and purification of secondary metabolites from medicinal plants.
4. Pharmacological applications and bioinformatics studies of secondary metabolites.

CHAPTER III

MATERIALS AND METHODS

3. MATERIALS AND METHODS:

3.1 Introduction

This chapter describes the methodology employed in this work, including the screening and isolation of Plant Growth Promoting Rhizobacteria from rhizospheric soil of medicinal plants such as Turmeric and Asparagus. Afterwards, using a pot culture experiment, it was determined how PGPR affected plant metrics and biological contents. Plant metabolites that were influenced by PGPR were then extracted and purified using different methods. Computational and experimental techniques are applied to delve deeper into its pharmacological characteristics.

3.2 Materials:

3.2.1 Soil

The rhizospheric soil samples were collected from the cultivated Turmeric farms of the Turmeric Research Section, "Mahatma Phule Krishi Vidyapeeth's Agriculture Research Centre", Kasbe Digraj, Dist. Sangli and from cultivated Asparagus farms of various localities in Kolhapur District.

3.2.2 Plant material

Turmeric rhizomes of the Salem variety and two months old cultivated plantlets of Asparagus were used for the pot culture experiments.

3.2.3 Chemicals and culture media

All the chemicals used in this study were highly purified and of analytical grade. All bacterial and fungal culture media such as nutrient agar (NA), calcium-adjusted Muller Hinton agar (MHA), brain heart infusion (BHI) broth, potato dextrose agar (PDA) and other media components were purchased from Himedia, India. Standard antibiotics discs, standard curcumin, curcuminoids, diosgenin were also purchased from HiMedia, India. Standard 4 Hydroxy 2 methylacetophenone was obtained from TCI, India while ascorbic acid (AR Grade), rutin, 2,2- Diphenyl-1-picrylhydrazyl (DPPH) were obtained from Himedia India. Filtration assembly and equipment were obtained from Axiva. Analytical grade TLC plates were obtained from Merck Millipore.

3.2.4 Bacterial cultures

Gram positive organisms: *Staphylococcus aureus* NCIM 2654, *Streptococcus mutans* NCIM 5660 and Gram negative: *Escherichia coli* NCIM 2832, *Proteus vulgaris* NCIM 2813 were purchased from National Collection of Industrially important Microorganism (NCIM) Pune, India and were maintained with refrigeration at the Department of Microbiology, Shivaji University, Kolhapur.

3.3 Screening of PGPR from rhizospheric soil of Medicinal plants

For the isolation of rhizome and root associated soil bacteria, the adhering soil (1 gm) was suspended in 100 ml of nutrient broth in an Erlenmeyer flask and shaken for 24 hrs on shaker at room temperature for enrichment. It was then serially diluted upto 10^{-5} to 10^{-10}, and from that 0.1 ml suspension was added to the Petri plate containing sterile nutrient agar media and spread by the sterile glass spreader in the laminar flow hood. Petri dishes were incubated at 30°C till visible growth appeared on the plates. Bacterial colonies were isolated following the standard microbiological techniques. The pure isolates were isolated after repeated streaking on the nutrient agar plate. The pure isolates were inoculated on the respective medium slants and after growth, they were maintained at 4°C in a freeze for further use in the Department of Microbiology, Shivaji University, Kolhapur.

3.4 Plant growth promoting attributes of PGPR:

3.4.1 Phosphate solubilization

The Pikovskay's agar medium containing tricalcium phosphate was spot-inoculated with the bacterial isolates, and the plates were then incubated at 28±2ºC for 2 to 3 days. The appearance of a transparent halo zone surrounding the bacterial isolates demonstrated their capacity to solubilize phosphate (Laslo et al., 2012).

3.4.2 Zinc solubilization

The bacterial isolates were grown separately on basal medium (Glucose-1gm, Ammonium sulphate-0.1gm, Potassium chloride-0.02gm, Dipotassium hydrogen phosphate-0.01gm, Magnesium sulphate-0.02gm, Distilled water -100ml, pH 7.0) supplemented with 0.1% insoluble zinc oxide. 10µl bacterial suspension was placed on a basal medium containing plates and plates were incubated at room temperature for 24, 48 and 72 hrs. After incubation zone of clearance were observed around

bacterial growth (Saravanan et al., 2004).

3.4.3 Potassium solubilization

To check potassium solubilization, isolates were inoculated on the modified Alexondrov's medium (Glucose- 0.5gm, Magnesium sulphate- 0.05gm, Ferric chloride- 0.0005gm, Calcium carbonate- 0.01gm, Tri- calcium phosphate- 0.2gm, Potassium alumino silicate- 0.2gm, Agar 1.5-2gm, distilled water- 100 mL) containing 0.2 % potassium alumino silicate as a potassium source and phenol red 0.05% as a pH indicator. The test organisms were inoculated on the media and incubated at 28 ± 2ºC for 24-72 hrs. After incubation the color change was observed due to the presence of pH indicator (Dhaked et al., 2017).

3.4.4 Production of IAA

Bacterial cultures were grown in the flasks containing Yeast extract mineral medium supplemented with 1 % mannitol, 0.01% $CaCl_2$ and different concentrations of L-Tryptophan (12.5, 37.5, 62.5, 75 mg/25ml) and kept at dark conditions for 48 hrs at room temperature on shaker. After incubation broth were centrifuged at (8000rpm, 10 min). 2 ml supernatant bacterial cultures were mixed with 2 drops of orthophosphoric acid and 4 ml of Salkowski reagent (50 ml, 35% of per chloric acid, 1 ml 0.5 M, $FeCl_3$ solution). Development of pink colour confirmed the Production of IAA (Brick et al.,1991).

3.4.5 Nitrogen fixation

The freshly grown potent isolates were streaked on N-free Asbhy's agar medium plates. The plates were incubated at room temperature for 48 hrs. formation of creamy white colonies indicates nitrogen fixation by the isolates. The Kjeldahl method was used to further quantify the fixed nitrogen. After adding a fresh inoculum of isolated PGPR to sterile, nitrogen-free Ashby's broth, the mixture was incubated for five days at 28 ±2°C and 120 rpm on a rotary shaker. The uninoculated broth was served as a control. Following incubation, the inoculated broth was centrifuged for 10 minutes at 5000 rpm to remove biomass, and the amount of Total Kjeldahl Nitrogen (TKN) was calculated by titration (Kumar et al., 2014).

3.4.6 NH_3 Production

To estimate NH3 production, the method suggested by Cappuccino and Sherman, (1992) was used. In brief, 50 µl of bacterial cell suspension was grown for 72 hours at 25°C in 30 ml of peptone broth (4%). Following incubation, 1 ml Nessler's reagent (50 gm potassium iodide, 35 ml saturated mercuric chloride, 25 ml distilled water, 400 ml potassium hydroxide (40%) was added. The presence of NH3 was demonstrated by the production of yellow to brown precipitate.

3.4.7 HCN Production

HCN Production was detected by the method of Kloepper et al. (1991). The bacterial cultures were streaked on King's B medium that contains 0.4% glycine. The plate's lid was lined with a Whatman filter paper No. 1 that had been dipped in a solution of 0.5% picric acid (in 2% sodium carbonate). Parafilm was used to seal the plates, which were then incubated for 72 hours at 28 ±2°C. HCN production was detected by the color changing from light brown to dark brown.

3.4.8 Siderophore Production

The Schwyn and Neilands (1987) approach was used to determine siderophore production. Bacterial suspension (10 µl) was inoculated on the Chrome azurol- S agar plate and incubated at 28 ±2ºC for 24, 48 and 72 hrs. The formation of a yellow orange hallow zone around the bacterial spot is the indication of siderophore production.

3.4.9 Salt tolerance

To test the salt tolerance of bacterial isolates, 100µl of 24 hrs old culture of isolates was inoculated into 10 ml Luria Broth containing 1%, 2%, 3%, 4%, 5%, 6%, 7%, 8%, 9%, 10% NaCl. After 24-48 hrs, the growth was examined by taking absorbance at 600 nm in a Spectrophotometer (UV/Vis) and their range of stress tolerance was detected (Tirry et al., 2021).

3.4.10 Exopolysaccharides (EPS) production

To detect exopolysaccharide production, the samples were cultured in optimized mineral salts medium with K_2HPO_4- 1.26gm, KH_2PO_4- 1.82gm, NH_4NO_3- 1gm, $MgSO_4.7H_2O$- 0.1gm, $MnSO_4$- 0.06gm, $CaCl_2.2H_2O$- 0.1gm, $FeSO_4.2H_2O$- 0.006gm, sodium molybdate- 0.1gm, NaCl- 0.15gm and Glucose- 0.02gm in 100 ml

of distilled water for 7 days incubation (Bramchari and Dubey, 2006). Following that, the 250 ml bacterial cultures were centrifuged for 20 minutes at 4°C and 10,000 rpm. Double the quantity of 95% ice-cold ethanol was added to the supernatant in order to remove the exopolysaccharides (Naseem & Bano, 2014).

3.5 Morphological, Cultural and Biochemical characteristics of bacterial isolates

Morphological, Cultural and Biochemical characteristics of bacterial isolates were studied on the basis of colony characters, Gram staining, motility, and biochemical tests such as citrate utilization, starch hydrolysis, nitrate reduction, catalase, oxidase and sugar fermentations including glucose, adonitol, arabinose. Further, antibiotic sensitivity testing was carried out utilizing the antibiotic impregnated discs method. The organisms have been categorized as resistant or sensitive based on their zone of inhibition, according to the DIFCO Manual, 10^{th} edition (1984).

3.6 Genotypic characterization of PGPR

The genomic DNA of potent PGPR were extracted using the conventional phenol/chloroform extraction method (Sambrook et al., 1989) and the 16S rRNA gene were amplified using universal primers 16F27 [5'-CCAGAGTTTGATCMTGGCTCAG-3'] and 16R1492 [5'-TACGGYTACCTTGTTACGACTT-3']. PEG-NaCl precipitation was used to purify the amplified 16S rRNA gene PCR products and it was then sequentially sequenced on an ABI®3730XL automated DNA sequencer (Applied Biosystems, Inc., Foster City, CA) as per the manufacturer's recommendations. The assembly was performed with the Lasergene package, andthe identification was done with the EzBioCloud database (Riera et al., 2017). Using the Nucleotide Basic Local Alignment Search Tool (BLAST) programme, the resulting sequences were processed and searched to find the best fit to sequences at the National Center for Biotechnology Information (NCBI) BLAST server (www.ncbi.nlm.nih.gov/BLAST). Multiple sequence alignment was performed using CLUSTALW software (Thompson et al., 1997) on the sequences that showed >98% resemblance. MEGA X was used to create a phylogenetic tree based on molecular analyses. Identified 16S rRNA sequence were deposited in GenBank with Accession number **MZ452064**, **OL739684, OL771442** and **OL656822.**

3.7 Pot culture experiment:

3.7.1 Inoculum preparation for Turmeric

With minor modifications, the inoculum was made as described Kaur et al. (2012). To maintain cell density at 10^8 CFU/ml of bacterial suspension, 1% activated charcoal powder was combined with 1% glucose and 0.5% NaCl. Turmeric rhizomes were surface sterilized with 70% alcohol and washed five to six times with sterile distilled water. Then coated with this inoculum and sowed in pots containing natural soil and sterile soil each.

3.7.2 Inoculum preparation for Asparagus

1 gm of carboxy methyl cellulose (adhesive), 10^8 CFU/ml of bacterial suspension, 1% glucose, and 0.5% NaCl were added into 90 ml of sterile distilled water to make the inoculum. Asparagus roots were surface sterilized with 70% alcohol and rinsed with sterile distilled water five to six times. The roots were then covered with inoculum and sown in pots containing naturaland sterile soil each.

3.7.3 Effect of PGPR on Turmeric

To demonstrate effect of PGPR on Turmeric, pot culture experiment was performed. The isolates used in present study were *Serratia nematodiphila* RGK and *Pseudomonas plecoglossicida* RGK. To study the influence of treatment of these isolates, the experiment was carried out in randomized block design (RBD) in triplicate by using air dried, sieved natural as well as sterile soil. Total 72 pots were used for experiment from that 36 for natural soil and 36 for sterile soil. Four types of treatments were given to rhizome before sowing -

T1 : Treatment with *Serratia nematodiphila* RGK

T2 : Treatment with *Pseudomonas plecoglossicida* RGK

T3: Co-culture of *Serratia nematodiphila* RGK and *Pseudomonas plecoglossicida* RGK

T4 : Control (Uninoculated)

The morphological parameters of plants were examined at 45, 90 and 180 days of sowing (Ambardar and Vakhlu, 2013).

3.7.4 Effect of PGPR on Asparagus

A pot culture experiment was carried out to demonstrate the effect of PGPR on Asparagus. The isolates used in this experiment were *Exiguobacterium acetylicum* RGK and *Enterobacter mori* RGK1. To study the influence of treatment of these isolates, the experiment was carried out in randomized block design (RBD) in triplicate by using air dried, sieved natural as well as sterile soil. Total 72 pots were used for experiment from that 36 for natural soil and 36 for sterile soil. Four types of treatments were given to plantlets before sowing

T1 : Treatment with *Exiguobacterium acetylicum* RGK

T2 : Treatment with *Enterobacter mori* RGK1

T3 : Co-culture of *Exiguobacterium acetylicum* RGK and *Enterobacter mori* RGK1

T4 : Control (Uninoculated)

The morphological parameters of plants were examined at 45, 90 and 180 days of sowing(Ambardar and Vakhlu, 2013).

3.7.5 Plant parameters:

The morphological plant parameters such as number of leaves, rhizome biomass, shoot length, root number, root biomass of both the plants from each pot were examined at 45, 90 and 180 days of sowing.

3.7.5.1 Plant parameters for Turmeric

Number of leaves- The leaf number was measured after 45, 90, and 180 days in net house conditions. All leaves, regardless of size, were counted, and the average number of leaves per plant were calculated.

Rhizome biomass- The extra water was removed by pressing it between the filter paper's folds. Following a 60°C drying process, the rhizomes' weight was measured and represented as gm/dry plant weight.

Shoot length- The plant's shoot length was measured in centimeters (cm) from the soil line tothe highest point of the plant.

3.7.5.2 Plant parameters for Asparagus

Root number - The data on root number was recorded after 45, 90 and 180 days in net house conditions. All the roots, regardless of their size were counted and average number of root per plant were calculated.

Root biomass - The roots were thoroughly washed and wiped off by putting them between the folds of filter paper. The roots were then dried at 60°C, and the weight was recorded in gm/dry weight of plant.

Shoot length - The plant's shoot length was measured in centimeters (cm) from the soil line to the highest point of the plant.

3.8 Extraction of secondary metabolites:

The uprooting of plants was done after 45, 90 and 180 days and proceeded for secondary metabolite extraction. After uprooting rhizomes and roots were washed with distilled water to remove adhered soil. It was then cut into small pieces and dried in oven at 40℃ to make fine powder. This powder was used for the metabolite extraction process. Different solvents and extraction techniques were used to extract plant secondary metabolites. Below are some additional effective extraction techniques.

3.8.1 Soxhlet Extraction

Soxhlet extraction was carried out using standard apparatus. 1 gm of powdered rhizomes with 250 ml of each hexane, methanol, acetone, petroleum ether, diethyl ether and ethanol as solvent were used with the extraction time of 8 hrs. The organic extracts were concentrated using hot plate and stored at 4℃ for further analysis.

3.8.2 Sonication for Turmeric and Asparagus

1 gm of sample was added to 10 ml of methanol in sealed tube and solution was treated in bath sonicator for 1 hr at room temperature, centrifuged at 5000 rpm at 4℃ for 10 min. Supernatant was collected for further analysis.

3.9 Preliminary qualitative phytochemical screening of crude extracts:

Preliminary qualitative phytochemical screening was performed with the prepared crude extracts of PGPR treated plants and control plants in natural and sterile soil, to assess the presence or absence of various classes of medicinally important secondary metabolites.

3.9.1 Analysis of total phenolic content

Wolfe et al. (2003) assessed the extracts' total phenolic content using the Folin-Ciocalteu technique. 12.5µl of plant extracts and 50µl of distilled water were

added to a 96-well microtiter plate. Following the addition of 12.5µl of Folin-Ciocalteu's phenol reagent, the plate was left at room temperature for 10 minutes. Following a 10 minute duration, 125µl of sodium carbonate 7% and 100µl of distilled water were added, resulting in a final volume of 300µl. The entire mixture was then allowed to stand at room temperature for 90 minutes in dark conditions. The total phenolic acid content was measured at 750 nm and represented as mg gallic acid equivalents (mg GA/gm) of the dry samples (Ahmad et al., 2015).

3.9.2 Analysis of flavonoids content

The method of Luximan and Rama (2002) was used to calculate the total flavonoid content of plant extracts. 150 µl of extracts and 150 µl 2% $AlCl_3$ was added to 96 well microtiter plate. Following a 10 minute dark incubation period, the plate was measured for absorbance at 367 nm. Rutin equivalents (RE)/gm of dry weight samples were used to express the total flavonoid content.

3.9.3 Analysis of saponins content

Using the method described by Hiai et al. in 1976, the saponin content was calculated. 5 ml of ice cold H_2SO_4 (72%) and 0.5 ml of 8% methanolic vanillin were added to 0.5 ml of asparagus plant extract and then the mixture was incubated in a water bath for 10 minutes at 60°C. After cooling, the absorbance at 544 nm was measured. The amount of total saponin was calculated as quil-A equivalents (QE)/gm of dry weight samples.

3.10 Purification of plant secondary metabolites:

Separation and purification of secondary metabolites from PGPR treated and non-treated plantswere done using following techniques

3.10.1 Purification of curcuminoids

Methanolic extract was subjected to silica gel column chromatography (60-120 mesh). To pack the column, silica gel was dissolved in chloroform: methanol (98:2) and filled upto 46 cm. Then sample was added on the top of gel and eluted with chloroform followed by chloroform: methanol with increasing polarity. All fractions were collected and subjected to UVspectrophotometry at 425 nm (Heffernan et al., 2017).

3.10.2 Thin layer chromatography (TLC) for curcuminoids

The collected fractions were tested on pre-coated Silica gel (Merck, Darmstadt, Germany) TLC plates along with standard curcuminoids. The plates were developed using pre- saturated TLC chamber for 1 hr. chloroform: methanol: formic acid (96:4:0.8 v/v/v) was used as mobile phase. Each plate was developed up to the height of about 12 cm. The plates were then removed and dried. Spots were analyzed and Rf values calculated (Zhang et al., 2008).

3.10.3 Purification of curcumin

Curcumin was further purified from separated spots on TLC. The uppermost spot which was of curcumin (based on Rf value) was scrapped, dissolved in methanol and kept in refrigerator overnight. The supernatant was then collected, evaporated and concentrated. It was used for further purification by silica gel column chromatography (Revathy et al., 2011).

3.10.4 Purification of diosgenin by acid hydrolysis

5 gm of Asparagus plant powder was hydrolyzed in 50 ml of 2 M sulphuric acid by heating under refluxation for 2 hrs. When the solution had cooled, 40% sodium hydroxide was added to neutralize it. The hydrolyzed product was then extracted with an equal quantity of chloroform (Wang et al., 2011; Yang et al., 2015). The extract was separated by a separating funnel and concentrated by evaporation at 60°C. The residue was dissolved in methanol and used for TLC on precoated silica gel for TLC analysis along with the standards.

3.10.5 Thin layer chromatography (TLC) for diosgenin

Thin-layer chromatography was performed on plates precoated with silica gel (Merck, Darmstadt, Germany). The samples were developed with hexane-acetone (8:2) as the mobile phase with a few minor modifications, dried to ensure that all solvents had evaporated, and detected with a 0.5:5 mixture of ethanol (8% vanillin) and sulfuric acid solution (70%) (Hardman, 1968).

3.10.6 High Performance Liquid Chromatography (HPLC)

For the purification of small organic molecules like drugs, peptides, microbial metabolites, plant metabolites and antibiotics, high-performance liquid chromatography (HPLC) is a highly effective and high-resolution technique (Smyth et

al., 2014; Dhanarajan et al., 2015). As part of the recovery of the purification method, HPLC was also used to quantify the metabolites.

3.10.6.1 For Curcumin

This method involves the interaction of liquid solvent in the tightly packed solid column or a liquid column. Parameter used during HPLC purification of Curcumin are given below in Table 3.1

Table 3.1: Parameter used for purification of Curcumin

Parameter used during HPLC purification of Curcumin

Column	C_{18}
Detector	Diode Array detector
Solvent system/Mobile phase	The mobile phase was 50:50 (v/v) acetonitrile and 2% acetic acid
Flow rate	0.5ml/min
Wavelength of detection	425nm
Sample volume	20 µl
Working temperature	25℃
Standard curcumin	100- 500 µg/ml

3.10.6.2 For Diosgenin

Parameter used during HPLC purification of Diosgenin are given below in Table 3.2

Table 3.2: Parameter used for purification of Diosgenin

Parameter used during HPLC purification of Diosgenin

Column	C_{25}
Detector	Diode Array detector
Solvent system/Mobile phase	The mobile phase was 10:90 (v/v) HPLC-grade water and acetonitrile
Flow rate	0.8ml/min
Wavelength of detection	194 nm
Sample volume	25 µl
Working temperature	27^0C
Standard diosgenin	20 – 100 µg/ml

3.10.7 Gas Chromatography-Mass spectroscopy (GC-MS/MS)

Phytocompounds were analyzed both qualitatively and quantitatively using Gas Chromatography Mass Spectroscopy (GC-MS/MS). Following the conversion of the materials to a gaseous form, analysis was done using the mass-to-charge ratio (Balamurugan et al., 2019). Curcuminoid fractions were subjected to GC-MS/MS analysis for compound identification. Helium was used as a carrier gas for the GC-MS/MS study of metabolites, which was performed utilizing an HS 2010 Plus (SHIMADZU) MS TQ 8050 mass detector, column, and SH-Rxi-5Sil MS (30mm × 0.25mm ID × 0.25µm). 1 µl of the sample was injected at a temperature of 250℃; the auxiliary was set at 290℃; the ion source was set at 280℃; the oven was set between 50℃ and 275℃; the GC ran for 38 minutes. The metabolites were identified by National Institute of Standard and Technology (NIST) database.

3.10.8 Liquid chromatography and mass spectroscopy (LC-MS/MS)

HPLC-Quadrupole-Orbitrap MS an Ultimate 3000-series HPLC hyphenated to a QExactive MS (ThermoFisher Scientific, Bremen, Germany) was used with a Waters HSST3 C18 (100 × 2.1 mm, 2.7 µm) column (Waters, USA), thermostated at 30°C. The mobile phase comprised the following: A: water and B: Acetonitrile, each containing 0.1% formic acid. With aflow rate of 0.4 mL/min, the gradient programme was set at 0–10 min/98% A, 11.1 min/2 % A, 16 min/2% A. The heated electrospray ionization (H-ESI, positive mode) parameters were as follows: sheath gas flow rate, 45; auxiliary gas flow rate, 8; sweep gas flow rate, 1; spray voltage, 3.50 kV; capillary temperature, 320 °C; S-lens RF level, 50.0 and heater temperature, 300°C. The MS analysis was performed in the ddMS2 mode. At three different resolutions of 70000 "Full Width at Half Maxima" (FWHM) (at m/z 200), FS was performed in the mass rangeof 100–1000 Da. This was followed by ddMS2 at 17500 resolution (at m/z 200) with stepped collision energy, operated at 10, 30 and 70 V. The automatic gain control (AGC)- targets for the ddMS2 methods were maintained at 1e6. In ddMS2 the m/z with scan range 100-1500 was used. (Originally developed by ThermoFisher Scientific). The software compound discoverer 3.2.0.421 was used for the data processing.

3.11 Analysis of Antioxidant Activity:

The total antioxidant capacity was calculated by measuring the sample's ability to scavenge free radicals using 2,2-Diphenyl-1-picrylhydrazyl (DPPH) according to the procedure described by Aquino et al. (2001). A 0.1 mM methanol DPPH solution was made, and a UV-vis spectrophotometer was used to detect the absorbance at 517 nm. A mixture of 10 µl plant extract and 290 µl DPPH was added to each well of 96-well microtiter plates. Following that, methanol was kept as a blank and the plate was incubated for 20 minutes at room temperature in the dark. Using a UV-vis spectrophotometer, the absorbance was determined at 517 nm. The experiment was conducted in triplicate. Percentage inhibition was calculated using the formula-

$$\% \text{ inhibition } = \frac{\text{A517Control – A517 Sample}}{\text{A517 control}} \; x\,100$$

The antioxidant capacity of the extracts using DPPH for free radical scavenging ability wasexpressed as mg ascorbic acid equivalent per gram of dry weight of sample.

3.12 Antimicrobial and antifungal activity of Phytocompounds:

Turmeric and Asparagus has long been considered as to have natural medicinal properties (Hoe seon lee, 2002). Antimicrobial studies were carried out on the pathogens included *Proteus vulgaris*, *Escherichia coli*, *Streptococcus mutans* and *Staphylococcus aureus.* Antifungal activity was checked by using *Pythium aphanidermatum*, *Aspergillus niger* and *Candida albicans* strains of fungus. The antimicrobial and antifungal activity was monitored in terms of zone of inhibition observed on agar plates of nutrient medium with 1.8% agar by using agar well diffusion method. The plates were incubated for 24 hrs at 37°C for bacteria and 48 hrs at 37°C for fungal cultures. Curcumin, curcuminoids, 4 hydroxy 2 methyl acetophenone, purified curcumin, purified curcuminoids, a combination of curcumin + 4 hydroxy 2 methyl acetophenone and diosgenin standard and purified diosgenin were used for testing purpose. After incubation results were recorded.

3.13 Minimum inhibitory concentration:

The Minimum inhibitory concentration (MIC) of purified metabolites (curcumin, curcuminoid and diosgenin), standard metabolites (curcumin, curcuminoid, 4 hydroxy 2 methyl acetophenone and diosgenin) and their combination (curcumin + 4 hydroxy 2 methyl acetophenone) was determined by using test pathogens as *P.*

vulgaris, E. coli, S. mutans and *S. aureus.* It was determined by twofold serial dilutions of metabolites in a Mueller-Hinton Broth medium. The test was carried out in 96 well microtitre plate with a standardized bacterial suspension of 0.5 McFarland's turbidity. The lowest concentration that completely inhibited the growth of the bacteria after 24 hrs was considered as the minimum inhibitory concentration (Bahari et al., 2017).

3.14 Effect of phytocompounds on test pathogen:

To assess the effect of these metabolites on pathogen growth, the test pathogen *S. aureus* NCIM 2654 was grown in the presence of purified metabolites (curcumin, curcuminoid, and diosgenin), standard metabolites (curcumin, curcuminoid, 4 hydroxy 2 methyl acetophenone, and diosgenin), and their combination (curcumin + 4 hydroxy 2 methyl acetophenone). Their effect on the development of bacteria was measured using an hourly interval of OD at 660 nm. The test culture with initial concentration of 0.5 McFarland was incubated for 12 hours in the presence of these metabolites. The OD values were compared with the control sample and a sterile BHI medium was used as blank. By taking absorbance readings every hour, the growth trend was obtained.

3.15 Biofilm inhibition study by using crystal violet assay:

The microtiter plate assay was used to optimize the conditions for biofilm production. Four human pathogenic strains were used for the study of biofilm inhibition by different phytocompounds. The experiment was performed with some modifications on pre-sterilized 96 well flat bottom polystyrene microtitre plates in triplicates as described earlier (Sharifian et al., 2020). Briefly, a 50µl of cell suspension with 0.5 OD at 600nm was inoculated in 150µl sterile BHI broth in each well. 100µl of purified metabolites (curcumin, curcuminoid and diosgenin), standard metabolites (curcumin, curcuminoid, 4 hydroxy 2 methyl acetophenone and diosgenin) and their combination (curcumin plus 4 hydroxy 2 methyl acetophenone) was added in respective wells. Then microtiter plate was incubated for 24 hrs at 37°C. Biofilms were fixed with 99% methanol after aspiration of planktonic cells. After two sterile phosphate buffer saline washes, the plates were dried. All wells were then filled with 200µl of crystal violet solution (0.1%). After 15 minutes, the extra crystal violet was removed, and the plates were washed twice and air dried. In order

to dissolve the cell-bound crystal violet, 33% acetic acid was used. Using a micro plate reader, the growth of the biofilm was observed in terms of OD 578 nm (Erba scan).

3.16 Biofilm inhibition study by scanning electron microscopy (SEM):

The effect of purified metabolites (curcumin, curcuminoid and diosgenin), standard metabolites (curcumin, curcuminoid, 4 hydroxy 2 methyl acetophenone and diosgenin) and their combination (curcumin + 4 hydroxy 2 methyl acetophenone) on biofilm inhibition was also investigated by the SEM technique. In this, a clean glass was cut into a square having dimensions 1 cm^2. They were washed in a 5% (v/v) Hiclean (Liquid soap, Hi-Media) solution for 30 minutes before being rinsed in ultrapure water to eliminate any leftover detergent. After airdrying for 30 minutes, the surfaces were immersed in 96% (v/v) ethanol for 10 minutes to eliminate any contaminants.

To prepare a sample for SEM, 2% glutaraldehyde solution was taken on slide. A test bacterial culture along with metabolites were used for the preparation of smear. The slides were kept in freezer overnight to fix the smear. On next day smear was washed with an ethanol dehydration series of 20 to 100% (v/v) (Ansari et al., 2021). The samples were then analyzed by SEM using VEGA3 TESCAN instrument.

3.17 *In silico* study:

3.17.1 Biological database

Since biological databases are an essential component of bioinformatics research, they offer structural data on macromolecules that can be used to study biological processes. Recent developments in computational technology and *in vitro* research have accelerated the development of biological databases and improved their quality. Databases can be categorized based on the types of data they contain. For example, there are several protein and peptide databases that include information on protein sequence, protein 3D structure, and protein families. These databases include Uniprot, Swiss-prot, and Protein Data Bank (PDB) (Ma L, 2015).

3.17.2 Protein Data Bank (PDB)

The ‘Protein Data Bank (PDB)’ was started in the 1970’s. Later, PDB was created by Brookhaven National Laboratory in 1971 as a global archive to store 3D

structural data of macromolecules (Berman et al., 2000). Before 1999, Brookhaven managed the PDB, but later that year a group called the Research Collaboratory of Structural Bioinformatics (RCSB PDB) took over management. The PDB contains the experimentally determined 3D structures of proteins, nucleic acids, carbohydrates, and complex assemblies (Burley et al., 2018). The PDB contains the xyz Cartesian coordinates of a macromolecule along with some additional details about the small-molecule ligands, some information about the data collection and structure refinement, and some structural descriptors (Berman et al., 2003).

3.17.3 Molecular Docking

The primary goal of a molecular docking study is to predict the structure of intramolecular complexes generated between two or more molecules (Thomsen and Christensen, 2006; Meyer and Schomburg 2008). Molecular docking is an effective technique for structure-based drug design and discovery, according to Sousa et al. (2006). The availability of more known protein crystal structures has driven interest in moleculardocking. The field of computational biology has advanced more recently. Molecular docking is a technique for predicting the preferred orientation of a receptor and ligand when they combine to create a stable complex (Lengauer and Rarey 1996). Molecular docking is a computational technique used to find possible binding conformation of ligand for interaction within binding pocket, most of docking protocols one of the partner is a protein and the other is a macromolecule such as DNA, RNA, protein, lipids and small organic molecules either natural or artificial (Ferreira et al.,2015). Depending on type of ligand different computational model with their search algorithm are required to solve the docking problem, genetic algorithm is most commonly used in many docking programs such as AutoDock, Gold is a type of stochastic algorithm apply theories of evolution and natural selection. In this study dock 6 program is used to predict binding mode and intramolecular interaction with the help of genetic algorithm and appropriate scoring function. Descriptor score, Hawkins generalized born (GB)/surface area (SA) score, and Amber score. The lowest score in each method was chosen for further examination. These algorithms were based on the Grid score in DOCK6. DOCK 6.7 was reasonably accurate and might be used to carry out additional extensive screening.

3.17.4 Molecular Dynamics (MD) simulation

Molecules are dynamic in nature this dynamic nature is essential for their functioning of protein, they exhibit variety of motion in both solution in the crystalline state (McCammon et. al.,1977). Molecular dynamics (MD) simulations are performed to investigate the structural conformation and stability of the protein and ligand bound state (Sivaramakrishnan et al., 2019). MD simulation is not only to study structure-function relationships of proteins at atomic level butalso behavior of the system in atomic detail that is the position of every atom as a function of time is computed by an algorithm that solves in an iterative fashion Newton's classical equation of motion.

$$F_i = m_i \, a_I$$

Where,

F_i- Force exerted on particle i,

m_i- Mass of particle i, and

a_i– Acceleration of particle i.

The equations are solved concurrently in small time steps. The system applies classical mechanics to describe the motion of atoms keeping temperature and pressure at defined values. These coordinates as a function of time are written to an output file at predefined time intervals and represented as the trajectory of the system to confirm the stability of the system.

3.17.5 MD simulation algorithm

There are numerous simulation algorithms that incorporate Newton's equation of motion. Among the most popular algorithms are the Verlet algorithm (Verlet, 1967) and its modification, the leap frog algorithm (Hockney, 1970), the Gear predictor-corrector algorithm (Gear et al., 1971), and the Beemann algorithm (Beemann, 1976). The reliable physical behavior of constraints is represented by bond vibrations and there are numerous algorithms are available. The SETTLE algorithm (Miyamoto and Kollman, 1992) is an analytical variant of the SHAKE algorithm, which is primarily used for small molecules. The SHAKE algorithm (Ryckaert et al., 1977) is a widely used algorithm for large molecules. Following an unconstrained update, LINear Constraint Solver (LINCS) algorithms reorder various bonds according to their exact lengths (Hess et al., 1997). Particle mesh Ewald (PME) was used to calculate long

rage Coulomb interactions between biomolecules (Essmann et al., 1995).

3.17.6 Topology generation

There are more atom types than elements, however the force field only covers atom types present in biological systems. The topology file illustrates the positions of the atoms as well as their interactions, such as bonds, angles, and dihedrals. These interactions are defined as fixed lists that are stored in the topology file (Spoel et al., 2005). Topology files are essential for nonstandard atoms, ions, and molecules. During the MD simulation, the topology file settings are applied to the atoms. As a result, additional molecular topology data are required for MD simulations of non-standard molecules such as ligands, ions, and lipids. The topology files for these non-standard molecules were included in the appropriate topology file after being directly downloaded from online servers or using AmberTools.

3.17.7 Force field (FF)

The term force field refers to the collection of variables and equations that are used to describe the characteristics of atoms and their bonded and nonbonded interactions. The potential function and parameter set for the force field are generated from either ab initio/semi-empirical quantum mechanical calculations or data from neutron electron, neutron and X-ray diffraction, Raman, NMR, and neutron spectroscopy studies (Gonzalez, 2011). The potential uses of the force field are classified into three categories: bonded, nonbonded, and restraints. The three types of bonding interactions that covalent bonds retain are bond distance, bond angle, and dihedral angles. Electrostatic and van der Waals interactions are examples of nonbonded interactions. Non-bonded potentials are described by the Lennard-Jones potential and the Coulomb interaction, according to Mackerell et al. (1998). Force fields such as AMBER (Cornell et al., 1995), CHARMM (Mackerell et al., 1998), GROMOS (Oostenbrink et al., 2004), and OPLS (Jorgensen et al., 1996) have been widely employed for biomolecule simulation over the last few years. The force field Amber ff99SBIldn was used in the present study.

3.17.8 Periodic boundary condition (PBC)

To minimise the effect of edges, periodic boundary conditions are used in finite and cubic systems (Fig. 3.1). GROMACS calculates far-off electrostatic interactions using the more precise lattice sum techniques, such as PME, Ewald Sum, and PPME (Berendsen et al., 1995; Darden et al., 1993). During the simulation, every direction of an atom in a PBC's primary cell is repeated. According to Bernendsen et al. (1995), an image cell that resembles an atom in terms of size, number, shape, location, and momentum is said to form an infinite lattice. It is simpler to compute the interactions between two given atoms when you have a graphic that illustrates the shortest path between them. Therefore, molecules act as an infinite system and are unrestricted in their movement inside the box (Hansson et al., 2002; Van der Spoel et al., 2005). MD simulation software provides numerous shapes of boxes but frequently used are cubic box.

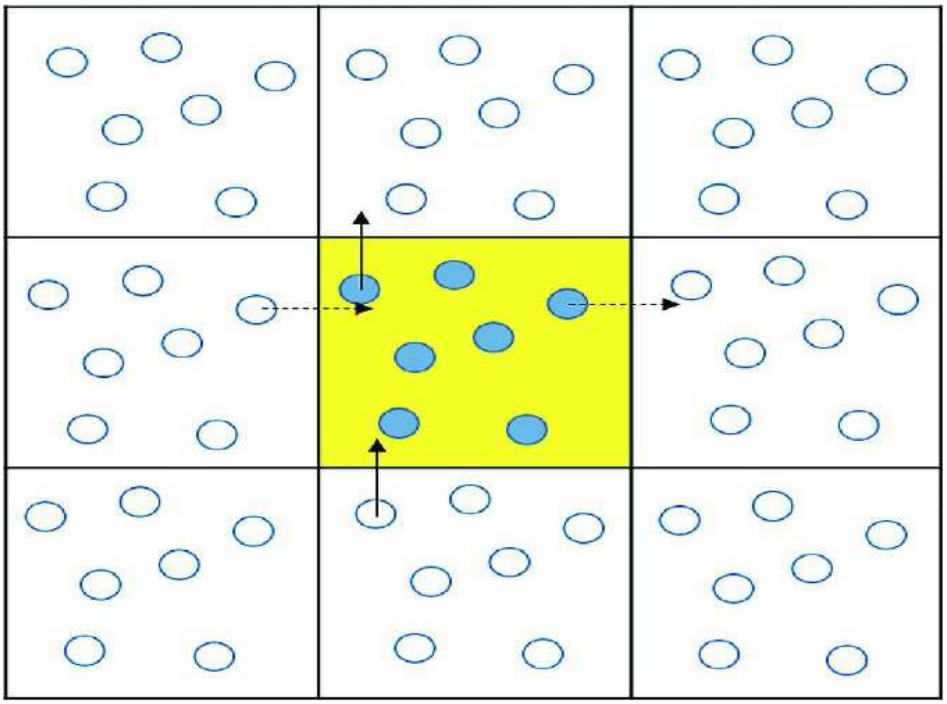

Fig. 3.1: Schematic representation of the idea of periodic boundary conditions. A particle which goes out from the simulation box by one side is reintroduced in the box by the opposite side. (Available from: https://www.researchgate.net/figure/Two-dimensional-representation-of-periodic-boundary-condition-The-central-cell-filled_fig3_322868494)

3.17.9 Thermodynamic ensembles and water model

A collection of all possible systems with a large variety of microscopic states and highly comparable thermodynamic states is called an ensemble. A system's thermodynamic state is composed of a small set of parameters known as thermodynamic ensembles (Brooks, 1995). Temperature (T), volume (V), pressure (P), energy (E), number of particles (N), and pressure (P) are some of these factors. Numerous configurations of thermodynamic ensembles exist, such as isothermal-isobaric (Gibbs) ensemble (NPT), microcanonical (NVE), and canonical ensembles (NVT) (Hunenberger 2005). An isothermal-isobaric, constant pressure and temperature (NPT) ensemble is frequently used to simulate macromolecules because it precisely resembles experimental circumstances. The number of molecules, pressure, and temperature are constant in this ensemble. As a result, it is critical to ensure that the temperature and pressure remain stable throughout the MD simulation time (Evans and Morriss 1983, Eslami and Plathe-Muller 2007).

Water is regarded as the most important solvent in nature. To explore a variety of perceptions, such as solvent dynamic behavior at protein surfaces and solvent effect related to biomolecule structural behavior, biomolecules are dissolved in water in the MD simulation (Marechal 2004, Fornili et al., 2012). The models TIP3-P (Transferable Intermolecular Potential 3-Point), TIP4-P (Transferable Interatomic Potential-4 Point) (Jorgensen et al., 1983), SPC (Simple Point Charge) (Berendsen et al., 1981), SPC/E (Extended Simple Point Charge) (Berendsen et al., 2005) were created for molecular simulations of water. These models feature three basically identical interaction fields with different Lennard-Jones (LJ) and Coulombic parameters in an attempt to replicate the bulk properties of water as shown in tests (Mark and Nilsson, 2001). Choice of water model depends on the nature of system and force field.

3.17.10 Energy minimization

Optimal molecule geometry can be obtained by minimizing energy by changing atomic potions in the molecule. In order to eliminate bad contacts, energy minimization can be used during system setup for MD simulation. The steepest-descent (SD) minimization method locates minima on the molecular potential energy surface using a first order derivative scheme (Wiberg 1965; van der Sopel et al., 2005). The steepest-descent approach uses the first order derivative to calculate the direction towards the

minimum, and this direction is always the inverse of the direction in which the gradient is steepest at the initial point. When the structure is far from the minimal configuration, the robust SD method is used to minimize the initial configuration. Energy minimization aims to relax the system by removing steric clashes. Energy minimization can also be done using the Newton-Raphson and conjugate-gradient methods, respectively. In order to find the best direction, the conjugate gradient method uses line search from the first derivative. As opposed to this, the Newton-Raphson method uses the second order derivative and the Hessian matrix to describe the curvature of the function (Hestenes and Eduard, 1952; Leach, 2001).

3.17.11 Binding energy calculation

MM-PBSA and MM-GBSA methods generally used to calculate binding energy between protein ligand complexes (Kumari et al., 2014), which is based on molecular mechanics Poisson−Boltzmann surface area (MM-PBSA) and Generalized Born/surface area (MM-GBSA) mostly used for calculation of interaction energy in biomolecule complexes.

Interaction free energy represent in equation as follows

$$\Delta G_{binding} = \Delta E_{MM} + \Delta G_{Solv}$$

Where, $G_{binding}$ is total binding energy of system

$$\Delta E_{MM} = E_{bonded} + E_{non}bonded = E_{bonded} + (\Delta G_{vdw} + \Delta G_{elec})$$

ΔG_{MM} is mean molecular mechanics includes van der waals interactions (ΔG_{vdw}) and electrostatic energies (ΔG_{elec})

$$\Delta G_{Solv} = \Delta G_{nps} + \Delta G_{ps}$$

ΔG_{Solv} is solvation energy includes both polar solvation energy (ΔG_{ps}) and non-polar solvationenergy (ΔG_{nps}).

3.17.12 MD simulation and analysis software

Various software used for performing molecular dynamic simulation. These are freelyand routinely used from GROMACS 2021.5 package. Commercial softwares such as AMBER and CHARMM are also used. Molecular visualization software used to visualize MD trajectories and molecules are Chimera, Rasmol, VMD, and PyMol.

3.18 Statistical analysis:

The obtained data were analyzed by one way Analysis of Variance (ANOVA). Values in figures and tables represent the arithmetic mean of the three replicates. Graph-pad prism software used for data analysis.

CHAPTER IV

RESULTS AND DISCUSSION

4.1 Screening, isolation and identification of plant growth promoting rhizobacteria

The part of this study published as:

YMER || ISSN : 0044-0477 http://ymerdigital.com

ISOLATION, CHARACTERIZATION AND IDENTIFICATION OF POTENT PLANT GROWTH PROMOTING RHIZOBACTERIA FROM *ASPARAGUS RACEMOSUS*

Ruddhi. R. Jagtap[1], Gajanan. V. Mali*[3,4], Kailas. D. Sonawane[1,2]

[1]Department of Microbiology, Shivaji University, Kolhapur (416004), Maharashtra, India.

[2]Department of Biochemistry, Shivaji University, Kolhapur (416004), Maharashtra, India

[3]Rayat Institute of Research and Development, Satara (415001), Maharashtra, India.

[4]Department of Microbiology, Bharati Vidyapeeth Deemed to be University, Yashwantrao Mohite College, Pune (411038), Maharashtra, India.

4.1.1 Introduction:

There are numerous types of microorganisms present in the soil, including bacteria, fungus, actinomycetes, and algae, which help to improve the soil's general quality and health. A source of microbial activity can be found in the rhizosphere, which receives nutrition from root secretions. Moreover, isolates from several genera, including *Bacillus, Serratia, Azospirillum, Pseudomonas, Clostridium, Azotobacter, Enterobacter,* and *Arthobacter,* have been demonstrated to possess PGPR properties (Kumar et al., 2014; Kloepper and Beauchamp, 1992). There are numerous ways that PGPR can directly and indirectly increase plant productivity. The direct mechanism involved the capability to fix nitrogen, synthesis of siderophores and phytohormones, solubilization of phosphate, and the biological regulation of diseased plants (Maougal et al., 2021). Plant- associated bacteria may provide an indirect benefit to plants by deterring the progress or interaction of plant pathogenic organisms through various mechanisms (such as rivalries for nutrition and space, antibiosis, formation of hydrolytic enzymes, and suppression of pathogen produced enzymes or toxins).

Plant-associated bacteria may induce plant defence mechanisms, which may also benefit plants (Laslo et al., 2012). PGPR, interact with plants and other microbes that can be either antagonistic or synergistic (Chauhan et al., 2021). PGPRs are useful to plants, as they arealso essential for maintaining the balance of the ecosystem. In recent years, PGPR has been extremely prevalently used as soil inoculants in environmentally friendly agriculture because they have a smaller negative influence on the surrounding environment and produced the highest possible crop yield (Kumar et al., 2016). According to Parveen et al, (2018) PGPR is aconstituent of the defensive microflora. They are beneficial to plants because they improve rootactivities, prevent disease, and speed up growth and development (Parveen et al., 2018). PGPRalso can potentially break down pesticides like endosulfan (Rani et al., 2021). In addition to this, they have antifungal properties (Kavitha et al., 2012). According to reports, they play a significant part in the production of secondary metabolites in plants (Kabera et al., 2014). Theeffects of PGPR on the phytoconstituents of medicinal plants are also documented (Egamberdieva and Teixeira, 2015).

Native medicinal shrubs of the genus Asparagus are members of the family Liliaceae and are valued for the therapeutic benefits of their stems, leaves, and roots. Around the globe,around 300 different species belong to the genus Asparagus (Negi et al.,

2010). Shatavari is thegeneric term for the plant that bears the scientific name *Asparagus racemosus* willd. This planthas a long history of usage as a female reproductive tonic because of its ability to protect the health of mothers and the developing fetus and stimulate increased lactation in breastfeeding women (Mfengwana and Mashele, 2020). *Asparagus racemosus* wild possesses curative properties that can be applied to treat a diverse range of diseases. According to the Ayurvedic literature (the database of Indian traditional remedies), it is a potent substance that can boost memory and intelligence and retain physical vigor and vitality. Additionally, the plant can be used as a demulcent to cure dyspepsia as well as a number of skin problems, wounds, and otherconditions (Patil, 2020). According to Sharafzadeh and Ordookhani (2011), the total phenol and flavonoid content was highest in plants grown in organic manure-treated soil, compost, and vermicompost-without using mineral or chemical fertilizer (Sharafzadeh and Ordookhani, 2011). According to research by Lastra et al, (2021), PGPR can inhibit fungal infections that reduce Asparagus productivity.

The current investigation demonstrates that inoculation of PGPR is an important agricultural approach that plays a significant role in protecting crops and promoting plant development in control of the diseases. As these isolates can tolerate high salt concentrations,they can be used as a biofertilizer in saline soil. They provide an option in place of conventionalagricultural practices that rely on synthetic fertilizers, antibiotics, herbicides and insecticides.

4.1.2. Material and method:

4.1.2.1 Isolation of PGPR from soil

Samples of soil (*A. racemosus* rhizospheric area) were collected from different locations in the districts of Kolhapur and Satara. To isolate PGPR, 100 ml of sterile nutrient broth was enriched with 1 gm of soil in a separate 250 ml Erlenmeyer flask. These flasks were continuously shaken at 30°C (at 120 rpm) for 24 hours. Following that, a 0.1 ml aliquot of a 10^{-5} to 10^{-8} dilution was spread on a sterile nutrient agar plate and incubated at 30°C for 24 hours.

4.1.2.2 Screening for Plant Growth-Promoting Activities:

4.1.2.3 Phosphate Solubilization

To assess their phosphate solubilization potential, all bacterial isolates were

streaked on Pikovskaya's agar plates and plates were incubated at 30°C for 48 hrs (Pikovskaya, 1948). After incubation, the transparent zone around the growth suggested that inorganic phosphate had been solubilized. Bacteria growing in Pikovskaya's broth were quantified, with a sterile uninoculated medium serving as a control. After 48 hours, the culture was collected by centrifuging it at 6000 rpm for 15 minutes to assess how much soluble phosphate was present in the supernatant (Fiske and Subbarow, 1925). Using the KH_2PO_4 standard curve, the amount of soluble phosphate was calculated.

4.1.2.4 Potassium solubilization

Potassium solubilizing isolates were inoculated in a modified Alexandrov's medium (Glucose- 0.5 gm, Magnesium sulfate- 0.05 gm, Ferric chloride- 0.005 gm, Calcium carbonate- 0.01 gm, Tricalcium phosphate- 0.2 gm, Potassium aluminosilicate- 0.2 gm, agar 1.5-2.0 gm, Double distilled water100 ml). The test organisms were seeded on the media and incubated for 48-72 hours at 28˚C. The colony's color variation and the diameter of the zone around it were both measured (Mahadevamurthy et al., 2016).

4.1.2.5 Zinc solubilization

To investigate the solubility of zinc, the isolates were spot-inoculated into an agar medium that included 0.1% of insoluble zinc compounds, like ZnO. Plates containing test microorganisms were incubated at 30°C for 48 hours. Further, the zone of clearance around the colonies were measured (Shakeel et al., 2015).

4.1.2.6 Production of indole-3-acetic acid (IAA)

Culturing the PGPR in yeast extract-mannitol-mineral salts broth enriched with various concentrations of tryptophan, at 28±1°C with constant shaking and it was used to quantify IAA production. Further, 5 ml of cultures were centrifuged at 10,000 rpm for 15 minutes at 4°C after 48 hours, and the supernatant was extracted (Brick et al., 1991). Two drops of orthophosphoricacid and 4 ml of Salkowski reagent (50 ml, 35% of perchloric acid, 1 ml 0.5 M $FeCl_3$ solution) were added to the supernatant (2 ml). IAA production is signified by the appearance of the cherry red color. A UV–Vis spectrophotometer was used to assess color at 540 nm. The concentration of IAA

was determined from a standard curve of IAA (50–300 µg/ml).

4.1.2.7 Ammonia Production

An actively growing PGPR culture was added in 30 ml of 4% peptone water. The entire set was then placed in an incubator at 30℃ for 48 hours. Following the completion of the bacterial growth, 0.3 ml of Nessler's reagent was added to each flask. The presence of a color range from brown to yellow indicates a successful ammonia production assay (Cappuccino and Sherman, 1992).

4.1.2.8 Siderophore Production

The chrome azurol S agar (CAS) was used to test the siderophore synthesis of isolates(Louden et al., 2011). All isolates were inoculated on chrome azurol S agar plates and incubated for 48 to 72 hrs at 30°C. After incubation, the emergence of a yellow-to-orange halo zone around the colony was considered positive for siderophore production

4.1.2.9 Hydrogen Cyanide Production

Using King's B medium, the isolates were tested for cyanide formation (King and Weinhold, 1995). Each bacterial isolate was placed on King's B agar plates amended with 1% glycine. The Petri plates were covered in parafilm and incubated at 30°C with a cover made of filter paper that had been moistened with a few drops of 10% NaCO3 and 1% picric acid (Lorck, 1948). Control plates without inoculation have been prepared. A change from yellow to brown filter paper was predicted to facilitate the production of HCN.

4.1.2.10 Exopolysaccharide Production

According to Nicolaus and team (1999), the exopolysaccharides production by isolates was evaluated qualitatively (Nicolaus et al., 1999). For that, bacterial strains were cultivated in 250 ml Erlenmeyer flasks containing 100 ml medium supplemented with Yeast extract- 1gm, Casamino acids- 0.75gm, Trisodium citrate- 0.3gm, KCl- 0.2gm, $MgSO_4.7H_2O$- 2 gm, $MnCl_2.4H_2O$- 0.036 mg, $FeSO_4.7H_2O$- 5 gm at 30°C for 48 hrs under shaking conditions at 120 rpm. After incubation the supernatant was extracted by centrifuging for 15 minutes at 4°C at 8000 rpm. The development of a precipitate was deemed positive for the synthesis of exopolysaccharidesafter adding

cold 100% ethanol dropwise under agitation.

4.1.2.11 Salt tolerance

To test for inherent resistance to salt stress, the isolated plant growth-promoting bacteria were used. The isolates were grown up for this purpose in flasks containing a nutrient broth supplemented with varying NaCl (1-7%) concentrations. Growth in NaCl-supplemented media was observed after the flasks had been incubated at 30°C for 48 hours (Bhise and Dandge, 2019).

4.1.2.12 Biochemical Characterization and Identification of isolates

A carbohydrate utilization test kit (KB 009, Hi-Media) was used to assess the PGPR's capacity to consume different types of carbohydrates, and 16S rRNA gene sequence analysis was used to identify the isolates showing the highest PGPR performance. The evolutionary history was ascertained by utilizing the neighbor-joining method and evolutionary analysis was conducted using MEGA X (Tamura et al., 2021). The partial 16S rRNA gene sequences were deposited into the GenBank database with accession numbers **OL771442** and **OL656822**.

4.1.2.13 Statistical analysis

The data is presented as means ± standard deviation (SD) for each of the three replicates. The data were analyzed by analysis of variance (ANOVA) utilizing the graph pad software in compliance with the Tukey comparison test ($p < 0.05$).

4.1.3. Results and Discussion:

4.1.3.1 Isolation of rhizobacterial strains PGPR

PGPR strains were isolated from soil attached to Asparagus roots employing the culture-dependent standard plate method. 20 rhizobacterial isolates were chosen based ondistinct colony morphologies and biochemical assays. Two PGPR isolates (Asp-A and Asp-B) with the highest plant growth promotion activity were preferred for physiological and biochemical investigation among the 20 isolates. Earlier studies also showed that plant symbiosis with rhizospheric microorganisms is an essential and critical component of environmentally friendly and efficient agriculture systems. Many bacteria found in the rhizosphere help plants thrives (Santoyo et al., 2021).

4.1.3.2 Phosphate solubilization

Phosphate solubilization was tested on all isolates. In Pikovskaya's agar plates, six isolates displayed a distinct zone, but the diameter of the zone was significant in Asp-A and Asp-B isolates. In a continuous culture medium, quantitative phosphate solubilization was carried out for 48 hrs. After 48 hours of incubation, Asp-A and Asp-B had the highest phosphate solubilization of 84.24 ±0.01 and 86.16 ±0.02 µg/ml. Data are shown as mean ± SD of three replicates (Table 4.1.1 Fig. 4.1.1, 4.1.2).

Hence, we observed that both PGPR strains, *Exiguobacterium acetylicum* strain RGK and *Enterobacter mori* strain RGK1, had an ability for P-solubilization. Phosphorus (P) is the second most important macronutrient after nitrogen (N), and it plays a significant function in plant growth and productivity. Due to insoluble forms of phosphorus, even in phosphorus-richsoil, the majority of the P is inaccessible to plants (Meena et al., 2015). *Pseudomonas, Enterobacter, Bacillus,* and endosymbiotic *Rhizobium* strains have been found to be highly efficient P- solubilizers in soil microbial flora.

Table 4.1.1: Solubilization of Phosphate and IAA production by *Exiguobacterium acetylicum* RGK (Asp-A) and *Enterobacter mori* RGK1 (Asp-B) after 48hrs. Data are shownas mean ± SD of three replicates.

Organism names	Solubilization of Phosphate µg/ml	IAA Production in µg/ml
Asp-A	84.24 ±0.01	90.11 ±0.1
Asp-B	86.16 ±0.02	253.45 ±0.01
Asp-C	31.35 ±0.01	8.45 ±0.02
Asp-D	24.30 ±0.03	33.45 ±0.01
Asp-E	25.90 ±0.01	6.55 ±0.03
Asp-F	31.67 ±0.02	38.45 ±0.02

Fig. 4.1.1: Solubilization of Phosphate on Pikovskaya's agar after 48 hrs where A) *Exiguobacterium acetylicum* RGK B) *Enterobacter mori* RGK1

4.1.3.3 Potassium and Zinc solubilization

Potassium releasing capacity was found in Asp-A and Asp-B isolates. The colour of the pH indicator changes as potassium was solubilized, and the resulting solubilization zone was recorded. After 72 hours of incubation at 28±2˚C, a range of diameter zone 20 mm to 30 mm was noted. The zinc solubilizing isolates were examined for effectiveness on TRIS minimal medium enriched with zinc source ZnO. The maximal solubilization zone of Asp-A was 18 mm where Asp-B was 22 mm in size. As a result, both isolates were capable of solubilizing potassium and zinc data presented in (Fig. 4.1.3, Table 4.1.2).

Earlier studies showed that *Burkholderia, Bacillus spp., Enterobacter spp., Paenibacillus mucilaginosus,* and other rhizospheric bacteria have been described as K-solubilizers and have a great capacity for mobilizing and solubilizing K from minerals (Meenaet al., 2016). According to Singh et al. (1998), increasing potassium application rates had a favorable and significant influence on fresh rhizome output (Singh et al., 1998). Similarly, zinc plays several dynamic roles in plants as crop growth, maturity, vigor, yield, and many physiological functions (Singh et al., 2020). Inoculating plants with various PGPR has resulted in improved growth and zinc content. This includes different strains of PGPR such as *Pseudomonas, Rhizobium, Bacillus, Azospirillum* (Kamran et al., 2017). Our results also showed that both the strains have ability to solubilize potassium and zinc.

4.1.3.4 Production of indole-3-acetic acid (IAA)

Rhizobacterial strains were examined for IAA quantification in tryptophan levels of 25, 50, 150, 200 and 250 µg/ml concentrations. The colorimetric investigations revealed that distinctive PGPR isolates differed substantially in their ability to produce IAA in the broth; isolates Asp-A and Asp-B produced the maximum IAA (Table 4.1.1, Fig. 4.1.2). Earlier study by Ghosh et al (2013) reported that increasing L-tryptophan concentration increased symbiotic growth and IAA production (Ghosh et al., 2013). IAA play a critical role in controlling plant development and growth. In many herbaceous plants, PGPR producing IAA in the rhizospheric soil is crucial for increasing the number of root tips and root surface area (Han et al., 2005).

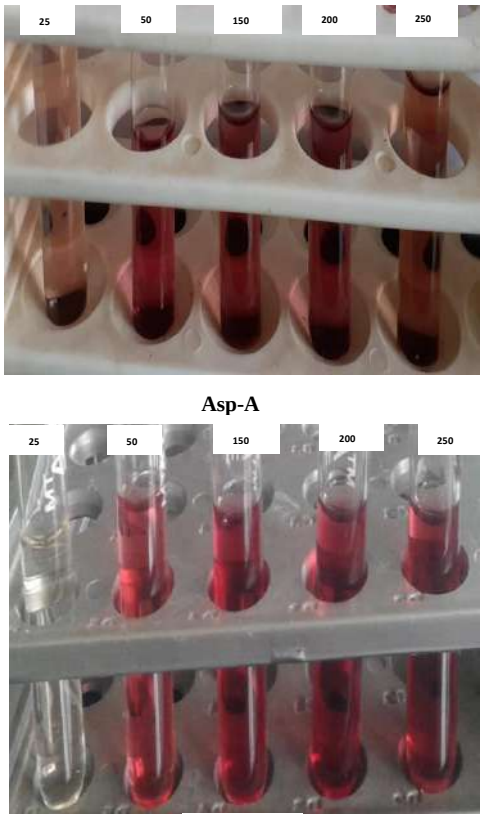

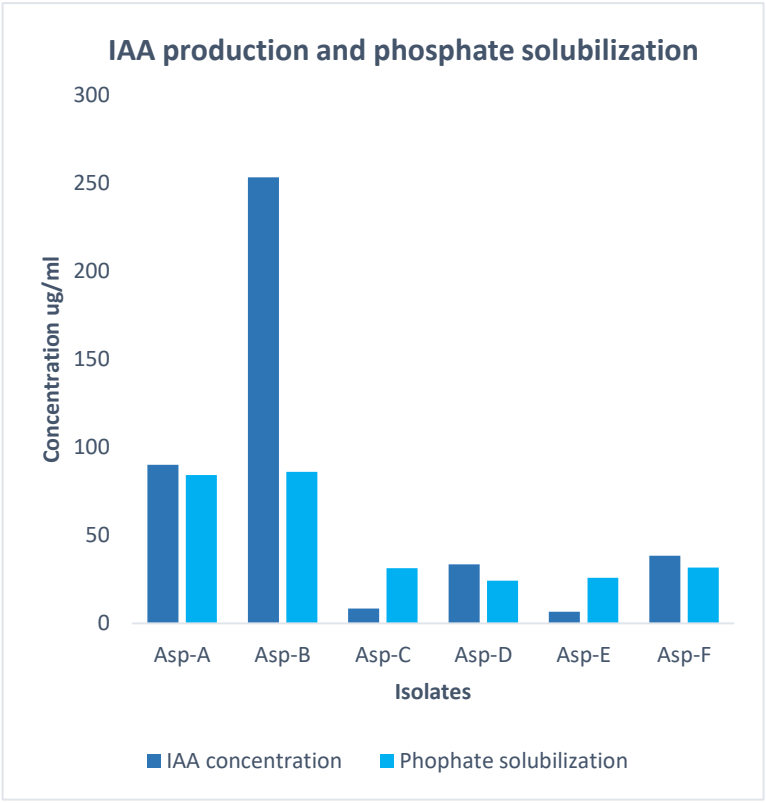

Fig. 4.1.2: A-Production of IAA (Qualitative), B- Production of IAA and solubilization of phosphate (Quantitative) after 48 hrs.

Table 4.1.2: Solubilization of Potassium and Zinc, Exopolysaccharide synthesis by *Exiguobacterium acetylicum* RGK (Asp-A) and *Enterobacter mori* RGK1(Asp-B) after 48hrs

Organism names	Exopolysaccharide production	Solubilization of Potassium	Solubilization of Zinc
Asp-A	+	+	+
Asp-B	+	+	+
Asp-C	+	-	-
Asp-D	-	-	-
Asp-E	-	+	-
Asp-F	-	-	-

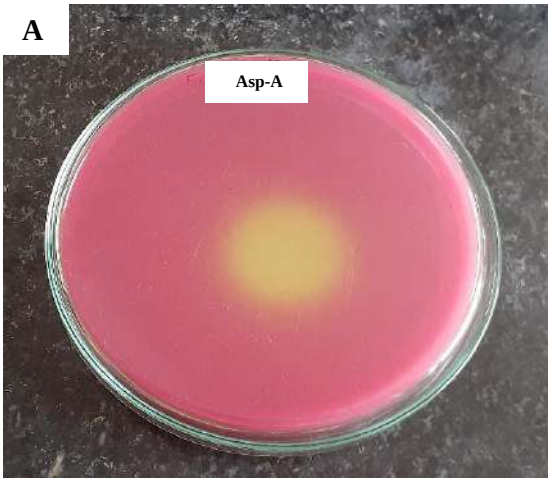

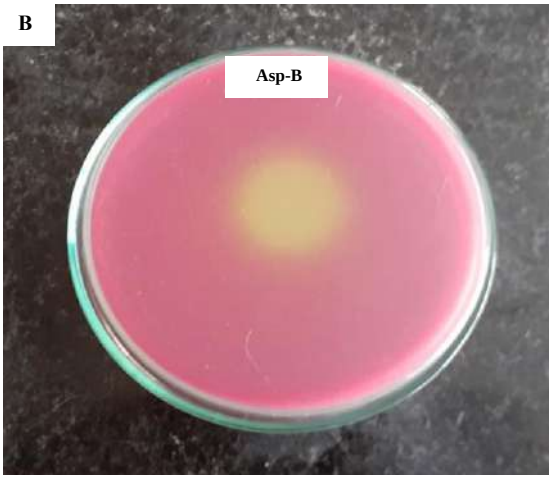

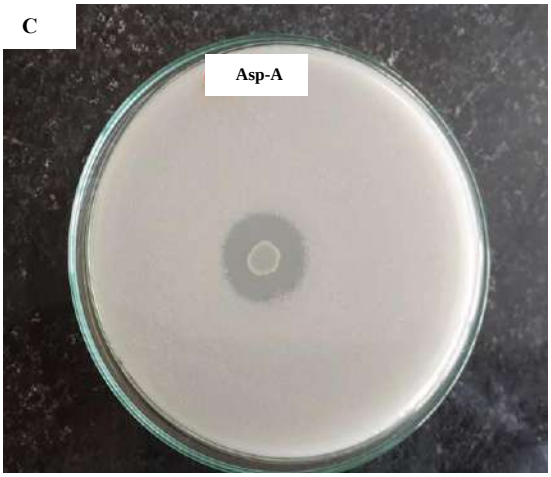

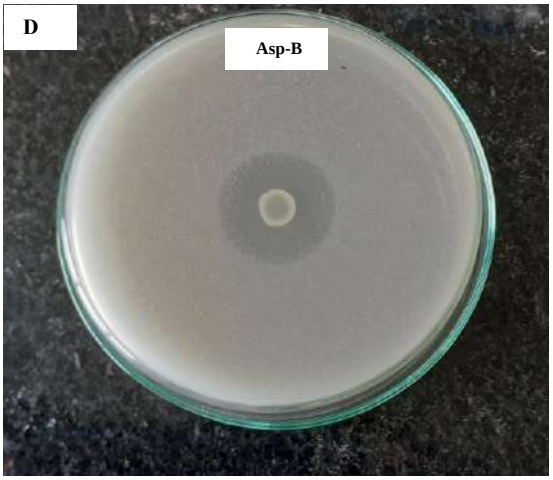

Fig. 4.1.3: A, B are solubilization of Potassium on modified Aleksandrov's k medium by *Exiguobacterium acetylicum* RGK (Asp-A) and *Enterobacter mori* RGK1(Asp-B) and C, D are Zinc solubilization by Asp-A and Asp-B after 72 hrs of incubation.

4.1.3.5 Siderophore, Ammonia, and Hydrogen Cyanide Production

Among the six isolates Asp-A and Asp-B can produce ammonia, hydrogen cyanide and siderophore on CAS agar medium, as illustrated in Fig. 4.1.4. Iron is one of the crucial elements for plant and microorganism development and appropriate functioning. Siderophore-producing isolates can improve plant growth by increasing iron availability to plants while decreasing iron availability to pathogenic fungi (Ahmad et al., 2008). Numerous studies have shown the critical function that bacterial strains that produce siderophores play in both biocontrol and growth promotion (Kumar et al., 2016a). Venkat et al. (2017) found that isolates of *Bacillus* and *Enterobacter* from soil that had been iron-enriched were good candidates to synthesize siderophores (Venkat et al., 2017).

PGPR converted organic nitrogen residues into soil organic matter, such as ammonia nitrifiers. Through ammonification, this PGPR releases ammonia (Geisselera et al., 2010). Similarly, hydrogen cyanide is a secondary metabolite that can be used to manage weeds biologically. The ability of HCN to block essential metalloenzymes, such as cytochrome c oxidase, impacts its toxicity (Alori and Babalola, 2018). In the current study, both PGPR isolates can synthesize siderophore, ammonia, and hydrogen cyanide.

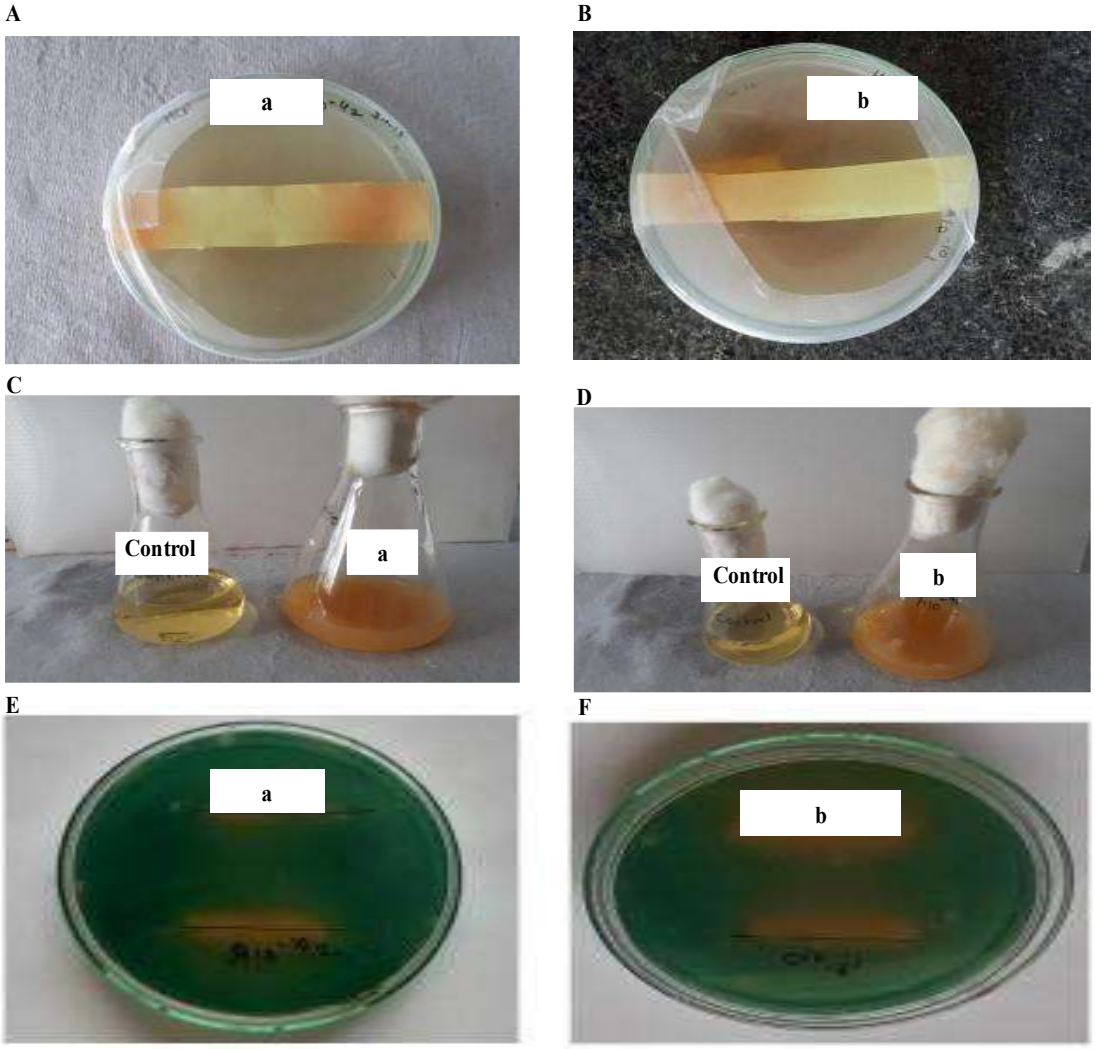

Fig. 4.1.4: A, B are HCN production, C, D are Ammonia production and E, F are Siderophore production by *E. acetylicum* RGK (a) and *E. mori* RGK1(b) respectively after 48 hrs of incubation.

4.1.3.6 Exopolysaccharide Production and Salt tolerance

After 72 hours, isolates were able to produce exopolysaccharides in the minimal medium. Asp-A and Asp-B were two of the six isolates that produced exopolysaccharides. Datarepresents in (Table 4.1.2). Earlier reports revealed that, exopolysaccharides generated by PGPR have been proven to impact plant growth and drought tolerance significantly. Exopolysaccharides have important roles in microbial aggregation, surface adhesion, desiccation resistance, plant-microbe interaction, and bioremediation (Khan and Bano, 2019).

In the presence of NaCl, six out of twenty bacteria showed a 3 % salt tolerance

capacity. Asp-A, on the other hand, could withstand up to a 5% salt concentration, whereas Asp-B could tolerate up to a 6% salt concentration. The trend indicates that these PGPR grows in high salt concentrations or high ionic strength environments and may provide salt tolerance to the host. Salt tolerance by endophytic plant growth promoting bacteria also reported by (Heydarian et al., 2018). Treatments with salt-tolerant PGPR like *B. pumilus* and *E. oxidotolerans* can be an effective approach in increasing biomass production and saponin levels in medicinal plants like *B. monnieri*, reported by (Bharti et al., 2013)

4.1.3.7 Biochemical Characterization and Identification of isolates

The most efficient plant growth-promoting rhizobacterial isolates were Asp-A (*E. acetylicum* RGK) and Asp-B (*E. mori* RGK1) (Table 4.1.3) summarizes the biochemical profile of the isolates. 16S rRNA sequencing analysis identified the isolates as *E. acetylicum* RGK and *E. mori* RGK1**.** (Fig. 4.1.5) shows the evolutionary tree of both the organisms.

Table 4.1.3: Biochemical characters of *Exiguobacterium acetylicum* RGK (Asp-A) and *Enterobacter mori* RGK1(Asp-B).

Biochemical activity	***Exiguobacterium acetylicum* RGK**	***Enterobacter mori* RGK1**
Gram nature	Gram positive	Gram negative
Glucose	+	+
Sucrose	+	+
Fructose	+	-
Maltose	+	-
Lactose	-	-
Starch utilization	-	-
Catalase	+	-
Gelatin hydrolysis	+	-
Raffinose utilization	-	+
Nitrate reduction	-	-

Citrate utilization	+	-
Urease	+	-
Oxidase	+	-
Salinity tolerance	5	6

+ present, - absent

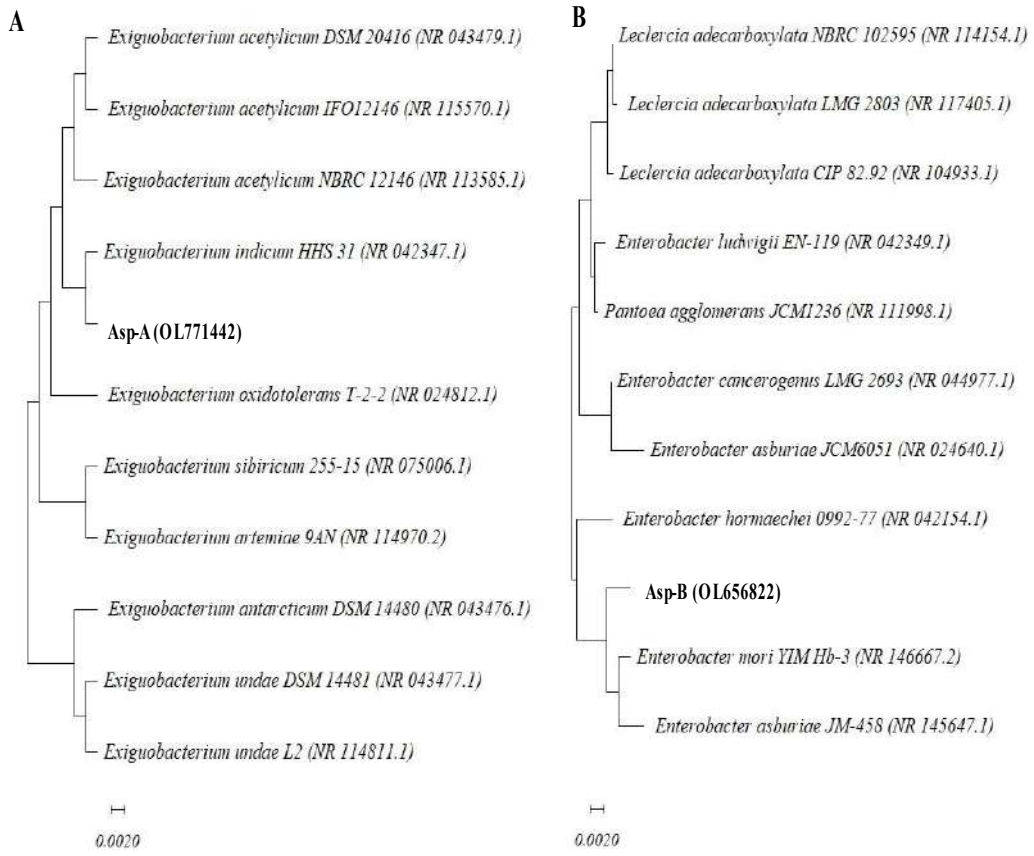

Fig. 4.1.5: Neighbor-joining phylogenetic tree based on16S rRNA gene sequence of the closely related isolates of (A) *Exiguobacterium acetylicum* RGK (B) *Enterobacter mori* RGK1, bootstrap values on each branch point indicates 1000 pseudo replicates.

4.1.4. Conclusions:

The current study involved the screening, isolation, and characterization of PGPR from the Asparagus plant's rhizosphere. By using the 16s rRNA method, the isolates were identified as *Exiguobacterium acetylicum* strain RGK and *Enterobacter mori* strain RGK1. The results of this study showed that the bacteria *Exiguobacterium acetylicum* RGK and *Enterobacter mori* RGK1 possess a variety of traits that aid in plant growth, such as the ability to solubilize phosphate, zinc and potassium, produce auxin, HCN, and ammonia, synthesize siderophores, and have a high tolerance to salt. The PGPR are appealing as biofertilizers and biopesticides as well as a cost-effective solution to sustainable agriculture. PGPR protects plants from phytopathogens and helps them grow and perform better. Although chemical fertilizers and pesticides are useful and practical for managing diseases and producing plants, they are hazardous to the environment, soil, plants, and human health. As a result, using these PGPR isolates as an inoculant can promote plant development. In conclusion, these PGPR could also be used as a biofertilizer in the future.

4.2 Impact of plant growth promoting rhizobacteria *Exiguobacterium acetylicum* RGK and *Enterobacter mori* RGK1 on secondary metabolites of *Asparagus racemosus*

Manuscript under preparation:

4.2.1 Introduction:

A significant variety of bacterial species have been investigated and proved to be advantageous to crop quality, plant growth, and yield, largely from the plant rhizosphere. These bacteria are referred to as Plant growth promoting rhizobacteria (PGPR) (Adnezhad et al., 2016). Rhizospheric bacteria that promote plant growth, including associative and symbiotic bacteria such as *Azotobacter* sp., *Alcaligenes* sp., *Azospirillum* sp., *Arthrobacter* sp., *Pseudomonas*sp., *Burkholderia* sp., *Klebsiella* sp., *Enterobacter* sp., and *Rhizobium* sp. (Mitra et al., 2016). Furthermore, some rhizospheric bacteria can induce plant growth by synthesizing plant growth promoting compounds like plant hormones or accelerating the uptake of specific nutrients from the environment like phosphorus, potassium, or nitrogen, which may help the plant fight pathogens (Lastra et al., 2021). They are also involved in a variety of key ecosystem processes (Adnezhad et al., 2016). PGPR has also proven to be an effective in addressing salinity and drought. The soil structure is altered by PGPR, which includes the growth of bacteria like *Azospirillum, Bacillus* sp., and *Pseudomonas*, as well as the production of EPS, which accumulates qualities that aid in the easy absorption of minerals and water (Kumar et al., 2022).

Asparagus racemosus is a member of the Asparagaceae family, often known as Shatavari. It is a woody climber that can reach heights of 1-2 metres. It is a popular herb in conventional medicine since steroidal saponins and sapogenins can be detected in many parts of the plant. (Jediya et al. 2022). The root of *A. racemosus* has numerous medicinal characteristics, according to the research of ancient classical Ayurvedic literature, and has been specifically indicated in situations of imminent abortion and as a galactagogue (Alok et al., 2013). It also has nutritive, anti-stress, antioxidant, antiulcer, antidiabetic, adaptogenic, anabolic, and immunomodulatory properties andis used in a variety of medicinal preparations have been reported (Sairam et al., 2003).

Asparagus is associated with several types of PGPR, which affect plant development directly or indirectly. The findings of various researchers demonstrated the ability of PGPR to actas a positive regulator. Under water-stressed conditions, seeds treated with PGPR produced excellent results in a variety of crop plants, including chickpea, maize, and asparagus (Umair et al., 2018). Similarly, *B. subtilis* PMB-034 was effective in controlling Fusarium wilt of asparagus bean and promoting crop growth (Ha et al., 2008). In addition to that vermicompost, have been shown to improve plant growth,

yields and germination, in greenhouse crops reported by Edwardsand Burrows, (1988).

The current study aimed to isolate and characterize potent PGPR from the Asparagus plant's rhizosphere, as well as to investigate the effects of their treatment on the growth parameters and biochemical content of Asparagus, both individually and in co-culture.

4.2.2 Materials and method:

4.2.2.1 Materials

Chemicals and solvents of the analytical grade were bought from Hi Media Laboratories in Mumbai, India. A standard diosgenin sample (20-100µg/ml) was prepared in methanol. Then, it was filtered using a 0.2 m Millipore filter that was obtained from Sigma Aldrich (Bangalore, India) to get rid of contaminants. For the pot culture experiments, 2 months old planlets of Asparagus were obtained from agriculture field at Sarud, Dist. Kolhapur, Maharashtra, India.

4.2.2.2 Screening and identification of PGPR

4.2.2.2.1 Sample collection and Screening of PGPR

For the current study, 20 soil samples were collected from Asparagus rhizospheres in Kolhapur and Satara districts of Maharashtra. The samples were brought to the lab for PGPR isolation in sterile polypropylene bags. For the purpose of enrichment, 100 ml of sterile nutrient broth were added to Erlenmeyer flasks containing 1 gm of soil from each sample. The flasks were then shaken at 120 rpm for 24 hrs at room temperature (27°C±2). In order to produce well-isolated colonies, the enriched samples were serially diluted in sterile distilled water. Then, 0.1 ml of each dilution was spread on sterile nutrient agar plates, and the plates were incubated for 24 hours at room temperature (27°C±2). After incubation well isolated colonies were obtained. To get pure cultures well isolated and pigmented colonies were selected and streaked over the same media. All bacterial isolates were stored at 4°C and phenotypic characterization was performed by examining their morphological, cultural, and biochemical properties according to Bergey's Manual of Determinative Bacteriology (Holt et al., 1994; Ahmad et al., 2008; Santoyo et al., 2021). The 16SrRNA gene sequence analysis was used to confirm the identification.

4.2.2.2.2 Genotypic identification of PGPR

The standard phenol/chloroform extraction procedure was used to extract the genomic DNA of potent PGPR, and universal primers 16F27 [5'-

CCAGAGTTTGATCMTGGCTCA G-3'] and 16R1492 [5'-TACGGYTACCTTGTTACGACTT-3'] were used for amplification of the 16S rRNA genes. After the amplification 16S rRNA gene, PCR products were purified using PEG-NaCl precipitation, and they were sequentially sequenced using an ABI®3730XL automated DNA sequencer (Applied Biosystems, Inc., Foster City, CA) in accordance with the manufacturer's instructions. The Lasergene package was used for assembly, and the EzBioCloud database was used for identification (Yoon et al., 2017). The obtained sequences were processed and searched using the Nucleotide Basic Local Alignment Search Tool (BLAST) programme to determine which sequences matched the results at the National Centre for Biotechnology Information (NCBI) BLAST server. (www.ncbi.nlm.nih.gov/BLAST). Multiple sequence alignment was performed using CLUSTALW software (Thompson et al., 1997) on the sequences that showed >98% resemblance. The phylogenetic tree was built using Mega X software(Tamura et al., 2021).

4.2.2.2.3 Plant growth promoting attributes of isolates

Bacterial isolates were examined for the growth promoting attributes such phosphate solubilization (Pikovskaya, 1948), zinc solubilization (Shakeel et al., 2015), Indole acetic acid (IAA) production (Bric et al., 1991), potassium solubilization (Mahadevamurthy et al., 2016), nitrogen fixation (Dashti et al., 1998), siderophore production (Louden et al., 2011), hydrogen cyanide (HCN) production (King and Weinhold, 1995), ammonia production (Cappuccino and Sherman, 1992), exopolysaccharide production (Nicolaus et al., 1999). Enzyme production in the isolates, including those of amylase, cellulase, and chitinase, was also examined. The ability of isolates to tolerate salt was tested using various NaCl concentrations (Tirry et al., 2021).

4.2.2.3 Antibiotic sensitivity test

Antibiotic impregnated paper disc diffusion method in seeded agar medium was used to test the antibiotic sensitivity of the bacterial isolates to drugs like Amikacin, Netilin, Co-trimaxazole, Streptomycin, Furazolidone, Kanamycin, Nalidixic acid, Nitrofurantoin, Tobramycin, Oxytetracyclin, Chloramphenicol, and Gentamycin (Barale et al., 2022). After an incubation period at room temperature (27^0C), plates were observed for zones of inhibition. The organisms were classified as resistant or sensitive based on the size of the zone of inhibition.

4.2.2.4 Pot culture experiment

4.2.2.4.1 Inoculum preparation

1 gm of carboxy methyl cellulose (adhesive), 10^8 CFU/ml of bacterial suspension, 1% glucose, and 0.5% NaCl were added into 90 ml of sterile distilled water to make the inoculum. Asparagus roots were surface sterilized with 70% alcohol and rinsed with sterile distilled water five to six times. The roots were then covered with inoculum and sown in pots containing natural and sterile soil each (Kumar et al., 2016).

4.2.2.4.2 Method of inoculation

The 2-month-old, healthy Asparagus plantlets were thoroughly cleaned with sterile distilled water at least 5 times, and they were surface sterilized with 70% ethanol 4 to 5 times. Before being sown in pots, the roots were kept in inoculum for 2 to 3 hours. The experiment was conducted in pots that were filled with sterile and naturally occurring soil that had been air-dried and sieved. The pots were arranged in naturalistic settings in a random pattern with 72 repetitions (36 for each treatment with natural soil and 36 for each treatment with sterile soil with corresponding controls), and they were periodically irrigated. Using a randomized block design (RBD), the experiment was run in triplicate to investigate the impact of treatment of both- the individual isolates and their co-culture. Four types of treatments were given to the rhizome before sowing-

T1 : Treatment with *Exiguobacterium acetylicum* RGK

T2: Treatment with *Enterobacter mori* RGK1

T3: Co-culture of *Exiguobacterium acetylicum* RGK and *Enterobacter mori* RGK1

T4: Control (Uninoculated)

The morphological parameters of plants were examined at 45, 90 and 180 days of sowing as perthe earlier report (Ambardar & Vakhlu, 2013).

4.2.2.5 Extraction and purification of secondary metabolites from Asparagus

In order to extract secondary metabolites, Asparagus plants were taken away from the pots after 45, 90, and 180 days. The roots were thinly sliced, dried at 40ºC in the oven, and then crushed into a fine powder. After adding 1 gm of sample to 10 ml of methanol in a sealed tube, the mixture was treated for 1 hour at room temperature in a bath sonicator. It was then centrifuged for 10 minutes at 5000 rpm and 4°C. For further analysis, supernatant was collected.

For purification 5 gm of Asparagus plant powder was hydrolysed in 50 ml of 2 M sulphuric acid by heating under refluxation for 2 hrs. 40% sodium hydroxide was used to neutralize the solution once it had cooled. Following hydrolysis, the product was extracted using an equal amount of chloroform (Wang et al., 2011; Yang et al., 2015). The extract was concentrated by evaporating it at 60°C after being separated using a separating funnel. The residue was dissolved in methanol and utilized for TLC on precoated silica gel with the standards, and the product was quantified using RP-HPLC.

4.2.2.6 Phytochemical analysis of Asparagus root extract

The Folin Ciocalteu reagent test (Lamuela-ravents, 1999) was used to assess the total phenolic content (TPC), using gallic acid as a standard. The measurement was given in mg gallic acid equivalents (GAE)/g of dry weight. Using rutin as a standard, the total flavonoid content (TFC) was calculated and represented as mg rutin equivalents (RE)/g dry weight (Zhishen et al., 1999). The capacity of each sample to scavenge free radicals in the presence of DPPH was also examined (Surveswaran et al., 2007).

4.2.2.7 Separation, detection and quantification of phytocompounds

Metabolites were separated using pre-coated silica gel thin layer chromatography (TLC) plates (Merck, Darmstadt, Germany). Samples were spotted on the plate, processed in a TLC chamber using hexane-acetone (8:2) as the mobile phase with a few minor modifications, dried to make sure all solvents had evaporated, and detected with a 0.5:5 mixture of ethanol (8% vanillin) and sulfuric acid solution (70%) and the RF values of metabolites were determined (Hardman, 1968). After that, the metabolites were recognized and quantified using HPLC on the methanolic extracts as well as GC-MS/MS analysis of the samples.

4.2.2.8 GC-MS / MS analysis of extracts

Samples were analyzed using GC-MS/MS utilizing GCMS-TQ8050Plus with HS 20 (SHIMADZU, Japan) that was outfitted with an MS detector. Helium was employed as a carrier gas at a flow rate of 1 ml per minute in a SH -Rxi - 5Sil MS column (30 mm × 0.25 mm ID × 0.25 µm). Method: Q3, scan, range: m/z 45–600, 1 µl sample was injected at 250°C, interphase temperature: 290°C, ion source temperature: 280°C, oven temperature: 50°C to 275°C, and GC running time: 52 min. The National Institute of Standards and Technology (NIST) Database was used to identify the metabolites.

4.2.2.9 Reverse phase high performance liquid chromatographic (RP-HPLC) analysis of diosgenin

JASCO's RP-HPLC system, which includes a quaternary pump, autosampler, and UV detector, was used to purify and measure diosgenin. As previously described (Schieffer, 2002), diosgenin purification was performed on a semi-preparative scale Hiber C25 column (250 4.6 mm, 5 m). With a flow rate of 0.8 ml/min and a total injection volume of 25 µl, the mobile phase was composed of acetonitrile and HPLC-grade water in a ratio of 10:90 (v/v). A UV detector detected the diosgenin at 194 nm. The linearity range of standards is determined by the standard diosgenin. Test solutions containing (20–100 µg/ml of standard diosgenin) have been prepared and injected three times as part of the linearity test. Diosgenin's correlation value (R2) was 0.9945.

4.2.2.10 Statistical analysis

The results were presented as mean values ± SD. Graph pad Prism version 5 software was used to do analysis of variance (ANOVA) techniques in order to detect variation differences. Tukey's comparison test showed significance at $p \leq 0.05$.

4.2.3 Results and discussion:

4.2.3.1 Phenotypic characterization and identification of PGPR

From the diverse soil samples, 20 different bacterial isolates were obtained. Based on their capacities to promote plant growth, 2 notable isolates were chosen for phenotypic characterization and identification. One of them was Gram negative and the other was Gram positive, both of them were rod-shaped and demonstrated the biochemical traits that are previously listed in Table 4.1.3 of Chapter 4.1. Based on 16S rDNA sequence analysis, they were identified as strains of *Exiguobacterium acetylicum* and *Enterobacter mori* and named *Exiguobacterium acetylicum* RGK and *Enterobacter mori* RGK1. The sequences has been deposited in the NCBI GenBank database under the accession numbers **OL771442** and **OL656822**, respectively (Fig. 4.1.5 from chapter 4.1). In the current investigation, strains of *Enterobacter mori* RGK1 and *Exiguobacterium acetylicum* RGK have been identified from the Asparagus rhizosphere to have the ability to promote plant growth. According to previous reports, PGPR produces a variety of vital metabolites for plants that support nutrient uptake and general plant vigour (Jabborova et al., 2020). In earlier investigations, plant growth-promoting *Enterobacter* spp. have been found in the rhizosphere of the Asparagus plant (Plate et al., 2010). Similarly,

Exiguobacterium spp. were isolated from the medicinal plant *Bacopa monnieri* (Bharti et al., 2013). These two PGPR strains were chosen based on a variety of their PGPR characteristics.

4.2.3.2 Plant growth promoting attributes of isolates

As mentioned in Chapter 4.1, these two isolates exhibited the highest levels of plant growth promoting properties such as phosphate solubilization, potassium solubilization, zinc solubilization, nitrogen fixation, indole acetic acid (IAA) production, hydrogen cyanide (HCN) production, ammonia production, siderophore production and exopolysaccharide synthesis. These isolates showed negative result for amylase and chitinase production where cellulase production was shown by *Exiguobacterium* spp. They were both resistant to salt concentration. *Exiguobacterium acetylicum* RGK tolerated up to 5.00% NaCl, while *Enterobacter mori* RGK1 tolerated up to 6.00% NaCl.

Many other studies have shown that PGPR has the ability to dissolve phosphorus, zinc, and potassium (Soto et al., 2019; Bagyalakshmi et al., 2017; Shakeel et al., 2015). Phosphate solubilization by numerous *Exiguobacterium* and *Enterobacter* species has also been documented (Saengsanga, 2018; Rajendran et al., 2012). Similar to phosphorus, potassium is a crucial macronutrient, and Meena et al. (2016) found that solubilizing potassium by PGPR improves plant development in a variety of commercial crops. According to Parveen et al. (2018), zinc also contributes to the metabolism of plants by acting as a cofactor in several enzyme activities.

In this work, both rhizobacteria strains synthesize siderophores and generate IAA when tryptophan is present. According to Kumari et al. (2018), IAA synthesis stimulates root system expansion and lengthening, which facilitates water and nutrient uptake. Our results are in line with earlier research which shows that PGPR, including *Exiguobacterium, Enterobacter, Pseudomonas,* and *Bacillus* can synthesizes IAA and siderophores (Lopez et al., 2019; Emmert & Handelsman, 1999; Rajendran et al., 2012). Both of the PGPRs used in this study are capable of fixing nitrogen and producing ammonia and HCN. Devi et al. (2022) claim that PGPR can produce siderophores, ammonia, and HCN, as well as able to fix nitrogen.

Both isolates in this investigation produced exopolysaccharides, which may be crucial for desiccation resistance, plant-microbe interactions, bioremediation and microbial aggregation. Under drought stress conditions, it has been shown that

inoculating plants with EPS-producing bacterial strains increases soil moisture content, leaf area, root and shoot length, plant biomass, and the amount of protein and sugar in the leaves (Naseem et al., 2014; Khan et al.,2017). Additionally, the salt tolerance of *Exiguobacterium acetylicum* RGK and *Enterobacter mori* RGK1 was up to 5% and 6%, respectively. Salinity is one of the most detrimental abiotic variables impacting crop development and output. Plant characteristics like root and shoot growth drought tolerance, and germination rate, are all enhanced by PGPR under salt stress. Previously, it was shown that plants exposed to salt were protected by PGPR, such as *Bacillus* sp. and *Pseudomonas* sp. (Chauhan et al., 2017).

4.2.3.3 Antibiotic sensitivity test

Results showed that both isolates were sensitive to Gentamycin, Kanamycin, Streptomycin, Tobramycin, furazolidone, Nalidixic acid, Co-trimoxazole and Amikacin where *Enterobacter mori* RGK1 resistant to nitrofurantoin. As listed in Table 4.2.1, *Exiguobacterium acetylicum* RGK showed 19 ±0.07mm, 19 ±0.05mm, 11 ±0.05mm, 21 ±0.07mm, 24 ±0.07mm, 17 ±0.07mm, 25 ±0.05mm, 17 ±0.04mm zone of inhibition respectively. In contrast, *Enterobacter mori* RGK1 showed 35 ±0.05mm, 23 ±0.07mm, 20 ±0.05mm, 6 ±0.04mm, 15 ±0.02mm, 2 ±0.08mm, 22 ±0.03mm, 30 ±0.07mm respectively. However, *Enterobacter mori* RGK1 was resistant to Nitrofurantoin (Saengsanga, 2018)

Table 4.2.1: Antibiotic resistivity of isolated PGPR strains against standard antibiotics and zone of inhibition (mm) given below

Antibiotics	***Exiguobacterium acetylicum* RGK**	***Enterobacter mori* RGK1**
Streptomycin	11 ± 0.05	20 ± 0.05
Oxytetracyclin	27 ± 0.06	30 ± 0.07
Gentamycin	19 ± 0.07	35 ± 0.05
Furazolidone	24± 0.07	15 ± 0.02
Co-trimoxazole	25 ± 0.05	22 ± 0.03
Amikacin	17 ± 0.04	30 ± 0.07
Tobramycin	21 ± 0.07	6 ± 0.04

Nitrofurantoin	19 ± 0.03	-
Kanamycin	19 ± 0.05	23 ± 0.07
Nalidixic acid	17 ±0.07	20±0.08

4.2.3.4 Pot culture experiment

A study on pot cultivation was conducted to determine the individual effect and the function of these PGPR in co-culture as well. The results showed that the co-culture's effect is superior to the individual application. Furthermore, the effect was more significant in natural soil than in sterile soil. Table 4.2.2a, 4.2.2b, and 4.2.2c show that after 45, 90, and 180 days of treatment, plants treated independently with *Exiguobacterium acetylicum* RGK, *Enterobacter mori* RGK1, and co-culture of both showed progressive increases in the shoot height, root number, and root biomass as compared to the control.

Previous research found that inoculating pea seeds with *Exiguobacterium* in pot trial conditions improved germination and growth parameters (Mishra et al., 2009). Similarly, co- inoculation of *Exiguobacterium* strains with *Trigonella foenum-graecum* promoted plant growth in terms of increased chlorophyll content, nodulation efficiency, root and shoot length, and noduledry weight (Rajendran et al., 2012). As with earlier research, *Enterobacter* could be used as a plant growth promoter to enhance crop production and yield. In addition to increasing plant growth, these bacteria were discovered to be antagonistic to plant pathogens (Lopez et al., 2019; Saengsanga, 2018). Similarly, inoculation with PGPR enhance seedling germination in asparagus reported by Liddycoat et al. (2009).

4.2.3.4.1 Effect on shoot height

E. acetylicum RGK, had shown the increment as 54, 102 and 109 % after 45, 90 and 180 days respectively in natural soil, while in sterile soil it showed the increment as 33, 82 and 105 % after same interval of days. Similarly, *E.mori* RGK1 it showed the increase in shoot height by 33, 54 and 79 % after 45, 90 and 180 days in natural soil. While in sterile soil it showed 15, 46 and 64 % of rise in the shoot height. Similarly, in case of treatment with co-culture of these PGPRs(*E.mori* RGK1+ *E. acetylicum* RGK) it showed the increase in the shoot height after 45, 90 and180 days as 120, 128 and 135% in natural soil while in sterile soil it showed as 106, 123 and 130 % increase after 45, 90 and 180 days when compared with its control (Table 4.2.2a).

4.2.3.4.2 Effect on root number

E. acetylicum RGK, had shown the enhanced root number after 45, 90 and 180 days as 35, 47 and 50% respectively in natural soil while in sterile soil it showed the increment as 33, 45 and57% after 45, 90 and 180 days. Similarly in case of treatment with *E.mori* RGK1 showed increament on the root number by 32, 35 and 39 % after 45, 90 and 180 days in natural soil. Whilein sterile soil it showed 22, 26 and 38 % increase in the root number. When Asparagus plant treated with co-culture of these PGPRs (*E.mori* RGK1 + *E. acetylicum* RGK) it showed increased root number after 45, 90 and 180 days as 58, 60 and 72% in natural soil while in sterile soil it showed as 53, 55 and 71 % increase after 45, 90 and 180 days when compare with its control (Table 4.2.2b).

4.2.3.4.3 Effect on root biomass

In case of treatment with *E. acetylicum* RGK, it showed the increment as 30, 35 and 56 % after 45, 90 and 180 days respectively in natural soil, while in sterile soil it showed the incrementas 25, 27 and 46 % after same interval of days, that is 45, 90 and 180. Similarly, *E.mori* RGK1, had shwon the increment in root biomass by 15, 17 and 37 % after 45, 90 and 180 days in naturalsoil, while in sterile soil it showed 12, 14 and 23 % of increase in the root biomass. When a Asparagus plant treated with co-culture of these PGPRs (*E.mori* RGK1+ *E. acetylicum* RGK) it showed the increased in root biomass after 45, 90 and 180 days as 54, 73 and 106% in natural soilwhile in sterile soil it showed as 50, 71 and 92 % increase after 45, 90 and 180 days when comparewith its control (Table 4.2.2c).

4.2.3.5 Phytochemical analysis of Asparagus extract

The phytochemical analysis of Asparagus extract is provided in Table 4.2.3a, 4.2.3b, 4.2.3c, and 4.2.3d in terms of total phenolic content (TPC) in mg/gm, total flavonoid content (TFC) in mg/gm, total saponin (SAP) mg/gm, and DPPH radical scavenging activity in percent inhibition. It reveals that after 45, 90, and 180 days the co-culture treated plants had higher phenolic, flavonoid, and saponin contents than the untreated plants. Furthermore, all of the samples demonstrated strong DPPH-targeting free radical scavenging activity. After 180 days, plants treated with individual PGPRs and co-cultures of PGPRs in natural soil showed higher TPC, TFC, SAP, and DPPH levels.

In the current investigation, we discovered that bacterial co-culture treatment raises the levels of total phenolic content, flavonoid content, saponin content, DPPH

radical scavenging, and diosgenin content. After 180 days, the combination of these PGPR enhanced the phenolic and flavonoid contents of natural and sterile soil by 31.6% and 27.1%, respectively, and by 46.2% and 42.8%, respectively. After 180 days, a co-culture treatment in natural and sterile soil revealed increased saponin content by 132% and 104.7%. The co-cultured plants showed increased antioxidant activity of between 55% and 36.6% in both types of soil.

According to Mitra et al. (2016), PGPR treatment increased phenolic content in *A.racemosus* (Mitra et al., 2016). There are a few reports on saponin content enhancement by PGPR. One of them is increased saponin content in *B. monnieri* plants after treatment with *Exiguobacterium oxidotolerans* (Bharti et al., 2013). Similarly, Jain et al. (2014) reported that the total phenolic and flavonoid content was increased in pea plants by *T. harzianum*, *P. aeruginosa*, and *B. subtilis*, both individually and in combination (Jain et al., 2014). Dobosz et al. (2011) reported an increase in *A officinalis* antioxidant capacity after fusarium treatment (Doboszet al., 2011). In the same way, Liu et al. (2018) reported increased antioxidant activity after treatment with single and consortium PGPR (Liu et al., 2018).

Table 4.2.2a: Shoot height of Asparagus after inoculation with PGPR

Parameter	Shoot height (cm) after 45, 90 and 180 days											
	Control			*E. acetylicum* RGK			*E.mori* RGK1			Co-culture of both these PGPR		
	Days			Days			Days			Days		
	45	90	180	45	90	180	45	90	180	45	90	180
Natural soil	20.83 ±0.6	22.5 ±0.4	45.9 ±0.9	32.17 ±0.8	45.5 ±0.4	96.33 ±3.9	27.83 ±0.2	34.83 ±0.6	82.67 ±2.5	45.83 ±2.3	51.5 ±1.8	108 ±4.3
Sterile soil	11 ±0.8	18.6 ±1.2	31 ±0.8	14.6 ±0.4	34 ±0.8	63.6 ±1.7	12.6 ±1.7	27.3 ±1.2	51 ±0.8	22.6 ±2.4	41.6 ±1.2	71.3 ±2.6
% Increase over control(N)	-	-	-	54	102	109	33	54	79	120	128	135
% Increase over control (S)	-	-	-	33	82	105	15	46	64	106	123	130

(N)=natural soil (S)=sterile soil. The values represent the average of three experiments ± SD. ANOVA using Tukey's comparison test yielded a significant difference from control group at $p \leq 0.05$, and the relative standard deviation for all values are less than 10

Table 4.2.2b: Root number of Asparagus after inoculation with PGPR

Parameter	Root number after 45, 90 and 180 days											
	Control			*E.acetylicum* RGK			*E.mori* RGK1			Co-culture of both these PGPR		
	Days			Days			Days			Days		
	45	90	180	45	90	180	45	90	180	45	90	180
Natural soil	5.67 ±0.4	11.83 ±1.3	18 ±0.4	7.6 ±0.6	17.5 ±1.8	27 ±1.6	7.5 ±0.4	15.1 ±0.8	25 ±1.3	9 ±0.4	19 ±2.1	31 ±0.8
Sterile soil	4.5 ±0.4	10.3 ±0.3	14 ±0.8	6 ±0.4	15 ±0.4	22 ±0.8	5.5 ±0.4	13 ±0.8	19 ±0.4	6.9 ±0.04	16 ±0.8	24 ±1.4
% Increase over control (N)	-	-	-	35	47	50	32	35	39	58	60	72
% Increase over control (S)	-	-	-	33	45	57	22	26	38	53	55	71

(N)=natural soil (S)=sterile soil. The values represent the average of three experiments ± SD. ANOVA using Tukey's comparison test yielded a significant difference from control group at $p \leq 0.05$, and the relative standard deviation for all values are less than 10.

Table 4.2.2c: Root biomass of Asparagus after inoculation with PGPR

Parameter	Root biomass (gm) after 45, 90 and 180 days											
	Control			*E. acetylicum* RGK			*E.mori* RGK1			Co-culture of both these PGPR		
	Days			Days			Days			Days		
	45	90	180	45	90	180	45	90	180	45	90	180
Natural soil	0.13 ±0.01	2.3 ±0.1	16 ±0.1	0.17 ±0.01	3.12 ±0.01	25 ±0.2	0.15 ±0.04	2.7 ±0.02	22 ±0.3	0.2 ±0.01	4 ±0.13	33 ±0.2
Sterile soil	0.08 ±0.08	1.57 ±0.04	13 ±0.1	0.1 ±0.01	2 ±0.02	19 ±0.2	0.09 ±0.01	1.80 ±0.08	16 ±0.1	0.12 ±0.05	2.7 ±0.03	25 ±0.2
% Increase over control(N)	-	-	-	30	35	56	15	17	37	54	73	106
% Increase over control (S)	-	-	-	25	27	46	12	14	23	50	71	92

(N)=natural soil (S)=sterile soil. The values represent the average of three experiments ± SD. ANOVA using Tukey's comparison test yielded a significant difference from control group at $p \leq 0.05$, and the relative standard deviation for all values are less than 10.

Table 4.2.3a: Total phenolic content of Asparagus plant inoculated with PGPR

	Phenolic content after 45, 90 and 180 days											
	Control			***E. acetylicum* RGK**			***E. mori* RGK1**			**Co-culture of both these PGPR**		
	Days			**Days**			**Days**			**Days**		
	45	**90**	**180**	**45**	**90**	**180**	**45**	**90**	**180**	**45**	**90**	**180**
Natural soil	3.46 ±0.02	4.60 ±0.04	5.32 ±0.01	3.7 ±0.01	5.1 ±0.07	6.1 ±0.09	3.5 ±0.01	4.9 ±0.06	5.7 ±0.09	3.8 ±0.05	5.9 ±0.01	7 ±0.02
Sterile soil	3.6 ±0.02	4.5 ±0.02	5.2 ±0.03	3.2 ±0.02	4.8 ±0.04	6 ±0.02	3.1 ±0.03	4.6 ±0.01	5.7 ±0.07	3.3 ±0.01	5.9 ±0.03	6.6 ±0.09
% Increase over control(N)	-	-	-	8	11.3	15.1	3.18	6.5	7.3	12.4	30	31.6
% Increase over control(S)	-	-	-	4.5	8.2	14	1.3	3.7	9.5	9.4	13.1	27.1

(N)=natural soil (S)=sterile soil. The values represent the average of three experiments ± SD. ANOVA using Tukey's comparison test yielded a significant difference from control group at $p \leq 0.05$, and the relative standard deviation for all values are less than 10.

Table 4.2.3b: Total flavonoid content of Asparagus plant inoculated with PGPR

	Flavonoid content after 45, 90 and 180 days											
	Control			***E. acetylicum* RGK**			***E. mori* RGK1**			**Co-culture of both these PGPR**		
	Days			**Days**			**Days**			**Days**		
	45	**90**	**180**	**45**	**90**	**180**	**45**	**90**	**180**	**45**	**90**	**180**
Natural soil	8.92 ±0.05	26.6 ±0.3	40 ±0.01	11.1 ±0.04	33.5 ±0.07	52.3 ±0.02	10 ±0.05	30.5 ±0.1	46 ±0.02	12 ±0.04	37.5 ±0.03	58.5 ±0.02
Sterile soil	6.6 ±0.03	20 ±0.02	35 ±0.05	8.2 ±0.03	24 ±0.09	43 ±0.02	7.2 ±0.05	22.2 ±0.1	40 ±0.01	8.2 ±0.03	27.2 ±0.02	50 ±0.03
% Increase over control(N)	-	-	-	24.8	25.5	30.7	12.1	14.2	15	34.5	40.5	46.2
% Increase over control (S)	-	-	-	23.8	20	22.8	8.7	11.5	14.2	24.3	36	42.8

(N)=natural soil (S)=sterile soil. The values represent the average of three experiments ± SD. ANOVA using Tukey's comparison test yielded a significant difference from control group at $p \leq 0.05$, and the relative standard deviation for all values are less than 10.

Table 4.2.3c: Total saponin content of Asparagus plant inoculated with PGPR

	Saponin content after 45, 90 and 180 days											
	Control			***E. acetylicum* RGK**			***E. mori* RGK1**			**Co-culture of both these PGPR**		
	Days			**Days**			**Days**			**Days**		
	45	**90**	**180**	**45**	**90**	**180**	**45**	**90**	**180**	**45**	**90**	**180**
Natural soil	84 ±0.08	100 ±0.02	115 ±0.05	92 ±0.3	132 ±0.3	158 ±1.2	89 ±0.2	118 ±0.03	140 ±0.1	100 ±0.4	189 ±0.4	267 ±2.1
Sterile soil	71 ±0.03	89 ±0.02	105 ±0.05	76 ±0.03	112 ±0.09	130 ±0.02	74 ±0.05	100 ±0.1	123 ±0.01	79 ±0.03	135 ±0.02	215 ±0.03
% Increase over control(N)	-	-	-	9.5	32	37.3	5.9	18	21.7	19	89	132
% Increase over control(S)	-	-	-	7.4	25.8	23.8	4.2	12.3	17.1	11.2	51.6	104.7

(N)=natural soil (S)=sterile soil. The values represent the average of three experiments ± SD. ANOVA using Tukey's comparison test yielded a significant difference from control group at $p \leq 0.05$, and the relative standard deviation for all values are less than 10.

Table 4.2.3d: Percent inhibition for DPPH activity of Asparagus plant inoculated with PGPR

	Percent inhibition for DPPH activity after 45, 90 and 180 days											
	Control			***E. acetylicum* RGK**			***E.mori* RGK1**			**Co-culture of both these PGPR**		
	Days			**Days**			**Days**			**Days**		
	45	**90**	**180**	**45**	**90**	**180**	**45**	**90**	**180**	**45**	**90**	**180**
Natural soil	25.2 ±0.06	30.7 ±0.04	38.2 ±0.14	28.7 ±0.01	36.02 ±0.04	48.5 ±0.01	28.3 ±0.06	35.9 ±0.1	45 ±0.07	29.3 ±0.04	36.2 ±0.06	59.5 ±0.07
Sterile soil	22.16 ±0.03	31.84 ±0.04	37.73 ±0.1	25 ±0.04	35 ±0.05	47.3 ±0.07	24 ±0.06	34 ±0.01	42 ±0.07	25 ±0.06	36 ±0.06	51 ±0.05
% Increase over control(N)	-	-	-	14.11	17.02	25.52	12.5	16.73	18	16.13	17.8	55
% Increase over control (S)	-	-	-	12.8	12.7	26.3	8.3	9.8	13.91	14.1	13.1	36.6

(N)=natural soil (S)=sterile soil. The values represent the average of three experiments ± SD. ANOVA using Tukey's comparison test yielded a significant difference from control group at $p \leq 0.05$, and the relative standard deviation for all values are less than 10

4.2.3.6 Separation and purification of PGPR induced phytocompounds

Diosgenin was purified using acid hydrolysis followed by solvent extraction. The obtained sample was evaporated and dissolved in methanol before being used for additional analyses such as TLC, GC-MS/MS, and RP-HPLC. The TLC profile revealed that the extracted compound matched with the standard diosgenin band on the pre-coated TLC silica-gel plate with an Rf value of 0.49. Similarly, GC-MS/MS results revealed that when Asparagus extracts were compared to untreated controls, the percent area of diosgenin in co-culture treated plants increased(5.71% area). Table 4.2.4 showed the GC-MS/MS identification of the compounds using the Wiley- NIST database based on retention time, peak area, molecular mass, and molecular formula. Fig.4.2.1. Previous research has also shown that acid hydrolysis followed by extraction in non-polar solvents yields a higher yield than traditional methods (Yang et al., 2016)**.** Similarly, in an earlier study of phytochemical analysis, a GC-MS based method was used to analyze *Asparagus racemosus* (Janani and Singaravadivel, 2014).

4.2.3.7 HPLC for diosgenin

Diosgenin was isolated from *A. racemosus* root by acid hydrolysis and analyzed with HPLC-UV detection. The retention time was noted at 17 min, and UV absorption of diosgenin occurs at 194 nm. Table 4.2.5 shows the concentrations of diosgenin after 45, 90, and 180 days and HPLC chromatograms are given in Fig. 4.2.2 Quantification of diosgenin was performed by using HPLC UV detection. Asparagus plant treated with *E. acetylicum* RGK had shown the enhanced diosgenin content after 45, 90 and 180 days as 0.05, 0.09 and 0.15 % respectively in natural soil while in sterile soil it showed the increment as 0.05, 0.09 and 0.13 % after 45, 90 and 180 days respectively. Further, treatment with *E. mori* RGK1 had shown the increment on the diosgenin content by 0.04, 0.09 and 0.12 % after 45, 90 and 180 days respectively in natural soil. While in sterile soil it showed 0.04, 0.09 and 0.11 % of the increase in the diosgenin content after 45, 90 and 180 days respectively. When an Asparagus plant treated with co-culture of these PGPRs (*E. acetylicum* RGK + *E. mori* RGK1) it showed the increased diosgenin content after 45, 90 and 180 days as 0.06, 0.09, and 0.28 % respectively in natural soil while in sterile soil it showed as 0.06, 0.09 and 0.19 % increase after 45, 90 and 180 days when compared with its control. An earlier study reported that the quantification of diosgenin was performed by using HPLC (Peiqin Li,2012).

Table 4.2.5: Diosgenin content after 45, 90 and 180 days

	Diosgenin content in percentage (%)					
	45 days		**90 days**		**180 days**	
	Natural soil	**Sterile soil**	**Natural soil**	**Sterile soil**	**Natural soil**	**Sterile soil**
Control	0.02	0.02	0.08	0.07	0.11	0.10
***E. acetylicum* RGK**	0.05	0.05	0.09	0.09	0.15	0.13
***E. mori* RGK1**	0.04	0.04	0.09	0.09	0.12	0.11
Co-culture of these PGPR	0.06	0.06	0.09	0.09	0.28	0.19

Table 4.2.4: Secondary metabolite profile identified by GC-MS/MS from PGPR treated Asparagus

Sr. No.	Name of Identified Compounds	Category	Retention time	Area%	Control	*Exiguobacterium acetylicum* RGK	*Enterobacter mori* RGK1	Co-culture of both PGPR
1	n-Hexadecanoic acid	Fatty acid	31.35	4± 21*	+	+	+	+
2	9,12-Octadecadienoic acid (Z,Z)-, methyl este	Fatty acid	34.89	5± 29.09*	+	+	+	-
3	Octadec-9-enoic acid	Fatty acid	48.24	7.24	+	-	+	+
4	Glycidyl palmitate	Fatty acid	38.01	0.2± 2.77*	+	+	+	-
5	n-Propyl 9,12-octadecadienoate	Fatty acid	33.68	0.71± 1.80*	+	-	+	-
6	Methyl 3-cis,9-cis,12-cis-octadecatrienoate	Fatty acid	41.08	1.10	-	+	-	+
7	Glycidyl oleate	Fatty acid	41.17	0.14± 2.77*	+	+	+	-
8	Glycidyl palmitate	Fatty acid	41.62	0.24± 3.78*	+	+	+	-
9	Butyl 9,12,15-octadecadienoate	Fatty acid	41.08	1.87	-	-	-	+
10	2,2-Dimethoxybutane	Alkane	3.2	0.37± 3.75*	-	+	+	+

11	Bicyclo[2.2.1]heptan-2-ol, 1,7,7-trimethyl-, (1S	Fatty acid	13.57	0.19± 1.19*	-	+	+	-
12	5-Hydroxymethylfurfural	furans	16.09	4.7 ± 55.41*	+	+	-	+
13	Oleic Acid	Fatty acid	35.01	0.66± 2.90	-	+	+	-
14	Octadecanoic acid	Fatty acid	35.55	0.7± 2.4	-	+	+	-
15	1,3-Propanediol, 2-(hydroxymethyl)-2-nitro-	Fatty acid	22.05	8± 26	-	+	-	+
16	Glycidol stearate	Fatty acid	41.64	0.83	-	-	-	+
17	Methyl 3-cis,9-cis,12-cis-octadecatrienoate	***methyl*** ester fatty acid	41.08	1.10	-	+	-	-
18	Sucrose	Disaccharide	49.25	73.69	-	+	-	-
19	Diosgenin	Saponin	44.09	1.27± 5.71*	-	+	-	+

Note: + denotes present, - denotes absent, *Exiguobacterium acetylicum* RGK+, Co-culture of both PGPR*

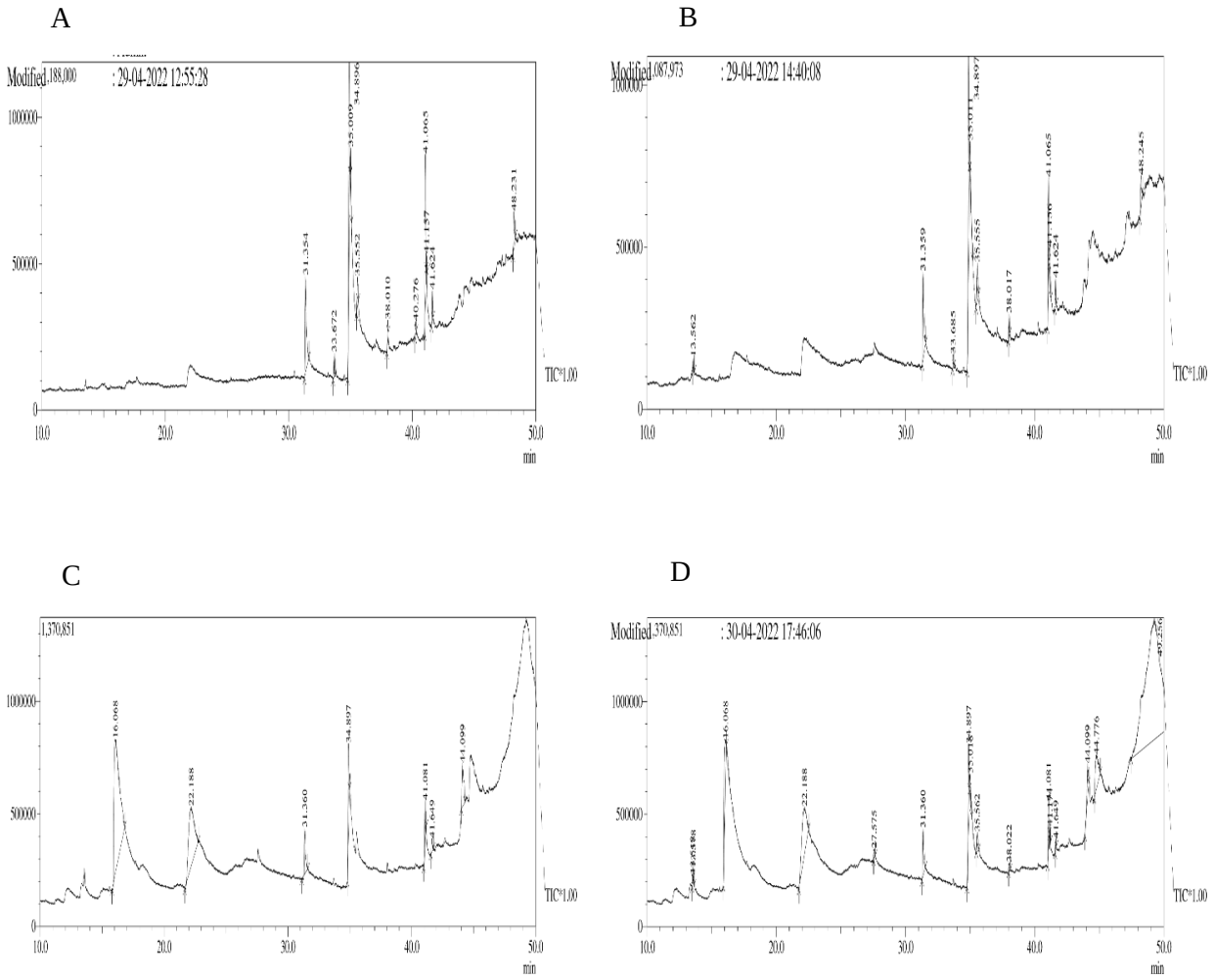

Fig.4.2.1: The gas chromatography–tandem mass spectrometry graph with various peaks of Asparagus where (a) Chromatogram of control Asparagus (uninoculated) (b) Chromatogram of *Enterobacter mori* RGK1 inoculated Asparagus (c) Chromatogram of *Exiguobacterium acetylicum* RGK inoculated Asparagus (d) Chromatogram of co-culture of both inoculated Asparagus

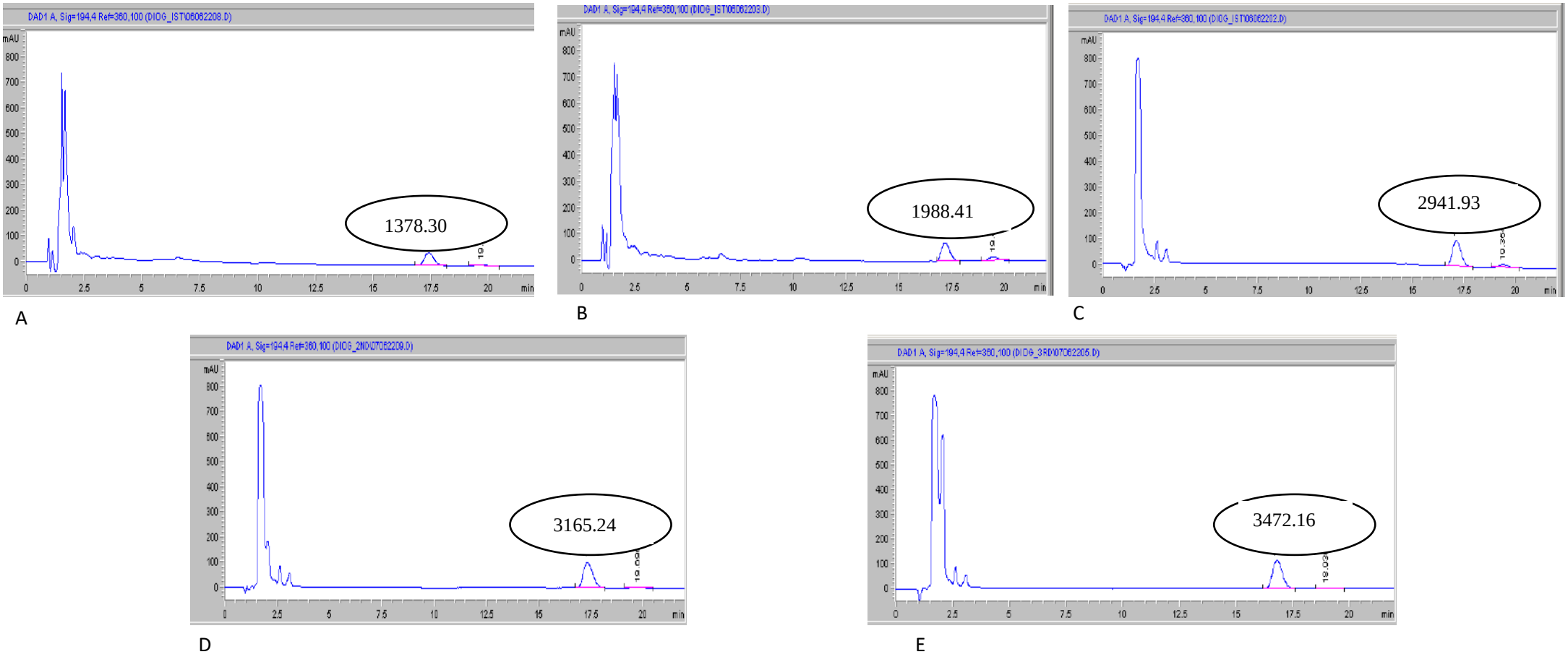

A B C D E

Fig.4.2.2: HPLC chromatogram of purified diosgenin at 194 nm. (A) Chromatogram of standard of diosgenin. (B) Chromatogram of control Asparagus (uninoculated). (C) Chromatogram of *Enterobacter mori* RGK1 inoculated Asparagus. (D) Chromatogram of *Exiguobacterium acetylicum* RGK noculated Asparagus. (E) Chromatogram of co-culture inoculated Asparagus

4.2.4 Conclusions:

In the present investigation, we found that PGPR treatment improved plant metrics and phytocompounds. Additionally, co-culture inoculations yielded better outcomes than a single inoculation. Furthermore, these findings reveal that the amount of phenolic compounds, flavonoids, and saponins has a positive relationship with anti-radical activities, meaning that the bioinoculants used on the Asparagus rhizosphere are effective. In the future, these phytocompounds could be employed as an effective treatment for a variety of diseases and therapeutic formulations, either alone or in combination with other relevant agents. This PGPR co-culture inoculation would be one of the best alternatives for a long-term Asparagus agroindustry.

The fundamental benefit of utilizing PGPR is that they have a twofold positive impact, working as both a full biofertilizer and a plant biofortifier, addressing nutritional shortages as well as agro-environmental concerns. In natural soil rather than sterile soil, we detected better plant metrics and phytocompounds in Asparagus after PGPR inoculation, both individualy and in co-culture. Although there have been a few publications on the presence of diosgenin in *A. racemosus* roots, we are the first to indicate that co-culture treatment increases diosgenin concentration in *A. racemosus* roots.

4.3 Impact of plant growth promoting rhizobacteria *Serratia nematodiphila* RGK and *Pseudomonas plecoglossicida* RGK on secondary metabolites of turmeric rhizome

The part of this study Published as:

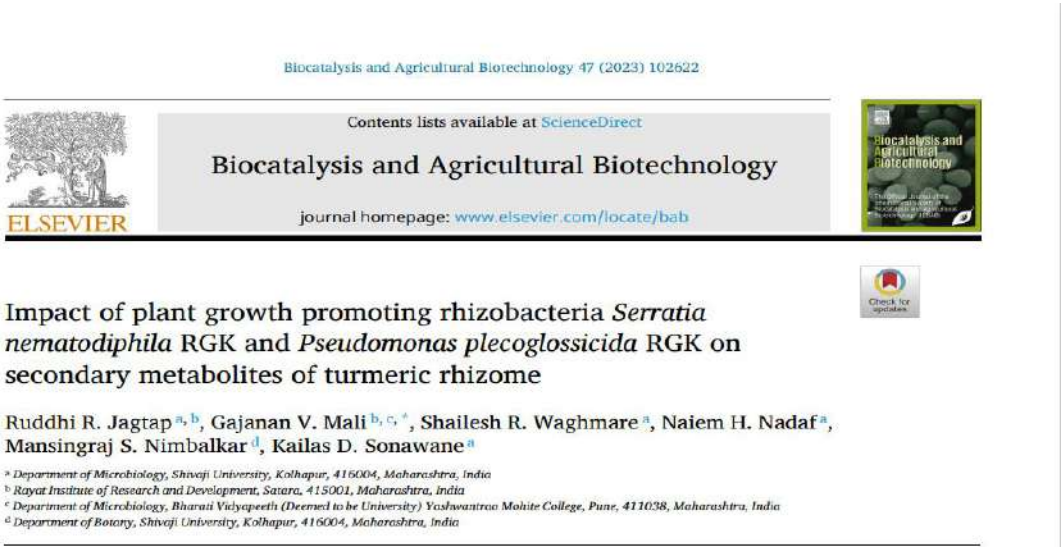

Biocatalysis and Agricultural Biotechnology 47 (2023) 102622

Contents lists available at ScienceDirect

Biocatalysis and Agricultural Biotechnology

journal homepage: www.elsevier.com/locate/bab

Impact of plant growth promoting rhizobacteria *Serratia nematodiphila* RGK and *Pseudomonas plecoglossicida* RGK on secondary metabolites of turmeric rhizome

Ruddhi R. Jagtap [a, b], Gajanan V. Mali [b, c, *], Shailesh R. Waghmare [a], Naiem H. Nadaf [a], Mansingraj S. Nimbalkar [d], Kailas D. Sonawane [a]

[a] Department of Microbiology, Shivaji University, Kolhapur, 416004, Maharashtra, India
[b] Rayat Institute of Research and Development, Satara, 415001, Maharashtra, India
[c] Department of Microbiology, Bharati Vidyapeeth (Deemed to be University) Yashwantrao Mohite College, Pune, 411038, Maharashtra, India
[d] Department of Botany, Shivaji University, Kolhapur, 416004, Maharashtra, India

4.3.1 Introduction:

Plant growth-promoting rhizobacteria (PGPR) are naturally existing soil bacteria that colonize plant roots actively and promote plant growth. Plant growth, plant health, soil fertility,carbon sequestration and phytoremediation are aided by these microbiomes colonizing the soiland plant surfaces (Adamczyk et al., 2019). These organisms are primarily associated with plant roots and help them to grow (Kloepper & Beauchamp, 1992). PGPR has recently become a viable approach considering its potential to produce essential phytohormones such as indoleacetic acid, gibberellic acid, cytokines, ethylene, and siderophores (Bharucha et al., 2013; Lotfiet al., 2022). PGPRs are also employed in the treatment of garbage (Yuan et al., 2020). Their ability to produce biofilms aids in their survival under stressful situations (Ansari et al., 2021).Moreover, some PGPR have demonstrated their ability to degrade pesticides (Rani et al., 2021). They also can withstand abiotic stress, which has beneficial impact on plant growth characteristics (Prasad, 2018). They are utilized as biofertilizers in many countries due to their capacity to solubilize potassium and zinc, and their usage is both environmentally and economically acceptable (Dhaked et al., 2017a). For decades, PGPR has piqued curiosity due to their multifunctional activities. They exhibit chemotactic behavior, as well as antagonism and synergism, with plant roots (Santoyo et al., 2021: Chauhan et al., 2021). Bacteria produceexopolysaccharides as well as function as a biocontrol agent (Chenniappan et al., 2019; Mohammed, 2018). *Bacillus subtilis*, one of the PGPR, is also recognized for its quorum sensing ability (Rosier et al., 2021).

Turmeric (*Curcuma longa*), a medicinally valuable plant, is a member of the *Zingiberaceae* family. It is a perennial spice with palmate leaves arranged alternately in two rows and an aromatic rhizome that is yellow to orange in color (Baranska et al., 2004). The rhizome includes a variety of secondary metabolites, the most common are curcuminoids, which are phenolic chemical compounds (Kumar et al., 2014). It is primarily well known for its therapeutic value. Even though curcumin has a long scientific history, it continues to attract scientist's interest.

Turmeric is associated with a number of PGPR, which influences plant development through direct or indirect mechanisms (Kumar et al., 2016). *Agrobacterium, Alcaligenes, Arthrobacter, Azotobacter, Azospirillum, Bacillus, Burkholderia, Enterobacter, Klebsiella, Pseudomonas,* and *Serratia* are the most

prevalent PGPR associated with turmeric (Kumar et al., 2018). Through an induced systemic resistance mechanism, PGPR increases secondary metabolites in plants. PGPR's synthesizes enzymes and secondary metabolites essential for the host's defence mechanisms (Kavitha et al., 2012). Many researchers have explored several biotechnological applications of PGPR. It includes an increase in the concentration of curcumin after treatment of *Pseudomonas fluorescens* and *Bacillus megaterium* (Boominathan and Sivakumaar, 2012). The co-culture application of PGPR is also more efficient than a single one(Kumar et al., 2019).

The current research work was undertaken with the objective of isolation and characterization of potent PGPR from the rhizosphere of the Turmeric plant and to investigate the effects of their treatment on the growth parameters and biochemical content of turmeric, both individually and in combination.

4.3.2 Material and method:

4.3.2.1 Materials

Analytical grade solvents and chemicals were purchased from Hi Media Laboratories, (Mumbai, India). A standard sample of curcumin was prepared in methanol (100-500µg/ml). To remove impurities, it was then filtered using a 0.2 µm Millipore filter obtained from SigmaAldrich (Bangalore, India). For the pot culture experiments, turmeric rhizomes of the Salem variety were obtained from Turmeric Research Department of Mahatma Phule Krishi Vidyapeeth's Agriculture Research Station at Kasabe Digraj, Dist. Sangli, Maharashtra, India.

4.3.2.2 Screening and identification of PGPR

4.3.2.2.1 Sample collection and Screening of PGPR

20 soil samples were obtained from Tumeric rhizospheres in Kolhapur, Sangli, andSatara districts of Maharashtra for the current study. Among them, five were from Kolhapur, eleven from Sangli while four were from Satara districts. The samples were transported to the laboratory in sterile polypropylene bags for the isolation of PGPR. 1 gm of soil from each sample was then transferred to Erlenmeyer flasks having 100 ml of sterile nutrient broth and shaken at 120 rpm for 24 hours at room temperature (270C±2) for enrichment. Serial dilutions of the enriched samples were carried out in sterile distilled water and 0.1 ml from each dilution was spread on the sterile nutrient agar plates and kept for incubation at room temperature (270C±2) for 24 hours to get well isolated colonies. Colonies with

diverse morphologies such as size, shape, margin, elevation, consistency, opacity, surface and pigmentation were picked and streaked over the same media to obtain the pure cultures. All the isolates of bacteria were preserved at 4°C and phenotypic characterization of isolates was carried out by studying their morphological, cultural and biochemical properties as per the Bergey's Manual of Determinative Bacteriology (Holt et al.,1994; Ahmad et al., 2008). Further identification was done by 16S rRNA gene sequence analysis.

4.3.2.2.2 Genotypic identification of PGPR

The genomic DNA of potent PGPR was extracted using the conventional phenol/chloroform extraction method, and the 16S rRNA genes were amplified using universal primers 16F27 [5'-CCAGAGTTTGATCMTGGCTCA G-3'] and 16R1492 [5'-TACGGYTACCTTGTTACGACTT-3']. Following amplification, the 16S rRNA gene PCR products were purified using PEG-NaCl precipitation, and ABI®3730XL automated DNA sequencer (Applied Biosystems, Inc., Foster City, CA) was used to sequence the results sequentially in accordance with the manufacturer's instructions. The EzBioCloud database was used for identification, and the Lasergene software was used for assembly (Yoon et al., 2017). The resultant sequences were processed and searched using the Nucleotide Basic Local Alignment Search Tool (BLAST) programme to determine which sequences matched the ones at the National Centre for Biotechnology Information (NCBI) BLAST server (www.ncbi.nlm.nih.gov/BLAST). For the sequences with >98% similarity, multiple sequence alignment was carried out using the CLUSTALW programme (Thompson et al., 1997). Using the neighbour joining approach and the Mega XI version of the distance matrix alignment tool (Tamura et al., 2021) with two different bootstrap values (*Serratia nematodiphila* RGK 0.50, and *Pseudomonas plecoglossicida* RGK 0.0010), the phylogenetic tree was constructed.

4.3.2.2.3 Plant growth promoting attributes of isolates

Bacterial isolates were screened for the growth promoting attributes such as Indole acetic acid (IAA) production (Bric et al., 1991), phosphate solubilization (Laslo et al., 2012), zinc solubilization (Saravanan et al., 2004)**,** potassium solubilization (Dhaked et al., 2017b), nitrogen fixation (Dashti et al., 1998), hydrogen cyanide (HCN) production (Lorck, 1948), siderophore production

(Schwyn & Neilands, 1987), ammonia production (Dhaked et al., 2017a), exopolysaccharide production (Naseem & Bano, 2014). The isolates were also checkedfor synthesis of enzymes such as chitinase, cellulase and amylase. Salinity tolerance of isolates was checked by using different concentrations of NaCl (Tirry et al., 2021).

4.3.2.3 Antibiotic sensitivity test

The bacterial isolates were tested for their sensitivity to the antibiotics such as Gentamycin, Amikacin, Kanamycin, Streptomycin, Netilin, Tobramycin, Co-trimaxazole, Furazolidone, Oxytetracyclin, Nitrofurantoin, Chloramphenicol and Nalidixic acid using antibiotic impregnated paper disc diffusion method in seeded agar medium (Barale et al., 2022). Plates were examined for zones of inhibition after incubation at room temperature (270C±2). Based on the diameter of zone of inhibition, the organisms were categorized as resistant or sensitive.

4.3.2.4 Antifungal activity

In vitro antifungal activity of bacterial isolates against fungal pathogen of Turmeric wastested. The pathogen was *Pythium aphanidermatum*, isolated and identified in the laboratory from naturally infected Turmeric plants (Kavitha et al., 2012). The bacterial isolates were streaked at one side of the potato dextrose agar medium in petri dish, and a mycelial disc (8 mm diameter) of five days old culture of *Pythium aphanidermatum* was put at the other side (Kavitha et al., 2010). The plates were incubated at room temperature (27 ±2°C) for 4 days andthe zone of inhibition was measured.

4.3.2.5 Pot culture experiment

4.3.2.5.1 Inoculum preparation

For the treatment of rhizomes, inoculum of each isolate was prepared in medium containing 1% activated charcoal powder, 1% glucose, and 0.5% NaCl. The cell density was adjusted to 10^8 CFU/ml as per MacFarland's standard (Teles et al., 2019)

4.3.2.5.2 Method of inoculation

The young and healthy rhizomes Salem variety were surface sterilized with 70% ethanol (4-5 times) and completely rinsed with sterile distilled water at least

five times. The rhizomes were kept in an inoculum for 2 to 3 hrs before sowing in pots. Experiment was carried out in pots filled with air dried and sieved natural as well as sterile soil. The pots were placed randomly with 72 repeats (36 for each treatment with natural soil and 36 for each treatment with sterile soil with their respective controls) in naturalistic environments and periodically irrigated. The experiment was performed in triplicate using a randomized block design (RBD) to examine the effects of treatment of both - the individual isolates and their co-culture. Four types of treatments were given to the rhizome before sowing -

T1 : Treatment with *Serratia nematodiphila* RGK

T2 : Treatment with *Pseudomonas plecoglossicida* RGK

T3 : Co-culture of *Serratia nematodiphila* RGK and *Pseudomonasplecoglossicida* RGK

T4 : Control (Uninoculated)

The morphological parameters of plants were examined at 45, 90 and 180 days of sowing as per the earlier report (Ambardar & Vakhlu, 2013).

4.3.2.6 Extraction of secondary metabolites from Turmeric

Rhizomes were uprooted from pots after 45, 90, and 180 days and cleaned to extract secondary metabolites. They were sliced into tiny pieces, dried in the oven at 40ºC and grindedto obtain a fine powder. The powder was used to extract secondary metabolites by an ultrasound assisted extraction procedure using methanol as a solvent. In this, 100 mg of dried rhizome powder was mixed with 10 ml of methanol in screw cap tube. The tubes were incubated at room temperature for 60 minutes in an ultrasonic clean bath (230 Volts, 50 Hz, Rivotek, RivieraGlass Pvt. Ltd., Mumbai, India). After centrifuging the solution for 10 minutes at 4500 rpm, the supernatant was recovered and evaporated to concentrate the sample. To evaluate secondary metabolite concentration, 2 ml methanol was added to dissolve the sample. Then, the samples were filtered through a 0.2 µm (Millipore) filter to eliminate contaminants before being used (Zhang et al., 2008).

4.3.2.7 Phytochemical analysis of Turmeric extract

Total phenolic content (TPC) was determined utilizing the Folin Ciocalteu reagent assay (Lamuela-ravents, 1999) using gallic acid as a standard and was

represented in mg gallic acid equivalents (GAE)/g dry weight. Using rutin as a standard, total flavonoid content (TFC)was calculated and reported as mg rutin equivalents (RE)/g dry weight (Zhishen et al., 1999). All the samples were also examined for their ability to scavenge free radicals in the presence of DPPH (Surveswaran et al., 2007).

4.3.2.8 Separation, detection and quantification of secondary metabolites

Pre-coated silica gel thin layer chromatography (TLC) plates were used to separate metabolites (Merck, Darmstadt, Germany). After saturation with mobile phase vapors for 1 hour, samples were spotted on the plate and processed in a TLC chamber with chloroform- methanol-formic acid (96:4:0.8 v/v/v) as a solvent system in a 20×20 cm glass (Borosil) flat bottom chamber. After the development of yellow colour spots, it was retrieved, air dried and the RF values of metabolites were determined. The metabolites were subsequently detected and quantified using HPLC on the methanolic extracts as well as GC-MS/MS analysis of samples were done.

4.3.2.9 GC-MS / MS analysis of extracts

The GC-MS/MS analysis of samples was carried out using GCMS-TQ8050Plus with HS 20 (SHIMADZU, Japan) equipped with an MS detector. Column used was SH -Rxi – 5SilMS with (30 mm × 0.25 mm ID × 0.25 μm) and helium as a carrier gas with flow rate 1ml/min.1 μl sample was injected at 250℃ temperature, interphase temperature was 290℃, ion sourcetemperature was set to 280℃, the oven temperature was 50℃ to 275℃ and GC running time was 38 min, Method-Q3, scan used and range-m/z 45–600. The metabolites were identified by National Institute of Standard and Technology (NIST) Database.

4.3.2.10 Reverse phase high performance liquid chromatographic (RP-HPLC) analysis of curcumin

Curcumin was purified and quantified using an RP-HPLC system by JASCO, including a quaternary pump, autosampler, and UV detector. Curcumin purification was carried out on asemi-preparative scale Hiber C18 column (250×4.6 mm, 5 μm) as previously reported with some modifications (Schieffer, 2002). The mobile phase was 50:50 (v/v) acetonitrile and 2% acetic acid, with a 0.5 ml/min flow rate and a

total injection volume of 20 µl. The peak of curcumin was detected by a UV detector at 425 nm. The standard curcumin determines the linearity range of standards. For the linearity test, test solutions containing (100- 500 µg/ml of curcumin) were produced and injected three times. It was found with high reproducibility inthe concentration range of 2-10 µg. Curcumin's correlation value (R2) was 0.9979.

4.3.2.11 Statistical analysis

The results were expressed as the mean values ± SD. Analysis of variance (ANOVA) techniques were used to determine variation differences by using Graph pad Prism version 5 Software. Significance was determined at $p \leq 0.05$ by Tukey's comparison test.

4.3.3 Results and discussion

4.3.3.1 Phenotypic characterization and identification of PGPR

A total number of 85 isolates of bacteria were obtained from the different soil samples. Among them two prominent isolates based on their plant growth promoting attributes were selected for phenotypic characterization and identification. Both of these were Gram negative,rod shaped showing biochemical characteristics as listed in Table 4.3.1. They were identified as strains of *Serratia nematodiphila* and *Pseudomonas plecoglossicida* based on 16S rDNA sequence analysis and named as *Serratia nematodiphila* RGK and *Pseudomonas plecoglossicida* RGK. The sequences were deposited in the NCBI GenBank database under the accession numbers **MZ452064** and **OL739684**, respectively (Fig. 4.3.1). PGPR is reported to generate a variety of essential metabolites for plants, which contribute in plant nutrition and overall plant vigor (Jabborova et al., 2020). In the present study strains of *Serratia nematodiphila* and *Pseudomonas plecoglossicida* having plant growth promoting potential areconfirmed from the Turmeric rhizosphere. In earlier studies also plant growth promoting *Pseudomonas* spp. were isolated from rhizosphere of Turmeric, Tomato and Wheat plant (Ansari et al., 2021; Takishita et al., 2018) whereas *Serratia nematodiphila* were isolated from pepperand rice plant (Kang et al., 2015; Khoa et al., 2016). These two PGPR strains were selected onthe basis of their various PGPR properties.

Table 4.3.1: Biochemical properties of potent isolates

Biochemical characters	*Pseudomonas plecoglossicida* RGK	*Serratia nematodiphila* RGK
Glucose	+	+
Adonitol	+	+
Arabinose	-	+
Catalase	+	+
Oxidase	-	+
Nitrate reduction	+	+
Starch hydrolysis	+	+
Citrate utilization	+	+

Note: + denotes Positive, - denotes Negative

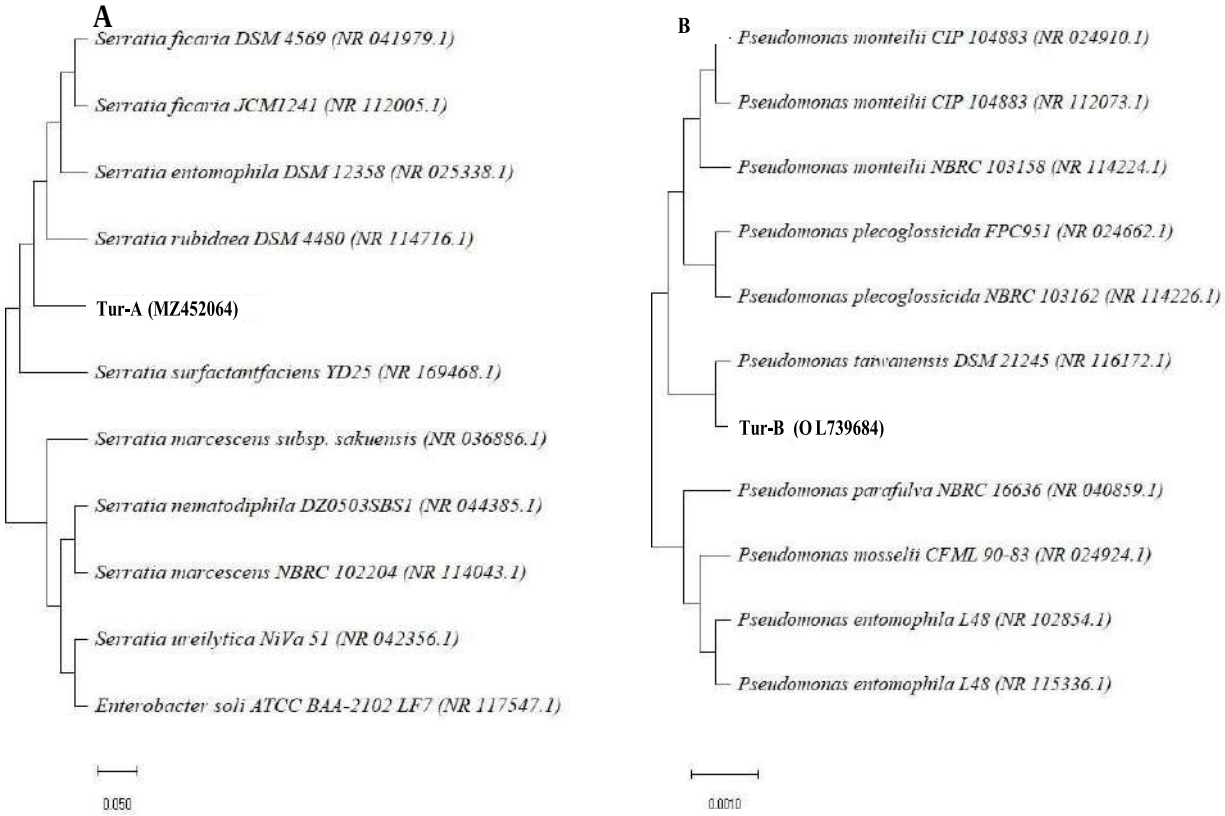

Fig. 4.3.1: Neighbor-joining phylogenetic tree based on16S rRNA gene sequence of the closelyrelated isolates of (A) *Serratia nematodiphila* RGK, (B) *Pseudomonas plecoglossicida* RGK bootstrap values on each branch point indicates 1000 pseudo replicates.

4.3.3.2 Plant growth promoting attributes of isolates

As indicated in Table 4.3.2, these two isolates showed maximum plant growth promoting characters such as phosphate solubilization, zinc solubilization, potassium solubilization, indole acetic acid (IAA) production, siderophore production, nitrogen fixation, hydrogen cyanide (HCN) production, ammonia production and exopolysaccharide synthesis. These isolates also showed amylase production, however *Serratia nematodiphila* RGK showed negative result for cellulase and chitinase production and *Pseudomonas plecoglossicida* RGK showed positive for these two enzymes production. Both of them were tolerant to high salt concentration. *Serratia nematodiphila* RGK tolerated up to 6.00% NaCl and *Pseudomonas plecoglossicida* RGK tolerated salt up to 7.00% NaCl.

Many other researchers also have demonstrated the potential of PGPR to dissolve phosphorus, potassium, and zinc (Soto et al., 2019; Bagyalakshmi et al., 2017; Shakeel et al., 2015). The solubilization of phosphate by numerous species of *Pseudomonas* and *Serratia* have also been documented (Sayyed et al., 2009; Khoa et al., 2016). Like phosphorous, potassium is also an important macronutrient, and its solubilization by PGPR enhances plant growth in anumber of commercial crops (Meena et al., 2016; Ajmal et al., 2021) has reported the solubilization of potassium by *Pseudomonas* and *Serratia*. Zinc also plays role in the plant metabolism by serving as a cofactor in number of enzyme processes (Parveen et al., 2018). Increase in zinc mobilization in wheat and soybean plants was found to be increased by treatment with *Bacillus, Pseudomonas,* and *Serratia* (Shakeel et al., 2015).

Both the strains of rhizobacteria in this work are producing IAA in the presence of tryptophan (Kumari et al., 2018) has reported the favorable impact of IAA synthesis on growthand elongation of root system, which aids in water and vital nutrients absorption. The results in our investigation are also in line with the earlier reports that shows the synthesis of IAA byPGPR such as *Serratia nematodiphila* NII-0928, *Pseudomonas* sp., *Agrobcterium tumifaciens, Burkholderia sp.,* and *Bacillus sp*. (Dastager & Ashok, 2011; Zhao et al., 2014).

Both the strains in our study are producing siderophores. Siderophores produced by rhizobacteria chelate Fe+3 and make it accessible to plants for growth. Several reports with regard to siderophore production by PGPR are well

documented. *P. fluorescence* NCIM5096 isolated from the groundnut field rhizosphere produced siderophores (Sayyed et al.,2009); *P. aeruginosa* isolated from the rhizosphere of a banana farm produced siderophore (Shaikh et al.,2014); ability of *S. nematodiphila* to produce siderophores helped to improve growth metrics of pepper plants (Kang et al.,2015).

Both the PGPRs in this work have ability to fix nitrogen as well as produce ammonia. Further *Serratia nematodiphila* RGK has the potential to produce HCN. According to Devi etal. (2022), PGPR can generate ammonia, siderophores, HCN, and N2 fixation. In one more study, bacteria isolated bacteria from the rhizosphere of the *L. hypogaea* plant were capable ofproducing HCN and fix nitrogen (Felestrino et al., 2017). Similarly, both the isolates in this study were producing exopolysaccharides, which may be crucial for bioremediation, microbialaggregation, plant-microbe interactions, and protection against desiccation. Enhanced soil moisture content, plant biomass, root and shoot length, leaf area, and leaf protein and sugar contents under drought stress conditions due to inoculation with EPS producing bacterial strains in plants such as maize and wheat is also previously reported (Naseem et al., 2014; Khanet al.,2017).

Isolates have also demonstrated enzyme synthesis which is in line with Jabborova et al., (2020) which demonstrated endophytic PGPR from ginger synthesize several enzymes. Further, *Serratia nematodiphila* RGK and *Pseudomonas plecoglossicida* RGK demonstrated up to 6% and 7% salt tolerance, respectively. Salinity is one of the most severe abiotic factors that affect crop development and yield. Under salt stress, PGPR has beneficial impacts on plant characteristics such as germination rate, drought tolerance, and root and shoot growth. Plants exposed to salt were protected by PGPR such as *Bacillus sp*. and *Pseudomonas sp*., (Chauhanet al., 2017).

Table 4.3.2: Plant growth promoting attributes of bacterial isolates

PGPR traits	***Pseudomonas plecoglossicida* RGK (OL739684)**	***Serratia nematodiphila* RGK (MZ452064)**
Phosphate solubilization	+	+
IAA production	+	+
Ammonia production	+	+
HCN production	-	+

Nitrogen fixation	+	+
Zinc solubilization	+	+
Potassium solubilization	+	+
Siderophore production	+	+
Salinity tolerance	7 %	6 %
Cellulase	+	-
Chitinase	+	-
Amylase	+	+
Exopolysaccharide production	+	+

Note: + denotes Positive, - denotes Negative

4.3.3.3 Antibiotic sensitivity test

Results showed that both isolates were sensitive to Gentamycin, Kanamycin, Streptomycin, Tobramycin and Amikacin. As listed in Table 4.3.3, *Serratia nematodiphila* RGK showed 20± 0.07mm, 24 ± 0.06mm,24 ± 0.07mm, 8 ± 0.04mm, 22 ± 0.07mm zone of inhibition respectively. In contrast, *Pseudomonas plecoglossicida* RGK showed 20 ± 0.05mm, 22 ± 0.07mm, 6 ± 0.02mm, 20 ± 0.03mm, 25 ± 0.06mm respectively. However, *Serratia nematodiphila* RGK was resistant to Oxytetracyclin, Furazolidone, Nitrofurantoin, and *Pseudomonas plecoglossicida* RGK shown resistance to Nitrofurantoin, Co-trimoxazole, Nalidixic acid. According to some previous reports, *Pseudomonas* and *Serratia* were likewise susceptible to the aforementioned drugs (Singh & Jha,2016; Capatina et al., 2022).

Table 4.3.3: Antibiotic resistivity of isolated PGPR strains against standard antibiotics andzone of inhibition (mm) given below

Antibiotics	***Pseudomonas plecoglossicida* RGK**	***Serratia nematodiphila* RGK**
Streptomycin	6 ± 0.02	24 ± 0.07
Oxytetracyclin	18 ± 0.07	-
Gentamycin	20 ± 0.05	20 ± 0.07
Furazolidone	15 ± 0.04	-
Co-trimoxazole	-	18 ± 0.05

Amikacin	25 ± 0.06	22 ± 0.07
Tobramycin	20 ± 0.03	8 ± 0.04
Nitrofurantoin	-	-
Kanamycin	22 ± 0.07	24 ± 0.06
Nalidixic acid	-	29 ± 0.07

4.3.3.4 Antifungal activity

As regard to the antifungal activity, fungistatic action was seen as a zone of growth inhibition in the area of the agar plate with bacterial inoculation. *Pseudomonas plecoglossicida* RGK shown antifungal activity against the fungus *Pythium aphanidermatum* while *Serratia nematodiphila* RGK doesn't showed it. *Pythium aphanidermatum* fungus, is responsible for rhizome rot of Turmeric. According to earlier study numerous species of *Pseudomonas* and *Serratia* have been demonstrated to exhibit antagonistic behavior towards different fungi and bacteria (Kumari et al., 2018; Passari et al., 2018; Khoa et al., 2016).

4.3.3.5 Pot culture experiment

Pot culture study was performed to determine the individual effect and the role of these PGPR in co-culture as well, and results revealed that the effect of co-culture is better than the individual application. Further, the effect was more in the natural soil than sterile soil. As demonstrated in Table 4.3.4a, 4.3.4b, 4.3.4c, rhizomes treated separately with *S. nematodiphila* RGK, *P. plecoglossicida* RGK and co-culture of both demonstrated progressive increase in the shoot height, leaf number, and rhizome biomass as compared to the control after45, 90 and 180 days. However, only the results after 180 days are described below.

The co-culture of *Serratia nematodiphila* RGK and *Pseudomonas plecoglossicida* RGK considerably increased the plant parameters in the pot culture experiment, and it was more than either strain alone and uninoculated control in both natural and sterile soil. Kumar et al., (2016) found that treatment with *P. fluorescens* CL12 improved plant development metrics including shoot height, leaf number, rhizome biomass, and curcumin content in *Curcuma longa*. Inoculation with diazotroph bacterial suspension (1:1 ratio of *Pseudomonas* and *Bacillus* sp.)

demonstrated considerable improvement in rhizome production (21%), plant height (5%), rhizome weight (60%) and soil microbial population over respective controls by (Suryadevara and Ponmurugan,2012) in natural soil. In another study it is found that when *Azotobacter, Bacillus, and Pseudomonas* were co-inoculated on a maize crop rather than whenthey were inoculated separately, the consortium significantly increased the dry weight of the maize (0.50 g plant-1) (Jarak et al., 2012). Under the pot culture experiment and field circumstances, the microbial consortia significantly affected the physiological and growth characteristics of the *Amaranthus* crop, as reported by Devi et al., (2022). As per the literature and practical investigations, combined inoculation produces successful outcomes when thereis a synergistic link between the microorganisms.

4.3.3.5.1 Shoot height

S. nematodiphila RGK had shwon the increament in shoot height by 61, 83 and 85 % after 45, 90 and 180 days in natural soil. While in sterile soil it showed 46, 80 and 81 % of rise in the shoot height. Similarly in case of treatment with *P. plecoglossicida* RGK the increment was 74, 90 and 95 % after 45, 90 and 180 days respectively in natural soil, while in sterile soil it showed the incerement as 65, 86 and 90 % after same interval of days. When a Turmeric plant treated with co-culture of these PGPRs (*S. nematodiphila* RGK + *P. plecoglossicida* RGK) it showed the increased in shoot height after 45, 90 and 180 days as 97, 110 and 116% in natural soil while in sterile soil it showed as 84, 100 and 113 % increase after 45, 90 and 180 days when compare with its control (Table 4.3.4a)

4.3.3.5.2 Leaf number

As regard to the leaf number, treatment with *S. nematodiphila* RGK showed the increment by 40, 46 and 60 % after 45, 90 and 180 days in natural soil. While in sterile soil it showed 25, 37.5 and 46 % of increase in the leaf numbers. Similarly in case of treatment with *P. plecoglossicida* RGK, it showed the enhanced leaves number after 45, 90 and 180 days as 32, 60 and 79% respectively in natural soil while in sterile soil it showed the increment as 25, 50 and 70 % after 45, 90 and 180 days. When a Turmeric plant treated with co-culture of these PGPRs (*S. nematodiphila* RGK + *P. plecoglossicida* RGK) it showed the increased leaves

number after 45, 90 and 180 days as 60, 66 and 114% in natural soil while in sterile soil it showed as 50, 62.5 and 106 % increase after 45, 90 and 180 days when compare with its control (Table 4.3.4b)

4.3.3.5.3 Rhizome biomass

In contrast, *S. nematodiphila* RGK had shown the increament in rhizome biomass by 29, 48 and 78 % after 45, 90 and 180 days in natural soil. While in sterile soil it showed 25, 45 and 56 % of increase in the rhizome biomass. Similarly in case of treatment with *P. plecoglossicida* RGK, it showed the increment as 41, 73 and 105 % after 45, 90 and 180 days respectively in natural soil, while in sterile soil it showed the increase as 37, 62 and 88 % after same interval of days, that is 45, 90 and 180. When a Turmeric plant treated with co-culture of these PGPRs (*S. nematodiphila* RGK + *P. plecoglossicida* RGK) it showed the increased in rhizome biomass after 45, 90 and 180 days as 76, 130 and 208 % in natural soil while in sterile soil it showed as 87, 127 and 188 % increase after 45, 90 and 180 days when compare with its control (Table 4.3.4c).

Table 4.3.4a: Shoot height of Turmeric after inoculation with PGPR

Parameter	Shoot height (cm) after 45, 90 and 180 days											
	Control			*S. nematodiphila* RGK			*P. plecoglossicida* RGK			Co-culture of both these PGPR		
	Days			Days			Days			Days		
	45	90	180	45	90	180	45	90	180	45	90	180
N	22.83 ±0.13	47.33 ±0.5	60.5 ±0.3	36.83 ±0.13	87 ±0.86	112 ±0.4	39.83 ±0.1	90.24 ±1.02	118 ±0.23	45 ±0.4	99.5 ±0.4	131 ±0.7
S	19.83 ±0.14	43 ±0.8	47 ±0.8	29 ±0.8	77.5 ±0.8	85.4 ±0.4	32.83 ±0.1	80 ±0.4	89.5 ±0.4	36.5 ±0.4	86.3 ±0.6	100 ±0.4
% Increase over control(N)	-	-	-	61	83	85	74	90	95	97	110	116
% Increase over control (S)	-	-	-	46	80	81	65	86	90	84	100	113

N (natural soil) S (sterile soil). The values represent the average of three experiments ± SD. ANOVA using Tukey's comparison test yielded a significant difference from control group at $p \leq 0.05$, and the relative standard deviation for all values are less than 10.

Table 4.3.4b: Leaf number of Turmeric after inoculation with PGPR

Parameter	Leaf number after 45, 90 and 180 days											
	Control			*S. nematodiphila* RGK			*P. plecoglossicida* RGK			Co-culture of both these PGPR		
	Days			Days			Days			Days		
	45	90	180	45	90	180	45	90	180	45	90	180
N	2.5 ±0.4	5 ±0.4	6 ±0.4	3.5 ±0.4	7.3 ±0.6	9.6 ±0.2	3.3 ±0.2	8 ±0.4	12.5 ±0.5	4 ±0.4	8.3 ±0.2	15 ±0.4
S	2 ±0.4	4 ±0.3	5 ±0.4	2.5 ±0.2	5.5 ±0.4	7.3 ±0.2	2.5 ±0.4	6 ±0.4	8.5 ±0.6	3 ±0.7	6.5 ±0.1	10.3 ±1.2
% Increase over control (N)	-	-	-	40	46	60	32	60	79	60	66	114
% Increase over control (S)	-	-	-	25	37.5	46	25	50	70	50	62.5	106

N (natural soil) S (sterile soil). The values represent the average of three experiments ± SD. ANOVA using Tukey's comparison test yielded a significant difference from control group at $p \leq 0.05$, and the relative standard deviation for all values are less than 10.

Table 4.3.4c: Rhizome biomass of Turmeric after inoculation with PGPR

Parameter	Rhizome biomass (gm) after 45, 90 and 180 days											
	Control			*S. nematodiphila* RGK			*P. plecoglossicida* RGK			Co-culture of both these PGPR		
	Days			Days			Days			Days		
	45	90	180	45	90	180	45	90	180	45	90	180
N	0.17 ±0.08	1.3 ±0.04	3.8 ±0.08	0.22 ±0.08	1.93 ±0.08	5.51 ±0.008	0.24 ±0.008	2.2 ±0.8	6.33 ±0.01	0.3 ±0.08	3 ±0.08	9.5 ±0.4
S	0.08 ±0.05	0.77 ±0.08	2.23 ±0.4	0.1 ±0.02	1.12 ±0.01	3.5 ±0.4	0.1 ±0.05	1.2 ±0.2	4.21 ±0.2	0.15 ±0.05	1.75 ±0.08	6.43 ±0.4
% Increase over control(N)	-	-	-	29	48	78	41	73	105	76	130	208
% Increase over control (S)	-	-	-	25	45	56	37	62	86	87	127	188

N (natural soil) S (sterile soil). The values represent the average of three experiments ± SD. ANOVA using Tukey's comparison test yielded a significant difference from control group at $p \leq 0.05$, and the relative standard deviation for all values are less than 10

4.3.3.6 Phytochemical analysis of Turmeric extract

In terms of total phenolic content (TPC), total flavonoid content (TFC) in mg/gm and DPPH radical scavenging activity in percent inhibition, the phytochemical analysis of Turmeric extract is given in Table 4.3.5a, 4.3.5b and 4.3.5c. It demonstrates that the co-culture treated plants had greater phenolic and flavonoid contents than untreated plants after 45, 90, and 180 days. Further, all of the samples showed significant free radical scavenging activity against DPPH. Plants treated with individual PGPRs and co-culture of PGPRs in natural soil had elevated TPC, TFC, and DPPH levels after 180 days.

In the current study we found that the treatment with bacterial co-culture increases the levels of total phenolic content, flavonoid content, DPPH radical scavenging, and curcumin content. In natural and sterile soil, a combination of these PGPR increased phenolic content by 42.5% and 39.2%, respectively, after 180 days while increase in flavonoid content was by 38.7% and 27.5%. In both types of soil, the plants treated with a co-culture demonstrated improved antioxidant activity by 53% and 51%. Devi et al., (2022) found that the co-culture increases total content of phenolics and flavonoids in the range of 0.67 to 1.07 and 0.998 to 1.029, respectively, in seeds of *Amaranthus hypochondrius* L. The results of Ham et al., (2022) demonstrated that the PGPR treatment of *G.aleppicum* increased the total phenol and flavonoid content. According to Dutta et al., (2016), the inoculation of turmeric plants with a bacterial and fungal consortia led to an increase in the total phenolic, flavonoid, antioxidant and curcumin contents in the rhizomes. As per the work by Jain et al., (2014), *Trichoderma harzianum*, *Pseudomonas aeruginosa*, and *Bacillus subtilis* individually and in consortia increased the amount of phenolic and flavonoids in pea plants. Similarly, *S. nematodiphila* has been shown to stimulate the antioxidative enzyme activity in *Solanum nigrum* (Wan et al., 2012).

Table 4.3.5a: Total phenolic content of Turmeric inoculated with PGPR

	Phenolic content after 45, 90 and 180 days (mg/gm)											
	Control			***S. nematodiphila* RGK**			***P. plecoglossicida* RGK**			**Co-culture of both these PGPR**		
	Days			**Days**			**Days**			**Days**		
	45	**90**	**180**	**45**	**90**	**180**	**45**	**90**	**180**	**45**	**90**	**180**
N	62.31 ±0.02	87 ±0.7	103.3 ±0.01	64.2 ±0.03	98.2 ±0.01	122.5 ±0.02	65.5 ±0.01	99 ±0.03	123 ±0.04	68.4 ±0.02	120 ±0.01	147.2 ±0.08
S	39.2 ±0.02	54.6 ±0.02	61.3 ±0.03	40 ±0.03	59 ±0.01	69 ±0.07	40.5 ±0.02	62 ±0.04	71.5 ±0.02	43 ±0.01	74 ±0.03	85 ±0.09
% Increase over control(N)	-	-	-	3.16	12.8	18.6	5.2	13.7	19	9.7	37.9	42.3
% Increase over control(S)	-	-	-	1.96	8.02	13.6	3.24	13.51	16.42	9.61	35.4	39.2

(N) natural soil (S) sterile soil. The values represent the average of three experiments ± SD. ANOVA using Tukey's comparison test yielded a significant difference from control group at $p \leq 0.05$, and the relative standard deviation for all values are less than 10

Table 4.3.5b: Total flavonoid content of Turmeric inoculated with PGPR

	Flavonoid content after 45, 90 and 180 days (mg/gm)											
	Control			***S. nematodiphila* RGK**			***P. plecoglossicida* RGK**			**Co-culture of both these PGPR**		
	Days			**Days**			**Days**			**Days**		
	45	**90**	**180**	**45**	**90**	**180**	**45**	**90**	**180**	**45**	**90**	**180**
N	203 ±0.07	217 ±0.03	239 ±0.06	213 ±0.05	231 ±0.02	284 ±0.01	205 ±0.01	248 ±0.01	292 ±0.01	221 ±0.06	265 ±0.01	332 ±0.05
S	170 ±0.01	201 ±0.05	235 ±0.06	175 ±0.08	213 ±0.05	282 ±0.08	172 ±0.06	225 ±0.08	278 ±0.06	185 ±0.04	240 ±0.01	300 ±0.04
% Increase over control(N)	-	-	-	5.1	6.5	18.1	0.8	14.1	21.9	8.6	22.3	38.7
% Increase over control(S)	-	-	-	2.7	5.6	19.8	0.6	11.5	18.1	8.3	19	27.5

(N) natural soil (S) sterile soil. The values represent the average of three experiments ± SD. ANOVA using Tukey's comparison test yielded a significant difference from control group at $p \leq 0.05$, and the relative standard deviation for all values are less than 10

Table 4.3.5c: Percent inhibition for DPPH activity of Turmeric inoculated with PGPR

	Percent inhibition for DPPH activity after 45, 90 and 180 days											
	Control			**S. *nematodiphila* RGK**			***P. plecoglossicida* RGK**			**Co-culture of both these PGPR**		
	Days			**Days**			**Days**			**Days**		
	45	**90**	**180**	**45**	**90**	**180**	**45**	**90**	**180**	**45**	**90**	**180**
N	11 ±0.03	34 ±0.08	41 ±0.02	14 ±0.2	43 ±0.01	52 ±0.1	13 ±0.1	49 ±0.06	59 ±0.02	15 ±0.2	52 ±0.6	63 ±0.5
S	10.35 ±0.02	30.13 ±0.02	39 ±0.03	12 ±0.01	34 ±0.02	47 ±0.07	11 ±0.01	41 ±0.03	54 ±0.5	14 ±0.02	43 ±0.06	59 ±0.01
% Increase over control(N)	-	-	-	25	22	26	10	42	43	35	48	53
% Increase over control (S)	-	-	-	15	12	20	6	36	38	35	42	51

(N) natural soil (S) sterile soil. The values represent the average of three experiments ± SD. ANOVA using Tukey's comparison test yielded a significant difference from control group at $p \leq 0.05$, and the relative standard deviation for all values are less than 10.

4.3.3.7 Separation of secondary metabolites

The TLC profile revealed three distinct spots with RF values of 0.28, 0.54 and 0.77. They were confirmed as bisdemethoxycurcumin, demethoxycurcumin and curcumin by comparison with the values in mixed standards. All of these spots showed fluorescence under UV light. Fig.4.3.2.

The curcumin and two additional curcuminoids, demethoxycurcumin and bisdemethoxycurcumin, are the most bioactive secondary metabolites and constitute the active component of turmeric (Wichitnithad & Rojsitthisak, 2009). In the present study separation ofthese compounds with the help of TLC was carried out.

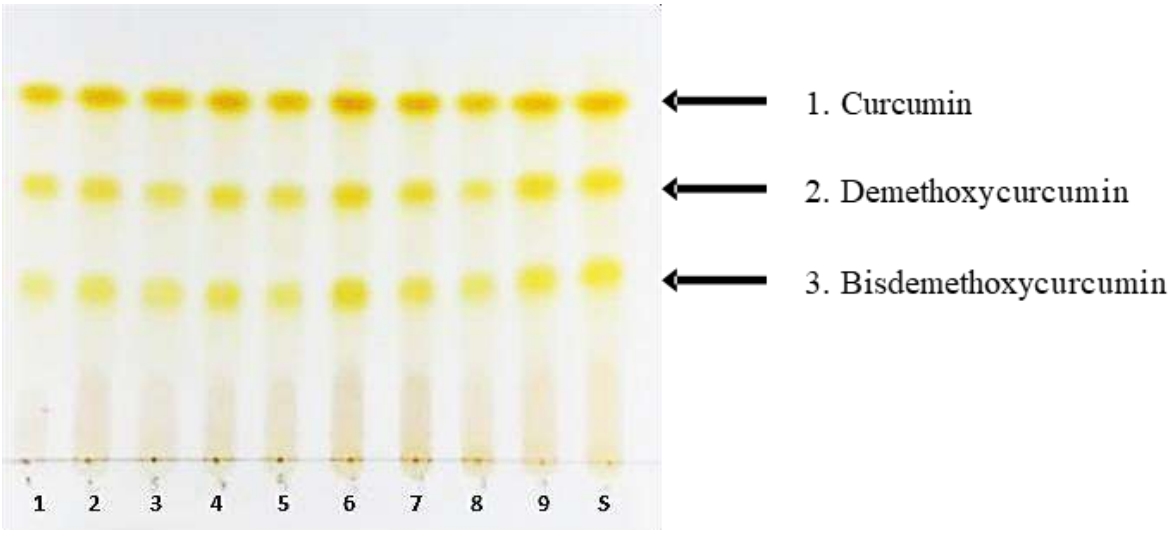

Fig.4.3.2: TLC profile showing separation of methanol extracts of *Curcuma longa* on silica gel TLC plate (20cm x 20cm). Where, S is mixed standards and 1-9 are rhizome extracts.

4.3.3.8 Extraction and analysis of secondary metabolites

4.3.3.8.1 GC-MS/MS analysis

The GC chromatogram shows retention durations, whereas MS analysis looks at compound fragmentation patterns, mass peaks, base peaks, m/z values, peak intensities and soon. A matching number of peaks were used in conjunction with these m/z values to confirm compound identification. The retention time, approximate concentration in the extract (peak area %), molecular weight, molecular formula and structures of identified secondary metabolites are depicted in the chromatograms Fig. 4.3.3 Total 22 metabolites were found in PGPR treated plant extracts. Control plants were showing 7 compounds, *P. plecoglossicida* RGK treated were showing 7, *S. nematodiphila* RGK treated plants were showing 12 compounds and consortia treated were showing 15 compounds. Among these, four were

sesquiterpenoids, one was triterpene, one was a derivative of hydrocarbon and two were phenols. The metabolites were identified by National Institute of Standard and Technology (NIST) Database and its abundance in percentage given in Table 4.3.6

In our investigation, we found that, in addition to curcumin, a few essential oils such as turmerone, phenolics such as 4-hydroxy 2-methyl acetophenone (ethanone), and sesquiterpenoids such as curlone (bisabolane) are elevated in co-culture treated plants as compared to untreated plants with biological activities. The analysis of these metabolites was performed with the assistance of GCMS. According to earlier research, PGPR inoculation with *Exiguobacterium oxidotolerans* increases the secondary metabolite bacoside-A in *Bacopa monnieri* L. (Bharti et al., 2013). A recently reported PGPR has also shown that rose scented geranium has enhanced plant characteristics and essential oil content in *Pelargonium graveolens cv. Bourbon*. (Dharni et al., 2014; Rahmoune et al., 2017). One of the known PGPRs, *Serratia sp*., can promote the development of plants by a variety of processes, including the synthesis of secondary metabolites including auxins, cytokinin, gibberellins, and HCN, as well as the solubilization of phosphate minerals. In a previous investigation, it was also shown that *S. nematodiphila* PEJ1011 can produce the plant hormone gibberellin (Kang et al., 2015).

4.3.3.8.2 RP-HPLC analysis

Curcumin content determined after 45, 90 and 180 days has been given in Table 4.3.7 UV absorbance was also examined at 425 nm. The UV detector showed curcumin peak at 425nm. Curcumin has an 11 minutes retention time. The purity of compound was determined by comparing it to a curcumin standard peak Fig.4.3.4 The HPLC analysis showed that increased curcumin content in individual PGPR treated plant as well as co-culture treated plant in natural soil after 180 days. Turmeric plant treated with *S. nematodiphila* RGK had shown the increment in the curcumin content by 5.8 % and 4.6% in natural and sterile soil respectively after 180 days. While, *P. plecoglossicida* RGK showed the enhanced curcumin content after 180 days by 4.8 % and 4.3% in natural and sterile soil respectively. Treatment with co-culture showed the increased curcumin content after 180 days in natural and sterile soil by 8.2% and 6.3% respectively.

In this study, co-culture inoculation significantly increased curcumin content as compared to a single bacterial treatment and a control. Dutta et al, (2016) found a considerably greater concentration of secondary metabolites (total phenolics, total flavonoids, and

curcumincontent) in turmeric rhizome. According to Kumar et al, (2016), *P. fluorescens* inoculations increased curcumin concentrations in Turmeric by 18% as compared to a control. The route of action of PGPR is currently not well understood, however in tomato, *P. fluorescens* exhibited chemotactic sensitivity to several amino acids (Oku et al., 2012). Turmeric rhizome contains phenolics like curcuminoids and sesquiterpenoids that may attract PGPR to the roots, resultingin improved nutrient intake and growth (Kumar et al., 2014). It is feasible to obtain a favorable response to *Pseudomonas plecoglossicida* RGK and *Serratia nematodiphila* RGK inoculation for curcumin production because PGPR serves as potent elicitors of key enzymes involved in secondary metabolite biosynthesis pathways, which are associated to plant defensive responsesagainst pathogenic infections (Wan et al., 2012).

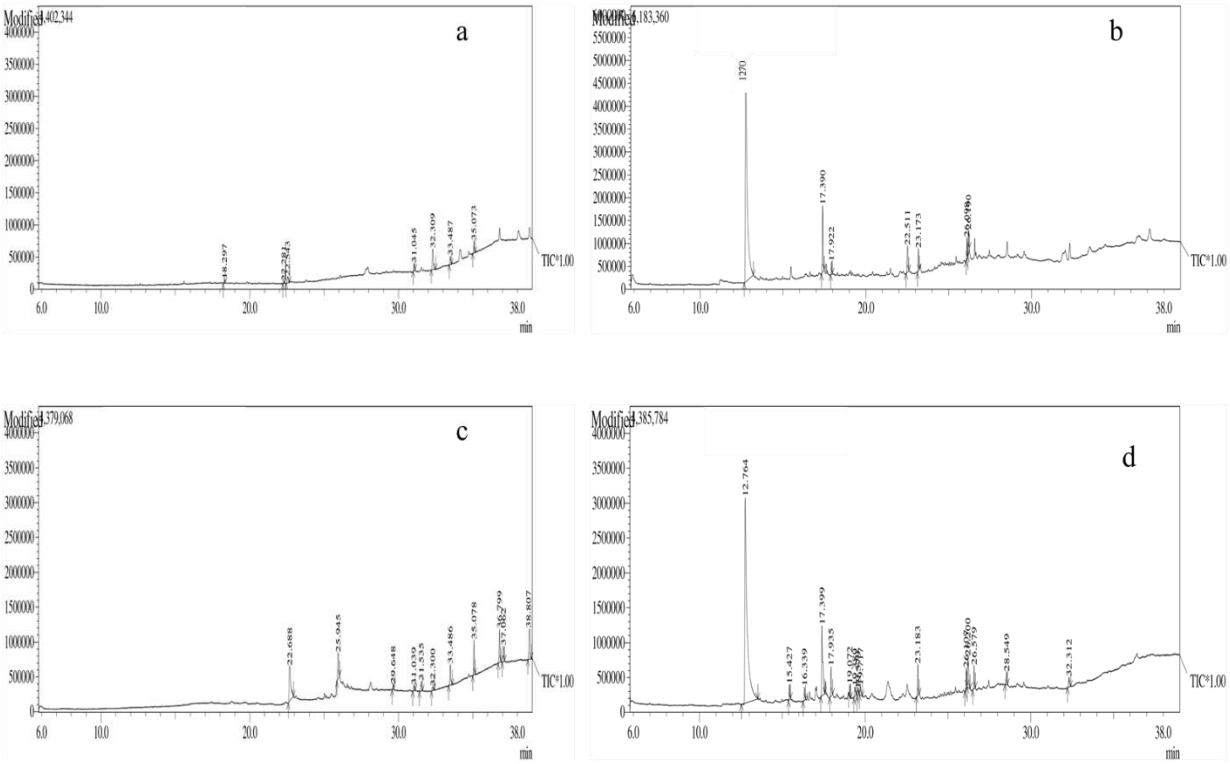

Fig. 4.3.3: The gas chromatography–tandem mass spectrometry graph with various peaks of *C. longa* where (a) Chromatogram of control Turmeric(uninoculated) (b) Chromatogram of *Pseudomonas plecoglossicida* RGK inoculated Turmeric (c) Chromatogram of *Serratia nematodiphila* RGK inoculated Turmeric (d) Chromatogram of co-culture of both inoculated Turmeric.

Table 4.3.6: Secondary metabolite profile of Turmeric identified by GC-MS/MS

S. No.	Name of Identified Compounds	Category	Retention time	Area%	Control	*P. plecoglossicida* RGK	*S. nematodiphila* RGK	Co-culture of both
1	Ethanone, 4-Hydroxy-2-methylacetophenone	Phenol	12.75	65± 77*	-	+	-	+
2	2,4-Di-tert-butylphenol	Phenol	15.42	1.35	-	-	-	+
3	Butyric acid, 2-phenyl-, dodec-2-en-1-yl ester	Fatty acid	16.33	1.18	-	-	-	+
4	aR-Turmerone	Sesquiterpene	17.93	8±10*	-	+	-	+
5	2-Methyl-6-(4-methyl enecyclohex-2-en-1-yl), curlone	Bisabolane	17.92	1± 3*	-	+	-	+
6	(Z)-.gamma.-Atlantone	Bisabolane	19.38	1.38	-	-	-	+
7	Isopropyl myristate	Fatty acid	19.57	0.44	-	-	-	+
8	Ethyl 14-methyl-hexa decanoate	Fatty acid	23.18	3.24	-	+	-	+
9	trans, trans-9,12-Octa decadienoic acid, propyl	Fatty acid	26.10	1.57	-	-	-	+
10	Ethyl Oleate	Ester of fatty acid	26.20	4.94	-	+	-	+

11	1-Hexadecanethiol	Alkane	26.57	2.05	-	-	-	+
12	Bis(2-ethylhexyl) phthalate	Esters of phthalic acid	32.13	1± 2*	+	-	+	+
13	Eicosane	Derivative of hydrocarbon	18.29	1± 4*	+	-	+	-
14	Tetracontane	N alkane	35	11± 16	+	-	+	-
15	Tetrapentacontane	N alkane	22.28	2.68	-	-	+	-
16	1, ,4-Cyclohexanediol, (Z)-,TMS derivative	Polyester resin	31.04	11.28	+	-	-	-
17	n-Hexadecanoic acid	Fatty acid	22.68	27.21	-	-	+	-
18	Dichloroacetic acid	Acid	25.94	12.13	-	-	+	-
19	1,3,5-Trisilacyclohexane	Acid	31.03	1.79	-	-	+	-
20	Dotriacontane	N alkane	33.48	7.09	-	-	+	-
21	Squalene	Triterpene	37.06	6.09	-	-	+	-
22	11,14-Eicosadienoic acid, methyl ester	Fatty acid	26.09	2.29	-	+	-	-

Note: + denotes present, - denotes absent, *P. plecoglossicida* RGK +, Co-culture of both *

Table 4.3.7: Curcumin content after 45, 90 and 180 days

	Curcumin content in percentage (%)					
	45 days		**90 days**		**180 days**	
	N	**S**	**N**	**S**	**N**	**S**
Control	0.6	0.12	2.6	2.1	4.01	2.4
***S. nematodiphila* RGK**	1.27	1.1	3.09	2.09	5.88	4.66
***P. plecoglossicida* RGK**	1.25	1.1	3.04	2.04	4.08	4.03
Co-culture of both PGPR	2.0	1.55	4.08	3.55	8.02	6.03

Note: N denotes (natural soil), S denotes (sterile soil).

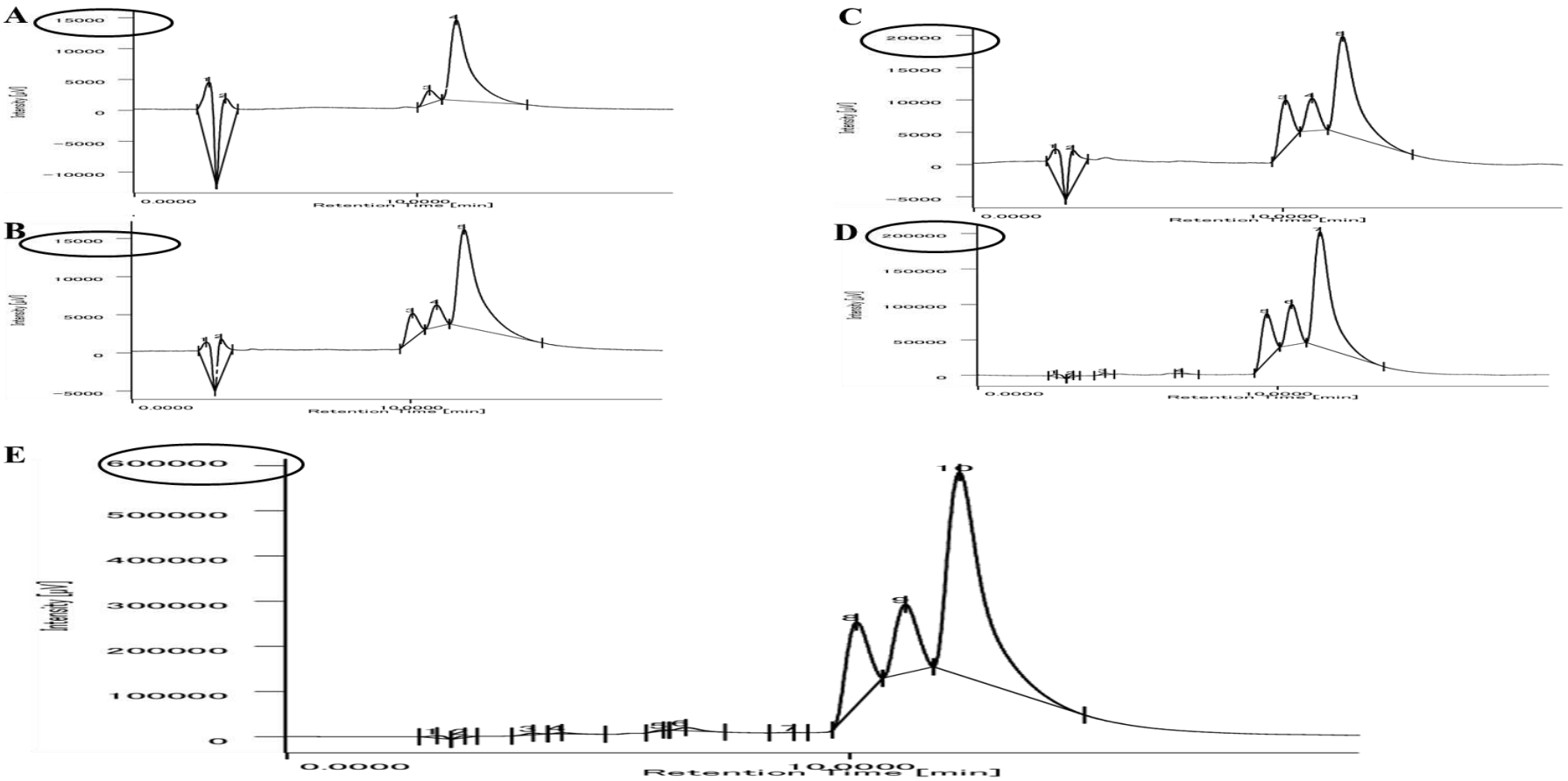

Fig. 4.3.4: HPLC chromatogram of Turmeric extracts at 425. (A) Chromatogram of standard ofcurcumin. (B) Chromatogram of control Turmeric (uninoculated). (C) Chromatogram of *Serratia nematodiphila* RGK inoculated Turmeric. (D) Chromatogram of *Pseudomonas plecoglossicida* RGK inoculated Turmeric. (E) Chromatogram of co-culture inoculated Turmeric.

4.3.4 Conclusions:

In the present study, we found that combination of both the PGPR inoculations yielded better effects than a single inoculation. Furthermore, these findings suggest that phenolic compounds and flavonoids have a favorable link with anti-radical activities, implying that the bioinoculants utilized on the Turmeric rhizosphere are efficacious. These phytochemicals can be used as an effective remedy for various ailments and drug formulations in the future, either alone or in combination with other suitable agents. This co-culture of PGPR inoculation would be one of the finest solutions for a sustained Turmeric agroindustry.

The primary benefit of employing PGPR is that they have a dual positive impact, acting as both a full biofertilizer and a biofortifier of plants, giving a remedy for nutritional deficiency and agro-environmental issues. Here we found enhanced plant parameters and phytocompounds in Turmeric following PGPR individually and in combination inoculation in natural soil rather than sterile soil. Our research revealed an interesting finding that after 180 days, the co-culture treated plant has a greater quantity of the secondary metabolite 4-hydroxy-2-methylacetophenone. We report here for the first time that 4-hydroxy-2-methylacetophenone is found in *Curcuma longa*, combined with a high percentage of curcumin.

4.4 Extraction, purification, quantification and bioactivity of secondary metabolites from PGPR treated *C. longa* and *A. racemosus*

Manuscript under preparation:

4.4.1 Introduction:

Plant secondary metabolites are mostly biosynthesized via three major pathways: the isoprenoid pathway, the shikimate pathway, and the polyketide pathway (Joulain 2021). The defense against biotic and abiotic stress is primarily mediated by the secondary metabolites of plants (Sun et al., 2019). Secondary metabolites and their derivatives such as phenolics, flavonoids, terpenes, saponins, alkaloids, glycosides, tannins, anthraquinones, essential oils, and steroids are examples of biologically active compounds (Egamberdieva & Teixeira da Silva, 2015). Plants are renewable resources that provide raw materials (such as lignocellulosic biomass) and phytochemicals (particularly secondary metabolites) for a variety of industrial applications, including textiles, building materials, pharmaceuticals, nutraceuticals, and cosmetics. Plants are thought to be essential for promoting the transition to a bio-economy that is less reliant on fossil fuels because of these characteristics (Guerriero et al., 2018).

A significant quantity of secondary metabolites are present in medicinal plants (John et al., 2014). According to Anandet al. (2019), these plants generate a wide range of secondary metabolites as a result of numerous metabolic processes, which are essential for enhancing the immune system in the treatment of illnesses. For instance, curcumin, a key ingredient in turmeric (Kumar et al., 2016 a, b), has been frequently used to both treat and prevent diabetes. It has been demonstrated that to maintain stable blood glucose levels, it increases postprandial serum insulin levels (Meng et al., 2013). Since the dawn of civilization, plant secondary metabolites (natural compounds) have been employed to treat a wide range of human illnesses, including chronic disorders (Kumar et al., 2021). These active compounds produced from plants are widely employed as secretagogues or insulin mimics(Patel et al., 2012). More than 25% of current medications are derived from plants, while natural product derivatives account for 60% of anti-cancer and 60% of anti-tumor drugs (Kumar et al., 2021).

The discovery of therapeutic agents and the identification of new sources of bioactive compounds depend on the phytochemical analysis of ethnomedicinal plants for secondary metabolites, which is a crucial area of fundamental research (Dutta, 2015). Several extraction methods were carried out in isolation of phytocompounds (Ibanez and Blazquez, 2021).For example, secondary metabolites such as phenolics, flavonoids and tannins can be separated and purified with help of repeated silica gel, RP-8, diaion, sephadex-LH20, MCI-gel, RP-18, and toyopearl chromatography columns (Chen et al.,

2017). Anticancer constituents that have been detected and isolated from terrestrial plants include brassinosteroids, polyphenols, and taxols (Greenwell & Rahman, 2015).

C. longa and *A. racemosus* were used in this study, and previously several extraction processes were used to isolate secondary metabolites from Turmeric, including steam distillation, soxhlet extraction, ultrasonic extraction, and solvent extraction (Ibanez and Blazquez, 2021). Traditionally, curcuminoids which are major component of Turmeric were extracted using solid-liquid or liquid-liquid extraction, followed by isolation using repeated column chromatography technology (Verghese and Joy, 1989). The separation of metabolites on column chromatography, such as silica gel column chromatography, is essentially based on polarity, with phenolic compounds containing more hydroxyl groups being more firmly adsorbed (Chen et al., 2017). Many studies have employed and reported on column chromatography for the discovery and identification of novel compounds, some of which have been associated to antibacterial, antimicrobial, and antifungal characteristics. Similarly, gas chromatography (GC and GC-MS) is a very potent analytical method for distinguishing the different components of essential oils. Mass spectrometry and retention indices have both been used to precisely identify the makeup of essential oils (Agostini-costa et al., 2012). Chaudhary et al, (2018) previously reported, the methods of diosgenin extraction from yams and high-performance liquid chromatography (HPLC)analysis are well-known and frequently employed (Chaudhary et al., 2018). A number of standard methods for detecting diosgenin and curcuminoids have been developed, including thin-layer chromatography (TLC). This technique has also been used successfully to obtain sufficient amounts of a substance to investigate its biological properties and detect its olfactory properties (Agostini-costa et al., 2012; Pushpakumari et al., 2014)

This study was designed to use an easy and effective method for extracting curcuminoidsand diosgenin from *C. longa* and *A. racemosus*, respectively. Curcumin was also purified by silicagel column chromatography, and diosgenin was acid hydrolyzed, and their quantification using HPLC was carried out as well. Furthermore, antibacterial, antifungal, and antibiofilm studies wereconducted.

4.4.2 Material and method:

4.4.2.1 Extraction of plant secondary metabolites

The uprooting of plants was done after 45, 90 and 180 days and proceeded for

secondary metabolite extraction. After uprooting rhizomes and roots were rinsed with distilled water to eliminate adhered soil. It was then cut into small pieces and dried in oven at 40℃ to make a fine powder. This powder was used for the metabolite extraction process. Different solvents and extraction techniques were used to extract plant secondary metabolites. Below are some additional effective extraction techniques.

4.4.2.1.1 Soxhlet Extraction

Soxhlet extraction was carried out using standard apparatus. 1 gm of powdered rhizomes with 250 ml of each hexane, methanol, acetone, petroleum ether, diethyl ether and ethanol as solvent were used with the extraction time of 8 hrs. The organic extracts were concentrated usinghot plate and stored at 4℃ for further analysis.

4.4.2.1.2 Sonication for Turmeric and Asparagus

In a sealed tube, 1 gm of sample was added to 10 ml of methanol. The mixture was then treated in a bath sonicator for 1 hour at room temperature and centrifuged at 5000 rpm for 10 minutes at 4 °C. Supernatant was collected for further analysis.

4.4.2.2 Purification of plant secondary metabolites

Separation and purification of secondary metabolites from PGPR treated and non-treated plantswere done using following techniques

4.4.2.2.1 Purification of curcuminoids by silica gel column chromatography

Methanolic extract was subjected to silica gel column chromatography (60-120 mesh). Topack the column, silica gel was dissolved in chloroform: methanol (98:2) and filled upto 46 cm. Then sample was added on the top of gel and eluted with chloroform followed by chloroform: methanol with increasing polarity. All fractions were collected and subjected to UV spectrophotometry at 425 nm (Heffernan et al., 2017).

4.4.2.2.2 Thin layer chromatography (TLC) for curcuminoids

The collected fractions were tested on pre-coated Silica gel (Merck, Darmstadt, Germany) TLC plates along with standard curcuminoid. The plates were developed using pre-saturated TLCchamber for 1 hr. chloroform: methanol (95:5 v/v) was used as mobile phase. Each plate was developed up to the height of about 12 cm. The plates were then removed and dried. Spots were analyzed and Rf values were calculated (Zhang et al., 2008; Peret-Almeida et al., 2005).

4.4.2.2.3 Purification of curcumin

Curcumin was further purified from separated spots on TLC. The uppermost spot which was of curcumin (based on Rf value) was scrapped, dissolved in methanol and kept in refrigeratorovernight. The supernatant was then collected, evaporated and concentrated. It was used for furtherpurification by silica gel column chromatography (Revathy et al., 2011).

4.4.2.2.4 High Performance Liquid Chromatography for curcumin

For the purification of small organic molecules like drugs, peptides, microbial metabolites,plant metabolites and antibiotics, high-performance liquid chromatography (HPLC) is a highly effective and high-resolution technique (Smyth et al., 2014; Dhanarajan et al., 2015). As part of the recovery of the purification method, HPLC was also used to quantify the metabolites. This method involves the interaction of liquid solvent in the tightly packed solid column or a liquid column. Parameter used during HPLC purification of Curcumin are given below in Table 4.4.1

Table 4.4.1: Parameter used for purification of Curcumin

Parameter used during HPLC purification of Curcumin

Column	C_{18}
Detector	Diode Array detector
Solvent system/Mobile phase	The mobile phase was 50:50 (v/v) acetonitrile and 2% acetic acid
Flow rate	0.5ml/min
Wavelength of detection	425nm
Sample volume	20 µl
Working temperature	25°C
Standard curcumin	100– 500 µg/ml

4.4.2.2.5 Purification of diosgenin by acid hydrolysis

5 gm of Asparagus plant powder was hydrolyzed in 50 ml of 2 M sulphuric acid by heating under refluxation for 2 hrs. After cooling, 40% sodium hydroxide was added to the solution to neutralize it. The hydrolysis product was then extracted using an equal

amount of chloroform (Wang et al., 2011; Yang et al., 2015). The extract was separated by a separating funnel and concentrated by 60°C evaporation. The residue was combined with the standards for TLC analysis after being dissolved in methanol and applied to precoated silica gel.

4.4.2.2.6 Thin layer chromatography (TLC) for diosgenin

Thin-layer chromatography was performed on plates precoated with silica gel (Merck, Darmstadt, Germany). The samples were developed with hexane-acetone (8:2) as the mobile phase with a few minor modifications, dried to ensure that all solvents had evaporated, and detected witha 0.5:5 mixture of ethanol (8% vanillin) and sulfuric acid solution (70%) (Hardman, 1968

4.4.2.2.7 High Performance Liquid Chromatography for Diosgenin

Parameter used during HPLC purification of Diosgenin are given below in Table 4.4.2

Table 4.4.2: Parameter used for purification of Diosgenin

Parameter used during HPLC purification of Diosgenin

Column	C_{25}
Detector	Diode Array detector
Solvent system/Mobile phase	The mobile phase was 10:90 (v/v) HPLC-grade water and acetonitrile
Flow rate	0.8ml/min
Wavelength of detection	194 nm
Sample volume	25 µl
Working temperature	27℃
Standard diosgenin	20 – 100 µg/ml

4.4.2.2.8 Gas Chromatography-Mass spectroscopy (GC-MS/MS)

Phytochemicals were analyzed qualitatively and quantitatively using gas chromatography-mass spectrometry (GC-MS/MS). The samples were transformed into a gaseous condition, and analysis based on the mass-to-charge ratio was then completed (Balamurugan et al., 2019). Curcuminoid fractions were subjected to GC-MS/MS analysis

for the purpose of compound identification. The HS 2010 Plus (SHIMADZU) MS TQ 8050 mass detector, column SH-Rxi-5Sil MS with (30mm 0.25mm ID 0.25m), and helium as a carrier gas were utilized in the GC-MS/MS study of metabolites. The temperature of the sample injection was 250°C, the auxiliary temperature was 290°C, the ion source temperature was set to 280°C, the oven temperature ranged from 50°C to 275°C, and the GC ran for 38-52 minutes. The metabolites were identified by National Institute of Standard and Technology (NIST) database.

4.4.2.2.9 Liquid chromatography and mass spectroscopy (LC-MS/MS)

ThermoFisher Scientific's Ultimate 3000-series MS was used for the HPLC-Quadrupole-Orbitrap analysis (Bremen, Germany). The subsequent was a part of the mobile phase: Formic acid is present in water and acetonitrile at 0.1% each. With a flow rate of 0.4 mL/min, the gradient programme was adjusted to 0-10 min/98% A, 11.1 min/2% A, and 16 min/2% A. The following values were used to calculate the heated electrospray ionisation (H-ESI, positive mode) parameters: capillary temperature, 320 °C; S-lens RF level, 50.0; sheath gas flow rate, 45; auxiliary gas flow rate, 8; sweep gas flow rate, 1; spray voltage, 3.50 kV; and heater temperature, 300 °C. The MS analysis was performed in ddMS2 mode. The mass range of 100-1000 Da was employed for FS at three different resolutions of 70000 "Full Width at Half Maxima" (FWHM) (at m/z 200). Then came ddMS2, which had stepped collision energy with a resolution of 17500 (at m/z 200) and operated at 10, 30, and 70 V. The 1e6 goals of the automatic gain control (AGC) were maintained for the ddMS2 approaches. The m/z was employed in ddMS2, which was initially created by ThermoFisher Scientific, and had a scan range of 100–1500. The data processing utilized the compound discoverer 3.2.0.421 programme.

4.4.2.3 Antimicrobial and antifungal activity of purified phytocompounds

Turmeric and Asparagus has long been considered as to have natural medicinal properties (Hoe seon lee, 2006). Antimicrobial studies were carried out on the pathogens including *Proteus vulgaris*, *Escherichia coli*, *Streptococcus mutans* and *Staphylococcus aureus.* Antifungal activity was checked by using *Pythium aphanidermatum*, *Aspergillus niger* and *Candida albicans* strains of fungus. The antimicrobial and antifungal activity was monitored in terms of zone of inhibition observed on agar plates of nutrient medium with 1.8% agar by using agar well diffusion method. The plates were incubated for 24 hrs

at 37℃ for bacteria and 48-72 hrs at 37℃ for fungal cultures. Curcumin, curcuminoids, 4 hydroxy 2 methyl acetophenone, purified curcumin, purified curcuminoids, combination of curcumin + 4 hydroxy 2 methyl acetophenone and diosgenin standard and purified diosgenin were used for testing purpose. After incubation results were recorded.

4.4.2.4 Minimum inhibitory concentration of phytocompounds

The Minimum inhibitory concentration (MIC) of purified metabolites (curcumin, curcuminoid and diosgenin), standard metabolites (curcumin, curcuminoid, 4 hydroxy 2 methyl acetophenone and diosgenin) and their combinations (curcumin + 4 hydroxy 2 methyl acetophenone) was determined by using test pathogens as *P. vulgaris, E. coli, S. mutans* and *S. aureus.* It was determined by twofold serial dilutions of metabolites in a Mueller-Hinton Broth medium. The test was carried out in 96 well microtitration plate with a standardized bacterial suspension of 0.5 McFarland's turbidity. The lowest concentration that completely inhibited the growth of the bacteria after 24 hrs was considered as the minimum inhibitory concentration (Bahariet al., 2017).

4.4.2.5 Effect of phytocompounds on test pathogen

The effect of phytocompounds on the growth of test pathogen *S. aureus* NCIM 2654 was assessed in the presence of purified plant metabolites (curcumin, curcuminoid and diosgenin), standard metabolites (curcumin, curcuminoid, 4 hydroxy 2 methyl acetophenone and diosgenin) and their combinations (curcumin + 4 hydroxy 2 methyl acetophenone). Their effect on bacterial growth was assessed by measuring OD at 660 nm against a time interval of 1 hr. The test culture at the initial concentration of 0.5 McFarland was incubated for 12 hours in the presence of these metabolites. The OD values were compared with the control sample. A sterile BHI medium was used as a blank. The growth pattern was obtained by taking absorbance at the time interval of 1 hr.

4.4.2.6 Biofilm inhibition study by using crystal violet assay

To improve the conditions for biofilm production, the microtiter plate assay was carried out. Four human pathogenic strains were employed in the study of biofilm suppression by various phytocompounds. As previously stated, (Sharifian et al., 2020), the experiment was carried out with a few changes on 96 well flat bottom polystyrene micro-titre plates that were previously sterilized. In each well, 150 µl of sterile BHI broth and 50 µl of cell suspension with 0.5 OD at 600 nm were used as inoculants. 100 µl of

purified metabolites (curcumin, curcuminoid and diosgenin), standard metabolites (curcumin, curcuminoid, 4 hydroxy 2 methyl acetophenone and diosgenin) and their combinations (curcumin plus 4 hydroxy 2 methyl acetophenone) was added in respective wells. Following that, the microtiter plate was incubated for 24 hours at 37°C. Planktonic cells were aspirated, and biofilms were then fixed in 99% methanol. Plates were air dried after being cleaned twice in sterile phosphate buffer saline. Then, 200 µl of 0.1 percent crystal violet solution was added to each well. After 15 minutes, the extra crystal violet was removed, the plates were cleaned twice, and they were air dried. Finally, 33% acetic acid was used to dissolve the cell-bound crystal violet. Using a micro plate reader (Erba scan), the growth of the biofilm was observed in terms of OD 578 nm.

4.4.2.7 Biofilm inhibition study by scanning electron microscopy (SEM)

The effect of purified metabolites (curcumin, curcuminoid and diosgenin), standard metabolites (curcumin, curcuminoid, 4-hydroxy 2-methylacetophenone and diosgenin) and their combinations (curcumin + 4- hydroxy 2 -methylacetophenone) on biofilm inhibition was also investigated by the SEM technique. In this, a clean glass was cut into a square having dimensions1 cm2. They were washed for 30 minutes in an ultrapure water rinse after being cleaned with a 5%(v/v) Hiclean (Liquid soap, Hi-Media) solution. The surfaces were immersed in 96% (v/v) ethanolfor 10 minutes to remove all impurities after being air dried for 30 minutes.

To prepare a sample for SEM, 2% glutaraldehyde solution was taken on slide. A test bacterial culture along with metabolites were used for the preparation of smear. The slides were kept in freezer overnight to fix the smear. On next day smear was washed with an ethanol dehydration series of 20 to 100% (v/v) (Galabova et al., 1996). The samples were then analyzed by SEM using VEGA3 TESCAN instrument.

4.4.3 Results and discussion:

4.4.3.1 Extraction of plant secondary metabolites

In the current study, Soxhlet extraction and sonication were used, and the resulting extract was used for purification and analysis of metabolites. Previously, Soxhlet extraction is used to ensure that curcumin and related compounds are extracted as completely as possible from turmeric root powder. Additionally, it eliminates the need to operate heavy glassware, heating, and cooling systems (Schieffer, 2002). To assess the

efficacy of the curcuminoid extraction methods under consideration, Soxhlet extraction was used as the baseline method. Soxhlet extraction is one of the most important and widely used extraction techniques, in which long extraction times at high temperatures aid in the extraction of the target compound, additionally, repeated contact of the solvent with turmeric can increase the extraction yield (Sahne et al., 2016). Although simpler, single or multiple ultrasonically-assisted extractions appear to leave a small but significant amount of secondary metabolites (Schieffer, 2002).

4.4.3.2 Purification of curcuminoids by silica gel column chromatography

In current study curcumin and curcuminoids were purified using silica gel column chromatography. Adsorption chromatography was performed for methanolic extracts using silica gel (60-120 mesh) and stepwise elution with chloroform and methanol CHCl3:CH3OH with increasing polarity with the flow rate of 1 ml/min. In our study, the chromatographic separation was done for curcumin as well as curcuminoids. A total of 40 fractions were collected and their OD was taken at 425 nm. Among the 40 fractions, fractions 10 to 25 demonstrated bioactivity and high absorbance at 425 nm, indicating that they contained purified curcuminoids. According to previous reports, separating curcumin and curcuminoids using silica gel column chromatography results in good yields (Peret-Almeida et al., 2005; Pushpakumari et al., 2014).

4.4.3.3 Thin layer chromatography

In the present study the TLC profile for the *C. longa* secondary metabolites shown three separate spots with retention factor (Rf) of 0.28, 0.54, and 0.77 for bisdemethoxycurcumin, demethoxycurcumin, and curcumin respectively (Fig. 4.3.2 from chapter 4.3) and were verified when compared to the levels in mixed standards. Under UV light, all of these dots fluoresced in comparison with standards. Similarly, in the case of diosgenin different solvent systems were used to conduct TLC analysis. In chloroform extracts produced from acid hydrolysis of roots of *A. racemosus*, retention factor for the diosgenin spot was 0.49 (Rf). (Fig.4.4.1). TLC is a simple and frequently used technique for purifying and identifying antibiotics, peptides, amino acids, plant pigments, and secondary metabolites in plants. Our findings are in line with previous reports for curcumin, curcuminoid and diosgenin (Laila et al., 2014; Peret-Almeida et al., 2005; Brain and hardman, 1968).

Fig. 4.4.1: TLC profile showing separation of purified secondary metabolites on Silica gel TLC plate where, S-standard diosgenin, D- purified diosgenin

4.4.3.4 Purification of curcumin

The spot with Rf value 0.77 was removed from the TLC separation as above mentioned, dissolved in methanol, and purified using silica gel column chromatography. A non isocratic elution profile was utilized with a constant mobile phase flow rate of 0.5 ml/min by progressively increasing the concentration of methanol in the chloroform-methanol mobile phase. Pure curcumin was extracted from the column using a pure chloroform solvent as a starting point. Subsequently increasing the methanol concentration, which elutes a mixture of remaining compounds. Fractions containing curcumin were collected, concentrated, and their UV absorbance at 425 nm was measured. These were then utilized for additional biological activities. As per earlier reports, curcumin has a wide range of therapeutic approaches. To examine the biological characteristics of individual curcumin, isolate compound of high purity is required (Heffernan et al., 2017).

4.4.3.5 Purification of diosgenin by acid hydrolysis

The acid concentration was an important factor in the hydrolysis reaction because it directly affected saponin yield. It was discovered that 50 ml of chloroform was sufficient to extract diosgenin, and that increasing the chloroform consumption did not increase the yield any further. Purified diosgenin is present in the upper layer of chloroform in the separating funnel, and the chloroform is evaporated at 60°C to yield a residual compound, which is then dissolved in methanol and used for TLC analysis. Previous research has also shown that acid hydrolysis followed by extraction in non-polar solvents yields a higher

yield than traditional methods (Yanget al., 2016).

4.4.3.6 HPLC analysis for curcumin and diosgenin

The HPLC approach was used to detect and quantify curcuminoids from the fractions of silica gel column chromatography. Separation by HPLC was done on reverse phase column by using mixtures of water and acetonitrile. Due to difference in the chemical structures of curcuminoids, their physicochemical properties and their functional qualities might differ. As a result, analysis of pure compounds and characterizing them separately in order to study their biological features is critical. Curcumin had eluted at 425 nm when analyzed with UVdetection by retention time of 11 min. The purity of the compound was assessed by comparing the extracted curcumin with curcumin standard. Curcumin content determined after 45, 90 and 180 days of each PGPR treated plant as depicted in chapter 4.3**.** Similar kind of work done by kumar et al. (2015) the reports stated that increased curcumin content after single and consortial treatment with PGPR to turmeric rhizome. Inoculations with *Pseudomonas fluorescens* raised turmeric's curcumin levels by 18% in comparison to a control, reported by Kumar et al. (2016).

HPLC results for diosgenin were shown in chapter 4.2 under results and discussion section. Earlier study reported that quantification of diosgenin was performed by using HPLC (Peiqin Li, 2012).

4.4.3.7 GC-MS/MS and LC-MS/MS analysis for curcumin and diosgenin

Analysis through GC-MS/MS to assess the similar compounds present in the fractions. The results for GC-MS/MS for Turmeric and Asparagus are given in chapter 4.3 and 4.2 respectively under results and discussion section. GC-MS/MS results revealed that when plant samples were compared to untreated control plants, the percent area of important phytocompounds in co-culture treated plants increased. Similar to this, we discovered a newer compound (4-hydroxy-2-methylacetophenone) in the co-culture and *Pseudomonas plecoglossicida*-treated *C. longa.* In an earlier study of phytochemical analysis, a GC-MS-based method was used to analyze *Asparagus racemosus* (Janani and Singaravadivel, 2014; Wang et al., 2011). Previous studies have shown that PGPR inoculation with *Exiguobacterium oxidotolerans* increases the secondary metabolite bacoside-A in *Bacopa monnieri* L. (Bharti et al., 2013).

Identification of curcumin and diosgenin were performed by using LC-MS/MS. The full scan in positive mode was used (scan range from m/z 200→m/z 700) to identify

the curcumin. With full scan mass spectra for the determination of curcumin precursor ion is [M+H]+ m/z 369. Under optimized HPLC and MS conditions, curcumin was detected. After optimization, the mass transitions were m/z 369→m/z 759 for curcumin. Fig.4.4.2 The earlier research by Xie et al. (2009) represents a verified LC-MS/MS based approach for figuring out how much curcumin is present in *Curcuma longa.* Because chromatographic separation coupled to mass spectrometry detection (LC- MS/MS) technologies offer great accuracy, repeatability, and sensitivity, they should be employed for precise measurement and detection of tiny quantities of curcuminoids and metabolites.

The voltage for the most significant abundance of diosgenin is [M+H]+ m/z 415.3. Fig.4.4.3 The retention time of 2.44 min was detected for diosgenin. These results led to the identification of the diosgenin by using the full scan in positive mode (scan range from m/z 200– m/z 450) and the precursor/product ion pair with a transition mass of m/z415.3/271.2. Similarly, earlier studies reported the determination of diosgenin from various plant sources by using LC- MS (Sarvin et al., 2018).

Fig.4.4.2: TIC of Curcumin

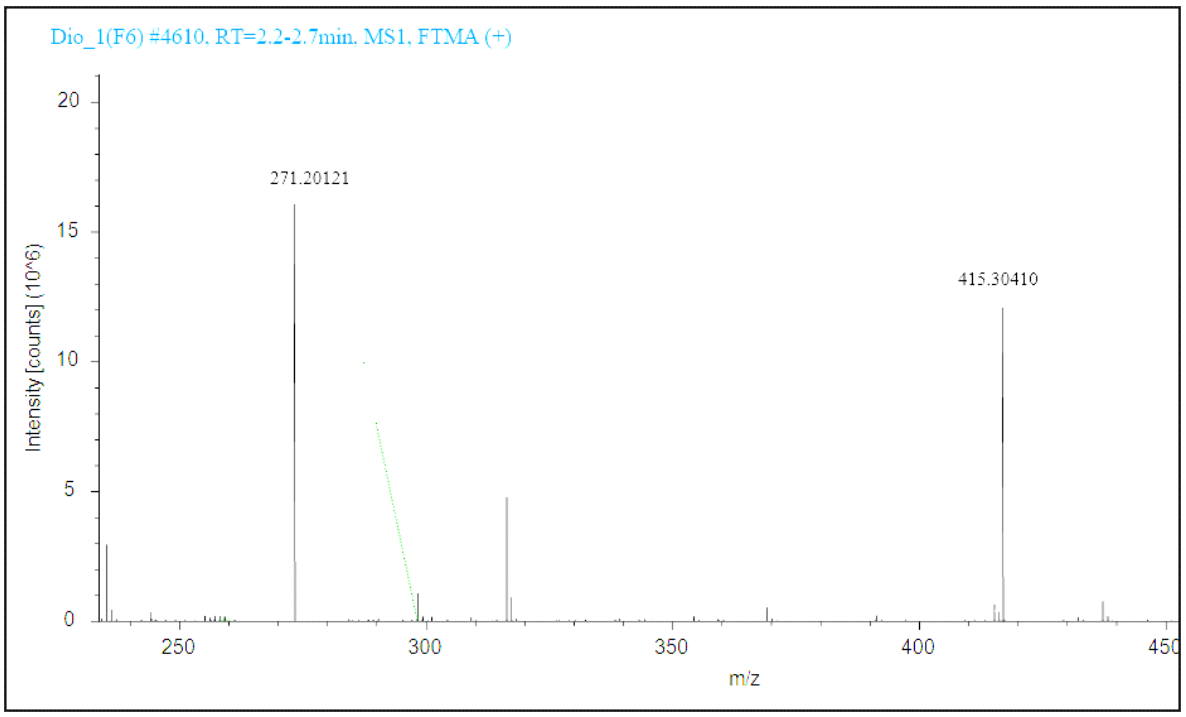

Fig.4.4.3: TIC of Diosgenin

4.4.3.8 Antibacterial and antifungal activity of phytocompounds

Curcumin, curcuminoids, 4-hydroxy-2-methylacetophenone, purified curcumin, purified curcuminoids, combination of curcumin + 4-hydroxy-2-methylacetophenone and diosgenin standard and purified diosgenin were tested against a variety of pathogens including *E. coli* NCIM2832, *Staphylococcus aureus* NCIM 2654, *Streptococcus mutans* NCIM 5660 and *Proteus vulgaris* NCIM 2813. Agar well diffusion method employed to check the antibacterial activity. The results are depicted in Table 4.4.3 Curcumin, curcuminoids, 4-hydroxy-2-methylacetophenone, purified curcumin, purified curcuminoids, combination of curcumin + 4-hydroxy-2-methylacetophenone and diosgenin standard and purified diosgenin showed highest antibacterial activity against *S. aureus* among all pathogens with diameter of zone of inhibition as 23.8 ±1.2, 23 ±2.7, 22.3 ±2.0, 24 ±0.5, 19.5 ±0.7, 27.8 ±0.70, 12.5 ±0.7 and 11 ±0.2 mm respectively. These results indicate that the combinational effect of curcumin + 4-hydroxy- 2-methylacetophenone is more inhibitory than the individual compound. We also demonstrated that purified compounds have inhibitory values close to the standard. Antifungal activity was tested against *Pythium aphanidermatum*, *Aspergillus niger* and *Candida albicans*, and findings were recorded in a Table 4.4.4. Curcumin, curcuminoids,

4-hydroxy-2-methylacetophenone, purified curcumin, purified curcuminoids, combination of curcumin + 4-hydroxy-2-methylacetophenone and diosgenin standard and purified diosgenin showed the highest antifungal activity against *A. niger* among all pathogens and the zone of inhibition was observed and noted as 13.8 ±1.2, 13 ±2.7, 12.3 ±2.0, 14 ±0.5, 14.5 ±0.7, 17.8 ±0.70, 14.5 ±0.7 and 11 ±0.2 mm respectively. According to our findings, the combined effect is more significant than a single treatment.

Many studies reported the antibacterial activity of Turmeric extracts, essential oil extracted from Turmeric and curcumin against pathogenic organisms (Khatun et al., 2021; Negi et al., 1999).Combinational effect of curcumin along with other phytocompounds showed the antibacterial effect against human pathogen (Sharma et al., 2013). Antifungal activity of *C. longa* against different fungi were also reported (Moghadamtousi et al., 2014).

Table 4.4.3: Antimicrobial activity of phytocompounds against Gram-positive and Gram-negative bacteria by agar well diffusion assay

Phytocompounds	**Inhibition zone in mm**			
	***S. aureus* NCIM 2654**	***S. mutans* NCIM 5660**	***P. vulgaris* NCIM 2813**	***E. coli* NCIM 2832**
Curcumin	23.8 ± 1.2	23.00±1.3	19 ±0.7	20 ±0.5
Curcuminoid	23.0 ± 2.7	22.5 ± 0.7	18 ±0.8	19 ±0.8
4-hydroxy-2-methylacetophenone	22.3±2.0	22 ± 0.2	16 ±1	17 ±0.7
Purified Curcumin	24.0 ± 0.5	23.5 ±0.3	18.5 ±0.8	19 ±0.3
Purified Curcuminoid	19.5 ± 0.7	22 ± 0.8	17 ±0.5	18 ±0.2
Curcumin+4-hydroxy-2-methylacetophenone	27.8 ± 0.70	26.00±1.4	20 ±0.6	21 ±0.2
Diosgenin	12.5 ± 0.7	10.12±0.3	12 ±1.2	11.5 ±0.6
Purified diosgenin	11 ± 0.2	10 ± 0.3	12 ±0.2	10 ±0.5

Table 4.4.4: Antifungal activity of phytocompounds against different fungi by agar well diffusion assay.

Phytochemicals	Inhibition zone in mm		
	Aspergillus niger	***Pythium aphanidermatum***	***Candida albicans***
Curcumin	13.8 ± 1.2	10.00 ± 1.3	17 ±0.7
Curcuminoid	13.0 ± 2.7	12.5 ± 0.7	15 ±0.8
4-hydroxy-2-methylacetophenone	12.3±2.0	08 ± 0.2	12 ±1
Purified Curcumin	14.0 ± 0.5	13.5 ± 0.3	15.5 ±0.8
Purified Curcuminoid	14.5 ± 0.7	12 ± 0.8	14 ±0.5
Curcumin + 4-hydroxy-2-methylacetophenone	17.8 ± 0.70	13.00 ± 1.4	17 ±0.6
Diosgenin	14.5 ± 0.7	12.12 ± 0.3	22 ±1.2
Purified diosgenin	11 ± 0.2	12± 0.3	20 ±0.2

4.4.3.9 Minimal Inhibitory concentration of phytocompounds

Minimum inhibitory concentration (MIC) was performed against a variety of human pathogens, including *S. aureus* NCIM 2654, *S. mutans* NCIM 5660, *P. vulgaris* NCIM 2813, and *E. coli* NCIM 2832. We continued our further investigation with *S. aureus* because among these pathogens, significant results were found for this species. *S. aureus* is an aerobic Gram-positive bacterium and has been found in a variety of diseases, including skin infections, endocarditis, toxic shock syndrome, osteomyelitis, and septicemia (Niu et al., 2018; Ippolito et al., 2010). MIC of curcumin, curcuminoids, 4-hydroxy-2-methylacetophenone, purified curcumin, purified curcuminoids, combination of curcumin + 4-hydroxy-2-methylacetophenone and diosgenin standard and purified diosgenin were 180, 200, 200, 200, 220, 160, 200 and 240 µg/ml respectively against *S. aureus* (Table 4.4.5).

Earlier studies reported the minimum inhibitory concentrations of curcumin against human pathogens (Gunes et al., 2016). MIC against *S. aureus* was reported by Park et al. (2005). Our results of MIC are in accordance to these findings.

Table 4.4.5: MIC against human pathogens

Phytocompounds	MIC in µg/ml			
	S. aureus **NCIM 2654**	***S. mutans*** **NCIM 5660**	***P. vulgaris*** **NCIM 2813**	***E. coli*** **NCIM2832**
Curcumin	180	200	220	300
Curcuminoid	200	220	240	300
4-hydroxy-2 methylacetophenone	200	240	240	310
Purified curcumin	200	220	260	320
Purified curcuminoid	220	240	240	340
Curcumin +4-hydroxy-2-methylacetophenone	160	200	240	280
Diosgenin	200	240	260	320
Purified diosgenin	240	260	260	300

4.4.3.10 Effect of phytocompounds on test pathogen

Growth curve experiment was performed to check the effect of purified metabolites (curcumin, curcuminoid and diosgenin), standard metabolites (curcumin, curcuminoid, 4-hydroxy-2-methylacetophenone and diosgenin) and their combinations (curcumin + 4-hydroxy-2-methylacetophenone) on the growth of *S. aureus* NCIM 2654. On the basis of MIC values of each metabolite, we selected *S. aureus* NCIM 2654 for this experiment. The experiment was performed to check inhibition potential of phytocompounds. The observed growth curve patterns (Fig. 4.4.4) showed the effective inhibition of *S. aureus* in presence of curcumin+4-hydroxy- 2-methylacetophenone over individual phytocompounds and control. The decrease in absorbance at 660 nm by *S. aureus* in the occurrence of phytocompounds showed that inhibition of growth of pathogen. Earlier reports also showed that growth of *S. aureus* was inhibited in the presence of curcumin (Wang et al., 2016).

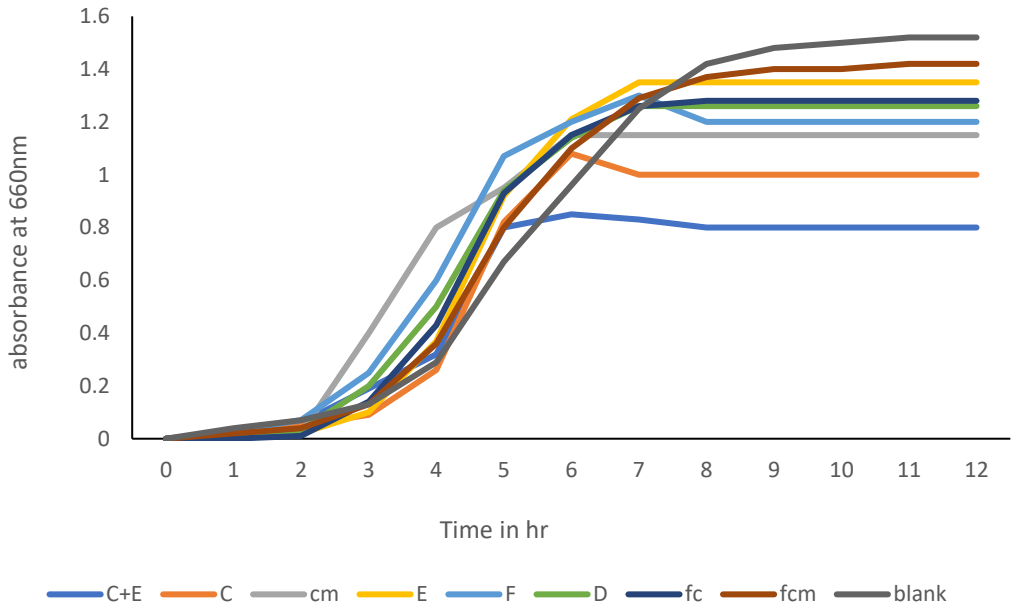

Fig.4.4.4: Growth curve of *S. aureus* in presence of different phytocompounds where C+E - curcumin+4-hydroxy-2-methylacetophenone, C-curcumin, cm- curcuminoids, E-4-hydroxy-2-methylacetophenone, F- purified diosgenin, D- diosgenin standard, fc- purified curcumin, fcm- purified curcuminoids.

4.4.3.11 Antibiofilm activity by using Crystal violet Assay

In order to investigate the biofilm inhibition activity of all phytocompounds, crystal violet assay was performed against biofilm forming pathogens. Biofilms in the wells containing curcumin, curcuminoids, 4-hydroxy-2-methylacetophenone, purified curcumin, purified curcuminoids, combination of curcumin + 4-hydroxy-2-methylacetophenone and diosgenin standard and purified diosgenin were easily detached from the base. It may be said that biofilms in the absence of phytocompounds were less disturbed by the staining process and adhered to the microplate wells more firmly. The OD was higher in the group lacking phytocompounds than in the group containing phytocompounds due to biofilm development. The combinational effect of curcumin + 4-hydroxy-2-methylacetophenone had shown better biofilm inhibition than individual treatment of metabolites as illustrated in Fig.4.4.5. These metabolites were showed better biofilm inhibition in case of *S. aureus* and *S. mutans* under *in vitro* and *in silico* studies.

S. aureus is known for biofilm-related infections, particularly in nosocomial infections (Jinet al., 2019), but *S. mutans* is more commonly connected with dental carries (Caroline et al., 2018). Bacteria associated with biofilm are resistant to the majority of

regularly used antibiotics, and they create extracellular polymeric substance (EPS) for cell-to-cell adhesion and biofilm growth, slowing the diffusion of conventional antibiotics (Nadaf et al., 2018). Attachment to cell surfaces, matrix development, and maturation are the phases in biofilm formation (Nadar and colleagues, 2022). Numerous earlier studies demonstrated that curcumin inhibits the growth of organisms that produce biofilms (Hu et al., 2013; Park et al., 2005).

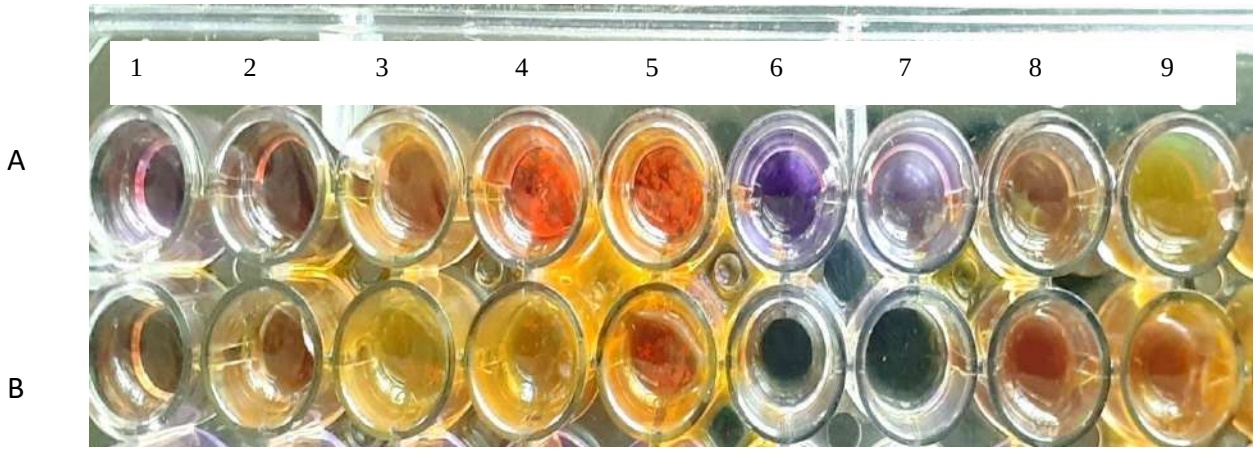

Fig.4.4.5: Crystal violet assay of biofilm for *S. mutans* (A) and *S. aureus* (B) where, 1) is control untreated cells 2) cells treated with curcumin 3) cells treated with curcuminoids 4) cells treated with purified curcumin 5) purified curcuminoid 6) cells treated with 4-hydroxy-2-methylacetophenone 7) cells treated with diosgenin 8) cells treated with curcumin + 4-hydroxy-2-methylacetophenone 9) cells treated with purified diosgenin.

4.4.3.12 Scanning electron microscopy (SEM) study for biofilm inhibition

The antibiofilm action of phytocompounds on *S. aureus* NCIM 2654 Fig. 4.4.6 was confirmed by SEM analysis. The disorganized adhesion of the organisms treated with phytocompounds is clearly visible, indicating a failure in aggregate formation and an inability to maintain their normal morphology in the presence of phytocompounds. The untreated cells had a smooth, undamaged surface that was spherical in shape, and they had a strong adherence to one another (Fig. 4.4.6-A). Cells lose their adhesion after being treated with all phytocompounds, and alterations to their morphology occur, with a combinational impact producing better results than an individualone. These observations lend credence to the results of the growth curve investigations.

One of the key steps in the production of biofilms, called quorum sensing or cell-to-cell communication, is where microorganisms may interact. Gram-positive and Gram-

negative microbes have been the subject of the most thorough research in this process (Waters and Bassler,2005; Eberhard et al., 1981; Sheikh et al., 2013; Vendeville et al., 2005). According to reports, the inhibitory effect of phytocompounds on quorum sensing and the formation of biofilms is a phenomenon that depends on the density of the bacteria (Filomena et al., 2013). Our findings, however, suggest that inhibiting adhesion may halt the development of biofilms right at their beginning, which may be more useful when developing fresh therapeutic approaches.

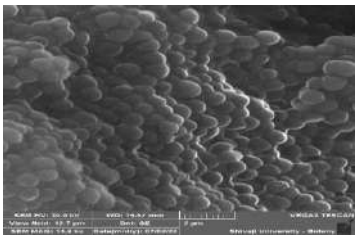

A

B

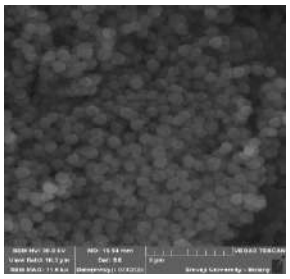

C

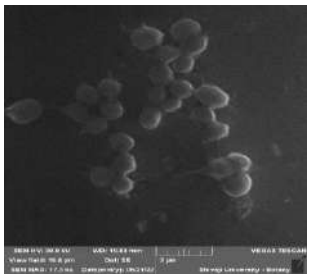

D

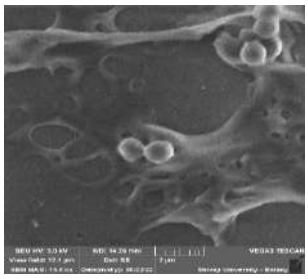

E

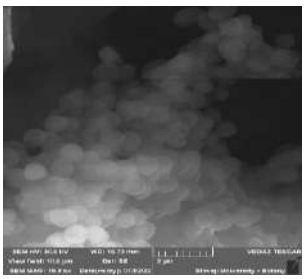

F

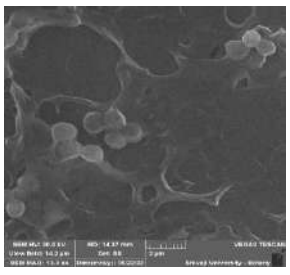

G

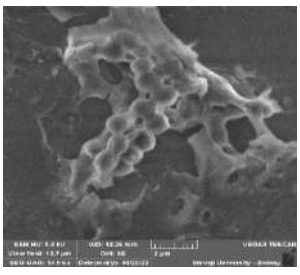

H

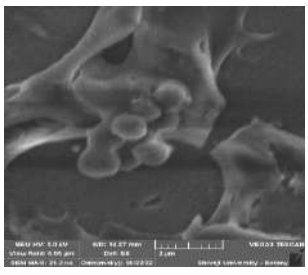

I

Fig.4.4.6: Scanning electron microscopic images of *S. aureus* cells after treatment with phytocompounds A) Untreated control cells B) cells treated with curcumin C) cells treated with curcuminoids D) cells treated with 4-hydroxy-2-methylacetophenone E) cells treated with purified curcumin F) cells treated with purified curcuminoid G) cells treated with combination of curcumin + 4-hydroxy-2-methylacetophenone H) cells treated with diosgenin I) cells treated with purified diosgenin

4.4.4 Conclusions:

The secondary metabolites from plants were extracted by using liquid, reflux, or ultrasonic extraction methods with an alcoholic solvent. The phytocompounds present in the extracts were separated by chromatographic method linked to mass spectrometer detection (LC-MS/MS) which offered accurate and reliable quantification and recognition of trace quantities of metabolites. Similarly, GC-MS/MS analysis provided insight into the variety of phytocompounds present in the extracts.

Individual and combinational effect of phytocompounds was investigated on Gram-positive and Gram-negative pathogens such as *S. aureus* NCIM 2654, *S. mutans* NCIM 5660 and *E. coli* NCIM 2832, *P. vulgaris* NCIM 2813 respectively. Further, we studied the inhibition of biofilm forming pathogens such as *S. aureus* and *S. mutans* by using phytocompounds. In this context, our biofilm inhibition experiment with crystal violet assay and SEM showed the inhibition of biofilm formation for all the phytocompounds significantly against *S. aureus*. Notably, the combinational effect of curcumin + 4-hydroxy-2-methylacetophenone showed significant antibacterial, antifungal, and anti-biofilm forming activity. Hence it concludes that the combinational effect of phytocompounds provides a better inhibition as compared to individual one.

4.5 Inhibition of *S. Aureus* and *S. Mutans* Sortase A by PGPR induced secondary metabolites from *C. longa: In-vitro* and *in-silico* approaches

The part of this study communicated to:

International Journal of Biological Macromolecules

Inhibition of S. Aureus and S. Mutans Sortase A by PGPR induced secondary metabolites from C. longa: In-vitro and in-silico approaches

--Manuscript Draft--

Manuscript Number:	
Article Type:	Research Paper
Section/Category:	Proteins and Nucleic acids

International Journal of Biological Macromolecules (Manuscript ID: IJBIOMAC-D-23-16762), Under Review

4.5.1 Introduction:

Staphylococcus aureus is an aerobic Gram-positive bacteria and has been found in a variety of diseases, including skin infections, endocarditis, toxic shock syndrome, osteomyelitis, and septicaemia (Niu et al., 2018; Ippolito et al., 2010; Lowy et al., 1998). Another Gram-positive endogenous pathogen, *Streptococcus mutans*, cariogenic bacteria live in biofilm and consequence in dental caries and other related disorders (Hu et al., 2013; Luo et al., 2017). Previously, it has been shown that *S. aureus* causes nosocomial infections, whereas *S. mutans* causes a variety of mild to severe infections (Chenna et al., 2008; Cvitkovitch et al., 2003). It has been found that cell adhesion protein sortases (SrtA) are extracellular transpeptidases highly conserved in Gram-positive bacteria that covalently attaches the secreted proteins to the peptidoglycan cell wall and essential for initiation of biofilm formation (McCafferty et al., 2010). So far, four isoforms of sortase have been identified: SrtA, SrtB, SrtC, and SrtD (Si et al., 2016; Nitulescu et al., 2021). Among them, the structure and catalytic mechanism of highly conserved SrtA has received promising target for anti-infective agents (Niu et al., 2018; Stoica et al., 2017). SrtA also plays an important role in the pathogenesis, invasions and biofilm formation in both of *S. aureus* and *S. mutans* (Hu et al., 2013). The biofilm is defined as dense aggregates of surface adherent microorganisms embedded in extracellular matrix composed by exopolysaccharide (EPS), and it is estimated that biofilms are reason for 65 percent of human bacterial infections (Cvitkovitch et al., 2003). The formation of biofilm involves two major steps: adhesion and maturation with proliferation (Fux et al., 2005; Costerton et al., 2003). SrtA catalyzed three steps sorting reaction: recognition, transesterification, and transpeptidation of LPXTG motif sorting signal (Ha et al., 2020; Cascioferro et al., 2015). Earlier studies of SrtA knockout *S. mutans* showed the decrease in adhesion, colonization, and biofilm formation and associated dental caries (Lee et al., 1989; Levesque et al., 2005). Hence, SrtA is being considered as a promising target in the development of drugs to treat these biofilm associated bacterial infections (Wang et al., 2019; Shulga et al., 2021).

The SrtA inhibition lead to diminution of attachment of various surface proteins that involved in cell adhesion, colonization and inhibition of biofilm formation (Nadaf et al., 2018; Richards et al., 2015;). Curcumin and its analogues have recently shown great *in-vitro* potential for reversing methicillin resistance in *Staphylococcus aureus* (Nitulescu et al., 2021). Several molecular modeling studies showed that curcumin analogues (Niu

et al., 2018; Park et al., 2005; Das et al., 2018; Nitulescu et al., 2017; Li et al., 2018) and other plant secondary metabolites inhibit SortaseA (Bi et al., 2016; He et al., 2017; Oniga et al., 2017; Salmanli et al., 2021; Nitlescue et al., 2017). SrtA's primary sequence includes an N-terminal signal peptide, a surface protein and a C-terminal sorting signal (Suree et al., 2009; Zong et al., 2004). The C-terminal sorting domain contains three subdomains: a LPXTG motif, second hydrophobic domain, and third charged tail (Si et al., 2016). These subdomains aid in the anchoring of microbial surface components recognizing adhesive matrix molecules (Cascioferro et al., 2015). In previous studies of sortase inhibition assay, it was discovered that curcumin effectively inhibited SrtA (Park et al., 2005). As per previous reports several SrtA conformations were observed, including the immobilized β 6/7 loop (formed by residues Thr156 to Lys177) in few docked complexes and open state conformations in apo form (Gao et al., 2016). The analysis of conformational diversity and binding pocket fluctuations assumes that the active site is not always the preferred site for binding for lead molecules reported (Gao et al., 2016). However, additional curcumin analogues have also been shown to inhibit SrtA (Sivaramakrishnan et al., 2019). Earlier studies showed the crude extracts of *C. longa* and *Psoralea* in methanol, inhibit the *S. aureus* (80%) and *S. mutans* (44.2%), respectively (Nitulescu et al., 2021). The SrtA inhibitor does not kill the bacteria, but it inhibits virulence and thus prevents infection caused by Gram-positive bacteria (Stoica et al., 2015.).

PGPR has also demonstrated their ability to increase the yield and content of plant secondary metabolites (Kumar et al., 2016; Bharati et al., 2013; Jagtap et al., 2023). When PGPR-treated plants are compared to untreated plants, they show a significant increase in plant growth and secondary metabolite production (Yadav et al., 2022; Cappellari et al., 2015). Considering pathogenic potential of biofilm forming pathogen and the great potential of PGPR in producing novel secondary metabolites which could inhibit the biofilm formation. Hence, our *in-vitro* and *in-silico* approaches to investigate the biofilm inhibition potential and molecular mechanism of SrtA inhibition by PGPR induced phytocompounds. It has been found that the all phytocompounds specifically in synergistic action showed significant biofilm inhibition activity. Hence, phytocompounds in synergy curcumin and 4 hydroxy 2 methyl acetophenone would pave the way for the development of novel lead molecules targeting Srt A to control biofilm formation by *S. aureus* and *S. mutans*.

4.5.2 Materials and methods:

4.5.2.1 Chemicals, bacterial strains and culture conditions

Chemicals such as glutaraldehyde, and crystal violet were purchased from (SRL, INDIA and Himedia,). Similarly, Muller hinton agar (MHA) and brain heart infusion (BHI) broth were bought from Himedia in India. The cultures of *Streptococcus mutans* NCIM 5660 and *Staphylococcus aureus* NCIM 2654 were bought from NCIM (National Collection of Industrial Microorganisms) Pune, India. These bacterial cultures were transferred to MHA plates, which were then incubated for 24 hours at 37°C. On the next day, pure cultures were obtained, transferred to slants, and maintained at 4°C in a refrigerator at the Department of Microbiology, Shivaji University in Kolhapur.

4.5.2.2 Molecular properties of phytocompounds

Phytocompounds such as curcumin, curcuminoids, 4-hydroxy 2-methylacetophenone isolated and identified in our previous study were used in this study (Jagtap et al., 2023). In order to predict pharmacological and toxicological prediction an *in-silico* approaches were used using ADME Lab2.0 online server (Bansode et al., 2019; Xiong et al., 2021).

4.5.2.3 Antibiofilm activity of PGPR induced phytocompounds

The microtiter plate assay based on crystal violet was performed for optimizing biofilm formation conditions (Toole et al., 1999). The biofilm formation assay was performed in triplicates using pre-sterilized 96 well flat bottom polystyrene micro-titre plates as described previously with minor modifications (Sharifian et al., 2020). Briefly, a 50 µl of cell suspension with optical density 0.5 at 600nm was inoculated in 150 µl sterile BHI broth in each well. The phytocompounds (curcumin, curcuminoids, 4 hydroxy 2 methyl acetophenone and their combinations- curcumin plus 4 hydroxy 2 methyl acetophenone) at 100 µl (300µg/ml) were added in respective wells. Then microtiter plates were incubated for 24 hrs at 37°C. After incubation media and planktonic cells were carefully aspirated then biofilms in microtitter plate was fixed with of 99% methanol. Thereafter, plates were rinsed with sterile phosphate buffer saline twice and air-dried. Then attached bacterial cells stained with 200 µl of 0.1 % (w/v) crystal violet solution and incubated at 15 min at room temperature. After incubation the excess stain was removed and plates were washed with PBS for twice and then air dried. Finally, the cell bound crystal violet was release by 33% acetic acid. Biofilm growth was monitored

by measuring absorbance at 578 nm using micro plate reader (Erba scan) (Thappeta et al., 2020).

4.5.2.4 Biofilm inhibition study by scanning electron microscopy (SEM)

In this, a clean glass was cut into a square having dimensions 1 cm^2 and washed with a solution of 5% (v/v) Hiclean (Liquid soap, Hi-Media) for 30 min and then rinsed in an ultrapure water to remove any remaining detergent. After air drying the surfaces for 30 min, they were immersed in 96% (v/v) ethanol for 10 min to remove all impurities. To prepare a sample for SEM, 2% glutaraldehyde solution was flood on slide. The bacteria *S. aureus* treated at 300µg/ml concentration of phytocompounds alone and in combination (curcumin and 4-hydroxy-2-methylacetophenone) were used for the preparation of smear. The slides were kept in freezer overnight to fix the smear. On next day smear was washed with an ethanol dehydration series of 20 to 100% (v/v) (Galabova et al., 1996). The samples were then analyzed by SEM using VEGA3 TESCAN instrument.

4.5.2.5 Structural analysis, refinement and validation of SrtA

The three-dimensional structures of SrtA of Gram positive *S. aureus* ($SrtA_{staph}$; PDB ID: 1T2P) and *S. mutans* ($SrtA_{strepto}$; PDB ID: 4TQX) were retrieved from the RCSB structural database (Zong et al., 2004; Richards et al., 2015). The residues from the missing loop region were constructed (5 conformations/loop) using the chimera modeler interface. The structure of SrtA from *S. mutans* had mutated residues, such as H139A, which were changed to wild type using the chimera's 'swapaa' module. The structures with the lowest DOPE (discrete optimised potential energy) scores were chosen and structural refinement was done using the Gromacs version 2018.2. The structural refinement parameters were derived from previous studies (Dhanavade et al., 2013; Parulekar and Sonawane 2017; Barale et al., 2019). The bad contacts along with steric clashes formed during modelling were removed through energy minimization using the steepest descent algorithm, followed by conjugate gradient. The both SrtA protein model with rebuilt loop from trajectories of unrestrained molecular dynamics (MD) simulation were stereochemicaly validated and secondary structural assignment were done using Structure Analysis and Verification Server 6 (SAVES) and by generating a Ramachandran plot (Sonawane et al., 2015; Laskowski et al., 1993; Cavaturu et al., 2019)

4.5.2.6 Binding mode analysis and intermolecular interactions of phytocompounds with SrtA

UCSF's dock6.9 docking tool was used to investigate the binding poses of phytocompounds to SrtA and their detailed intermolecular interactions. The energy minimised and validated structures of both SrtA from MD simulations trajectories were subjected to local docking and then blind docking. Both SortaseA protein were prepared using 'dockprep' module of UCSF chimera by adding hydrogens and assigning charges. Three-dimensional structures of all the phytocompounds were obtained from the PubChem small molecule database in SDF format and open babel was used to converted in pdb (Singh et al., 2014; Kim et al., 2016; O'Boyle et al., 2011), Curcumin (CID 969516), demethoxycurcumin (CID 5324476), Bisdemethoxycurcumin (CID 5315472), 4-hydroxy 2-methyl acetophenone (CID 160512), and ar-turmerone (CID 70133). For convenience, we have referred to these phytocompounds as C1, C2, C3, C4, and C5 respectively, throughout the manuscript.

The known SrtA inhibitors Carvone (Car) for $SrtA_{Staph}$ and Transchalcone (TC) for $SrtA_{Strepto}$ were chosen as controls for comparison with phytocompounds of *C. longa*. All Ligands (Phytocompounds) and Car, TC for docking protocol were prepared using UCSF Chimera 'dockprep' tool. The spheres (grid) were generated using the 'sphgen' tool, and the binding pocket was defined using both the largest sphere and active site residues, Cys184, His120, Arg197 of $SrtA_{Staph}$ and His139, Cys205, Arg213 of $SrtA_{Strepto}$ (Maia et al., 2020). To study detailed binding modes, the conformations were clustered based on grid score and conformation with lowest grid score subjected for investigation of intermolecular interactions. Docking studies of Curcumin (C1) and 4-hydroxy 2-methyl acetophenone (C4) with both SrtA in synergistic were also implemented, as our experimental studies showed significant anti-biofilm activity of C1 and C4 in synergistic as compare to alone. The efficacy of dual inhibitors is well established (Mannu et al., 2014), earlier studies also suggest the binding of compounds other than active site of SrtA alter its activity (Gao et al., 2016). The Maestro suite was used to construct the 2D SrtA and phytocompounds interaction diagrams (Hajbabaie et al., 2021). The structural stability, intermolecular interactions, and binding affinity of docked complexes ($SrtA_{Staph}$-Car, $SrtA_{Staph}$-C1, $SrtA_{Staph}$-C2, $SrtA_{Staph}$-C3, $SrtA_{Staph}$ -C4, $SrtA_{Staph}$ -C5, $SrtA_{Staph}$ -C1+C4) were investigated by performing all atom MD simulation in explicit solvent.

4.5.2.7 MD simulations of SrtA in complex with phytocompounds to assess structural stability

All the $SrtA_{Staph}$-Car, $SrtA_{Staph}$-C1, $SrtA_{Staph}$-C2, $SrtA_{Staph}$-C3, $SrtA_{Staph}$-C4, $SrtA_{Staph}$-C5, $SrtA_{Staph}$-C1+C4, $SrtA_{Strepto}$-TC, and $SrtA_{Strepto}$-C1, $SrtA_{Strepto}$-C2, $SrtA_{Strepto}$-C3, $SrtA_{Strepto}$-C4, $SrtA_{Strepto}$-C5, $SrtA_{Strepto}$-C1+C4 complexes from lowest grid score were selected for MD simulation using GROMACS 2018.2 on Linux platform (Abraham et al., 2015). The partial charges on the ligand structures were calculated in antechamber using the quantum mechanics method (Katsori et al., 2011), and the force field parameters for all ligands were generated using the generalised amber force field (GAFF). The topology files for all 14 docked complexes (listed above) were generated using the Amber ff99SB-ILDN force field in Ambertool21's 'xleap' module (Niu et al., 2018; Gao et al., 2016). ParmEd tool was used to convert Amber topology files to Gromacs (http://parmed.github.io/ParmEd)). TIP3P water model was used to solvate the docked complexes, and the required numbers of counter ions were added to neutralise charges on the solvated systems. The energy of these systems were minimised using the steepest descent method, followed by the conjugate gradient method. Energy-minimized systems were equilibrated over 1ns using a canonical 'NVT' ensemble and an isothermal-isobaric 'NPT' ensemble. Furthermore, for each of the systems under consideration, an unrestrained MD simulation was run for 100ns. The cut-off values for treating long/short range interactions, as well as other input parameters for MD, were derived from previous studies (Parulekar and Sonawane, 2018; Dhanavade and Sonawane, 2014; Jalkute et al., 2013; Sonawane et al., 2021; Bansode et al., 2019; Dhanavade et al., 2013). The simulation trajectories were recorded every 2fs, and the trajectories were analysed for structural stabilities using Gromacs tools such as 'gmx_rms', 'gmx_rmsf', gmx_hbond and so on. Other third-party tools, such as 'vmd,' were also used where necessary. UCSF Chimera1.15 was used to analyse the individual snapshots and to generate quality images. Biovia Discovery studio visualizer 2021 was used to investigate intermolecular interactions at the atomic level.

4.5.2.8 Binding energy calculation and key residue contributions in binding energy of phytocompounds with SrtA

Binding free energy estimation provides a measure of binding affinities between protein-ligand complexes. With a single trajectory approach and either the MMPBSA or MMGBSA methods, it is now possible to estimate relative binding energy effectively. To

calculate relative binding free energy, we used the recently released 'gmx MMGBSA' tool (Tresanco et al., 2021; Miller et al, 2012).

To calculate the binding free energy, the MMGBSA method employs the following equations:

$$\Delta G_{Bind} = < G_{com} > - < G_{Rec} > - < G_{Lig} >$$

However, classical thermodynamic equation of binding energy is;

$$\Delta G_{Bind} = \Delta H - T\Delta S$$

Where ΔH is enthalpy of binding and $T\Delta S$ is conformational entropy after ligand binding.

$$\Delta H = \Delta E_{MM} + \Delta G_{sol}$$

The enthalpic contribution in the binding free energy ΔE_{MM} is calculated by;

$\Delta E_{MM} = \Delta E_{bonded+\Delta E_{nonbonded}} = \left(\Delta E_{bond} + \Delta E_{angle} + \Delta E_{dihedral}\right) + (\Delta E_{ele} + \Delta E_{vdW})$

and, $$\Delta G_{sol} = \Delta G_{polar\ (GB)} + \Delta G_{non-polar}$$

After reimaging the periodic boundary conditions, the stable trajectory observed between 60ns and 100ns of the entire MD simulation period was extracted and used for binding free energy calculation. By performing residue decomposition energy, the contribution of individual residues to the binding free energy was also investigated. This would aid in the investigation of conserved binding pocket interactions in our docked complexes versus their respective controls.

4.5.2.9 Principle component analysis (PCA) and dynamic cross correlation map

We looked for dynamic differences during stable complex formations by both the sortases $SrtA_{staph}$ and $SrtA_{strepto}$, which would provide key insights into the significant dynamic information and inter residue / inter domain correlation of proteins in 2D, in addition to structural stability and intermolecular interactions. Dynamic cross correlation matrices over representative snapshots from stable trajectories (60 to 100 ns) were plotted using the CPPTRAJ module of antechamber to observe the correlation in the dynamics of $SrtA_{staph}$ and $SrtA_{strepto.}$ GNUPLOT was used to create the 2D plot. Principal component analysis (PCA) is a well-established statistical method for studying protein dynamics and describing functionally important protein motions. To test the collective motion and obtain extreme conformations from stable trajectories, principal component analysis was used.

4.5.3. Results and Discussion:

4.5.3.1 Molecular properties of phytocompounds

The phytocompounds such as curcumin, demethoxycurcumin, bisdemethoxycurcumin, 4-hydroxy-2-methylacetophenone, and ar-turmerone were detected in our previous studies of GC-MS/MS and RP-HPLC analysis of PGPR treated *C. longa* (Jagtap et al., 2023). These compounds individually and in combination were investigated for anti-biofilm activity in this study. To determine drug-likeness of physicochemical, pharmacological, Lipinski rule and toxicity properties of these selected compounds have been assessed using ADME Lab2.0 online server. It has been discovered that the molecules of all five compounds pass through the Lipinski rule and exhibit drug-like behaviour. The ADMET profile highlights the therapeutic potential of all of the chosen molecules (Table 4.5.1). Fig. 4.5.1A depicts the 2D structures of the PGPR-treated phytocompounds with PubChem ID.

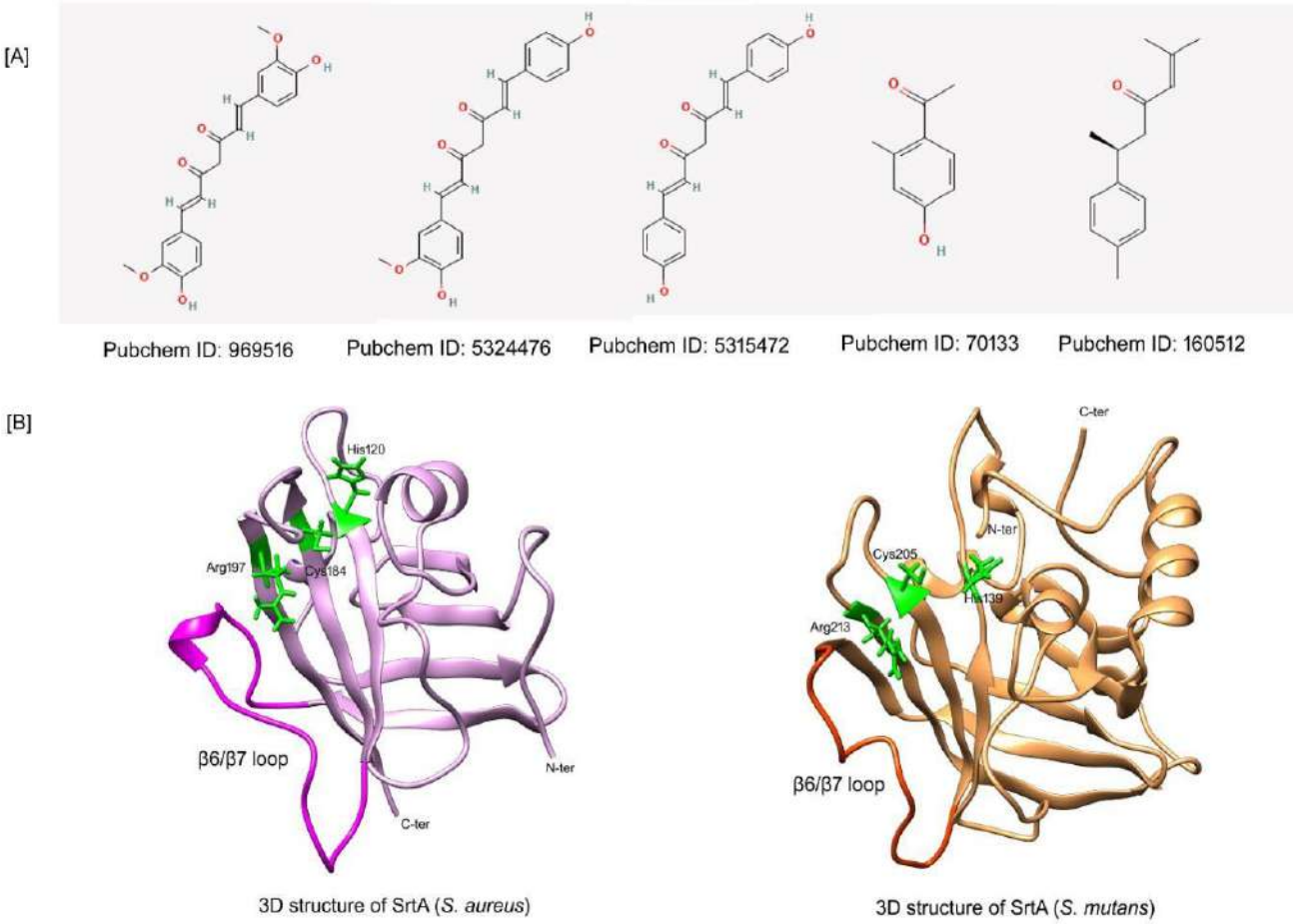

Fig. 4.5.1: The 2D representation of the PGPR treated phytocompounds with PubChem ID and the three-dimensional representation of the relaxed conformation of $SrtA_{staph}$ and $SrtA_{strepto}$.

Table 4.5.1: The ADMET profile of PGPR induced phytocompounds, as well as their PubChem ID, are listed below

Name	PubChem ID	Molecular weight	LogP	SkinSen	Ames	DILI	Carcinogenicity	LC_{50}	Lipinski	Pfizer
Carvone	7439	150.22	2.136	0.041	0.029	0.455	0.432	3.777	Accepted	Accepted
Transchalcone	139036268	208.26	2.987	0.952	0.818	0.668	0.627	5.908	Accepted	Accepted
Curcumin	969516	368.38	2.742	0.958	0.234	0.895	0.706	6.191	Accepted	Accepted
Demethoxycurcumin	5324476	338.36	2.786	0.96	0.41	0.877	0.611	6.13	Accepted	Accepted
Bisdemethoxycurcumin	5315472	308.33	2.847	0.967	0.613	0.843	0.457	6.05	Accepted	Accepted
4 hydroxy 2 methyl acetophenone	160512	150.17	1.771	0.347	0.12	0.462	0.556	3.515	Accepted	Accepted
Ar turmerone	70133	216.32	4.11	0.925	0.015	0.259	0.475	4.57	Accepted	Rejected

4.5.3.2 Antibiofilm activity of PGPR induced phytocompounds from *C. longa*

In order to investigate the biofilm inhibition activity of all phytocompounds, crystal violet assay was performed against biofilm forming *S. aureus* and *S. mutans*. The wells containing curcumin, curcuminoids, 4 hydroxy 2 methyl acetophenone, along with combination of curcumin and 4 hydroxy 2 methyl acetophenone showed the biofilm inhibition activity. Notably, profound anti-biofilm activity was observed for synergistic action of curcumin and 4 hydroxy 2 methyl acetophenone. It may be stated that biofilms without phytocompounds were more securely adhered to the micro plate wells and were less disrupted in staining procedure. The higher absorbance of crystal violet of untreated well of bacteria indicate well established biofilm. However, when bacteria in well treated with curcumin, curcuminoids, 4-hydroxy- 2-methylacetophenone at 300µg/ml concentration the decrease in absorbance was observed which implies the inhibition of biofilm. The profound biofilm inhibition activity was observed for the combination of curcumin and 4 hydroxy 2 methyl acetophenone. These results suggest that the combination of curcumin and 4 hydroxy 2 methyl acetophenone are more effective than alone of phytocompounds as an anti-biofilm activity (Fig. 4.5.2). Hence, these metabolites alone and in their combination are manifested to inhibit the biofilm formation by *S. aureus* and *S. mutans*.

S. aureus is known for biofilm-related infections, particularly in nosocomial infections (Gould 2009), but *S. mutans* is more commonly connected with dental carries (Caroline et al., 2018). Bacteria associated with biofilm are resistant to the majority of regularly used antibiotics, and they create extracellular polymeric substance (EPS) for cell-to-cell adhesion and biofilm growth, slowing the diffusion of conventional antibiotics (Nadaf et al., 2018). Attachment to cell surfaces, matrix development, and maturation are the phases in the biofilm formation (Nadar et al., 2022). Several earlier studies demonstrated that alone curcumin inhibits the growth of biofilm producing organisms (Hu et al., 2013; Park et al., 2005). However, our both *in-vitro* and *in-silico* studies showed significant biofilm inhibition activity of phytocompounds in combination against *S. aureus* as compare to alone targeting adhesion protein SrtA.

4.5.3.3 Biofilm inhibition study by scanning electron microscopy (SEM)

To confirm the anti-biofilm activity of phytocompounds on *S. aureus* NCIM

2654, SEM analysis was implemented. The SEM analysis of untreated *S. aureus* showed more organised and dense bacterial biofilm (chapter 4- Fig.4.4.6A). The untreated cells had a smooth, undamaged surface that was spherical in shape, contributing in their strong adherence to one another (chapter 4-Fig. 4.4.6A). The disorganized adhesion of the bacteria was clearly visible in bacteria treated with phytocompounds (chapter 4-Fig. 4.4.6 B-D,G), indicating impediment in formation of aggregate and an inability to maintain their normal morphology. SEM analysis also revealed that, after the treatment of curcumin and 4-hydroxy-2-methylacetophenone alone cell number get drastically reduced as compare to control (chapter 4-Fig. 4.4.6 A, B, G). Notably, combination of curcumin and 4-hydroxy-2-methylacetophenone showed profound effect on cell morphology and cell number, the cell number get reduced as compared to all experiment in this study. Similarly, cells loses their adhesion after being treated with all phytocompounds, and alterations to their morphology was observed, our results suggest the synergistic impact of phytocompounds better than an individual on biofilm inhibition. These observations lend credence to the results of the growth curve investigations.

One of the key steps in the production of biofilms, called quorum sensing or cell-to-cell communication, where microorganisms may interact with each other. Gram positive and Gram-negative microbes have been the subject of the most thorough research in this process (Waters and Bassler, 2005; Eberhard et al., 1981; Sheikh et al., 2013; Vendeville et al., 2005). According to reports, the inhibitory effect of phytocompounds on quorum sensing and the formation of biofilms is a phenomenon that depends on the density of the bacteria (Filomena et al., 2013). Our findings, however, suggest that inhibiting adhesion may halt the development of biofilms right at their beginning, which may be more useful when developing fresh therapeutic approaches. Earlier several studies showed the role of sortaseA (SrtA) in attachment of surface protein involved in adhesion of cell to host and subsequent biofilm formation (Hu et al., 2013; Wang et al., 2019; He et al., 2017).

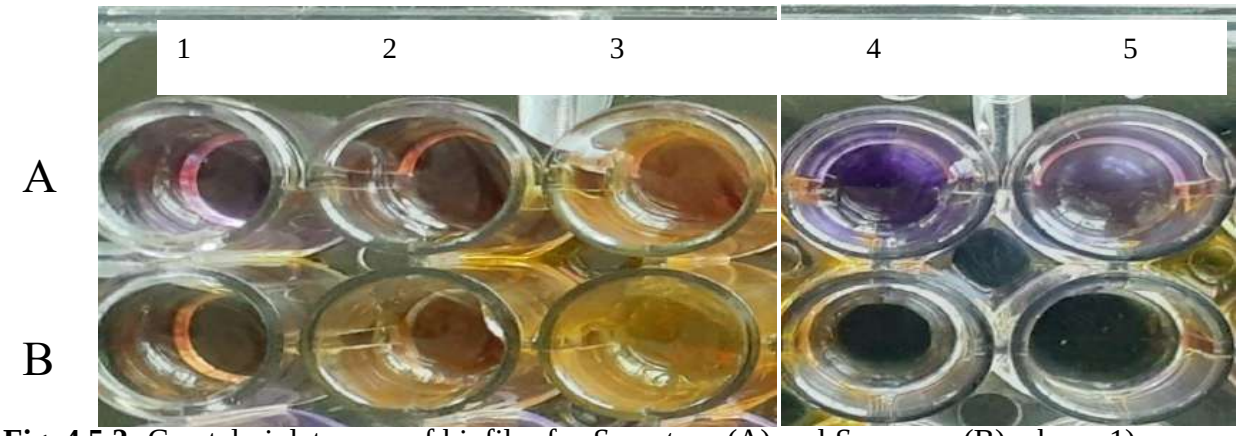

Fig. 4.5.2: Crystal violet assay of biofilm for *S. mutans* (A) and *S. aureus* (B) where, 1) is control untreated cells 2) cells treated with curcumin 3) cells treated with curcuminoids 4) cells treated with 4-hydroxy-2-methylacetophenone 5) cells treated with curcumin + 4-hydroxy-2 methylacetophenone

4.5.3.4 Structural analysis, refinement and validation of SrtA

In order to investigate the mechanism of inhibition of sortaseA (SrtA) from both *S. aureus* and *S. mutans* by phytocompounds molecular modelling techniques were used. The structural stability of SrtA was evaluated by MD simulation and analysis of conformational stability parameters such as root mean square deviation (RMSD), root mean square fluctuation (RMSF) and radius of gyration (Rg). The overall quality of SrtA structure was validated using, the ERRAT score, ramachandran plot along with the stereochemical properties of $SrtA_{staph}$ and $SrtA_{strepto}$. The ERRAT scores of $SrtA_{staph}$ and $SrtA_{strepto}$ conformations are 97 and 95 percent, respectively, indicating that the tertiary structure is of high quality. The Ramachandran plot shows that 98.6 percent of the residues ($SrtA_{staph}$) and 98.9 percent of the residues ($SrtA_{strepto}$) occupy the most allowed and additionally allowed region in the plot (Fig.4.5.3). It is worth noting that after structural refinement in free form of $SrtA_{staph}$ and $SrtA_{strepto}$, no single residue occupies a disallowed region in either sortases.

The N-terminal signal peptide of SrtA was removed in this study due to its flexibility and positioned away from the primary binding pocket. The result, suggests that both of these models of $SrtA_{staph}$ and $SrtA_{strepto}$ have good stereochemical properties as well as native secondary structural folds in the tertiary structure (Fig.4.5.1B). The calculated Q-means of $SrtA_{staph}$ and $SrtA_{strepto}$ are 0.7 and 0.62, respectively, indicating

the model's reliability. The ProSA analysis results of SrtA$_{staph}$'s showed Z-score of -5.93, and -4.89 for SrtA$_{strepto}$, confirming the good overall quality of the 3D structures. The structural quality of protein is also supported by the local quality, which is estimated using the knowledge-based energy value for all amino acids in SrtA$_{staph}$ and SrtA$_{strepto}$ which are less than 0. These results suggest both SrtA$_{staph}$ and SrtA$_{strepto}$ have fewer high energy regions in their relaxed conformations. The relaxed conformation of SrtA$_{staph}$ and SrtA$_{strepto}$ (Fig. 4.5.1B) is represented in three dimensions, highlighting the β 6/7 loop and key active residues in stick form (shown in green).

4.5.3.5 Binding mode analysis and intermolecular interactions of phytocompounds with SrtA

Docking studies aid in elucidating binding poses and estimating binding affinity as observed in previous studies (Dhanavade et al., 2013; Parulekar and Sonawane 2017; Barale et al., 2019). SrtA$_{Staph}$ and SrtA$_{strepto}$ energetically refined structures were used to investigate binding mode and explore intermolecular interactions of phytocompounds at the atomic level using UCSF's dock6.9. The docking studies were also conducted using carvone (car) as control for SrtA$_{Staph}$ and transchalcone (TC) for SrtA$_{strepto}$. Our docking protocol reproduced and showed similar type of binding and interaction of carvone (Car) and transchalcone (TC) molecules with SrtA$_{Staph}$ and SrtA$_{strepto}$ respectively, validating our docking protocol also. Curcumin, demethoxy curcumin, bisdemethoxy curcumin, 4 hydroxy 2 methyl acetophenone, and ar-turmerone bind to the binding pocket residues of SrtA$_{staph}$ and SrtA$_{strepto}$ and represented as SrtA$_{Staph}$-C1, SrtA$_{Staph}$-C2, SrtA$_{Staph}$-C3, SrtA$_{Staph}$-C4, SrtA$_{Staph}$-C5, and in combination SrtA$_{Staph}$-C1+C4, and for SrtA$_{strepto}$-C1, SrtA$_{strepto}$-C2, SrtA$_{strepto}$-C3, SrtA$_{strepto}$-C4, SrtA$_{strepto}$-C5 and in combination SrtA$_{Strepto}$-C1+C4 respectively. Binding affinity to the SrtA$_{Staph}$ was estimated in decreasing order to be C1 > C2 > C3 > C5 > Car > C4 > C1+C4 and for SrtA$_{Strepto}$ it was estimated to be C2 > C3 > C1 > C1+C4 > TC > C5 > C4. The grid score, van der Waals energy, and repulsive energy of phytocompounds Car, TC, C1, C2, C3, C4, C5, C1+C4 (combination) and bound to both the SrtA$_{Staph}$ and SrtA$_{strepto}$ are listed in Table 4.5.2. These result showed the curcumin (C1) has a much stronger binding to SrtA$_{Staph}$ than car (control), however, curcumin analogue demethoxy curcumin (C2) reflects much stronger binding towards SrtA$_{strepto}$ than TC (control), the binding mode of all phytocompounds depicted in Fig. 4.5.4A and 4.5.4B The analysis of intermolecular interactions suggests that the

formation of stable complexes is primarily triggered by conserved non-bonded contacts with the key binding pocket residues reported in previous studies (Nadaf et al., 2018; Bi et al., 2016; Chenna et al., 2008). The fact that hydrophobic and hydrogen bonding interactions facilitates the formation of stable complexes in all complexes (Table 4.5.3). In both SrtA$_{Staph}$ and SrtA$_{strepto}$ complexes, the residues Thr, Lys, Ala, and Glu (156 to 177) of the β 6/7 loop play a critical role in loop opening and closing as compared to other neighbouring residues. Docking results showed interacting residues of SrtA$_{Staph}$ Glu105, Cys184, Arg 197, Lys62 and for SrtA$_{strepto}$ Cys205, His139, Arg213, Ser138 found in interaction with phytocompounds.

C4 binds at the active site of SrtA in complex SrtA$_{Staph}$-C1+C4, whereas C1 binds at an alternate binding pocket adjacent to the primary binding pocket of SrtA. Previous studies showed the compounds have been bind at other than active site of SrtA (Gao et al., 2016). Our findings of forming a stable ternary complex with SrtA$_{Staph}$ and SrtA$_{strepto}$ of C1 and C4 respective are consistent with previous reports. In the complex SrtA$_{Strepto}$-C1+C4, both C1 and C4 occupy in same binding pocket and exhibit conserved non-bonded interactions, as reported in the crystal structure (Wallock et al., 2015). Fig. 4.5.5 depicts non-bonded interactions in the studied complexes in two dimensions.

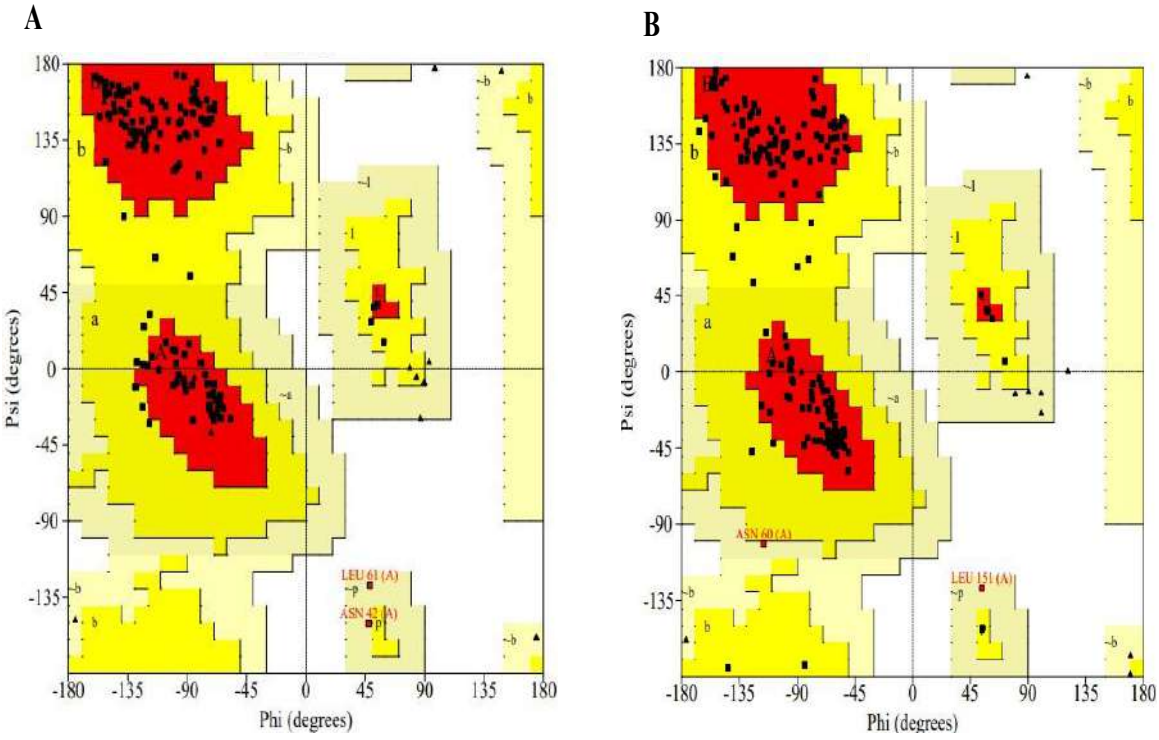

Fig. 4.5.3: Ramachandran plot of SrtA$_{staph}$ (A) and SrtA$_{strepto}$ (B) model with rebuilt loop.

Table 4.5.2: Molecular docking of phytocompounds with active site residues of $SrtA_{staph}$ and $SrtA_{strepto}$-using Dock6.9

	Compound name	**Grid Score**	**Vwd energy**	**Energy repulsive**
$SrtA_{staph}$	Carvone (Car)	-21.06	-21.31	3.97
	Curcumin(C1)	-34.55	-29.10	14.18
	Demethoxycurcumin(C2)	-32.29	-28.02	10.49
	Bisdemethoxycurcumin(C3)	-31.24	-27.11	4.85
	4-hydroxy-2-methylacetophenone (C4)	-19.49	-17.28	2.60
	Ar-turmerone(C5)	-21.47	-21.03	9.79
	Curcumin + 4-hydroxy-2-methylacetophenone (C1+C4)	-18.74	-18.74	2.12
$SrtA_{strepto}$	Transchalcone (Tc)	-23.05	-22.21	2.85
	Curcumin(C1)	-31.38	-29.96	11.39
	Demethoxycurcumin(C2)	-32.73	-30.33	4.30
	Bisdemethoxycurcumin(C3)	-31.99	-28.46	3.64
	4-hydroxy-2-methylacetophenone (C4)	-18.59	-15.55	1.76
	Ar-turmerone(C5)	-21.40	-20.08	8.01
	Curcumin + 4-hydroxy-2-methylacetophenone (C1+C4)	-23.31	-23.31	13.99

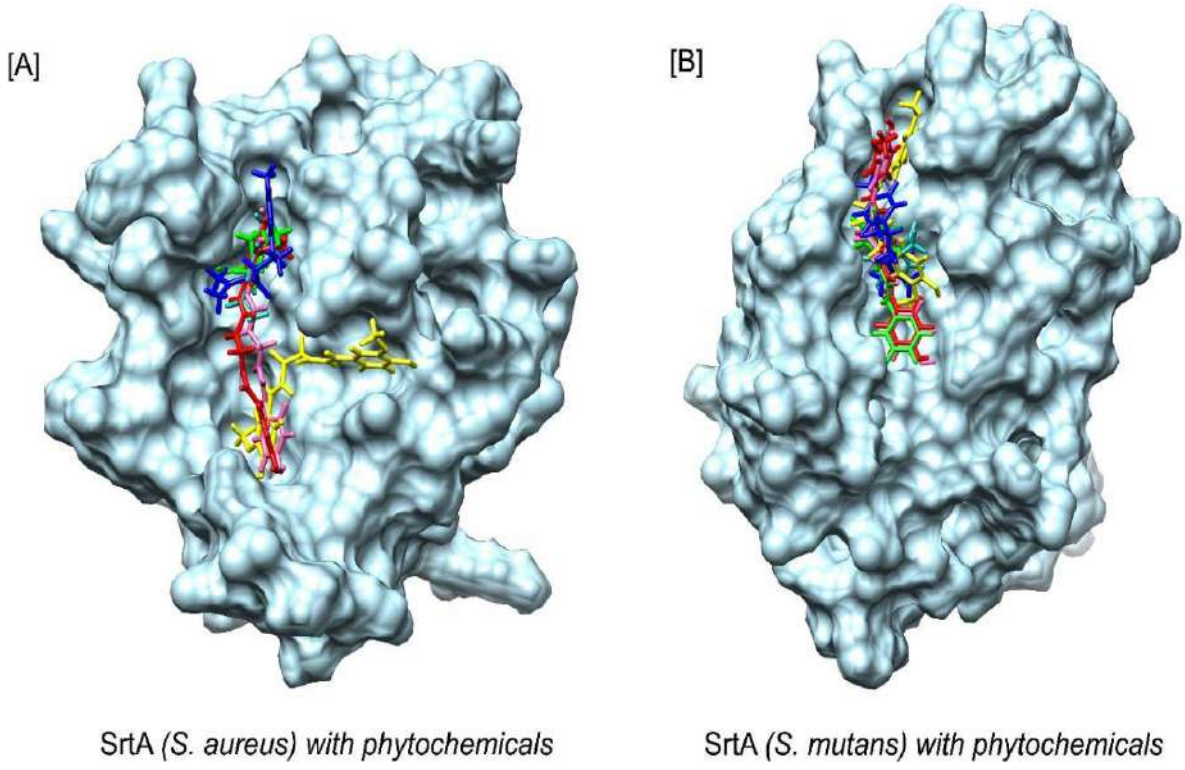

Fig. 4.5.4: The surface view depicts the binding mode of all phytocompounds bound to $SrtA_{staph}$ and $SrtA_{strepto}$

Table 4.5.3: Hydrogen bonding interactions of phytocompounds with $SrtA_{staph}$ and $SrtA_{strepto}$ in docking

	Compound name	**Interaction**	**Distance(Å)**
$SrtA_{staph}$	Carvone (Car)	ALA92 HN…O1 UNK	3.07726
	Curcumin(C1)	LEU169 HN… O3 UNK GLY167 O … H13 UNK VAL168 H… O3 UNK	2.68979 2.4078 2.00886
	Demethoxycurcumin(C2)	LEU169 HN…O5 UNK ARG197 H…O3 UNK ALA104 O…H15 UNK	2.04411 2.64559 2.71909
	Bisdemethoxycurcumin(C3)	LEU169 HN…O3 UNK	2.51404
	4-hydroxy-2-methylacetophenone C4)	GLY192 O…H10 UNL TRP194 HD1… C5 UNL ILE182 HD12… O2	2.22369 2.788 2.854

		UNL	
	Ar-turmerone(C5)	-	-
	Curcumin + 4-hydroxy-2-methylacetophenone (C1+C4)	LEU169 H …O3 UNK VAL168 H…H UNK VAL166 C20… H UNK SER109 HB2… O4 UNK ALA 92 HB3…H UNL TRP194 H… O2 UNL ARG 197 HD2… O2 UNL GLY192 O… H5 UNL	1.737 1.654 2.630 2.009 2.674 2.369 2.941 2.688
SrtA*strepto*	Transchalcone (Tc)	HIS140 H…O1 UNK THR204 H… O1UNK CYS205 H… O1 UNK HIS139 HA… O1 UNK	2.35582 2.71581 2.42955 2.94051
	Curcumin(C1)	ALA210 H… O5 UNK SER138 O… H15 UNK ASP68 O… H18 UNK	3.04136 3.03284 2.56842
	Demethoxycurcumin(C2)	HIS140 H…O4 UNK	2.41686
	Bisdemethoxycurcumin(C3)	HIS140 H… O2UNK HIS139 H…O2 UNK	2.24961 2.88918
	4-hydroxy-2-methylacetophenone (C4)	THR204 H… O1 UNL CYS205 H… O1 UNL SER138 O… H10 UNL HIS139 H… O2 UNL	2.56819 2.32768 2.66199 2.91423
	Ar-turmerone(C5)	ASN113 H… O1 UNK HIS139 H… O1UNK	2.91684 2.47309
	Curcumin + 4-hydroxy-2-methylacetophenone (C1+C4)	CYS205 H… O1 UNK SER138 O… H1 UNK HIS139 H… O2 UNK HIS139 HE1… O2 UNL CYS205 H… H1 UNL THR204 HG1… H1 UNL	2.32768 2.172 2.91423 2.914 2.599 1.920

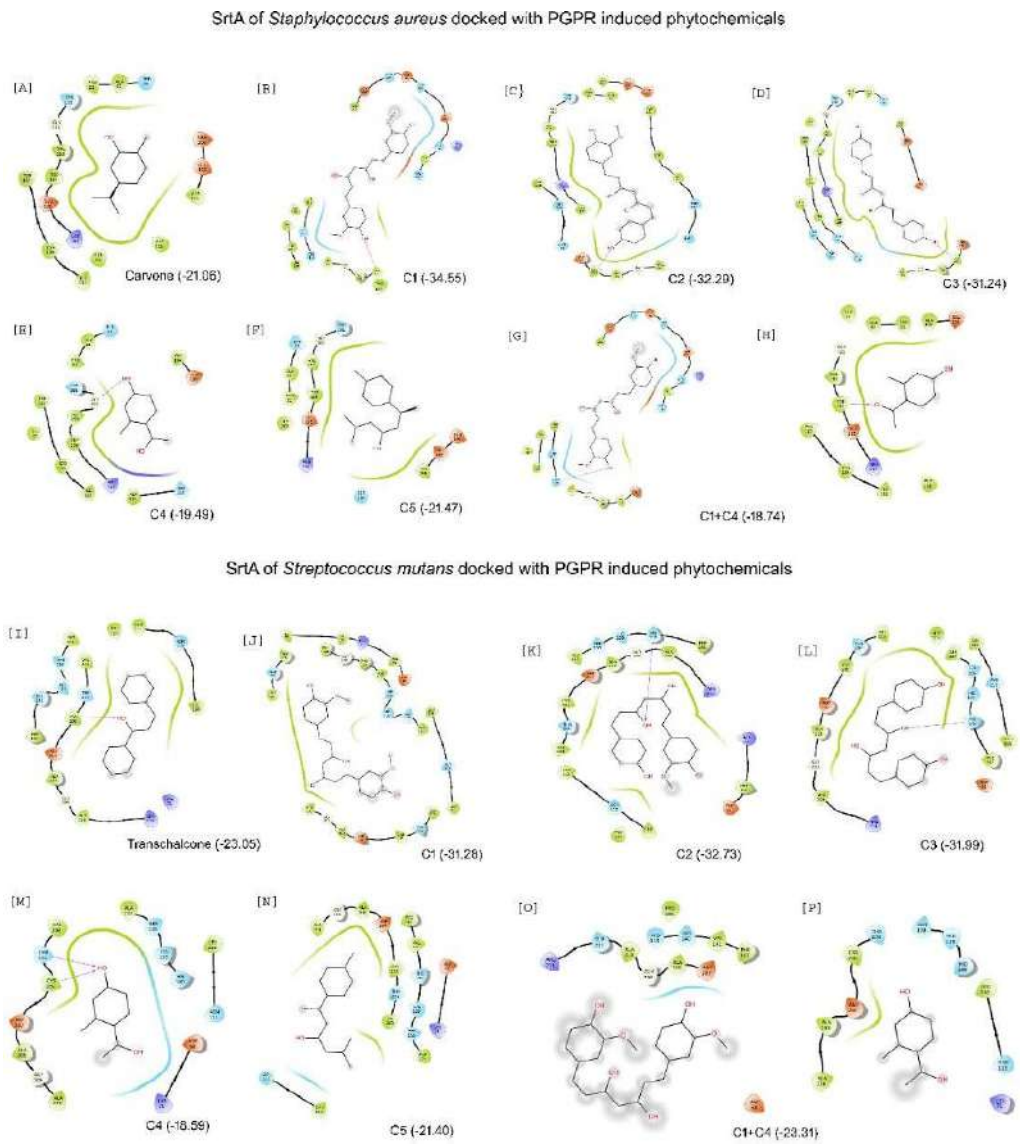

Fig. 4.5.5: Nonbonded interactions in the complexes studied are represented in 2D

4.5.3.6 MD simulations of SrtA in complex with phytocompounds to assess structural stability

MD simulation helps to generate ensemble of configurations, assessment of structural stability of ligand bound proteins, further in free energy calculations and ligand induced conformational changes. MD simulations of 100 ns performed for all the docked complexes namely SrtA$_{Staph}$-Car, SrtA$_{Strepto}$-TC, SrtA$_{Staph}$-C1, SrtA$_{Staph}$-C2, SrtA$_{Staph}$-C3, SrtA$_{Staph}$-C4, SrtA$_{Staph}$-C5, SrtA$_{Staph}$-C1+C4, SrtA$_{Strepto}$-C1, SrtA$_{Strepto}$-C2, SrtA$_{Strepto}$-C3, SrtA$_{Strepto}$-C4, SrtA$_{Strepto}$-C5, SrtA$_{Strepto}$-C1+C4 to investigate their structural stability and

intermolecular interactions. The trajectories of all simulated complexes were examined for the quality and dependability of the MD parameters. Throughout the simulation, the potential energy, temperature, and pressure were all analysed to ensure the quality of all the trajectories. The data show that the pressure and temperature remained constant at 300K and 1bar, respectively, and that the potential energy fluctuated less during MD. As a result, we believe that all of the MD simulation trajectories are properly equilibrated.

The parameters that explain structural stability have been studied, including RMSD, RMSF, Rg, and solvent accessible surface area (SASA). Calculating the RMSD of proteins allows for the quantification of the degree of conformational changes that may occur during MD simulations with respect to the starting structure as a reference. An average RMSD of SrtA$_{Staph}$ and SrtA$_{Strepto}$ in complex with all phytocompounds fall within a range of 2 and 2.5Å, respectively (Fig. 4.5.6A and 4.5.6B; Table 4.5.4). This RMSD analysis of SrtA from both the pathogens reflects the structural stability. The complex of SrtA$_{Staph}$-Car has a higher RMSD of 2.3 when compared to other complexes bound to SrtA$_{Staph}$. Overall, we found that after the equilibrium period of 0 ns to 60 ns, all of the simulated complexes were well stabilized. The complexes SrtA$_{Staph}$-C5 and SrtA$_{Strepto}$-C5 have higher RMSD values, owing to the flexibility of the N-terminal domain (NTD). RMSF analysis of C-alpha of residues of SrtA from both pathogens in complex with all phytocompounds showed similar kind of residue fluctuation except for the complex SrtA$_{Strepto}$-C5 (Fig. 4.5.6D). In SrtA$_{Staph}$ complexed with phytocompounds, the N-terminal region shows maximum fluctuations with RMSF values up to 5.5 Å, whereas the fluctuation of SrtA$_{Strepto}$ shows the highest RMSF value of 12 Å. As seen in the RMSF plot, the maximum RMSF value in SrtA$_{Strepto}$ is primarily due to the N-terminal flexibility of the SrtA$_{Strepto}$-C5 complex. Overall, the stability of SrtA was attained during MD simulation due to facilitation of stable complexation of phytocompounds with the residues Thr156 to Lys177 of SrtA$_{Staph}$ and Thr184 to Asn198 of SrtA$_{Strepto}$ within the loop β 6/7 (Fig. 4.5.6C and 4.5.6D). Additionally, our results highlight the much lower fluctuations and more stability of SrtA from both the pathogen, when complexed with both curcumin and 4-hydroxy 2-methyl acetophenone (C1and C4). The reported key residues of both SrtA$_{Staph}$ and SrtA$_{Strepto}$ His, Cys, and Arg, show less fluctuation. This emphasises the importance of these binding pocket residues in the formation of stable protein-ligand complexes.

Another parameter that contributes to overall spatial arrangement of secondary structure in protein is Rg, which represents the folding and unfolding pattern and compactness of protein-ligand complexes. A comparison of the Rg values of all the complexes shows that the control complexes in our study, SrtA$_{Staph}$-Car and SrtA$_{Strepto}$-TC, have larger deviation in Rg values, indicating that these complexes are unstable, most likely due to poor binding pocket interactions (Fig. 4.5.7A and 4.5.7B). The SrtA$_{Strepto}$-C5 complex exhibits partial unfolding for up to 30ns before adopting compact globular shapes during the simulation (Fig. 4.5.7B). As a result, we believe that the partial unfolding at the N-terminus of SrtA$_{Strepto}$ may cause some conformational changes at the binding pocket, enhancing the interactions. The Rg value of the ternary complexes SrtA$_{Staph}$-C1+C4 and SrtA$_{Strepto}$-C1+C4 is relatively stable, indicating that the binding of curcumin (C1) and 4-hydroxy 2-methyl acetophenone (C4) promotes the formation of compact globular conformations (Fig. 4.5.7A and 4.5.7B). Except for SrtA$_{Strepto}$ -C5 and SrtA$_{Strepto}$-TC, the complexes of phytocompounds bound to SrtA$_{Strepto}$ showing similar folding pattern as revealed by a steady decrease in Rg values during the simulation from 16.15 to 15.8. (Fig. 4.5.7B). However, phytocompounds bound to SrtA$_{Staph}$ exhibit Rg value variations (Rg value ranges between 14.5 and 15.1), resulting in a different folding pattern in all complexes. As a result, we propose that SrtA$_{Staph}$ undergoes significant conformational changes during MD simulations, resulting in the formation of stable complexes. In order to evaluate compactness of SrtA, we calculate solvent accessible surface area (SASA), which is thought to be important for intermolecular interactions within globular molecules. It aids in determining the protein's accessibility to the solvent. The stability of SrtA was observed in a similar trend of hydrophobic SASA as that of Rg values which was observed in all complexes (Fig. 4.5.7C and 4.5.7D). Increased SASA has been observed for complexes SrtA$_{Strepto}$-C5 and SrtA$_{Strepto}$-TC, revealing the unfolding caused by interruption of hydrophobic interactions in non-polar residues. The SASA plot reveals a moderate fluctuation in the SASA of all complexes, indicating its importance in the formation of stable complexes

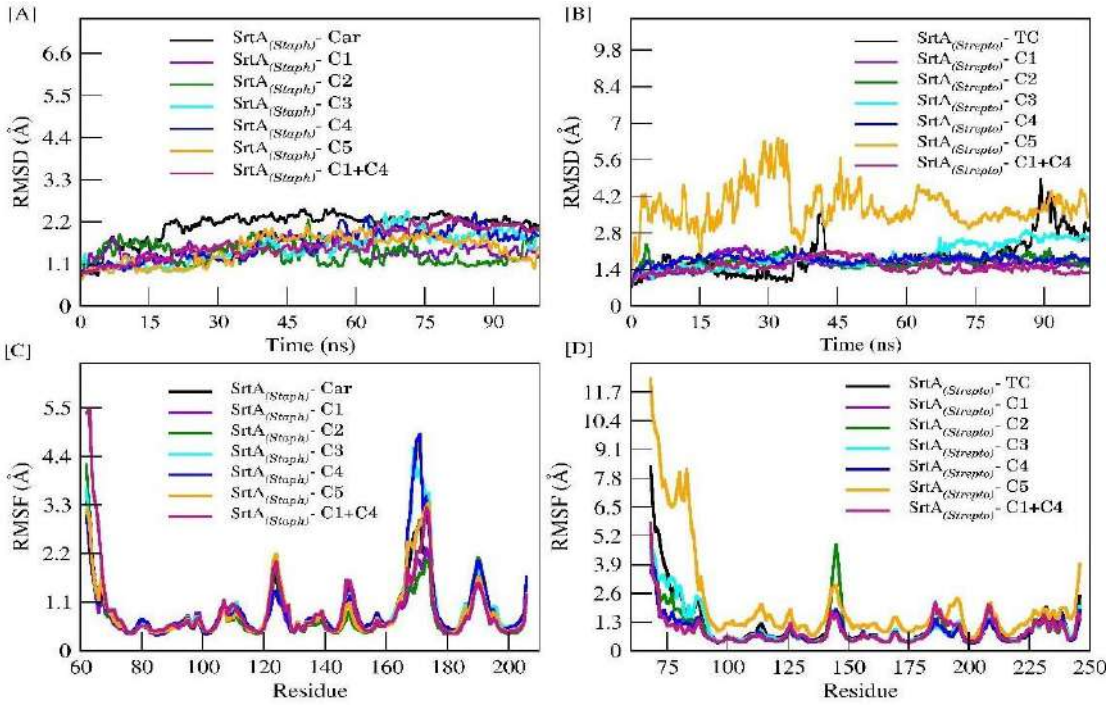

Fig. 4.5.6: The structural stability of simulated complexes was investigated by plotting the backbone RMSD of all complexes. A) $SrtA_{staph}$ B) $SrtA_{strepto}$ and C) $SrtA_{staph}$ D) $SrtA_{strepto}$ and their comparative RMSF

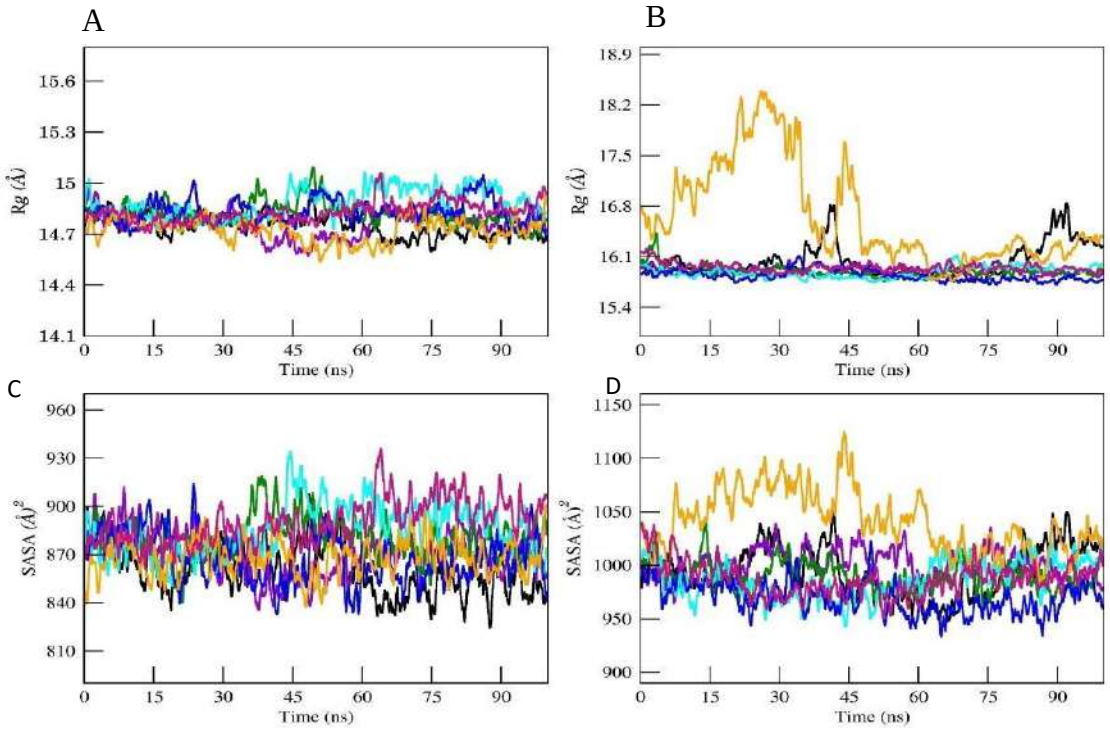

Fig. 4.5.7: The radius of gyration of A) $SrtA_{staph}$ B) $SrtA_{strepto}$ and solvent accessible area of all C)$SrtA_{staph}$ D) $SrtA_{strepto}$ complexes.

Table 4.5.4: Analysis of MD trajectories for average RMSD, RMSF and Rg of SrtA*staph* and SrtA*strepto* over 100 ns.

	Name of organisms					
	Staphylococcus aureus			*Streptococcus mutans*		
	RMSD(Å)	**RMSF(Å)**	**Rg**	**RMSD(Å)**	**RMSF(Å)**	**Rg**
C1	1.4 ±0.02	0.8 ±0.04	14.7 ±0.009	1.6 ±0.02	0.9 ±0.05	15.9 ±0.006
C2	1.3 ±0.02	0.7 ±0.04	14.8 ±0.008	1.6 ±0.02	0.9 ±0.07	15.8 ±0.009
C3	1.5 ±0.04	0.9 ±0.07	14.8 ±0.01	1.9 ±0.04	1.0 ±0.07	15.8 ±0.008
C4	1.6 ±0.04	0.9 ±0.07	14.8 ±0.008	1.7 ±0.01	0.8 ±0.05	15.8 ±0.008
C5	1.4 ±0.03	0.8 ±0.06	14.7 ±0.008	3.8 ±0.07	2.1 ±0.19	16.6 ±0.06
C1+C4	1.6 ±0.04	0.9 ±0.07	14.8 ±0.007	1.6 ±0.02	0.8 ±0.05	15.9 ±0.008
Car	2.1 ±0.03	0.8 ±0.05	14.7 ±0.008	-	-	-
Tc	-	-	-	1.8 ±0.07	1.1 ±0.09	16.0 ±0.02

4.5.3.7 Molecular interactions contributes in inhibition of SrtA

Hydrogen bonding interactions are crucial in protein-ligand interactions among the other non-bonded interactions. The number of hydrogen bonds formed with SrtA*Staph* and SrtA*Strepto* by phytocompounds during the MD simulation was plotted against time (Fig. 4.5.8). The hydrogen bond analysis showed the complexes SrtA*Strepto*-C1, SrtA*Strepto* -C2, and SrtA*Strepto* -C1+C4 maximum number of H-bonds with SrtA, with a total of six, four of which are consistent during the MD simulation. Compound C5 (ar-turmerone) interacts poorly with both sortases, SrtA*Staph* and SrtA*Strepto*. The calculated minimum distance between the ligand and protein demonstrates that in complex SrtA*Staph*–C1,

$SrtA_{Staph}$–C4, $SrtA_{Staph}$–C1+C4, $SrtA_{Strepto}$-C1, $SrtA_{Strepto}$-C1+C4 phytocompounds maintain close contacts with SrtA forming stable non-bonded contacts during the MD simulation. The compound C5 exhibits increased distance in both the sortases $SrtA_{Staph}$ and $SrtA_{Strepto}$ due to significant conformational changes expressed during the dynamics (RMSD, RMSF, Rg, and SASA) responsible for the weak non-bonded interactions. Overall, the complexes such as $SrtA_{Staph}$-C1+C4 and $SrtA_{Strepto}$-C1+C4 have the minimum distances, indicating the stability of ternary complex formed by C1 and C4 further these interactions are stable and conserved during the simulation. In conclusion, the results of analysis of molecular interactions during docking, MD simulation showed the structural stability of SrtA in complex with Curcumin (C1), and 4-hydroxy 2-methyl acetophenone (C4) and in their combination. These results are consistent with our biofilm inhibition assay by crystal violet and SEM, hence we believe that Curcumin, and 4 hydroxy 2 methyl acetophenone in combination would be effective to inhibit SrtA and for biofilm inhibition.

The number of contacts quantifies interactions between spatially closed amino acids that are not sequentially next to each other in the protein's primary sequence. The percentage of contacts that are preserved reflects the stability of the protein-ligand complexes. We looked at the total number of contacts to learn more about the structural stability of the simulated complexes. Except for phytocompounds C5 complexed with both $SrtA_{Staph}$ and $SrtA_{Strepto,}$ all complexes showed a steady increase in the number of contacts. In $SrtA_{Staph}$ and $SrtA_{Strepto}$, the number of contacts formed by C1, C2, C3, and C4 are significantly greater than that of the controls, Car and TC. However, the ternary complex formed by C1 and C4 in $SrtA_{Staph}$ and $SrtA_{Strepto}$ shows a consistent number of contacts with relatively less fluctuations, highlighting the importance of both of these compounds in SrtA inhibition. The non-bonded interactions between phytocompounds and SrtA following MD simulation are illustrated in Fig. 4.5.9A and Fig.4.5.9B.

In order to evaluate the consistency of non-bonded interactions of phytocompounds with SrtA we compare the starting docked conformation of SrtA and final confirmation from MD simulation. Table 4.5.5 list all of the important hydrogen and non-bonded interactions that influence stable complex formation. The interactions observed in our simulated SrtA complexes with phytocompounds were also compared to the control complexes and previously reported interactions (Katsipis et al., 2020, Bi et

al., 2016, Zong et al., 2004). This analysis reveals that residues from the β 6/7 loop, such as Lys, Asp, Gly, Gln, Leu, Val, and Thr, play an important role in the formation of stable complexes. During the MD simulations, we observed that hydrophobic interactions outweighed the H-bonding interactions. In addition, number of intermolecular interactions in all complexes has increased at the end of MD simulation as compared to the initial starting conformation.

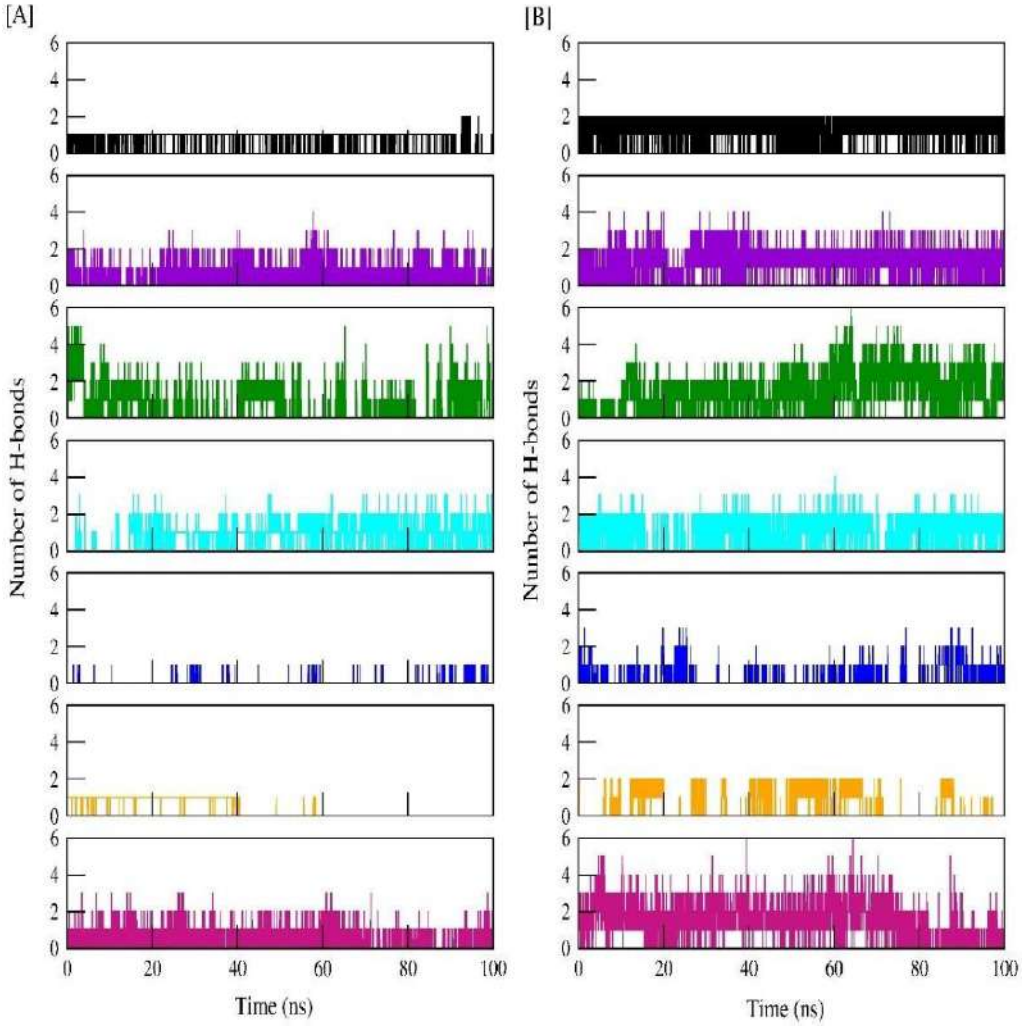

Fig. 4.5.8: Hydrogen bond interactions observed in complexes of PGPR induced phytocompounds in A)$SrtA_{staph}$ B) $SrtA_{strepto}$

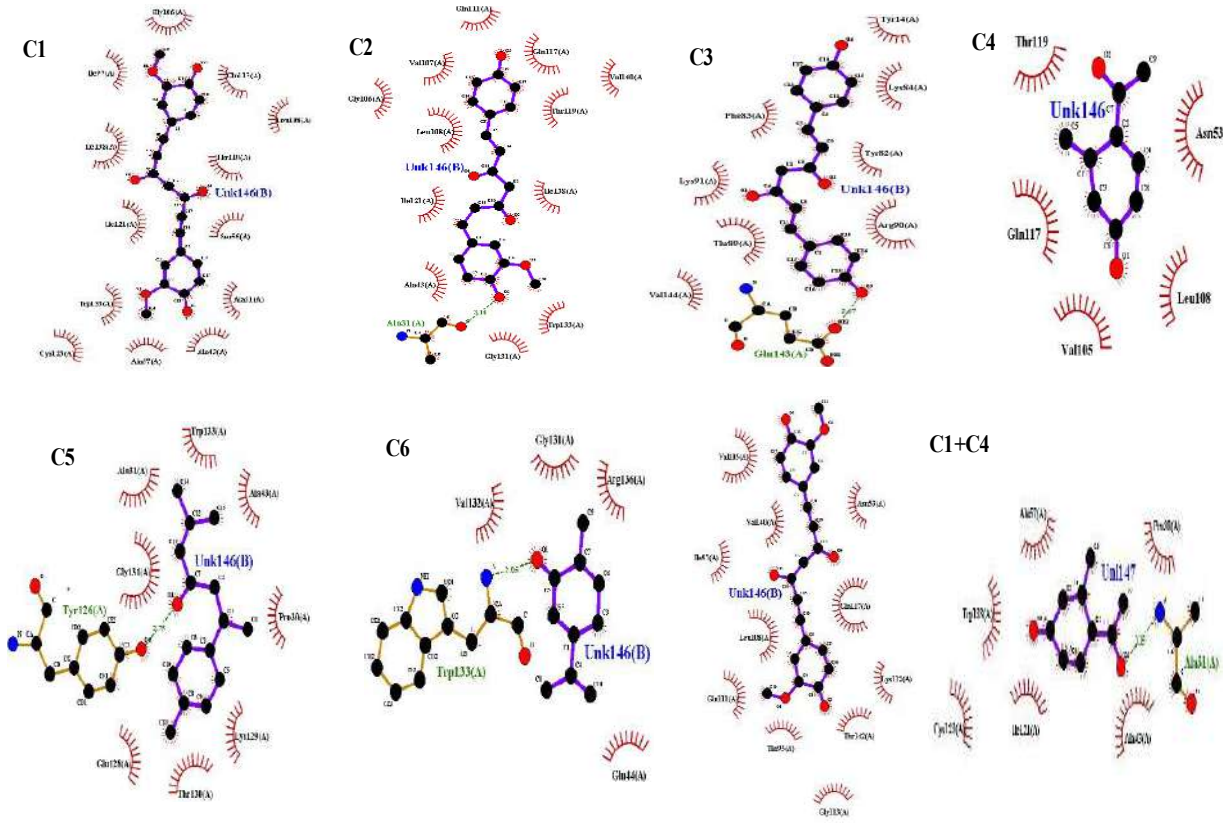

Fig. 4.5.9A: Nonbonded interactions in the complexes of $SrtA_{staph}$ studied after MD simulation are represented in 2D

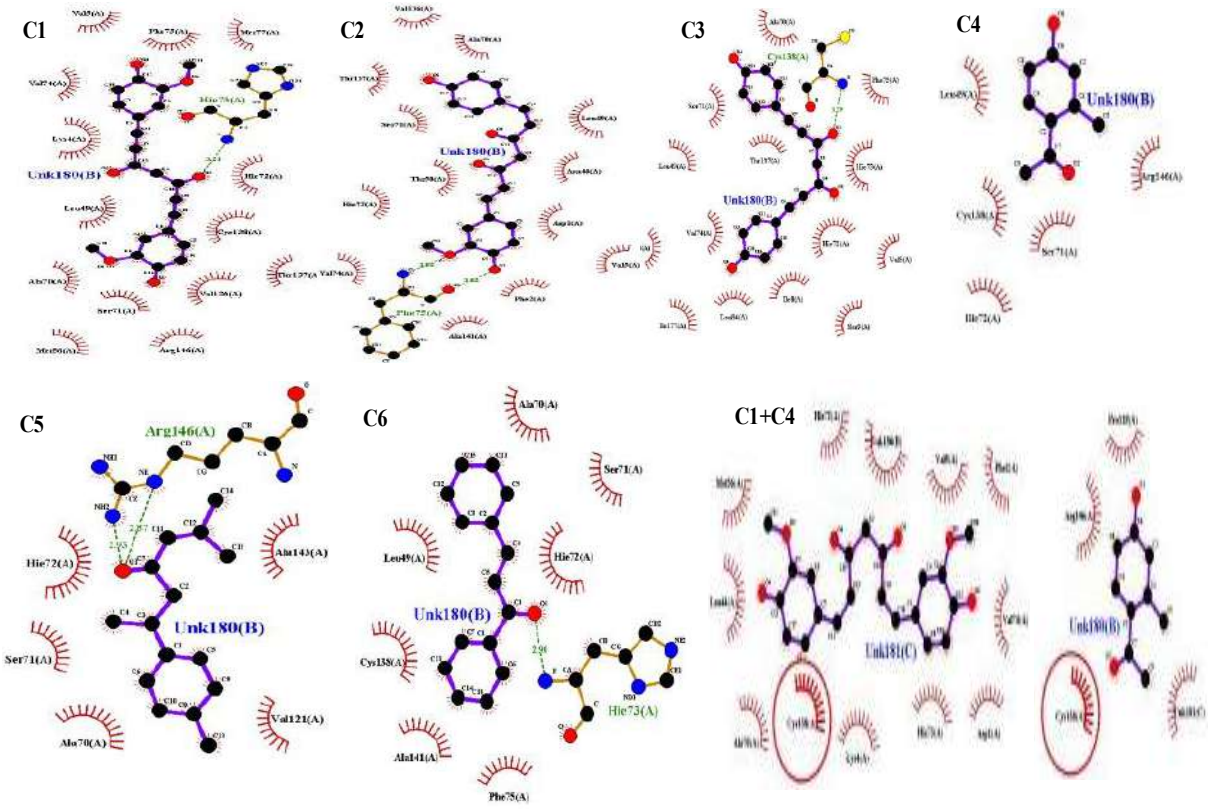

Fig. 4.5.9B: Nonbonded interactions in the complexes of $SrtA_{strepto}$ studied after MD simulation are represented in 2D.

Table 4.5.5: Hydrogen bond interactions of phytocompounds with $SrtA_{staph}$ and $SrtA_{strepto}$ during MD simulations.

	Compound name	**Interaction**	**Distance(Å)**
$SrtA_{staph}$	Carvone (Car)	TRP194 H… O1 UNK VAL193 H… O1 UNK TRP194 HD… O1 UNK	1.99652 2.88217 2.72136
	Curcumin(C1)	GLY167 HN… O1 UNK SER116 OG…O6 UNK TRP194 HD1… O2 UNK	2.41154 3.0304 2.7939
	Demethoxycurcumin(C2)	ALA92 H… O2 UNK TRP194 HE1…O2 UNK ARG197 HE… O2 UNK	2.88586 2.65387 2.66132 2.38455

		GLY192 O… H17 UNK	
	Bisdemethoxycurcumin(C3)	GLU204 OE2…H15 UNK	1.72421
	4-hydroxy-2-methylacetophenone (C4)	ILE182 HD12 … O2 UNL TRP194 HD1… C5 UNL GLY192 O… H10 UNL	2.854 2.788 2.224
	Ar-turmerone(C5)	TYR187 HH…O1 UNK	1.81662
	Curcumin + 4-hydroxy-2-methylacetophenone (C1+C4)	ASN114 HD22… O6 UNK GLY174 HA1… O3 UNK VAL166 HB… O4 UNK VAL201 HG12… O6 UNK GLN178 HG3… O6 UNK ALA 92 H… O2 UNL TRP194 HD1… O1 UNL PRO91 HB2… O1 UNL	3.09247 2.66458 2.682 2.838 2.792 2.586 2.297 2.406
SrtA*strepto*	Transchalcone (Tc)	HIS140 H…O1 UNK CYS205 H…O1 UNK HIS139 HA…O1 UNK	1.90111 2.76199 2.64532
	Curcumin(C1)	HIS140 HN…O5 UNK CYS205 HN… O5 UNK LYS71 HE1… O6 UNK	2.31886 2.36848 2.26958
	Demethoxycurcumin(C2)	PHE142 H… O1 UNK PHE142 O…H14 UNK VAL141 HA… O1 UNK PHE142 O…H16 UNK	2.00704 2.10119 2.71378 2.92132
	Bisdemethoxycurcumin(C3)	HIS140 HN…O2 UNK CYS205 HN… O2 UNK	2.53223 2.38858
	4-hydroxy-2-methylacetophenone (C4)	ALA137 H…C5 UNL LEU111 HD1…H10 UNL	2.25865 2.781
	Ar-turmerone(C5)	ARG213 HE… O1 UNK	1.93355 2.08737

		ARG213 HH21…O1 UNK	
	Curcumin + 4-hydroxy-2-methylacetophenone (C1+C4)	LEU111 HD1… H14 UNK MET123 HE… CH10 UNK HIS139 HE1… CH1 UNK ALA137 HB1… CH10 UNK PRO185 O… H1 UNL ARG213 HD3… O2 UNL	2.968 2.125 2.512 2.054 1.896 2.902

4.5.3.8 Effect of phytocompounds on secondary structure of SrtA$_{staph/strepto.}$

The Dictionary of secondary structure of protein (DSSP) tool was used to analyse the distortions in the secondary structural changes during the MD simulation. Complexes of phytocompounds C1, C2, C3, C4, and C5 with SrtA$_{staph}$ exhibit fewer deviations at the secondary structural level; interestingly, all of the β-sheets maintain their structures throughout the simulations (Fig. 4.5.10A). The β 6/7 loop formed by the residues Thr156-Lys177 undergoes structural transitions during the MD and contributes significantly to stable interactions with phytocompounds. SrtA$_{staph}$ also formed a short-lived helix in this β 6/7 loop in a ternary complex of C1+C4). This short-lived helix is expected to give the binding pocket rigidity by forming stable H-bonding interactions. Furthermore, complex SrtA$_{staph}$-C1+C4 exhibits closure movement by the β 6/7 loop and N-terminal helix, whereas complex SrtA$_{staph}$- Car β 6/7 loop and N-terminus move away from each other. As a result of the closure movement of β 6/7 at the active site, we observed the most non-bonded interactions in SrtA$_{staph}$–C1+C4. During the MD simulation of complex SrtA$_{Strepto}$–C5, the N-terminal helix loses its helicity completely and transitions to turn. As seen in the RMSD, RMSF, and Rg plots, increased flexibility of the N-terminal region is responsible for the larger deviation in structural stability of the SrtA$_{Strepto}$–C5 complex. This N-terminal helix's helicity varies moderately in other complexes, namely SrtA$_{Strepto}$-C1, SrtA$_{Strepto}$–C2, SrtA$_{Strepto}$–C3, and SrtA$_{Strepto}$–C4, whereas in complex SrtA$_{Strepto}$-C1+C4 helicity is well maintained throughout the simulation (Fig. 4.5.10B). The complex N-terminal helix in complexes SrtA$_{Strepto}$– C2 and SrtA$_{Strepto}$-C1+C4 exhibits scissoring movement, promoting the opening and closing of the binding pocket and enhancing non-bonded interactions during simulation. Other secondary structure components exhibit the

fewest variations in the structure. The minimum distance between the residues has also been used to estimate the local conformational changes at the binding pocket. As a result, the SrtA*Strepto*–C1+C4 complex is more stable than other complexes.

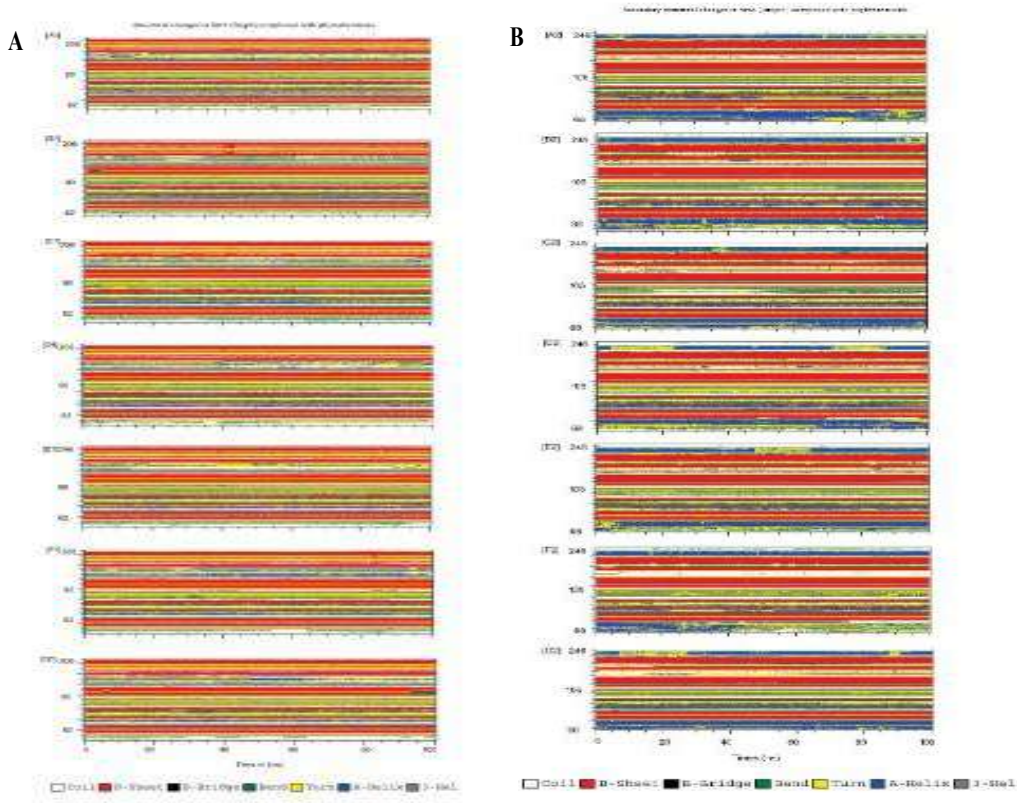

Fig. 4.5.10: The distortions in the secondary structure observed during MD simulation were noted in SrtA*staph*(A) and SrtA*strepto*(B) using DSSP of all the studied phytocompounds.

4.5.3.9 Binding energy calculation using MM/GBSA and SrtA residue contribution in binding

The binding free energy provides a reliable estimate of the protein-ligand binding affinities. In this context we used the MM/GBSA method to calculate binding free energy; the individual components that contribute to binding energy are listed in (Table 4.5.6a and 4.5.6b). The compounds in complex with SrtA*staph* are found the binding energy order of in descending order C1+C4>, C1>C3>C5>C2>Car>C4, whereas compounds in complex with SrtA*Strepto* showed a binding energy order of C3>C1>C1+C4>C2>TC>C5>C4. In our study, the majority of the compounds have

higher binding affinity than the control (Car and TC) to $SrtA_{staph}$ and $SrtA_{Strepto}$, respectively. A newer phytocompound 4-hydroxy 2-methyl acetophenone from our previous study with the smallest molecular weight of 150.17 and the smallest size has the lowest binding affinity with $SrtA_{staph}$ and $SrtA_{Strepto}$. However, when compared to the other compounds studied, the combination of C1 and C4 complexed with $SrtA_{staph}$ ($SrtA_{staph}$–C1+C4) exhibits significantly higher binding affinity. The compounds C1, C3, and C1+C4 with comparable binding energy values were observed to $SrtA_{strepto}$, but based on the overall MD analysis e.g. structural stability, intermolecular interactions, and conformational changes at the structural level. Thus, we propose that the combination of curcumin and 4-hydroxy 2-methyl acetophenone is more effective and favours the formation of stable complexes. As a result, the curcumin and 4-hydroxy 2-methyl acetophenone combination of these compounds would be regarded as the best possible inhibition for both sortases, $SrtA_{staph}$ and $SrtA_{strepto}$. We also performed residue decomposition analysis to determine the contribution of individual residues to the binding energy (Fig.4.5.11A and 4.5.11B). According to this data, the residues involved in the stable non-bonded interactions such as van der Waals and electrostatic during the MD which contribute significantly in the total binding energy. The β 6/7 loop residues for $SrtA_{staph}$ and $SrtA_{strepto}$ are Ile 158, Gly 167, Leu 169, Gln 178, and Pro 185, Val 188, and Thr 204, respectively. Similarly, the active site residues for $SrtA_{staph}$ and $SrtA_{strepto}$ are Cys 184, Arg 197, and His 139, Cys 205, Arg 213, contributes the most to the binding energy, emphasising the importance of this flexible loop in the formation of stable complexes.

Table 4.5.6 a: The relative binding energy of phytocompounds in binding with $SrtA_{staph}$.

Compound name	**ΔTOTAL(SD)**	**ΔVDWAALS**	**ΔEEL**	**ΔEGB**	**ΔESURF**	**ΔGGAS**	**ΔGSOLV**
Carvone	-18.97±0.21	-20.29	-8.11	12.17	-2.75	-28.40	9.43
Curcumin	-31.84±2.83	-36.75	-17.05	27.21	-5.24	-53.81	21.97
Demethoxycurcumin	-22.71±3.92	-29.63	-9.38	20.67	-4.37	-39.01	16.30
Bisdemethoxycurcumin	-27.90±1.79	-32.18	-16.02	25.13	-4.83	-48.20	20.30
4-hydroxy-2-methylacetophenone	-13.47±0.82	-17.10	-8.44	14.64	-2.57	-25.54	12.07
Ar-turmerone	-23.62±0.44	-21.47	-2.78	3.53	-2.90	-24.25	0.63
Curcumin + 4-hydroxy-2-methylacetophenone	-62.34±0.36	-71.23	-5.16	22.43	-8.38	-76.39	14.05

Table 4.5.6 b: The relative binding energy of phytocompounds in binding with SrtA*strepto*.

Compound name	ΔTOTAL	ΔVDWAALS	ΔEEL	ΔEGB	ΔESURF	ΔGGAS	ΔGSOLV
Transchalcone	-29.55± 0.75	-5.24	0.0	13.73	-4.18	-34.79	9.55
Curcumin	-53.84±1.46	-60.24	-9.62	22.10	-6.08	-69.86	16.02
Demethoxycurcumin	-36.85± 2.04	-41.98	-26.55	37.85	-6.17	-68.53	31.68
Bisdemethoxycurcumin	-56.81±0.46	-61.86	-1.45	12.38	-5.87	-63.31	6.50
4-hydroxy-2-methylacetophenone	-16.37±1.24	-14.95	-1.99	2.97	-2.39	-16.95	0.58
-Ar-turmerone	-25.79±1.80	-26.48	-14.70	19.14	-3.76	-41.18	15.38
Curcumin + 4-hydroxy-2-methylacetophenone	-51.39±0.42	-45.71	-3.87	5.02	-6.82	-49.59	-1.80

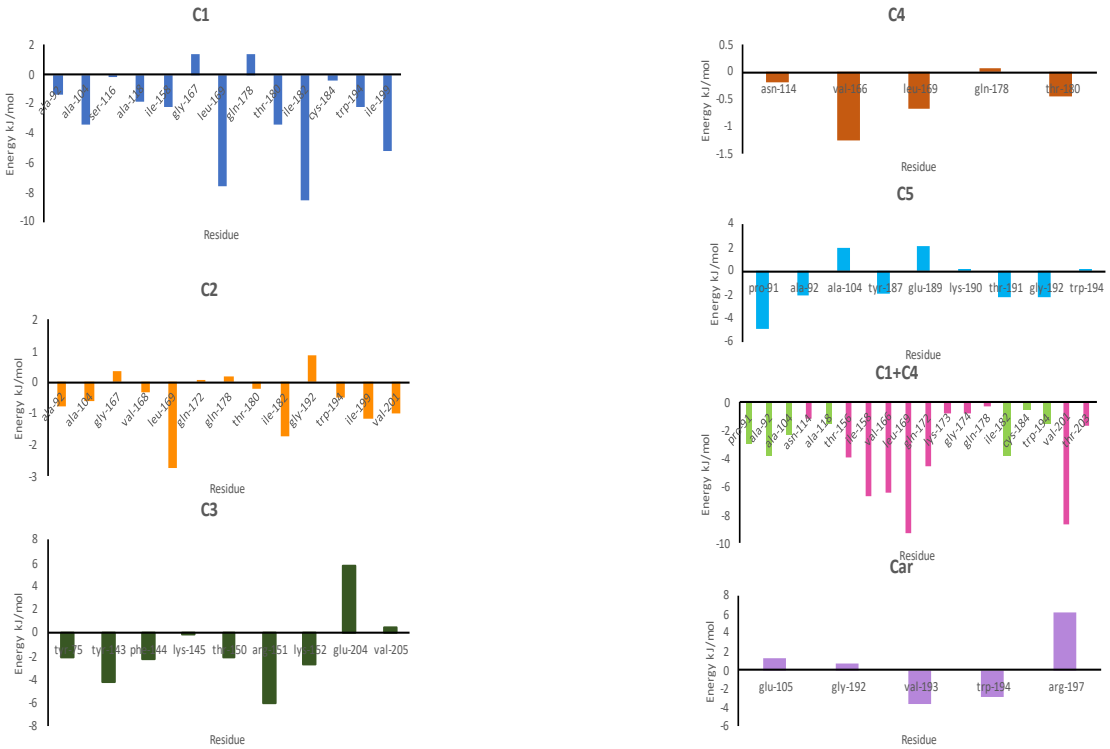

Fig. 4.5.11A: The energy contribution of residues from SrtA*staph* complexes to binding free energy in kJ/mol

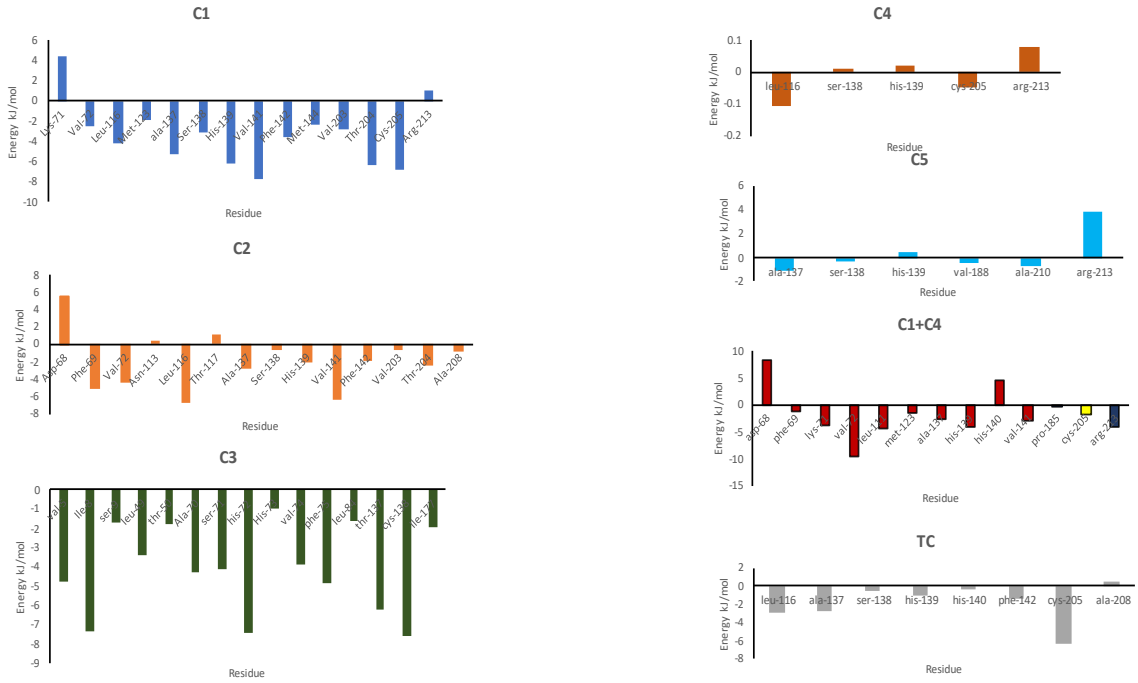

Fig. 4.5.11B: The energy contribution of residues from SrtA*strepto* complexes to binding free energy in kJ/mol

4.5.3.10 Principle component analysis (PCA) and dynamic cross correlation map

The coordinated motions of SrtA*staph* and SrtA*strepto* caused by the binding of phytocompounds from *C. longa* were recorded in order to gain important insights into the significant dynamic information and inter residue and inter domain correlation of SrtA*staph* and SrtA*strepto*. The dynamic cross correlation map in 2D for all complexes is depicted in Fig. 4.5.12 Individual residue self-correlation in all complexes shows a strong positive correlation with itself (Fig.4.5.12). The control complex i.e. SrtA*staph* – Car exhibits overall negative correlation in various regions of the SrtA*staph*, whereas the amplitude of negative correlation in complex SrtA*strepto*–TC is relatively smaller. The ternary complex SrtA*strepto*–C1+C4 has a negative correlation with the N-terminal region, indicating that the β 6/7 loop has a significant dynamic nature that facilitates the stable interactions of curcumin and 4-hydroxy 2-methyl acetophenone at the primary and alternate binding pockets of SrtA*staph*. A similar negative correlation has been observed in another ternary complex, SrtA*staph*–C1+C4, but the amplitude of the negative correlation is much lower. However, the SrtA*staph*–C5 and SrtA*strepto*–C5 show a moderately positive correlation with the N-terminal region at β 6/7 loop and our MD results show that the dynamics of these

two complexes are unstable. Thus, the negative co-operative motion of the β 6/7 loop with the N-terminal region has a significant influence on the stability of SrtA complexes with phytocompounds.

In order to observe the conformational dynamics, we extracted the extreme conformations of SrtA using PCA from the stable trajectory observed during the simulation. The compact globular shape has been adopted in complexes SrtA$_{strepto}$–C1+C4 and SrtA$_{strepto}$–C2, owing to the scissoring motion exerted by bending the N-terminal domain towards the binding pocket. The extended conformation of the β 6/7 loop has been observed in complex SrtA$_{staph}$–C1+C4, which promotes proper folding of this SrtA$_{staph}$ to form a compact globular shape. The open and close states have been observed in the binding pocket region of SrtA$_{staph}$ and SrtA$_{strepto}$ complexes where large phytocompounds such as C1, C2, and C3 occupy the binding pocket.

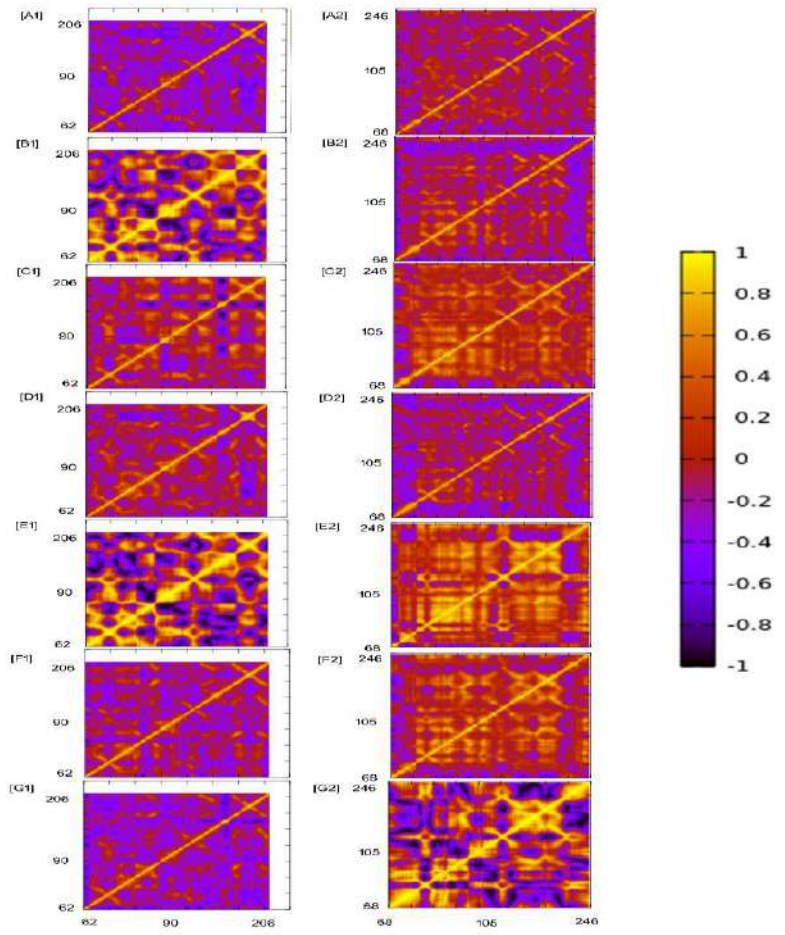

Fig. 4.5.12: Concerted motion analysed using dynamic cross corelation map for all complexes where (A1 to G1) for SrtA$_{staph}$ and (A2 to G2) for SrtA$_{strepto}$

4.5.4 Conclusions:

Thus, in the present work, we studied the inhibition of biofilm forming pathogens such as *S. aureus* and *S. mutans* by using PGPR induced phytocompounds of *C. longa*. In this context, our biofilm inhibition experiment with crystal violet and SEM showed the inhibition of biofilm formation for all the phytocompounds from *C. longa*. Notably, the synergistic action of curcumin and 4-hydroxy 2 methylacetophenone showed significant anti-biofilm forming activity. Further, we targeted the adhesion protein SrtA from both the *S. aureus* and *S. mutans* to study the inhibition mechanism using molecular modelling methods. Our docking studies revealed varying binding sites for phytocompounds and combination of binding of phytocompounds significantly lowers the binding energy of overall complex implies the synergistic inhibition mechanism of phytocompounds. MD simulation and MM-GBSA binding energy calculation studies showed the stability of SrtA in all phytocompounds specifically for ternary complexes of combined curcumin and 4-hydroxy-2-methylacetophenone.

Thus, we propose that binding of Curcumin and 4-hydroxy-2-methylacetophenone to the binding pocket and alternate site, respectively, attains a high stability in ternary complex of SrtA as compare to other phytocompounds alone that inhibits SrtA more effectively than individual compounds. Thus, this study would pave the way for the development of PGPR-induced secondary metabolite therapeutic approaches by targeting SrtA to control biofilm related infectious diseases.

CHAPTER V

SUMMARY AND CONCLUSIONS

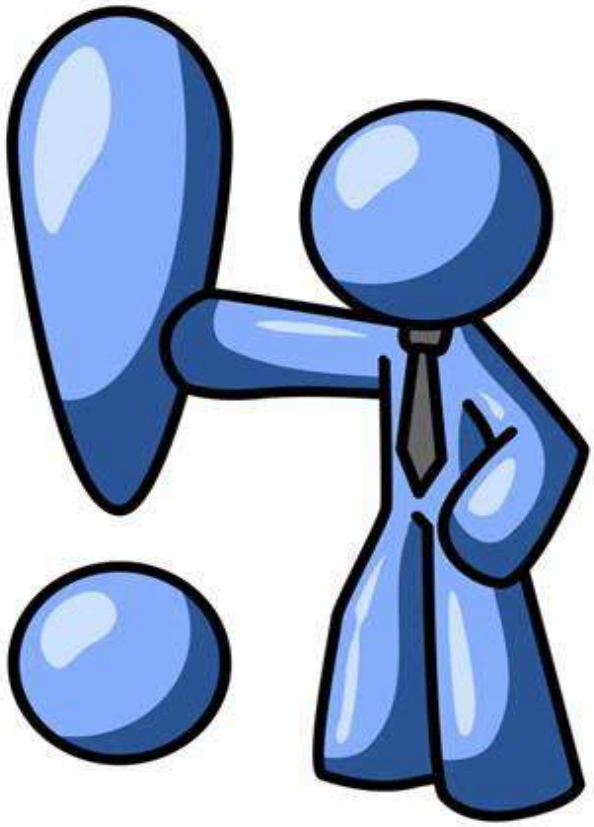

SUMMARY AND CONCLUSIONS:

5.1 Summary:

In the present study, we have selected two medicinal plants - namely are *Curcuma longa* (Turmeric) and *Asparagus racemosus* (Asparagus). Phytochemical analysis of Turmeric has revealed a large number of compounds, including curcumin, volatile oil, and curcuminoids, all of which have potent pharmacological properties. Curcuminoid which is a group of phenolic compounds, represented in the quantities ranging from 2 to 5 % of the dry weight, as a functional secondary metabolite. Asparagus has saponins ranging from 5 to 7 % of dry weight as a major secondary metabolite.

The present work resulted in the isolation of novel strains of plant growth-promoting rhizobacteria from the rhizosphere of two medicinal plants - Turmeric and Asparagus with maximum plant growth-promoting traits. The isolated PGPR strains were characterized on the basis of their morphological and biochemical properties. Further, they were identified by the molecular characterization by 16S rRNA analysis. The Turmeric rhizosphere isolates were identified as strains of *Serratia nematodiphila* and *Pseudomonas plecoglossicida* while Asparagus rhizosphere isolates were identified as the strains of *Exiguobacterium acetylicum* and *Enterobacter mori*. These isolates were designated as *Serratia nematodiphila* RGK, *Pseudomonas plecoglossicida* RGK, *Exiguobacterium acetylicum* RGK and *Enterobacter mori* RGK1. These strains were used for pot culture studies. A pot culture study demonstrated that PGPR treatment improved the growth, yield, and phytocompounds of Asparagus and Turmeric. Additionally, these phytocompounds were purified after extraction and tested for different *in vitro* biological activities as well as *in silico* study.

Curcumin and curcuminoids were purified and separated by using chromatographic techniques such as silica gel chromatography, TLC and by using RP-HPLC-UV detection. Additionally, diosgenin was purified by acid hydrolysis and quantified on RP-HPLC-UV detection. Furthermore, phytocompounds were identified by using GC-MS/MS, and LC-MS/MS as well, the results showed an increase in the concentration of chief phytocompounds such as curcumin and diosgenin. The computational approach used in this study elucidated the mechanism of inhibition of the SortaseA enzyme which is a key adhesion protein involved in biofilm formation.

These phytocompounds individually as well as in combination also showed

antibacterial and antifungal activity. Additionally, antibiofilm activity of these phytocompounds against Gram positive pathogens like *S. aureus* and *S. mutans* was also checked in the current study. Crystal violet assay revealed the biofilm formed by bacteria as well as inhibitory action of phytocompounds against these pathogenic organisms, so these phytocompounds may be used as drug molecules in the future.

The combinational effect of phytocompounds (Curcumin + 4-hydroxy-2 methylacetophenone) inhibits the enzyme (SrtA) by forming a ternary complex which shows better results over control inhibitors and this combination also gives similar results in wet-lab experiments. Hence, the present work opens a new avenue and creates scope for evaluation of other applications of PGPR-induced plant secondary metabolites from Turmeric and Asparagus in pharmaceutical applications, agricultural and food industries.

5.2 Conclusions:

- The screening of PGPR from the rhizospheric soil of two medicinal plants such as *C. longa* and *A. racemosus* resulted in the isolation of four potent PGPRs which were used for further studies based on their PGPR traits.
- The phenotypic and genotypic characterization of isolated PGPR identified them as strains of *Serratia nematodiphila*, *Pseudomonas plecoglossicida*, *Exiguobacterium acetylicum* and *Enterobacter mori*. These isolates were designated as *Serratia nematodiphila* RGK, *Pseudomonas plecoglossicida* RGK, *Exiguobacterium acetylicum* RGK and *Enterobacter mori* RGK1.
- The 16S rRNA sequences were submitted to the NCBI GenBank and Accession Numbers were obtained as - **MZ452064, OL739684, OL771442** and **OL656822** respectively.
- Biochemical characterization of these strains shows that they are capable to utilize various sugars.
- *Pseudomonas plecoglossicida* RGK can tolerate 7% NaCl along with exopolysaccharide production.
- A pot culture study revealed that PGPR treatment improved the growth and yield of Turmeric and Asparagus. These plants are then subjected to extraction and purification procedures.
- Soxhlet extraction and sonication used here may give several metabolites from PGPR-treated and control plants. Further, these extracts were used for purification.

- Silica gel column chromatography and TLC method yielded good results for curcumin purification, while RP-HPLC determination revealed the maximum amount of curcumin (8.02%) produced in co-culture treated plants.
- Similarly, acid hydrolysis yields a significant amount of diosgenin, and RP-HPLC results showed that the largest level of diosgenin (0.28%) was found in co-culture treated plants.
- GC-MS/MS analysis of the purified extracts gave an idea about the diversity of known and established phytocompounds in the plant extracts. In this study, we report for the first time a presence and elevated concentration of a new phytocompound (4-hydroxy-2 methylacetophenone) in the co-culture treated Turmeric plant.
- PGPR treated plants also showed strong free-radical scavenging activity and its inoculation enhanced phenolic content in Turmeric rhizome while saponin content in Asparagus root mainly co-culture treatment gives these kinds of results. An overall increase in phenolic and flavonoid content in both plants was observed.
- Individual and combinational effect of purified phytocompounds was checked on Gram-positive and Gram-negative pathogens such as *S. aureus* NCIM 2654, *S. mutans* NCIM 5660 and *E. coli* NCIM 2832, *Proteus vulgaris* NCIM 2813 respectively. The minimum inhibitory concentration of each phytocompounds against these pathogens was checked and it concludes that the combinational effect of phytocompounds provided a better inhibition as compared to an individual one.
- The bacterial growth curve assay was performed for *S. aureus* which is prominent organism in biofilm formation. It was performed in presence of standard plant metabolites and purified fractions to investigate the inhibition effect of phytocompounds. The obtained growth curve patterns showed the effective inhibition of the microorganism in presence of individual and combination of phytocompounds as compare control.
- The result of biofilm biomass assay indicated a reduced production of biofilm biomass in pathogens when treated with individual and combinational phytocompounds. These phytocompounds not only reduced the biofilm biomass but also reduced the microcolony formation.
- The present study also includes *in silico* study of biofilm-forming protein SrtA from *S. aureus* and *S. mutans.* The binding mode analysis by using molecular docking and MD simulation showed that phytocompounds may be bound to other site than the active site in combinational effect.

- Docking with dock 6 explored the molecular interactions, showing the involvement of hydrogen bonding and hydrophobic contacts of phytocompounds with SrtA.
- MD simulation showed ligand-induced conformational changes. We also emphasize the significance of the β 6/7 loop's scissoring and closure movement, which facilitates the opening and closing of the binding pocket region for stable complex formation in SrtA.
- As a result, we believe that PGPR-treated plant secondary metabolites would be great candidates for SrtA suppression and that combining curcumin and 4-hydroxy 2-methyl acetophenone would encourage better control of these pathogens.
- Thus, this study would pave the way for the development of PGPR-induced secondary metabolite therapeutic approaches by targeting SrtA to control biofilm related infectious diseases.

CHAPTER VI

REFERENCES

Abraham, M., Murtola, T., Schulz, R., Pall, S., Smith, J., Hess, B., Lindah, E. (2015). Gromacs: high-performance molecular simulations through multi-level parallelism from laptops to supercomputers, *SoftwareX* **1**, 219–25.

Adamczyk, M., Hagedorn, F., Wipf, S., Donhauser, J., Vittoz, P., Rixen, C., Frossard, A., Theurillat, J. P., & Frey, B. (2019). The soil microbiome of Gloria Mountain summits in the Swiss Alps. *Frontiers in Microbiology* **10**, 1080.

Agan, L. and Akariah, K. (2002). Improved HPLC Method for the Determination of Curcumin, Demethoxycurcumin, and Bisdemethoxycurcumin. *Journal of Agricultural and Food Chemistry* **50**, 3668–3672.

Agarwal, E., Brattain, M., Chowdhury, S. (2013). Cell survival and metastasis regulation by Akt signaling in colorectal cancer. *Cellular Signalling* **25**, 1711–1719.

Aggarwal, B., Yuan, W., Li, S., Gupta, S. (2013). Curcumin-free turmeric exhibits anti-inflammatory and anticancer activities : Identification of novel components of turmeric. *Molecular Nutrition Food Research* **57,** 1529–1542.

Aggarwal, S., Ichikawa, H., Takada, Y., Sandur, S.K., Shishodia, S., Aggarwal, B.B., (2006). Curcumin (diferuloylmethane) down-regulates expression of cell proliferation and antiapoptotic and metastatic gene products through suppression of I-kappa B-alpha kinase and Akt activation. *Molecular Pharmacology* **69**, 195–206.

Agostini-Costa, S., Vieira, R., Bizzo, H., Silveira, D., Gimenes, M. (2012). Secondary metabolites. *Chromatography and its applications* **1**, 131-164.

Agrawal, D., Saikia, D., & Tiwari, R. (2008). Demethoxycurcumin and its Semisynthetic Analogues as Antitubercular Agents. *Planta Med*. **74,** 1828-1831.

Ahmad, A., Robinson, A., Duensing, A., van Drunen, E., Beverloo, H., Weisberg, D., Hasty, P., Hoeijmakers, J., & Niedernhofer, L. (2008). ERCC1-XPF Endonuclease Facilitates DNA Double-Strand Break Repair. *Molecular and Cellular Biology* **28,** 5082–5092.

Ahmad, F., Ahmad, I., Khan, M. (2005). Indole acetic acid production by the indigenous isolates of *Azotobacter* and Flourescent *Pseudomonas* in the presence and absence of tryptophan. *Turk J Biol* **29,** 29–34.

Ahmad, F., Ahmad, I., Khan, M. (2008). Screening of free-living rhizospheric bacteria for their multiple plant growth promoting activities. *Microbiol Research* **163,**173–181.

Ahmad, S., Maziah, M. (2015). Total Antioxidant Capacity, Total Phenolic Compounds and the Effects of Solvent Concentration on Flavonoid Content in *Curcuma longa* and *Curcuma xanthorhhiza* Rhizomes. *Medicinal & Aromatic Plants* **3,** 156.

Ajmal, A., Saroosh, S., Mulk, S., Hassan, M., Yasmin, H., Jabeen, Z., Nosheen, A., Shah, S., Naz, R., Hasnain, Z., Qureshi, T., Waheed, A., & Mumtaz, S. (2021). Bacteria

isolated from wastewater irrigated agricultural soils adapt to heavy metal toxicity while maintaining their plant growth promoting traits. *Sustainability* **13,** 7792.

Akhtar, S., Mekureyaw, M., Pandey, C., and Roitsch, T. (2020). Role of cytokinins for interactions of plants with microbial pathogens and pest insects. *Front. Plant Sci*. **10,** 1777.

Alibi, S., Crespo, D., Navas, J. (2021). Plant-Derivatives Small Molecules with Antibacterial Activity. *Antibiotics* (Basel) **10,** 231.

Alok, S., Jain, S., Verma, A., Kumar, M., Mahor, A., & Sabharwal, M. (2013). Plant profile, phytochemistry and pharmacology of *Asparagus racemosus* (Shatavari): A review. *Asian Pacific Journal of Tropical Disease* **3,** 242–251.

Alori, E., & Babalola, O. (2018). Microbial inoculants for improving crop quality and human health in Africa. *Frontiers in Microbiology* **9,** 1–12.

Al-snafi, A. E. (2015). The pharmacological importance of *Asparagus officinalis* - A review. *Pharm. Biol* **5,** 93–98.

Amalraj, A., Pius, A., Gopi, S. (2016). Biological activities of curcuminoids, other biomolecules from turmeric and their derivatives e A review. Journal of Traditional and Complementary Medicine. **7,** 205-233.

Ambardar, S., and Vakhlu, J. (2013). Plant growth promoting bacteria from *Crocus sativus* rhizosphere. *World Journal of Microbiology and Biotechnology* **29,** 2271–2279.

Anand, K., Kumari, B., and Mallick M. (2016). Phosphate solubilizing microbes: An effective and alternative approach as bio-fertilizers. *International Journal of Pharmacy and Pharmaceutical Sciences* **8**, 37–40.

Anand, U., Jacobo-Herrera, N., Altemimi, A., Lakhssassi, N., (2019). A comprehensive review on medicinal plants as antimicrobial therapeutics: potential avenues of biocompatible drug discovery. *Metabolites* **9,** 258.

Anandaraj, M., and Dinesh, R. (2008). Use of microbes for spices production. In: Parthasarathy VA, Kandiannan K, Srinivasan V, editors. *Organic spices* New Delhi: New India Publishing Agency, 101–32.

Andy, A., Masih, S., & Gour, V. (2020). Isolation, screening and characterization of plant growth promoting rhizobacteria from rhizospheric soils of selected pulses. *Biocatalysis and Agricultural Biotechnology* **27,** 101685.

Ansari, F., Jabeen, M., & Ahmad, I. (2021). *Pseudomonas azotoformans* FAP5, a novel biofilm-forming PGPR strain, alleviates drought stress in wheat plant. *International Journal of Environmental Science and Technology* **18,** 3855–3870.

Aquino, R., Morellis, S., Lauro, M., Abdo, S., Saija, A., Tomaino, A. (2001). Phenolic constituents and antioxidant activity of an extract of Anthurium vesicular leaves. *Journal of Natural Products* **64,** 1019-1023.

Aratanechemuge, Y., Komiya, T., & Moteki, H. (2002). Selective induction of apoptosis by ar-turmerone isolated from turmeric (*Curcuma longa* L) in two human leukemia cell lines, but not in human stomach cancer cell line. *International Journal of Molecular Medicine* **9,** 481–484.

Arora, N., & Verma, M. (2017). Modified microplate method for rapid and efficient estimation of siderophore produced by bacteria. *3 Biotech* **7,** 381.

Austin, M., and Noel, J. (2003). The chalcone synthase superfamily of type III polyketide synthases. *Nat Prod Rep* **20,** 79–110.

Baek, S., Choi, B., Nam, S., Kim, H. (2018). Inhibition of monoamine oxidase A and B by demethoxycurcumin and bisdemethoxycurcumin. *Journal of Applied Biological Chemistry* **61,** 187–190.

Bagyalakshmi, B., Ponmurugan, P., & Balamurugan, A. (2017). Potassium solubilization, plant growth promoting substances by potassium solubilizing bacteria (KSB) from southern Indian Tea plantation soil. *Biocatalysis and Agricultural Biotechnology* **12,** 116–124.

Bahari, S., Zeighami, H., Mirshahabi, H., Roudashti, S., Haghi, F. (2017). Inhibition of *Pseudomonas aeruginosa* quorum sensing by subinhibitory concentrations of curcumin with gentamicin and azithromycin. *Integrative Medicine Research* **10,** 21–28.

Bajpai, V., Majumder, R., Park, J. (2016). Isolation and purification of plant secondary metabolites using column-chromatographic technique. *Bangladesh Journal of Pharmacology **11,*** 844–848.

Bakker, P., Doornbos, R., Zamioudis, C., Berendsen, R., Pieterse, C. (2013). Induced Systemic Resistance and the rhizosphere microbiome. *Plant Pathology Journal* **29,** 136–143.

Bal, H., Nayak, L., Das, S., and Adhya, K. (2013). Isolation of ACC deaminase producing PGPR from rice rhizosphere and evaluating their plant growth promoting activity under salt stress. *Plant and Soil* **366,** 93–105.

Balamurugan V, Sheerin F, Velurajan S. (2019). A guide to phytochemical analysis. *IJARIIE* **5,** 236-245.

Banchio, E., Bogino, P., Zygadlo, J., Giordano, W. (2008). Plant growth promoting rhizobacteria improve growth and essential oil yield in *Origanum majorana* L. *Biochemical* Systematics and *Ecology* **36,** 766–771.

Bandopadhyay, S. (2019). Optimization of biofertilizer production and its application in plants using pot culture technique. *Journal of Pure and Applied Microbiology* **13,** 2159–2167.

Bandyopadhyay, P., Yadav, B., Kumar, S., Kumar, R., Kogel, K., Kumar, S. (2022). *Piriformospora indica* and *Azotobacter chroococcum* consortium facilitates higher

acquisition of N, P with improved carbon allocation and enhanced plant growth in *Oryza sativa*. *Journal of Fungi* **8,** 453.

Bansode, P., Anantacharya, R., Dhanavade, M., Kamble, S., Barale, S. Sonawane, K., Nayak, D., Rashinkar, G. (2019). Evaluation of drug candidature: In silico ADMET, binding interactions with CDK7 and normal cell line studies of potentially anti-breast cancer enamidines, *Computational Biology and Chemistry*, **83**, 107-124.

Barale, S., Ghane, S., Sonawane, K. (2022). Purification and characterization of antibacterial surfactin isoforms produced by *Bacillus velezensis* SK. AMB Express **12,** 7.

Barale, S., Parulekar, R., Fandilolu, P., Dhanavade, M., and Sonawane, K. (2019). Molecular Insights into Destabilization of Alzheimer's Aβ Protofibril by Arginine Containing Short Peptides: A Molecular Modeling Approach. *ACS Omega* **4,** 892-903.

Baranska, M., Schulz, H., Rosch, P., Strehle, M. A., & Popp, J. (2004). Identification of secondary metabolites in medicinal and spice plants by NIR-FT-Raman microspectroscopic mapping. *Analyst* **129,** 926–930.

Batista, J., Pessoa, V., Brito F., Rocha, C., Gurgel L., Ramos, A., Barbosa, M., Silva, J., Marinho, E., Cavalcanti, B. (2021). Anti-mrsa activity of curcumin in planktonic cells and biofilms and determination of possible action mechanisms. *Microbial Pathogenesis* **155,** 104892.

Beattie G. (2006). Survey, molecular phylogeny, genomics and recent advances. *Plant-Associated Bacteria* 1-56.

Bednarikova, Z., Gancar, M., Wang, R., Zheng, L., Tang, Y., Luo, Y., Huang, Y., Spodniakova, B., Ma, L., Gazova, Z. (2021). Extracts from Chinese herbs with anti-amyloid and neuroprotective activities. *International Journal of Biological Macromolecules* **179**, 475–484.

Beemann, D. (1976). Some multistep methods for use in molecular dynamics simulations. *Journal of Computational Physics* **20,** 130-139.

Beevers, C., and Huang, S. (2011). Pharmacological and clinical properties of curcumin. *Botanics: Targets and Therapy* **1,** 5-18.

Begum, A., Knv, R., Dutt, R. Giri, K., Sindhu, K., Umera, f., Gowthami, G., Kumar, V., Naveen N., and Shaffath, S. (2017). Phytochemical screening and thin layer chromatography of indian *Asparagus officinalis* Linn. *International Journal of Advanced Research* **5,** 1520-1528.

Behnsen, J., and Raffatellu, M. (2016). Siderophores: More than stealing iron. *M Bio* **15,** 1906-1916.

Beneduzi A, Ambrosini A, Passaglia L. (2012). Plant growth-promoting rhizobacteria (PGPR): Their potential as antagonists and biocontrol agents. *Genetics and Molecular Biology* **35,** 1044–1051.

Bensalim, S., Nowak, J., Asiedu, S. (1998). A plant growth promoting rhizobacterium and temperature effects on performance of 18 clones of potato. *Am J Potato Res* **75,** 145–152.

Berendsen, R., Pieterse, C., Bakker, P. (2012). The rhizosphere microbiome and plant health. *Trends Plant Sci* **17,** 478–486.

Berman, H., Henrick, K., Nakamura, H. (2003). Announcing the worldwide Protein Data Bank. *Nat Struct Mol Biol* **10,** 980–980.

Berman, H., Westbrook, J., Feng, Z., Gilliland, G., Bhat, T., Weissig, H., Shindyalov, I., Bourne, P. (2000). The Protein Data Bank. *Nucleic Acids Research* **28,** 235–242.

Bhandare, V. & Ramaswamy, A. (2016). Identification of possible siRNA molecules for TDP43 mutants causing amyotrophic lateral sclerosis: in silico design and molecular dynamics study. *Comput Biol Chem* **61**, 97-108.

Bharti, N., Yadav, D., Barnawal, D., Maji, D., Kalra, A. (2013). *Exiguobacterium oxidotolerans*, a halotolerant plant growth promoting rhizobacteria, improves yield and content of secondary metabolites in *Bacopa monnieri* (L.) Pennell under primary and secondary salt stress. *World Journal of Microbiology and Biotechnology* **29,** 379–387.

Bharucha, U., Patel, K., & Trivedi, U. B. (2013). Optimization of Indole Acetic Acid Production by *Pseudomonas putida* UB1 and its Effect as Plant Growth-Promoting Rhizobacteria on Mustard (*Brassica nigra*). *Agriculture research* **2,** 215–221.

Bhattacharyya, C., Banerjee, S., Acharya, U., Mitra, A., Mallick, I., Haldar, A., Haldar, S., Ghosh, A. (2020). Evaluation of plant growth promotion properties and induction of antioxidative defense mechanism by tea rhizobacteria of Darjeeling, India. *Scientific Reports*, **10,** 1–19.

Bhattacharyya, P., & Jha, D. (2012). Plant growth-promoting rhizobacteria (PGPR): Emergence in agriculture. *World Journal of Microbiology and Biotechnology* **28,** 1327–1350.

Bhise, K., and Dandge, B. (2019). Mitigation of salinity stress in plants using plant growth promoting bacteria. *Symbiosis* **79,** 191-204.

Bhutani, K., Paul, A., Fayad, W., Linder, S. (2010). Apoptosis inducing activity of steroidal constituents from *Solanum xanthocarpum* and *Asparagus racemosus*. *Phytomedicine* **17,** 789–793.

Bi, C., Dong, X., Zhong, X., Cai, H., Wang, D., Wang, L. (2016). Acacetin Protects Mice from *Staphylococcus aureus* Bloodstream Infection by Inhibiting the Activity of Sortase A, *Molecules.* **21**, 1285.

Bijitha, P., and Suseela, R. (2019). *Burkholderia cepacia* strain iisrclrb5, a promising bioagent for the management of rhizome rot of turmeric (*Curcuma longa* L.) *International Journal of Agricultural Science and Research* **9,** 2250-0057.

Blagojevic, P., Radulovic, N., Boylan, F., & Resources, N. (2011). Volatiles of *Curcuma mangga* Val & Zijp (Zingiberaceae) from Malaysia. *Chemistry and Biodiversity* **8,** 2005–2014.

Boominathan, U., Sivakumaar, P. (2012). A liquid chromatography method for the determination of curcumin in PGPR inoculants *Curcuma longa* L. plant. *Int J Pharm Sci Res* **3,** 4438–4441.

Boominathan, U., Sivakumaar, P. (2012). Induction of systemic resistance by mixtures of rhizobacterial isolates against *Pythium aphanidermatum*. *Res J Biotechnol* **7,** 192–197.

Bopana, N., Saxena, S. (2007). *Asparagus racemosus*- Ethnopharmacological evaluation and conservation needs. *Journal of Ethnopharmacology* **110,** 1–15.

Bottini, R., Cassan, F., Piccoli, P. (2004). Gibberellin production by bacteria and its involvement in plant growth promotion and yield increase. Appl Microbiol Biotechnol **65,** 497–503.

Bourgaud, F., Gravot, A., Milesi, S. and Gonteir, E. (2001). Production of plant secondary metabolites: a historical perspective. *Plant Science* **161,** 839-851.

Bramchari, P. and Dubey, S. (2006). Isolation and characterization of exopolysaccharides produced by *Vibrio harveyi* strain VB23. *Lett Appl Microbiol* **43,** 571-577.

Brick, J., Bostock, R., Silverstone, S., (1991). Rapid in situ assay for indole acetic acid production by bacteria immobilized on nitrocellulose membrane. *Appl Environ Microbiol* **57,** 535-538.

Brooks, C. (1995). Methodological advances in molecular dynamics simulations of biological systems. *Curr Opin Struct Biol* **5,** 211-215.

Burley, S., Berman, H., Christie, C., Duarte, J., Feng, Z., Westbrook, J., Zardecki, C., (2018). RCSB Protein Data Bank: Sustaining a living digital data resource that enables breakthroughs in scientific research and biomedical education: RCSB Protein Data Bank. *Protein Science* **27,** 316–330.

Cakmakc, R., Mosber, G., Hazal, A., Firat, M., & Baboo, A. (2020). The Effect of Auxin and Auxin - Producing Bacteria on the Growth, Essential Oil Yield, and Composition in Medicinal and Aromatic Plants. *Current Microbiology* **77,** 564-577.

Cao, L., Zhou, Z., Sun, J., Li, C., Zhang, Y. (2021) Altering Sterol Composition Implied That Cholesterol is Not Physiologically Associated With Diosgenin Biosynthesis in *Trigonella foenum-graecum*. *Frontiers in Plant Science* **12,** 1-11.

Capatina, D., Feier, B., Hosu, O., Tertis, M., & Cristea, C. (2022). Analytical methods for the characterization and diagnosis of infection with *Pseudomonas aeruginosa*: A critical review. *Analytica Chimica Acta* **1204,** 1-33.

Cappuccino, J.G., Sherman, N. (1992). Biochemical activities of microorganisms. Microbiology, A Laboratory Manual. The Benjamin/Cummings Publishing Co, California, USA

Caroline, A., Dias, P., Aparecida, S., Corona, M., Cristina, M. (2018). Photodiagnosis and Photodynamic Therapy Effect of aPDT on *Streptococcus mutans* and *Candida albicans* present in the dental biofilm :Systematic review. *Photodiagnosis and Photodynamic Therapy* **21,** 363–366.

Cas, M., & Ghidoni, R. (2019). Dietary curcumin: Correlation between bioavailability and health potential. *Nutrients* **11,** 1–14.

Cascioferro, S., Ra, D., Maggio, B., Raimondi, M., Schillaci, D., & Daidone, G. (2015). Sortase A Inhibitors : Recent Advances and Future Perspectives. *Journal of Medicinal Chemistry* **58,** 9108–9123.

Cavuturu, B., Bhandare, V., Ramaswamy, A., & Arumugam, N. (2019). Molecular dynamics of interaction of Sesamin and related compounds with the cancer marker β-catenin: an in silico study. *Journal of Biomolecular Structure and Dynamics* **37,** 877–891.

Chaaban, A., Richardi, V., Carrer, A., Brum, J., Cipriano, R., Martins, C., Silva, M., Deschamps, C., & Molento, M. (2019). Insecticide activity of *Curcuma longa* (leaves) essential oil and its major compound α-phellandrene against *Lucilia cuprina* larvae (Diptera: Calliphoridae): Histological and ultrastructural biomarkers assessment. *Pesticide Biochemistry and Physiology* **153**, 17–27.

Chandra, S., Askari, K., & Kumari, M. (2018). Optimization of indole acetic acid production by isolated bacteria from *Stevia rebaudiana* rhizosphere and its effects on plant growth. *Journal of Genetic Engineering and Biotechnology* **16,** 581–586.

Chaudhary, S., Chaudhary, P., Syed, B., Misra, R., Bagali, P., Vitalini, S., & Iriti, M. (2018). Validation of a method for diosgenin extraction from fenugreek (*Trigonella foenum-graecum* L.). *Acta Scientiarum Polonorum, Technologia Alimentaria* **17,** 377–385.

Chauhan, A., Maheshwari, D., Dheeman, S., Bajpai, V. (2017). Termitarium-Inhabiting *Bacillus* spp. Enhanced Plant Growth and Bioactive Component in Turmeric (*Curcuma longa* L.). *Current Microbiology* **74,** 184–192.

Chauhan, A., Saini, R., Sharma, C. (2021). Plant growth promoting rhizobacteria and their biological properties for soil enrichment and growth promotion. *Journal of Plant Nutrition* **45,** 273– 299.

Chen, B., Luo, S., Wu, Y., Ye, J., Wang, Q., Xu, X., Pan, F., Khan, K., Feng, Y., & Yang, X. (2017). The effects of the endophytic bacterium *Pseudomonas fluorescens* Sasm05

and IAA on the plant growth and cadmium uptake of Sedum alfredii hance. *Frontiers in Microbiology* **8,** 1–13.

Chen, C., Jin, S., Xiang, X., Wang, X., Shi, Q., Yang, M., Ji, S., Huang, R., & Song, C. (2017). Enrichment and Cytotoxic Activity of Curcuminoids from Turmeric Using Macroporous Resins. *Journal of Food Science* **82,** 2024–2030.

Chenna, B., Shinkre, B., King, J., Lucius, A., Narayana, S. & Velu, S. (2008). Identification of novel inhibitors of bacterial surface enzyme *Staphylococcus aureus* Sortase A. *Bioorganic & Medicinal Chemistry Letters* **18,** 380–385.

Chenniappan, C., Narayanasamy, M., Daniel, G., Ramaraj, G., Ponnusamy, P., Sekar, J., Ramalingam, P. (2019). Biocontrol efficiency of native plant growth promoting rhizobacteria against rhizome rot disease of turmeric. *Biol. Control* **129,** 55–64.

Ciura, J., Szeliga, M., Grzesik, M., & Tyrka, M. (2017). Next-generation sequencing of representational difference analysis products for identification of genes involved in diosgenin biosynthesis in fenugreek (*Trigonella foenum - graecum*). *Planta* **245,** 977–991.

Clancy, K., Melvin, J., McCafferty, D. (2010). Sortase transpeptidases: insights into mechan- ism, substrate specificity, and inhibition. *Biopolymers* **94,** 385–396.

Corbiere, C., Liagre, B., Bianchi, A., Bordji, K., Dauca, M., Netter, P., Beneytout, J. (2003). Different contribution of apoptosis to the antiproliferative effects of diosgenin and other plant steroids, hecogenin and tigogenin, on human 1547 osteosarcoma cells. *International Journal of Oncology* **22,** 899–905.

Cornell, W., Cieplak, P., Bayly, C., Gould, I., Merz, K., Ferguson, D., Spellmeyer, D., Fox, T., Caldwell, J., Kollman, P. (1995). A second generation force field for the simulation of proteins, nucleic acids, and organic molecules. *J Am Chem Soc* **117,** 5179-5197.

Costerton, W., Veeh, R., Shirtliff, M, Pasmore. M., Post, C., Ehrlich, G. (2003). The application of biofilm science to the study and control of chronic bacterial infections. *J. Clin Invest* **112,** 1466–1477.

Crozier, A., Kamiya, Y., Bishop, G., Yokota, T. (2000). Biosynthesis of hormones and elicitor molecules. Biochemistry and molecular biology of plants. *American Society of Plant Physiology* 850–929.

Cvitkovitch, D., Li, Y., Ellen, R., Cvitkovitch, D., & Ellen, R. (2003). Quorum sensing and biofilm formation in *Streptococcal infections*. *The Journal of Clinical Investigation* **112,** 1626–1632.

Darden, T., York, D., Pedersen, L. (1993). Particle mesh Ewald: An N -log(N) method for Ewald sums in large systems. *J Chem Phys* **98**, 10089-10092.

Darzi, M. (2012). Effect of biofertilizers application on quantitative and qualitative yield of fennel (*Foeniculum vulgare*) in a sustainable production system. *IJACS* **4,**187–192.

Das, R., & Mehta, D. (2018). Microbial Biofilm and Quorum Sensing Inhibition: Endowment of Medicinal Plants to Combat Multidrug-Resistant Bacteria. *Current Drug Targets*, **19,** 1916–1932.

Dashti, N., Zhang, F., Hynes, R., Smith, D. & Bellevue, S. (1998). Plant growth promoting rhizobacteria accelerate nodulation and increase nitrogen fixation activity by field grown soybean (*Glycine max* L.) under short season conditions. *Plant and Soil* **200,** 205–213.

Dastager, S. & Ashok, C. (2011). Potential plant growth-promoting activity of *Serratia nematodiphila* NII-0928 on black pepper (*Piper nigrum* L.). *World J Microbiol Biotechnol* **27,** 259–265.

De Christo Scherer, M., Marques, F., Figueira, M., Peisino, M., Schmitt, E., Kondratyuk, T., Endringer, D., Scherer, R. & Fronza, M. (2019). Wound healing activity of terpinolene and α-phellandrene by attenuating inflammation and oxidative stress in vitro. *Journal of Tissue Viability* **28,** 94–99.

De la Lastra, E., Camacho, M. & Capote, N. (2021). Soil bacteria as potential biological control agents of Fusarium species associated with asparagus decline syndrome. *Applied Sciences* **11,** 8356.

Del Rosario Cappellari, L., Santoro, M., Reinoso, H., Travaglia, C., Giordano, W. & Banchio, E. (2015). Anatomical, Morphological, and Phytochemical Effects of Inoculation with Plant Growth- Promoting Rhizobacteria on Peppermint (*Mentha piperita*). *Journal of Chemical Ecology* **41,** 149–158.

Devi, R., Kaur, T., Kour, D. & Nath, A. (2022). Microbial consortium of mineral solubilizing and nitrogen fixing bacteria for plant growth promotion of amaranth (*Amaranthus hypochondrius* L.). *Biocatalysis and Agricultural Biotechnology* **43,** 102404.

Dhaked, B., Triveni, S., Reddy, R. & Padmaja, G. (2017a). Isolation and Screening of Potassium and Zinc Solubilizing Bacteria from Different Rhizosphere Soil. *International Journal of Current Microbiology and Applied Sciences* **6**, 1271–1281.

Dhanarajan, G., Rangarajan, V., Sridhar, P., Sen, R. (2016). Development and Scale- up of an Efficient and Green Process for HPLC purification of antimicrobial homologues of commercially important microbial lipopeptides. *ACS Sustain Chem Eng* **4,** 6638–6646.

Dhanasekaran, S., Rameshthangam, P., Venkatesan, S., Singh, S. & Vijayan, S. (2018). In Vitro and In Silico Studies of Chitin and Chitosan Based Nanocarriers for Curcumin and Insulin Delivery. *Journal of Polymers and the Environment,* **26,** 4095–4113.

Dhanavade, M. and Sonawane, K. (2014). Insights into the molecular interactions between aminopeptidase and amyloid beta peptide using molecular modeling techniques. *Amino acids* **46,**1853–1866.

Dhanavade, M., Jalkute, C., Barage, S., Sonawane, K. (2013). Homology modeling, molecular docking and MD simulation studies to investigate role of cysteine protease from *Xanthomonas campestris* in degradation of Aβ peptide, *Computers in Biology and Medicine*. **43**, 2063-2070.

Dharni, S., Kumar, A., Samad, A. & Dhar, D. (2014). Impact of plant growth promoting *Pseudomonas monteilii* PsF84 and *Pseudomonas plecoglossicida* PsF610 on metal uptake and production of secondary metabolite (monoterpenes) by rose-scented geranium (*Pelargonium graveolens* cv. bourbon) grown. Chemosphere **117,** 433–439.

Dobbelaere, S., Croonenborghs, A., Thys, A., Ptacek, D., Vanderleyden, J., Dutto, P., Labandera-Gonzalez, C., Caballero-Mellado, J., Aguirre, J., Kapulnik, Y. (2001). Responses of agronomically important crops to inoculation with *Azospirillum*. *Australian Journal of Plant Physiology* **28,** 871–879.

Dobbelaere, S., Vanderleyden, J., Okon, Y. (2003). Plant growth-promoting effects of diazotrophs in the rhizosphere. *Critical Review of Plant Science* **22,** 107–149.

Dobosz, B., Drzewiecka, K., Waskiewicz, A., Irzykowska, L., Bocianowski, J., Karolewski, Z., Kostecki, M., Kruczynski, Z., Krzyminiewski, R., Weber, Z., Golinski, P. (2011). Free Radicals, Salicylic Acid and Mycotoxins in *Asparagus* after Inoculation with Fusarium. *Applied Magnetic Resonance* **41,**19–30.

Dutta, B. (2015). Study of secondary metabolite constituents and curcumin contents of six different species of genus Curcuma. *Journal of Medicinal Plants Studies* **3,** 116–119.

Dutta, S. & Neog, B. (2016). Accumulation of secondary metabolites in response to antioxidant activity of turmeric rhizomes co-inoculated with native arbuscular mycorrhizal fungi and plant growth promoting rhizobacteria. *Scientia Horticulturae* **204,** 179–184.

Eberhard, A., Burlingame, L., Eberhard, C., Kenyon, L., Nealson, H., Oppenheimer, J. (1981). Structural identification of autoinducer of *Photobacterium fischeri* luciferase. *Biochem* **20,** 2444–2449.

Edwards, C. and Burrows, I. (1988). The potential of earthworm composts as plant growth media In: Earthworms in Environmental and Waste Management. SPB Academic Publ. b.v, The Netherlands, 211-220.

Egamberdieva, D., Shrivastava, S., Varma, A. (2015). Plant-Growth-Promoting Rhizobacteria (PGPR) and Medicinal Plants. *Soil Biology* **42,** 1-16.

Egamberdieva, D., Teixeira da Silva, J. (2015). Medicinal Plants and PGPR: A New Frontier for Phytochemicals. *Soil Biology* **42,** 287–303.

El, S., Koraichi, S., Latrache, H., Hamadi, F. (2012). Scanning Electron Microscopy (SEM) and Environmental SEM: Suitable Tools for Study of Adhesion Stage and Biofilm Formation. *Scanning Electron Microscopy* **35,** 717-730.

Emmert, E. & Handelsman, J. (1999). Biocontrol of plant disease: A Gram-positive perspective. *FEMS Microbiology Letters*, **171,** 1–9.

Eslami, H., Muller-Plathe F. (2007). Molecular dynamics simulation in the grand canonical ensemble. *J Comput Chem* **28,** 1763-1773.

Essmann, U., Perera, L., Berkowitz, M., Darden, T., Lee, H., Pedersen, L. (1995). A smooth particle mesh Ewald method. *The Journal of Chemical Physics* **103,** 8577–8593.

Etesami, H., Emami, S., & Alikhani, H. A. (2017). Potassium solubilizing bacteria (KSB): Mechanisms, promotion of plant growth, and future prospects - a review. *Journal of Soil Science and Plant Nutrition* **17**, 897–911.

Evans, D. and Morriss, G. (1983). Isothermal/Isobaric molecular dynamics ensemble. *Physics Letter* **98,** 433-436.

Falcinelli, B., Marconi, O., Maranghi, S., Lutts, S., Rosati, A., Famiani, F., Benincasa, P. (2017). Effect of Genotype on the Sprouting of Pomegranate (*Punica granatum* L.) Seeds as a Source of Phenolic Compounds from Juice Industry by-Products. *Plant Foods for Human Nutrition* **72**, 432–438.

Fanaei, H., Khayat, S., Kasaeian, A., Javadimehr, M. (2016). Effect of curcumin on serum brain-derived neurotrophic factor levels in women with premenstrual syndrome: a randomized, double-blind, placebo-controlled trial. *Neuropeptides* **56,** 25-31.

Fatahiya, M., Fadzilah, A., Hassan, F., Tet, S., Kamyar, S., Mikio, M. and Nurul B. (2018). In Silico and In Vitro Study of the Bromelain-Phytochemical Complex Inhibition of Phospholipase A2 (Pla2). *Molecules* **23,** 73.

Felestrino, E., Santiago, I., Freitas, L., Rosa, L., Ribeiro, S. & Moreira, L. (2017). Plant growth promoting bacteria associated with *Langsdorffia Hypogaea* Rhizosphere-Host biological interface: A neglected model of bacterial prospection. *Frontiers in Microbiology* **8,** 1–15.

Ferreira, F., Aparecida, S., Mossini, G., Maery, F., Ferreira, D., Arrotéia, C., Luciana, C., Nakamura, C. & Junior, M. (2013). The inhibitory Effects of *Curcuma longa* L . Essential Oil and Curcumin on *Aspergillus flavus* Link Growth and Morphology *Scientific World Journal* **20**, 343804.

Ferreira, L., Santos, R., Oliva, G. and Andricopulo, A. (2015). Molecular Docking and Structure-Based Drug Design Strategies. *Molecules* **20,** 13384-13421.

Filomena, N., Florinda, F., Raffaele, C., (2013). Quorum Sensing and Phytochemicals. *Int. J. Mol. Sci*. **14,** 12607-12619.

Fiske H, and Subbarow Y. (1925). The colorimetric determination of phosphorus. *J. biol. Chem* **66**, 375-400.

Fornili, A., Autore, F., Chakroun, N., Martinez, P., Fraternali, F. (2012). Protein-Water

Interactions in MD Simulations: POPS/POPSCOMP Solvent Accessibility Analysis, Solvation Forces and Hydration Sites. *Methods Mol Biol* **819,** 375-392.

Fu, W., Liu, J., Zhang, M., Li, J., Hu, J., Xu, L. & Dai, G. (2018). Isolation, purification and identification of the active compound of turmeric and its potential application to control cucumber powdery mildew. *The Journal of Agricultural Science* **156,** 358–366.

Fumes, A., da Silva Telles, P., Corona, S., Borsatto, M. (2018). Effect of aPDT on *Streptococcus mutan*s and *Candida albicans* present in the dental biofilm: Systematic review, *Photodiagnosis Photodyn Ther.* **21**, 363-366.

Fux, C., Costerton, J., Stewart, P., Stoodley, P. (2005). Survival strategies of infectious biofilms. Trends *Microbiology* **13,** 34-40.

Galabova, D., Tuleva, B., Spasova, D. (1996). Permeabilization of *Yarrowia lipolytica* cells by triton X-100. *Enzyme and Microbial Technology* **18,** 18–22.

Gamalero, E. & Glick, B. (2011). Plant Nutrient Management. *Bacteria in Agrobiology* Book

Gangurde, A., Kundaikar, H., Javeer, S., Jaiswar, D., Degani, M. & Amin, P. (2015). Enhanced solubility and dissolution of curcumin by a hydrophilic polymer solid dispersion and its insilico molecular modeling studies. *Journal of Drug Delivery Science and Technology* **29,** 226–237.

Gao, C., Uzelac, I., Gottfries, J., Eriksson, A. (2016). Exploration of multiple Sortase A protein conformations in virtual screening. *Scientific reports* **6**, 1–14.

Garg, A., Faheem, M. and Singh, S. (2021). Role of medicinal plant in human health disease. *Asian J Plant Sci Res* **11,**19-21.

Ge, C., Radnezhad, H., Abari, M., Sadeghi, M. and Kashi, G. (2016). Effect of biofertilizers and plant growth promoting bacteria on the growth characteristics of the herb Asparagus officinalis. *Applied Ecology and Environmental Research* **14**, 547–558.

Gear, C. (1971). Numerical initial value problems in ordinary differential equations Prentice-Hall, Inc., Englewood cliffs N. J., Chapter 2. 17-253.

Geisselera, D., Horwath, R., Joergensen, G. and Ludwig, B. (2010). Pathways of nitrogen utilization by soil microorganisms. *Soil Biology* **42,** 2058– 2067.

Gharib, F., Moussa L. and Massoud, O. (2008). Effect of compost and bio-fertilizers on growth, yield and essential oil of sweet marjoram (*Majorana hortensis*) plant. *International Journal of Agricultural Biology* **10,** 381-387.

Ghorbanpour, M., Hatami, M. and Khavazi, K. (2013). Role of plant growth promoting rhizobacteria on antioxidant enzyme activities and tropane alkaloid production of Hyoscyamus niger under water deficit stress. *Turk J Biol* **37,** 350–360.

Glick, B. (1995). The enhancement of plant growth by free living bacteria. *Canadian Journal of Microbiology* **41,** 109–114.

Gohel, R., Solanki, B., Gurav, N., Patel, G., Patel, B. (2015). Isolation and characterization of shatavarin iv from root of asparagus. *Innovare academic sciences* **7**, 6–9.

González, M. (2011). Force fields and molecular dynamics simulations. *Collection SFN* **12,** 169-200.

Gould, I. (2009). Antibiotic resistance: the perfect storm, *Int J Antimicrob Agents.* **34,** Suppl 3:S2-5.

Gray, E., Smith, D. (2005). Intracellular and extracellular PGPR: commonalities and distinctions in the plant–bacterium signaling processes. *Soil biology and Biochemistry* **37,** 395–412.

Greenwell, M. and Rahman, P. (2015). Medicinal Plants: Their Use in Anticancer Treatment. *International Journal of Pharmaceutical Sciences* and *Research* **6,** 4103–4112.

Guerra, A., Hoyos, C., Velasquez, J., Acosta, L., Rojo, P., Maria, A., Giraldo, V. & Mar, A. (2019). The nanotech potential of turmeric (*Curcuma longa* L.) in food technology : A review. *Critical Reviews in Food Science and Nutrition* **0,** 1–13.

Guerriero, G., Berni, R., Munoz-sanchez, J., Apone, F., Abdel-salam, E., Qahtan, A., Alatar, A. & Cantini, C. (2018). Production of Plant Secondary Metabolites: Examples, Tips and Suggestions for Biotechnologists. *Genes* **9,** 309.

Guller, P., Karaman, M., Guller, U., Aksoy, M. & Kufrevioglu, O. (2021). A study on the effects of inhibition mechanism of curcumin, quercetin, and resveratrol on human glutathione reductase through in vitro and in silico approaches. *Journal of Biomolecular Structure and Dynamics* **39**, 1744–1753.

Gunamalai, L. & Vanila, D. (2014). Insilico analysis of neem secondary metabolites against clumping factor A of *Staphylococcus aureus*. *International Journal of Pharmaceutical Sciences Review and Research* **29**, 232–235.

Gunes, H., Gulen, D., Mutlu, R., Gumus, A., Tas, T. and Topkaya A. (2016). Antibacterial effects of curcumin : An in vitro minimum inhibitory concentration study. *Toxicology and Industrial Health* **32**, 246–250.

Gupta, S. and Rashotte, A. (2012). Down-stream components of cytokinin signaling and the role of cytokinin throughout the plant. *Plant Cell Rep* **31,** 801–812.

Gupta, S., Sung, B., Kim, J., Prasad, S., Li, S., Aggarwal, B. (2013). Multitargeting by turmeric, the golden spice: From kitchen to clinic. *Mol. Nutr. Food Res* **57,** 1510–1528.

Ha, M., Huang, Y., & Huang, J. (2008). Influence of organic amendment and *Bacillus subtilis* on mineral nutrient uptake of asparagus bean in two field soils. *Plant*

Pathology Bulletin 17, 289–296.

Ha, M., Yi, S. & Paek, S. (2020). Design and Synthesis of Small Molecules as Potent Staphylococcus aureus Sortase A Inhibitors. *Antibiotics* **9,** 706.

Haghi, G., Hatami, A. and Mehran, M. (2012). Determination of Shatavarin IV in Root Extracts of Asparagus racemosus by HPLC-UV. *Analytical Chemistry Letters* **2**, 1–6.

Hajbabaie, R., Harper, M., Rahman, T. (2021). Establishing an Analogue Based In Silico Pipeline in the Pursuit of Novel Inhibitory Scaffolds against the SARS Coronavirus 2 Papain-Like Protease, *Molecules.* **26,** 1134.

Hakeem, K. and Akhtar, M. (2016). Plant, soil and microbes: Mechanisms and molecular interactions. *Plant, Soil Microbes* **2,** 1–439.

Ham, S., Yoon, A., Oh, H. & Park, Y. (2022). Plant Growth-Promoting Microorganism *Pseudo arthrobacter* sp. NIBRBAC000502770 Enhances the Growth and Flavonoid Content of *Geum aleppicum*. *Microorganisms* **10,** 1241.

Hameed, A., Egamberdieva, D., Abd-Allah, E., Hashem, A., Kumar, A., Ahmad, P. (2014). Salinity stress and arbuscular mycorrhizal symbiosis in plants. In: Miransari M (ed) Use of microbes for the alleviation of soil stresses. Springer, New York, pp 139–159.

Hamizah, A., Kartini, H., Izzaty, N., Latip, J., & Embi, N. (2020). Data on antiplasmodial and stage-specific inhibitory effects of Aromatic (Ar)-Turmerone against Plasmodium falciparum 3D7. *Data in Brief* **33,** 106592.

Han, J., Sun, L., Dong, X., Cai, Z., Sun, X., Yang, H., Wang, Y., Song, W. (2005). Characterization of a novel plant growth-promoting bacteria strain *Delftia tsuruhatensis* HR4 both as a diazotroph and a potential biocontrol agent against various plant pathogens. *Syst Appl Microbiol* **28,** 66–76.

Hansson, T., Oostenbrink, C., van Gunsteren, W. (2002). Molecular dynamics simulations. *Curr Opin Chem Biol* **12,** 190-196.

Hardman, K. and R. (1968). An improved method of densitometric thin layer chromatography as applied to the determination of sapogenin in dioscorea tubers *Determination sapogenin*. **38,** 355–363.

Hashemi, M., Behboodian, B., Karimi, E. (2022). Enhancing biosynthesis and bioactivity of *Trachyspermum ammi* seed essential oil in response to drought and *Azotobacter chroococcum* stimulation. *Chem. Biol. Technol. Agric*. **9**, 26.

Hayat, R., Ali, S., Amara, U., Khalid, R., & Ahmed, I. (2010). Soil beneficial bacteria and their role in plant growth promotion: A review. *Annals of Microbiology* **60**, 579–598.

Hayes P, Jahidin, A, Lehmann R, Penman K, Kitching W, De Voss J. (2008). Steroidal saponins from the roots of *Asparagus racemosus*. *Phytochemistry* **69,** 796–804.

Hazra, K., Mandal, A., Mondal, D., Ravte, R., Hazra, J., & Rao, M. (2020). Seasonal dynamics of shatavarin-iv, a potential biomarker of asparagus racemosus by HPTLC: Possible validation of the ancient ayurvedic text. *Indian Journal of Traditional Knowledge* **19,** 174–181.

He, W., Zhang, Y., Bao, J., Deng, X., Batara, J., Casey, S., Guo, Q., Jiang, F., Fu, L. (2017) Synthesis, biological evaluation and molecular docking analysis of 2-phenyl-benzofuran-3-carboxamide derivatives as potential inhibitors of *Staphylococcus aureus* Sortase A, Bioorg *Med Chem*. **25,** 1341-1351,

Heffernan, C., Ukrainczyk, M., Gamidi, R., Hodnett, B., Rasmuson, A. (2017). Extraction and Purification of Curcuminoids from Crude Curcumin by a Combination of Crystallization and Chromatography. *Organic Process Research & Development* **21,** 821-826.

Hermenau R. (2018). Gramibactin is a bacterial siderophore with a diazeniumdiolate ligand system. *Nat Chem Biol* **14,** 841–843.

Hess, B., Bekker, H., Berendsen, H. and Fraaije, J. (1997). LINCS: a linear constraint solver for molecular simulations. *J Comput Chem* **18,** 1463–1472.

Hestenes, M. and Eduard, S. (1952). Methods of Conjugate Gradients for Solving Linear Systems. *J Res Natl Bur Stand* **49,** 410-436.

Heydarian, Z., Gruber, M., Glick, B., Hegedus, D. (2018). Gene expression patterns in roots of *Camelina sativa* with enhanced salinity tolerance arising from inoculation of soil with plant growth promoting bacteria producing 1-aminocyclopropane-1-carboxylate deaminase or expression the corresponding acds gene. *Frontiers in Microbiology* **9,** 1–15.

Hiai, S., Oura, H. and Nakajima, T. (1976). Color Reaction of Some Sapogenins and Saponins with Vanillin Sulfuric Acid. *Planta Medica* **29,** 116-122.

Hildah, M., & Sitheni M. (2020). Medicinal Properties of Selected Asparagus Species: A Review. In Phytochemicals in Human Health. *Intech Open*.

Hockney R. (1970). The potential calculation and some applications, in: Alder, B., Fernbach, S., Rotenberg, M. (eds.): *Methods in Computational Physics* **9,** 136.

Hofstad, G., Van Der Marugg, J., Verjans, G. (1986). Characterization and structural analysis of the siderophore produced by the PGPR *Pseudomonas putida* strain wcs358. Plenum press 71–75.

Holt, J., Krieg, N. and Sneath, P. (1994). Berger's manual of determinative bacteriology. 9th ed. Williams & Wilkins, Baltimore, MD, USA

Hu, P., Huang, P., Chen, M. (2013). Curcumin reduces *Streptococcus mutans* biofilm formation by inhibiting sortase A activity. *Archives of Oral Biology* **58,** 1343–1348.

Hu, Y., Xia, Z., Sun, Q., Orsi, A., Rees, D. (2005). A new approach to the pharmacological regulation of memory: sarsasapogenin improves memory by elevating the low

muscarinic acetylcholine receptor density in brains of memory-deficit rat models. *Brain Res* **1060,** 26–39.

Hunenberger, P. (2005). Thermostat Algorithms for Molecular Dynamics Simulations. *Adv Polym Sci* **173,** 105-149.

Huyskens-keil, S., Hassenberg, K., Herppich. (2011). Impact of postharvest UV-C and ozone treatment on textural properties of white asparagus (*Asparagus officinalis* L.). *Journal of Applied Botany and Food Quality* **84,** 229 – 234.

Ilangovan, U., Ton-That, H., Iwahara, J., Schneewind, O., & Clubb, R. (2001). Structure of sortase, the transpeptidase that anchors proteins to the cell wall of *Staphylococcus aureus*. *Proc Natl Acad Sci* **98**, 6056-6061.

Inghorn A. (2004). Constituents of *Asparagus officinalis* Evaluated for Inhibitory Activity against Cyclooxygenase *Journal of Agricultural and Food Chemistry* **52,** 2218−2222.

Ipek, M., Pirlak, L., Esitken, A., Figen, D., Turan M., Sahin, F. (2014). Plant growth promoting rhizobacteria (PGPR) increase yield, growth and nutrition of strawberry under high-calcareous soil conditions. *Journal of Plant Nutrition* **37,** 990–1001.

Ippolito, G., Leone, S., Lauria, F., Nicastri E, Wenzel R. (2010). Methicillin-resistant *Staphylococcus aureus*: the superbug. *International Journal of Infectious Disease* **14,** S7–S11.

Islam, F., Yasmeen, T., Ali, Q., Ali, S., Arif, S., Hussain, S., Rizvi, H. (2014). Influence of *Pseudomonas aeruginosa* as PGPR on oxidative stress tolerance in wheat under Zn stress. *Ecotoxicology and Environmental Safety* **104**, 285–293.

Islam, S., Akanda, A., Prova, A., Islam, M., Hossain, M. (2016). Isolation and identification of plant growth promoting rhizobacteria from cucumber rhizosphere and their effect on plant growth promotion and disease suppression. *Frontiers in Microbiology* **6,** 1360.

Itatiaia, S., Samambaia, C., Itatiaia, S. (2016). Physicochemical/photophysical characterization and angiogenic properties of *Curcuma longa* essential oil. *Annals of the Brazilian Academy of Sciences* **88,** 1889–1897.

Jabborova, D., Wirth, S., Kannepalli, A., Narimanov, A., Desouky, S., Davranov, K., Sayyed, R., Enshasy, H., Malek, R., Syed, A., & Bahkali, A. (2020). Co-inoculation of rhizobacteria and biochar application improves growth and nutrientsin soybean and enriches soil nutrients and enzymes. *Agronomy* **10,** 1142.

Jackson, K., Brown M. (1966). Behaviour of *Azotobacter chroococcum* introduced into the plant rhizosphere. Ann. Inst. Pasteur, Paris. **3**, 108–112.

Jacqueline, L., Luis, J., Ignacio, R., & Martín, J. (2022). A Look at Plant-Growth-Promoting Bacteria. *Plants*, **12**, 1668.

Jagatha, B., Mythri, R., Vali, S., & Bharath, M. (2008). Curcumin treatment alleviates the effects of glutathione depletion in vitro and in vivo: Therapeutic implications for

Parkinson's disease explained via in silico studies. *Free Radical Biology and Medicine* **44**, 907–917.

Jagtap, R., Mali, G., Waghmare, S., Nadaf, N., Nimbalkar, M., Sonawane, K. (2023). Impact of plant growth promoting rhizobacteria *Serratia nematodiphila* RGK and *Pseudomonas plecoglossicida* RGK on secondary metabolites of turmeric rhizome, *Biocatalysis and Agricultural Biotechnology.* **47,** 102622.

Jain, A., Singh, A., Chaudhary, A., Singh, S., Singh, H. (2014). Modulation of nutritional and antioxidant potential of seeds and pericarp of pea pods treated with microbial consortium. *Food Res. Int.* **64,** 275–282.

Jain, A., Verma, S., Kumar, A., Mahor, M., Sabharwal, M. (2013). Plant profile, phytochemistry and pharmacology of *Asparagus racemosus* (Shatavari): A review. *Asian Pacific J. Trop. Dis.* **3,** 242–251.

Janani, S. R., Analytical, A. F., & Kunjithapatham, S. (2014). Screening of Phytochemical and GC-MS Analysis of some Bioactive constituents of *Asparagus racemosus. International Journal of PharmTech Research* **6**, 428-432.

Jarak, M., Mrkovacki, N., Bjelic, D., Joscaron, D., Hajnal-Jafari, T., Stamenov, D. (2012). Effects of plant growth promoting rhizobacteria on maize in greenhouse and field trial. *African Journal of Microbiology Research* **6,** 5683–5690.

Jasim, B., Joseph, A., John, C., Mathew, J., Radhakrishnan, E. (2014). Isolation and characterization of plant growth promoting endophytic bacteria from the rhizome of *Zingiber officinale. 3 Biotech* **4**, 197204.

Jayaprakasha, G., Jagan Mohan Rao, L., & Sakariah, K. (2005). Chemistry and biological activities of *C. longa*. *Trends in Food Science and Technology* **16**, 533–548.

Jediya, H., Joshi, M., Sharma, S., Gurjar, M., Aalam, H. (2022). Effect of phytobiotic feed additives garlic (*Allium sativum*), Ashwagandha (*Withania somnifera*) and Shatavari (*Asparagus racemosus*) on haematology in broiler. *The Pharma Innovation Journal* **11**, 1908–1911.

Jenardhanan, P., Mannu, J., Mathur, P. (2014). The structural analysis of MARK4 and the exploration of specific inhibitors for the MARK family: a computational approach to obstruct the role of MARK4 in prostate cancer progression. *Molecular BioSystems*, **10,** 1845.

Jesus, M., Martins, A., Gallardo, E., & Silvestre, S. (2016). Diosgenin: Recent Highlights on Pharmacology and Analytical Methodology. *Journal of Analytical Methods in Chemistry*, **2016,** 16.

Jha, Y., Dehury, B., Kumar, S., Chaurasia, A., Singh, U., Yadav, M., Angadi, U., Ranjan, R., Tripathy, M., Subramanian, R., Kumar, S., & Simal-Gandara, J. (2022). Delineation of molecular interactions of plant growth promoting bacteria induced β-1,3-glucanases and guanosine triphosphate ligand for antifungal response in rice: a molecular dynamics approach. *Molecular Biology Reports* **49**, 2579–2589.

Ji, S., Kim, J., Lee, C., Seo, H., Chun, S., Oh, J., Park, G., (2019). Enhancement of vitality and activity of a plant growth-promoting bacteria (PGPB) by atmospheric pressure non-thermal plasma. *Scientific Reports* **9,** 1–16.

Jin, S., Song, C., Jia, S., Li, S., Zhang, Y., Chen, C., Feng, Y., Xu, Y., Xiong, C., Xiang, Y., & Jiang, H. (2017). An integrated strategy for establishment of curcuminoid profile in turmeric using two LC–MS / MS platforms. *Journal of Pharmaceutical and Biomedical Analysis* **132,** 93–102.

John, K., Ayyanar, M., Jeeva, S., Suresh, M., Enkhtaivan, G., & Kim, D. (2014). Metabolic Variations, Antioxidant Potential, and Antiviral Activity of Different Extracts of *Eugenia singampattiana* (an Endangered Medicinal Plant Used by Kani Tribals, Tamil Nadu, India) Leaf. *BioMed Research International* **2014,** 11.

Jorgensen, W., Maxwell, D., Tirado-Rives, J. (1996). Development and testing of the OPLS all-atom force field on conformational energetics and properties of organic liquids. *Journal of American Chemical Society* **118,** 11225-11236.

Joulain, D. (2021). Jasminum grandiflorum flowers- Phytochemical complexity and its capture in extracts: a review. *Flavour and Fragrance Journal* **36,** 526-553.

Jung, D., Park, H., Byun, H., Park, Y., Kim, T., Kim, B., Um, S., & Pyo, S. (2010). Diosgenin inhibits macrophage-derived inflammatory mediators through downregulation of CK2, JNK, NF-κB and AP-1 activation. *International Immunopharmacology* **10**, 1047–1054.

Jurenka, J, Ascp, M. (2009). Anti-inflammatory Properties of Curcumin, a Major Constituent of *Curcuma longa*: A Review of Preclinical and Clinical Research. *Alternative Medicine Review* **14,** 141-153.

Kabera, N., Semana, E., Mussa, R. and He X. (2014). Plant secondary metabolites: biosynthesis, classification, function and pharmacological properties. *J Pharm Pharmacol* **2,** 377-392.

Kahlon, A., Negi, A., Kumari, R., (2014). Identification of 1-chloro-2- formyl indenes and tetralenes as novel anti-staphylococcal agents exhibiting sortase A inhibition. *Applied Microbiology and Biotechnology* **98,** 2041–51.

Kalaycıoglu, Z., Gazioglu, I., & Erim, F. (2017). Comparison of antioxidant, anticholinesterase, and antidiabetic activities of three curcuminoids isolated from *Curcuma longa* L. *Natural Product Research* **31,** 2914-2917.

Kamat, J., Boloor, K., Devasagayam, P., Venkatachalam, S. (2000). Antioxidant properties of *Asparagus racemosus* against damage induced by gamma-radiation in rat liver mitochondria. *Journal of Ethnopharmacology* **71,** 425–435.

Kaminek, M., Motyka, V., Vankova, R. (1997). Regulation of cytokinin content in plant cells. *Physiol Plant* **101,** 689–700.

Kamran, S., Shahid, I., Baig, D., Rizwan, M., Malik, K. & Mehnaz, S. (2017).

Contribution of zinc solubilizing bacteria in growth promotion and zinc content of wheat. *Frontiers in Microbiology* **8,** 2593.

Kang, S., Bilal, S., Shahzad, R., Kim, Y. & Park, C. (2020). Producing Endophytic *Klebsiella pneumoniae* YNA12 as a Bio-Herbicide for Weed Inhibition : Special Reference with Evening Primroses. *Plants* **9,** 761.

Kang, S., Latif, A., Waqas, M., You, Y., Hamayun, M., Joo, G., Shahzad, R., Choi, K., & Lee, I. (2015). Gibberellin-producing *Serratia nematodiphila* PEJ1011 ameliorates low temperature stress in *Capsicum annuum* L . *European Journal of Soil Biology* **68**, 85–93.

Kankate, M., Tekale, V., Thakare, P. (2018). Adoption of Improved Cultivation Practices of Turmeric in Yavatmal District. *International Journal of Current Microbiology and Applied Science* **7,** 640–647.

Karnwal A. (2011) Plant growth promoting activity of *Bacillus* spp. on turmeric. The annals of "valahia" university of targoviste.

Karthikeyan, B., Joe, M., Jaleel, C. (2009). Response of some medicinal plants to vesicular arbuscular mycorrhizal inoculations. *Journal of Scientific Research* **1,** 381–386.

Karthikeyan, B., Sakthivel, U., Narayanan, J. (2013). Role of plant growth promoting rhizobacteria for commercially grown medicinal plants. *Bacteria in agrobiology: crop productivity* **2,** 65–76.

Kasai, T. and Sakamura, S. (1981). N-Carboxymethyl-L-serine, a new acidic amino acid from Asparagus (*Asparagus officinalis*) shoots. *Agriculture and Biological Chemistry* **45,** 1483-1485.

Kashyap, P., Muthusamy, K., Niranjan, M., Trikha, S., & Kumar, S. (2020). Sarsasapogenin : A steroidal saponin from *Asparagus racemosus* as multi target directed ligand in Alzheimer ' s disease. *Steroids* **153,** 108529.

Katsipis, G., Tsalouxidou, V., Halevas, E., Geromichalou, E., Geromichalos, G., & Pantazaki, A. (2021). In vitro and in silico evaluation of the inhibitory effect of a curcumin-based oxovanadium (IV) complex on alkaline phosphatase activity and bacterial biofilm formation. *Applied Microbiology and Biotechnology* **105**, 147–168.

Katsori, M., Chatzopoulou, M., Dimas, K., Kontogiorgis, C., Patsilinakos, A., Trangas, T., & Hadjipavlou-Litina, D. (2011). Curcumin analogues as possible anti-proliferative & anti-inflammatory agents. *European Journal of Medicinal Chemistry*, **46,** 2722–2735.

Katsuyama, Y., Kita, T., & Horinouchi, S. (2009). Identification and characterization of multiple curcumin synthases from the herb *Curcuma longa*. *FEBS Letters* **583**, 2799–2803.

Kaur, S., Anu, G., & Satinder, K. (2012). Assessing the Benefits of Azotobacter Bacterization in Sugarcane : A Field Appraisal. *Sugar Tech* **14,** 61–67.

Kavitha, K., Nakkeeran, S., & Chandrasekar, G. (2012). Rhizobacterial-mediated induction of defense enzymes to enhance the resistance of turmeric (*Curcuma longa* L) to *Pythium aphanidermatum* causing rhizome rot. *Archives of Phytopathology and Plant Protection* **45,** 199–219.

Khaerunnisa, S., Kurniawan, H., Awaluddin, R., Suhartati, S., Soetjipto, S. (2020). Potential Inhibitor of COVID-19 Main Protease (Mpro) From Several Medicinal Plant Compounds by Molecular Docking Study Molecular Docking, ADME-Toxicity Prediction, and Evaluation of Curcumin Derivative Compound as Inhibitor Inflamation on Rheumathoid Arth. *Preprints.org*.

Khan, & Bano, A. (2019). Exopolysaccharide producing rhizobacteria and their impact on growth and drought tolerance of wheat grown under rainfed conditions. Plos One **12,** 1–19.

Khan, F., Bamunuarachchi, N. I., Tabassum, N., & Kim, Y. M. (2021). Caffeic Acid and Its Derivatives: Antimicrobial Drugs toward Microbial Pathogens. *Journal of Agricultural and Food Chemistry* **69,** 2979–3004.

Khan, M., Zaidi, A., & Musarrat, J. (2014). Phosphate solubilizing microorganisms: Principles and application of microphos technology. *Phosphate Solubilizing Microorganisms: Principles and Application of Microphos Technology* 1–297.

Khanna, K., Lakshmi, V., Sharma, A., Gandhi, S., Ali, H. & Ahmad, P. (2019). Supplementation with plant growth promoting rhizobacteria (PGPR) alleviates cadmium toxicity in *Solanum lycopersicum* by modulating the expression of secondary metabolites. *Chemosphere* **230**, 628–639.

Khatun, M., Nur, A., Biswas, S., Khan, M., Amin, Z. (2021). Assessment of the anti-oxidant, anti-inflammatory and anti-bacterial activities of different types of turmeric (*Curcuma longa*) powder in Bangladesh. *Journal of Agriculture and Food Research* **6,** 100201.

Khoa, N., Giau, N., Tuan, T. (2016). Effects of *Serratia nematodiphila* CT-78 on rice bacterial leaf blight caused by *Xanthomonas oryzae* pv.oryzae. *Biological Control* **103,** 1–10.

Khorasani, A., Sani, W., Philip, K., Taha, R., Rafat, A. (2010). Antioxidant and antibacterial activities of ethanolic extracts of *Asparagus officinalis* cv. Mary Washington: Comparison of in vivo and in vitro grown plant bioactivities *African journal of biotechnology* **9,** 8460–8466.

Kim, J., Mistry, B., Shin, H. & Kang, S. (2021). Anti-biofilm activity of N-Mannich bases of berberine linking piperazine against *Listeria monocytogenes*. *Food Control*, **121**,107668.

Kim, S., Kang, O., Lee, Y., Han, S., & Ahn, Y. (2016). Hepatoprotective Effect and

Synergism of Bisdemethoycurcumin against MCD Diet-Induced Nonalcoholic Fatty Liver Disease in Mice. *Plos one* **16,** 1–15.

Kim, S., Thiessen, P., Bolton, E., Chen, J., Fu, G., Gindulyte, A., Han, L., He, J., He, S., Shoemaker, B., Wang, J., Yu, B., Zhang, J., Bryant, S. (2016). PubChem Substance and Compound databases. *Nucleic acids Res.* **44**, D1202–D1213

King, F., Weinhold, F. (1995). Structure and spectroscopy of (HCN) n clusters: Cooperative and electronic delocalization effects in C–H···N hydrogen bonding. *The Journal of chemical physics* **103,** 333-347.

Kishore, A., Kumar, S., Pratap, P., Kumar, A., Pandey, K., Kumar, A. & Yadav, H. (2018). Biotechnological aspects of plants metabolites in the treatment of ulcer : A new prospective. *Biotechnology Reports* **18,** 256.

Kita, T., Imai, S., Sawada, H., Kumagai, H., Seto, H. (2008). The biosynthetic pathway of curcuminoid in turmeric (*Curcuma longa*) as revealed by 13C-labeled precursors. *Bioscience, Biotechnology and Biochemistry* **72,** 1789–1798.

Kloepper, J. & Beauchamp, C. (1992). A review of issues related to measuring colonization of plant roots by bacteria. *Canadian Journal of Microbiology* **38,** 1219–1232.

Kloepper, J. (1993). Plant growth promoting rhizobacteria as biological agents. In: FB Metting (eds) Soil microbial ecology: application in agricultural and environmental management, *Jr. Marcel Dekker* 255-274.

Kloepper, J., Lifshitz, R., Zablotowicz, R. (1989). Free-living bacterial inocula for enhancing crop productivity. *Trends Biotechnol* **7,** 39-43.

Knobloch, J. & Horstkotte, M. (2002). Evaluation of different detection methods of biofilm formation in *Staphylococcus aureus*. *Medical Microbiology and Immunology* **191,** 101–106.

Kuan, K., Othman, R., & Rahim, K. (2016). Plant Growth-Promoting Rhizobacteria Inoculation to Enhance Vegetative Growth, Nitrogen Fixation and Nitrogen Remobilisation of Maize under Greenhouse Conditions. *PLoS One* **11,** 1–19.

Kugler, S., Cooper, R., Boessneck, J., Kusel, K., & Wichard, T. (2020). Rhizobactin B is the preferred siderophore by a novel *Pseudomonas* isolate to obtain iron from dissolved organic matter in peatlands. *BioMetals* **33**, 415–433.

Kumar, A., Maurya, B., Raghuwanshi, R. (2014a). Isolation and characterization of PGPR and their effect on growth, yield and nutrient content in wheat (*Triticum aestivum* L.). *Biocatalysis and Agricultural Biotechnology* **3**, 121–128.

Kumar, A., Singh, A., Kaushik, M., Mishra, S., Raj, P., Singh, P., Pandey, K. (2017). Interaction of turmeric (*Curcuma longa* L.) with beneficial microbes: a review. *3 Biotech* **7,** 1–8.

Kumar, A., Singh, R., Giri, D., Singh, P. & Pandey, K. (2014). Effect of *Azotobacter*

chroococcum CL13 inoculation on growth and curcumin content of turmeric (*Curcuma longa* L). *International Journal of Current Microbiology and Applied Sciences* **3**, 275–283.

Kumar, A., Singh, V., Singh, M., Singh, P., Singh, S., Pandey, K. (2016). Isolation of plant growth promoting rhizobacteria and their impact on growth and curcumin content in *Curcuma longa* L. *Biocatalysis and Agricultural Biotechnology* **8,** 1–7.

Kumar, P., and Dubey R. (2012). Plant Growth Promoting Rhizobacteria for biocontrol of phytopathogens and yield enhancement of *Phaseolus vulgaris*. *Journal of Current Perspectives in Applied Microbiology* **1,** 6–38.

Kumar, P., Kamle, M., Maurya, P., Singh, R. (2019). Beneficial Uses and Applications of Plant Growth-Promoting Rhizobacteria in Sustainable Agriculture. *Microbiology for Sustainable Agriculture, Soil Health, and Environmental Protection* 81–104.

Kumar, R., Swapnil, P., Meena, M., Selpair, S., & Yadav, B. (2022). Plant Growth-Promoting Rhizobacteria (PGPR): Approaches to Alleviate Abiotic Stresses for Enhancement of Growth and Development of Medicinal Plants. *Sustainability* **14,** 15514.

Kumar, S., Mehla, R., Dang, A. (2008). Use of Shatavari *Asparagus Racemosus* as a Galactopoietic and Therapeutic Herb a Review. *Agricultural Reviews* **29,** 132 – 138.

Kumar, V., Kumar, A., Pandey, K. & Roy, B. (2015). Isolation and characterization of bacterial endophytes from the roots of *Cassia tora* L. *Annals of Microbiology*, **65,** 1391–1399.

Kumari, P., Meena, M., & Upadhyay, R. (2018). Characterization of plant growth promoting rhizobacteria (PGPR) isolated from the rhizosphere of *Vigna radiata* (mung bean). *Biocatalysis and Agricultural Biotechnology* **16,** 155–162.

Kumari, R., Kumar, R., Lynn, A. (2014). G-mmpbsa-A GROMACS tool for high-throughput MM-PBSA calculations. *Journal of Chemical Information and Modeling* **54**, 1951–1962.

Lamuela-ravents, R. (1999). 2,6-di-tert-butyl-4-hydroxytoluene. *Methods in enzymology* **299,** 152–178.

Lan, C., Chen, X., Zhang, Y., Wang, W., Liu, Y., Cai, Y., Ren, H., Zheng, S., Zhou, L., Zeng, C. (2018). Curcumin prevents strokes in stroke-prone spontaneously hypertensive rats by improving vascular endothelial function. *BMC Cardiovasc. Disord.* **18,** 1–10.

Laskowski, R., MacArthur, M., Moss, D., Thornton, J. (1993) PROCHECK—a program to check the stereochemical quality of protein structures, *J Appl Cryst.* **26**, 283–291.

Laslo, E., Gyorgy, E., Mara, G., Tamas, E., Abraham, B., & Lanyi, S. (2012). Screening of plant growth promoting rhizobacteria as potential microbial inoculants. *Crop Protection* **40,** 43–48.

Lastra, D., Camacho, M., Capote, N. (2021). Soil bacteria as potential biological control agents of Fusarium species associated with asparagus decline syndrome. *Applied Sciences* **11,** 8356.

Leach A. (2001). Molecular Modelling: Principles and Applications, second edition

Lee, H. (2006). Antimicrobial Properties of Turmeric (*Curcuma longa* L.) Rhizome-Derived ar-Turmerone and Curcumin. *Food science Biotechnology* **15,** 559-563.

Lee, J., Park, J., Cho, H., Joo, S., Cho, M., Lee, J. (2013). Anti-biofilm activities of quercetin and tannic acid against *Staphylococcus aureus. Biofouling* **29,** 491-499.

Lee, K., Shin, D., Yoon, J., Kang, H., Oh, K. (2002). Expression of a transpeptidase for cell wall sorting reaction, from sortase, *Staphylococcus aureus* ATCC 6538p in *Escherichia coli J. Microbiol. Biotechnol* **12,** 530-533.

Lee, S., Progulske, A., Erdos, G., Piacentini, D., Ayakawa, G., Crowley, P., Bleiweis, A. (1989) Construction and characterization of isogenic mutants of *Streptococcus mutans* deficient in major surface protein antigen P1 (I/II), *Infect Immun*. **57**, 3306-13.

Lee, S., Song, I., Lee, J., Yang, W., Oh, K. & Shin, J. (2014). Sortase A inhibitory metabolites from the roots of *Pulsatilla koreana*. *Bioorganic and Medicinal Chemistry Letters* **24**, 44–48.

Lekshmi, P., Arimboor, R., Indulekha, P. & Menon, A. (2012). Turmeric (*Curcuma longa* L.) volatile oil inhibits key enzymes linked to type 2 diabetes. *International Journal ofFood Sciences and Nutrition* **63**, 832–834.

Levesque, C., Voronejskaia, E., Huang, Y., Mair, R., Ellen, R., Cvitkovitch, D. (2005). Involvement of sortase anchoring of cell wall proteins in biofilm formation by *Streptococcus mutans, Infect Immun*. **73** 3773-7.

Li, B., Li, X., Lin, H., & Zhou, Y. (2018). Curcumin as a Promising Antibacterial Agent: Effects on Metabolism and Biofilm Formation in *S. mutans*. *BioMed Research International* **2018,** 4508709.

Li, L., Aggarwal, B., Shishodia, S., Abbruzzese, J., Kurzrock, R., (2004). Nuclear factor-kappaB and I-kappaB kinase are constitutively active in human pancreatic cells, and their down-regulation by curcumin (diferuloylmethane) is associated with the suppression of proliferation and the induction of apoptosis. *Cancer* **101,** 2351–2362.

Li, R., Xiang, C., Zhang, X., Guo, D., Ye, M. (2010). Chemical Analysis of the Chinese Herbal Medicine Turmeric (*Curcuma longa* L). *Current Pharmaceutical Analysis* **6,** 256–268.

Li, S., & Wang, P. (2011). Chemical composition and product quality control of turmeric (*Curcuma longa* L). *Pharmaceutical Crops* **2,** 28-54.

Liddycoat S, Wolyn D. (2009). Field evaluation of asparagus crowns and germinating seeds inoculated with plant growth-promoting rhizobacteria. *Canadian Journal of*

Plant Science **89**, 1133–1138.

Liu, W., Huang, X., Qi, Q., Dai, Q.S., Yang, L., Nie, F., Lu, N., Gong, D., Kong, L., Guo, Q., (2009). Asparanin A induces G2/M cell cycle arrest and apoptosis in human hepatocellular carcinoma HepG2 cells. *Biochem. Biophys. Res. Commun*. **381**, 700–705.

Lopez, S., Pastorino, G., Malbran, I., & Balatti, P. (2019). Enterobacteria isolated from an agricultural soil of Argentina promote plant growth and biocontrol activity of plant pathogens. *Revista de La Facultad de Agronomia* **118**, 022.

Lorck, H. (1948). Production of Hydrocyanic Acid by Bacteria. *Physiologia Plantarum* **1**, 142–146.

Lotfi, N., Soleimani, A., Cakmakcı, R., Vahdati, K., & Mohammadi, P. (2022). Characterization of plant growth-promoting rhizobacteria (PGPR) in Persian walnut associated with drought stress tolerance. *Scientific Reports* **12**, 1–13.

Louden, C., Haarmann, D., Lynne, M. (2011). Use of blue agar CAS assay for siderophore detection. *Journal of microbiology & biology education* **12**, 51-53.

Lowy F. (1998). *Staphylococcus aureus* infections. *N Engl J Med* **8,** 520–532.

Lucy, M., Reed, E., Glick, B. (2004). Applications of free living plant growth promoting rhizobacteria. *Antonie Van Leeuwenhoek* **86,** 1– 25.

Luo, H., Liang, D., Bao, M., Sun, R., Li, Y., Li, J., Wang, X., Lu, K., & Bao, J. (2017). In silico identi fi cation of potential inhibitors targeting *Streptococcus mutans* sortase A. *International Journal of Oral Science* **9,** 53–62.

Luthra, P., Kumar, R., & Prakash, A. (2009). Demethoxycurcumin induces Bcl-2 mediated G2/M arrest and apoptosis in human glioma U87 cells. *Biochemical and Biophysical Research Communications* **384**, 420–425.

Luximon-Ramma, A., Bahorun, T., Soobrattee, M., Aruom, O. (2002). Antioxidant activities of phenolic, proanthocyanidin, and flavonoid components in extracts of *Cassia fistula*. *Journal of Agricultural and Food Chemistry* **50,** 5042-5047.

Ma, L. (2015). Biological Databases for Human Research. *Genomics, Proteomics & Bioinformatics* **13**, 55–63.

Mack, D., Becker, P., Chatterjee, I., Dobinsky, S., Knobloch, J., Peters, G., Rohde, H., & Herrmann, M. (2004). Mechanisms of biofilm formation in Staphylococcus epidermidis and *Staphylococcus aureus*: functional molecules, regulatory circuits, and adaptive responses. *International Journal of Medical Microbiology* **294,** 203–212.

MacKerell, A., Bashford, D., Bellott, Dunbrack R., Evanseck, J., Field, M., Fischer, S., Gao, J., Guo, H., Ha, S., Joseph-McCarthy, D. (1998). All-atom empirical potential for molecular modeling and dynamics studies of proteins. *J Phys Chem B* **102,** 3586-3616.

Mahadevamurthy, M., Channappa, M., Sidappa, M., Raghupathi, S., Nagaraj, K. (2016). Isolation of phosphate solubilizing fungi from rhizosphere soil and its effect on seed growth parameters of different crop plants. *J. Appl. Biol. Biotechnol,* **4**, 22-26.

Mahattanadul, S., Nakamura, T., Panichayupakaranant, P., & Phdoongsombut, N. (2009). Comparative antiulcer effect of Bisdemethoxycurcumin and Curcumin in a gastric ulcer model system. *Phytomedicine* **16,** 342–351.

Maheshwari, D, and Dheeman, S. (2014). Phytohormone-Producing PGPR for Sustainable Agriculture. *Bacterial Metabolites in Sustainable Agroecosystem, Sustainable Development and Biodiversity* 12.

Maia, E., Medaglia, L., da Silva, A., Taranto, A. (2020). Molecular Architect: A User-Friendly Workflow for Virtual Screening, *ACS Omega*. **5**, 6628-6640.

Malik, K., Bilal, R., Mehnaz, S., Rasul, G., Mirza, M., & Ali, S. (1997). Association of nitrogen-fixing, plant-growth-promoting rhizobacteria (PGPR) with kallar grass and rice. *Plant and Soil* **194,** 37–44.

Malleswari, D., Bagyanarayana, G. (2013). In vitro screening of rhizobacteria isolated from the rhizosphere of medicinal and aromatic plants for multiple plant growth promoting activities. *J Microbiol Biotech Res* **3,** 84–91.

Manca de Nadra, M., Strasser, A., de Saad A., de Ruiz Holgado, P., Oliver, G. (1985). Extracellular polysaccharide production by *Lactobacillus bulgaricus* CRL 420. *Milchwissenschaft* **40,** 409-411.

Mandal, S., Nandy, A., Pal, M., Saha, B. (2000). Evaluation of antibacterial activity of *Asparagus racemosus* Willd. root. *Phytotherapy Research* **14,** 118–119.

Maougal, T., Kechid, M., Ladjabi, C., Djekoun, A. (2021). PGPR Characteristics of Rhizospheric Bacteria to Understand the Mechanisms of Faba Bean Growth. *Proceedings* **66,** 27.

Marechal, Y. (2004). Water and biomolecules: an introduction. *J Mol Struct* **70,** 207-210.

Maria D. and Maria A. (2021). *Curcuma longa L.* Rhizome Essential Oil from Extraction to Its Agri-Food Applications: A Review. *Plants* **10,** 44.

Mark, P. and Nilsson, L. (2001). Structure and dynamics of the TIP3P, SPC, and SPC/E water models 298 K. *J Phys Chem A* **105,** 9954-9960.

Masuda, T., Isobe, J., Jitoe, A., Nakatani, N. (1992). Antioxidative curcuminoids from rhizomes of *Curcuma xanthorrhiza*. *Phytochemistry* **31,** 3645–3647.

Matloubi, Z., Hassan, Z. (2020). HSA-curcumin nanoparticles: a promising substitution for Curcumin as a Cancer chemoprevention and therapy. *J. Pharm. Sci.* **28,** 209–219.

Mattos, J., Castro, H., Alves, G. & Amorim, L. (2015). The Use of DNA Extraction for Molecular Biology and Biotechnology Training : A Practical and Alternative Approach. *Creative Education* **6,** 762-772.

Mayak, S., Tirosh, T., Glick, B. (2004). Plant growth-promoting bacteria that confer resistance to water stress in tomatoes and peppers. *Plant Science* **166,** 525–530.

Mazumdar, D., Saha, S., Ghosh, S. (2019). Isolation, screening and application of a potent PGPR for enhancing growth of Chickpea as affected by nitrogen level. *International Journal of Vegetable Science* **0**, 1–18.

Mazumder, M., Borah, A., & Choudhury, S. (2020). Inhibitory potential of plant secondary metabolites on anti-Parkinsonian drug targets: Relevance to pathophysiology, and motor and non-motor behavioural abnormalities. *Medical Hypotheses* **137**, 109544.

McCammon, J., Gelin, B. and Karplus, M. (1977). Dynamics of folded proteins. *Nature* **267**, 585-590.

Meena, V., Maurya, B. and Verma, J. (2014a). Does a rhizospheric microorganism enhance K^+ availability in agricultural soils. *Microbiological Research* **169,** 337-347.

Meena, V., Maurya, B., Verma, J., & Meena, R. (2016). Potassium-Solubilizing Microorganism in Evergreen Agriculture: An Overview. *Potassium solubilizing microorganisms for sustainable agriculture* 1–331.

Mehrafarin, A., Ghaderi, A., Rezazadeh, S., Naghdi, B., Nourmohammadi, G., (2010). Bioengineering of important secondary metabolites and metabolic pathways in fenugreek (*Trigonella foenum-graecum* L.). *J. Med. Plant*. **9**, 1–18.

Mehrotra, N., Sabarinath, S., Suryawanshi, S., Raj, K., & Gupta, R. (2009). LC – UV Assay for Simultaneous Estimation of Aromatic Turmerone, a/b-Turmerone and Curlone : Major Bisabolane Sesquiterpenes of Turmeric Oil in Rabbit Plasma for Application to Pharmacokinetic Studies. *Chromatographia* **69,** 1077–1082.

Meizarini, A., Siswandono, Riawan, W., & Rahayu, R. (2018). In silico and in vivo anti-inflammatory studies of curcuminoids, turmeric extract with zinc oxide, and eugenol. *Tropical Journal of Pharmaceutical Research* **17**, 269–275.

Meng, B., Li, J., Cao, H. (2013). Antioxidant and anti-inflammatory activities of curcumin on diabetes mellitus and its complications. *Cur. Phar. Des*. **19,** 2101–2113.

Meng, F., Zhou, Y., Ren, D., & Wang, R. (2018). Turmeric : A Review of Its Chemical. In Natural and Artificial Flavoring Agents and Food Dyes. Elsevier Inc. London, UK, 299–350.

Meyer, M., & Schomburg, D. (2008). Protein Interactions. *Biotechnology*, **5,** 87–108.

Miller, B., McGee, T., Swails, J., Homeyer, N., Gohlke, H., Roitberg, A. (2012). MMPBSA.py: An Efficient Program for End-State Free Energy Calculations, *J Chem Theory Comput***. 8**, 3314-21.

Mishra P. (2009). Isolation, spectroscopic characterization and molecular modeling studies of mixture of *Curcuma longa*, ginger and seeds of fenugreek. *Int. J. Pharm Tech Res*. **1,** 79–95.

Mishra, P., Kundu, E. & Gupta, A. (2009). *Exiguobacterium acetylicum* strain 1P (MTCC 8707) a novel bacterial antagonist from the North Western Indian Himalayas. *World J Microbiol Biotechnol* **25,** 131–137.

Mishra, R., Prakash, O., Alam, M., Dikshit, A. (2010). Influence of plant growth promoting rhizobacteria (PGPR) on the productivity of *Pelargonium graveolens* L. herit. *Recent Res Sci Technol* **2,** 53–57.

Mitra, D., Sharma, K., Uniyal, N., Chauhan, A., & Sarkar, P. (2016). Study on Plant Hormone (Indole-3-Acetic Acid) Producing Level and Other Plant Growth Promotion Ability (PGPA) by *Asparagus racemosus* L. Rhizobacteria. *Journal of Chemical and Pharmaceutical Research* **8**, 995–1002.

Mitra, S., Prakash, N. & Sundaram, R. (2012). Shatavarins (containing Shatavarin IV) with anticancer activity from the roots of *Asparagus racemosus*. *Indian Journal of Pharmacology* **44,** 732–736.

Miyamoto, S., Kollman, P. (1992). Settle: An analytical version of the SHAKE and RATTLE algorithm for rigid water models. *J Comput Chem* **13,** 952-962.

Moghadamtousi, S., Kadir, H., Hassandarvish, P., Tajik, H., Abubakar, S., Zandi, K. (2014). Review on antibacterial, antiviral, and antifungal activity of curcumin. *BioMed Research International*. **2014,** 186864.

Mohamed, F., Abd Majid, F., Ismail, H., Wong, T., Shameli, K., Miyake, M., Ahmad Khairudin, N. (2018). In Silico and In Vitro Study of the Bromelain-Phytochemical Complex Inhibition of Phospholipase A2 (Pla2) Fatahiya. *Molecules* **23,** 73.

Mohammed, A. (2018). Effectiveness of exopolysaccharides and biofilm forming plant growth promoting rhizobacteria on salinity tolerance of faba bean (*Vicia faba* L.). *African Journal of Microbiology Research* **12**, 399–404.

Mohankumar, K., Sridharan, S., Pajaniradje, S., Singh, V., Ronsard, L., Banerjea, A., Somasundaram, D., Coumar, M., Periyasamy, L. & Rajagopalan, R. (2015). BDMC-A, an analog of curcumin, inhibits markers of invasion, angiogenesis, and metastasis in breast cancer cells via NF-κB pathway-A comparative study with curcumin. *Biomedicine and Pharmacotherapy* **74**, 178–186.

Mohite, B. (2013). Isolation and characterization of indole acetic acid (IAA) producing bacteria from rhizospheric soil and its effect on plant growth. *Journal of Soil Science and Plant Nutrition* **13**, 638–649.

Mostert, M., Schoeman, A., Van Merwe, M. (2000). Isolation, characterization and insect growth inhibitory activity of major turmeric constituents and their derivatives against *Schistocerca gregaria* (Forsk) and *Dysdercus koenigii* (Walk). *Pest Management Science* **56**, 1086–1092.

Mustarichie, R., Levita, J. and Febriani, D. (2013). In-Silico Study of Curcumin, Demethoxycurcumin and Xanthorrizol as Skin Whitening Agents. *World Journal of Pharmaceutical Sciences* **1,** 72-80.

Nadaf, N., Parulekar, R., Patil, R., Gade, T., Momin, A., Waghmare, S., Dhanavade, M., Akalpita, U., Sonawane, K. (2018). Biofilm inhibition mechanism from extract of *Hymenocallis littoralis*. *Journal of Ethnopharmacology* **222,** 121-132.

Nadar, S., Khan, T., Patching, S. & Omri, A. (2022). Development of Antibiofilm Therapeutics Strategies to Overcome Antimicrobial Drug Resistance. *Microorganisms* **10**, 1–28.

Nagaraju, Y., Triveni, S., Reddy, R., Sagar, B., Kumar, B., Chari, K., Jhansi, P. (2016). Screening of zinc solubilizing, potassium releasing bacterial and fungal isolates from different rhizosphere soils *International Journal for Research in Applied Science & Engineering Technology* **11,** 2187–2192.

Nandakumar, D., Nagaraj, V., Vathsala, P., Rangarajan, P. and Padmanaban, G. (2006). Curcumin-artemisinin combination therapy for Malaria. *Antimicrobial Agents and Chemotherapy* **50,** 1859–1860.

Naseem, H., Bano, A. (2014). Role of PGPR and their Exopolysaccharide (EPS) in drought tolerance of maize. *Journal of Plant Interactions* **9**, 689-701.

Nazir, R., Gupta, S., Dey, A., Kumar, V., Gupta, A., Shekhawat, M., Goyal, P., & Pandey, D. (2022). In vitro tuberization, genetic, and phytochemical fidelity assessment of *Dioscorea deltoidea*. *Industrial Crops and Products* **175**, 114174.

Nazzaro, F., Fratianni, F., Coppola, R. (2013). Quorum sensing and phytochemicals, *Int J Mol Sci*. **14,** 12607-12619.

Negi, J., Singh, P., Joshi, G., Rawat, M., Bisht, V. (2010). Chemical constituents of Asparagus. *Pharmacognosy reviews* **8,** 215-220.

Negi, P., Jayaprakasha, G., Rao, L., & Sakariah, K. (1999). Antibacterial Activity of Turmeric Oil : A Byproduct from Curcumin Manufacture. *Journal of agricultural and food chemistry* **47,** 4297−4300.

Nicolaus, B., Panico, A., Lama, L., Romano, I., Manca, C., De Giulio A., Gambacorta, A. (1999). Chemical composition and production of exopolysaccharides from representative members of heterocystous and non-heterocystous cyanobacteria. *Phytochemistry* **52**, 639-647.

Nithyapriya, S., Lalitha, S., Sayyed, R., Reddy, M., Dailin, D., El Enshasy, H., Luh Suriani, N., & Herlambang, S. (2021). Production, purification, and characterization of bacillibactin siderophore of *Bacillus subtilis* and its application for improvement in plant growth and oil content in sesame. *Sustainability* **13,** 5394.

Nitulescu, G., Margina, D., Zanfirescu, A., Olaru, O., & Nitulescu, G. (2021). Targeting bacterial sortases in search of anti-virulence therapies with low risk of resistance development. *Pharmaceuticals* **14,** 415.

Nitulescu, G., Nicorescu, I., Olaru, O. & Ungurianu, A. (2017). Molecular Docking and Screening Studies of New Natural Sortase A Inhibitors. *International Journal of Molecular Sciences* **18,** 2217.

Niu, X., Gao, Y., Yu, Y., Yang, Y., Wang, G., & Sun, L. (2018). Molecular Modeling reveals the inhibition mechanism and structure-activity relationship of curcumin and its analogues to *Staphylococcal aureus* Sortase A. *Journal of Biomolecular Structure and Dynamics* **37,** 1220-1230.

O'Boyle, N., Banck, M., James, C., Morley, C., Vandermeersch, T., Hutchison, G. (2011). Open Babel: An open chemical toolbox. *J. Cheminform.* **3,** 33.

Ogungbe, I. & Setzer, W. (2016). The Potential of secondary metabolites from plants as drugs or leads against protozoan neglected diseases-Part III: In-Silico molecular docking investigations. *Molecules* **21,** 1389.

Oku, S., Komastu, A., Tajima, T., Nakashimada, Y., Kato, J., (2012). Identification of chemotaxis sensory proteins for aminoacids in *Pseudomonas fluorescens* Pf0-1 and their involvement in chemotaxis to tomato root exudates and root colonization. *Microbes Environ*. **27,** 462-469.

Okuda-hanafusa, C., Uchio, R., Fuwa, A., Kawasaki, K., Muroyama, K., Yamamoto, Y., & Murosaki, S. (2019). Turmeronol A and turmeronol B from *Curcuma longa* prevent inflammatory mediator production by lipopolysaccharide-stimulated RAW264.7 macrophages, partially via reduced NF-κB signaling. *Food and function* **10,** 5779-5788.

Olanrewaju, O., Glick, B., & Babalola, O. (2017). Mechanisms of action of plant growth promoting bacteria. *World Journal of Microbiology and Biotechnology* **33**, 1–16.

Oniga, S., Araniciu, C., Palage, M., Popa, M., Chifiriuc, M., Marc, G., Pirnau, A., Stoica, C., Lagoudis, I., Dragoumis, T., Oniga, O. (2017). New 2-Phenylthiazoles as Potential Sortase A Inhibitors: Synthesis, Biological Evaluation and Molecular Docking. *Molecules* **27,** 1827.

Onlom, C., Nuengchamnong, N., Phrompittayarat, W., Putalun, W., Waranuch, N., Ingkaninan, K. (2017). Quantification of saponins in *Asparagus racemosus* by HPLC-Q-TOF-MS/MS. *Nat. Prod. Commun.* ***12***, 7–10.

Oostenbrink, C., Villa, A., Mark, A., Van Gunsteren, W. (2004). Biomolecular Force Field Based on the Free Enthalpy of Hydration and Solvation: The GROMOS ForceField Parameter Sets 53A5 and 53A6. *Journal of Computational Chemistry* **25,** 1656– 76.

O'Toole, G., Pratt, L., Watnick, P., Newman, D., Weaver, V., Kolter, R. (1999). Genetic approaches to study of biofilms, *Methods Enzymol*. **310**, 91-109.

Pandiyan, G., Leela, V., Eswari, S., Ramachandran, M., Ranganathan, V., Visha, P. (2022). Evaluation of Shatavarin IV Compound from Methanolic Extract of *Asparagus racemosus* by High Performance Thin Layer Chromatography. *J. Phytopharm*. **11,** 89–91.

Pant, G., Panwar, M., Negi, D., Rawat, M., Morris, G. (1988). Spirostanol glycoside from fruits of *Asparagus officinalis*. *Phytochemistry* **27,** 3324–3325.

Paramesha, M., Priyanka, N., Crassina, K., Shetty, N. (2021). Evaluation of diosgenin content from eleven different Indian varieties of fenugreek and fenugreek leaf powder fortified bread. *J. Food Sci. Technol*. **58,** 4746–4754.

Parewa, H., Yadav, J., Rakshit, A., Meena, V., Karthikeyan, N. (2014). Plant Growth Promoting Rhizobacteria Enhance Growth and Nutrient Uptake of Crops. *Agric Sustain Dev*. **2,**101-116.

Park, B., Kim, J., Kim, M., Lee, S., Takeoka, G., Oh, K. (2005). *Curcuma longa* L. constituents inhibit sortase A and *Staphylococcus aureus* cell adhesion to fibronectin. *Journal of Agricultural and Food* **53**, 9005–9009.

Parmar, P., Sindhu, S. (2013). Potassium solubilization by rhizosphere bacteria: influence of nutritional and environmental conditions. *J. Microbiol. Res.* **3,** 25-31.

Parulekar, R., Sonawane, K. (2018). Molecular modeling studies to explore the binding affinity of virtually screened inhibitor toward different aminoglycoside kinases from diverse MDR strains. *Journal of Cellular Biochemistry* **119**, 2679–2695.

Parveen, H., Singh, A., Khan, A., Prasad, B., & Pareek, N. (2018). Influence of plant growth promoting rhizobacteria on seed germination and seedling vigour of green gram. *Int J Chem Stud* **6**, 611–618.

Passari, A., Lalsiamthari, P., Zothanpuia, Leo, V., Mishra, V., Yadav, M., Gupta, V. & Singh, B. P. (2018). Biocontrol of Fusarium wilt of *Capsicum annuum* by rhizospheric bacteria isolated from turmeric endowed with plant growth promotion and disease suppression potential. *European Journal of Plant Pathology* **150**, 831–846.

Patel, B. (2015). Isolation and characterization of shatavarin IV from root of *Asparagus racemosus* willd. *International Journal of Pharmacy and Pharmaceutical Sciences* **7,** 362-365.

Patel, D., Prasad, S., Kumar, R., Hemalatha, S., (2012). An overview on antidiabetic medicinal plants having insulin mimetic property. *Asi.Pac.J.Trop.biomed*. **2,** 320–333.

Patil D, (2020). Shatpushpa: One solution for various female health issues: A Review. *Natl. J. Res. Ayurved Sci*. **8,** 1105–1114.

Patil, D., Gautam, M., Gairola, S., Jadhav, S., & Patwardhan, B. (2014). HPLC/Tandem mass spectrometric studies on steroidal saponins: An example of quantitative

determination of shatavarin IV from dietary supplements containing *Asparagus racemosus*. *Journal of AOAC International* **97,** 1497–1502.

Peiqin, Li. (2012). Quantitative determination of diosgenin in *Dioscorea zingiberensis* cell cultures by microplate-spectrophotometry and high-performance liquid chromatography. *African Journal of Pharmacy and Pharmacology* **6,** 15.

Peret-Almeida, L., Cherubino, A., Alves, R., Dufosse, L., & Gloria, M. (2005). Separation and determination of the physico-chemical characteristics of curcumin, demethoxycurcumin and bisdemethoxycurcumin. *Food Research International* **38**, 1039–1044.

Perez-Montano, F., Alias-Villegas, C., Bellogin, R., Cerro, P., Espuny, M., Guerrero, I., Baena, F., Ollero, F., Cubo, T. (2014). Plant growth promotion in cereal and leguminous agricultural important plants: from microorganism capacities to crop production. *Microbiol. Res*. **169**, 325–336.

Pikovskaya, I. (1948). Mobilization of phosphorus in soil in connection with vital activity of some microbial species. *Microbiologiya* **17,** 362-370.

Ponnusamy, S., Zinjarde, S., Bhargava, S., Rajamohanan, P. & Ravikumar, A. (2012). Discovering Bisdemethoxycurcumin from *Curcuma longa* rhizome as a potent small molecule inhibitor of human pancreatic alpha-amylase, a target for type-2 diabetes. *Food Chemistry* **135,** 2638–2642.

Prabhukarthikeyan, S., Manikandan, R., Durgadevi, D., Keerthana, U., Harish, S., Karthikeyan, G., Raguchander, T. (2017). Bio-suppression of turmeric rhizome rot disease and understanding the molecular basis of tripartite interaction among *Curcuma longa*, *Pythium aphanidermatum* and *Pseudomonas fluorescens*. *Biol. Control* **111,** 23–31.

Prasad, M., Srinivasan, R. & Chaudhary, M. (2019). Plant Growth Promoting Rhizobacteria (PGPR) for Sustainable Agriculture: Perspectives and Challenges. *PGPR Amelioration in Sustainable Agriculture* 129-157.

Prasad, S., Aggarwal, B. (2011). Turmeric, the Golden spice from traditional medicine to modern medicine. In: Benzie IFF, Wachtel-Galor S (eds) Herbal medicine. *Biomolecular and clinical aspects*, 2nd edn. CRC Press, Boca Raton, 1-26.

Pushpakumari, K., Naijo, Varghese. and Kavitha, Kottol. (2014). Purification and separation of individual curcuminoids from spent. *International Journal of Pharmaceutical Sciences and Research* **5,** 3246–3254.

Rahman, M., Khan, K. (2019). In silico based unraveling of New Delhi metallo- β - lactamase (NDM-1) inhibitors from natural compounds : a molecular docking and molecular dynamics simulation study. *J. Biomol. Struct. Dyn***. 0,** 1–11.

Rahmoune, B., Morsli, A., Khelifi-Slaoui, M., Khelifi, L., Strueh, A., Erban, A., Kopka, J., Prell, J. & Van Dongen, J. (2017). Isolation and characterization of three new PGPR and their effects on the growth of Arabidopsis and Datura plants. *Journal of*

Plant Interactions **12,** 1–6.

Raina, V., Srivastava, S., Jain, Ł., Ahmad, A., Syamasundar, K. & Aggarwal, K. (2002). Essential oil composition of *Curcuma longa* L . roma from the plains of northern India. *Flavour And Fragrance Journal* **17,** 99–102.

Rajendran, G., Patel, M. & Joshi, S. (2012). Isolation and characterization of nodule-associated *Exiguobacterium* sp. from the root nodules of fenugreek (*Trigonella foenum-graecum*) and their possible role in plant growth promotion. *International Journal of Microbiology* **2012,** 8.

Ramamoorthy, V., Viswanathan, R., Raguchander, T., Prakasam, V. & Samiyappan, R. (2001). Induction of systemic resistance by plant growth promoting rhizobacteria in crop plants against pests and diseases. *Crop Protection* **20,** 1-11.

Rani, R., Kumar, V., Gupta, P., Chandra, A. (2021). Potential use of *Solanum lycopersicum* and plant growth promoting rhizobacterial (PGPR) strains for the phytoremediation of endosulfan stressed soil. *Chemosphere* **279,** 130589.

Rani, S. (2014). Trigonelline and diosgenin attenuate ER stress, oxidative stress-mediated damage in pancreas and enhance adipose tissue PPAR c activity in type 2 diabetic rats *Mol Cell Biochem* **396,**161–174.

Rarey, M., Kramer, B., Lengauer, T., Klebe, G. (1996). A fast flexible docking method using an incremental construction algorithm. *J. Mol. Biol*. **261,** 470-489.

Rarnsewak, R., Dewitt, D. & Nair, M. (2000). activities of Curcumins I-III from *Curcuma longa*. *Phytomedicine* **7**, 303–308.

Reiter, B., Sessitsch, A. (2006). Bacterial endophytes of the wildflower *Crocus albiflorous* analyzed by characterization of isolates and by a cultcultivation-independent roach. *Can J Microbiol* **52,**140–149.

Revathy, S., Elumalai, S., Benny, M., & Antony, B. (2011). Isolation, Purification and Identification of Curcuminoids from Turmeric (*Curcuma longa* L.) by Column Chromatography. *Journal of Experimental Sciences* **2**, 21–25.

Riaz, U., Murtaza, G., Anum, W., Samreen, T., Sarfraz, M., Nazir, M. (2021). Plant Growth-Promoting Rhizobacteria (PGPR) as Biofertilizers and Biopesticides. *Microbiota and Biofertilizers* 181-196.

Riera, N., Handique, U., Zhang, Y., Dewdney, M. & Wang, N. (2017). Characterization of antimicrobial-producing beneficial bacteria isolated from Huanglongbing escape citrus trees. *Frontiers in Microbiology* **8**, 1–12.

Rizvi, A., Ahmed, B., Khan, M., El-Beltagi, H., Umar, S. & Lee, J. (2022). Bioprospecting Plant Growth Promoting Rhizobacteria for Enhancing the Biological Properties and Phytochemical Composition of Medicinally Important Crops. *Molecules* **27**, 1–31.

Rodrigues, J., Prather, K., Kluskens, L. & Rodrigues, L. (2015). Heterologous Production

of Curcuminoids. *Microbiology and Molecular Biology Reviews* **79**, 39–60.

Rodriguez, H. & Fraga, R. (1999). Phosphate solubilizing bacteria and their role in plant growth promotion. *Biotechnology Advances* **17,** 319–339.

Rosier, A., Beauregard, P. & Bais, H. (2021). Quorum Quenching Activity of the PGPR *Bacillus subtilis* UD1022 Alters Nodulation Efficiency of Sinorhizobium meliloti on *Medicago truncatula*. *Frontiers in Microbiology* **11,** 596299.

Roychowdury, D., Paul, M. & Banerjee, S. (2015). Isolation Identification and Partial Characterization of Nitrogen Fixing Bacteria from Soil and then the Production of Biofertilizer. *International Journal of Current Microbiology and Applied Sciences* **4**, 808-815.

Ryckaert, J., Ciccotti, G., Berendsen, H. (1977). Numerical integration of the cartesian equations of motion of a system with constraints; molecular dynamics of n-alkanes. *J Comput Phys* **23,** 327-341.

Saengsanga, T. (2018). Isolation and Characterization of Indigenous Plant Growth-Promoting Rhizobacteria and Their Effects on Growth at the Early Stage of Thai Jasmine Rice (*Oryza sativa* L. KDML105). *Arabian Journal for Science and Engineering* **43**, 3359–3369.

Saharan, B. & Nehra, V. (2011). Plant Growth Promoting Rhizobacteria: A Critical Review. *Life Sci. Med. Res* **2011**, 1–30.

Sahne, F., Mohammadi, M., Najafpour, G. & Moghadamnia, A. (2016). Enzyme-assisted ionic liquid extraction of bioactive compound from turmeric (*Curcuma longa* L.): Isolation, purification and analysis of curcumin. *Industrial Crops & Products* **95**, 686-694.

Saikia, L. & Upadhyaya, S. (2011). Antioxidant activity, phenol and flavonoid content of *A. racemosus* Willd. a medicinal plant grown using different organic manures. *Res. J. Pharm. Biol. Chem. Sci* **2**, 457-463.

Sairam, K., Priyambada, N. & Goel, R. (2003). Gastroduodenal ulcer protective activity of *Asparagus racemosus.* An experimental, biochemical and histological study. *Journal of Ethnopharmacology* **86**, 1-10.

Saito, K. & Matsuda, F. (2010). Metabolomics for functional genomics, systems biology, and biotechnology. *Annu Rev Plant Bio* **l61**, 463–89.

Salamone, I., Hynes, R. & Nelson, L. (2001). Cytokinin production by plant growth promoting rhizobacteria and selected mutants. *Can J Microbiol* **47**, 404–411.

Saleem, H., Sarfraz, M., Ahsan, H., Khurshid, U., Kazmi, S., Zengin, G., Locatelli, M., Ahmad, I., Abdallah, H., Mahomoodally, M., Rengasamy, K. & Ahemad, N. (2020). Secondary metabolites profiling, biological activities and computational studies of *Abutilon figarianum* webb (Malvaceae). *Processes* **8**, 336.

Salmanli, M., Tatar Yilmaz, G., Tuzuner, T. (2021). Investigation of the antimicrobial activities of various antimicrobial agents on *Streptococcus Mutans* Sortase A through computer-aided drug design (CADD) approaches, *Comput Methods Programs Biomed.* **212**, 106454.

Sanchita, Singh, G. & Sharma, A. (2014). In silico study of binding motifs in squalene synthase enzyme of secondary metabolic pathway Solanaceae family. *Molecular Biology Reports* **41**, 7201–7208.

Sandhya, V., Ali, S., Grover, M., Kishore, N. & Venkateswarlu, B. (2009). *Pseudomonas* sp. strain P45 protects sunflowers seedlings from drought stress through improved soil structure. *J Oilseed Res* **26**, 600–601.

Sangeetha, M., Mal, N., Atmaja, K., Sali, V. & Vasanthi, H. (2013) Chemico-Biological Interactions PPAR's and Diosgenin a chemico biological insight in NIDDM. *Chem. Biol. Interact* **206**, 403–410.

Santoro, M., Zygadlo, J., Giordano, W. & Banchio, E. (2011). Volatile organic compounds from rhizobacteria increase biosynthesis of essential oils and growth parameters in peppermint (*Mentha piperita*). *Plant Physiol Biochem* **49**, 1177–1182.

Santoyo, G., Urtis-Flores, C., Loeza-Lara, P., Orozco-Mosqueda, M. & Glick, B. (2021). Rhizosphere colonization determinants by plant growth-promoting rhizobacteria (Pgpr). *Biology* **10**, 1–18.

Saravanan, V., Subramoniam, S. & Raj, S. (2004). Assessing in vitro solubilization potential of different zinc solubilizing bacterial (zsb) isolates. *Brazilian journal of microbiology* **35**, 121–125.

Sarvin, B., Fedorova, E., Shpigun, O., Titova, M. & Nikitin, M. (2018). LC-MS determination of steroidal glycosides from *Dioscorea deltoidea* Wall cell suspension culture: Optimization of pre-LC-MS procedure parameters by Latin Square design. *Journal of Chromatography B*, **1080**, 64–70.

Sattari, N., Pahlavan, Y. & Bozorg, A. (2018). Effects of humic acid and plant growth-promoting rhizobacteria (PGPR) on induced resistance of canola to *Brevicoryne brassicae* L. *Bulletin of Entomological Research* **109**, 479-489.

Saxena, V. & Chourasia, S. (2001). A new isoflavone from the roots of *Asparagus racemosus. Fitoterapia* **72**, 307-309.

Sayyed, R. Z. (Ed.). (2019). Plant Growth Promoting Rhizobacteria for Sustainable Stress Management. *Rhizobacteria in Biotic Stress Management* Springer Nature **13.**

Schieffer, G. (2002). Pressurized liquid extraction of curcuminoids and curcuminoid degradation products from turmeric (*Curcuma longa*) with subsequent HPLC assays. *Journal of Liquid Chromatography and Related Technologies* **25**, 3033–3044.

Schippers, B., Bakker, A., Bakker, P. & Van, P. (1990). Beneficial and deleterious effects of HCN-producing *Pseudomonad*s on rhizosphere interactions. *Plant and Soil* **129,** 75-83.

Schmidt, R., Koberl, M., Mostafa, A., Ramadan, E., Monschein, M., Jensen, K., Bauer, R. & Berg, G. (2014). Effects of bacterial inoculants on the indigenous microbiome and secondary metabolites of chamomile plants. *Frontiers in Microbiology* **5**, 1–11.

Schwyn, B. & Neilands, J. (1987). Universal chemical assay for the detection and determination of siderophores. *Analytical Biochemistry* **160**, 47–56.

Setzer, W., Sama, W., Essien, E., Olayemi, J., Ekundayo, O., Ajaiyeoba, E., Sama, W., Walker, T. & Setzer, W. (2008). Larvicidal Activity of Turmerone-Rich Essential Oils of *Curcuma longa,* Leaf and Rhizome from Nigeria on Anopheles gambiae. Pharmaceutical Biology **46**, 279-282.

Shah, A., Nazari, M., Antar, M., Msimbira, L., Naamala, J., Lyu, D., Rabileh, M., Zajonc, J. & Smith, D. (2021). PGPR in Agriculture: A Sustainable Approach to Increasing Climate Change Resilience. *Frontiers in Sustainable Food Systems* **5**, 1–22.

Shaikh, S. & Saraf, M. (2017). Biofortification of *Triticum aestivum* through the inoculation of zinc solubilizing plant growth promoting rhizobacteria in field experiment. *Biocatalysis and Agricultural Biotechnology* **9**, 120–126.

Shakeel, M., Rais, A., Hassan, M. & Hafeez, F. (2015). Root Associated *Bacillus* sp. Improves Growth, Yield and Zinc Translocation for Basmati Rice (*Oryza sativa*) Varieties. *Frontiers in Microbiology* **6**, 1–12.

Shameer, S., Prasad, T.N.V.K.V (2018). Plant growth promoting rhizobacteria for sustainable agricultural practices with special reference to biotic and abiotic stresses. *Plant Growth Regulation* **84**, 603–615.

Shao, Y., Poobrasert, O., Kennelly, E., Chin, C., Ho, C., Huang, M., Garrison, S. & Cordell, G. (1997). Steroidal saponins from *Asparagus officinalis* and their cytotoxic activity. *Planta. Med.* **63**, 258-262.

Sharafzadeh, S. & Ordookhani, K. (2011). Organic and bio fertilizers as a good substitute for inorganic fertilizers in medicinal plants farming. *Australian Journal of Basic and Applied Sciences* **5**, 1330–1333.

Sharifian, P., Yaslianifard, S., Fallah, P., Aynesazi, S., Bakhtiyari, M. & Mohammadzadeh, M. (2020). Investigating the effect of nano-curcumin on the expression of biofilm regulatory genes of *Pseudomonas aeruginosa*. *Infection and Drug Resistance* **13**, 2477–2484.

Sharma, O. (1976). Antioxidant activity of curcumin and related compounds. *Biochemical Pharmacology* **25**, 1811–1812.

Sharma, V. & Sarkar, I. (2013). Bioinformatics opportunities for identification and study of medicinal plants. *Briefings in Bioinformatics* **14**, 238–250.

Sheikh, I., Capoor, M. & Khatoon, F. (2013). Phytochemical analysis and growth inhibiting effects of *Cinnamomum cassia* bark on some pathogenic fungal isolates. *J Chem. Pharma. Res* **5**, 25-32.

Shulga, D., Kudryavtse, K. (2021). Selection of Promising Novel Fragment Sized *S. aureus* SrtA Noncovalent Inhibitors Based on QSAR and Docking Modeling Studies, *Molecules*. **26** 7677,

Si, L., Li, P., Liu, X. & Luo, L. (2016). Chinese herb medicine against Sortase A catalyzed transformations, a key role in gram-positive bacterial infection progress, *Journal of Enzyme Inhibition and Medicinal Chemistry* **31,** 184-196.

Siddiqui, I., Shaukat, S., Sheikh, I. & Khan, A. (2006). Role of cyanide production by *Pseudomonas fluorescens* CHA0 in the suppression of root-knot nematode, Meloidogyne javanica in tomato. *World J Microbiol Biotechnol* **22**, 641–650.

Singh, M., Hamid, A., Maurya, A., Prakash, O., Khan, F., Kumar, A., Aiyelaagbe, O., Negi, A. & Bawankule, D. (2014). Journal of Steroid Biochemistry and Molecular Biology Synthesis of diosgenin analogues as potential anti-inflammatory agents. *Journal of Steroid Biochemistry and Molecular Biology* **143**, 323–333.

Singh, M., Singh, D., Gupta, A. & Pandey, K. (2019). Plant Growth Promoting Rhizobacteria: Application in Biofertilizers and Biocontrol of Phytopathogens. *PGPR Amelioration in Sustainable Agriculture* Chapter **3,** 41-66.

Singh, R. & Jha, P. (2016). The Multifarious PGPR *Serratia marcescens* CDP-13 Augments Induced Systemic Resistance and Enhanced Salinity Tolerance of Wheat (*Triticum aestivum* L). PLoS ONE **11,** e0155026.

Singh, R., Singh, P., Li, H., Song, Q., Guo, D., Solanki, M., Verma, K., Malviya, M., Song, X., Lakshmanan, P. & Yang, L. (2020). Diversity of nitrogen-fixing rhizobacteria associated with sugarcane : a comprehensive study of plant-microbe interactions for growth enhancement in *Saccharum* spp. *BMC Plant Biology* **20,** 1–21.

Singh, T., Sahai, V., Goyal, D., Prasad, M., Yadav, A., Shrivastav, P., Ali, A. & Dantu, P. (2020). Identification, Characterization and Evaluation of Multifaceted Traits of Plant Growth Promoting Rhizobacteria from Soil for Sustainable Approach to Agriculture. *Current Microbiology* **77**, 3633–3642.

Sivaramakrishnan, M., Jagadeesan, V. & Ruban, S. (2019). Screening of curcumin analogues targeting Sortase A enzyme of *Enterococcus faecalis* : a molecular dynamics approach. *Journal of Proteins and Proteomics* **10**, 245–255.

Siviero, A., Gallo, E., Maggini, V., Gori, L., Mugelli, A., Firenzuoli, F. & Vannacci, A. (2015). Curcumin, a golden spice with a low bioavailability. *J Herb Med* **5**, 57–70.

Smyth, T., Rudden, M., Tsaousi, K., Marchant, R. & Banat, I. (2014). Protocols for the Isolation and Analysis of Lipopeptides and Bioemulsifiers. In: McGenity T, Timmis K, Nogales B (eds) Hydrocarbon and Lipid Microbiology Protocols. *Springer*

Protocols Handbooks, Springer, Heidelberg.

Sonawane, K., Barale, S., Dhanavade, M., Waghmare, S., Nadaf, N., Kamble, S., Mohammed, A., Makandar, A., Fandilolu, P., Dound, A., Naik, N., More, V. (2021). Structural insights and inhibition mechanism of TMPRSS2 by experimentally known inhibitors Camostat mesylate, Nafamostat and Bromhexine hydrochloride to control SARS-coronavirus-2: a molecular modeling approach, *Inform. Med. Unlocked* **24**, 100597.

Soni, V., Mehta, A., Ratre, Y., Tiwari, A., Amit, Singh, R., Sonkar, S., Chaturvedi, N., Shukla, D. & Vishvakarma, N. (2020). Curcumin, a traditional spice component, can hold the promise against COVID-19. *Eur. J. Pharmacol* **886**, 173551.

Soto, J., Ortiz, J., Herrera, H., Fuentes, A., Almonacid, L. & Charles, T. (2019). Enhanced arsenic tolerance in *Triticum aestivum* inoculated with arsenic-resistant and plant growth promoter microorganisms from a heavy metal-polluted soil. *Microorganisms* **7**, 348.

Sousa, S., Fernandes, P. & Ramos, M. (2006). Protein–ligand docking: current status and future challenges. *Proteins* **65**, 15–26.

Srivastava, P., Shukla, A. & Kalunke, R. (2018). Comprehensive metabolic and transcriptomic profiling of various tissues provide insights for saponin biosynthesis in the medicinally important *Asparagus racemosus. Sci. Rep*. **8**, 1–13.

Su, H., Horvat, R. & Jilani, G. (1982). Isolation, Purification, and Characterization of Insect Repellents from Curcuma. *J. Agric. Food Chem.* **30,** 290-292.

Su, Z., Cai, S., Liu, J., Zhao, J., Liu, Y., Yin, J. & Zhang, D. (2021). Root-Associated Endophytic Bacterial Community Composition of *Asparagus officinalis* of Three Different Varieties. *Indian J. Microbiol* **61**, 160–169.

Sun, J., Cui, G., Ma, X., Zhan, Z., Ma, Y., Teng, Z., Gao, W., Wang, Y., Chen, T., Lai, C., Zhao, Y., Tang, J., Lin, H., Shen, Y., Zeng, W., Guo, J. & Huang, L. (2019). An integrated strategy to identify genes responsible for sesquiterpene biosynthesis in turmeric. *Plant Molecular Biology* **101**, 221–234.

Suree, N., Liew, C., Villareal, V., Thieu, W., Fadeev, E., Clemens, J. & Clubb, R. (2009). The structure of the *Staphylococcus aureus* sortase- substrate complex reveals how the universally conserved LPXTG sorting signal is recognized. *J Biol Chem* **284**, 24465-24477.

Surveswaran, S., Cai, Y., Corke, H. & Sun, M. (2007). Systematic evaluation of natural phenolic antioxidants from 133 Indian medicinal plants. *Food Chemistry* 102, 938–953.

Suryadevara, N., Ponmurugan, P. (2012). Response of turmeric to plant growth promoting rhizobacteria (PGPR) inoculation under different levels of nitrogen. *Int J Biol Technol* **3,** 39–44.

Swamy, M., Pokharen, N., Dahal, S. & Anuradha, M. (2011). Phytochemical and antimicrobial studies of leaf extract of *Euphorbia neriifolia*. *J Med Plants Res* **5**, 5785–5788.

Takishita, Y., Charron, J. & Smith, D. (2018). Biocontrol rhizobacterium Pseudomonas sp. 23S induces systemic resistance in Tomato (*Solanum lycopersicum* L.) against bacterial Canker *Clavibacter michiganensis* subsp. michiganensis. *Frontiers in Microbiology* **9**, 1–14.

Tal, B., Tamir, I., Rokem, J. & Goldberg, I. (1984). Isolation and characterization of an intermediate steroid metabolite in diosgenin biosynthesis in suspension cultures of *Dioscorea deltoidea* cells. *Biochem. J* **219**, 619 - 24.

Tamura, K., Stecher, G. & Kumar, S. (2021). MEGA11: Molecular Evolutionary Genetics Analysis Version 11. *Mol Biol Evol* **38**, 3022–3027.

Tanaka, K., Kuba, Y., Ina, A., Watanabe, H. & Komatsu, K. (2008). Prediction of cyclooxygenase inhibitory activity of Curcuma rhizome from chromatograms by multivariate analysis. *Chemical and Pharmaceutical Bulletin* **56**, 936–940.

Taufique, T., Mayda, U. & Mehraj, H. (2014). Yield performance and phytochemical screening of three asparagus varieties. *Bangladesh Research Publication Journal* **10**, 196-201.

Taylor, P., Joe, B., Vijaykumar, M., Lokesh, B., Joe, B. (2004). Biological Properties of Curcumin-Cellular and Molecular Mechanisms of Action of Curcumin. *Crit Rev Food Sci Nutr* **44**, 97-111.

Tchuisseu, G., Berger, B., Patz, S., Fankem, H. & Ruppel, S. (2018). Data on molecular identification, phylogeny and in vitro characterization of bacteria isolated from maize rhizosphere in Cameroon. *Data in Brief* **19**, 1410–1417.

Teles, A., Dulce, T., Mouchrek, A., Abreu-silva, A., Calabrese, S. & Almeida-souza, F. (2019), Cinnamomum zeylanicum, Origanum vulgare, and Curcuma longa Essential Oils: Chemical Composition, Antimicrobial and Antileishmanial Activity. *Evid Based Complement Alternat Med* **2019**, 2421695.

Thappeta, K., Zhao, L., Nge, C., Crasta, S., Leong, C., Ng, V., Kanagasundaram, Y., Fan, H. & Ng, S. (2020). In-silico identified new natural sortase a inhibitors disrupt *S. aureus* biofilm formation. *International Journal of Molecular Sciences* **21**, 1–18.

Thewles, A., Parslow, R. & Coleman, R. (1993). Effect of diosgenin on biliary cholesterol transport in the rat. *Biochemical Journal* **291**, 793–798.

Thompson, J., Gibson, T., Plewniak, F., Jeanmougin, F. & Higgins, D. (1997). The CLUSTAL_X windows interface: flexible strategies for multiple sequence alignment aided by quality analysis tools. *Nucleic Acids Res* **25**, 4876–4882.

Thomsen, R., Christensen, M. (2006). MolDock: a new technique for high-accuracy molecular docking. *J Med Chem.* **49,** 3315–3321.

Tirry, N., Kouchou, A., Laghmari, G., Lemjereb, M., Hnadi, H., Amrani, K., Bahafid, W. & El Ghachtouli, N. (2021). Improved salinity tolerance of *Medicago sativa* and soil enzyme activities by PGPR. *Biocatalysis and Agricultural Biotechnology* **31,**101914.

Tonnesen, H.H. (1992). Chemistry of curcumin and curcuminoids. *Phenolic Compounds in Food and their Effect on Health. I*: **506,** 143 153.

Toussaint, J., Kraml, M., Nell, M., Smith, S., Smith, F., Steinkellner, S., Schmiderer, C., Vierheilig, H. & Novak, J. (2008). Effect of *Glomus mosseae* on concentrations of rosmarinic and caffeic acids and essential oil compounds in basil inoculated with *Fusarium oxysporum* f. sp. basilici. *Plant Pathol* **57**, 1109–1116.

Tsai, S., Huan, C., Chyau, C., Weng, C. & Mau, J. (2011). Composition and Antioxidant Properties of Essential Oils from Curcuma rhizome. *Asian Journal of Arts and Sciences* **2,** 57–66.

Umair, M., Muhammad, I., Muhammad, S., Adeela, A., Farooq, A. & Sikandar, H. (2018). A brief review on plant growth promoting rhizobacteria (PGPR): a key role in plant growth promotion. *Plant Protection* **2**, 77–82.

Upadhyay, S., Phukan, U., Mishra, S. & Shukla, R. (2014). De novo leaf and root transcriptome analysis identified novel genes involved in Steroidal sapogenin biosynthesis in *Asparagus racemosus.* *BMC Genomics* **15**, 746.

Valdes-Tresanco, M., Valiente, P., Moreno, E. (2021). gmx_MMPBSA: A New Tool to Perform End-State Free Energy Calculations with GROMACS, *J Chem Theory Comput.* **17**, 6281-6291.

Van Loon, L. & Glick, B. (2004). Increased plant fitness by rhizobacteria. In *Molecular ecotoxicology of plants* 170, 177–205.

Van, Der., Lindahl, E., Hess, B., Groenhof, G., Mark, A. & Berendsen, H. (2005). GROMACS: fast, flexible, and free. *J Comput Chem* **26**, 1701-1718.

Varma, A., Prasad, R. & Tuteja, N. (2017). Promotion and Value Addition to Some Important Medicinal Plants Under Saline Condition by Intervention of a Novel Mycorrhizal Formulation. *Mycorrhiza - eco-physiology, secondary metabolites, nanomaterials: Fourth Edition* 1–334.

Vasagade, S., Patil, S., Patil, S. & Shubham, A. (2021). Study on Rhizospheric Bacterial Exopolysaccharide and Its Application in Plant Growth Promoters and Antimicrobial Activity. *International Journal of Research in Engineering and Science (IJRES)* **9**, 59–66.

Vasudha, S., Shivesh, S. & Prasad, S. (2013). Harnessing PGPR from rhizosphere of prevalent medicinal plants in tribal areas of Central India. *Res J Biotechnol* **8**, 76–85.

Velavan, S., Nagulendran, K., Mahesh, R. & Begum, H. (2007). In vitro antioxidant

activity of *Asparagus racemosus* root. *Pharmacognecy* **3**, 26–33.

Velhal, C. (2014). Effect of Rhizobium Based Biofertilizer Combined with *Saccharomyces cerevisiae* on the Growth of Hyacinth Bean. *International Journal of Plant & Soil Science* **3**, 959–968.

Vendeville, A., Winzer, K., Heurlier, K., Tang, C. & Hardie, K. (2005). Making 'sense' of metabolism: autoinducer-2, LuxS and pathogenic bacteria. *Nat Rev Microbiol* **3,** 383-96.

Vendeville, A., Winzer, K., Heurlier, K., Tang, C., Hardie, K. (2005). Making 'sense' of metabolism: autoinducer-2, LuxS and pathogenic bacteria, *Nat Rev Microbiol*. **3,** 383-96.

Venkat, S., Soumya, S., Agarwal, H. & Divya, D. (2017). Characterization and optimization of bacterium isolated from soil samples for the production of siderophores. *Resour Effic Technol* **3**, 434-439.

Venkata, M., Sripathy, R., Anjana, D., Somashekara, N., Krishnaraju, A., Krishanu, S., Murali, M., RamaVerma, S. & Ramchand, C. (2012). In silico, in vitro and in vivo assessment of safety and anti-inflammatory activity of curcumin. *American Journal of Infectious Diseases* **8**, 26–33.

Verghese, J. & Joy, M. (1989). Isolation of the colouring matter from dried turmeric (*Curcuma longa* L.) with ethyl acetate. *Flavour Frag J* **4**, 31–2.

Verlet, L. (1967). Computer experiments on classical fluids. I. Thermodynamical properties of Lenard-Jones molecules. *Physical Review* **159**, 98-103.

Verma, H., Sonbhadra, D., Singh, S., White, J. & Kumar, A. (2021). Biocontrol Potential of Microbial Consortia: Approaches in Food Security and Disease Management. In: Kumar, A. (eds) *Microbial Biocontrol: Sustainable Agriculture and Phytopathogen Management*. Springer, Cham. 187-203

Verma, J. (2010). Impact of plant growth promoting rhizobacteria on crop production. *Int J Agric Res* **5**, 954–983.

Verma, V., Patel, R., Deshmukh, N., Jha, A., Ngachan, S., Singha, A. & Deka, B. (2019). Response of ginger and turmeric to organic versus traditional production practices at different elevations under humid subtropics of north-eastern India. *Ind. Crops Prod* **136**, 21–27.

Vijayalakshmi, K., Nadhiya, K., Haripriya, D. & Ranjani, R. (2014). In silico docking analysis of secondary metabolites of *Bauhinia variegata* and *Garcinia cambogia* with retinol-binding protein 4 as target for obesity. *International Journal of Pharmacognosy and Phytochemical Research* **6**, 636–642.

Vinayarani, G. & Prakash, H. (2018). Growth Promoting Rhizospheric and Endophytic Bacteria from *Curcuma longa* L. as Biocontrol Agents against Rhizome Rot and Leaf Blight Diseases *Plant Pathol. J.* **34**, 218–235.

Vinayarani, G., Madhusudhan, K. & Prakash, H. (2019). Induction of systemic resistance in turmeric by rhizospheric isolate *Trichoderma asperellum* against rhizome rot disease. *J. Plant Pathol* **101**, 965–980.

Wagner, L., Jonatas, F., Oliveira, R., Esteves, S. & Camargo, A. (2020). *Curcuma longa* L. (turmeric), *Rosmarinus officinalis* L. (rosemary), and *Thymus vulgaris* L. (thyme) extracts aid murine macrophages (RAW 264.7) to fight *Streptococcus mutans* during in vitro infection. *Archives of Microbiology* **202**, 2269-2277.

Walia, M., Batra, N. & Goyal, S. (2014). Isolation and characterization of plant growth promoting rhizobacteria and their application in plant growth. *Legume Research* **37**, 72–78.

Wallock, R., Marles, W., Clarke, D., Maitra, A., Dodds, M., Hanley, B. & Campopiano, D. (2015). Molecular basis of *Streptococcus mutans* sortase A inhibition by the flavonoid natural product trans-chalcone. *Chem Commun (Camb)* **51**, 10483-10485.

Wan, Y., Luo, S., Chen, J., Xiao, X., Chen, L. & Zeng, G. (2012). Chemosphere Effect of endophyte-infection on growth parameters and Cd-induced phytotoxicity of Cd-hyperaccumulator *Solanum nigrum* L . *Chemosphere* **89**, 743–750.

Wang, E. & Martinez, R. (2000). *Sesbania herbacea*-Rhizobium huautlense nodulation in flooded soils and comparative characterization of *S. herbacea*-nodulating rhizobia in different environments. *Microb Ecol* **40**, 25–32.

Wang, J., Li, H., Pan, J., Dong, J., Zhou, X. Niu, X., Deng, X. (2018). Oligopeptide Targeting Sortase A as Potential Anti-infective Therapy for *Staphylococcus aureus*, *Front Microbiol***. 9,** 245.

Wang, J., Shi, Y., Jing, S., Dong, H., Wang, D., Wang, T. (2019). Astilbin Inhibits the Activity of Sortase A from *Streptococcus mutans. Molecules.* **24,** 465.

Wang, L., Wang, X. & Zhao, B. (2011). Simultaneous Analysis of Diosgenin and Sarsasapogenin in *Asparagus officinalis* Byproduct by Thin-layer Chromatography. *Phytochem Anal* **22,** 14–17.

Wang, N., Wang, Z., Tootle, S., Philip, T. & Zhao, Z. (2012). Curcumin promotes cardiac repair and ameliorates cardiac dysfunction following myocardial infarction. *Br. J. Pharmacol* **167**, 1550–1562.

Wase, N. & Wright, P. (2008). Systems biology of cyanobacterial secondary metabolite production and its role in drug discovery. *Expert Opinion on Drug Discovery* **3**, 903–929.

Waters, C. & Bassler, B. (2005). Quorum sensing: cell-to-cell communication in bacteria. *Ann Rev Cell Developmental Biol* **21**, 319-46.

Werner, T. & Schmulling, T. (2009). Cytokinin action in plant development. *Curr Opin Plant Biol* **12**, 527-38.

Weyens, N., Van, L., Taghavi, S., Newman, L. & Vangronsveld, J. (2009). Exploiting plant microbe partnerships to improve biomass production and remediation. *Trends Biotechnol* **27**, 591-598.

Wiberg, K. (1965). A scheme for strain energy minimization application to the cycloalkanes. *J Am Chem Soc* **87**, 1070-1078.

Wichitnithad, W., Rojsitthisak, P., Ichitnithad, W., Jongaroonngamsang, N., Pummangura, S. and Rojsitthisak, P. (2009). A simple isocratic HPLC method for the simultaneous determination of curcuminoids in commercial turmeric extracts. *Phytochem. Anal* **20**, 314-319.

Wolfe, K., Wu, X. & Liu, R. (2003). Antioxidant Activity of Apple Peels. *Journal of Agricultural and Food Chemistry* **51**, 609-614.

Xekarfotakis, N., Chatzistathis, T., Mola, M., Demirtzoglou, T. & Monokrousos, N. (2021). The effects of different fertilization practices in combination with the use of PGPR on the sugar and amino acid content of *Asparagus officinalis*. *Horticulturae* **7**, 507.

Xie, Z., Ma, X. & Gang, D. (2009). Modules of co-regulated metabolites in turmeric (*Curcuma longa*) rhizome suggest the existence of biosynthetic modules in plant specialized metabolism. *Journal of Experimental Botany* **60**, 87–97.

Xiong, G., Wu, Z., Yi, J., Fu, L., Yang, Z., Hsieh, C., Yin, M., Zeng, X., Wu, C., Lu, A., Chen, X., Hou, T., Cao, D. (2021). ADMETlab 2.0: an integrated online platform for accurate and comprehensive predictions of ADMET properties. *Nucleic Acids Res*. **49**, W5-W14.

Xu, L., Shang, Z., Lu, Y., Li, P., Sun, L., Guo, Q., Bo, T., Le, Z., Bai, Z., Zhang, X., Qiao, X., & Ye, M. (2020). Analysis of curcuminoids and volatile components in 160 batches of turmeric samples in China by high-performance liquid chromatography and gas chromatography-mass spectrometry. *Journal of Pharmaceutical and Biomedical Analysis* **188**, 1–7.

Yadav, P., Kadam, K., Bhingare K. & Patil, M. (2018). Standardization and quantification of curcumin from *Curcuma longa* extract using UV visible spectroscopy and HPLC. *Journal of Pharmacognosy and Phytochemistry* **7,** 1913–1918.

Yang, C., Huang, S., Yang, X. & Jia, Z. (2004). Nor-lignans and steroidal saponins from *Asparagus gobicus*. *Planta Med* **70**, 446-51.

Yang, H., Yin, H., Shen, Y., Xia, G., Zhang, B., Wu, X., Cai, B. & Tam, J. (2016). A more ecological and efficient approach for producing diosgenin from *Dioscorea zingiberensis* tubers via pressurized biphase acid hydrolysis. *Journal of Cleaner Production* **131**, 10–19.

Yang, H., Yin, H., Wang, X., Li, Z., Shen, Y. & Jia, X. (2015). In situ pressurized biphase acid hydrolysis, a promising approach to produce bioactive diosgenin from the

tubers of *Dioscorea Zingiberensis*. *Pharmacognosy Magazine* **11**, 636–642.

Yilmaz, A. & Karik, U. (2022). AMF and PGPR enhance yield and secondary metabolite profile of basil (*Ocimum basilicum* L.). *Industrial Crops and Products*, **176**, 114327.

Yodkeeree, S., Chaiwangyen, W., Garbisa, S. & Limtrakul, P. (2009). Curcumin, demethoxycurcumin and bisdemethoxycurcumin differentially inhibit cancer cell invasion through the down-regulation of MMPs and uPA. *J. Nutr. Biochem*. **20**, 87–95.

Yoon, S., Ha, S., Kwon, S., Lim, J., Kim, Y., Seo, H. & Chun, J. (2017). Introducing EzBioCloud : a taxonomically united database of 16S rRNA gene sequences and whole-genome assemblies. *Int J Syst Evol Microbiol* **67**, 1613–1617.

Yuan, Y., Chu, D., Fan, J., Zou, P., Qin, Y., Geng, Y., Cui, Z., Wang, X., Zhang, C., Li, X., Clark, J., Li, Y. & Wang, X. (2020). Ecofriendly conversion of algal waste into valuable plant growth- promoting rhizobacteria (PGPR) biomass. *Waste Management* **120**, 576 – 584.

Yue, G., Kwok, H. & Lee, J. (2015). Novel anti-angiogenic effects of aromatic- turmerone, essential oil isolated from spice. *Journal of Functional Foods* **15**, 243–253.

Zainab, B., Ayaz, Z., Alwahibi, M., Khan, S., Rizwana, H., Soliman, D., Alawaad, A. & Mehmood A. (2020). In-silico elucidation of *Moringa oleifera* phytochemicals against diabetes mellitus. *Saudi Journal of Biological Sciences* **27**, 2299–2307.

Zhang, S., Guan, J., Yang, Q., Liu, G., Cheng, J. & Li, P. (2008). Analysis Qualitative and quantitative analysis of four species of Curcuma rhizomes using twice development thin layer chromatography. *Journal of Pharmaceutical and Biomedical* **48**, 1024–1028.

Zhao, Y., Cartabia, A., Lalaymia, I. & Declerck, S. (2022). Arbuscular mycorrhizal fungi and production of secondary metabolites in medicinal plants. *Mycorrhiza* **32**, 3–4.

Zhishen, J., Mengcheng, T., Jianming, W., The determination of flavonoid contents in mulberry and their scavenging effects on superoxide radicals, *Food Chemistry* **64**, 555-559.

Zong, Y., Bice, T., Ton-That, H., Schneewind, O. & Narayana, S. (2004). Crystal structures of *Staphylococcus aureus* Sortase A and its substrate complex. *Journal of Biological Chemistry* **279**, 31383–31389.

CHAPTER VII

RESEARCH PUBLICATIONS AND PRESENTATIONS

Paper Published (02):

1. **Ruddhi R. Jagtap**, Gajanan V. Mali and Kailas D. Sonawane. (2022) Isolation, characterization and identification of potent plant growth promoting rhizobacteria from *Asparagus racemosus.* **YMER, 21,** || ISSN : 0044-0477

2. **Ruddhi R. Jagtap**, Gajanan V. Mali, Shailesh R. Waghmare, Naiem H. Nadaf, Mansingraj S. Nimbalkar, and Kailas D. Sonawane. (2023) Impact of plant growth promoting rhizobacteria *Serratia nematodiphila* RGK and *Pseudomonas plecoglossicida* RGK on secondary metabolites of turmeric rhizome. **Biocatalysis and Agricultural Biotechnology, 47**, 102622. DOI: 10.1016/j.bcab.2023.102622.

Manuscript Communicated (01):

3. **Ruddhi. R. Jagtap**, Gajanan. V. Mali, Sagar S. Barale and Kailas. D. Sonawane. Inhibition of *S. Aureus* and *S. Mutans* Sortase A by PGPR induced secondary metabolites from *C. longa: In-vitro* and *in-silico* approaches **International Journal of Biological Macromolecules (Manuscript ID: IJBIOMAC-D-23-16762),** Under Review

Conferences Attended/ Paper Presented:

1. Participated in two days National conference-2019: Research and innovations in healthcare & Business Management Organised by Rashtriya Shikshan Mandal's CDGIM, Pune, 5 & 6th November 2019
2. **Ruddhi. R. Jagtap**, Gajanan.V. Mali, Kailas. D. Sonawane, Effect of Plant Growth Promoting Rhizobacteria on Turmeric. Interdisciplinary International Conference on 'Research Interventions and Technological Advancements In Plant Sciences (RITAPS,2021)' jointly organized by Association of Plant Science Researchers, Dehradun and PG department of Botany, Shri Pancham Khemraj Mahavidyalaya, Sawantwadi on 26th and 27th March, 2021.
3. Participated in two days International conference on 'Infectious Diseases and Immunopathology', organized by Department of Biotechnology, Savitribai Phule Pune University, Pune, 22nd to 24thApril 2021.

4. Completed one online certificate course on HPC Shiksha -Basics of High Performance Computing, conducted by Indian Institute of Technology Goa.
5. Participated in two days 3rd International Multidisciplinary Conference on Emerging Trends in Humanities, Commerce, Management, Science and Technology (IMCET-2021) organized by the Balwant College, Vita Dist. Sangli (MS) on 23rd – 24th December 2021.
6. **Ruddhi. R. Jagtap**, Gajanan.V. Mali, Kailas. D. Sonawane, Effect of Plant Growth Promoting Rhizobacteria on Secondary Metabolites of Medicinal Plant. International E-conference on the "Frontiers in Microbiology" organized by Vasantdada Patil Arts, commerce and science college in association with Microbiologists society, India on 17th and 18th January 2022.
7. **Ruddhi. R. Jagtap**, Gajanan.V. Mali, Kailas. D. Sonawane, Effect of Plant Growth Promoting Rhizobacteria on Secondary Metabolites of Medicinal Plant. National Conference on Recent trends in pure and applied sciences (RTPAS-2022) organized by internal quality assurance cell, Bharati Vidyapeeth's Dr. Patangrao Kadam Mahavidyalaya, Sangli. on 21st and 22nd January 2022.
8. **Ruddhi. R. Jagtap,** Gajanan.V. Mali, Kailas. D. Sonawane, Effect of Plant Growth Promoting Rhizobacteria on Secondary Metabolites of *Asparagus racemosus* one-day national conference on "Biodiversity and biosciences" organized by Rayat Shikshan Sanstha's Balwant College, Vita on 29 th December 2022.
9. **Ruddhi. R. Jagtap,** Gajanan.V. Mali, Kailas. D. Sonawane, SrtA inhibition by PGPR treated plant secondary metabolites from *C. longa*: A Structural perspectives, Symposium on "Accelerating Biology 2023: Discovery to Delivery" organized by HPC M & BA Group, C-DAC, Pune, India from 28th Feb to 2nd March 2023.
10. Participated in the workshop cum hands-on training on techniques on biogenic synthesis of nanomaterials organized by the School of Nanoscience and Biotechnology, Department of Biochemistry, and Department of Botany, Shivaji University, Kolhapur held during 20-24 Feb 2023 under the DBT-BUILDER SUK program.

STUDIES ON SECONDARY METABOLITES OF *C. LONGA* AND *A. RACEMOSUS* INFLUENCED BY PLANT GROWTH PROMOTING RHIZOBACTERIA

A THESIS SUBMITTED TO

SHIVAJI UNIVERSITY, KOLHAPUR

FOR THE DEGREE OF

DOCTOR OF PHILOSOPHY

IN

MICROBIOLOGY

UNDER THE FACULTY
OF
SCIENCE AND TECHNOLOGY

BY

MISS. RUDDHI RAJENDRA JAGTAP
M.Sc., SET, NET-ICAR

UNDER THE GUIDANCE OF

Dr. GAJANAN VISHNU MALI
M. Sc., Ph. D
Rayat Institute of Research and Development, Satara

AND

CO-GUIDANCE OF

Prof. (Dr.) KAILAS DASHRATH SONAWANE
M. Sc., Ph. D
Head,
Department of Biochemistry,
Shivaji University, Kolhapur.

2023

1. Recommendations:

Plant growth promoting rhizobacteria (PGPR) are naturally occurring soil bacteria that aggressively colonise plant roots and benefit plants by promoting growth. Several PGPR inoculants that are currently on the market appear to stimulate growth through at least one mechanism, including the prevention of plant disease (Bioprotectants), enhanced nutrient uptake (Biofertilizers), siderophore production (Biostimulants), and phytohormone production (Biofertilizers). The use of PGPR offers a desirable alternative to chemical fertilizers, pesticides, and dietary supplements, and the majority of these isolates significantly increase overall plant growth. The use of PGPRs for medicinal plant cultivation is a promising approach. These medicinal plants and their secondary metabolites have been used as one of the key sources for medicines and other health-related issues.

2. Conclusions:

The present work has resulted in the isolation of potent PGPR strains from the rhizosphere of medicinal plants such as *Curcuma longa* L. and *Asparagus racemosus* Willd. These PGPR identified as strains of *Serratia nematodiphila* RGK, *Pseudomonas plecoglossicida* RGK, *Exiguobacterium acetylicum* RGK and *Enterobacter mori* RGK1. The strain showed broad-spectrum antimicrobial activity against both Gram-positive and Gram-negative human pathogens. Biochemical characterization of these strains shows that they are capable to utilize various sugars. *Serratia nematodiphila* RGK and *Pseudomonas plecoglossicida* RGK can tolerate 7% NaCl along with exopolysaccharide production. Further these PGPR used for pot cultures studies, individually and in combination and found that PGPR treatment improved the growth and yield of Asparagus and Turmeric plants. Further, these plants were taken in order to extract secondary metabolites. Following extraction, metabolites were purified using acid hydrolysis and silica gel column chromatography. After that, HPLC, GC-MS/MS, and LC-MS/MS analysis were performed on the purified metabolites. One new phytocompound with increased level was found in the turmeric plant treated by the co-culture of both the isolated PGPR. In addition to this, studies on the antimicrobial, antifungal, antioxidant, and anti-biofilm properties of purified metabolites gave good results. Individual and combined effect of phytocompounds against Gram-positive and Gram-negative pathogens were also gave good results. The present study also includes *in silico* study of biofilm-forming protein SrtA from *S. aureus* and *S. mutans.* Thus, the present study will serve as a foundation for the development of similar therapeutic approaches (PGPR-induced phytocompounds) for controlling biofilm production by the Gram-positive pathogens such as *S. aureus* and *S. mutans*

3. Summary:

The present thesis was aimed to isolate bacterial strains of potent PGPR from the rhizosphere of *Curcuma longa* L. and *Asparagus racemosus* Willd. The *in-vitro* studies showed that these PGPR have ability to enhance plant growth and secondary metabolites of Asparagus and Turmeric plants. The present study includes extraction, purification, quantification and identification of plant secondary metabolites which was influenced by PGPR. The various analytical techniques were used to study these secondary metabolites. Purification of these metabolites were carried out by silica gel column chromatography and acid hydrolysis. Furthermore, phytocompounds were identified by using GC-MS/MS, and LC-MS/MS as well, the results showed an increase in the concentration of chief phytocompounds such as curcumin and diosgenin. These purified metabolites were tested for antimicrobial activity using a variety of microbiological assays, including Agar well diffusion and MIC, as well as antifungal and anti-biofilm inhibition activity. The mechanism of inhibition of Sortase A enzyme, which is essential for biofilm formation, was elucidated using molecular modelling techniques. The combinational effect of phytocompounds (curcumin + 4-hydroxy-2 methylacetophenone) inhibits the enzyme by forming a ternary complex which shows better results over control inhibitors and this combination also gives similar results in wet-lab experiments.

4.Future Findings:

- In this study, pot culture experiments were conducted, but it will be interesting to see if the potent PGPR, such as *Serratia nematodiphila* RGK, *Pseudomonas plecoglossicida* RGK, *Exiguobacterium acetylicum* RGK, and *Enterobacter mori* RGK1, will have the same effects in field trials.
- It will be fascinating to see these potent strains of isolated PGPRs used on a large scale by the production of biofertilizer in future research.
- According to the current study, isolated PGPR influenced plant secondary metabolites, and these enhanced metabolites were used for a variety of purposes. It will be interesting to see if these metabolites can be used for various purposes, such as anti-cancer and anti-insecticidal, as in the previous study, a variety of uses for plant secondary metabolites were reported.
- The antimicrobial activity and selectivity of secondary metabolites can be improved by combining them with nanoparticles.
- Hence, the present work opens a new avenue and creates scope for evaluation of other applications of PGPR-induced plant secondary metabolites from Turmeric and Asparagus in pharmaceutical applications, agricultural and food industries.